THE SYNTHESIS AND LATE-STAGE DIVERSIFICATION OF THE CYANTHIWIGIN NATURAL PRODUCT CORE AND SYNTHETIC INSIGHTS DERIVED THEREIN

Thesis by

Kelly E. Kim

In Partial Fulfillment of the Requirements

for the Degree of

Doctor of Philosophy

CALIFORNIA INSTITUTE OF TECHNOLOGY

Pasadena, California

2017

(Defended December 16, 2016)

Kelly E. Kim

ORCID: 0000-0002-4132-2474

To Mom, Dad, and Roger

and

To Steven

ACKNOWLEDGEMENTS

Scientific research is by nature a collaborative endeavor, incorporating the painstaking efforts of many contributors. While the preparation of this thesis has at times seemed like the ultimate solitary activity, its completion would not have been possible without the input, guidance, and support of many people.

First and foremost, I would like to thank my advisor, Professor Brian Stoltz. I feel extremely fortunate to have joined the Stoltz group, as Brian is a phenomenal mentor. From my first meeting with him, I was exhilarated by Brian's enthusiasm for chemistry and the training of young scientists, a quality that has been instrumental to my success in graduate school. There have been many instances where I entered Brian's office confused and frustrated by setbacks in my research, and each time I exited feeling invigorated and eager to try out all the ideas we had discussed. As I acclimated to the often overwhelming nature of scientific research during my early years in graduate school, these moments of clarity helped keep me excited about my work and focused on answering the important questions.

Brian's knowledge of chemistry is awe-inspiring, as is his talent for motivating his students to produce their very best work. Under his tutelage, I have cultivated a keen eye for professionalism in executing, writing, and presenting scientific research. However, perhaps even more admirable is his ability to connect with students on a human level and understand that the pursuit of academic excellence is most possible when one's personal life is intact. This is one of Brian's mentorship qualities that I most appreciate and one that has significantly contributed to the overall success of my graduate training.

For his support during my most uncertain times, I am deeply grateful, and I hope to emulate his mentorship style in my future career.

I am also fortunate to have enjoyed much wisdom and encouragement from the members of my dissertation committee throughout my graduate studies. As the committee chair, Professor Robert Grubbs has been continuously supportive of my work, collaborating on several of my research projects and ensuring that all of my graduate degree progress meetings have occurred smoothly and in a timely fashion. I am also very grateful for Professor Harry Gray's constant dedication to my training, providing much-appreciated encouragement on my exit proposals and always taking the time to discuss my progress and career goals any time I stop by his office. Professor Sarah Reisman, the newest member of my committee, has tirelessly offered her feedback on a diverse range of topics including research concerns, post-Caltech plans, and Women in Chemistry event-planning and committee management over the past several years.

I have also benefitted enormously from my involvement in the NSF Center for Stereoselective C–H Functionalization (CCHF) over the past four years. The weekly videoconferences and annual meetings became defining activities of my graduate school experience, and I am fortunate to have met many wonderful students, postdocs, professors, and industrial chemists through this program. While the Center is quite large and encompasses too many individuals to name specifically, I would like to thank CCHF Director Professor Huw Davies (Emory) for getting the Center established, and Dr. Dan Morton for tirelessly working to ensure Center-wide events ran smoothly. Additionally, I must thank my CCHF collaborators: Professor Justin Du Bois, Dr. Ashley Adams, and Nicholas Chiappini (Stanford), along with many other individuals with whom I've shared

insightful conversations about chemistry and life. I will certainly miss the cross-institutional discussions that I've grown accustomed to through the CCHF.

I am also grateful for the many teaching opportunities I've had at Caltech and would like to thank Professors Nathan Lewis, Geoffrey Blake, Douglas Rees, Peter Dervan, Daniel O'Leary, Gregory Fu, and Brian Stoltz for allowing me to serve as a teaching assistant for their courses. I am especially appreciative of Professor O'Leary's active role in cultivating and supporting my interest in pursuing a career at a PUI .

The research described in this thesis would not have been possible without the expertise of synthetic and spectroscopic wizards Dr. Scott Virgil and Dr. David VanderVelde. Dr. Virgil's assistance was instrumental in my efforts to reproduce Dr. John Enquist's synthesis of the cyanthiwigin natural product core. As a relatively inexperienced second-year graduate student at the time, I learned a great deal from Dr. Virgil's careful analyses of experimental setups for sensitive reactions, particularly the Negishi cross-coupling and RCM/cross-metathesis transformations. Moving forward, this knowledge enabled me to perform the entire synthetic sequence repeatedly with minimal trouble, which was vital to the success of the cyanthiwigin diversification project. Although I have yet to meet him, Dr. John Enquist also graciously answered in great detail many of my emails asking for advice on certain synthetic steps.

Similarly, Dr. VanderVelde's devotion to educating me in multi-dimensional NMR analysis was a key component of my research, as most of the compounds generated from the cyanthiwigin diversification project required the use of 2D NMR experiments for unambiguous structural determination. Compared to the overwhelming confusion I felt the first several times I attempted to interpret 2D NMR data, the ease with which I

acquire and analyze these spectra today is a testament to Dr. VanderVelde's substantial contributions to my graduate training.

Along the same lines, Dr. Mona Shagholi and Naseem Torian have tirelessly provided assistance in the acquisition of mass-spectrometry data and have always done so kindly and patiently, even when my samples were overly dilute. Furthermore, I am grateful to Dr. Michael Takase and Lawrence Henling for helping in the acquisition of X-ray crystallography data and for taking the time to scrutinize my samples even when they were not of good enough quality for X-ray diffraction.

I ascribe much of my current interest in chemistry to the masterfully designed courses that captured my attention early in college. Professor J. Michael McBride's Freshman Organic Chemistry course at Yale was a challenging but fascinating beginning to university coursework and organic chemistry during my first semester in the fall of 2007. Professor McBride's thoughtful approaches to lectures and his insistence that students always ask the questions "How do you know?" and "Compared to what?" taught me to engage with the scientific process and think critically. Furthermore, the course's unorthodox diligence in scrutinizing the historical backgrounds of important concepts in chemistry showcased the progressing sophistication of chemical research methods, helping me appreciate the significance of modern advances in this evolutionary process.

My interest in chemistry was bolstered by my enjoyment of the accompanying laboratory course. The instructor, Dr. Christine DiMeglio, advised me in choosing courses for the chemistry major and employed me as an aide in the teaching labs. She also provided me with my first opportunities for original chemical experimentation when she tasked me with optimizing a low-yielding procedure used in the lab courses.

Furthermore, Dr. DiMeglio supported my application to the DAAD RISE summer internships program, an experience that ultimately led to my decision to pursue graduate studies in chemistry. For her unwavering support and instrumental role in my early laboratory education, I am most grateful.

I'm also very fortunate to have had the opportunity to work in three differently focused research labs as an undergraduate. I am grateful to Dr. Hal Blumenfeld for enlightening me to the practice of scientific research, albeit in a non-chemistry field. I am indebted to Dr. Max Bielitza and Prof. Dr. Jörg Pietruszka for introducing me to research in organic synthesis and for inspiring me to continue my training in chemistry after college. Finally, I am appreciative of Prof. Nilay Hazari for taking me on as the first undergraduate student in his lab, introducing me to organometallic chemistry research, and for sharing all of his insightful anecdotes about his time as a postdoc at Caltech.

Over the past five years, I have shared lab space with many remarkable graduate students, postdoctoral scholars, and undergraduate students. When I first joined the group, I benefitted tremendously from the expertise of older students in my bay and in the office. My hoodmate, Christopher Haley, spent much time helping me set up my hood and showing me where to find anything I needed in the lab. He also taught me many little tricks for running columns that I still use today. Dr. Grant Shibuya, Dr. Doug Behenna, Allen Hong, Nathan Bennett, Alex Goldberg, Jonny Gordon, and Jeff Holder were also phenomenal sources of advice on tricky work-ups, problematic separations, or elaborate reaction set-ups. Depsite only overlapping with them for a few months, Dr. Kristy Tran, Hosea Nelson, and Chris Gilmore were highly encouraging of me as a new student in the group, and I enjoyed many uplifting conversations with them.

Being trapped at the desk next to mine in the small office, Allen Hong was a great sport about answering all of my inane first-year questions. Despite working on a completely different project than mine, Allen served as an in-lab mentor for me, often supplying much-needed advice on my research and on grad school in general, including introducing me to a vital aspect of my Caltech experience: post-subgroup Tuesday flautas at Ernie's. I especially appreciated his weeks-long campaign to combat my night-owl tendencies through the promise of a morning piece of candy if I made it to lab before 9 AM (at which I was moderately successful). Even after departing Caltech during my second year, Allen has remained a good friend and mentor, providing encouragement and advice on postdoctoral and fellowship applications, paper submissions, and more. He is also the creator of some of the best-looking figures and templates I've seen, and I often follow his example when creating official documents such as CVs, thesis outlines, etc.

One of the best parts about starting in a new lab as part of a big class of graduate students is forming special bonds with the other students in your year. Nick O'Connor, Seojung Han, and Anton Toutov have been fantastic classmates, and we spent many an evening in lab talking about chemistry and musing over what to expect from graduate school. These discussions were supplemented with extracurricular video game nights at my apartment and margarita nights at Amigos. I greatly enjoyed the many conversations I've had with Nick, Seojung, and Anton about chemistry and life over the past several years, and wish them all the best in their future endeavors.

Having secured my friendship early on in our first year with the (reimbursed) purchase of a bottle of whipped cream vodka, Nick O'Connor has been one of my closest friends at Caltech. Fellow night owls, Nick and I have worked late into the night on

various occasions, providing each other with good company and humor. In addition to being a close confidante and fellow opponent of the word "vignette," Nick is one of the most intelligent and well-read people I know, and his passion for historical biographies, obscure named reactions, and Wikipedia exploration is unparalleled among our peers. I feel privileged to have been able to share as much of our graduate school experiences as we did, having undergone candidacy exams, fourth-year meetings, postdoc and fellowship applications, proposal exams, and thesis writing in roughly identical timelines. I will certainly miss our spirited discussions when we part ways and wish him the best at UC Berkeley and beyond. I am confident that he will do amazing things with his career.

After she joined the lab in my third year, Sam Shockely and I struck up a fast friendship, as we were both baymates and desk neighbors. Extremely hard-working and intelligent, Sam hit the ground running in her graduate studies, and her enthusiasm for science and efficiency in the lab breathed new life into me during my post-candidacy third-year slump. In addition to inspiring me to work more cleanly with her insanely tidy fume hood and desk, Sam took an active role in helping me fight the "grad school 15" by introducing me to a rich variety of group fitness classes at the Caltech gym and joining me in the Alhambra Pumpkin Run 10K. Sam's energy and zest for science is effusive, and I know that she will continue to inspire others while enjoying wildly successful graduate and post-graduate careers.

I am fortunate to have worked with talented individuals on several projects. I greatly enjoyed working with Yiyang Liu on the decarbonylative dehydration of fatty acids and with Doug Duquette, Dr. Alex Marziale, Dr. Marc Liniger, Dr. Yoshitaka Numajiri, and Rob Craig on the low-catalyst enantioselective allylic alkylation. I also

appreciate Jiaming Li's nitrite screening contributions to the aldehyde-selective Tsuji–Wacker oxidations project and Dr. Xiangyou Xing's insights into allylic C–H oxidation for the comparative C–H functionalization project. Dr. Boger Liu, with whom I overlapped for several years in the lab, provided a font of knowledge and inspiration. Finally, I thank Yuka Sakazaki for allowing me the opportunity to serve as a mentor in the lab and wish her the best in her future career.

While it is challenging to name every single person whose presence in lab has influenced me over the past five years, I would also like to thank Nina Vrielink, Beau Pritchett, Dr. Christian Eidamshaus, Chung Whan Lee, Corey Reeves, Dr. Pamela Tadross, Austin Wright, Elizabeth Goldstein, Steven Loskot, Shoshana Bachmann, Christopher Reimann, Dr. Eric Welin, Dr. Caleb Hethcox, Kelvin Bates, Katerina Korch, Dr. Masaki Hayashi, Dr. Kazato Inanaga, Dr. Yuji Sumii, Dr. Noriko Okamoto, Dr. Jimin Kim, Dr. Max Klatte, Dr. Hendrik Klare, Julian West, and Moriam Masha for providing friendship, proofreading services, good conversations, and fond memories over the past several years. I am especially grateful to Christopher Haley, Yutaro Saito, Yuka Sakazaki, and Dr. Denis Kroeger for having been wonderful hoodmates. Additionally, I have enjoyed years of stimulating conversation in the "small office" with Doug Duquette, Nick O'Connor, Sam Shockley, David Schuman, Alex, Sun, Dr. Gerit Pototschnig, Christopher Haley, Dr. Guillaume Lapointe, Lukas Hilpert, Allen Hong, Dr. Jared Moore, Nathan Bennett, Chris Gilmore, Dr. Marchello Cavitt, Dr. Daisuke Saito, and Dr. Justin Hilf. I will look back with fond memories on the many summers of CCE softball, culminating with a championship victory this past year, thanks to a wonderful team and Beau's tireless efforts as captain. I enjoyed attending MTG events with Doug and will

miss “shamblesharking” with him as well as receiving all sorts of random religious figurines from his apartment complex. I wish all the best for the first- and second-year students who are just beginning their graduate school adventures.

My discussions about science, graduate school, and life with friends outside of the Stoltz lab have also greatly enriched my experience by providing opportunities to view my work outside of the usual contexts. I am deeply grateful to Dr. Pablo Guzmán for his unwavering support and encouragement throughout the years and to Dr. Alissa Hare, Dr. Nathan Schley, Dr. James Blakemore, Anton Toutov, Kevin Shen, Marc Serra, Tania Darnton, Helen Yu, Matthew Chalkley, Dr. David Romney, and Dr. Charisma Bartlett for engaging me in thought-provoking and insightful conversations. I was also fortunate to have many interesting discussions with my cousin, Cedric Flamant, with whom I overlapped at Caltech for four years as he earned his bachelor’s degree.

I would also like to thank Delores Bing for serving as a fantastic director of the Caltech Chamber Music Program, in which I participated throughout my time at Caltech. I am indebted to Robert Ward for encouraging me to participate in the program during a chance encounter my first week on campus in 2011. Were it not for his encouragement, I would not have discovered the great joy that playing chamber music has brought me over the past five years. My participation in the chamber program provided me with an outlet to engage my musical interests and disconnect from the stresses of research, without which I would surely have grown disillusioned. I am deeply grateful to my coaches Robert Ward, Kirsten Joel, Michael Kreiner, Delores Bing, and Martin Chalifour for enriching my musical education, and I feel fortunate to have met many wonderful musician-scientists through this program. My performances with Sean Symon, Ian

Wong, Joe Iverson, and Sarah Jeong, are among my favorite musical memories so far, and our conversations about music and science have been similarly unforgettable.

The Caltech Division of Chemistry and Chemical Engineering is blessed with a fantastic and caring staff. Agnes Tong facilitated navigation of the administrative processes involved in completing the PhD degree. Her geniune concern for students and dedication to their happiness and success is always apparent, and she has been a great friend to me these past several years. Alison Ross has also been tremendously helpful in this position and is a great resource for students. Jeff Groseth has rejuvenated many a malfunctioning stir plate, UV lamp, or rotovap in impressive fashion. Likewise, Rick Gerhart has repaired countless broken columns, manifolds, and the like over the years, and the Caltech community is surely sad to see him go despite wishing him the best in his retirement. Joe Drew has facilitated the ordering and shipping of various chemical parcels and has assisted me in locating misplaced packages on several occasions. In addition to taking care of many computer-related needs, Silva Virgil has been an amazing friend, and I've greatly enjoyed the wonderful holiday parties and opera outings that she and Scott have hosted over the years. Last but certainly not least, I am grateful for all of the work Lynne Martinez does to keep our group operating smoothly and to facilitate fellowship applications for students. To all of these staff members, I extend my sincere gratitude for their dedication to the Caltech community and for assisting with the completion of my thesis work.

Finally, I would like to thank my family for their unconditional support, love, and patience. My parents have consistently inspired me with their incredible work ethic and dedication to caring for my brother and me. I am especially grateful for the positive

thinking abilities that I learned from my mother, as I soon came to realize the importance of staying positive in the midst of the uncertainty and failure that inevitably accompanies scientific research. Likewise, the perseverence and determination that I learned from my father have also proven essential in the completion of this dissertation. Throughout my life, my older brother, Roger, has inspired me with his enthusiasm for learning and commitment to excellence. His passion for medicine and science is effusive, and my conversations with him often leave me feeling invigorated and eager to achieve my best work in the lab. I am also fortunate to have amazingly supportive aunts and uncles living on the West Coast who have made my time here very comfortable. I thank Aunt Valinda, Aunt Rebecca, Aunt Daphne, Aunt Kathryne, Uncle Andy, Uncle Allen, Aunt Jane, and their spouses, for reaching out to me many times over the years.

I would also like to acknowledge my boyfriend, Steven Banks, who has supported me continuously throughout my time at Caltech, despite living over 1000 miles away. Gamely weathering my rants about graduate school and research while serving as a scapegoat for the lab's collective criticisms of Microsoft software, Steven has always encouraged me to follow my dreams and stood by me through the most harrowing moments in my graduate studies. I appreciate being able to regularly talk to someone outside of science, as these conversations provide a break from the immersion experience of graduate school while also affording unique insight into my work from an outside perspective. I look forward to finally joining Steven in Seattle next month.

Overall, the work described herein would not have been possible without the contributions and support of all those listed above and many others not specifically mentioned by name. To each and every one of them, I offer my most heartfelt gratitude.

ABSTRACT

Inspired by the therapeutic properties of many natural products and the ever-growing need for novel medicines, research programs for the late-stage diversification of complex molecular scaffolds have risen in popularity over the past few decades. In addition to generating a wide range of non-natural compounds for biological evaluation, these research efforts provide valuable synthetic insights into the preapration and reactivity of structurally intricate molecules. After a brief summary of the various strategies for late-stage diversification, examples of previous studies toward the derivatization of natural product-inspired scaffolds are highlighted.

A second-generation synthesis of the cyanthiwigin natural product core employing recently developed technologies is described. Re-optimization of the key double asymmetric catalytic alkylation transformation facilitates large-scale operations, and application of the aldehyde-selective Tsuji–Wacker oxidation enables productive recycling of an advanced intermediate. Together, these modifications expedite the preparation of the tricyclic cyanthiwigin framework on multi-gram scale.

The aldehyde-selective Tsuji–Wacker reaction is demonstrated to be effective for the oxidation of terminal alkenes bearing quaternary carbons at the allylic or homoallylic position. The synthetic utility of this method is extended through further transformation of the crude aldehyde products, permitting catalytic conversion of hindered terminal olefins to a variety of other synthetically useful functional groups.

With access to large quantities of the cyanthiwigin natural product core, a comparative study of various methods for intermolecular C–H oxidation was conducted. Examination of the reactivity of the cyanthiwigin framework under established conditions for allylic C–H acetoxylation, C–H hydroxylation, C–H amination, C–H azidation, and C–H chlorination reveals significant steric and electronic influences and suggests that functionalization is guided by innate reactivity within the substrate.

Finally, the preparation of several non-natural cyanthiwigin–gagunin hybrid molecules from the cyanthiwigin core is described. Preliminary studies toward the biological activities of synthetic intermediates are presented, and future directions for the synthesis of novel cyanthiwigin–gagunin hybrids are outlined.

PUBLISHED CONTENT AND CONTRIBUTIONS

Kim, K. E.; Stoltz, B. M. "A Second-Generation Synthesis of the Cyanthiwigin Natural Product Core." *Org. Lett.* **2016**, *18*, 5720–5723. DOI: 10.1021/acs.orglett.6b02962.

K.E.K. participated in the conception of the project, all experimental work described, data acquisition and analysis, and manuscript preparation. Permission has been secured from the American Chemical Society for use of this material.

Kim, K. E.; Li, J.; Grubbs, R. H.; Stoltz, B. M. "Catalytic Anti-Markovnikov Transformations of Hindered Terminal Alkenes Enabled by Aldehyde-Selective Wacker-Type Oxidation." *J. Am. Chem. Soc.* **2016**, *138*, 13179–13182. DOI: 10.1021/jacs.6b08788.

K.E.K. participated in the conception of the project, all experimental work described, data acquisition and analysis, and manuscript preparation. Permission has been secured from the American Chemical Society for use of this material.

Marziale, A. N.; Duquette, D. C.; Craig, R. A., II; Kim, K. E.; Liniger, M.; Numajiri, Y.; Stoltz, B. M. "An Efficient Protocol for the Palladium-Catalyzed Asymmetric Decarboxylative Allylic Alkylation Using Low Palladium Concentrations and a Palladium(II) Precatalyst." *Adv. Synth. Catal.* **2015**, *357*, 2238–2245. DOI: 10.1002/adsc.201500253.

K.E.K. participated in experimental work, data acquisition and analysis, and mansucript preparation. Permission has been secured from Wiley-VCH for use of this material.

TABLE OF CONTENTS

LIST OF FIGURES

CHAPTER 1

CHAPTER 2

APPENDIX 3

CHAPTER 3

APPENDIX 4

APPENDIX 5

CHAPTER 4

APPENDIX 7

APPENDIX 8

APPENDIX 9

CHAPTER 5

APPENDIX 11

LIST OF SCHEMES

CHAPTER 1

CHAPTER 2

APPENDIX 1

APPENDIX 2

CHAPTER 3

APPENDIX 4

CHAPTER 4

APPENDIX 6

CHAPTER 5

APPENDIX 10

LIST OF TABLES

CHAPTER 2

CHAPTER 3

CHAPTER 4

APPENDIX 8

CHAPTER 5

APPENDIX 12

LIST OF ABBREVIATIONS

$[\alpha]_D$	angle of optical rotation of plane-polarized light
Å	angstrom(s)
Ac	acetyl
AIBN	azobis-(isobutyronitrile)
ALA	1 M aqueous solution of aminolevulinic acid
amp	ampicillin
APCI	atmospheric pressure chemical ionization
app	apparent
aq	aqueous
Ar	aryl group
atm	atmosphere(s)
bipy	2,2'-bipyridyl
Bn	benzyl
Boc	*tert*-butoxycarbonyl
bp	boiling point
br	broad
Bu	butyl
i-Bu	*iso*-butyl
n-Bu	butyl or *norm*-butyl
t-Bu	*tert*-butyl
Bn	benzyl
BQ	1,4-benzoquinone

Bz	benzoyl
c	concentration of sample for measurement of optical rotation
^{13}C	carbon-13 isotope
/C	supported on activated carbon charcoal
°C	degrees Celsius
calc'd	calculated
CAN	ceric ammonium nitrate
cap	caprolactam
Cbz	benzyloxycarbonyl
CCDC	Cambridge Crystallographic Data Centre
CDI	1,1'-carbonyldiimidazole
cf.	consult or compare to (Latin: *confer*)
CFL	compact fluorescent light
cm^{-1}	wavenumber(s)
cod	1,5-cyclooctadiene
comp	complex
conc.	concentrated
CSI	chlorosulfonyl isocyanate
d	doublet
D	dextrorotatory
Da	Dalton(s)
dba	dibenzylideneacetone
pmdba	bis(4-methoxybenzylidene)acetone

dmdba	bis(3,5-dimethoxybenzylidene)acetone
DBU	1,8-diazabicyclo[5.4.0]undec-7-ene
DCE	1,2-dichloroethane
DDQ	2,3-dichloro-5,6-dicyano-1,4-benzoquinone
de	diastereomeric excess
DIAD	diisopropyl azodicarboxylate
DMAD	dimethyl acetylenedicarboxylate
DMAP	4-dimethylaminopyridine
DMDO	dimethyldioxirane
DME	1,2-dimethoxyethane
DMF	*N*,*N*-dimethylformamide
DMP	Dess–Martine periodinane
DMSO	dimethylsulfoxide
dppf	1,1'-bis(diphenylphosphino)ferrocene
dppp	1,3-bis(diphenylphosphino)propane
dr	diastereomeric ratio
ee	enantiomeric excess
E	trans (entgegen) olefin geometry
EC_{50}	median effective concentration (50%)
EDCI	1-ethyl-3-(3-dimethylaminopropyl)carbodiimide
e.g.	for example (Latin: *exempli gratia*)
EI	electron impact
ESI	electrospray ionization

Et	ethyl
et al.	and others (Latin: *et alii*)
FAB	fast atom bombardment
g	gram(s)
h	hour(s)
^{1}H	proton
^{2}H	deuterium
^{3}H	tritium
[H]	reduction
HFIP	hexafluoroisopropanol
HMDS	hexamethyldisilamide or hexamethyldisilazide
HMPA	hexamethylphosphoramide
$h\nu$	light
HPLC	high performance liquid chromatography
HRMS	high resolution mass spectrometry
Hz	hertz
IC_{50}	half maximal inhibitory concentration (50%)
i.e.	that is (Latin: *id est*)
IPTG	1 M aqueous solution of isopropyl-β-D-thiogalactoside
IR	infrared spectroscopy
J	coupling constant
k	rate constant
kcal	kilocalorie(s)

kg	kilogram(s)
L	liter or neutral ligand
L	levorotatory
LA	Lewis acid
LB	lysogeny broth
LB_{amp}	LB with 100 μg/mL amp
LB_{amp}/agar	a gel consisting of 1.6% (w/v) agar in LB_{amp}.
LD_{50}	median lethal dose (50%)
LDA	lithium diisopropylamide
LTMP	lithium 2,2,6,6-tetramethylpiperidide
m	multiplet or meter(s)
M	molar or molecular ion
m	meta
μ	micro
m-CPBA	*meta*-chloroperbenzoic acid
Me	methyl
mg	milligram(s)
MHz	megahertz
min	minute(s)
mL	milliliter(s)
mol	mole(s)
mp	melting point
Ms	methanesulfonyl (mesyl)

MS	molecular sieves
m/*z*	mass-to-charge ratio
N	normal or molar
NBS	*N*-bromosuccinimide
nm	nanometer(s)
NMO	4-methylmorpholine *N*-oxide
NMR	nuclear magnetic resonance
nOe	nuclear Overhauser effect
NOESY	nuclear Overhauser enhancement spectroscopy
o	ortho
[O]	oxidation
p	para
PCC	pyridinium chlorochromate
PDC	pyridinium dichromate
Ph	phenyl
pH	hydrogen ion concentration in aqueous solution
PHOX	phosphinooxazoline
pin	pinacol
pK_a	acid dissociation constant
PMB	*para*-methoxybenzyl
ppm	parts per million
PPTS	pyridinium *para*-toluenesulfonate
Pr	propyl

i-Pr	isopropyl
n-Pr	propyl or *norm*-propyl
psi	pounds per square inch
py	pyridine
q	quartet
R	alkyl group
R	rectus
r	selectivity = [major stereoisomer – minor stereoisomer]/[major stereoisomer + minor stereoisomer]
RCM	ring-closing metathesis
ref	reference
R_f	retention factor
s	singlet or seconds
s	selectivity factor = $k_{rel(fast/slow)} = \ln[(1 - C)(1 - ee)]/\ln[(1 - C)(1 + ee)]$, where C = conversion
S	sinister
sat.	saturated
SEM	2-(trimethylsilyl)ethoxymethyl
t	triplet
tacn	1,4,7-trimethyl-1,4,7-triazacyclo-nonane
TB	terrific broth
TB_{amp}	TB with 100 μg/mL amp
TBAF	tetra-*n*-butylammonium fluoride
TBAT	tetra-*n*-butylammonium difluorotriphenylsilicate

TBDPS	*tert*-butyldiphenylsilyl
TBHP	*tert*-butylhydroperoxide
TBME	*tert*-butylmethyl ether
TBS	*tert*-butyldimethylsilyl
tbsbp	*tert*-butyl sulfonyl bridged prolinate
temp	temperature
TES	triethylsilyl
Tf	trifluoromethanesulfonyl
TFA	trifluoroacetic acid
THF	tetrahydrofuran
TIPS	triisopropylsilyl
TLC	thin layer chromatography
TMEDA	*N*,*N*,*N*',*N*'-tetramethylethylenediamine
TMS	trimethylsilyl
TOF	time-of-flight
tol	tolyl
t_r	retention time
Ts	*para*-toluenesulfonyl (tosyl)
UV	ultraviolet
w/v	weight per volume
v/v	volume per volume
X	anionic ligand or halide
Z	cis (zusammen) olefin geometry

CHAPTER 1

Late-Stage Diversification of Natural Product Scaffolds:

A Tool for Synthetic and Biological Studies

1.1 INTRODUCTION

The following chapter is intended to present an overview of complex molecule diversification, including the motivations for conducting these studies, the various strategies developed for this purpose, and highlights of published reports. Considering the vast breadth of study in this open-ended and active research area, the present discussion will focus on strategies that involve late-stage diversification of natural product-inspired scaffolds. References for reviews and examples of studies using alternative strategies will be provided as appropriate.

1.2 OVERVIEW OF COMPLEX MOLECULE DIVERSIFICATION

Fine-tuned over thousands of centuries for specific biological roles,[1] natural products served therapeutic purposes from the dawn of the most rudimentary medical practices in

human civilization and continue to inspire drug development in today's highly technical world.[2] Tremendous advances in synthetic chemistry and biology research over the past half-century have greatly enhanced understanding of many biological processes for which natural products were evolved. The de-mystification of many natural products' roles in biology has enabled the performance of detailed studies correlating molecular structure with biological function, thereby providing the scientific community with opportunities to plan research strategies around the conclusions drawn from these investigations.[3] In line with this phenomenon, the past few decades have witnessed a surge in research programs aiming to derivatize complex molecules with the ultimate goal of discovering novel therapeutics and the concomittant aim of establishing powerful methodologies to facilitate complex molecule synthesis. Overall, the synthetic and medicinal insights gleaned from this type of research originate from a unique perspective complementary to those of pure total synthesis and methods development programs.

1.2.1 MOTIVATIONS

Central to any research program is the impact of the findings on the scientific community and beyond. The goals of complex molecule diversification programs are multi-faceted but center largely around studying the biological activities of non-natural structurally intricate compounds and preparing large quantities of the complex precursors to the aforementioned non-natural compounds. While the primary aim of using organic synthesis to study biology is of great significance to medicinal chemistry and drug development, the seemingly peripheral goal of executing multi-step synthesis of complex molecules should not be underestimated in its potential for generating impactful

information of high relevance to the chemical community. Together, the biological and synthetic implications derived from these investigations are what motivate scientists to devote significant effort to the diversification of complex molecular scaffolds.

1.2.1.1 BIOLOGICAL CONSIDERATIONS

Natural products have served therapeutic purposes for many centuries, and today most FDA-approved drugs available are small molecules, many of which are based on natural products.[2,4] Given the intimate relationship between complex molecules and drug development, a central theme of most research efforts in complex molecule diversification entails the biological evaluation of the derivative compounds generated. The specific disease area investigated can either be targeted based on knowledge of the biological activities of related known compounds (as is the case with natural product-based strategies) or left open to as wide a range as possible (as is the case with classic diversity-oriented synthesis approaches). In all cases, developing an understanding of the three-dimensional configurations of the complex molecule derivatives, especially in the context of interaction with the biological agent to be studied, is of paramount importance if meaningful conclusions about biological activity are to be made. Under the appropriate circumstances, unexpected observations in biological investigations could lead to significant discoveries about the mechanisms of activity among complex molecules and contribute to the potential for a given compound to form the basis of a drug development program.

1.2.1.2 SYNTHETIC CONSIDERATIONS

As a more immediate consideration, diversification studies also provide a foundation from which to develop an efficient and reliable synthetic route for accessing a complex molecular scaffold in large quantities. Unless the compound to be diversified is commercially available or accessible through semi-synthesis, a highly effective multi-step synthesis is generally required for the overall research program to succeed. While this consideration may resemble those of a traditional total synthesis project, the amount of late-stage material required for a successful diversification project generally exceeds what is necessary to complete a total synthesis since the number of potential targets is essentially limitless.[5] As such, constant optimization of the synthetic route to the main scaffold is common in diversification programs and often leads to the development of new methodologies or strategies to expedite the synthesis.

Once the core scaffold has been obtained in sizeable quantities, diversification studies also provide a viewpoint from which to examine the reactivities of complex frameworks. Unexpected outcomes of traditionally straightforward reactions often form the basis of efforts to adapt pre-established methodologies for the transformations of complex molecules, contributions which are likely to find use in many other synthetic endeavors. Another important synthetic consideration in the later stages of diversification projects is the characterization of all the non-natural compounds synthesized. Since accurate knowledge of molecular structure is vital to the validity of the structure-activity relationship (SAR) studies that form the backbone of biological assessment, significant effort should be expended on elucidating the intricate, unknown structures of the complex derivatives prepared. As no reference data exists for these non-natural compounds,

structure elucidation is often achieved through multi-dimensional NMR spectroscopy, X-ray crystallography, and high-resolution mass spectrometry, among other means.

1.2.2 STRATEGIES

Many approaches toward the diversification of complex molecules have been documented over the years. While each account bears unique nuances that evade classification, it can be useful to demarcate the myriad examples into three distinct categories: 1) natural product derivatization, 2) diversity-oriented synthesis, and 3) natural product scaffold diversification (Figure 1.1). Although all three types share similar attributes, the key differentiating factor is the nature of the scaffold to be diversified. This, along with subtle discrepancies in the motivations and philosophies, serves to delineate these strategies and highlight the major contributions of each approach.

Figure 1.1 Overview of strategies for complex molecule library preparation

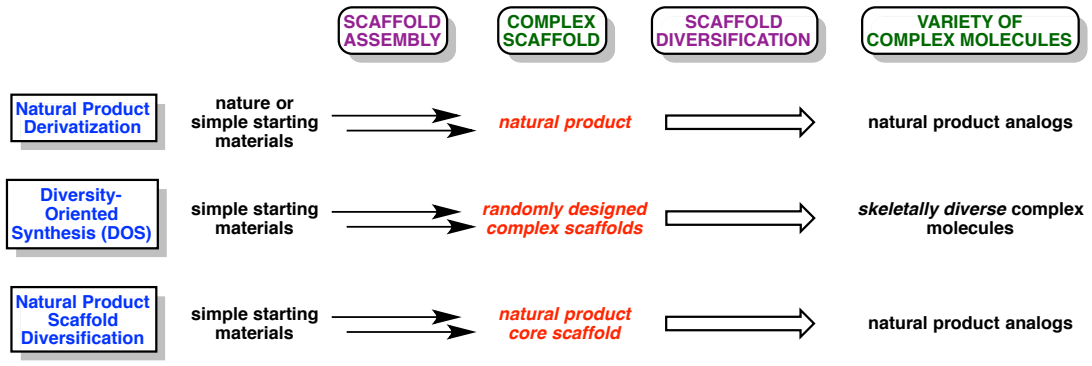

1.2.2.1 NATURAL PRODUCT DERIVATIZATION

Natural products are central to modern drug discovery efforts, as evidenced by the success of pharmaceuticals such as paclitaxel (anticancer), artemisinin (antimalarial), daptomycin (antibacterial), and morphine (analgesic).[6] While natural products and their derivatives have comprised many small molecule drugs since the 1940s,[7] interest in developing natural products as therapeutics began to wane in the 1990s due to challenges in identifying new biologically potent natural agents.[8] Furthermore, advances in synthetic methods enabling the rapid assembly of diverse molecular architectures encouraged the transition away from reliance on natural products and toward synthetic scaffolds.[9] However, extensive research over the last few decades has revealed that the considerable structural differences between typical synthetic scaffolds and natural products correspond to substantial disparities in biological activity.[10] Specifically, the differences in ring system complexity, percentage of sp^3-hybridized carbons, heteroatom content, and number of stereocenters contributed to significant structural variations that resulted in the synthetic scaffolds and natural products targeting different macromolecular receptors.[11]

Given the potential to complement the therapeutic benefits of synthetically derived lead molecules, enthusiasm for natural product research has been rejuvenated over the past decade. Armed with modern synthetic methods and techniques for conducting detailed SAR studies, chemists are well situated to build on the foundation established by previous natural product and synthetic scaffold research. Current research programs to create natural product analogs target compounds that incorporate the structural

complexity and physicochemical properties of natural products while employing efficient routes that enable rapid construction of the scaffold.

Figure 1.2 Starting points for derivatization studies: selected natural products available through A) commercial suppliers, B) extraction, or C) semi-synthesis

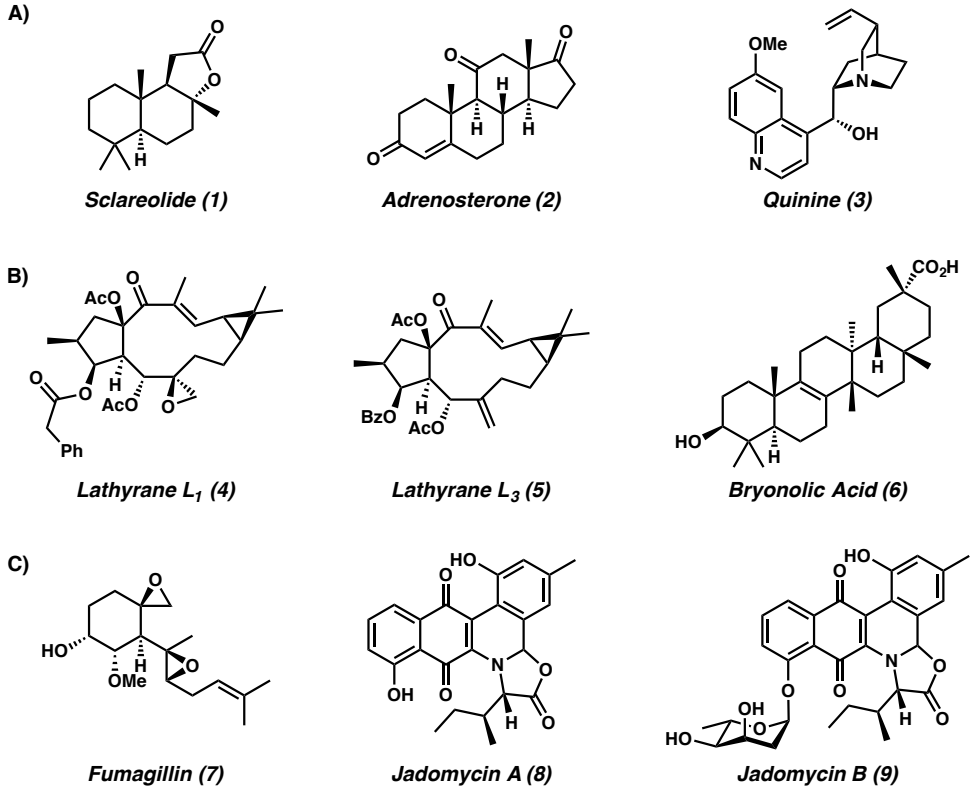

Considering the therapeutic effects exhibited by many natural products, one reasonable strategy for generating libraries of compounds for medicinal evaluation involves the direct modification of natural products themselves. Many are available from commercial suppliers, facilitating their use as starting points for library assembly.[12] For instance, numerous diversification studies have been carried out on the commercially available natural products sclareolide (**1**),[13] adrenosterone (**2**),[14] and quinine (**3**),[14,15] generating an abundance of derivatives in large enough quantities for extensive biological

evaluation (Figure 1.2A). Natural products obtained through extraction have also served as fine starting points for diversification studies, such as those conducted on the lathyrane diterpenoids L_1 (**4**) and L_3 (**5**)[16] and bryonolic acid (**6**),[17] among others (Figure 1.2B). Additionally, Furlan and co-workers demonstrated that extracts containing mixtures of several natural products could also be conveniently transformed into useful diversified analogs that could be screened for biological activity, further encouraging the use of natural products as library progenitors.[18]

Synthetically, natural products can be accessed through total synthesis or semi-synthesis, which entails enzymatic generation of the desired natural product. While diversification studies based on natural products arising from total synthesis have been accomplished, the high step counts of many total syntheses hinder the applicability of this strategy for accessing natural products as diversification scaffolds. In contrast, semi-synthesis has emerged as a useful approach toward this end, permitting facile production of compounds such as fumagillin (**7**)[19] and jadomycins A (**8**) and B (**9**)[20] to be used as diversification scaffolds (Figure 1.2C).

1.2.2.2 DIVERSITY-ORIENTED SYNTHESIS

Aiming to discover small molecules with therapeutic properties orthogonal to those of both natural products and pharmaceutical proprietary compounds,[21] diversity-oriented synthesis (DOS) is a relatively new research area, rising to prominence only within the past 15 years. DOS has been defined as "the deliberate, simultaneous, and efficient synthesis of more than one target compound in a diversity-driven approach."[22] The central principles of DOS assert that traditionally undruggable disease-related targets like

protein-protein interactions (PPIs) and protein-DNA interactions may be conquered by the ideally crafted small molecule therapeutic which differs in just the right aspects from currently available pharmaceuticals.[23] Since structure and function are generally related in small molecule therapeutics, DOS programs seek to vary as many aspects of compound libraries as possible, including scaffold structures, stereochemistry, and scaffold substituents.[19a] In effect, the DOS approach is opposite to that of the natural product derivatization strategy. Rather than seeking to uncover a derivative with enhanced potency toward a particular disease agent as natural product derivatization programs often do, DOS programs aim to study as many potential targets for therapeutic intervention as possible with the goal of elucidating their amenabilities to small molecule modulation. In accordance with this philosophy, DOS strategies seek to derivatize a wide range of molecular scaffolds rather than just one.

The ultimate goal of DOS is to explore the entirety of bioactive chemical space using functionally diverse small molecules. While this aim remains largely utopian in nature due to the astronomically high number of compounds this would encompass (about 10^{63} compounds of mass < 500 Da),[24] the recent adaptation of solid-phase synthetic methods to organic synthesis has made the rapid assembly of thousands of complex molecules a reality. Originally developed for polypeptide synthesis in the 1960s,[25] solid-phase techniques have simplified the purification processes for organic compounds,[26] enabling hundreds of reactions to be carried out in parallel, a logistical impossibility using traditional purification methods (e.g. silica gel column chromatography). While an exhaustive review of the myriad examples of DOS is outside the scope of this discussion,

there are numerous documented accounts[27] in addition to reviews[28] summarizing the successes and challenges of this growing area of research.

1.2.2.3 NATURAL PRODUCT-INSPIRED SCAFFOLDS/LIBRARIES

The final strategy for complex molecule library preparation to be discussed entails the modification of natural product-inspired scaffolds, often available as intermediates in a synthetic route to the natural product or independently designed to mimic the structure of a biologically potent natural product. Described by Danishefsky as "diverted total synthesis,"[5] this tactic incorporates advantageous qualities of both the natural product derivatization and DOS approaches to complex molecule diversification. Namely, the natural product-inspired scaffold can be strategically selected or designed to include a more diverse set of functional handles (reminiscent of DOS strategy) while still retaining the core structure of a biologically active natural product (similar to natural product derivatization). Furthermore, as an intermediate to the natural product, the chosen scaffold is more easily accessible through synthesis than the natural product in quantities appropriate for biological study. In this way, compounds generated through diversification of natural product-*based* scaffolds (not the natural products themselves) provide avenues for studying the biological activities of natural product families that may be challenging to access through total synthesis (for instance due to low-yielding endgame transformations).

Along the same lines, the natural product-inspired approach allows for the examination of natural product family hybrids as potential therapeutics. It is often the case that two or more natural product families share core structures but exhibit varying

biological activities. As such, combining salient features (e.g. oxidation states, substitution patterns, functional groups) of both families on the common carbon skeleton creates "hybrid" molecules that may exhibit heightened potency or even novel activity. Specific examples of the natural product-inspired scaffold diversification are outlined in the following section.

1.3 PREVIOUS DIVERSIFICATION STUDIES

True to the open-ended nature of this research area, there exists an abundance of literature detailing the diversification of complex molecules, and an exhaustive review of these studies would be highly impractical. Instead, the present discussion will focus on accounts that employ the natural product-inspired scaffold diversification strategy since this approach is the most relevant to the research described in the later chapters of this text. The following sections present highlights from studies based on one of three approaches: 1) diversification of a late-stage intermediate in a natural product total synthesis, 2) diversification of a scaffold independently designed to mimic a natural product core, or 3) diversification of a scaffold to access hybrid molecules between two or more natural products.

1.3.1 SCAFFOLD AS AN INTERMEDIATE IN TOTAL SYNTHESIS

Diversification studies often originate seamlessly from natural product total synthesis research programs due to the ready availability of complex late-stage intermediates. Furthermore, total synthesis and diversification projects enjoy a symbiotic relationship in

that diversification of a late-stage intermediate for biological screening purposes also provides insights into core reactivity that may prove critical to the eventual success of the total synthesis.

1.3.1.1 FÜRSTNER'S BUTYLCYCLOHEPTYLPRODIGIOSIN SYNTHESIS

Produced by various strains of the *Serratia* and *Streptomyces* bacteria,[29] the prodigiosin alkaloids have attracted great interest due to their potential as immunosuppressive agents for organ transplants[30] and as promising anticancer agents.[31] Aiming to settle a decade-long structural disagreement among isolation chemists[32] while illuminating the biological profile of a less abundant member of the natural product family, Fürstner and co-workers embarked on a total synthesis of butylcycloheptylprodigiosin (**10**).[33] They envisioned accessing the natural product through cross-coupling of triflate **11**, which would also serve as a scaffold from which to generate prodigiosin analogs through treatment with various cross-coupling partners (Scheme 1.1) Key intermediate **11**, in turn, could be prepared from aldehyde **12**, which would require an intricate sequence of transformations for assembly due to challenges associated with the inherent strain of the *ortho*-pyrrolophane core. Noting the thermodynamic and kinetic disfavorability of nine-membered rings,[34] Fürstner and co-workers opted for a strategy that assembled the carbocycle as soon as possible. As such, they planned to access aldehyde **12** via oxidation of bicycle **13**, which could be prepared through an "aza-Heck" cyclization of oxime **14** similar to that pinoeered by Narasaka and co-workers.[35]

*Scheme 1.1 Fürstner's retrosynthetic analysis of butylcycloheptylprodigiosin (**10**)*

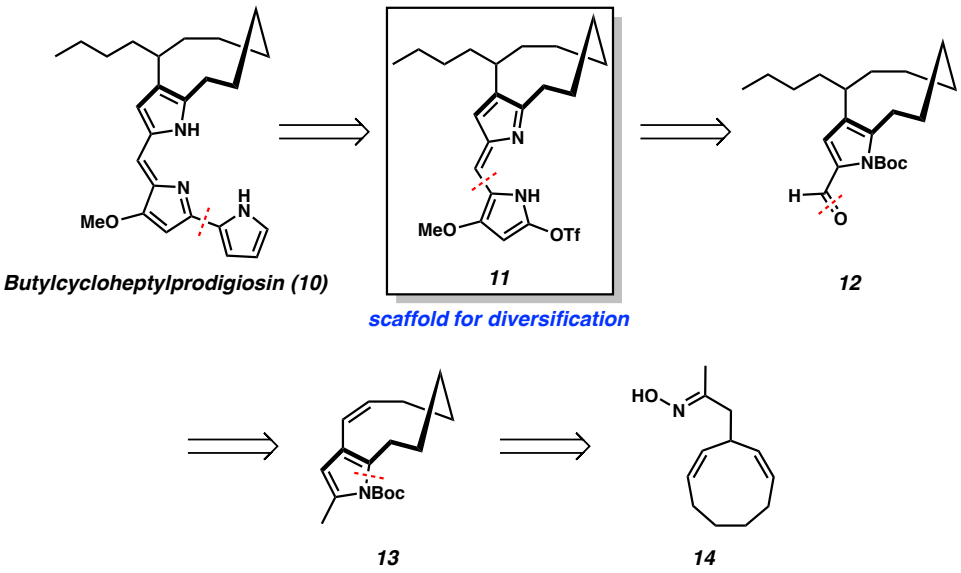

In the forward direction, Fürstner and co-workers converted cyclooctanone (**15**) to (*Z*,*Z*)-cyclononadienone (**16**) over six steps and next accessed oxime **14** through a five-step sequence (Scheme 1.2). Treatment of **14** with pentafluorobenzoyl chloride afforded **17**, the substrate for the key Narasaka–Heck cyclization. Gratifyingly, cyclization occurred smoothly and was viable on multigram scale. Surprisingly, however, pyrrole formation was not observed, with bicyclic imine **18** arising as the major product instead. To induce aromatization, Fürstner and co-workers adopted a thermodynamic deprotonation/reprotonation procedure mediated by potassium hydride. The resulting labile pyrrole (**19**) was immediately *N*-protected, forming bicyclic intermediate **13**.

Scheme 1.2 Preparation of bicyclic intermediate ***13***

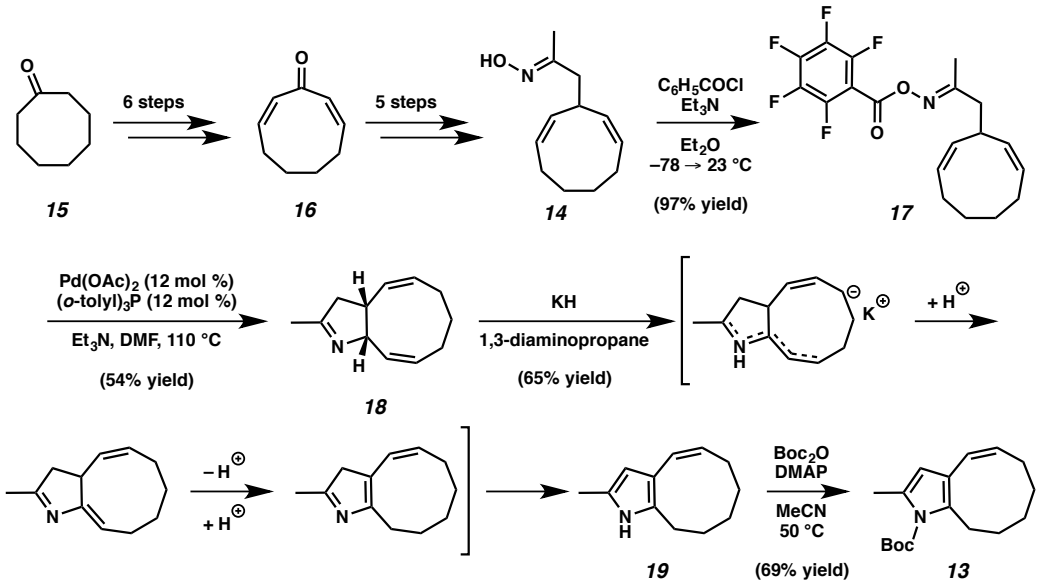

With bicyclic pyrrole **13** in hand, Fürstner and co-workers proceeded to install the butyl side chain onto the carbocyclic framework by way of alkene oxidation followed by Wittig olefination and hydrogenation. Unfortunately, attempts to oxidize the olefin in the nine-membered ring by means of Wacker oxidation,[36] rhodium-catalyzed hydroboration, or oxymercuration proved unsuccessful. Finally, stoichiometric hydroboration using BH_3•THF followed by stepwise oxidation with H_2O_2 and subsequent Dess–Martin oxidation[37] enabled access to ketone **20** along with undesired isomer **21** (Scheme 1.3). Separation of the two isomers by flash chromatography enabled **20** to serve as the platform for the endgame strategy. Interestingly, Wittig olefination of ketone **20** was only possible in refluxing toluene, which was attributed to steric shielding of the carbonyl moiety. The resulting mixture of *E* and *Z* geometric isomers of alkene **22** was then

treated with Crabtree's catalyst[38] under hydrogen atmosphere, effecting regioselective hydrogenation to furnish compound **23** in excellent yield.

Scheme 1.3 Introduction of the n-butyl substituent into the carbocyclic framework

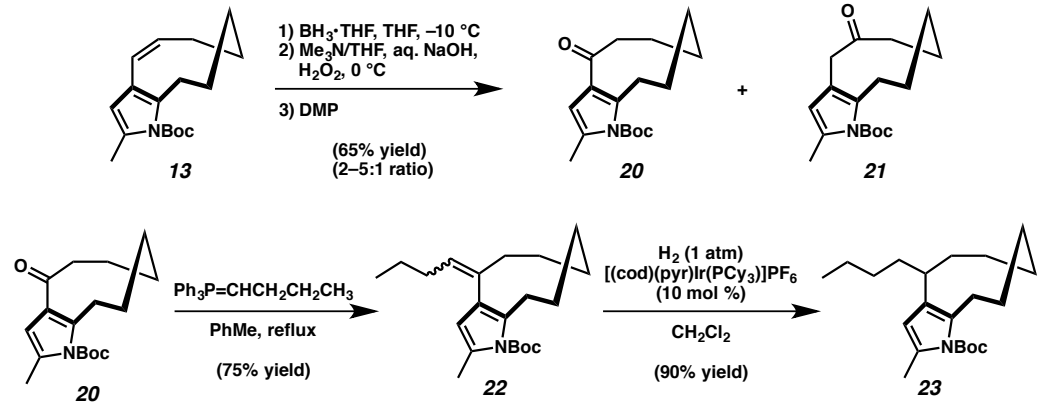

Completion of the total synthesis of **10** was achieved in four steps from pyrrole **23**. While initial efforts to oxidize **23** using standard conditions with cerium ammonium nitrate (CAN) proved unsuccessful, careful optimization revealed that use of dimethoxyethane (DME) as the reaction solvent was critical. Under these conditions, oxidation occurred smoothly, furnishing desired aldehyde **12** in good yield along with over-oxidation product **24**, which was readily removed through flash chromatography (Scheme 1.4). Base-promoted aldol condensation of **12** and commercially available lactam **25** with concomittant removal of the Boc protecting group afforded compound **26**, and subsequent treatment with triflic anhydride induced π-system reorganization to supply vinyl triflate **11**. The final Suzuki coupling was carried out using boronic acid **27**, catalytic [$Pd(PPh_3)_4$], and superstoichiometric LiCl under previously optimized conditions,[39] delivering the prodigiosin **10** in 23 steps overall from cyclooctanone.

*Scheme 1.4 Completion of the total synthesis of butylcycloheptylprodigiosin (**10**)*

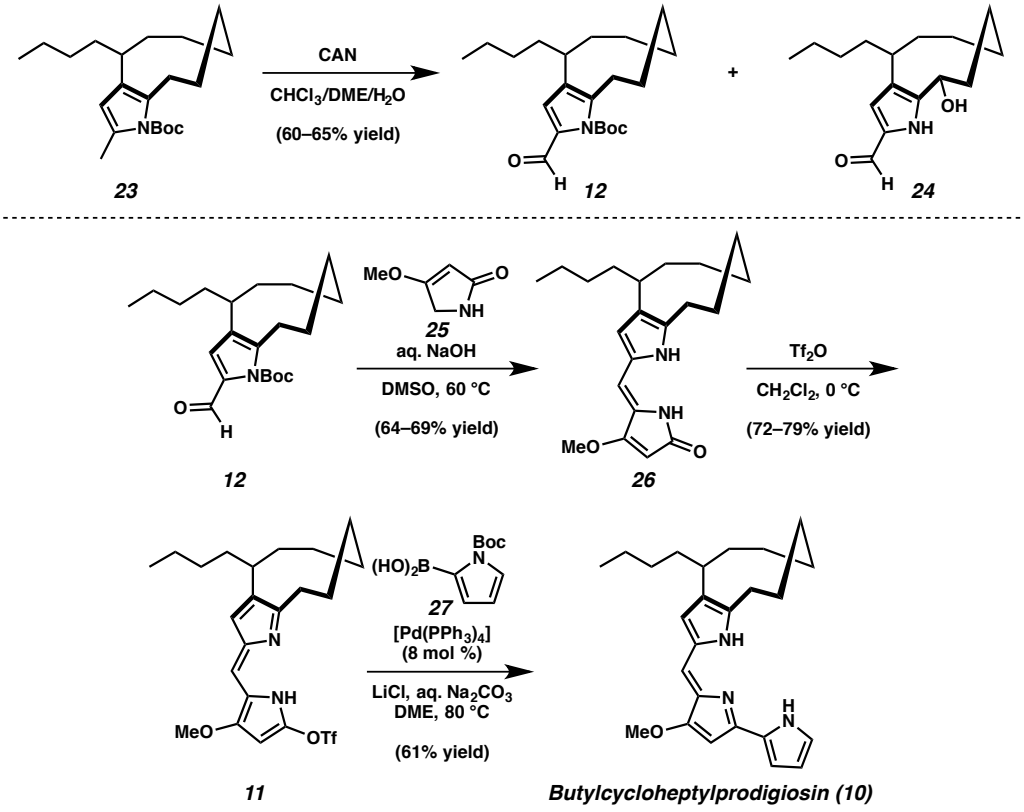

Having accomplished the total synthesis of **10** and reaffirmed the structure proposed by the original isolation chemists, Fürstner and co-workers turned their attention to the diversification of late-stage intermediate **11**. Given the therapeutic properties of simplified prodigiosin analogs PNU-156804 (**28**), which was shown by in vivo studies to act as an immunosuppressant,[30] and GX15-070 (**29**), which was recently advanced into phase I/II clinical trials for treatment of refractory chronic lymphoid leukemia (Figure 1.3),[40] Fürstner and co-workers surmised that variation of the final cross-coupling partner with **11** could generate a variety of biologically active prodigiosin analogs. To this end, triflate **11** was treated with boronic acid derivatives **30**–**33** under the same cross-coupling

conditions employed in the synthesis of **10**, generating analogs **34**–**37** in good to excellent yields (Scheme 1.5).

Figure 1.3 Simplified prodigiosin analogs exhibiting therapeutic properties

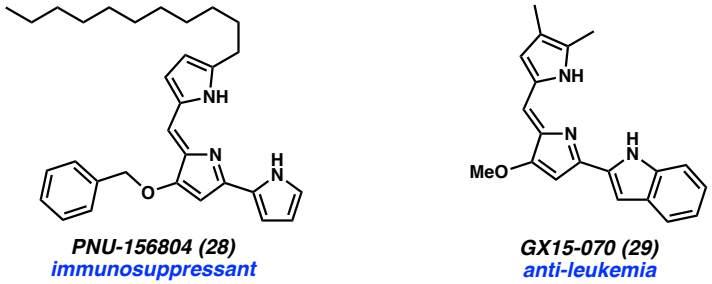

*Scheme 1.5 Diversification of intermediate scaffold **11***

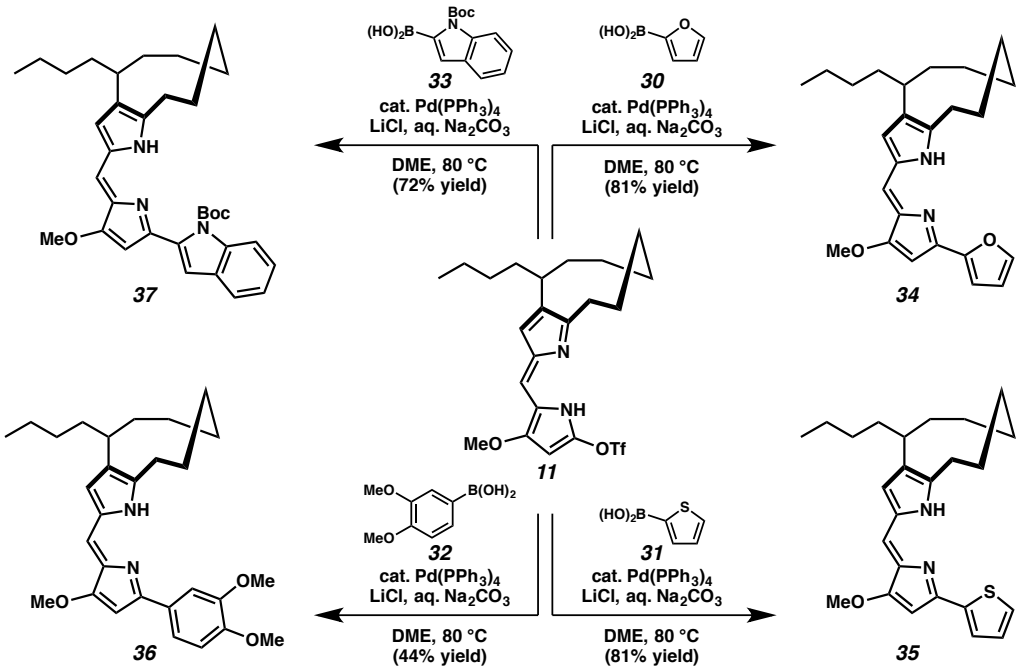

While the natural prodigiosins display nuclease-like activity, inducing oxidative DNA cleavage,[29] incubation of the non-natural prodigiosin analogs **34**–**37** with purified double-stranded plasmid DNA of the bacteriophage *Φ*X174 in the presence of $Cu(OAc)_2$ resulted

in a distinct lack of nuclease ability in any of the synthetic analogs, as indicated by agarose gel electrophoresis.[41] Notably, under the same conditions, prodigiosin **10** effected single-strand DNA cleavage, in accordance with previous studies. Based on these observations, Fürstner and co-workers concluded that the terminal pyrrole present in the natural prodigiosins is critical to the biological potency of the compounds, as formal replacement with other electron-rich arenes resulted in loss of nuclease activity despite the similarity in overall electronic distribution within the heterocyclic perimeter.

1.3.1.2 BARAN'S INGENOL SYNTHESIS

Polyoxygenated terpenoid natural products are potent biological agents in a variety of therapeutical areas, including oncology, immunology, and infectious diseases.[42] Due to the challenges associated with obtaining these compounds from their natural sources,[43] many synthetic chemists have targeted these important molecules in total synthesis research programs.[44] In 2013, Baran and co-workers completed the total synthesis of ingenol (**38**),[45] a plant-derived diterpenoid featuring a unique [4.4.1]bicycloundecane core.[46] Encouraged by the anticancer and anti-HIV activities displayed by ingenol esters,[47] the Baran group entered into a collaborative effort with LEO Pharma, the producer of the pharmaceutical known as Picato (ingenol metabutate), an FDA-approved treatment for actinic keratosis, a pre-cancerous skin affliction.[48] Under the auspices of this industrial–academic collaboration, the Baran group designed a synthetic route to ingenol (**38**) with two explicit goals: 1) brevity for the sake of commercial viability and 2) amenability to the production of analogs.

Taking cues from biosynthesis[49] and past synthetic studies,[50] Baran's retrosynthetic analysis of **38** accesses the natural product through allylic oxidation and deprotection of carbonate **39**, which would be assembled via stereoselective dihydroxylation and vinylogous pinacol rearrangement of **40**. Tetracycle **40** could be prepared through Grignard addition to **41**, the complex intermediate which would later serve as a scaffold for diversification studies. This core structure could be constructed readily from ethynyl magnesium bromide (**42**), commodity chemical (+)-3-carene (**43**), and aldehyde **44** (Scheme 1.6).

*Scheme 1.6 Baran's retrosynthetic analysis of ingenol (**38**)*

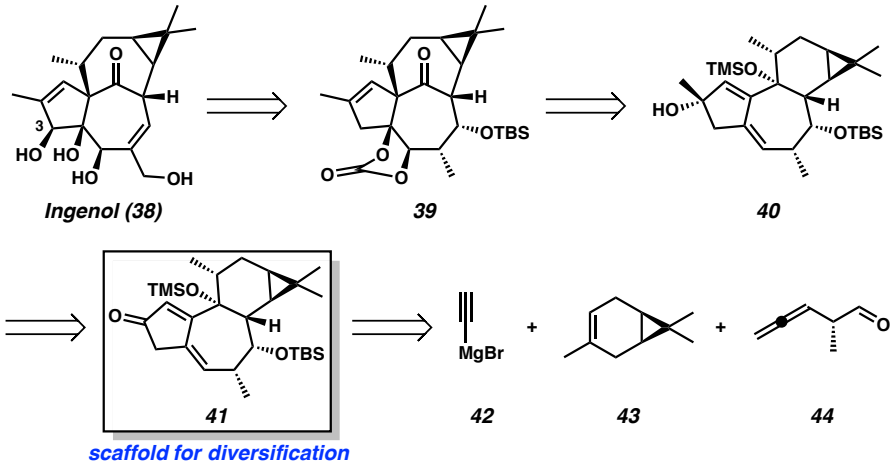

The forward synthesis began with chlorination and ozonolysis of **43** to generate ketone **45**, followed by tandem methylation and aldol reaction with aldehyde **44** to access allene compound **46** (Scheme 1.7). Addition of ethynlmagnesium bromide (**42**) furnished diol **47**, which was treated sequentially with TBS triflate and TMS triflate to incur stepwise protection of the two hydroxyls, thereby suppressing undesired reactivity in the

subsequent transformation. Subjection of bis-protected diol **48** to conditions for allenic Pauson–Khand cyclization[51] resulted in formation of the key tetracyclic intermediate, **41**.

*Scheme 1.7 Assembly of core scaffold **41***

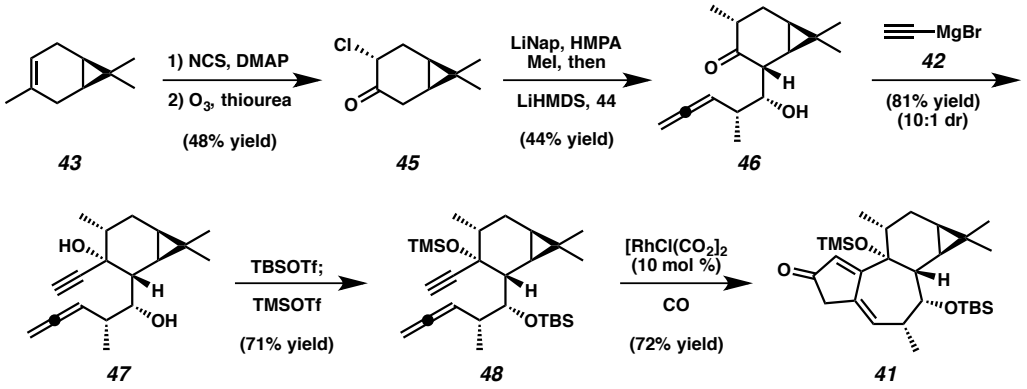

*Scheme 1.8 Completion of the total synthesis of ingenol (**38**)*

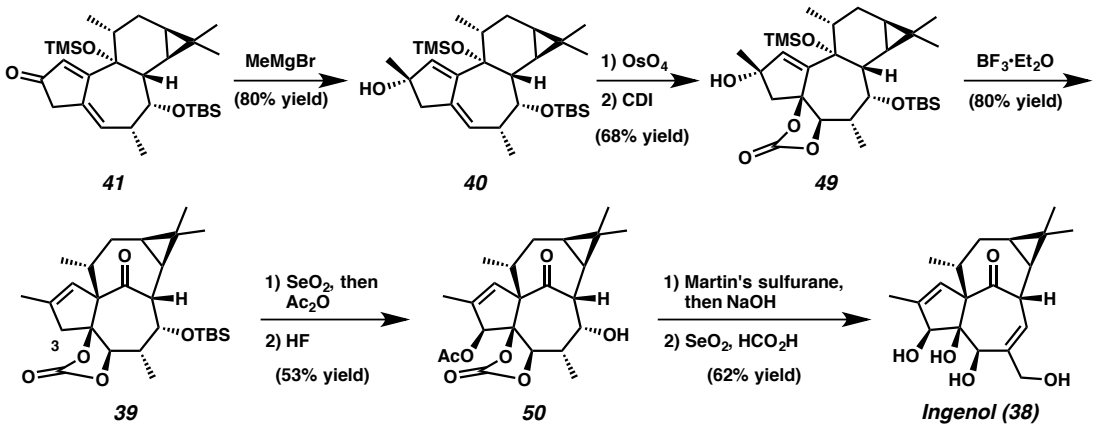

Key intermediate **41** was advanced to carbonate **49** by methylation to produce alcohol **40**, followed by osmium-mediated hydroxylation and protection using *N*,*N*-carbonyldiimidazole (CDI) (Scheme 1.8). After numerous efforts to induce the key vinylogous pinacol rearrangement of **49**, Baran and co-workers found that treatment with BF_3•Et_2O at low temperature effected the desired transformation, assembling the

rearranged core structure **39** in high yield. Subsequent allylic oxidation by SeO_2 and acylation followed by alcohol deprotection delivered acetate **50**. Completion of the total synthesis was achieved through concomittant global deprotection and alcohol elimination using Martin's sulfurane, followed by allylic oxidation using Shibuya's conditions to avoid overoxidation.[52] Overall, Baran and co-workers accomplished the total synthesis of ingenol (**38**) in 14 steps and 1.2% overall yield from **43**.

*Scheme 1.9 Oxidative diversification of scaffold **39** (four steps from core scaffold **41**)*

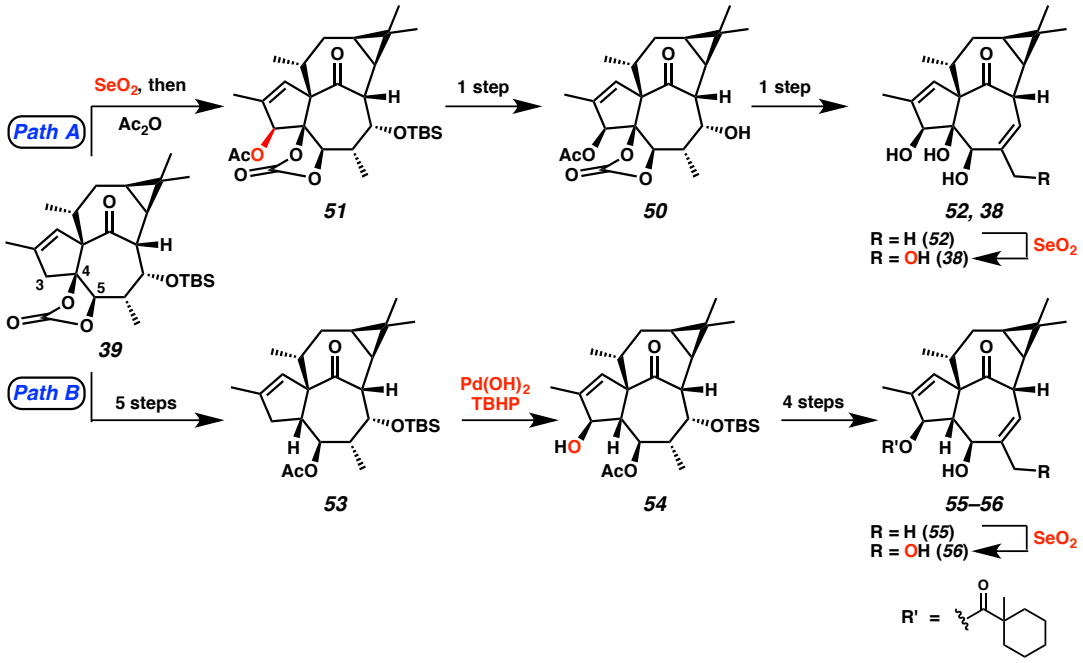

Having met their first goal of crafting a concise synthesis of **38**, Baran and co-workers set their sights on the second goal of preparing ingenane analogs for biological evaluation.[53] Specifically, they aimed to systematically assess the role of the four hydroxyl groups in the biological profile of **38**. To this end, they carried out a series of transformations on carbonate **39**, the preparation of which was greatly facilitated by the

development of a catalytic protocol for the previously stoichiometric osmium dihydroxylation of **40**. Two main pathways for diversification were pursued: Path A involved elaboration to 20-deoxyingenol (**52**) and ingenol (**38**) while Path B entailed the preparation of 4-deoxyingenanes **55** and **56** (Scheme 1.9).

*Scheme 1.10 Elaboration of core scaffold **41** into scaffold **58***

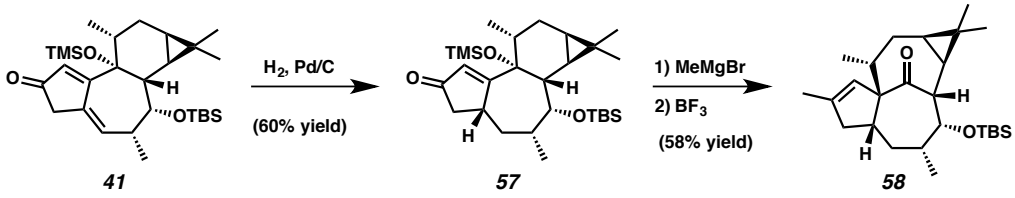

*Scheme 1.11 Oxidative diversification of scaffold **58** (three steps from core scaffold **41**)*

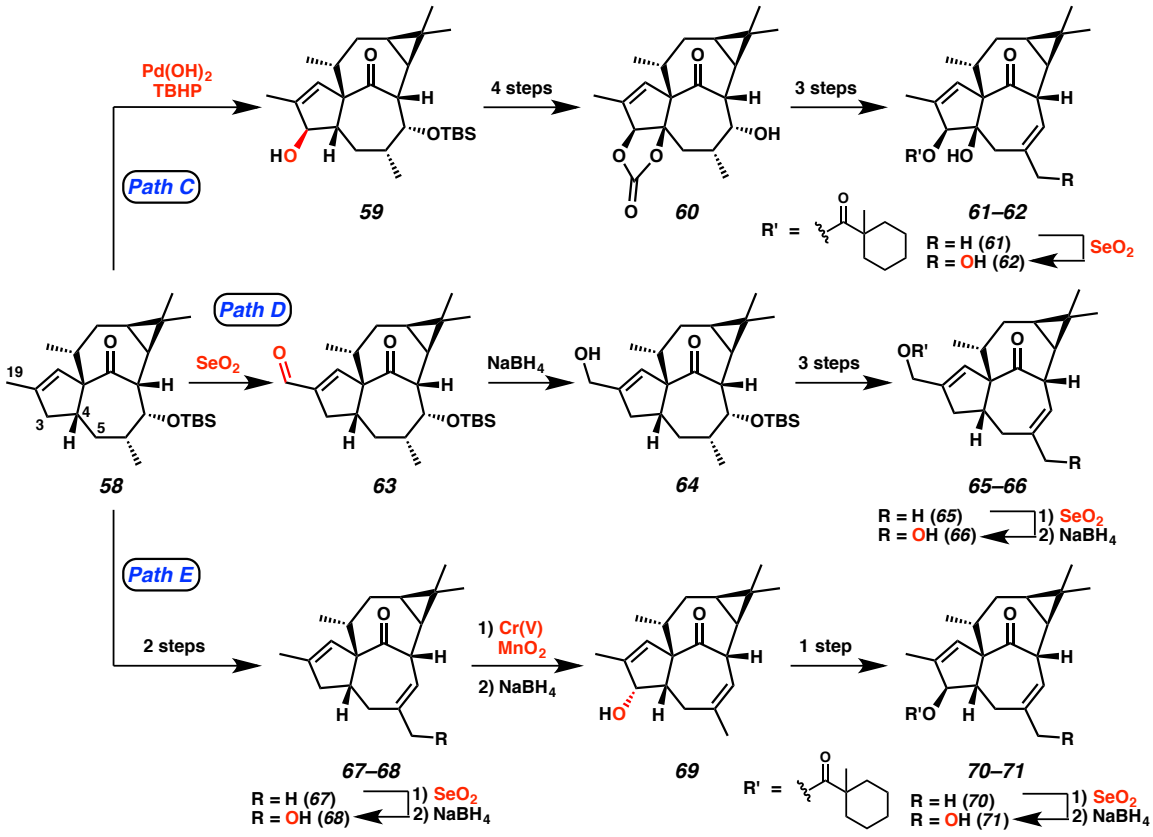

To access less-oxidized analogs, Baran and co-workers elaborated scaffold **41** into **58** by way of regioselective hydrogenation followed by Grignard addition and vinylogous pinacol rearrangement (Scheme 1.10). Interestingly, treatment of **58** with $Pd(OH)_2$ and *tert*-butyl hydroperoxide (TBHP)[54] resulted in oxidation at the C3 position to form allylic alcohol **59**, whereas treatment with SeO_2 effected oxidation at the C19 position, generating aldehyde **63** (Scheme 1.11). This divergency in reactivity formed the basis of Paths C and D, which led to the production of 5-deoxyingenanes **61–62** and **65–66**, respectively. A third pathway, Path E, was accessible through alcohol deprotection and subsequent dehydration to form diene **67**. Curiously, **67** proved unreactive under the $Pd(OH)_2$/TBHP conditions used for C3 oxidation in Path C but underwent C3 oxidation with the opposite facial selectivity when subjected to the Baran group's recently developed Cr(V)-based conditions,[55] generating allylic alcohol **69**. Stereochemical inversion at C3 was accomplished using a Mitsunobu reaction, enabling access to analogs **70** and **71**.

With the ingenol analogs in hand, Baran and co-workers investigated the ability of these compounds to activate human recombinant protein kinase C (PKCδ), stimulate IL-8 release in primary epidermal keratinocytes, and induce oxidative burst in polymorphonuclear leukocytes (neutrophils) based on a previously developed screening cascade. The PKC enzymes play an essential role in mediating cell metabolism, growth, and apoptosis. The PKCδ isoform has been indicated as a tumor suppressant in keratinocytes[56] and is necessary for the attraction of neutrophils, immune cells essential to the antitumor mechanism of Picato.[57] Collaborative studies with scientists at LEO Pharma revealed that the C4 and C5 hydroxyl moieties are critical to the ability of the

ingenol-based compounds to activate PKCδ and stimulate IL-8 release.[53] While the absence of oxygenation at only one of the two positions resulted in only moderate reduction of potency, deoxygenation at both C4 and C5 resulted in a significant loss in activity, with analogs **66** and **68** exhibiting low or nonexistent activity.

Interestingly, however, the ability to induce neutrophil oxidative burst was not influenced by the oxidation patterns at C4 and C5. Despite its inactivity in the PKCδ and IL-8 assays, analog **66** exhibited high potency in the oxidative burst studies, an unexpected observation due to previously established correlations between PKCδ activation and oxidative burst induction.[58] Through these findings, the authors surmised that a PKC isoform other than PKCδ is operative in oxidative burst induction in neutrophils, a hypothesis that was tested by examining the ability of the ingenol analogs to activate PKCβII. As predicted, analogs **66** and **71** were active in nanomolar concentrations. Together, these studies showcase the potential that natural product-based diversification programs have to offer in guiding total synthesis projects and exploring the structure-activity relationships of these non-naturally occurring molecules.

1.3.2 INDEPENDENTLY DESIGNED NATURAL PRODUCT SCAFFOLD

Rather than arising as an intermediate in a total synthesis, an independently designed natural product scaffold is created with the specific intention of use as a starting point for diversification studies. This nuance in research plan may result in subtle discrepancies in functional handles present in an independently designed scaffold as compared to a total synthesis intermediate scaffold. For instance, an independently designed scaffold may strategically include an olefin or carbonyl for use as a versatile diversification handle

when these functionalities might be unnecessary or even detrimental in a total synthesis route and therefore excluded in a late-stage intermediate.

1.3.2.1 SUN'S IBOGAMINE-INSPIRED TETRAHYDROAZEPINO INDOLES

The iboga alkaloid natural products display important biological activities including *N*-methyl-D-aspartate (NMDA) receptor antagonism and opioid (k) receptor agonism.[59] Structurally, the iboga alkaloids feature seven-membered azepino[4,5-*b*]indole ring systems present in various other biologically active natural products.[60] Noting the correlation between the azepino indole framework and biological potency, Sun and co-workers sought to prepare the iboga alkaloid core (**73**) and append a substituted hydantoin motif to access a set of diversified compounds (**74**) (Figure 1.4).[61] Given the biologically privileged nature of hydantoin[62] and the biological activity of the iboga alkaloids, the combination of the two motifs was hypothesized to result in access to therapeutically interesting iboga analogs.

*Figure 1.4 Ibogamine-inspired core scaffold **73** and targeted diversified products **74***

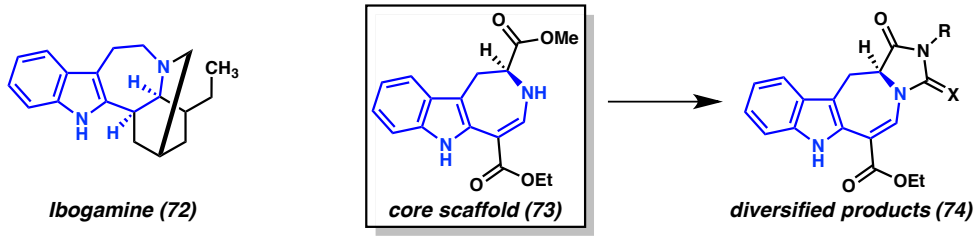

Building on previously reported efforts toward azepino indole scaffolds, Sun and co-workers developed a concise synthetic route toward **73** that avoids several drawbacks of

previously established strategies,[55b,63] including prolonged reaction times, use of toxic reagents, and poor yields. Their retrosynthetic plan involved accessing the diversified hydantoin-fused tetrahydroazepino compounds (**74**) through urea formation from tricycle **73** and subsequent intramolecular cyclization to form the D ring (hydantoin moiety). Core scaffold **73** would be obtained through ring expansion of tricycle **75** (via intramolecular *N*-alkylation and aziridine ring-opening), which could be assembled by Pictet–Spengler condensation of L-tryptophan methyl ester **76** and bromopyruvate **77** (Scheme 1.12).

*Scheme 1.12 Sun's retrosynthetic analysis of hydantoin-fused tetrahydroazepino compounds **74***

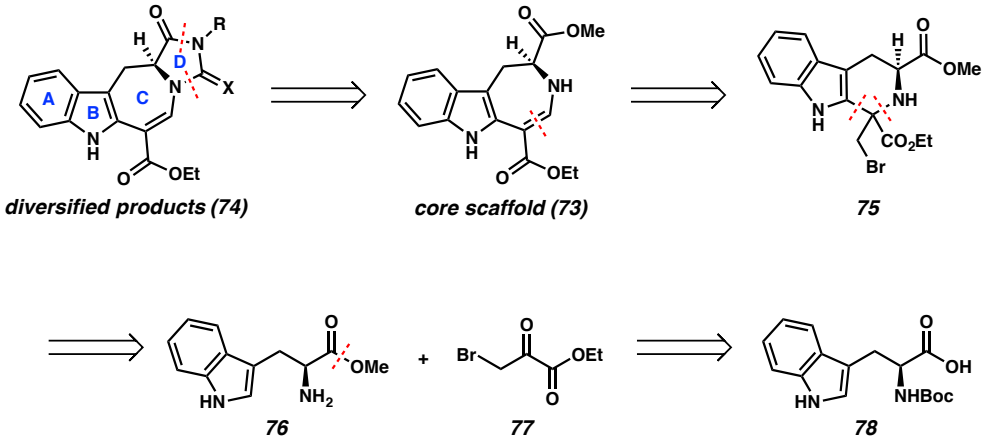

Preparation of core scaffold **73** was achieved rapidly, beginning with esterification of L-tryptophan (**78**) followed by Pictet–Spengler condensation with bromopyruvate **77**, with both transformations proceeding in excellent yield. Although the tricyclic product of the Pictet–Spengler reaction was formed as a 1:1 mixture of diastereomers, both isomers were efficiently converted into scaffold **73**, albeit under drastically different conditions. Interestingly, the (*1S,3S*) diastereomer **75a** rearranged readily to **73** under

acidic conditions at ambient temperature, whereas the (*1R,3S*) diastereomer **75b** required refluxing basic media to undergo the desired transformation. With key scaffold **73** in hand, Sun and co-workers proceeded to examine the final cyclization event. Disppointingly, initial efforts to effect hydantoin formation using *tert*-butyl isocyanate and various bases in a variety of solvents either proved unsuccessful or resulting in only low yields of desired tetracycle **74a** (Scheme 1.13).

*Scheme 1.13 Preparation of scaffold **79** and initial efforts at product (**74a**) formation*

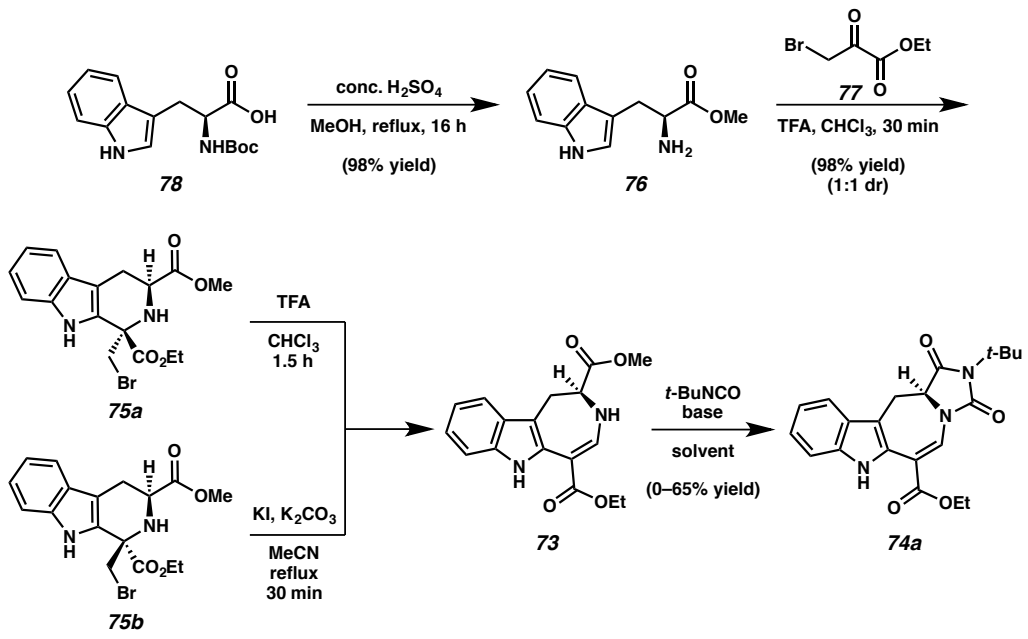

Hypothesizing that delocalization of the nitrogen lone pair through the α,β-unsaturated ethyl ester in **73** was causing low nitrogen nucleophilicity (and therefore low yields of **74**), Sun and co-workers sought to remove the olefinic moiety to facilitate cyclization. Accordingly, treatment of **73** with $NaBH_3CN$ afforded **79** as a mixture of diastereomers which reacted smoothly with *tert*-butyl isocyanate at ambient temperature,

delivering tetracycle **80** as a diastereomeric mixture. After exploration of a number of oxidants, reinstation of the olefin was achieved using DDQ (Scheme 1.14).

*Scheme 1.14 Strategy for accessing tetracyclic product **74a** in higher yield*

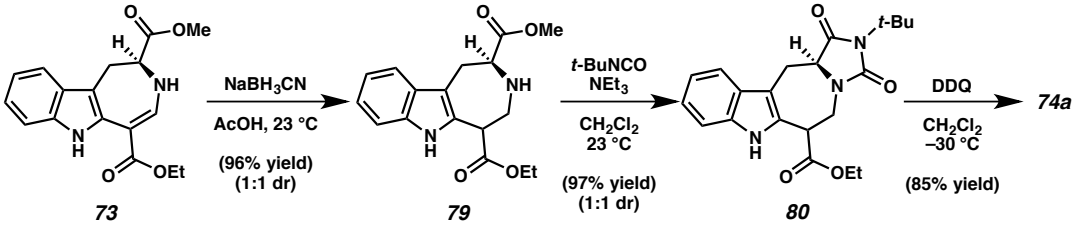

*Scheme 1.15 Diversification of scaffold **79** and oxidation to generate varied tetracyclic products **74***

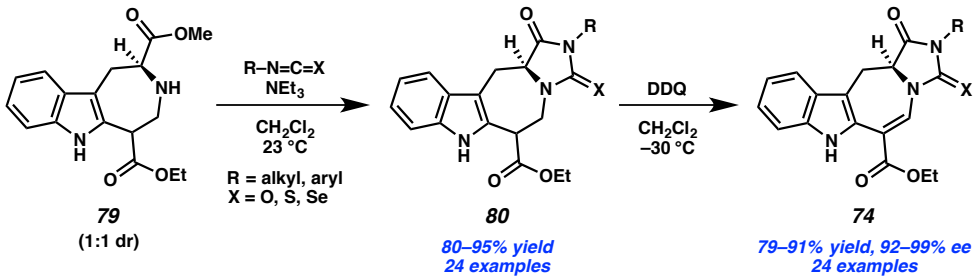

Having elucidated the optimal conditions for this critical sequence of transformations, Sun and co-workers were able to access 24 different tetracyclic compounds (**80**) by using variously substituted isocyanates in the cyclization reaction. Further oxidation of these compounds using DDQ afforded the desired analogs **74** in good to excellent yields (Scheme 1.15). Although the authors do not comment on the biological activities of the compounds generated from these investigations, this contribution provides a good example of strategy for diversifying a natural product-inspired scaffold prepared explicitly for the purposes of creating a library of complex molecules, rather than en route to a total synthesis.

1.3.3 DIVERSIFICATION TO PRODUCE NATURAL PRODUCT HYBRIDS

Unique from the previously discussed guiding principles for diversification programs is the strategy of producing hybrid molecules that contain structural features from two or more different families of natural products. With more than one natural product class to inspire diverse structural design, the possibilities are vast for generating derivatives with a wide range of biological activities.

1.3.3.1 PATERSON'S DICTYOSTATIN/DISCODERMOLIDE HYBRIDS

Cancers are among the foremost causes of death in the developed world, and as such, a great deal of effort has been invested in developing treatments for these devastating afflictions. Decades of research have shown that the study of natural products effective in attenuating cell growth through cellular microtubule inhibition is a viable approach toward diminishing the effects of cancer.[64] Indeed, after its discovery in 1962, the diterpenoid natural product paclitaxel (**81**, Figure 1.5)[65] proved to be a competent chemotherapeutic, gaining FDA approval as the pharmaceutical known as Taxol in 1992 and enjoying widespread clinical use.[66] Unfortunately, the taxane class of cytotoxic drugs tend to suffer from low solubility in aqueous media and the rise of drug resistance in patients, ultimately impeding their efficacy as cancer treatments.[67] Given promising leads in the study of cellular microtubule inhibition, there has been a surge of interest among the chemical community in identifying new microtubule-stabilizing agents (MSA) with mechanisms of activity similar to that of Taxol.

While some research groups adopted the strategy of creating direct analogs of Taxol by modifying substituents around the taxane core,[68] Paterson and co-workers took a different approach. Noting that the marine sponge-derived polyketides dictyostatin (**82**)[69] and discodermolide (**83**)[70] share the same microtubule-stabilizing mechanism as Taxol while maintaining efficacy against Taxol-resistant cancer cell lines, Paterson recognized that the two natural products could serve as parent compounds for the design of dictyostatin/discodermolide hyrid molecules.[71] While discodermolide had been synthesized[72] and deemed unfit for clinical use due to pulmonary toxicity revealed in a Phase I clinical trial by Novartis,[73] Paterson envisioned that blending structural features of discodermolide with those of dictyostatin could result in the production of uniquely active therapeutics.[74]

Figure 1.5 Natural products exhibiting microtubule-stabilizing activity

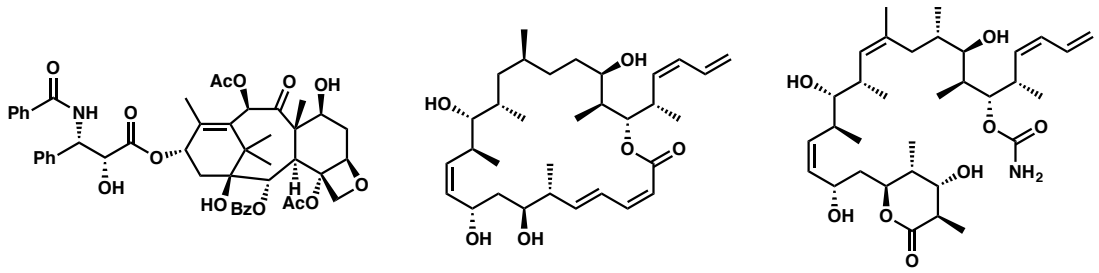

Paclitaxel/Taxol (81) ***Dictyostatin (82)*** ***Discodermolide (83)***

Based on previous investigations by the Canales group into the conformations of paclitaxel, discodermolide, and dictyostatin at the taxoid binding site,[75] Paterson designed dictyostatin/discodermolide hybrid **84**. Canales's studies indicated that structural similarities between discodermolide and dictyostatin corresponded with the three-dimensional regions of greatest overlap in the taxoid binding site. Furthermore, the most

significant spatial discrepancies arose from the δ-lactone and dienoate moieties in discodermolide and dictyostatin, respectively. Because dictyostatin exhibited superior biological activity,[76] Paterson opted to furnish the regions of greatest difference (C1 to C7) with structural features from dictyostatin (highlighted in green) while modeling the regions of closest overlap (C8 to C26) after discodermolide (highlighted in purple) (Scheme 1.16). In doing so, Paterson sought to capture the bioactive potency of dictyostatin while retaining the advantageous binding properties shared by both natural products. Retrosynthetically, Paterson envisioned assembling the macrocyclic core of hybrid **84** using Still–Gennari olefination of known compounds **85** and **86** to form the C10–C11 alkene followed by a cross-coupling/macrolactonization event.

*Scheme 1.16 Paterson's retrosynthetic strategy for dictyostatin/discodermolide hybrid **84***

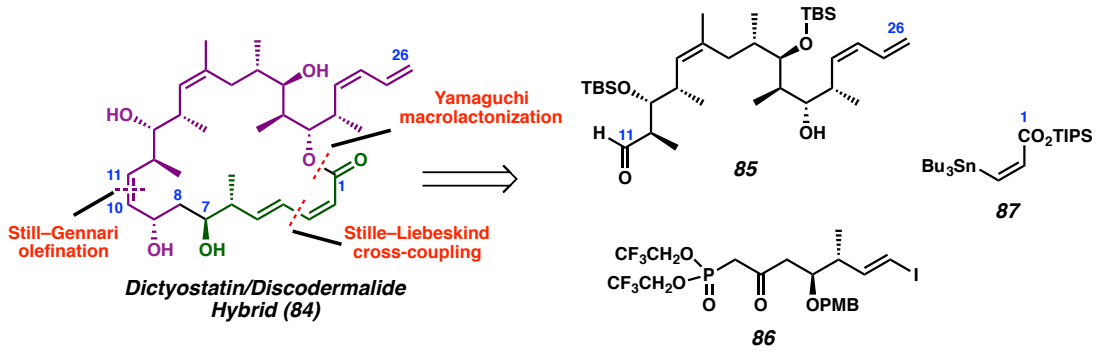

Preparation of hybrid **84** began with previously optimized Still–Gennari olefination of **85** and **86**, which proceeded in good yield and selectivity. Cleavage of the PMB ether using DDQ followed by stereoselective CBS reduction of the enone and acetonide protection afforded vinyl iodide **89** in good yield. Copper-mediated Stille–Liebeskind cross-coupling[77] between **89** and stannane **87** followed by macrolactonization under

modified Yamaguchi conditions[78] delivered the fully protected macrocycle (**90**). Global deprotection in acidic media supplied desired dictyostatin/discodermolide hybrid **84**.

Having prepared hybrid **84** along with several other analogs not highlighted in this discussion, Paterson and co-workers turned their attention to the creation of "triple" hybrids, that is, compounds bearing structural features of three different natural products. Taking cues once again from Canales's binding model of the taxanes, Paterson noted that the C13 side chain of paclitaxel occupies a sizeable pocket of the binding site that remains empty in the discodermolide and dictyostatin binding models. Recognizing that the C7 and C9 hydroxyls of hybrid **84** point in the direction of this pocket, Paterson hypothesized that appendage of the paclitaxel C13 side chains onto the discodermolide/dictyostatin hybrid (**84**) would generate novel triple hybrids that would provide further insights into the binding interactions of the taxanes.

*Scheme 1.17 Synthesis of dictyostatin/discodermolide hybrid **84***

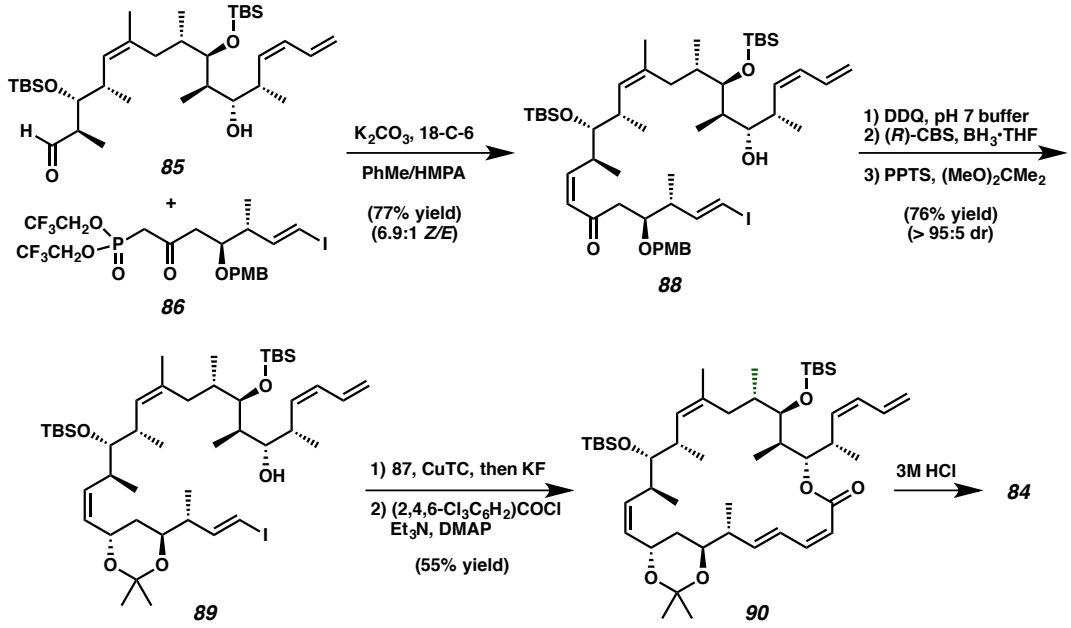

Treatment of fully protected macrocycle **90** with pyridinium *p*-toluenesulfonate (PPTS) effected removal of the acetonide protecting group to furnish 1,3-diol **91**, the scaffold from which an array of triple hybrids would be constructed. In accordance with a previously developed protocol for side-chain introduction,[79] diol **91** was treated with NaHMDS followed by either lactam **92a** or **92b**. The resulting mixture of inseparable C7-esterified and C9-esterified isomers was subjected to TBS deprotection conditions (HF•pyr, pyridine), affording triple hybrids **93** and **94**, which were separated by careful HPLC purification.

*Scheme 1.18 Diversification of scaffold **91** to access "triple" hybrids including Taxol features*

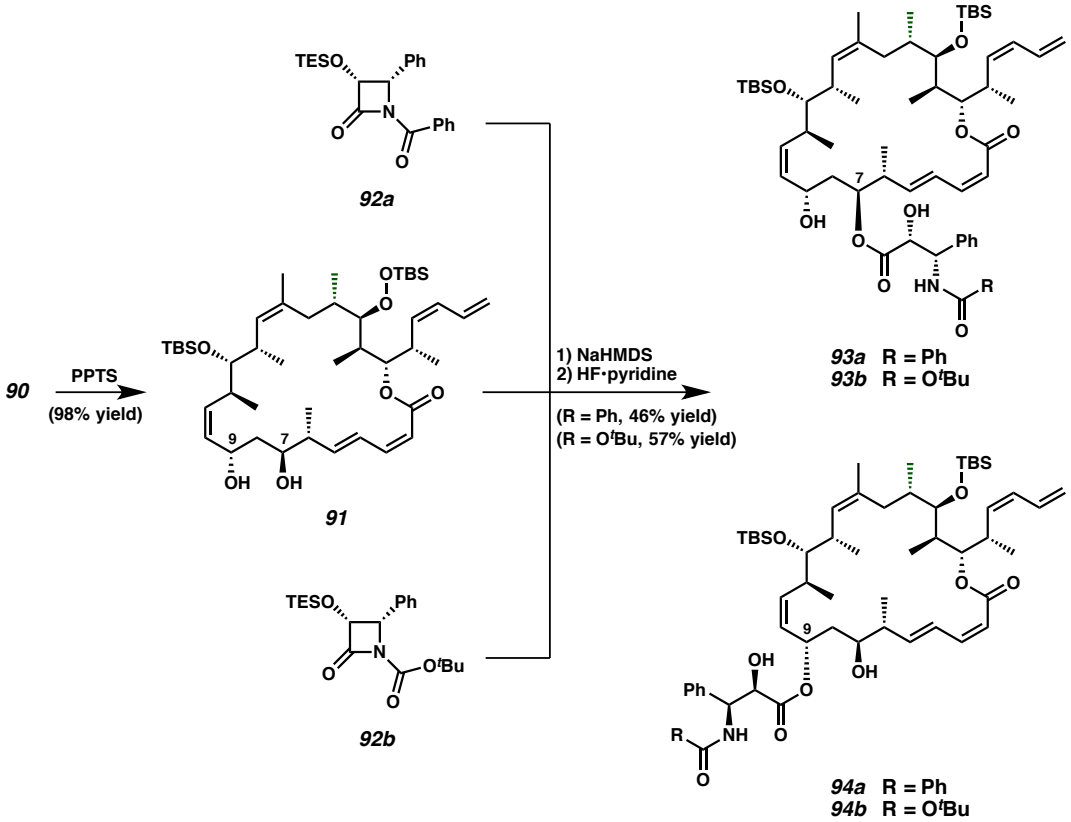

Unfortunately, attempts to characterize these compounds by NMR spectroscopy were hampered by the apparent lability of the newly installed side chains. Paterson and co-workers found that triple hybrids **93** and **94** underwent transesterification in DMSO, producing a mixture of C9 and C7 esters in an approximately 2:1 ratio. Since DMSO is a common solvent for biological assays, these observations invalidated any future biological studies on these hybrids, as any sample would likely contain an isomeric mixture of compounds. The lability of the ester side chains was further highlighted by the regeneration of the original double hybrid **84** when triple hybrids **93** and **94** were allowed to stand as solutions in methanol over 72 hours.

*Scheme 1.19 Preparation of methyl-capped triple hybrids **97** and **100***

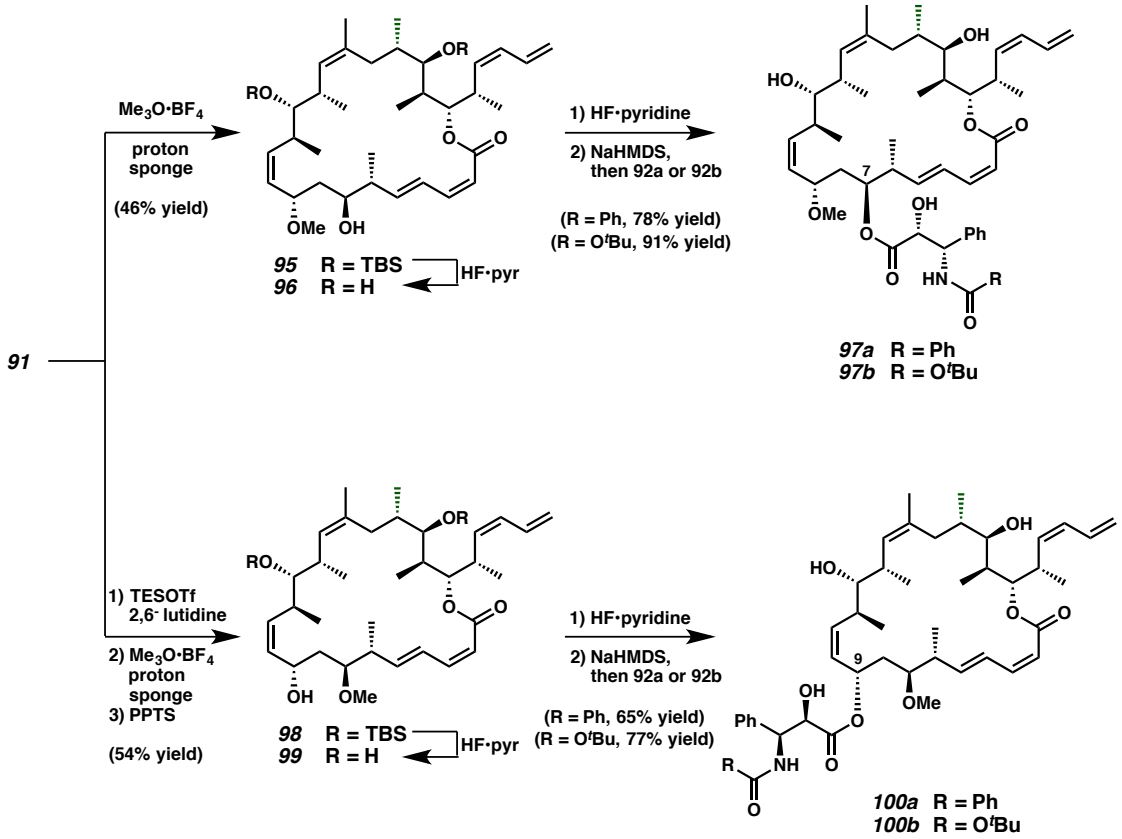

To prevent this undesired reactivity without substantially altering the biological profile of the triple hybrids, Paterson and co-workers sought to cap the C9 or C7 hydroxyl as a methyl ether. Selective methylation of the more nucleophilic C9 hydroxyl of **91** using Meerwein's salt and proton sponge enabled access to methyl ether **95**, and subsequent TBS deprotection and esterification with either lactam **92a** or **92b** afforded the C7-esterified triple hybrid **97a** or **97b**, respectively. Access to the C9-esterified triple hybrids **100a** and **100b** was achieved through regioselective C9-silylation, followed by methylation of the C7 hydroxyl and TES deprotection to generate methyl ether **98**. Once again, TBS deprotection and esterification with either lactam **92a** or **92b** delivered triple hybrid **100a** or **100b**, respectively.

With an abundance of taxane derivatives in hand, Paterson and co-workers proceeded to investigate the biological profiles of the hybrid molecules. To this end, they compared the activities of the double and triple hybrid molecules to those of the parent compounds (taxol, discodermolide, and dictyostatin) in assays against human cancer cell lines AsPC-1 (pancreatic), DLD-1 (colon), PANC-1 (pancreatic), and NCI/ADR-Res (taxol-resistant ovarian). These studies revealed double hybrid **84** and its structural derivative, 9-methoxy analog **96**, to be the most potent of all the synthetic compounds, with both exhibiting low nanomolar cytotoxicities in taxol-sensitive and taxol-resistant cell lines. With an IC_{50} value between that of discodermolide and dictyostatin across all cell lines, hybrid **84** was identified as a promising lead compound for further diversification studies. Notably, none of the triple hybrids displayed appreciable cytotoxicity, indicating that the addition of the side chains did not enhance tubulin-binding ability.

1.4 CONCLUSIONS

The diversification of complex scaffolds contributes a wealth of knowledge to the chemical community, as attested to by the surge in enthusiasm for these types of research programs over the last two decades. The contributions of diversification studies to chemical science are twofold. From a synthetic perspective, the preparation of complex scaffolds for diversification often reveals unexpected patterns of reactivity, inspiring methods development and synthetic insight from which future researchers are likely to benefit. Additionally, the observed reactivity of a complex scaffold under established conditions for various transformations contributes valuable information for practitioners of complex molecule synthesis. From a biological perspective, the creation of myriad compounds resembling biologically active complex molecules enables detailed study of structure-activity relationships, systematically increasing the collective understanding of medicinal chemistry and ultimately leading to the next major therapeutic breakthrough. Given these considerable motivating factors, it is likely that diversification projects will soon become mainstays of most synthesis-oriented research programs.

1.5 NOTES AND REFERENCES

(1) Paterson, I.; Anderson, E. A. *Science* **2005**, *310*, 451–453.

(2) (a) Newman, D. J.; Cragg, G. M. *J. Nat. Prod.* **2007**, *70*, 461–477; (b) Butler, M. S. *Nat. Prod. Rep.* **2008**, *25*, 475–516.

(3) (a) Schreiber, S. L. *Bioorg. Med. Chem.* **1998**, *6*, 1127–1152; (b) Schreiber, S. L. *Chem. Eng. News* **2003**, *81*, 51–60; (c) Stockwell, B. R. *Nat. Rev. Genet.* **2000**, *1*, 116–125; (d) O'Connor, C. J.; Laraia, L.; Spring, D. R. *Chem. Soc. Rev.* **2011**, *40*, 4332–4345.

(4) (a) Lacaná, E.; Amur, S.; Mummanneni, P.; Zhao, H.; Frueh, F. W. *Clin. Pharmacol. Ther.* **2007**, *82*, 466–471; (b) Nelson, A. L.; Dhimolea, E.; Reichert, J. M. *Nat. Rev. Drug Discovery* **2010**, *9*, 767–774.

(5) (a) Njardarson, J. T.; Gaul, C.; Shan, D.; Huang, X.-Y.; Danishefsky, S. J. *J. Am. Chem. Soc.* **2004**, *126*, 1038–1040; (b) Shimokawa, J. *Tetrahedron Lett.* **2014**, *55*, 6156–6162.

(6) Morrison, K. C.; Hergenrother, P. J. *Nat. Prod. Rep.* **2014**, *31*, 6–14.

(7) Newman, D. J.; Cragg, G. M. *J. Nat. Prod.* **2012**, *75*, 311–335.

(8) (a) Baltz, R. H. *Curr. Opin. Pharmacol.* **2008**, *8*, 557–563; (b) Li, J. W.-H.; Vederas, J. C. *Science* **2009**, *325*, 161–165.

(9) (a) Cooper, T. W.; Campbell, I. B.; Macdonald, S. J. *Angew. Chem., Int. Ed.* **2010**, *49*, 8082–8091; (b) Welsch, M. E.; Snyder, S. A.; Stockwell, B. R. *Curr. Opin. Chem. Biol.* **2010**, *14*, 347–361.

(10) (a) Hann, M. M.; Leach, A. R.; Harper, G. *J. Chem. Inf. Comput. Sci.* **2001**, *41*, 856–864; (b) Shelat, A. A.; Guy, R. K. *Nat. Chem. Biol.* **2007**, *3*, 442–446; (c) Hert, J.; Irwin, J. J.; Laggner, C.; Keiser, M. J.; Shoichet, B. K. *Nat. Chem. Biol.* **2009**, *5*, 479–483.

(11) Lachance, H.; Wetzel, S.; Kumar, K.; Waldmann, H. *J. Med. Chem.* **2012**, *55*, 5989–6001.

(12) For derivatization studies on teicoplanin and vancomycin, see: (a) Pathak, T. P.; Miller, S. J. *J. Am. Chem. Soc.* **2013**, *135*, 8415–8422; (b) Yoganathan, S.; Miller, S. J. *J. Med. Chem.* **2015**, *58*, 2367–2377.

(13) (a) de la Torre, M. C.; García, I.; Sierra, M. A. *J. Org. Chem.* **2003**, *68*, 6611–6618; (b) de la Torre, M. C.; García, I.; Sierra, M. A. *Chem.–Eur. J.* **2005**, *11*, 3659–3667.

(14) Huigens, R. W., III; Morrison, K. C.; Hicklin, R. W.; Flood, T. A., Jr.; Richter, M. F.; Hergenrother, P. J. *Nat. Chem.* **2013**, *5*, 195–202.

(15) Song, C. E. *Cinchona Alkaloids in Synthesis and Catalysis*. Wiley: 2009.

(16) For isolation procedure, see: Appendino, G.; Tron, G. C.; Cravotto, G.; Palmisano, G.; Jakupovic, J. *J. Nat. Prod.* **1999**, *62*, 76–79. For diversification study, see: Appendino, G.; Tron, G. C.; Jarevång, T.; Sterner, O. *Org. Lett.* **2001**, *3*, 1609–1612.

(17) For isolation procedure, see: Barker, E. C.; Gatbonton-Schwager, T. N.; Han, Y.; Clay, J. E.; Letterio, J. J.; Tochtrop, G. P. *J. Nat. Prod.* **2010**, *73*, 1064–1068. For diversification studies, see: (a) Ignatenko, V. A.; Han, Y.; Tochtrop, G. P. *J. Org. Chem.* **2013**, *78*, 410–418; (b) Ignatenko, V. A.; Tochtrop, G. P. *J. Org. Chem.* **2013**, *78*, 3821–3831.

(18) (a) López, S. N.; Ramallo, I. A.; Sierra, M. G.; Zacchino, S. A.; Furlan, R. L. E. *Proc. Natl. Acad. Sci. U.S.A.* **2007**, *104*, 441–444; (b) García, P.; Ramallo, I. A.; Salazar, M. O.; Furlan, R. L. E. *RSC Adv.* **2016**, *6*, 57245–57252.

(19) For semi-synthesis, see: (a) Hanson, F. R.; Eble, T. E. *US Patent* 2652356, 1950; (b) Tarbell, D. S.; Carman, R. M.; Chapman, D. D.; Cremer, S. E.; Cross, A. D.;

Huffman, K. R.; Kunstmann, M.; McCorkindale, N. J.; McNally, J. G., Jr.; Rosowsky, A.; Varino, F. H. L.; West, R. L. *J. Am. Chem. Soc.* **1961**, *83*, 3096–3113. For diversification study, see: Balthaser, B. R.; Maloney, M. C.; Beeler, A. B.; Porco, J. A., Jr.; Snyder, J. K. *Nat. Chem.* **2011**, *3*, 969–973.

(20) Dupuis, S. N.; Robertson, A. W.; Veinot, T.; Monro, S. M. A.; Douglas, S. E.; Syvitski, R. T.; Goralski, K. B.; McFarland, S. A.; Jakeman, D. L. *Chem. Sci.* **2012**, *3*, 1640–1644.

(21) (a) Galloway, W. R. J. D.; Isidro-Llobet, A.; Spring, D. R. *Nat. Commun.* **2010**, *1*, 80; (b) Tan, D. S. *Nat. Chem. Biol.* **2005**, *1*, 74–84; (c) Burke, M. D.; Schreiber, S. L. *Angew. Chem., Int. Ed.* **2003**, *43*, 46–58.

(22) Spring, D. R. *Org. Biomol. Chem.* **2003**, *1*, 3867–3870.

(23) (a) Ng, P. Y.; Tang, Y.; Knosp, W. M.; Stadler, H. S.; Shaw, J. T. *Angew. Chem., Int. Ed.* **2007**, *46*, 5352–5355; (b) Rottmann, M.; McNamara, C.; Yeung, B. K. S.; Lee, M. C. S.; Zou, B.; Russell, B.; Seitz, P.; Plouffe, D. M.; Dharia, N. V.; Tan, J.; Cohen, S. B.; Spencer, K. R.; González-Páez, G. E.; Lakshminarayana, S. B.; Goh, A.; Suwanarusk, R.; Jegla, T.; Schmitt, E. K.; Beck, H.-P.; Brun, R.; Nosten, F.; Renia, L.; Dartois, V.; Keller, T. H.; Fidock, D. A.; Winzeler, E. A.; Diagana, T. T. *Science* **2010**, *329*, 1175–1180; (c) Cruz, D.; Wang, Z.; Kibbie, J.; Modlin, R.; Kwon, O. *Proc. Natl. Acad. Sci. U.S.A.* **2011**, *108*, 6769–6774.

(24) Bohacek, R. S.; McMartin, C.; Guida, W. C. *Med. Res. Rev.* **1996**, *16*, 3–50.

(25) Merrifield, R. B. *J. Am. Chem. Soc.* **1963**, *85*, 2149–2154.

(26) (a) Leznoff, C. C.; Wong, J. Y. *Can. J. Chem.* **1972**, *50*, 2892–2893; (b) Camps, F.; Castells, J.; Ferrando, M. J.; Font, J. *Tetrahedron Lett.* **1971**, *12*, 1713–1714; (c) Crowley, J. I.; Rapoport, H. *J. Am. Chem. Soc.* **1970**, *92*, 6363–6365; (d) Yedida, V.; Leznoff, C. C. *Can. J. Chem.* **1980**, *58*, 1144–1150.

(27) For selected DOS studies, see: (a) Goess, B. C.; Hannoush, R. N.; Chan, L. K.; Kirchhausen, T.; Shair, M. D. *J. Am. Chem. Soc.* **2006**, *128*, 5391–5403; (b) Oguri, H.; Hiruma, T.; Yamagishi, Y.; Oikawa, H.; Ishiyama, A.; Otoguro, K.; Yamada, H.; Omura, S. *J. Am. Chem. Soc.* **2011**, *133*, 7096–7105.

(28) For reviews on DOS, see: (a) Schreiber, S. L. *Science* **2000**, *287*, 1964–1969; (b) O'Connor, C. J.; Beckmann, H. S. G.; Spring, D. R. *Chem. Soc. Rev.* **2012**, *41*, 4444–4456.

(29) (a) Fürstner, A. *Angew. Chem., Int. Ed.* **2003**, *42*, 3582–3603; (b) Manderville, R. A. *Curr. Med. Chem. Anti-Cancer Agents* **2001**, *1*, 195–218; (c) Pérez-Tomás, R.; Montaner, B.; Llagostera, E.; Soto-Cerrato, V. *Biochem. Pharmacol.* **2003**, *66*, 1447–1452.

(30) (a) Nakamura, A.; Magae, J.; Tsuji, R. F.; Yamasaki, M.; Nagai, K. *Transplantation* **1989**, *47*, 1013–1016; (b) Magae, J.; Miller, M. W.; Nagai, K.; Shearer, G. M. *J. Antibiot.* **1996**, *49*, 86–90; (c) Stepkowski, S. M.; Nagy, Z. S.; Wang, M.-E.; Behbod, F.; Erwin-Cohen, R.; Kahan, B. D.; Kirken, R. A. *Transplant. Proc.* **2001**, *33*, 3272–3273; (d) Stepkowski, S. M.; Erwin-Cohen, R. A.; Behbod, F.; Wang, M.-E.; Qu, X.; Tejpal, N.; Nagy, Z. S.; Kahan, B. D.; Kirken, R. A. *Blood* **2002**, *99*, 680–689; (e) D'Alessio, R.; Bargiotti, A.; Carlini, O.; Colotta, F.; Ferrari, M.; Gnocchi, P.; Isetta, A.; Mongelli, N.; Motta, P.; Rossi, A.; Rossi, M.; Tibolla, M.; Vanotti, E. *J. Med. Chem.* **2000**, *43*, 2557–2565; (f) Mortellaro, A.; Songia, S.; Gnocchi, P.; Ferrari, M.; Fornasiero, C.; D'Alessio, R.; Isetta, A.; Colotta, F.; Golay, J. *J. Immunol.* **1999**, *162*, 7102–7109.

(31) (a) Boger, D. L.; Patel, M. *J. Org. Chem.* **1988**, *53*, 1405–1415; (b) Detailed information about the cytotoxic properties of prodigiosins assayed in the standard 60-cell line panel are available at the homepage of the National Cancer Institute, Bethesda, at http://www.dtp.nci.nih.gov.

(32) For the original structural assignments, see: (a) Gerber, N. N. *J. Antibiot.* **1975**, *28*, 194–199; (b) Tsao, S.-W.; Rudd, B. A. M.; He, X.-G.; Chang, C.-J.; Floss, H. G. *J. Antibiot.* **1985**, *38*, 128–131. For the opposing assignment, see: Laatsch, H.; Kellner, M.; Weyland, H. *J. Antibiot.* **1991**, *44*, 187–191.

(33) Fürstner, A.; Radkowski, K.; Peters, H.; Seidel, G.; Wirtz, C.; Mynott, R.; Lehmann, C. W. *Chem.–Eur. J.* **2007**, *13*, 1929–1945.

(34) Galli, C.; Mandolini, L. *Eur. J. Org. Chem.* **2000**, 3117–3125.

(35) (a) Tsutsui, H.; Kitamura, M.; Narasaka, K. *Bull. Chem. Soc. Jpn.* **2002**, *75*, 1451–1460; (b) Tsutsui, H.; Narasaka, K. *Chem. Lett.* **1999**, 45–46; (c) Zaman, S.; Kitamura, M.; Narasaka, K. *Bull. Chem. Soc. Jpn.* **2003**, *76*, 1055–1062; (d) Tsutsui, H.; Narasaka, K. *Chem. Lett.* **2001**, 526–527; (e) Chiba, S.; Kitamura, M.; Saku, O.; Narasaka, K. *Bull. Chem. Soc. Jpn.* **2004**, *77*, 785–796; (f) Narasaka, K.; Kitamura, M. *Eur. J. Org. Chem.* **2005**, 4505–4519.

(36) (a) Tsuji, J. *Palladium Reagents and Catalysts: Innovations in Organic Synthesis*, Wiley, New York, **1996**; (b) Trost, B. M.; Van Vranken, D. L. *Chem. Rev.* **1996**, *96*, 395–422; (c) *Handbook of Organopalladium Chemistry for Organic Synthesis* (Ed.: Negishi, E.), Wiley New York, **2002**.

(37) (a) Dess, D. B.; Martin, J. C. *J. Org. Chem.* **1983**, *48*, 4155–4156; (b) Meyer, S. D.; Schreiber, S. L. *J. Org. Chem.* **1994**, *59*, 7549–7552.

(38) Crabtree, R. H.; Felkin, H.; Fillebeen-Khan, T.; Morris, G. E. *J. Organomet. Chem.* **1979**, *168*, 183–195.

(39) Fürstner, A.; Grabowski, J.; Lehmann, C. W. *J. Org. Chem.* **1999**, *64*, 8275–8280.

(40) (a) Dairi, K.; Tripathy, S.; Attardo, G.; Lavallée, J.-F. *Tetrahedron Lett.* **2006**, *47*, 2605–2606; (b) For further investigations on mono-indole analogs, see: Baldino, C. M.; Parr, J.; Wilson, C. J.; Ng, S.-C.; Yohannes, D.; Wasserman, H. H. *Bioorg. Med. Chem. Lett.* **2006**, *16*, 701–704.

(41) For previous studies using these conditions, see: (a) Fürstner, A.; Krause, H. *J. Org. Chem.* **1999**, *64*, 8281–8286; (b) Park, G.; Tomlinson, J. T.; Melvin, M. S.; Wright, M. W.; Day, C. S.; Manderville, R. A. *Org. Lett.* **2003**, *5*, 113–116; (c) Melvin, M. S.; Tomlinson, J. T.; Saluta, G. R.; Kucera, G. L.; Lindquist, N.; Manderville, R. A. *J. Am. Chem. Soc.* **2000**, *122*, 6333–6334; (d) Melvin, M. S.; Calcutt, M. W.; Noftle, R. E.; Manderville, R. A.; *Chem. Res. Toxicol.* **2002**, *15*, 742–748.

(42) Koehn, F. E.; Carter, G. T. *Nat. Rev. Drug Discov.* **2005**, *4*, 206–220.

(43) (a) Mountford, P. in *Green Chemistry in the Pharmaceutical Industry*, Dunn, P. J.; Wells, A. S.; Williams, M. T., Eds. Wiley, Weinheim, Germany, **2010**: pp. 145–160; (b) Paddon, C. J.; Westfall, P. J.; Pitera, D. J.; Benjamin, K.; Fisher, K.; McPhee, D.; Leavell, M. D.; Tai, A.; Main, A.; Eng, D.; Polichuk, D. R.; Teoh, K. H.; Reed, D. W.; Treynor, T.; Lenihan, J.; Jiang, H.; Fleck, M.; Bajad, S.; Dang, G.; Dengrove, D.; Diola, D.; Dorin, G.; Ellens, K. W.; Fickes, S.; Galazzo, J.;

Gaucher, S. P.; Geistlinger, T.; Henry, R.; Hepp, M.; Horning, T.; Iqbal, T.; Kizer, L.; Lieu, B.; Melis, D.; Moss, N.; Regentin, R.; Secrest, S.; Tsuruta, H.; Vasquez, R.; Westblade, L. F.; Xu, L.; Yu, M.; Zhang, Y.; Zhao, L.; Lievense, J.; Covello, P. S.; Keasling, J. D.; Reiling, K. K.; Renninger, N. S.; Newman, J. D. *Nature* **2013**, *496*, 528–532.

(44) (a) Zhu, C.; Cook, S. P. *J. Am. Chem. Soc.* **2012**, *134*, 13577–13579; (b) Kuwajima, I.; Tanino, K. *Chem. Rev.* **2005**, *105*, 4661–4670; (c) Winkler, J. D.; Rouse, M. B.; Greaney, M. F.; Harrison, S. J.; Jeon, Y. T. *J. Am. Chem. Soc.* **2002**, *124*, 9726–9728; (d) Tanino, K.; Onuki, K.; Asano, K.; Miyashita, M.; Nakamura, T.; Takahashi, Y.; Kuwajima, I. *J. Am. Chem. Soc.* **2003**, *125*, 1498–1500; (e) Nickel, A.; Maruyama, T.; Tang, H.; Murphy, P. D.; Greene, B.; Yusuff, N.; Wood, J. L. *J. Am. Chem. Soc.* **2004**, *126*, 16300–16301.

(45) Jørgensen, L.; McKerrall, S. J.; Kuttruff, C. A.; Ungeheuer, F.; Felding, J.; Baran, P. S. *Science* **2013**, *341*, 878–882.

(46) Hecker, E. *Cancer Res.* **1968**, *28*, 2338–2348.

(47) (a) Ogbourne, S. M.; Suhrbier, A.; Jones, B.; Cozzi, S.-J.; Boyle, G. M.; Morris, M.; McAlpine, D.; Johns, J.; Scott, T. M.; Sutherland, K. P.; Gardner, J. M.; Le, T. T. T.; Lenarczyk, A.; Aylward, J. H.; Parsons, P. G. *Cancer Res.* **2004**, *64*, 2833–2839; (b) Fujiwara, M.; Ijichi, K.; Tokuhisa, K.; Katsuura, K.; Shigeta, S.;

Konno, K.; Wang, G. Y.; Uemura, D.; Yokota, T.; Baba, M. *Antimicrob. Agents Chemother.* **1996**, *40*, 271–273; (c) Vasas, A.; Rédei, D.; Csupor, D.; Molnár, J.; Hohmann, J. *Eur. J. Org. Chem.* **2012**, *2012*, 5115–5130.

(48) U.S. Food and Drug Administration, *2012 Novel New Drugs Summary* (FDA, Washington, DC, 2013); www.fda.gov/downloads/Drugs/DevelopmentApprovalProcess/DrugInnovation/UCM337830.pdf.

(49) Schmidt, R. J. *J. Linn. Soc. Bot.* **1987**, *94*, 221–230.

(50) (a) Rigby, J. H.; Moore, T. L. *J. Org. Chem.* **1990**, *55*, 2959–2962; (b) Kierkus, P. C.; Rigby, J. H.; Heeg, M. J. *Acta Cryst.* **1990**, *C46*, 521–522; (c) Heeg, M. J.; Moore, T. L.; Rigby, J. H. *Acta Cryst.* **1991**, *C47*, 198–200.

(51) Brummond, K. M.; Chen, H.; Fisher, K. D.; Kerekes, A. D.; Rickards, B.; Sill, P. C.; Geib, S. J. *Org. Lett.* **2002**, *4*, 1931–1934.

(52) Shibuya, K. *Synth. Commun.* **1994**, *24*, 2923–2941.

(53) Jin, Y.; Yeh, C.-H.; Kuttruff, C. A.; Jørgensen, L.; Dünstl, G.; Felding, J.; Natarajan, S. R.; Baran, P. S. *Angew. Chem., Int. Ed.* **2015**, *54*, 14044–14048.

(54) Yu, J.-Q.; Corey, E. J. *J. Am. Chem. Soc.* **2003**, *125*, 3232–3233.

(55) Wilde, N. C.; Isomura, M.; Mendoza, A.; Baran, P. S. *J. Am. Chem. Soc.* **2014**, *136*, 4909–4912.

(56) D'Costa, A. M.; Robinson, J. K.; Maududi, T.; Chaturvedi, V.; Nickoloff, B. J.; Denning, M. F. *Oncogene* **2006**, *25*, 378–386.

(57) Challacombe, J. M.; Suhrbrier, A.; Parsons, P. G.; Jones, B.; Hampson, P.; Kavanagh, D.; Rainger, G. E.; Morris, M.; Lord, J. M.; Le, T. T. T.; Hoang-Le, D.; Ogbourne, S. M. *J. Immunol.* **2006**, *177*, 8123–8132.

(58) Grue-Sørensen, G.; Liang, X.; Månsson, K.; Vedsø, P.; Sørensen, M. D.; Soor, A.; Stahlhut, M.; Bertelsen, M.; Engell, K. M.; Högberg, T. *Bioorg. Med. Chem. Lett.* **2014**, *24*, 54–60.

(59) (a) Popik, P.; Glick, S. D. *Drugs Future* **1996**, *21*, 1109–1115; (b) Repke, D. B.; Artis, D. R.; Nelson, J. T.; Wong, E. H. F. *J. Org. Chem.* **1994**, *59*, 2164–2171.

(60) (a) Maisonneuve, I. M.; Glick, S. D. *Pharmaol. Biochem. Behav.* **2003**, *75*, 607–618; (b) Chen, P.; Cao, L.; Li, C. *J. Org. Chem.* **2009**, *74*, 7533–7535.

(61) Barve, I. J.; Dalvi, P. B.; Thikekar, T. U.; Chanda, K.; Liu, Y.-L.; Fang, C.-P.; Liu, C.-C.; Sun, C.-M. *RSC Adv*. **2015**, *5*, 73169–73179.

(62) (a) Moloney, G. P.; Martin, G. R.; Matthews, N.; Milne, A.; Hobbs, H.; Dosworth, S.; Sang, P. Y.; Knight, C.; Williams, M.; Maxwell, M.; Glen, R. C. *J. Med. Chem*. **1999**, *42*, 2504–2526; (b) Somsák, L.; Kovács, L.; Tóth, M.; Ösz, E.; Szilágyi, L.; Györgydeák, Z.; Dinya, Z.; Docsa, T.; Tóth, B.; Gergely, P. *J. Med. Chem*. **2001**, *44*, 2843–2848; (c) Thenmozhiyal, J. C.; Wong, P. T.-H.; Chui, W.-K. *J. Med. Chem*. **2004**, *47*, 1527–1535; (d) Sergent, D.; Wang, Q.; Sasaki, N. A.; Ouazzani, J. *Bioorg. Med. Chem. Lett*. **2008**, *18*, 4332–4335.

(63) (a) Flatt, B.; Martin, R.; Wang, T.-L.; Mahaney, P.; Murphy, B.; Gu, X.-H.; Foster, P.; Li, J.; Pircher, P.; Petrowski, M.; Schulman, I.; Westin, S.; Wrobel, J.; Yan, G.; Bischoff, E.; Daige, C.; Mohan, R. *J. Med. Chem*. **2009**, *52*, 904–907; (b) Kuehne, M. E.; Bohnert, J. C.; Bornmann, W. G.; Kirkemo, C. L.; Kuehne, S. E.; Seaton, P. J.; Zebovitz, T. C. *J. Org. Chem*. **1985**, *50*, 919–924; (c) Zheng, L.; Xiang, J.; Bai, X. *J. Heterocycl. Chem*. **2006**, *43*, 321–324.

(64) (a) Koehn, F. E.; Carter, G. T. *Nat. Rev. Drug Discovery* **2005**, *4*, 206–220; (b) Butler, M. S. *Nat. Prod. Rep*. **2008**, *25*, 475–516; (c) Newman, D. J.; Cragg, G. M. *J. Nat. Prod*. **2007**, *70*, 461–477; (d) Paterson, I.; Anderson, E. A. *Science* **2005**, *310*, 451–453; (e) Cragg, G. M.; Kingston, D. G. I.; Newman, D. J. *Anticancer Agents From Natural Products*, Taylor&Francis, Boca Raton, **2005**.

(65) Nicolaou, K. C.; Dai, W.-M.; Guy, R. K. *Angew. Chem., Int. Ed. Engl.* **1994**, *33*, 15–44.

(66) Gueritte-Voegelein, F.; Guenard, D.; Lavelle, F.; Le Goff, M. T.; Mangatal, L.; Potier, P. *J. Med. Chem.* **1991**, *34*, 992–998.

(67) Orr, G. A.; Verdier-Pinard, P.; McDaid, H.; Horwitz, S. B. *Oncogene* **2003**, *22*, 7280–7295.

(68) (a) Chaudhary, A. G.; Rimoldi, J. M.; Kingston, D. G. I. *J. Org. Chem.* **1993**, *58*, 3798–3799; (b) Kingston, D. G. I.; Chaudhary, A. G.; Chordia, M. D.; Gharpure, M.; Gunatilaka, A. A. L.; Higgs, P. I.; Rimoldi, J. M.; Samala, L.; Jagtap, P. G.; Giannakakou, P.; Jiang, Y. Q.; Lin, C. M.; Hamel, E.; Long, B. H.; Fairchild, C. R.; Johnston, K. A. *J. Med. Chem.* **1998**, *41*, 3715–3726; (c) Altstadt, T. J.; Fairchild, C. R.; Golik, J.; Johnston, K. A.; Kadow, J. F.; Lee, F. Y.; Long, B. H.; Rose, W. C.; Vyas, D. M.; Wong, H.; Wu, M.-J.; Wittman, M. D. *J. Med. Chem.* **2001**, *44*, 4577–4583.

(69) (a) Pettit, G. R.; Cichacz, Z. A.; Goa, F.; Boyd, M. R.; Schmidt, J. M. *J. Chem. Soc., Chem. Commun.* **1994**, 1111–1112; (b) Isbrucker, R. A.; Cummins, J.; Pomponi, S. A.; Longley, R. E.; Wright, A. E. *Biochem. Pharmacol.* **2003**, *66*,

75–82; (c) Paterson, I.; Britton, R.; Delgado, O.; Wright, A. E. *Chem. Commun.* **2004**, 632–633.

(70) (a) Gunasekera, S. P.; Gunasekera, M.; Longley, R. E.; Schulte, G. K. *J. Org. Chem.* **1990**, *55*, 4912–4915; (b) ter Haar, E.; Kowalski, R. J.; Hamel, E.; Lin, C. M.; Longley, R. E.; Gunasekera, S. P.; Rosenkranz, H. S.; Day, B. W. *Biochemistry* **1996**, *35*, 243–250; (c) Kowalski, R. J.; Giannakakou, P.; Gunasekera, S. P.; Longley, R. E.; Day, B. W.; Hamel, E. *Mol. Pharmacol.* **1997**, *52*, 613–622.

(71) For selected previous studies on dictyostatin analogs, see: (a) Shin, Y.; Choy, N.; Balachandran, R.; Madiraju, C.; Day, B. W.; Curran, D. P. *Org. Lett.* **2002**, *4*, 4443–4446; (b) Jung, W.-H.; Harrison, C.; Shin, Y.; Fournier, J.-H.; Balachandran, R.; Raccor, B. S.; Sikorski, R. P.; Vogt, A.; Curran, D. P.; Day, B. W. *J. Med. Chem.* **2007**, *50*, 2951–2966; (c) Paterson, I.; Gardner, N. M.; Poullennec, K. G.; Wright, A. E. *Bioorg. Med. Chem. Lett.* **2007**, *17*, 2443–2447.

(72) Mickel, S. J.; Niederer, D.; Daeffler, R.; Osmani, A.; Kuesters, E.; Schmid, E.; Schaer, K.; Gamboni, R.; Chen, W.; Loeser, E.; Kinder, F. R., Jr.; Konigsberger, K.; Prasad, K.; Ramsey, T. M.; Repič, O.; Wang, R.-M.; Florence, G.; Lyothier, I.; Paterson, I. *Org. Process Res. Dev.* **2004**, *8*, 122–130.

(73) (a) Mita, A.; Lockhart, A. C.; Chen, T.-L.; Bochinski, K.; Curtright, J.; Cooper, W.; Hammond, L.; Rothenberg, M.; Rowinsky, E.; Sharma, S. *J. Clin. Oncol.* **2004**, *22*, 2025–2025; (b) Mita, A.; Lockhart, A. C.; Chen, T. *Proc. Am. Soc. Clin. Oncol.* **2004**, *23*, 133.

(74) Paterson, I.; Naylor, G. J.; Gardner, N. M.; Guzmán, E.; Wright, A. E. *Chem.–Asian J.* **2011**, *6*, 459–473.

(75) Canales, A.; Matesanz, R.; Gardner, N. M.; Andreu, J. M.; Paterson, I.; Díaz, J. F.; Jiménez-Barbero, J. *Chem.–Eur. J.* **2008**, *14*, 7557–7569.

(76) Buey, R. M.; Barasoain, I.; Jackson, E.; Meyer, A.; Giannakakou, P.; Paterson, I.; Mooberry, S.; Andreu, J. M.; Díaz, J. F. *Chem. Biol.* **2005**, *12*, 1269–1279.

(77) Allred, G. D.; Liebeskind, L. S. *J. Am. Chem. Soc.* **1996**, *118*, 2748–2749.

(78) Inanaga, J.; Hirata, K.; Saeki, H.; Katsuki, T.; Yamaguchi, M. *Bull. Chem. Soc. Jpn.* **1979**, *52*, 1989–1993.

(79) (a) Ojima, I.; Habus, I.; Zhao, M.; Zucco, M.; Park, Y. H.; Sun, C. M.; Brigaud, T. *Tetrahedron* **1992**, *48*, 6985–7012; (b) Ojima, I.; Sun, C. M.; Zucco, M.; Park, Y. H.; Duclos, O.; Kuduk, S. *Tetrahedron Lett.* **1993**, *34*, 4149–4152.

CHAPTER 2[†]

A Second-Generation Synthesis of

the Cyanthiwigin Natural Product Core

2.1 INTRODUCTION

Recognizing the vast potential of late-stage diversification research programs for the study of biologically active complex molecules as outlined in the previous chapter, our group is interested in conducting such studies using a late-stage intermediate in our previously reported syntheses of cyanthiwigins F, B, and G.[1] The cyanthiwigin natural product framework is an ideal scaffold for late-stage diversification studies due to its structural complexity and inclusion of multiple handles for diversification as well as the existence of a concise synthetic route for its preparation. However, many new technologies have been developed that we realized could be exploited to further expedite preparation of the cyanthiwigin core, an important aim given the sizable quantities needed for diversification studies. This chapter presents the challenges in large-scale

[†] Portions of this chapter have been reproduced with permission from *Org. Lett.* **2016**, *18*, 5720–5723 and the supporting information found therein.

synthesis faced in the original route and presents the solutions we devised to address them.

2.1.1 BACKGROUND AND PREVIOUS SYNTHESIS

Isolated from the marine sponges *Epipolasis reiswigi* and *Myrmedioderma styx*, the 30 known cyanthiwigins constitute part of a larger class of diterpene natural products called the cyathanes, which display a vast array of biological properties including antimicrobial activity, antineoplastic action, stimulation of nerve growth factor synthesis, and κ-opioid receptor agonism.[2] The cyanthiwigins themselves exhibit a range of biological activities against such disease agents as HIV-1 (cyanthiwigin B), lung cancer and leukemia cells (cyanthiwigin C), and primary tumor cells (cyanthiwigin F).

*Figure 2.1 Cyathane carbon skeleton (**101**) and selected cyanthiwigin natural products*

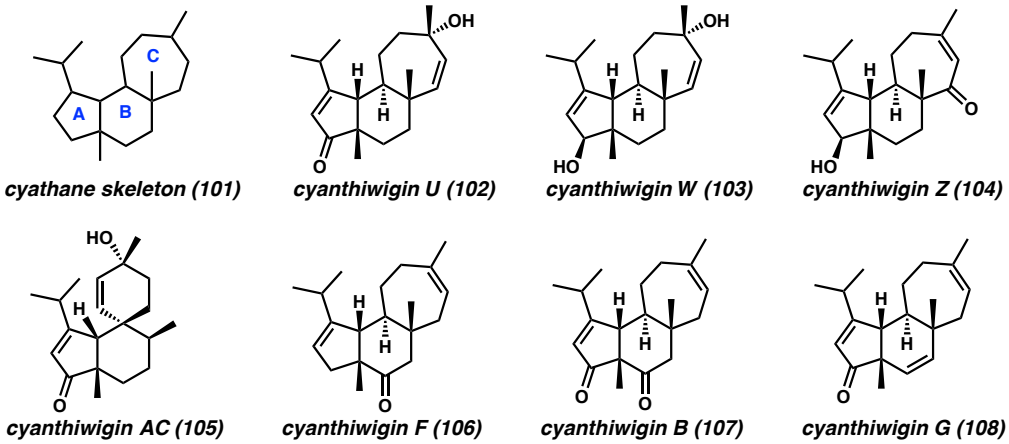

In addition to these interesting biological properties, their structural complexity has made the cyanthiwigins attractive target molecules for total synthesis.[2c] Specifically, the cyanthiwigins contain four contiguous stereocenters, including two quaternary

stereocenters at the A–B and B–C ring junctures of the tricyclic carbon skeleton (**101**, Figure 2.1). The first cyanthiwigin total synthesis was reported in 2005, when the Phillips group completed the synthesis of cyanthiwigin U (**102**),[3] and they later employed their strategy to access cyanthiwigin W (**103**) and cyanthiwigin Z (**104**).[4] Cyanthiwigin AC (**105**), a unique member of the natural product family featuring a spirocyclic framework instead of the 5–6–7 tricyclic fused core, was prepared by the Reddy laboratory in 2006,[5] and in 2008 our group accomplished the synthesis of cyanthwigin F (**106**),[1a] later applying the core strategy to access cyanthiwigin B (**107**)[1b] and cyanthiwigin G (**108**).[1b]

Scheme 2.1 Stoltz's retrosynthetic analysis of cyanthiwigin F

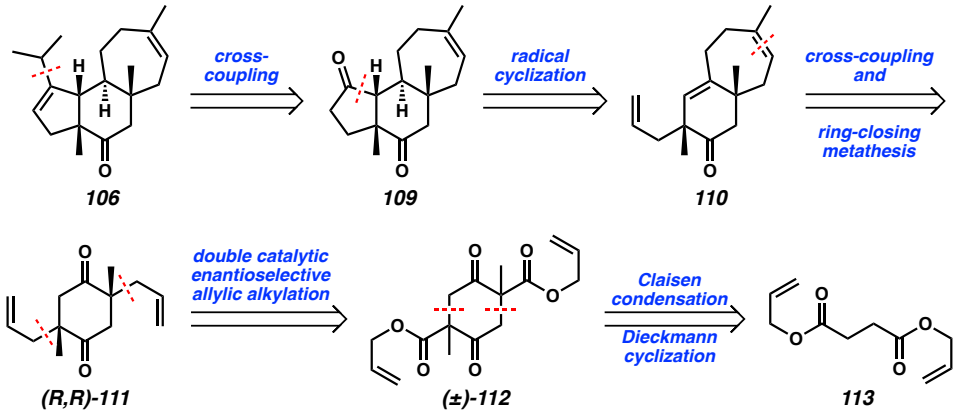

Our group's retrosynthetic strategy toward cyanthiwigin F (**106**) focused on early construction of the central B-ring and rapid installation of the two all-carbon quaternary stereocenters at the A–B and B–C ring junctures of the natural product (Scheme 2.1). Late-stage construction of the five-membered A-ring to form tricyclic diketone **109** could be accomplished from bicyclic ketone **110**, which would be assembled through triflation, cross-coupling, and ring-closing metathesis (RCM) of diketone **111**. Critically, this

symmetrical intermediate could be accessed through our group's enantioselective decarboxylative allylic alkylation methodology,[6] allowing the two quaternary stereocenters to be established from symmetrical bis-(β-ketoester) **112**, which itself would be constructed from diallyl succinate (**113**) by way of tandem Claisen condensation/ Dieckmann cyclization.

Scheme 2.2 Stoltz's synthesis of cyanthiwigins F, B, and G (2008, 2011)

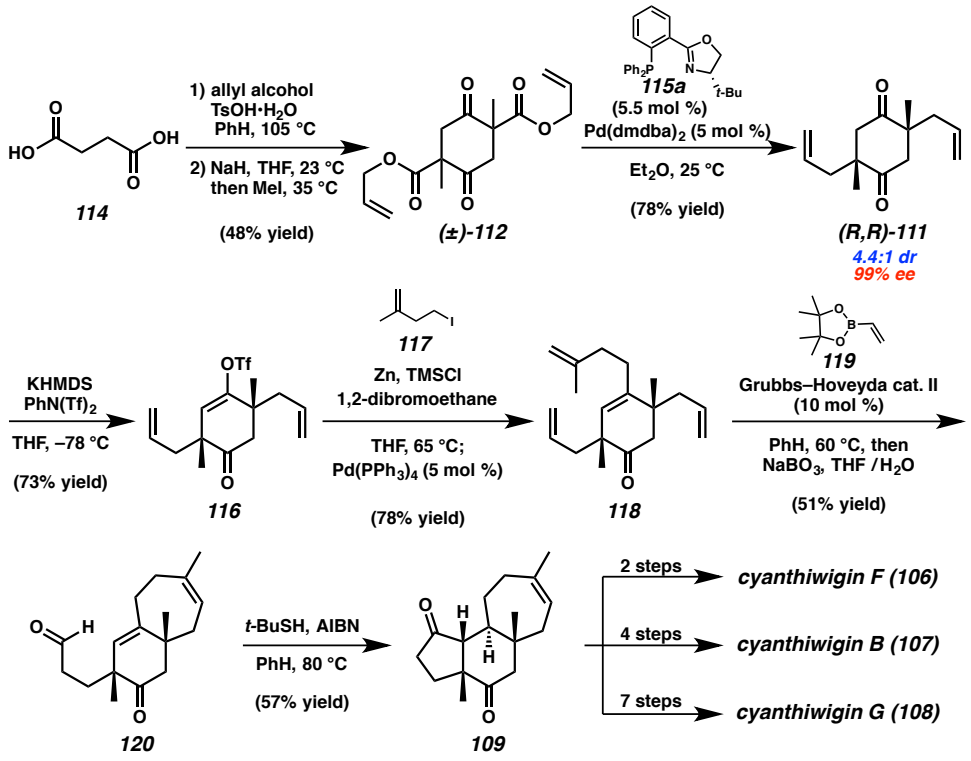

The forward synthesis began with preparation of diallyl succinate (**113**) from succinic acid (**114**) via double Fischer esterification. Subsequent treatment of **113** with sodium hydride induced tandem Claisen condensation/Dieckmann cyclization, and quenching with methyl iodide furnished bis-(β-ketoester) **112** as a 1:1 mixture of meso and racemic diastereomers. This mixture was subjected to conditions for Pd-catalyzed

enantioselective allylic alkylation, which gratifyingly delivered diketone *(R,R)*-**111** in high yield and diastereoselectivity and excellent enantioselectivity.[7] Significantly, this unusual transformation exemplified a powerful application of stereoablative enantioselective alkylation methodology, enabling concurrent selective installation of two stereocenters from a complex mixture of diastereomers. Desymmetrization of **113** via monotriflate formation generated vinyl triflate **116** as a suitable substrate for Negishi coupling with alkyl iodide **117**, allowing access to tetraene **118**. Ring-closing metathesis (RCM)[8] to assemble the seven-membered C ring followed by cross-metathesis with boronic ester **119** and subsequent oxidation furnished bicyclic aldehyde **120**. Finally, A ring formation was achieved through radical cyclization of **120**. The resulting tricyclic diketone **109** was elaborated to cyanthiwigins F, B, and G in 2, 4, and 7 steps, respectively.[9] Notably, no protecting groups were used in this concise 7-step route to tricycle **109**.

2.1.2 CHALLENGES IN LARGE-SCALE SYNTHESIS

With this efficient route to the cyanthiwigin carbon framework available, we recognized an opportunity to employ tricycle **109** as a scaffold from which to conduct late-stage diversification studies. To accomplish this, the synthetic sequence outlined in Scheme 2.2 would need to be repeated on a large scale to generate sizable quantities of **109**. While the conversion of succinic acid (**114**) to bis-(*β*-ketoester) **112** was readily performed on 100-gram scale, the ensuing double catalytic enantioselective alkylation proved cumbersome on large scale due to relatively high catalyst and ligand loadings and low reaction concentrations (0.01 M) necessitated by poor catalyst solubility in diethyl

ether, the optimal solvent for stereoselectivity. Similarly, while vinyl triflate formation and subsequent Negishi coupling to generate tetraene **118** proceeded smoothly on large scale, another bottleneck arose at the formation of bicyclic aldehyde **120**. Although the initial RCM progressed rapdily with full conversion, the ensuing cross-metathesis was sluggish. A significant amount of intermediate **110** was routinely isolated even after prolonged reaction times and use of excess **119**. Re-subjection of **110** to cross-metathesis conditions with **119** generally produced low yields, returning large quantities of **110**.

2.2 MODIFIED SYNTHETIC TRANSFORMATIONS

We envisioned that these obstacles to the large-scale preparation of tricycle **109** could be overcome using modern technologies developed after our group devised the initial synthetic route to **109** in 2008. For the reasons described in the previous section, we focused our efforts on the two most problematic transformations: 1) the double asymmetric decarboxylative alkylation and 2) the formation of bicyclic aldehyde **120**.

2.2.1 DOUBLE ASYMMETRIC DECARBOXYLATIVE ALKYLATION

Despite producing desired *(R,R)*-**111** in good yields and selectivities, the key double asymmetric decarboxylative alkylation suffered from two major limitations to scaling: 1) relatively high loadings of catalyst $Pd(dmdba)_2$ and phosphinooxazoline (PHOX) ligand **115a**, both of which are available only through multistep preparations, and 2) low reaction concentrations (0.01 M) required due to low catalyst solubility in diethyl ether, the optimal solvent for maximizing stereoselectivity. Indeed, performance of this

transformation on 15 g of substrate **112** required 2 g of $Pd(dmdba)_2$, 1 g of PHOX ligand **115a**, and over 3 L of solvent, an experimentally risky setup, considering the potential for diethyl ether to ignite in large volumes.

Table 2.1 Effect of the PHOX ligand on the double catalytic enantioselective allylic alkylation of ***112***

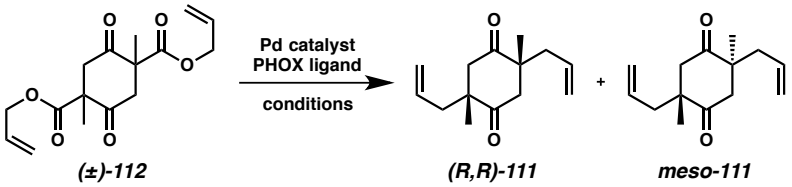

Entry	Pd cat. (mol %)	PHOX (mol %)	Solvent	Conc	Temp	Yield	dr	ee
1	$Pd(dmdba)_2$ (5.0)	***115a*** (5.5)	Et_2O	0.01 M	25 °C	78%	4.4 :1	99%
2	$Pd(dmdba)_2$ (5.0)	***115a*** (5.5)	2:1 PhMe:Hex	0.10 M	25 °C	75%	3.4:1	99%
3	$Pd(dmdba)_2$ (5.0)	***115b*** (5.5)	Et_2O	0.01 M	25 °C	92%	4.3:1	99%
4	$Pd(OAc)_2$ (0.25)	***115a*** (2.5)	TBME	0.10 M	40 °C	83%	2.2:1	97%
5	$Pd(OAc)_2$ (0.25)	***115b*** (2.5)	TBME	0.10 M	40 °C	93%	3.5:1	99%

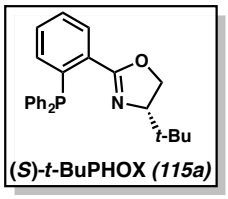

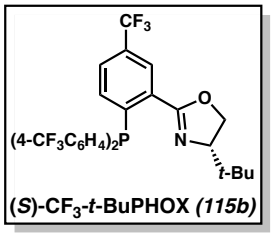

To address these issues, we investigated different solvent systems at a higher concentration of substrate **112** (0.10 M) and found that using a 2:1 mixture of toluene and hexane resulted in yields and ee's comparable to those of the original reaction conditions (Table 2.1, Entry 1) but markedly lower dr (Entry 2). Variation of the PHOX ligand showed that use of the electron-poor ligand (*S*)-CF_3-*t*-BuPHOX (**115b**)[10] in the catalytic system resulted in significantly higher yields, dr's, and ee's (Entry 3). Pleased by this improvement, we also sought to lower the loadings of Pd catalyst and PHOX ligand by application of our group's recently developed protocol for enantioselective alkylation that employs drastically lower loadings of catalyst and ligand.[11] Notably, the Pd precatalyst used in this protocol, $Pd(OAc)_2$, is commercially available, obviating the need to prepare

$Pd(dmdba)_2$. Although initial application of the standard conditions using ligand **115a** provided *(R,R)*-**111** in unsatisfactory dr (Entry 4), the use of ligand **115b** once again resulted in a dramatic improvement (Entry 5).

Encouraged by this observation, we set out to elucidate the optimal reaction conditions using the new catalyst system. To this end, we examined several different solvent systems and temperatures (Table 2.2). The yield was not substantially affected by decreasing the temperature from 40 to 30 °C (Entries 1–2), but the use of diethyl ether as the solvent resulted in lower yields (Entry 3). Interestingly, the use of toluene as the solvent greatly improved both the yield and dr (Entry 4), but the previously optimal solvent system, 2:1 toluene/hexane significantly impeded the reaction (Entry 5). Finally, we discovered that lowering the temperature further to 25 °C in toluene supplied the optimal yield and dr (Entry 6).

Table 2.2 Optimization of the low-catalyst-loading conditions for enantioselective alkylation

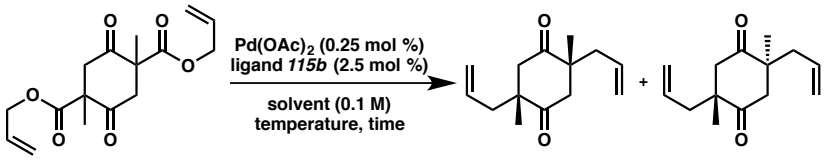

Entry	Solvent	Temperature	Time	Yield	dr	ee
1	TBME	40 °C	5 h	93%	3.5:1	99%
2	TMBE	30 °C	5 h	97%	3.6:1	99%
3	Et_2O	30 °C	5 h	88%	3.7:1	99%
4	PhMe	30 °C	5 h	99%	4.3:1	99%
5	2:1 PhMe:Hex	30 °C	24 h	45%	2.8:1	97%
6	PhMe	25 °C	16 h	97%	4.9:1	99%

We were pleased to find that the reoptimized conditions for the double catalytic enantioselective allylic alkylation were also effective on a large scale. When 10 g (32.4 mmol) of bis(*β*-ketoester) **112** was subjected to the new alkylation conditions, the desired diketone *(R,R)*-**111** was formed in 94% yield with good dr and excellent ee (Scheme 2.3). Remarkably, only 20 mg of Pd catalyst and 480 mg of PHOX ligand were required, greatly facilitating the scaling of this crucial step. Furthermore, only 250 mL of solvent was required for this large-scale reaction, permitting simple set-up and avoiding the saftey issues associated with large volumes of solvent. Overall, the modified conditions produced diketone *(R,R)*-**111** in higher yield with comparable selectivity while requiring 10 times less solvent, less than half the amount of PHOX ligand, and 20 times less Pd than the original conditions. Moreover, the use of a commercial Pd source eliminated the need to prepare $Pd(dmdba)_2$, further expediting the synthesis of the cyanthiwigin core (**109**).

*Scheme 2.3 Large-scale preparation of diketone **111** using the modified alkylation conditions*

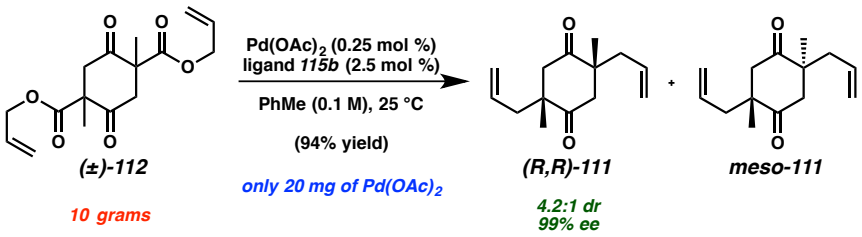

2.2.2 FORMATION OF THE PENULTIMATE BICYCLIC ALDEHYDE

Having succesfully applied the low-catalyst-loading allylic alkylation procedure to the preparation of diketone **111**, we turned our attention to the other transformation in

need of modification: the formation of bicyclic aldehyde **120**. As previously described, the cross-metathesis between RCM product **110** and vinylboronic ester **119** catalyzed by modified Grubbs–Hoveyda catalyst **121** proceeded sluggishly, generally returning sizable amounts of unreacted **110** (Scheme 2.4A). We hypothesized that the suboptimal performance of the reaction was due to unfavorable steric interactions arising from bulky boronic ester **119** with the quaternary stereocenter proximal to the site of reactivity in bicyclic triene **110**. Noting the efficiency of the aldehyde-selective Tsuji–Wacker reaction developed by the Grubbs group,[12] we hypothesized that this robust methodology could be used to convert the accumulated quantities of bicycle **110** to aldehyde **120**. Gratifyingly, this hypothesis was validated by the successful oxidation of **110** to aldehyde **120** in moderate yield under nitrite-modified Tsuji–Wacker conditions (Scheme 2.4B). Notably, this approach toward the preparation of **110** not only enabled productive recycling of the accrued **110** but also circumvented the preparation of boronic ester **119**, which was generally preferred over purchase due to cost and purity considerations.

*Scheme 2.4 Preparation of bicyclic aldehyde **120***

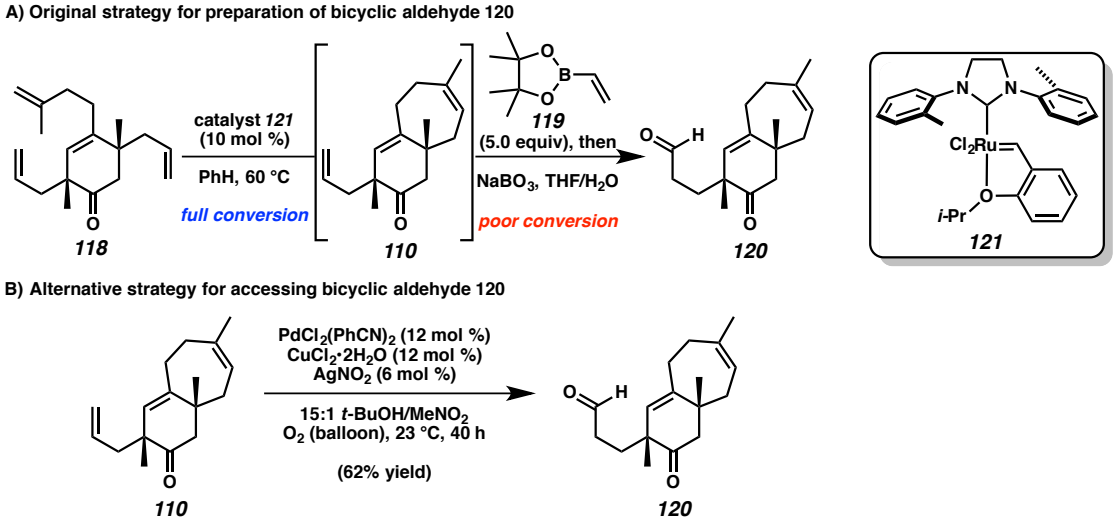

2.2.3 COMPLETION OF THE CYANTHIWIGIN CORE

With bicyclic aldehyde **120** in hand, we proceeded to the final step of the synthesis of **109**, azobis-(isobutyronitrile) (AIBN)-initiated radical cyclization to form the A-ring.[13] Initial attempts to effect the transformation using the original conditions tended to provide **109** in low yields, an observation attributed to possible loss of the *tert*-butylthiol propagator through evaporation facilitated by the elevated temperature. To mitigate this issue, we found that the use of *tert*-dodecanethiol as the propagator resulted in more consistent yields and avoided the odor associated with *tert*-butylthiol (Scheme 2.5).

*Scheme 2.5 Completion of the synthesis of **109** through radical cyclization of **120***

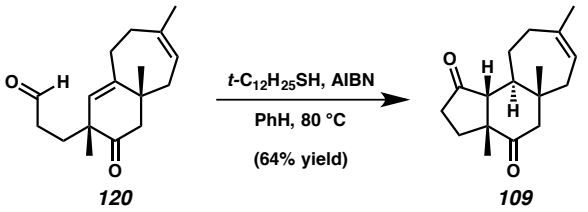

120 *109*

2.3 CONCLUDING REMARKS

In summary, we have developed a second-generation synthesis of the cyanthiwigin natural product core (**109**) using catalytic methodologies that have been developed within the past several years.[14] These modifications have proven essential in scaling the synthetic route, effectively setting the stage for late-stage diversification studies of the complex tricyclic framework.

2.4 EXPERIMENTAL SECTION

2.4.1 MATERIALS AND METHODS

All reactions were performed at ambient temperature (23 °C) unless otherwise noted. Reactions requiring external heat were modulated to the specified temperatures indicated by using an IKAmag temperature controller. All reactions were performed in glassware flame-dried under vacuum and allowed to cool under nitrogen or argon. Solvents were dried by passage over a column of activated alumina with an overpressure of argon gas.[15] Tetrahydrofuran was distilled directly over benzophenone and sodium, or else was dried by passage over a column of activated alumina with an overpressure of argon gas. Anhydrous *tert*-butanol and nitromethane were purchased from Sigma Aldrich in sure-sealed bottles and used as received unless otherwise noted. Commercial reagents (Sigma Aldrich or Alfa Aesar) were used as received with the exception of palladium(II) acetate (Sigma Aldrich) which was stored in a nitrogen-filled govebox. Grubbs's Ru catalyst **121**[8] was donated by Materia Inc. and used without further purification. (*S*)-*t*-BuPHOX (**115a**),[16] (*S*)-CF_3-*t*-BuPHOX (**115b**),[10] 4-iodo-2-methyl-1-butene (**117**),[17] vinyl boronate ester **119**,[18] and bis(3,5-dimethoxydibenzylideneacetone)palladium[19] were prepared according to known methods. All other chemicals and reagents were used as received. Compounds purified by flash chromatography utilized ICN silica gel (particle size 0.032–0.063 mm) or SiliCycle® Silia*Flash*® P60 Academic Silica Gel (particle size 40–63 μm; pore diameter 60 Å). Thin-layer chromatography (TLC) was performed using E. Merck silica gel 60 F254 pre-coated plates (0.25 mm) and visualized by UV fluorescence quenching, *p*-anisaldehyde, or alkaline permanganate staining. NMR spectra were

recorded on a Varian Mercury 300 spectrometer (at 300 MHz for ^{1}H NMR and 75 MHz for ^{13}C NMR), a Varian Inova 500 spectrometer (at 500 MHz for ^{1}H NMR and 126 MHz for ^{13}C NMR), or a Bruker AV III HD spectrometer equipped with a Prodigy liquid nitrogen temperature cryoprobe (at 400 MHz for ^{1}H NMR and 101 MHz for ^{13}C NMR), and are reported relative to residual $CHCl_3$ (δ 7.26 for ^{1}H NMR, δ 77.16 for ^{13}C NMR) or C_6H_6 (δ 7.16 for ^{1}H NMR, δ 128.06 for ^{13}C NMR). The following format is used for the reporting of ^{1}H NMR data: chemical shift (δ ppm), multiplicity, coupling constant (Hz), and integration. Data for ^{13}C NMR spectra are reported in terms of chemical shift. IR spectra were recorded on a Perkin Elmer Spectrum Paragon 1000 spectrometer, and data are reported in frequency of absorption (cm^{-1}). High-resolution mass spectra were obtained from the Caltech Mass Spectral Facility, or else were acquired using an Agilent 6200 Series TOF mass spectrometer with an Agilent G1978A Multimode source in ESI, APCI, or MM (ESI/APCI) ionization mode. Analytical chiral gas chromatography was performed with an Agilent 6850 GC using a G-TA (30 m x 0.25 mm) column (1.0 mL/min carrier gas flow). Analytical achiral gas chromatography was performed with an Agilent 6850 GC using a DB-WAX (30 x 0.25 mm) column (1.0 mL/min carrier gas flow). Preparatory reverse-phase HPLC was performed on a Waters HPLC with Waters Delta-Pak 2 x 100 mm, 15 μm column equipped with a guard, employing a flow rate of 1 mL/min and a variable gradient of acetonitrile and water as eluent. HPLC visualization was performed by collecting 1 mL fractions after initial injection and analyzing each fraction via TLC. Optical rotations were measured with a Jasco P-1010 polarimeter at 589 nm using a 100 mm path-length cell.

2.4.2 PREPARATIVE PROCEDURES

2.4.2.1 PREPARATION OF BIS-(β-KETOESTER) 112

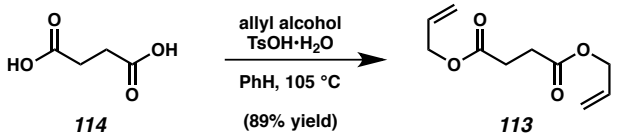

114 *113*

Diallyl Succinate (113). To a solution of succinic acid (**114**, 40.0 g, 338.7 mmol) in benzene (300 mL) was added TsOH • H_2O (0.21 g, 1.2 mmol, 0.003 equiv). After brief mixing, allyl alcohol (70 mL, 1.01 mol, 3.00 equiv) was added to the reaction, and the flask was fitted with a Dean–Stark trap and reflux condenser under nitrogen. The reaction was heated to 105 °C and allowed to reflux over 12 h. After collection of 13 mL H_2O from the Dean–Stark trap, the reaction was allowed to cool to room temperature and was quenched by slow treatment with saturated $NaHCO_{3(aq)}$ until gas evolution halted. The phases were separated, and the organic layer was washed with saturated $NaHCO_{3(aq)}$ (2 x 40 mL) and brine (2 x 30 mL). The combined organic layers were dried over $MgSO_4$, and solvent was removed in vacuo after filtration. The resulting colorless oil was dried under high vacuum to afford diallyl succinate (**113**, 59.8 g, 89% yield). This material was carried into the next step without further purification: R_f = 0.35 (10% Et_2O in pentane); ^{1}H NMR (300 MHz, $CDCl_3$) δ 5.90 (ddt, *J* = 17.3, 10.5, 5.6 Hz, 2H), 5.31 (ddt, *J* = 17.0, 1.6, 1.3 Hz, 2H), 5.23 (ddt, *J* = 10.4, 1.3, 1.1 Hz, 2H), 4.60 (ddd, *J* = 5.9, 1.3, 1.3 Hz, 4H), 2.67 (s, 4H); ^{13}C NMR (75 MHz, $CDCl_3$) δ 172.0, 132.1, 118.5, 65.5, 29.2; IR (Neat film, NaCl) 3086, 2942, 1738, 1649, 1413, 1377, 1271, 1157, 990, 932 cm^{-1}; HRMS (EI) *m/z* calc'd for $C_{10}H_{14}O_4$ $[M]^+$: 198.0892, found 198.0888.

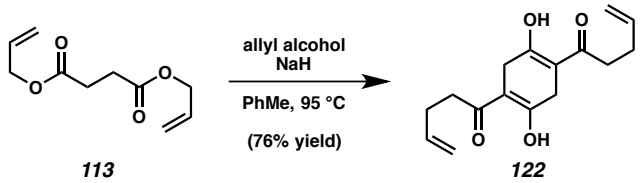

113 ***122***

Diallyl Succinylsuccinate (122). To a flame dried flask under argon was added NaH (60% in mineral oil, 25.0 g, 630.6 mmol, 2.50 equiv) and toluene (125 mL). To this was added, dropwise, neat allyl alcohol (4.14 mL, 70.6 mmol, 0.28 equiv) with vigorous stirring. After gas evolution had ceased, neat diallyl succinate (**113**, 50.0 g, 252.2 mmol, 1.00 equiv) was added dropwise, and the reaction was heated to 95 °C. The reaction flask was fitted with a reflux condenser, and reaction was allowed to proceed over 10 h. After ca. 15 min, an additional portion of toluene (125.0 mL) was added to the reaction to ensure fluidity of the mixture. Once the reaction had completed by TLC, the flask was cooled to room temperature, and the solvent was removed in vacuo. The crude solid was immediately suspended in CH_2Cl_2, and then acidified by addition of 2 N $HCl_{(aq)}$ (350 mL). The biphasic mixture was allowed to stir over 2 h, after which time all solids had dissolved. The phases were separated, and the aqueous layer was extracted with CH_2Cl_2 (2 x 50 mL). The combined organic layers were dried over $MgSO_4$ and filtered, and solvent was removed in vacuo to yield a crude orange solid. The crude residue was recrystallized twice from a mixture of petroleum ether and acetone to afford diallyl succinylsuccinate (**122**) as a flaky white solid (26.9 g, 76% yield) that matched previously reported characterization data:[1] R_f = 0.6 (15% ethyl acetate in hexanes) ^{1}H NMR (300 MHz, $CDCl_3$) δ 12.11 (s, 2H), 5.95 (dddd, *J* = 17.1, 10.7, 5.7, 5.7 Hz, 2H), 5.35 (ddt, *J* = 17.3, 1.6, 1.3 Hz, 2H), 5.27 (ddt, *J* = 10.4, 1.3, 1.3 Hz, 2H), 4.69 (ddd,

J = 5.3, 1.3, 1.3 Hz, 4H), 3.22 (s, 4H); ^{13}C NMR (75 MHz, $CDCl_3$) δ 170.8, 168.8, 131.7, 118.4, 93.1, 65.2, 28.5; IR (Neat film, NaCl) 1666, 1647, 1684, 1451, 1389, 1329, 1219, 1204, 1133, 1061, 961, 843, 783 cm^{-1}; HRMS (EI) *m/z* calc'd for $C_{14}H_{16}O_6$ $[M]^+$: 280.0947, found 280.0948.

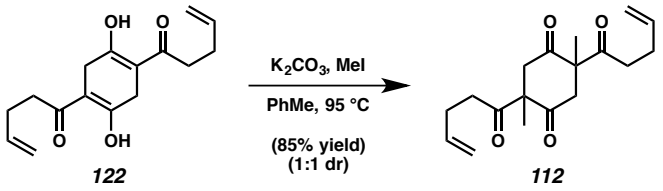

Bis(*β*-ketoester) 112. Prior to use in the reaction, acetone was dried by stirring it over anhydrous calcium sulfate, and then passing the solvent over a short plug of silica. Potassium carbonate (5.80 g, 43.9 mmol, 4.10 equiv) and diallyl succinylsuccinate (**122**, 3.00 g, 10.7 mmol, 1.00 equiv) were suspended in acetone (21.3 mL). After addition of solvent to the solids, the reaction mixture was fitted with a reflux condenser and then was heated to 50 °C. To this mixture was added methyl iodide (3.40 mL, 54.5 mmol, 5.10 equiv). The reaction was stirred vigorously to ensure completion. (Note: If reaction is not stirred, or if stirring is not efficient, potassium carbonate will collect into a solid aggregate and the reaction will halt. Breaking up these solid collections with a spatula is typically enough to reinitiate reaction, though in some cases additional methyl iodide may be required.) After 6 h, the reaction was allowed to cool and then was passed through filter paper. The remaining solids were washed with additional CH_2Cl_2 to ensure complete solvation of any precipitated product trapped within the potassium carbonate. The collected organic layers were combined and concentrated to yield an amorphous semi-solid, which was purified over silica gel using 15% → 20% ethyl acetate in hexanes

as eluent. Compound **112** was afforded as two diastereomers in a 1 : 1 ratio. The less polar diastereomer (by TLC analysis with 20% ethyl acetate in hexanes) was obtained as a white, fluffy solid, and the more polar diastereomer was obtained as a thick, yellow oil (1.4 g for each diastereomer, 2.8 g for combined diastereomers, 85% yield) that matched previously reported characterization data.[1] **Diastereomer A**: R_f = 0.30 (20% ethyl acetate in hexanes); ^{1}H NMR (300 MHz, $CDCl_3$) δ 5.84 (dddd, *J* = 17.3, 10.4, 5.8, 5.8 Hz, 2H), 5.30 (app dq, *J* = 17.3, 1.3 Hz, 2H), δ 5.26 (app dq, *J* = 10.4, 1.3 Hz, 2H), δ 4.60 (app ddd, *J* = 5.9, 1.3, 1.3 Hz, 4H), δ 3.14 (d, *J* = 15.2 Hz, 2H), δ 2.80 (d, *J* = 15.2 Hz, 2H), δ 1.43 (s, 6H); ^{13}C NMR (75 MHz, $CDCl_3$) δ 201.8, 170.6, 131.0, 119.7, 66.8, 57.6, 48.1, 20.8; IR (Neat film, NaCl) 2988, 2940, 1749, 1708, 1420, 1375, 1281, 1227, 1132, 1076, 911, 809, 744 cm^{-1}; HRMS (EI) *m/z* calc'd for $C_{16}H_{20}O_6$ [M^+]: 308.1260, found 308.1263. **Diastereomer B**: R_f = 0.20 (20% ethyl acetate in hexanes); ^{1}H NMR (300 MHz, $CDCl_3$) δ 5.88 (dddd, *J* = 17.1, 10.4, 5.7, 5.7 Hz, 2H), δ 5.31 (app dq, *J* = 17.2, 1.5 Hz, 2H), δ 5.27 (app dq, *J* = 10.3, 1.5, 2H), δ 4.62 (app ddd, *J* = 5.4, 1.5, 1.5 Hz, 4H), δ 3.47 (d, *J* = 15.6 Hz, 2H), δ 2.63 (d, *J* = 15.9 Hz, 2H), δ 1.46 (s, 6H); ^{13}C NMR (75 MHz, $CDCl_3$) δ 202.5, 169.9, 131.1, 119.1, 66.7, 56.6, 47.1, 21.5; IR (Neat film, NaCl) 3088, 2984, 2940, 1747, 1722, 1649, 1454, 1422, 1381, 1275, 1233, 1196, 1110, 984, 934 cm^{-1}. HRMS (EI) *m/z* calc'd for $C_{16}H_{20}O_6$ [M^+]: 308.1260, found 308.1263.

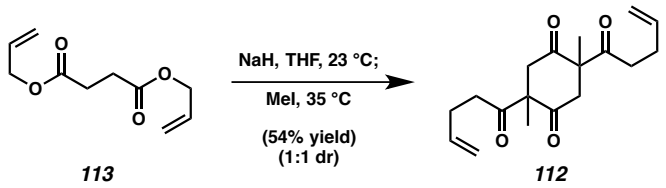

113 ***112***

Alternative Preparation of Bis(*β*-ketoester) 112. A flame dried round bottom flask was charged with NaH (60% in mineral oil, 4.44 g, 111.0 mmol, 2.2 equiv). The flask was briefly vacuum purged, and then was backfilled with argon. The solid NaH was then suspended in freshly distilled (or freshly dispensed) THF (40 mL). The resulting suspension was cooled to 0 °C in an ice water bath. After cooling, the NaH slurry was treated with a THF solution (20 mL) of diallyl succinate (**113**, 10.0 g, 50.4 mmol) added via cannula. The reaction was allowed to gradually warm to room temperature overnight (12 h). The next morning the reaction was heated to 40 °C to encourage completion of the Claisen condensation/Dieckmann cyclization process. After 24 h at this temperature, TLC analysis revealed total consumption of diallyl succinate (**113**). The reaction was cooled to 35 °C, and then a single portion of MeI (8.16 mL, 131.2 mmol, 2.6 equiv) was introduced via syringe. After an additional 12 h at 35 °C, the reaction was quenched with saturated $NH_4Cl_{(aq)}$ (40 mL). The organic layer was separated from the aqueous layer, and the aqueous layer was extracted with CH_2Cl_2 (3 x 40 mL). The combined organic layers were washed with brine (40 mL), dried over $MgSO_4$, and filtered. The crude material obtained upon removal of solvent in vacuo was further purified via column chromatography over silica using 15% → 20% ethyl acetate in hexanes as eluent. Compound **112** was afforded as two diastereomers in a 1 : 1 ratio, again as both a white solid and a clear oil (2.1 g for each diastereomer, 4.2 g for combined diastereomers, 54% yield). All spectroscopic data was identical to that reported above.

2.4.2.2 OPTIMIZATION OF THE DOUBLE CATALYTIC ENANTIOSELECTIVE ALLYLIC ALKYLATION

Table 2.3 Investigation of the influence of Pd catalyst and PHOX ligand

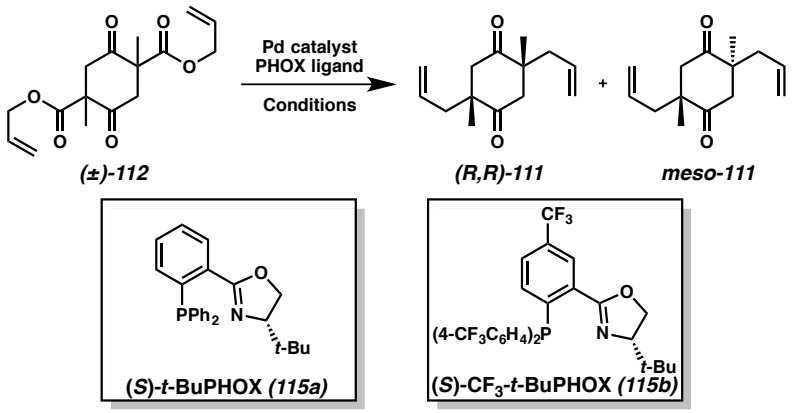

Entry	Pd cat. (mol %)	PHOX (mol %)	Solvent	Conc.	Temp.	Yield	d.r.	ee
1	$Pd(dmdba)_2$ (5.0)	*115a* (5.5)	Et_2O	0.01 M	25 °C	78%	4.4 : 1.0	99%
2	$Pd(dmdba)_2$ (5.0)	*115a* (5.5)	2:1 PhMe:Hex	0.10 M	25 °C	75%	3.4 : 1.0	99%
3	$Pd(dmdba)_2$ (5.0)	*115b* (5.5)	Et_2O	0.01 M	25 °C	92%	4.3 : 1.0	99%
4	$Pd(OAc)_2$ (0.25)	*115a* (2.5)	TBME	0.10 M	40 °C	83%	2.2 : 1.0	97%
5	$Pd(OAc)_2$ (0.25)	*115b* (2.5)	TBME	0.10 M	40 °C	93%	3.5 : 1.0	99%

Diketone 111. In a nitrogen-filled glovebox, a 20-mL scintillation vial equipped with a magnetic stir bar was charged with palladium catalyst and PHOX ligand. The solids were diluted with solvent (amount based on indicated concentration of substrate), the vial was sealed with a Teflon-lined cap, and the mixture was stirred at ambient temperature (25 °C) in the glovebox for 30 minutes. Neat bis-β-ketoester **112** was added to the mixture,[20] and the vial was once again sealed and heated to the indicated temperature for the specified amount of time. Reaction progress was monitored by TLC. Upon full

conversion of the substrate to the desired product, the reaction was allowed to cool to ambient temperature and removed from the glovebox. Concentration in vacuo followed by purification by silica gel column chromatography (3% ethyl acetate in hexanes) afforded diketone **111** as a colorless oil that matched previously reported characterization data:[1] R_f = 0.38, 10% ethyl acetate in hexanes; ^{1}H NMR ($CDCl_3$, 300 MHz) δ 5.68 (dddd, *J* = 18.3, 10.2, 6.9, 6.9 Hz, 2H), 5.17–5.09 (comp. m, 3H), 5.07–5.04 (m, 1H), 2.82 (d, *J* = 14.7 Hz, 2H), 2.38 (d, *J* = 15 Hz, 2H), 2.34 (app ddt, *J* = 13.2, 6.9, 1.0 Hz, 2H), 2.09 (app ddt, *J* = 13.5, 7.8, 0.9 Hz, 2H), 1.10 (s, 6H); ^{13}C NMR ($CDCl_3$, 126 MHz) δ 212.8, 132.4, 120.0, 49.4, 48.4, 43.8, 24.3; IR (Neat Film, NaCl) 3078, 2978, 1712, 1640, 1458, 1378, 1252, 1129, 1101, 998, 921 cm^{-1}; HRMS (ESI+) *m/z* calc'd for $C_{14}H_{20}O_2$ $[M]^+$: 220.1463, found 220.1466; $[\alpha]^{25}_D$ –163.1 (*c* 0.52, CH_2Cl_2). Diastereomeric ratio and enantiomeric excess were determined by GC analysis. Chiral GC assay (GTA column): 100 °C isothermal method over 90 min. Retention times: 67.7 min (Major enantiomer, C_2 diastereomer), 74.1 min (Minor enantiomer, C_2 diastereomer), 77.4 min (*meso* diastereomer). Achiral GC assay (DB-Wax column): 100 °C isotherm over 2.0 min, ramp 5 °C/min to 190 °C, then 190 °C isotherm for 10.0 min. Retention times: 18.5 min (C_2 diastereomer), 18.7 min (*meso* diastereomer).

Table 2.4 Investigation of the influence of solvent and temperature

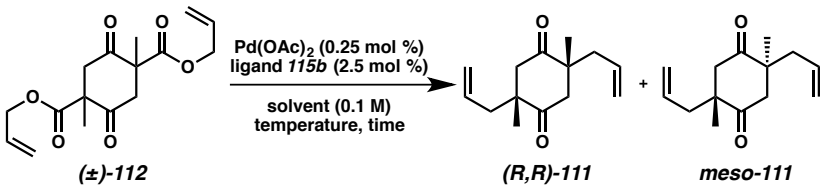

Entry	Solvent	Temperature	Time	Yield	d.r.	ee
1	TBME	40 °C	5 h	93%	3.5 : 1.0	99%
2	TMBE	30 °C	5 h	97%	3.6 : 1.0	99%
3	Et_2O	30 °C	5 h	88%	3.7 : 1.0	99%
4	PhMe	30 °C	5 h	99%	4.3 : 1.0	99%
5	2:1 PhMe:Hex	30 °C	24 h	45%	2.8 : 1.0	97%
6	PhMe	25 °C	16 h	97%	4.9 : 1.0	99%

Allylic Alkylation Procedure. In a nitrogen-filled glovebox, $Pd(OAc)_2$ (1.4 mg, 6.3 μmol) was weighed into a 20-mL scintillation vial and dissolved in solvent (10 mL). In a separate 1-dram vial, (*S*)-CF_3-*t*-Bu-PHOX (**115b**) (3.7 mg, 6.3 μmol) was dissolved in solvent (1 mL). To a 2-dram vial equipped with a magnetic stir bar, 1.0 mL of the $Pd(OAc)_2$ solution was added (14 μg, 0.63 μmol, 0.25 mol %) followed by 1.0 mL of the (*S*)-CF_3-*t*-BuPHOX solution (3.7 mg, 6.3 μmol, 2.5 mol %), washing with an additional 0.5 mL of solvent. The vial was sealed with a Teflon-lined cap, and the mixture was stirred at ambient temperature (25 °C) in the glovebox for 30 minutes. Neat bis-*β*-ketoester **112** (77 mg, 0.25 mmol, 1.0 equiv) was added to the mixture, and the vial was once again sealed and heated to the indicated temperature for the specified amount of time. Reaction progress was monitored by TLC. Upon full conversion of the substrate to the desired product (R_f = 0.38, 10% ethyl acetate in hexanes), the reaction was allowed to

cool to ambient temperature and removed from the glovebox. Concentration in vacuo followed by purification by silica gel column chromatography (3% ethyl acetate in hexanes) afforded diketone **111** as a colorless oil that matched previously reported characterization data (see above).

2.4.2.3 SCALE-UP OF THE DOUBLE CATALYTIC ENANTIOSELECTIVE ALLYLIC ALKYLATION

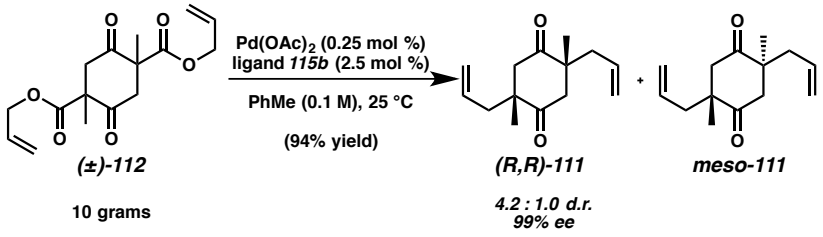

Large-Scale Allylic Alkylation Procedure. An oven-dried 500-mL round-bottom flask equipped with a magnetic stir bar was cooled to room temperature under vacuum in the antechamber of a nitrogen-filled glovebox. In the glovebox, the flask was charged with $Pd(OAc)_2$ (18 mg, 0.081 mmol, 0.25 mol %), (*S*)-CF_3-*t*-BuPHOX (**115b**) (480 mg, 0.81 mmol, 2.5 mol %), and toluene (300 mL). The flask was capped with a rubber septum, secured with electrical tape, and the contents were stirred at ambient temperature (25 °C) in the glovebox. After 1 hour, the septum was removed, and neat bis-(β-ketoester) **112** (10 g, 32 mmol, 1.0 equiv) was added to the bright yellow solution in one portion. The flask was re-sealed, and stirring continued at ambient temperature for 48 hours, at which time the reaction was removed from the glovebox and concentrated in vacuo to a dark orange oil. Purification by silica gel column chromatography (3% ethyl

acetate in hexanes) afforded pure diketone **111** as a colorless oil (6.7 g, 94% yield) that matched previously reported characterization data (see above).

2.4.2.4 PREPARATION OF TETRAENE 118

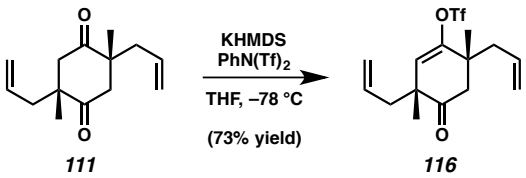

Triflate 116. A flask was charged with potassium bis(trimethylsilyl)amide (1.49 g, 7.49 mmol, 1.10 equiv) in the glovebox, and then was transferred to a manifold line outside of the glovebox under argon. The solids were dissolved in THF (180 mL), and the resulting solution was stirred while being cooled to –78 °C. To this alkaline solution was added, dropwise, neat diketone **111** (1.50 g, 6.80 mmol, 1.00 equiv). The solution immediately turned yellow, and viscosity increased. Deprotonation was allowed over 30 min, after which time the anionic solution was transferred by cannula into a solution of *N*-phenyl bis(trifluoromethane)sulfonimide (2.91 g, 8.17 mmol, 1.20 equiv) in THF (60 mL) at –78 °C. Reaction was allowed to proceed at this temperature over 6 h, after which time the mixture was brought to room temperature. The anionic reaction was quenched with brine (100 mL). The phases were separated, and the aqueous layer was extracted with diethyl ether (3 x 100 mL) and ethyl acetate (1 x 100 mL). The combined organic layers were washed with brine (2 x 50 mL), dried over $MgSO_4$, and the solvent was removed in vacuo after filtration. The crude oil obtained was loaded onto a silica gel column and eluted with 2% Et_2O in pentane. This afforded triflate **116** as a colorless oil

(1.75 g, 73% yield) that matched previously reported characterization data:[1] R_f = 0.40 (5% ethyl acetate in hexanes); ^{1}H NMR (500 MHz, $CDCl_3$) δ 5.77–5.58 (comp. m, 2H), 5.63 (s, 1H), 5.22–5.03 (comp. m, 4H), 2.71 (d, *J* = 14.3 Hz, 1H), 2.40 (d, *J* = 14.4 Hz, 1H), 2.49–2.30 (comp. m, 2H), 2.24 (app ddt, *J* = 13.5, 6.9, 1.3 Hz, 1H), 2.09 (app ddt, *J* = 13.8, 8.24, 1.2 Hz, 1H), 1.22 (s, 3H), 1.19 (s, 3H); ^{13}C NMR (125 MHz, $CDCl_3$) δ 209.6, 152.0, 132.6, 132.1, 122.9, 120.6, 119.7, 49.2, 48.9, 43.8, 43.0, 42.1, 25.2, 24.6; IR (Neat film, NaCl) 3081, 2980, 2934, 1721, 1673, 1641, 1457, 1416, 1214, 1141, 1010, 923.6, 895.2, 836.2 cm^{-1}; HRMS *m/z* calc'd for $C_{15}H_{19}O_4SF_3$ [M^+]: 352.0956, found 352.0949; $[\alpha]^{25}_D$ –6.5 (*c* 1.15, CH_2Cl_2).

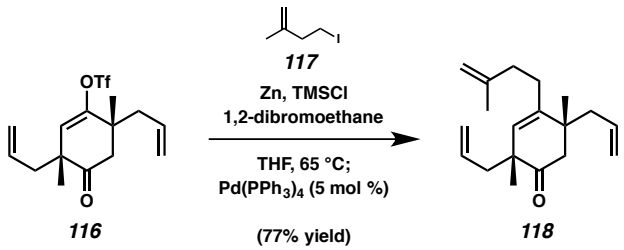

Tetraene 118. A flame-dried Schlenk flask equipped with a magnetic stir bar was charged with zinc dust (0.70 g, 11 mmol, 7.5 equiv) and evacuated and backfilled with argon (3x) before addition of THF (30 mL). Trimethylsilyl chloride (59 μL, 0.47 mmol, 0.33 equiv) and 1,2-dibromoethane (0.15 mL, 1.7 mmol, 1.2 equiv) were added sequentially to the suspension by syringe, and the flask was sealed and heated to 65 °C. After 15 minutes, the mixture was cooled to 23 °C, and neat alkyl iodide **117** (0.27 mL, 2.1 mmol, 1.5 equiv) was added by syringe. The flask was re-sealed and heated to 65 °C for 2 hours. Meanwhile, in a nitrogen-filled glovebox, a separate flame-dried conical flask was charged with a solution of triflate **116** (0.50 g, 1.4 mmol, 1.0 equiv) and

tetrakis(triphenylphosphine)palladium(0) (82 mg, 0.071 mmol, 0.05 equiv) in THF (16 mL). This solution was added to the suspension in the Schlenk flask at 23 °C, the flask was sealed, and the resulting olive green mixture was heated to 65 °C. After 3 hours, the reaction was cooled to 23 °C and filtered over a pad of Celite, washing with excess diethyl ether (150 mL). The filtrate was diluted with brine and extracted with diethyl ether (4 x 50 mL), and the combined organics were washed sequentially with brine (50 mL) and saturated sodium thiosulfate (3 x 50 mL). The organic layer was dried over magnesium sulfate before filtration and concentration in vacuo. The crude residue was purified by silica gel column chromatography (1% → 2% → 3% Et_2O in hexanes) to afford pure tetraene **118** as a colorless oil (0.30 g, 77% yield) that matched previously reported characterization data:[1] R_f = 0.50 (5% ethyl acetate in hexanes); ^{1}H NMR ($CDCl_3$, 500 MHz) δ 5.77–5.61 (comp. m, 2H), 5.20 (s, 1H), 5.10–4.97 (comp. m, 4H), 4.74 (d, *J* = 8.8 Hz, 2H), 2.56 (d, *J* = 13.5 Hz, 1H), 2.40–2.13 (comp. m, 8H), 2.05–1.98 (m, 1H), 1.77 (s, 3H), 1.09 (s, 3H), 1.04 (s, 3H); ^{13}C NMR ($CDCl_3$, 126 MHz) δ 214.4, 145.5, 142.5, 134.1, 134.0, 128.6, 118.6, 117.9, 110.1, 49.5, 48.7, 44.4, 44.3, 43.2, 36.5, 28.6, 26.5, 24.7, 22.7; IR (Neat Film, NaCl) 3076, 2996, 2928, 2360, 1715, 1639, 1455, 1376, 1320, 1298, 1261, 1229, 1138, 1093, 996, 916, 887 cm^{-1}; HRMS (ESI+) *m/z* calc'd for $C_{19}H_{28}O$ $[M]^+$: 272.2140, found 272.2138; $[\alpha]^{25}_D$ –72.4 (*c* 0.22, CH_2Cl_2).

2.4.2.5 PREPARATION OF BICYCLIC ALDEHYDE 120

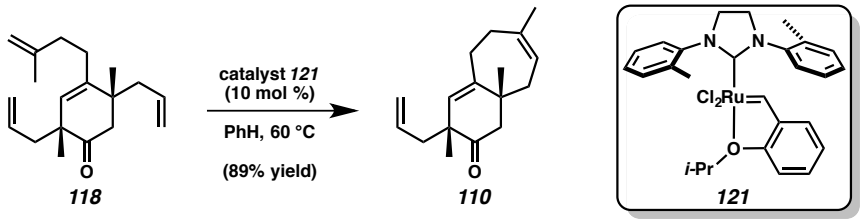

Bicyclic Triolefin 110. To a flame dried flask was added tetraolefin **118** (160 mg, 588 mmol, 1.00 equiv). This oil was dissolved in benzene (5 mL), and then azeotroped from this solvent. This process was repeated three times, and then the resulting residue was dissolved in benzene (28 mL) and sparged with argon for 30 min. After the sparge time had elapsed, a single portion of Grubbs–Hoveyda catalyst **121** (34.0 mg, 59.0 μmol, 0.10 equiv) was added to the solution. The reaction was then heated to 40 °C. (Note: tetraolefin **118** and bicyclic triolefin **110** are difficult to separate by TLC in a wide variety of solvent systems, and frequently are seen to co-spot. In order to afford more efficient separation via TLC, the use of silver nitrate treated silica gel TLC plates is very effective.) After 20 min at 40 °C, the reaction had completed by TLC, and so was quenched via the addition of ethyl vinyl ether (20 mL). The solvents were removed in vacuo, and the resulting crude mixture was purified via chromatography over silica gel using 0.5% → 1.0% → 1.5% → 3.0% Et_2O in petroleum ether as eluent. This afforded bicyclic triene **110** as a colorless oil (128 mg, 89% yield) that matched previously reported characterization data:[1] R_f = 0.50 (5% ethyl acetate in hexanes); ^{1}H NMR (500 MHz, $CDCl_3$) δ 5.64 (dddd, *J* = 16.8, 10.2, 8.4, 6.5 Hz, 1H), 5.33 (dddd, *J* = 6.9, 5.4, 2.9, 1.5 Hz, 1H), 5.19 (s, 1H), 5.01–4.93 (comp. m, 2H), 2.73 (dd, *J* = 13.4, 0.6 Hz, 1H), 2.53 (dddd, *J* = 13.2, 11.7, 5.3, 0.6 Hz, 1H), 2.45–2.39 (m, 2H), 2.22–2.17 (m, 1H), 2.22 (app

ddt, J = 13.5, 8.4, 0.9 Hz, 1H), 2.11–2.03 (m, 2H), 2.11 (app ddt, J = 13.5, 6.5, 1.4 Hz, 1H), 2.03 (d, J = 13.5 Hz, 1H), 1.65 (s, 3H), 1.10 (s, 3H), 0.95 (s, 3H); ^{13}C NMR (125 MHz, $CDCl_3$) δ 216.6, 145.3, 138.5, 134.0, 129.2, 120.2, 117.8, 51.7, 49.0, 46.3, 44.9, 37.4, 29.5, 28.1, 25.8, 23.7; IR (Neat film, NaCl) 3076, 2961, 2927, 1711, 1639, 1452, 1372, 1225, 1163, 997, 916 cm^{-1}; HRMS (EI) m/z calc'd for $C_{17}H_{24}O$ [M^+]: 244.1827, found 244.1821; $[\alpha]^{25}_D$ –96.7 (*c* 1.33, CH_2Cl_2).

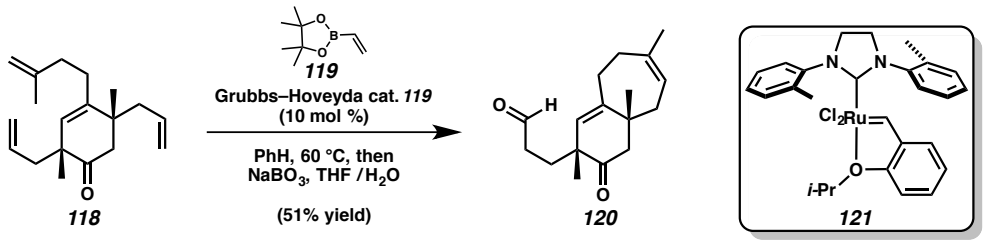

Bicyclic Aldehyde 120. A flame-dried round-bottom flask equipped with a magnetic stir bar was charged with tetraene **118** (0.25 g, 0.92 mmol, 1.0 equiv). Dry benzene (2 mL) was added, then evaporated under vacuum. This azeotropic drying procedure was repeated two additional times, and the resulting material was then dried under high vacuum and backfilled with argon, before dilution with benzene (10 mL). A solution of Grubbs–Hoveyda catalyst **121** (26 mg, 0.046 mmol, 0.05 equiv) in THF (10 mL) was added slowly, and the resulting mixture was stirred at 25 °C. After 1 hour, boronate ester **119** (0.78 mL, 4.6 mmol, 5.0 equiv) was added dropwise, and another portion of catalyst **121** (26 mg, 0.046 mmol, 0.05 equiv) in THF (10 mL) was added. The olive green mixture was heated to 40 °C. After 20 hours, the reaction was cooled to 0 °C, and ethyl vinyl ether (0.4 mL) was added to quench remaining catalyst. Volatiles were removed in vacuo, and the resulting residue was passed through a plug of silica, eluting with 20%

ethyl acetate in hexanes (300 mL). Upon concentration, the resulting oil was diluted with THF (30 mL) and water (30 mL), treated with sodium perborate monohydrate (0.55 g, 5.5 mmol, 6.0 equiv), and stirred at 23 °C for 1.5 hours. The phases were separated, and the aqueous layer was extracted with ethyl acetate (4 x 50 mL). The combined organics were washed with brine and dried over magnesium sulfate. Upon filtration and concentration, the crude reside was purified by silica gel column chromatography (5% ethyl acetate in hexanes) to furnish pure aldehyde **120** as a colorless oil (0.11 g, 46% yield) that matched previously reported characterization data:[1] R_f = 0.20 (10% ethyl acetate in hexanes); ^{1}H NMR (500 MHz, $CDCl_3$) δ 9.71 (app t, *J* = 1.3 Hz, 1H), 5.38–5.31 (m, 1H), 5.15 (s, 1H), 2.70 (d, *J* = 13.6 Hz, 1H), 2.59–2.32 (comp. m, 5H), 2.12 (d, *J* = 13.8 Hz, 1H), 2.24–2.04 (comp. m, 2 H), 1.89–1.64 (comp. m, 3 H), 1.67 (s, 3H), 1.12 (s, 3H), 0.97 (s, 3H); ^{13}C NMR (125 MHz, $CDCl_3$) δ 215.5, 201.6, 146.4, 138.7, 129.0, 120.1, 51.6, 47.7, 39.9, 37.6, 37.2, 33.1, 29.6, 27.8, 25.9, 23.9; IR (Neat film, NaCl) 2960, 2927, 2360, 2341, 1711–1710 (overlapping peaks), 1452, 1374, 1296, 1163 cm^{-1}; HRMS (EI) *m/z* calc'd for $C_{17}H_{24}O_2$ [M^+]: 260.1776, found 260.1784; $[\alpha]^{25}_D$ –83.5 (*c* 1.09, CH_2Cl_2).

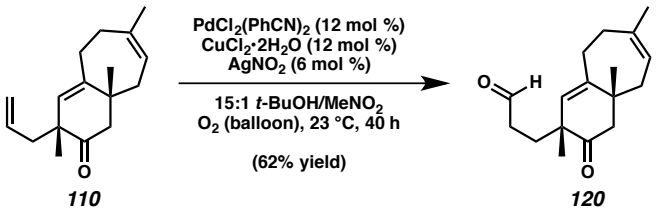

110 *120*

Alternative Preparation of Bicyclic Aldehyde 120. To a flame-dried 25-mL round-bottom flask with a magnetic stir bar were added bis(benzonitrile)palladium(II) chloride (5.7 mg, 0.015 mmol, 0.12 equiv), copper(II) chloride dihydrate (2.6 mg, 0.015 mmol, 0.12 equiv), and silver nitrite (1.2 mg, 0.0075 mmol, 0.06 equiv). The flask was capped

with a rubber septum, and *tert*-butyl alcohol (2.3 mL) and nitromethane (0.20 mL) were added sequentially by syringe. The mixture was stirred at 23 °C and sparged with oxygen gas (balloon) for 3 minutes. Alkene **110** (30 mg, 0.12 mmol, 1.0 equiv) was added dropwise by syringe, and the reaction mixture was sparged with oxygen for another minute. The reaction was stirred under oxygen atmosphere at 23 °C for 20 hours, at which time another half portion of the catalyst system (2.9 mg Pd, 1.3 mg Cu, 0.6 mg Ag) was added to the reaction mixture. After 20 hours, the reaction mixture was diluted with water (4 mL) and extracted with dichloromethane (3 x 5 mL). The organic extracts were dried over sodium sulfate, then filtered and concentrated in vacuo. The crude residue was purified by silica gel column chromatography (3% ethyl acetate in hexanes), furnishing aldehyde **120** as a colorless oil (20 mg, 62% yield) that matched previously reported characterization data (see above).

2.4.2.6 PREPARATION OF TRICYCLIC DIKETONE 109

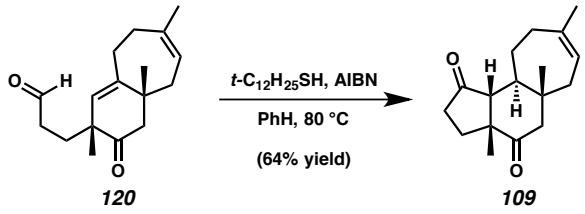

120 *109*

Tricyclic Diketone 109. A flame-dried Schlenk flask equipped with a magnetic stir bar was charged with aldehyde **120** (20 mg, 0.076 mmol, 1.0 equiv). Dry benzene (2 mL) was added, and then evaporated under vacuum. This azeotropic drying procedure was repeated two additional times, and the resulting material was then dried under high

vacuum and backfilled with argon. *tert*-Dodecanethiol (54 μL, 0.23 mmol, 3.0 equiv) and azobisisobutyronitrile (19 mg, 0.12 mmol, 1.5 equiv) were added, and the resulting mixture was diluted with benzene (5 mL), then freeze-pump-thawed (3x) and backfilled with argon. The flask was sealed, and the contents were heated to 80 °C. After 48 hours, the reaction was cooled to 23 °C and concentrated in vacuo. The crude oil was purified by silica gel column chromatography (5.0% → 7.5% → 10.0% ethyl acetate in hexanes) to afford tricyclic diketone **109** as an amorphous solid (13 mg, 64% yield) that matched previously reported characterization data:[1] R_f = 0.40 (10% ethyl acetate in hexanes); ^{1}H NMR ($CDCl_3$, 500 MHz) δ 5.33 (ddq, *J* = 5.13, 5.13, 1.71 Hz, 1H), 2.65 (d, *J* = 14.5 Hz, 1H), 2.55–2.49 (m, 1H), 2.41–2.28 (m, 2H), 2.27–2.21 (m, 1H), 2.20–2.12 (m, 1H), 2.02 (d, *J* = 14.5 Hz, 1H), 2.01–1.93 (m, 2H), 1.89 (dd, *J* = 12.2, 1.2 Hz, 1H), 1.83–1.72 (m, 3H); 1.74 (s, 3H), 1.09 (s, 3H), 0.70 (s, 3H); ^{13}C NMR ($CDCl_3$, 126 MHz) δ 218.0, 212.8, 142.6, 121.0, 63.2, 52.6, 51.0, 47.8, 42.3, 40.1, 34.4, 32.4, 31.4, 25.4, 24.1, 21.7, 17.3; IR (Neat Film, NaCl) 2961, 2926, 2868, 1735, 1705, 1576, 1453, 1380, 1149 cm^{-1}; HRMS (ESI+) *m/z* calc'd for $C_{17}H_{24}O_2$ $[M]^+$: 260.1777, found 260.1776; $[\alpha]^{25}_D$ –158.6 (*c* 0.925, CH_2Cl_2).

2.5 NOTES AND REFERENCES

(1) (a) Enquist, J. A., Jr.; Stoltz, B. M. *Nature* **2008**, *453*, 1228–1231; (b) Enquist, J. A., Jr.; Virgil, S. C.; Stoltz, B. M. *Chem.–Eur. J.* **2011**, *17*, 9957–9969.

(2) (a) Green, D.; Goldberg, I.; Stein, Z.; Ilan, M.; Kashman, Y. *Nat. Prod. Lett.* **1992**, *1*, 193–199; (b) Peng, J.; Walsh, K.; Weedman, V.; Bergthold, J. D.; Lynch, J.; Lieu, K. L.; Braude, I. A.; Kelly, M.; Hamann, M. T. *Tetrahedron* **2002**, *58*, 7809–7819; (c) Enquist, J. A., Jr.; Stoltz, B. M. *Nat. Prod. Rep.* **2009**, *26*, 661–680.

(3) Pfeiffer, M. W. B.; Phillips, A. J. *J. Am. Chem. Soc.* **2005**, *127*, 5334–5335.

(4) Pfeiffer, M. W. B.; Phillips, A. J. *Tetrahedron Lett.* **2008**, *49*, 6860–6861.

(5) Reddy, T. J.; Bordeau, G.; Trimble, L. *Org. Lett.* **2006**, *8*, 5585–5588.

(6) (a) Behenna, D. C.; Stoltz, B. M. *J. Am. Chem. Soc.* **2004**, *126*, 15044–15045; (b) Behenna, D. C.; Mohr, J. T.; Sherden, N. H.; Marinescu, S. C.; Harned, A. M.; Tani, K.; Seto, M.; Ma, S.; Novák, Z.; Krout, M. R.; McFadden, R. M.; Roizen, J. L.; Enquist, J. A., Jr.; White, D. E.; Levine, S. R.; Petrova, K. V.; Iwashita, A.; Virgil, S. C.; Stoltz, B. M. *Chem.–Eur. J.* **2011**, *17*, 14199–14223; (c) Behenna, D. C.; Liu, Y.; Yurino, T.; Kim, J.; White, D. E.; Virgil, S. C.; Stoltz, B. M. *Nat.*

Chem. **2012**, *4*, 130–133; (d) Reeves, C. M.; Eidamshaus, C.; Kim, J.; Stoltz, B. M. *Angew*. *Chem., Int*. *Ed*. **2013**, *52*, 6718–6721; (e) Liu, Y.; Han, S.-J.; Liu, W.-B.; Stoltz, B. M. *Acc*. *Chem*. *Res*. **2015**, *48*, 740–751; (f) Craig, R. A., II; Loskot, S. A.; Mohr, J. T.; Behenna, D. C.; Harned, A. M.; Stoltz, B. M. *Org*. *Lett*. **2015**, *17*, 5160–5163.

(7) Diketone **111** is isolated as an inseparable mixture of *(R,R)* and meso stereoisomers, with a negligible amount of the *(S,S)* isomer observed. The diastereomers are separated later in the synthetic sequence upon the formation of tricycle **109**.

(8) The RCM and cross-metathesis reactions were carried out using a modified version of Grubbs–Hoveyda catalyst II (**121**, Scheme 2.4A). For details, see: Stewart, I. C.; Ung, T.; Pletnev, A. A.; Berlin, J. M.; Grubbs, R. H.; Schrodi, Y. *Org*. *Lett*. **2007**, *9*, 1589–1592.

(9) The double catalytic enantioselective allylic alkylation strategy was also applied by our group to the synthesis of the carbocyclic core of the gagunin natural product family. For details, see: Shibuya, G. M.; Enquist, J. A., Jr.; Stoltz, B. M. *Org*. *Lett*. **2013**, *15*, 3480–3483.

(10) McDougal, N. T.; Streuff, J.; Mukherjee, H.; Virgil, S. C.; Stoltz, B. M. *Tetrahedron Lett*. **2010**, *51*, 5550–5554.

(11) Marziale, A. N.; Duquette, D. C.; Craig, R. A., II; Kim, K. E.; Liniger, M.; Numajiri, Y.; Stoltz, B. M. *Adv. Synth. Catal.* **2015**, *357*, 2238–2245.

(12) (a) Wickens, Z. K.; Morandi, B.; Grubbs, R. H. *Angew. Chem., Int. Ed.* **2013**, *52*, 11257–11260; (b) Wickens, Z. K.; Skakuj, K.; Morandi, B.; Grubbs, R. H. *J. Am. Chem. Soc.* **2014**, *136*, 890–893.

(13) Yoshikai, K.; Hayama, T.; Nishimura, K.; Yamada, K.; Tomioka, K. *J. Org. Chem.* **2005**, *70*, 681–683.

(14) Kim, K. E.; Stoltz, B. M. *Org. Lett.* **2016**, *18*, 5720–5723.

(15) Pangborn, A. B.; Giardello, M. A.; Grubbs, R. H.; Rosen, R. K.; Timmers, F. J. *Organometallics* **1996**, *15*, 1518–1520.

(16) Krout, M. R.; Mohr, J. T.; Stoltz, B. M. *Org. Synth.* **2009**, *86*, 181–193.

(17) Helmboldt, H.; Köhler, D.; Hiersemann, M. *Org. Lett.* **2006**, *8*, 1573–1576.

(18) For development and synthetic application of the vinyl boronate cross-metathesis, see: (a) Morrill, C.; Funk, T. W.; Grubbs, R. H. *Tetrahedron Lett.* **2004**, *45*, 7733–7736; (b) Morrill, C.; Grubbs, R. H. *J. Org. Chem.* **2003**, *68*, 6031–6034;

(c) Njardarson, J. T.; Biswas, K.; Danishefsky, S. J. *Chem. Commun.* **2002**, 2759–2761.

(19) Fairlamb, I. J. S.; Kapdi, A. R.; Lee, A. F. *Org. Lett.* **2004**, *6*, 4435–4438.

(20) Substrate **112** is formed as a 1:1 mixture of the racemic and meso diastereomers, which are readily separable by silica gel column chromatography. The double catalytic enantioselective alkylation is effective on the diastereomeric mixture of **112**, but for ease of operation a single diastereomer was used for screening experiments.

APPENDIX 1

Synthetic Summary for the Cyanthiwigin Natural Product Core

*Scheme A1.1 Original synthesis of the cyanthiwigin core (**109**)*

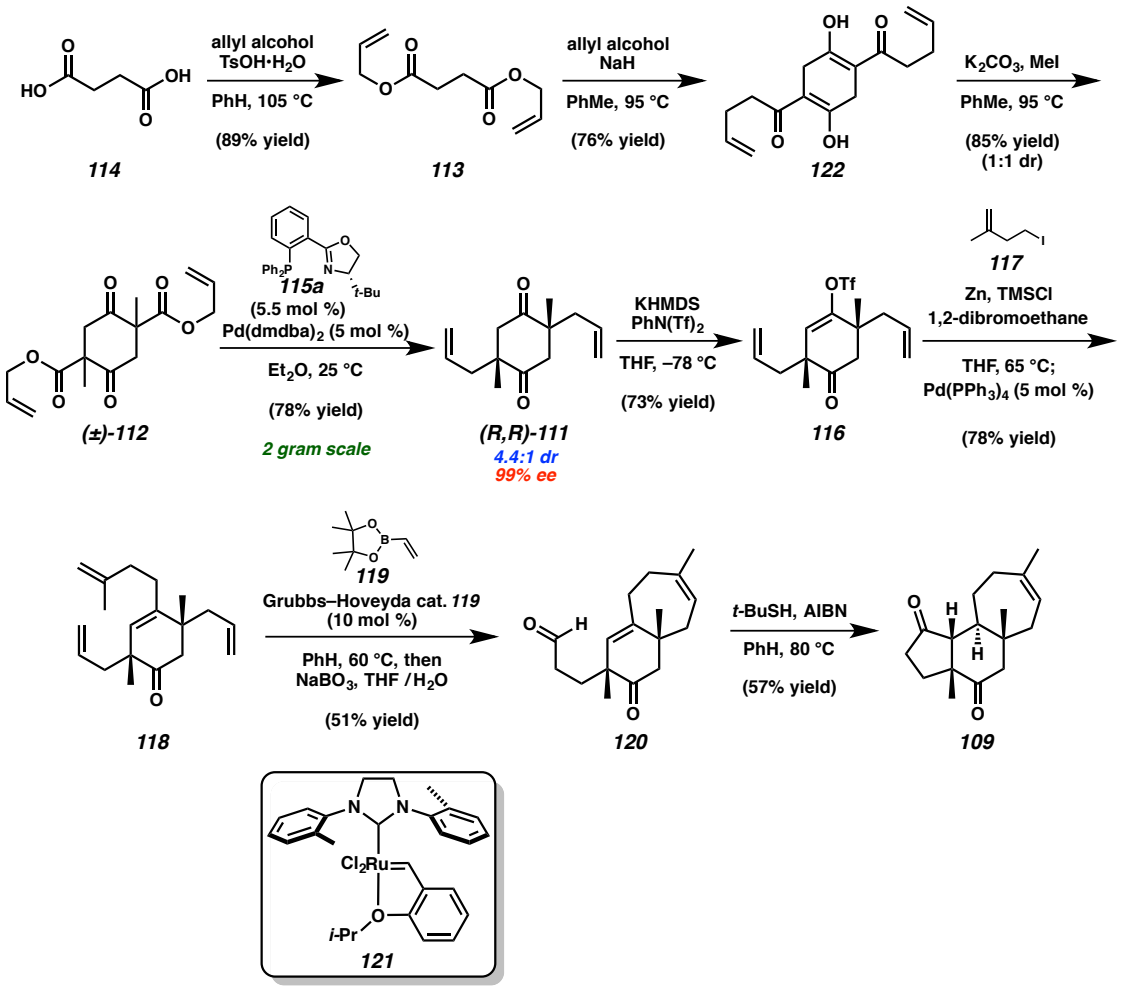

*Scheme A1.2 Modified synthesis of the cyanthiwigin core (**109**)*

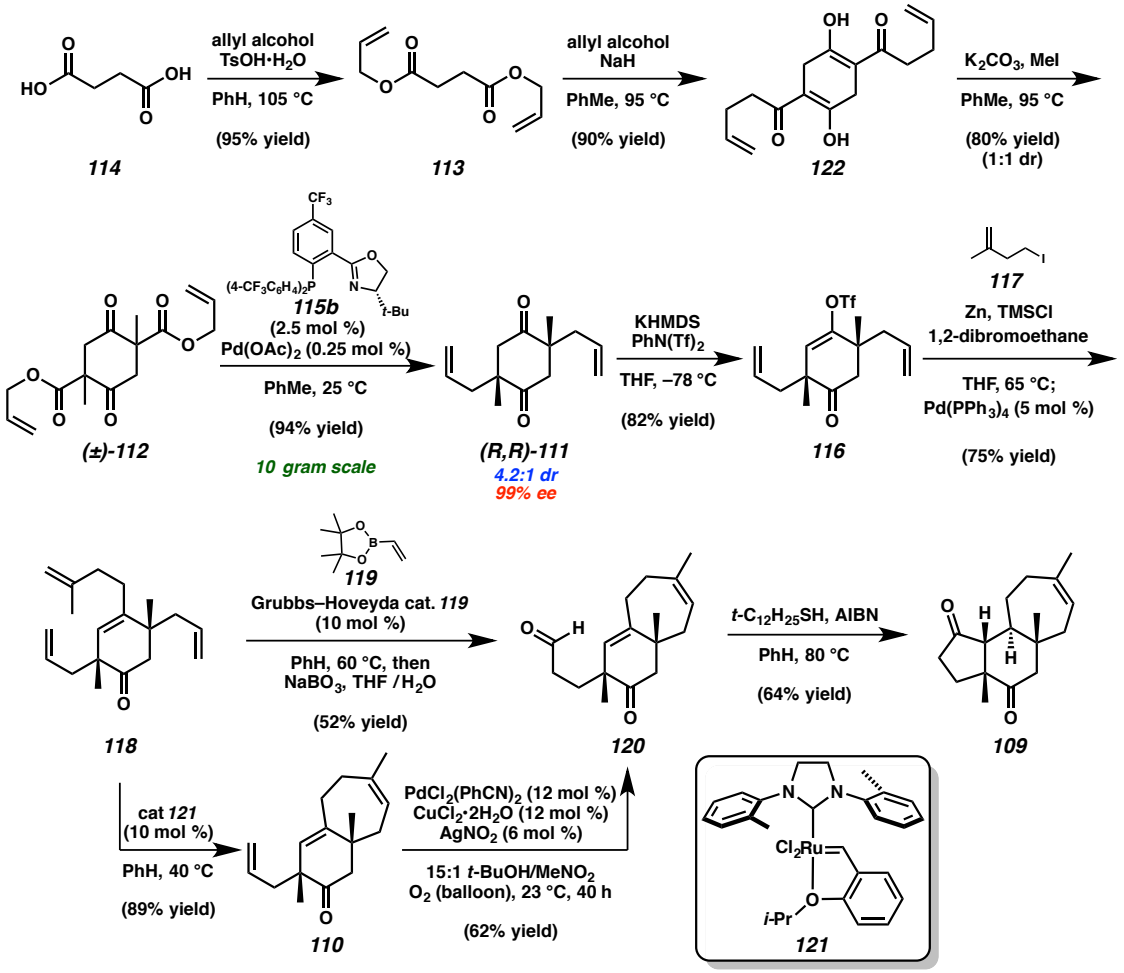

APPENDIX 2

Synthetic Efforts toward Cyanthiwigin F

A2.1 INTRODUCTION AND BACKGROUND

Through our group's synthetic route, cyanthiwigin F (**106**) is accessible from tricycle **109** in two steps.[1] Selective triflation of the A-ring ketone supplied vinyl triflate **123** (Scheme A2.1), which was subjected to cross-coupling conditions to afford the natural product. Unfortunately, the cross-coupling proved quite challenging and was generally plagued by low yields and side product formation. After extensive exploration of transition metal catalysts (e.g., Pd, Cu, Ni) and isopropyl coupling partners (e.g., *i*-PrZnI, *i*-PrMgCl, *i*-PrLi), the combination of [Pd(dppf)Cl_2], *i*-PrMgCl, and CuCN generated **106** as a 1.8:1 mixture (favoring the natural product) with the commonly observed reductive deoxygenation product **122** (Scheme A2.2). The two compounds were inseparable through silica gel column chromatography, with characterization-quality samples attainable only through reverse-phase HPLC.

*Scheme A2.1 Conversion of tricyclic diketone **109** to vinyl triflate **123***

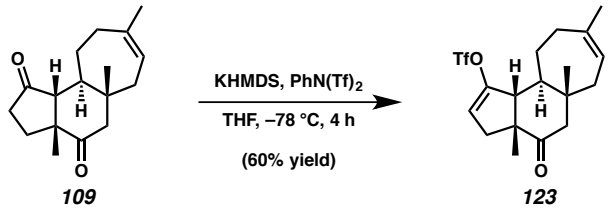

109 *123*

Scheme A2.2 Previously optimized conditions for the final cross-coupling to form cyanthiwigin F

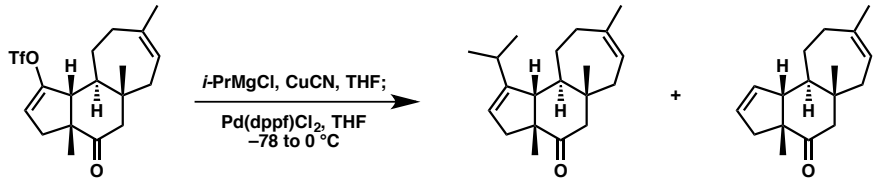

123 *cyanthiwigin F (106)* (41% yield) *124* (23% yield)

A2.2 EFFORTS TOWARD MODIFIED ISOPROPYL INSTALLATION

In light of these challenges, we sought to identify a superior alternative to the conditions described above. To this end, we pursued several strategies for the installation of the isopropyl unit.

A2.2.1 DIRECT INSTALLATION VIA CROSS-COUPLING

We began by investigating cross-coupling conditions for the direct installation of the isopropyl unit distinct from those previously examined by our group. Narasaka and co-workers documented an interesting strategy for this transformation (i.e., conversion of vinyl triflate to isopropyl) in their synthesis of sordarin (Scheme A2.3A).[2] Treatment of vinyl triflate **125** with *i*-PrMgCl and a higher-order thienyl-derived cuprate reagent in the presence of HMPA delivered the desired cross-coupling product (**126**) in good yield

along with only small amounts of the reduction side-product (**127**). Unfortunately, when these conditions were applied to triflate **123**, we observed formation of the desired natural product (**106**) contaminated with reduction product **124** as a 1.7:1 ratio favoring **106**. The yields of each product were nearly identical to those obtained from our group's previously optimized conditions (cf. Scheme A2.3B).

Scheme A2.3 Isopropyl installation using a higher-order cuprate reagent

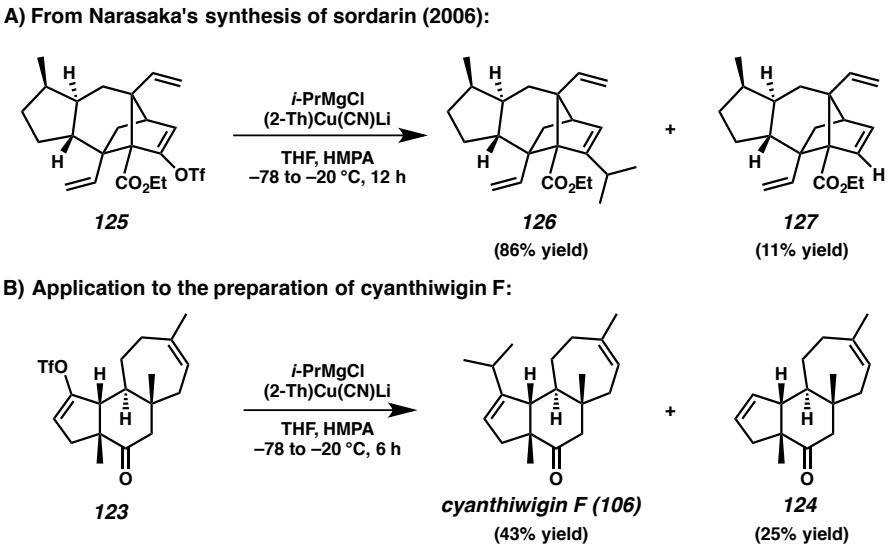

We next examined isopropyl installation using conditions developed by Biscoe and co-workers for Pd-catalyzed cross-coupling of secondary alkyl azastannatrane nucleophiles with aryl chlorides, bromides, iodides, and triflates.[3] Disappointingly, subjection of vinyl triflate **123** to these conditions using isopropyl-azastannatrane **128** resulted in predominantly the undesired reduction product (**124**) with only trace amounts of the natural product observed (Scheme A2.4).

*Scheme A2.4 Isopropyl installation using Biscoe's azastannatrane reagent (**128**)*

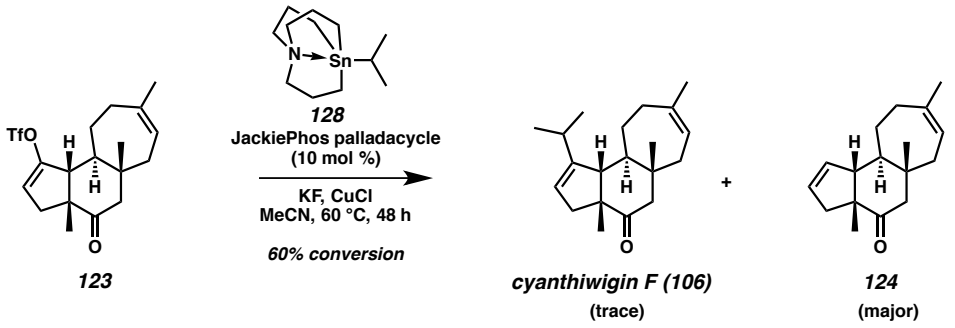

A2.2.2 TWO-STEP INSTALLATION VIA CROSS-COUPLING

Given the apparent difficulties in direct installation of the isopropyl unit, we turned our attention to two-step strategies. One such approach entailed cross-coupling vinyl triflate **123** with an isopropenyl fragment followed by selective hydrogenation to furnish the natural product. To this end, we examined various conditions for cross-coupling, beginning with Corey's Cu-assisted conditions.[4] Despite good conversion of **123**, the desired product (**129**) was contaminated with an unidentified by-product that was unfortunately inseparable from the desired compound likely arising from rearrangement of the isopropenyl fragment (Scheme A2.5A). Fortunately, application of traditional conditions for Stille coupling furnished **129**, albeit in modest yield. Subjection of this compound to superstoichiometric Lindlar's catalyst under hydrogen atmosphere enabled formation of trace amounts of the natural product (**106**).

Noting the challenges associated with cross-coupling using isopropenyl partners, we reasoned isopropyl installation might be accomplished using a different two-step approach: vinylation followed by hydromethylation using a procedure developed by the Baran group.[5] We were pleased to find that treatment of **123** with tributylvinylstannane

under Stille conditions afforded the desired vinylated compound **130** in good yield. Disappointingly, however, attempts to effect hydromethylation using the conditions reported by Baran and co-workers were ineffective (Scheme A2.6).

Scheme A2.5 Efforts toward isopropenylation followed by hydrogenation to form ***106***

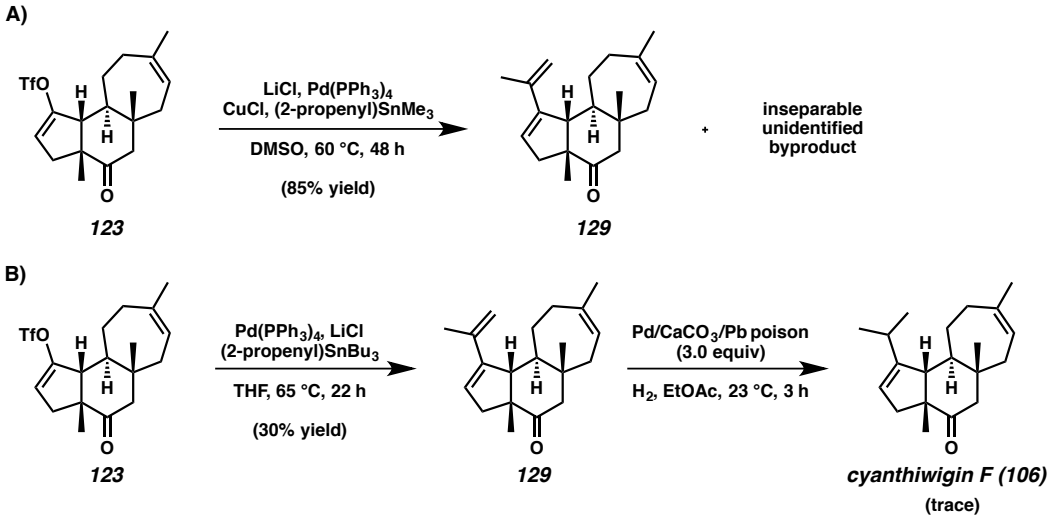

Scheme A2.6 Efforts toward vinylation followed by hydromethylation to form ***106***

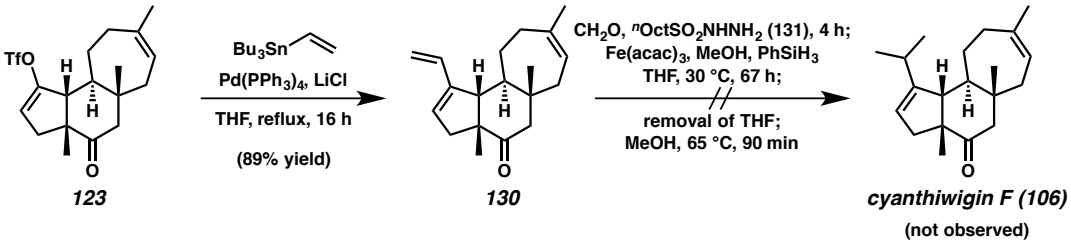

Our final approach toward completing the synthesis of cyanthiwigin F through a two-step sequence aimed to reverse the final cross-coupling partners by way of boronate ester **132** (Scheme A2.7A). Regrettably, this strategy remained unexplored due to the

overwhelming dominance of proto-detriflation in efforts to prepare **132** from **123** (Scheme A2.7B).

*Scheme A2.7 Efforts toward cross-coupling partner reversal via boronate ester **132***

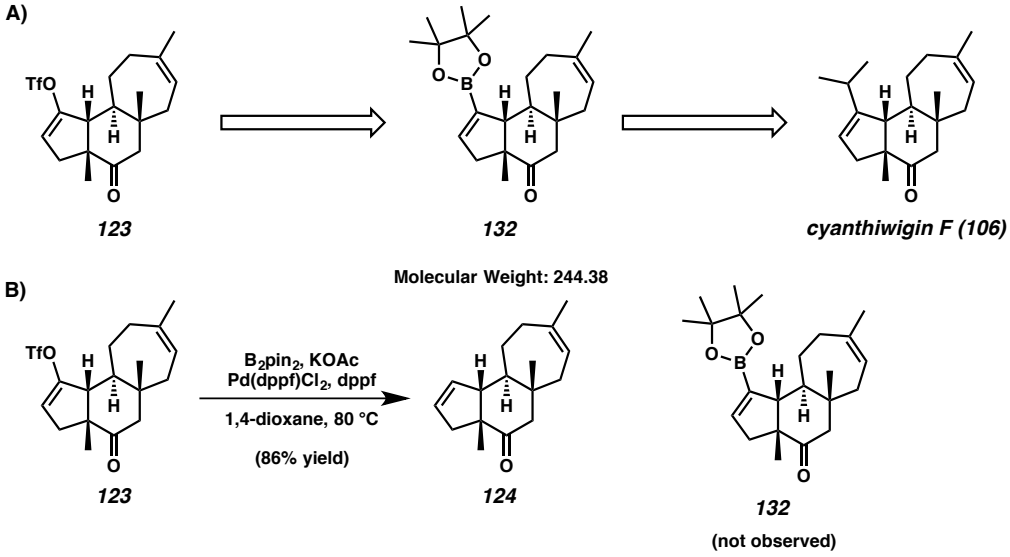

A2.2.3 ISOPROPYL GRIGNARD ADDITION

Finally, we directed our attention away from cross-coupling strategies and investigated a Grignard addition/dehydration approach. We envisioned that addition of an isopropyl Grignard reagent to the A-ring carbonyl and subsequent dehydration of the resulting alcohol (**133**) using Burgess reagent or Martin's sulfurane would generate the natural product (Scheme A2.8A). While treatment of diketone **109** with *i*-PrMgCl resulted in no reaction, product formation was observed using *i*-PrLi. Unfortunately, this compound did not appear to be the desired product (**133**) (Scheme A2.8B).

Scheme A2.8 Efforts toward Grignard addition followed by dehydration to form ***106***

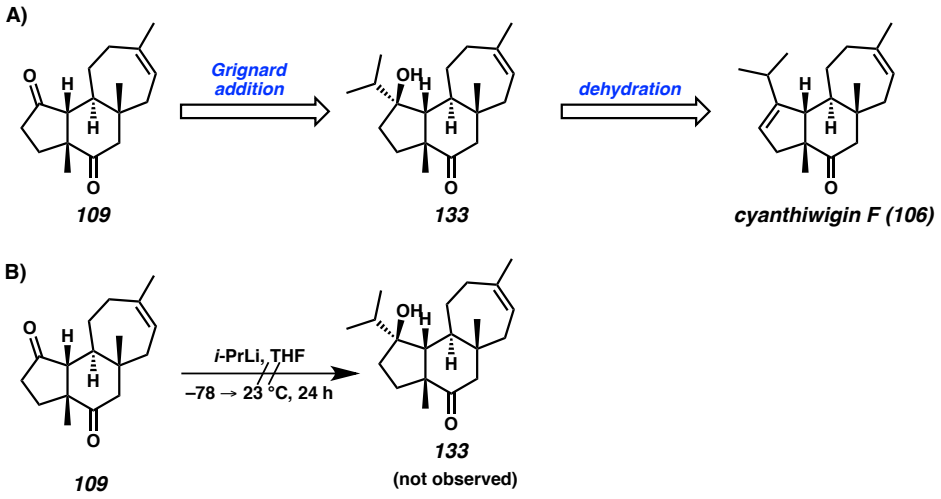

A2.3 FUTURE DIRECTIONS

As showcased in these investigations in addition to the original optimization studies, the installation of an isopropyl fragment at a sterically hindered site remains a major synthetic challenge. Indeed, a recent example of this issue was reported by Zhou and co-workers in their synthesis of hamigerin B,[6] further underscoring the need for new technologies to assist in the resolution of this difficult transformation. In contrast to the synthetic transformations amenable to modification that were described in the preceding chapter, it is clear through these studies that methodologies for isopropyl cross-couplings have remained underdeveloped over the past decade. As such, the development of new methodologies for this challenging reaction would contribute a great service to the synthetic community.

A2.4 EXPERIMENTAL SECTION

A2.4.1 MATERIALS AND METHODS

All reactions were performed at ambient temperature (23 °C) unless otherwise noted. Reactions requiring external heat were modulated to the specified temperatures indicated by using an IKAmag temperature controller. All reactions were performed in glassware flame-dried under vacuum and allowed to cool under nitrogen or argon. Solvents were dried by passage over a column of activated alumina with an overpressure of argon gas.[7] Tetrahydrofuran was distilled directly over benzophenone and sodium, or else was dried by passage over a column of activated alumina with an overpressure of argon gas. Anhydrous *tert*-butanol and nitromethane were purchased from Sigma Aldrich in sure-sealed bottles and used as received unless otherwise noted. Azastannatrane **128**[3] and octane-1-sulfonohydrazide were prepared according to known methods.[5] All other chemicals and reagents were used as received. Compounds purified by flash chromatography utilized ICN silica gel (particle size 0.032–0.063 mm) or SiliCycle® Silia*Flash*® P60 Academic Silica Gel (particle size 40–63 μm; pore diameter 60 Å). Thin-layer chromatography (TLC) was performed using E. Merck silica gel 60 F254 pre-coated plates (0.25 mm) and visualized by UV fluorescence quenching, *p*-anisaldehyde, or alkaline permanganate staining. NMR spectra were recorded on a Varian Mercury 300 spectrometer (at 300 MHz for ^{1}H NMR and 75 MHz for ^{13}C NMR), a Varian Inova 500 spectrometer (at 500 MHz for ^{1}H NMR and 126 MHz for ^{13}C NMR), or a Bruker AV III HD spectrometer equipped with a Prodigy liquid nitrogen temperature cryoprobe (at 400 MHz for ^{1}H NMR and 101 MHz for ^{13}C NMR), and are reported relative to residual $CHCl_3$ (δ 7.26 for ^{1}H NMR, δ 77.16 for ^{13}C NMR) or C_6H_6 (δ 7.16 for ^{1}H NMR, δ 128.06

for ^{13}C NMR). The following format is used for the reporting of ^{1}H NMR data: chemical shift (δ ppm), multiplicity, coupling constant (Hz), and integration. Data for ^{13}C NMR spectra are reported in terms of chemical shift. IR spectra were recorded on a Perkin Elmer Spectrum Paragon 1000 spectrometer, and data are reported in frequency of absorption (cm^{-1}). High-resolution mass spectra were obtained from the Caltech Mass Spectral Facility, or else were acquired using an Agilent 6200 Series TOF mass spectrometer with an Agilent G1978A Multimode source in ESI, APCI, or MM (ESI/APCI) ionization mode. Analytical chiral gas chromatography was performed with an Agilent 6850 GC using a G-TA (30 m x 0.25 mm) column (1.0 mL/min carrier gas flow). Analytical achiral gas chromatography was performed with an Agilent 6850 GC using a DB-WAX (30 x 0.25 mm) column (1.0 mL/min carrier gas flow). Preparatory reverse-phase HPLC was performed on a Waters HPLC with Waters Delta-Pak 2 x 100 mm, 15 μm column equipped with a guard, employing a flow rate of 1 mL/min and a variable gradient of acetonitrile and water as eluent. HPLC visualization was performed by collecting 1 mL fractions after initial injection and analyzing each fraction via TLC. Optical rotations were measured with a Jasco P-1010 polarimeter at 589 nm using a 100 mm path-length cell.

A2.4.2 PREPARATIVE PROCEDURES

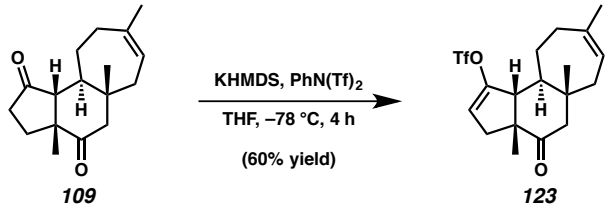

109 *123*

Tricyclic Triflate 123. To a flame-dried flask under argon was added tricyclic diketone **109** (250 mg, 0.960 mmol, 1.0 equiv). Dry PhH (5 mL) was added, then evaporated under vacuum. This azeotropic drying procedure was repeated two additional times, and the resulting material was then dried under high vacuum briefly, then dissolved in THF (10 mL). A separate flame dried flask under argon was charged with potassium bis(trimethylsilyl)amide (211 mg, 1.06 mmol, 1.1 equiv) and THF (10 mL). The flask containing diketone **109** was cooled to –78 °C, and the basic solution was cannula transferred into the cooled solution containing the substrate diketone via a positive pressure of argon. Deprotonation was allowed over 30 min. After this time had elapsed, a solution of *N*-phenyl bis(trifluoromethane)sulfonimide (395 mg, 1.10 mmol, 1.15 equiv) in THF (10 mL) was cannula transferred to the anionic solution under a positive pressure of argon. After 3 h, the reaction was quenched via addition of a solution of saturated $NaHCO_{3\,(aq)}$. The phases were separated, and the aqueous layer was extracted with Et_2O (3 x 30 mL). The combined organic layers were washed, sequentially, with 2 N $NaOH_{(aq)}$ (30 mL), 2 N $HCl_{(aq)}$ (30 mL), and brine (2 x 30 mL). The organic layers were then dried over $MgSO_4$, and the solvent was removed in vacuo after filtration. The crude material was purified over silica gel using 0.5% → 1.0% ethyl acetate in hexanes as eluent to afford triflate **123** as a white solid (226 mg, 60% yield)

that matched previously reported characterization data:[1] R_f = 0.45 (10% ethyl acetate in hexanes); ^{1}H NMR (500 MHz, C_6D_6) δ 5.16 (ddq, *J* = 5.1, 1.7, 1.7 Hz, 1H), 5.08 (dd, *J* = 3.0, 2.0 Hz, 1H), 2.07 (dd, *J* = 10.7, 2.2 Hz, 1H), 2.02 (br. t, *J* = 13.3 Hz, 1 H), 1.94–1.86 (m, 3H), 1.90 (s, 1H), 1.85 – 1.79 (m, 1H), 1.74 (app ddt, *J* = 14.8, 6.8, 1.5 Hz, 1H), 1.59 (s, 3H), 1.57 (d, *J* = 3.4 Hz, 1H), 1.54 (d, *J* = 3.4 Hz, 1H), 1.38–1.31 (m, 1H), 1.35 (dd, *J* = 14.4, 8.5 Hz, 1H), 1.23 (s, 3H), 0.44 (s, 3H); ^{13}C NMR (125 MHz, C_6D_6) δ 209.8, 153.2, 141.9, 121.4, 116.0, 57.6, 54.1, 54.0, 51.2, 41.6, 38.1, 36.5, 32.5, 26.2, 25.0, 23.6, 16.8; IR (Neat film, NaCl) 2932, 1709, 1656, 1423, 1382, 1245, 1211, 1141, 1097, 927 cm^{-1}; HRMS (EI) *m/z* calc'd for $C_{17}H_{23}F_3O_4S$ [M$^+$]: 392.1269, found 392.1273; $[\alpha]^{25}_D$ – 101.9 (*c* 0.63, CH_2Cl_2).

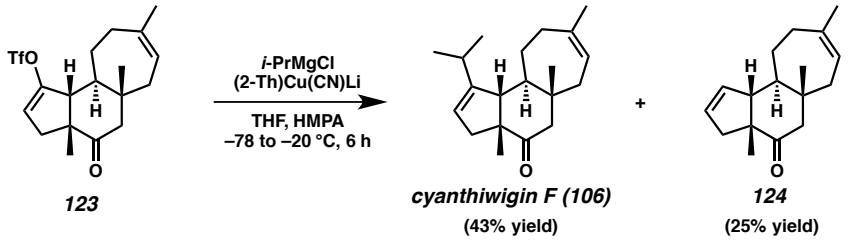

Cyanthiwigin F (106) and Reduction Product (124). A flame-dried flask under argon was charged with lithium 2-thienylcyanocuprate solution (0.25 M in THF, 0.31 mL, 0.0787 mmol, 3.09 equiv) and cooled to –78 °C. Isopropyl magnesium chloride solution (2.0 M in THF, 40 μL, 0.0765 mmol, 3.0 equiv) and HMPA (50 μL) were added, and the resulting mixture was warmed to 0 °C, generating a homogeneous mixture. The reaction was re-cooled to –78 °C, and a solution of tricyclic vinyl triflate **123** (10 mg, 0.0255 mmol, 1.0 equiv) in THF (1.3 mL) was added. The resultingmixture was warmed to –20 °C over 3 hours and then maintained at this temperature for an additional 3 hours.

After this time, the reaction was quenched via addition of a solution of saturated $NH_4Cl_{(aq)}$ and filtered over a pad of Celite. The filtrate was extracted with Et_2O (3 x 10 mL), and the combined organic layers were washed, sequentially, with water (20 mL) and brine (20 mL). The organic layers were then dried over $MgSO_4$, and the solvent was removed in vacuo after filtration. The crude material was purified over silica gel using 0.5% → 1.0% Et_2O in hexanes as eluent to afford a 1.7:1 mixture of **106** and **124** as a white solid (5.0 mg, 68% combined yield)

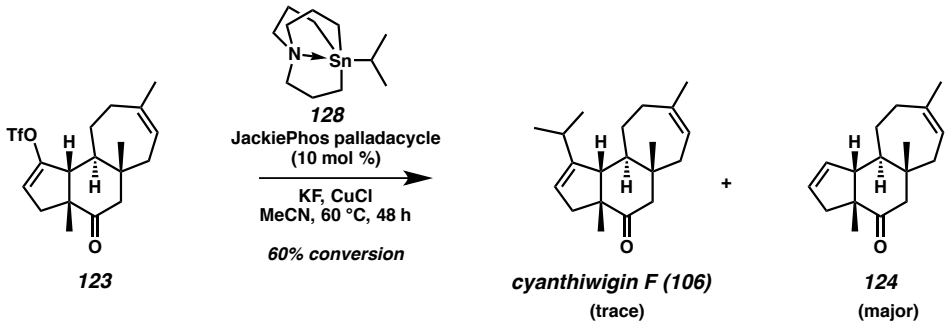

Cyanthiwigin F (106) and Reduction Product (124). A flame-dried Schlenk tube was charged with JackiePhos palladacycle (2.6 mg, 2.29 μmol, 0.10 equiv), potassium fluoride (2.7 mg, 0.0458 mmol, 2.0 equiv), and copper(I) chloride (4.5 mg, 0.0458 mmol, 2.0 equiv). To this mixture was added a solution of azastannatrane **128** (10.4 mg, 0.0344 mmol, 1.5 equiv) and tricyclic vinyl triflate **123** (9.0 mg, 0.0229 mmol, 1.0 equiv) in degassed MeCN (1.0 mL). The reaction vessel was sealed and heated to 60 °C. After 46 hours, heating was discontinued, and the reaction mixture was diluted with Et_2O (5 mL) and washed sequentially with saturated $KF_{(aq.)}$ (10 mL) and brine (10 mL). The organic layers were then dried over Na_2SO_4, and the solvent was removed in vacuo after

filtration. The crude material was purified over silica gel using 0.5% → 1.0% Et_2O in hexanes as eluent to afford a mixture of **106** and **124** (major).

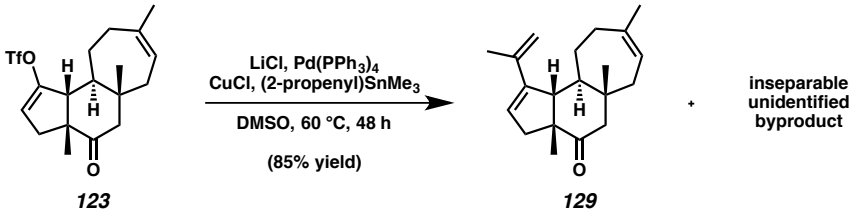

Modified Stille Coupling. In a nitrogen-filled glove box, a flame-dried vial was charged with $Pd(PPh_3)_4$ (2.6 mg, 2.29 μmol, 0.10 equiv), CuCl (11.3 mg, 0.115 mmol, 5.0 equiv), and DMSO (1.0 mL). The resulting mixture was stirred for 5 minutes before a solution of tricyclic vinyl triflate **123** (9.0 mg, 0.0229 mmol, 1.0 equiv) and trimethyl(2-propenyl)stannane (9.1 mg, 0.0275 mmol, 1.2 equiv) in DMSO was added. The vial was sealed with a Teflon-lined cap and electrical tape, and its contents were stirred at 25 °C (ambient temperature in the glove box) for 1 hour, then heated to 60 °C. After 70 hours, heating was discontinued, and the reaction vial was removed from the glove box. The reaction mixture was diluted with Et_2O (5 mL) and washed with a mixture of 5:1 brine/NH_4OH (5% aq.) (10 mL total volume). The phases were separated, and the aqueous layer was extracted with Et_2O (2 x 20 mL). The combined organic layers were washed, sequentially, with water (2 x 20 mL) and brine (2 x 20 mL). The organic layers were then dried over Na_2SO_4, and the solvent was removed in vacuo after filtration. The crude material was purified over silica gel using 2.0% ethyl acetate in hexanes as eluent to afford tricycle **129** along with an unidentified by-product as a colorless oil (5.5 mg, 85% yield).

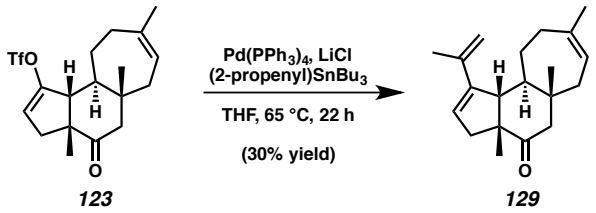

123 ***129***

Dehydrocyanthiwigin F (129). In a nitrogen-filled glove box, a flame-dried vial was charged with $Pd(PPh_3)_4$ (2.6 mg, 1.96 μmol, 0.10 equiv), LiCl (2.6 mg, 0.0608 mmol, 3.1 equiv), and THF (0.5 mL). To the resulting slurry was added a solution of tricyclic vinyl triflate **123** (7.7 mg, 0.0196 mmol, 1.0 equiv) and tributyl(2-propenyl)stannane (4.0 mg, 0.0196 mmol, 1.0 equiv) in THF (1.0 mL). The vial was sealed with a Teflon-lined cap and electrical tape and heated to 70 °C. After 22 hours, during which time the bright yellow solution became colorless, heating was discontinued, and the reaction vial was removed from the glove box. The reaction mixture was diluted with pentane (4 mL) and washed sequentially with water (10 mL), 10% aq. NH_4OH (10 mL), water (10 mL), and brine (10 mL). The organic layers were then dried over $MgSO_4$, and the solvent was removed in vacuo after filtration. The crude material was purified over silica gel using 1.0% Et_2O in hexanes as eluent to afford dehydrocyanthiwigin F (**129**) as a white amorphous solid (1.7 mg, 30% yield): R_f = 0.59 (20% ethyl acetate in hexanes); ^{1}H NMR (500 MHz, $CDCl_3$) δ 5.74 (dd, *J* = 3.5, 2.0 Hz, 1H), 5.33 (m, 1H), 4.90 (s, 2H), 2.77 (d, *J* = 16.9 Hz, 1H), 2.50 (d, *J* = 14.7 Hz, 1H), 2.48 (d, *J* = 10.8 Hz, 1H), 2.21–2.15 (m, 2H), 2.04 (d, *J* = 14.7 Hz, 1H), 2.03 (dd, *J* = 3.6, 17.0 Hz, 1H), 1.95–1.90 (m, 1H), 1.92 (s, 3H), 1.87–1.78 (m, 1H), 1.74–1.69 (m, 1H), 1.72 (s, 3H), 1.58 (m, 1H), 1.10 (s, 3H), 1.07–1.02 (m, 1H), 0.73 (s, 3H); ^{13}C NMR (101 MHz, $CDCl_3$) δ 215.6, 151.1, 142.4, 142.0, 124.9, 121.3, 113.0, 57.7, 55.3, 55.0, 54.5, 42.9, 42.2, 37.9, 33.2, 27.0, 25.0, 22.3, 21.5, 17.5; IR (Neat film, NaCl) 2922, 2851, 1703, 1456, 1384, 1292, 1074, 886, 814

cm^{-1}; HRMS (FAB+) *m/z* calc'd for $C_{20}H_{29}O$ $[M+H]^+$: 285.2218, found 285.2246; $[\alpha]^{25}_D$ –48.9 (*c* 0.17, $CHCl_3$).

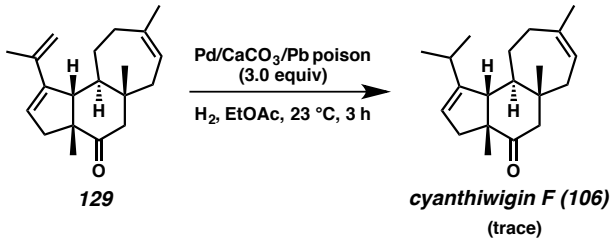

Hydrogenation Procedure. To a flame-dried flask was added a solution of tricycle **129** (1.7 mg, 5.98 μmol, 1.0 equiv) in ethyl acetate (1.0 mL) and Lindlar's catalyst (2.0 mg, 0.0188 mmol, 3.0 equiv). The reaction vessel was evacuated under reduced pressure (~400 Torr) and backfilled with hydrogen gas (3x). After stirring for 4 hours at 23 °C under hydrogen atmosphere, the reaction mixture was filtered over a pad of silica gel, eluting with 20% ethyl acetate in hexanes, and the filtrate was concentrated in vacuo, affording an inseparable mixture of **106** and **129**.

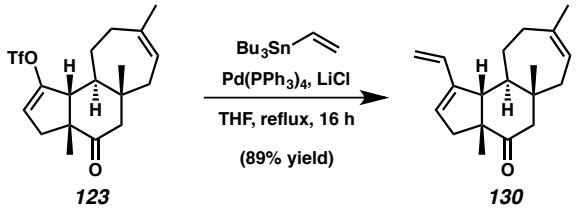

Tricyclic tris-olefin 130. In a nitrogen-filled glove box, a flame-dried vial was charged with $Pd(PPh_3)_4$ (0.3 mg, 0.29 μmol, 0.02 equiv), LiCl (1.9 mg, 0.045 mmol, 3.1 equiv), and THF (0.5 mL). To the resulting slurry was added a solution of tricyclic vinyl triflate **123** (5.7 mg, 0.0145 mmol, 1.0 equiv) and tributyl(vinyl)stannane (4.6 mg, 0.0145 mmol, 1.0 equiv) in THF (1.0 mL). The vial was sealed with a Teflon-lined cap and

electrical tape and heated to 70 °C. After 18 hours, during which time the bright yellow solution became colorless, heating was discontinued, and the reaction vial was removed from the glove box. The reaction mixture was diluted with pentane (4 mL) and washed sequentially with water (10 mL), 10% aq. NH_4OH (10 mL), water (10 mL), and brine (10 mL). The organic layers were then dried over $MgSO_4$, and the solvent was removed in vacuo after filtration. The crude material was purified over silica gel using 1.0% Et_2O in hexanes as eluent to afford tricyclic tris-olefin **130** as a white amorphous solid (3.5 mg, 89% yield): R_f = 0.32 (10% Et_2O in hexanes); ^{1}H NMR (400 MHz, $CDCl_3$) δ 6.53 (dd, *J* = 17.6, 10.9 Hz, 1H), 5.76 (m, 1H), 5.33 (m, 1H), 5.16–5.03 (m, 2H), 2.75 (d, *J* = 17.2 Hz, 1H), 2.50 (d, *J* = 14.8 Hz, 1H), 2.41 (d, *J* = 11.1 Hz, 1H), 2.18 (m, 2H), 2.07–2.03 (m, 1H), 2.04–1.99 (m, 1H), 1.97–1.89 (m, 2H), 1.74–1.68 (m, 1H), 1.73 (s, 3H), 1.62–1.57 (m, 1H), 1.09 (s, 3H), 1.07 (m, 1H), 0.74 (s, 3H); ^{13}C NMR (101 MHz, $CDCl_3$) δ 215.4, 149.1, 142.4, 135.4, 128.3, 121.3, 114.4, 57.2, 55.4, 54.9, 54.5, 42.6, 42.1, 37.8, 33.0, 27.1, 25.0, 22.4, 17.4.

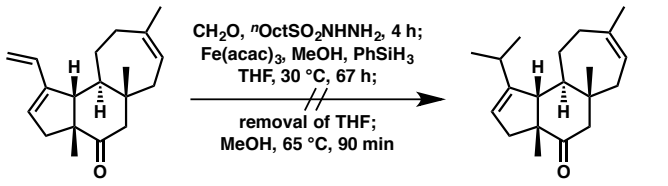

130 ***cyanthiwigin F (106)*** **(not observed)**

Hydromethylation Procedure. To a solution of formaldehyde (8.0 μL, 0.0777 mmol, 6.0 equiv) in THF (2 mL) under argon was added octane-1-sulfonohydrazide (13.5 mg, 0.0647 mmol, 5.0 equiv) at 23 °C. The resulting solution was stirred for 4 hours, after which time it was added to a solution of tricycle **130** (3.5 mg, 0.0129 mmol, 1.0

equiv) and $Fe(acac)_3$ (9.1 mg, 0.0258 mmol, 2.0 equiv) in THF (0.6 mL) and MeOH (1.0 μL, 0.0258 mmol, 2.0 equiv). The resulting mixture was degassed by freeze-pump-thaw (2x) before the addition of phenylsilane (6.4 μL, 0.0516 mmol, 4.0 equiv). After two more iterations of the freeze-pump-thaw procedure, the reaction was heated to 30 °C and stirred under argon atmosphere for 36 hours. After this time, the volatiles were removed in vacuo, and the reaction vessel was purged with argon before addition of degassed methanol (1.5 mL). The resulting solution was heated to 62 °C. After 90 minutes, the reaction mixture was concentrated in vacuo, and the residue was diluted with ethyl acetate (5 mL) and washed with brine (5 mL). The organic layer was separated, dried over $MgSO_4$, filtered, and concentrated to a crude residue. Signals characteristic of the desired product (**106**) were not visible in the crude material by ^1H NMR or TLC analysis.

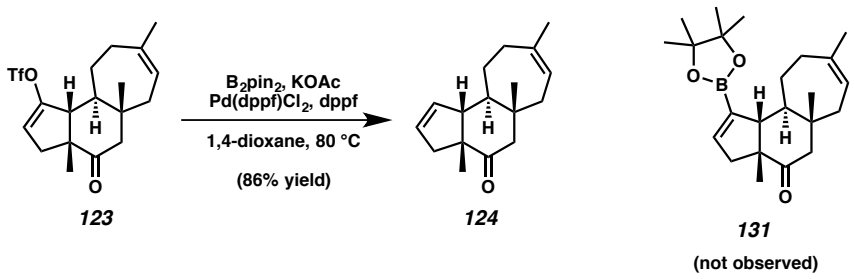

Unsuccessful Effort to form Boronate Ester 131. In a nitrogen-filled glove box, a flame-dried 1-dram vial was charged with bis(pinacolato)diboron (7.3 mg, 0.0286 mmol, 1.1 equiv), $Pd(dppf)Cl_2$ (1.6 mg, 0.772 μmol, 0.08 equiv), potassium acetate (7.6 mg, 0.0777 mmol, 3.0 equiv), and dppf (1.2 mg, 0.772 μmol, 0.09 equiv). To this mixture was added a solution of vinyl triflate **123** (10.1 mg, 0.0257 mmol, 1.0 equiv) in 1,4-dioxane (1.0 mL). The vial was sealed with a Teflon-lined cap and electrical tape, and then heated to 80 °C. After 75 hours, heating was discontinued, and the reaction vessel

was removed from the glove box. The reaction mixture was diluted with hexanes and filtered over a pad of silica gel, eluting with dichloromethane. The filtrate was concentrated and purified over silica gel column chromatography (1% Et_2O in hexanes) to afford reduction product **124** (4.9 mg, 86% yield), which matched previously reported characterization data.

A2.5 NOTES AND REFERENCES

(1) (a) Enquist, J. A., Jr.; Stoltz, B. M. *Nature* **2008**, *453*, 1228–1231; (b) Enquist, J. A., Jr.; Virgil, S. C.; Stoltz, B. M. *Chem.–Eur. J.* **2011**, *17*, 9957–9969.

(2) Chiba, S.; Kitamura, M.; Narasaka, K. *J. Am. Chem. Soc.* **2006**, *128*, 6931–6937.

(3) Li, L.; Wang, C.-Y.; Huang, R.; Biscoe, M. R. *Nat. Chem.* **2013**, *5*, 607–612.

(4) Han, X.; Stoltz, B. M.; Corey, E. J. *J. Am. Chem. Soc.* **1999**, *121*, 7600–7605.

(5) Dao, H. T.; Li, C.; Michaudel, Q.; Maxwell, B. D.; Baran, P. S. *J. Am. Chem. Soc.* **2015**, *137*, 8046–8049.

(6) Lin, H.; Xiao, L.-J.; Zhou, M.-J.; Yu, H.-M.; Xie, J.-H.; Zhou, Q.-L. *Org. Lett.* **2016**, *18*, 1434–1437.

(7) Pangborn, A. B.; Giardello, M. A.; Grubbs, R. H.; Rosen, R. K.; Timmers, F. J. *Organometallics* **1996**, *15*, 1518–1520.

APPENDIX 3

Spectra Relevant to Appendix 2:

Synthetic Efforts toward Cyanthiwigin F

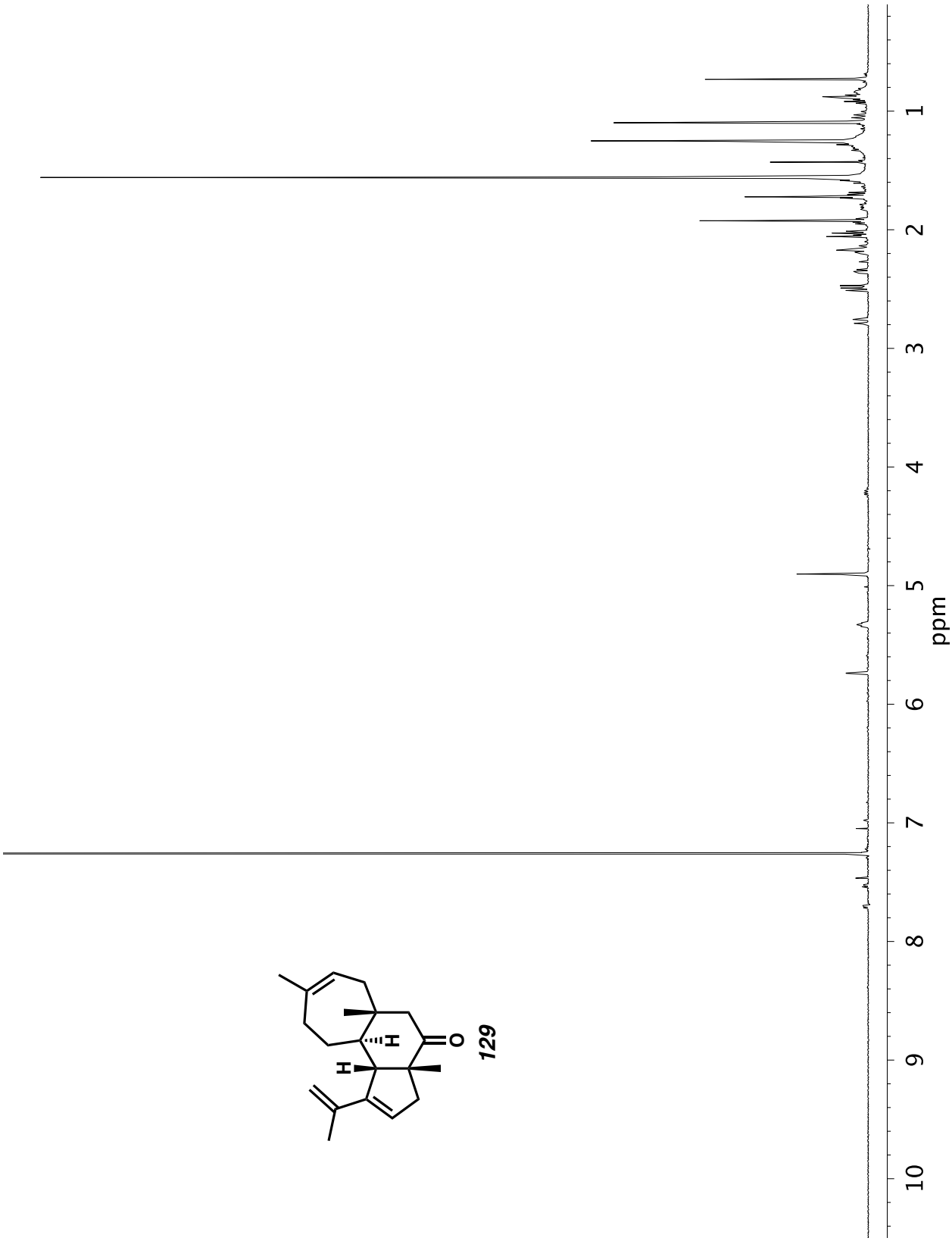

Figure A3.1. ^{1}H NMR (500 MHz, $CDCl_3$) of compound **129**.

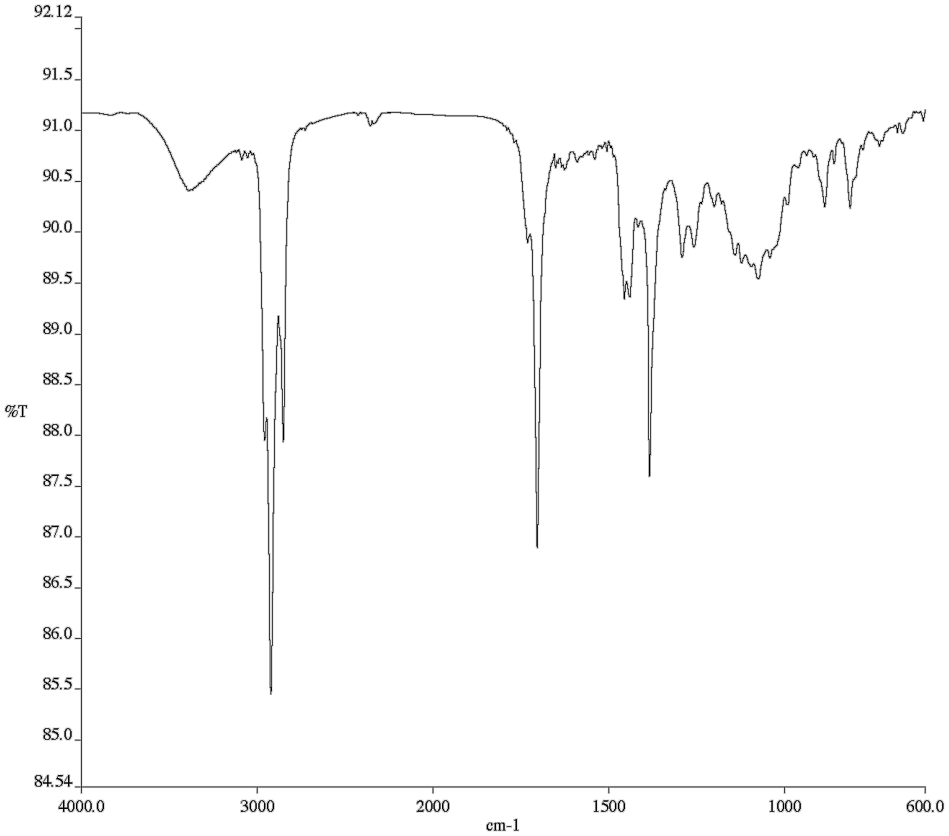

Figure A3.2. Infrared spectrum (Thin Film, NaCl) of compound **129**.

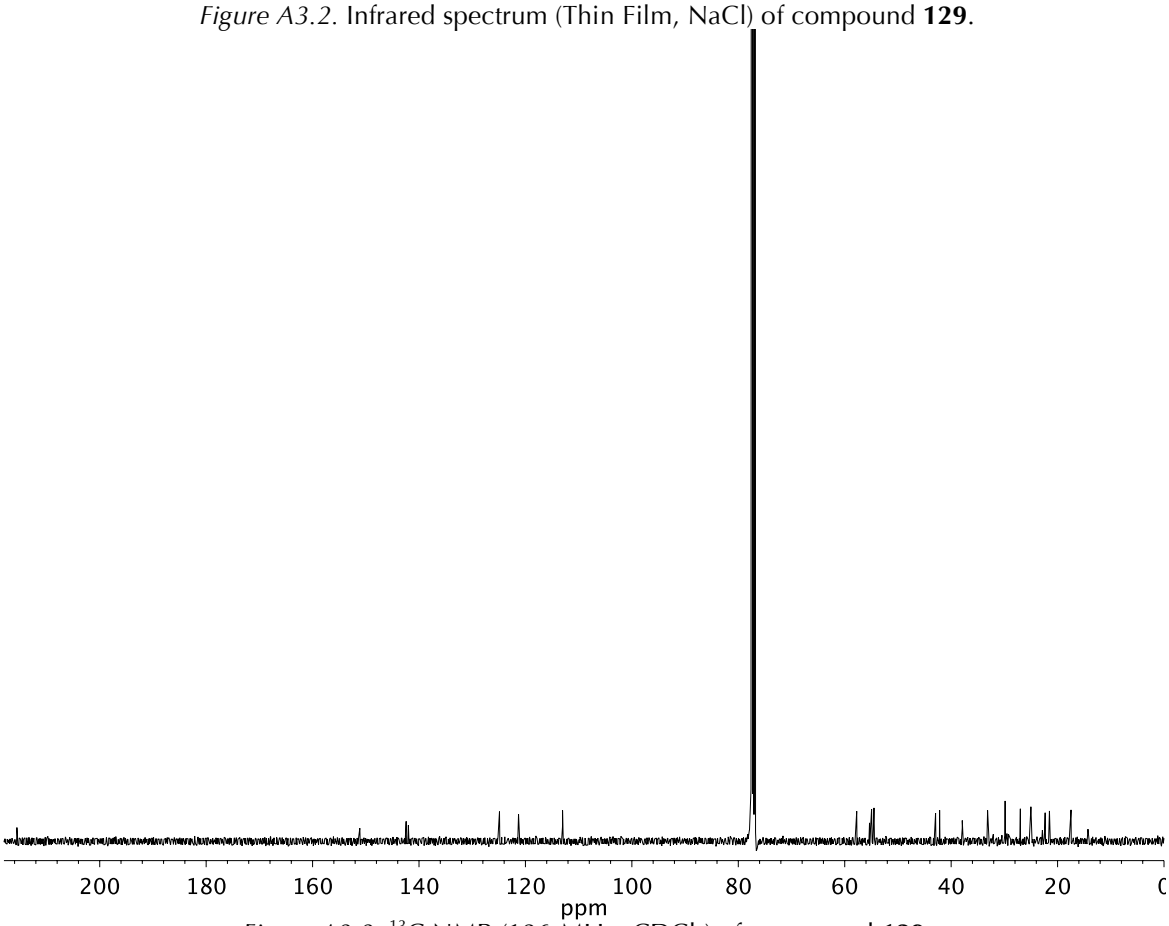

Figure A3.3. ^{13}C NMR (126 MHz, $CDCl_3$) of compound **129**.

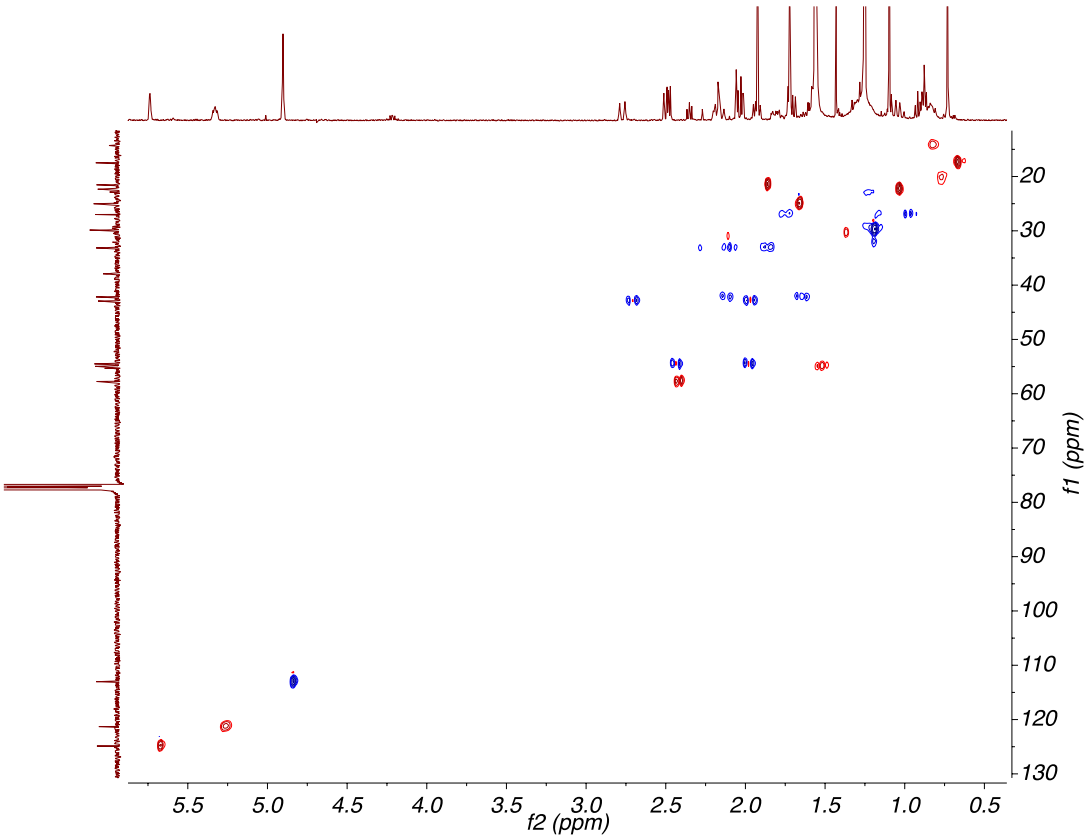

Figure A3.4. HSQC (500, 101 MHz, $CDCl_3$) of compound **129**.

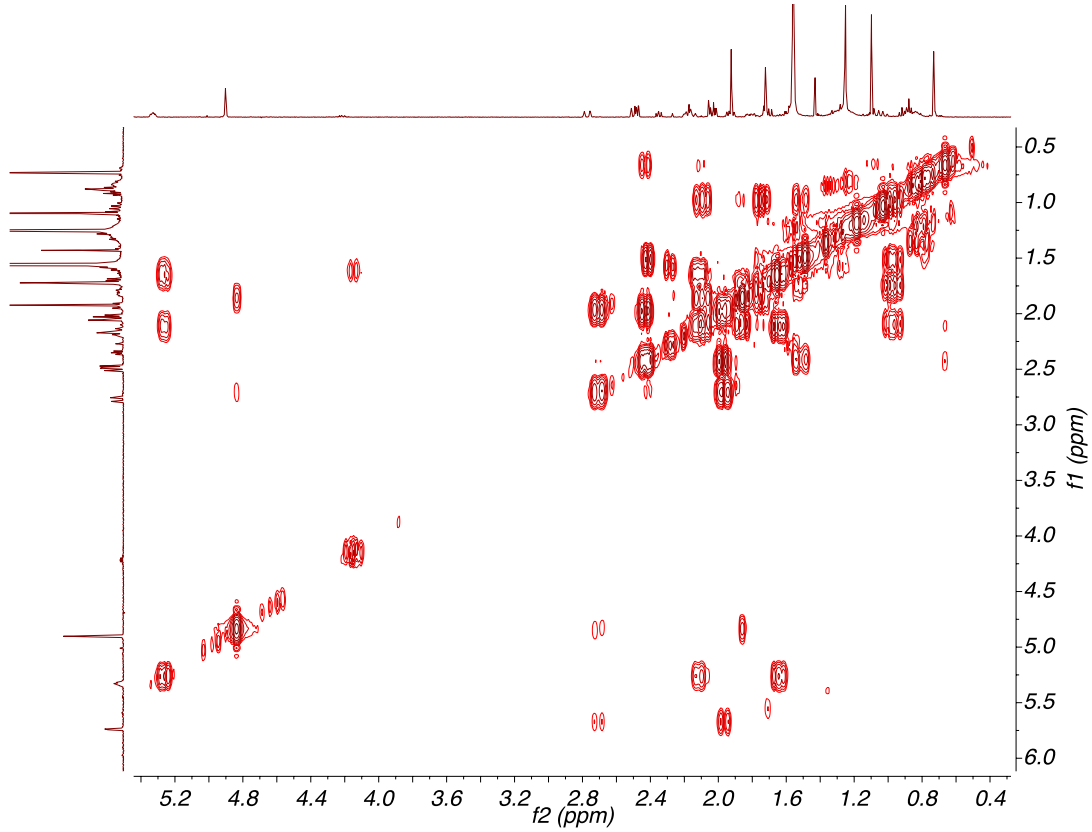

Figure A3.5. COSY (500 MHz, $CDCl_3$) of compound **129**.

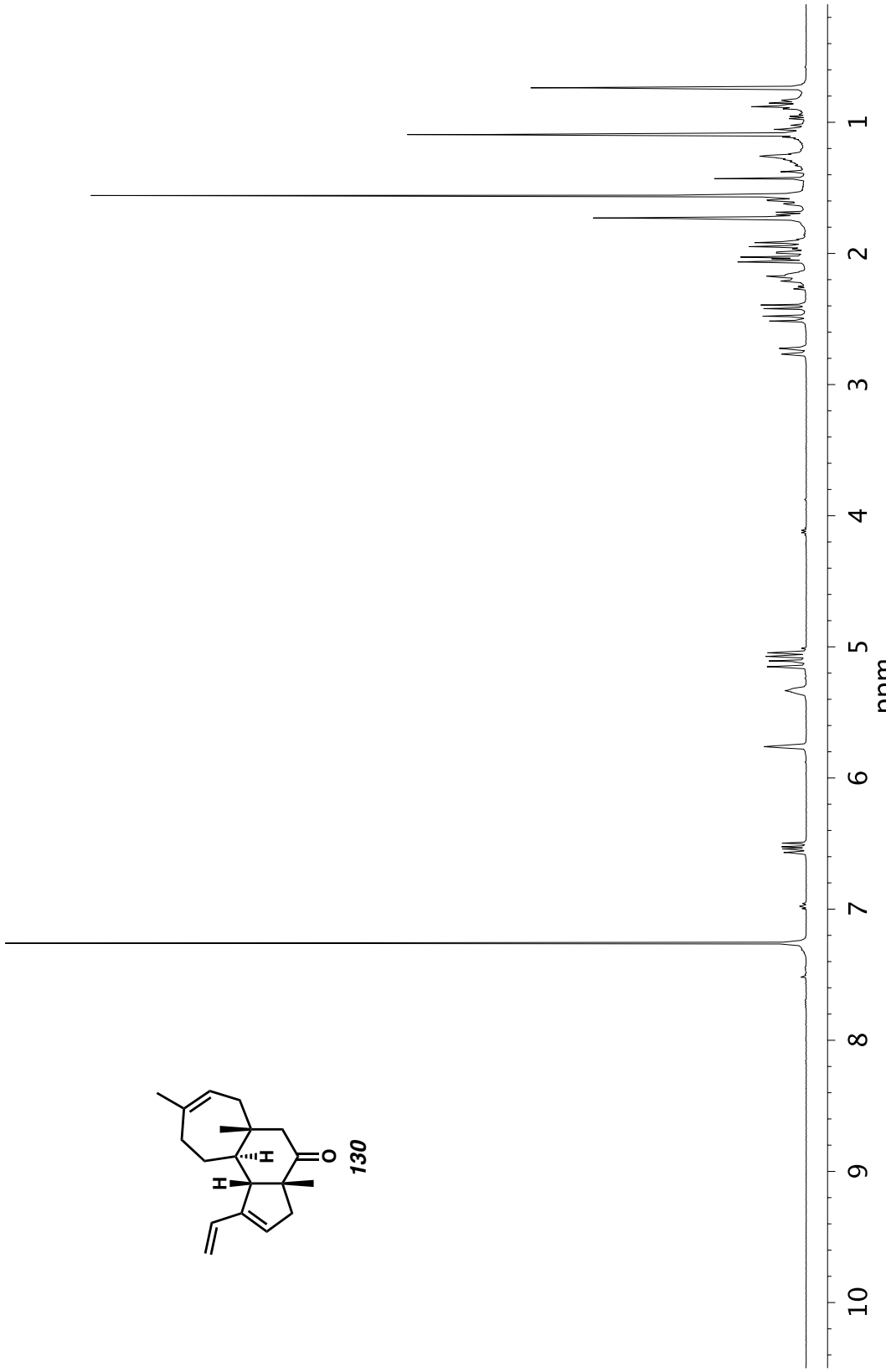

Figure A3.6. ^{1}H NMR (400 MHz, $CDCl_3$) of compound **130**.

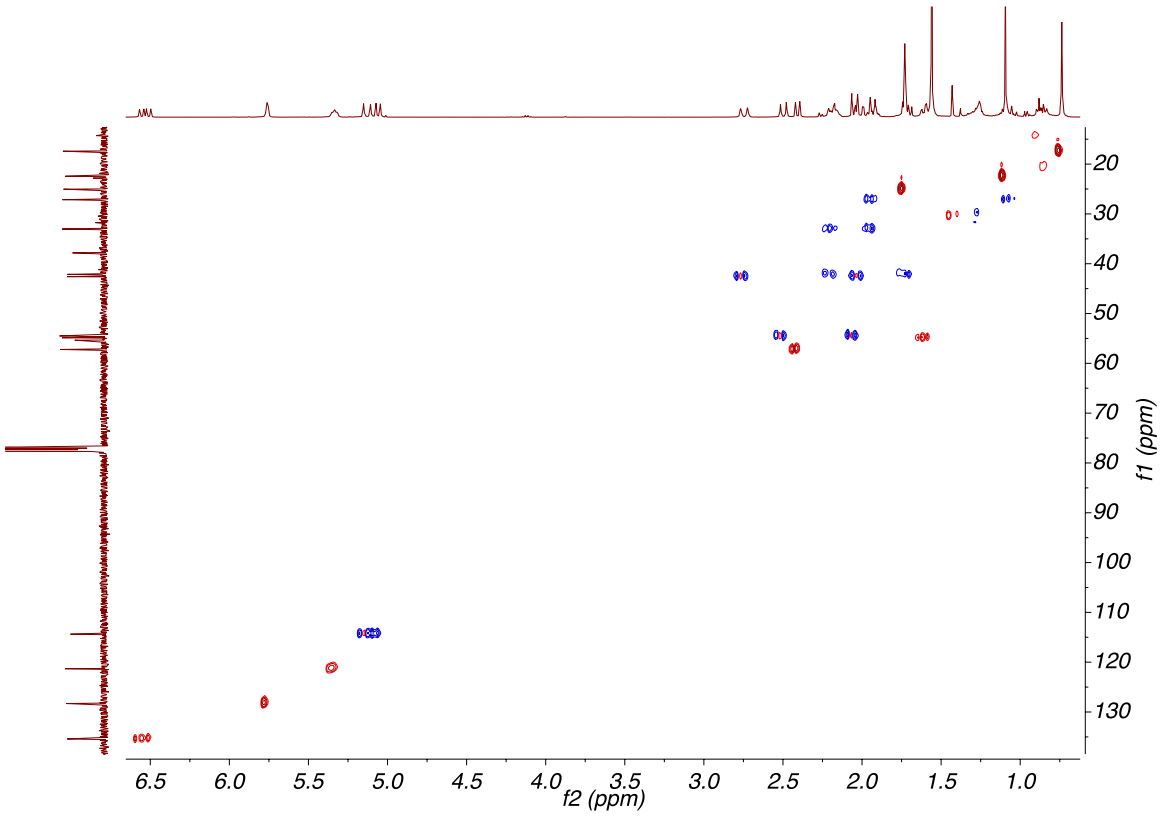

Figure A3.7. HSQC (400, 101 MHz, $CDCl_3$) of compound **130**.

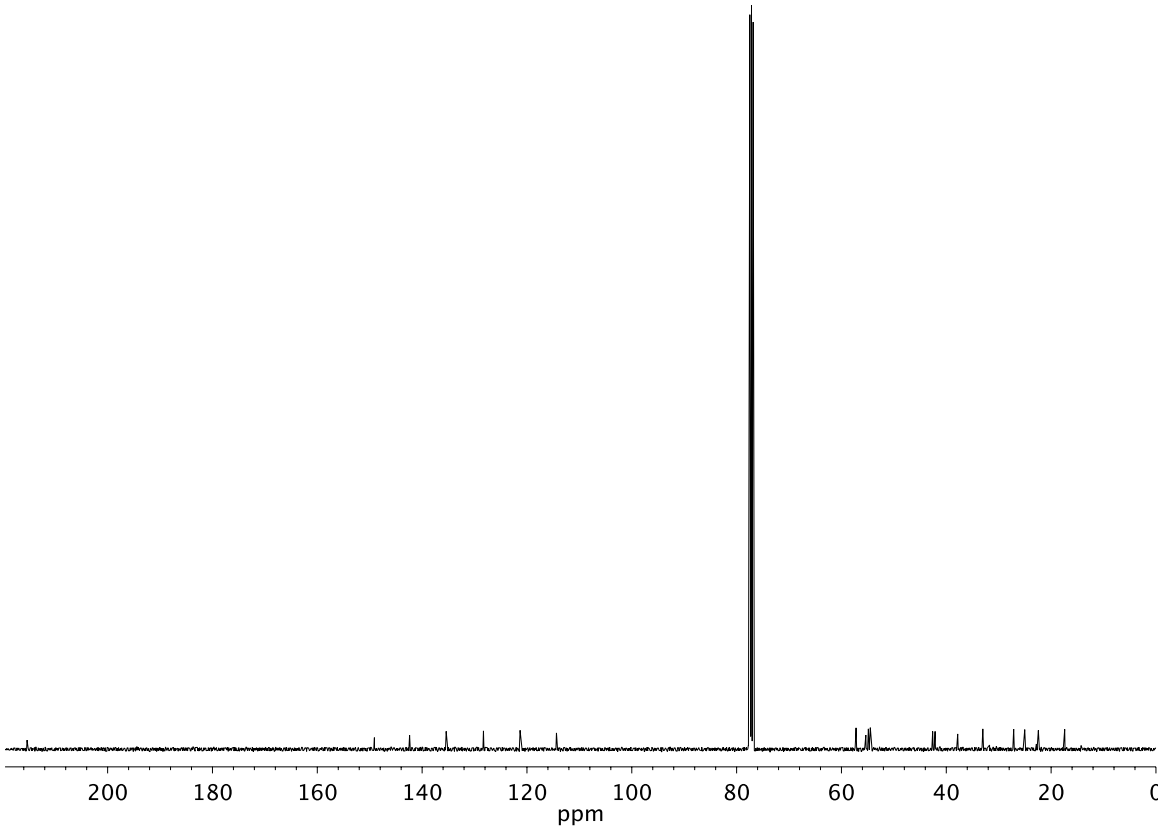

Figure A3.8. ^{13}C NMR (101 MHz, $CDCl_3$) of compound **130**.

CHAPTER 3[†]

The Aldehyde-Selective Tsuji–Wacker Oxidation:

A Tool for Facile Catalytic Transformations of Hindered Terminal Olefins

3.1 INTRODUCTION

Inspired by the success of the aldehyde-selective Tsuji–Wacker oxidation in our second-generation synthesis of the cyanthiwigin natural product core, we decided to explore the utility of this remarkable transformation in the oxidation of various sterically hindered substrates and to probe the broader applicability of the reaction in chemical synthesis. The results of these investigations are described herein.

3.1.1 BACKGROUND

The use of transition metal catalysts in the preparation of organic compounds has enabled previously unattainable transformations, streamlining otherwise cumbersome synthetic sequences. Although most early applications of transition metal catalysis did

[†] Portions of this chapter have been reproduced with permission from *J. Am. Chem. Soc.* **2016**, *138*, 13179–13182 and the supporting information found therein. © 2016 American Chemical Society.

not involve Pd,[1] the discovery of the Wacker process in 1956 stimulated interest in the use of Pd catalysts in synthesis.[2,3] Since then, Pd has emerged as one of the leading transition metals in the catalysis of organic transformations.[4] The popularity of Pd-catalyzed processes is largely due to the wide breadth of organic substrates capable of coordination to Pd, which allows for the promotion of many different types of transformations. Furthermore, Pd-catalyzed reactions often occur with high stereospecificity since they rarely proceed through radical-based pathways.[1]

While Pd catalysis has enhanced many areas of organic synthesis, the selective oxidation of olefins represents an exceptionally important accomplishment due to the ubiquity of alkenes in organic building blocks and their versatility as functional handles. Among the various methods of functionalizing olefins, the Wacker process has proven especially useful for industrial production of acetaldehyde from ethylene and is formally one of the oldest known methods for C–H oxidation. The application of this robust transformation to a broader range of substrates, known as the Tsuji–Wacker reaction, has facilitated the conversion of terminal olefins to methyl ketones with such high regioselectivity that terminal olefins may often be viewed as masked methyl ketones.[5]

The synthetic utility of the Tsuji–Wacker oxidation stems from its efficiency and broad functional group compatibility, and modifications to the original conditions have further expanded its applications.[6,7,8] While traditional Tsuji–Wacker conditions exhibit Markovnikov regioselectivity, forming mainly methyl ketone products (**135**) with only trace amounts of aldehyde (**136**) (Scheme 3.1A), a notable modification reported by the Grubbs group reverses this trend, enabling selective formation of aldehydes as the major products instead (Scheme 3.1B).[9] Early investigations into aldehyde-selective Tsuji–

Wacker processes required biased alkene substrates,[5,10] but Grubbs and co-workers found that use of $AgNO_2$ as a co-catalyst with $PdCl_2(PhCN)_2$ and $CuCl_2 \bullet 2H_2O$ in 15:1 *t*-BuOH/$MeNO_2$ enabled conversion of unbiased terminal alkenes to aldehydes in high yields and selectivities.[11] They further illustrated the catalyst-controlled nature of their system by accomplishing oxidation with high aldehyde selectivity on substrates bearing Lewis-basic directing groups that influence regioselectivity under traditional Tsuji–Wacker conditions.[12]

Scheme 3.1 A) Traditional Tsuji–Wacker selectivity. B) Aldehyde-selective Tsuji–Wacker oxidation

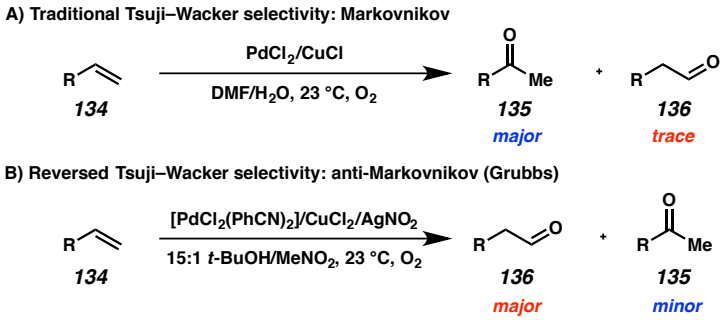

Despite the robustness of the nitrite-modified Tsuji–Wacker reaction, limitations remain. Specifically, oxidation of substrates bearing proximal steric hindrance, such as quaternary carbons, has yet to be demonstrated. Quaternary carbons are prevalent in many structurally complex and biologically interesting organic compounds (Figure 3.1A). The synthetic challenges presented by these sterically demanding motifs have inspired our group to develop a number of strategies for their construction via catalytic enantioselective decarboxylative allylic alkylation, among other methods.[13] While these methods have been employed to great effect in total synthesis,[14,15] the allylic alkylation products (**139**) are also unique substrates for methodological studies given that many

traditionally robust reactions often become problematic under the extreme steric constraints.[16] Structurally, the allyl moiety supplies a versatile functional handle, and the proximal quaternary stereocenter provides a basis from which to examine methodologies that are resilient enough to overcome the high steric demand (Figure 3.1B).

Figure 3.1 A) Examples of natural products containing quaternary carbons. B) Typical products of enantioselective decarboxylative allylic alkylations.

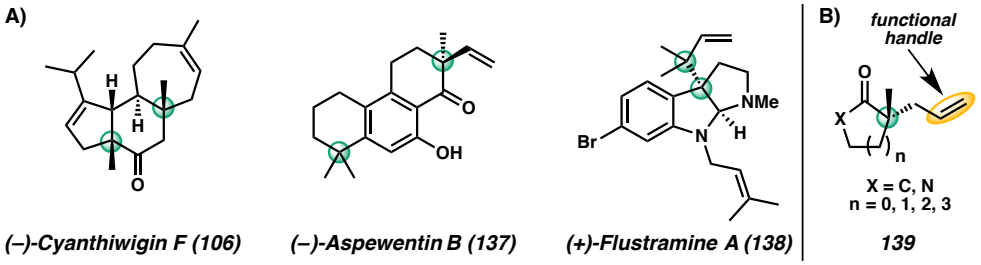

*Scheme 3.2 Example of a common two-step oxidation strategy from Danishefsky's synthesis of guanacastepene A (**142**)*

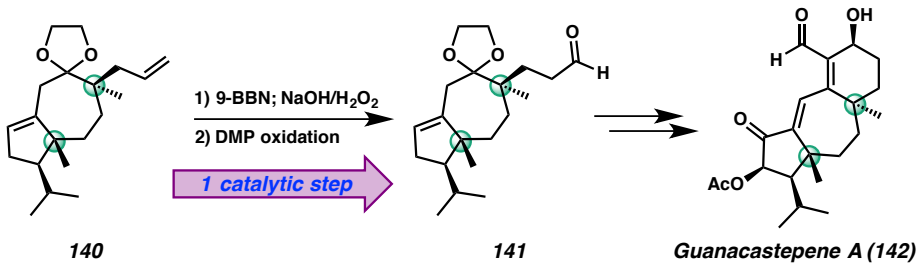

Examples of sterically encumbered substrates are often absent from methodology reports, impeding their utility in complex molecule synthesis. Indeed, the oxidation of hindered terminal alkenes to the corresponding aldehydes is often accomplished in two stoichiometric steps: hydroboration–oxidation, followed by Dess–Martin or Swern oxidation (Scheme 3.2). However, with the modern capabilities of the nitrite-modified Tsuji–Wacker reaction, we hypothesized this sequence could be achieved in a single

catalytic step, thereby streamlining synthetic strategy and generating less waste compared to the stoichiometric processes.

3.2 EXAMINATION OF THE NITRITE CO-CATALYST

We began our investigations by examining the effect of different nitrite sources on the reactivity of malonate derivative **143a** (Figure 3.2). Although various nitrite sources gave comparable yields of desired aldehyde **144a** (Entries 2–7), we found that $AgNO_2$ gave the optimal overall yield and selectivity for this hindered system (Entry 8).[17] Notably, the exclusion of any nitrite source severely impeded oxidation (Entry 1), corroborating theories concerning the critical role nitrite plays in this transformation.[9,11]

*Figure 3.2 Investigation of different nitrite sources in the aldehyde-selective Tsuji–Wacker. Oxidation yield is the sum of the yields of **144a** and **145a**.*

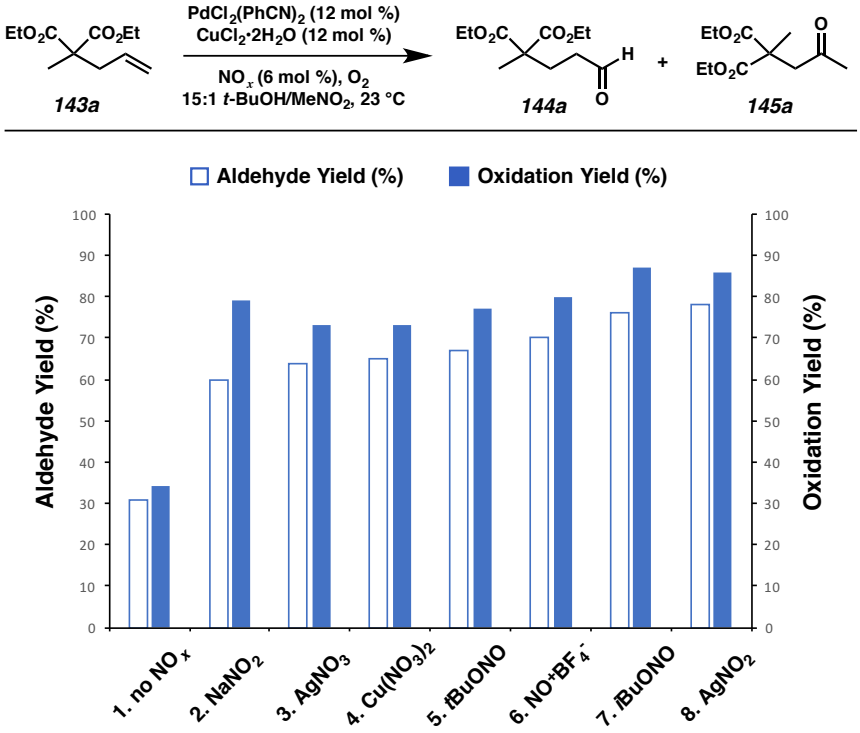

3.3 OXIDATION OF HINDERED TERMINAL ALKENES

Having elucidated the optimized reaction conditions, we explored the reactivity of various substrates bearing proximal quaternary carbons in the aldehyde-selective Tsuji-Wacker oxidation, beginning with alkenes bearing quaternary carbons at the homoallylic position and later examining substrates with allylic quaternary carbons.

3.3.1 HOMOALLYLIC QUATERNARY ALKENES

Beginning our investigations on allylated malonate derivatives, we were delighted to find that substrates containing ester and nitrile functionalities readily underwent oxidation to the corresponding aldehyde products in excellent yields and high selectivities (Table 3.1, Entries 1–3). Although alcohols were incompatible with the reaction conditions,[18] TBS-ether **143d** was a competent substrate for the transformation, furnishing aldehyde **144d** in high yield (Entry 4). Vinylogous ester **143e** and caprolactone derivative **143f** were also reactive under the conditions, affording aldehydes **144e** and **144f** in good yield (Entries 5–6). Tetralone-derived substrates **143g–143i** also performed well in the reaction (Entries 7–9), although the more sterically congested alkene of **143h** required prolonged reaction time for full conversion (Entry 8). Notably, deoxytetralone derivative **135j** also proved to be a competent substrate, demonstrating that the presence of a carbonyl functionality adjacent to the quaternary carbon is not necessary for oxidation to proceed (Entry 10).[19]

Table 3.1 Substrate scope of the aldehyde-selective Tsuji–Wacker oxidation on hindered alkenes

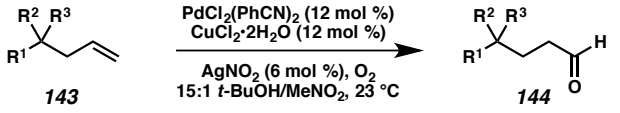

Entry[a]	Alkene Substrate	Aldehyde Product	Yield
1	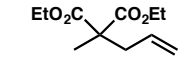 143a	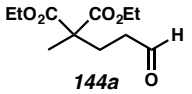 144a	90%[b]
2	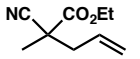 143b	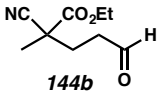 144b	81%
3	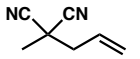 143c	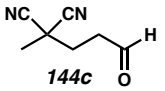 144c	89%
4	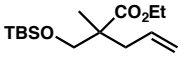 143d	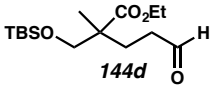 144d	87%
5	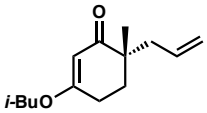 143e	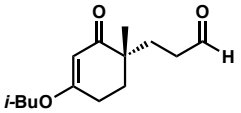 144e	60%[d,f]
6	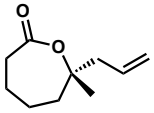 143f	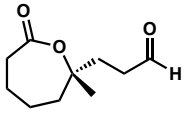 144f	67%[c]
7	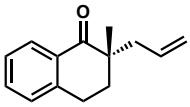 143g	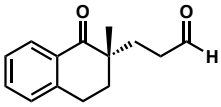 144g	80%[c]
8	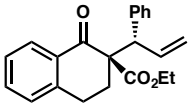 143h	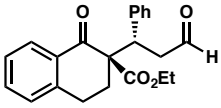 144h	75%[b,e,g]
9	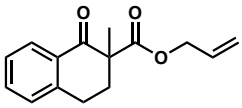 143i	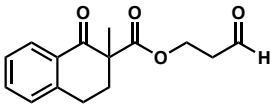 144i	74%[c]
10	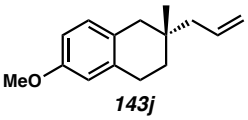 143j	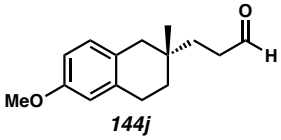 144j	63%[c]

[a]Reactions performed on 0.2 mmol of **143** at 0.05 M over 7–17 h. Isolated yields. [b]Methyl ketone observed, 91–96% aldehyde selectivity. [c]Enal observed, 80–97% aldehyde selectivity. [d]Enal observed, 67% aldehyde selectivity. [e]Reaction time = 40 h. [f]Conducted on 0.08 mmol of **143e**. [g]Conducted on 0.06 mmol of **143h**.

3.3.2 ALLYLIC QUATERNARY ALKENES

Remarkably, alkenes bearing quaternary carbons at the allylic position were also suitable substrates for oxidation (Table 3.2). For instance, α-vinylic ketone **146a** was oxidized to aldehyde **147a** in high yield (Entry 1). Bulkier substitution at the allylic position was also tolerated, with α-vinylic ester **146b** reacting smoothly to generate aldehyde **147b** in good yield (Entry 2). Gratifyingly, oxidation of complex organic molecules was also possible, as conversion of aspewentin B derivative **146c**[20] to aldehyde **147c** proceeded in moderate yield (Entry 3).

Table 3.2 Aldehyde-selective Tsuji–Wacker oxidation of allylic quaternary alkenes

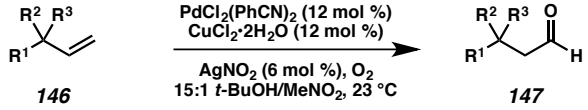

Entry[a]	Alkene Substrate	Aldehyde Product	Yield
1	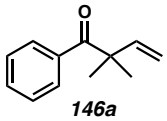 **146a**	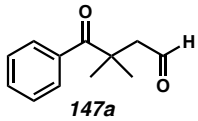 **147a**	85%[b]
2	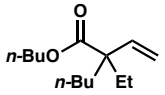 **146b**	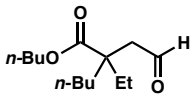 **147b**	69%[b]
3	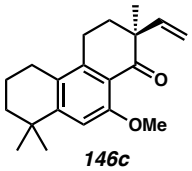 **146c**	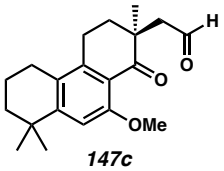 **147c**	64%[c]

[a]Reactions performed on 0.2 mmol of **146** at 0.05 M over 20–48 h. Isolated yields. [b]Methyl ketone observed, 88–91% aldehyde selectivity. [c]Conducted on 0.07 mmol of **146c**.

3.4 FORMAL ANTI-MARKOVNIKOV HYDROAMINATION

Inspired by the robustness of this transformation on such sterically encumbered substrates, we recognized an opportunity to expand the synthetic impact of the nitrite-modified Tsuji–Wacker reaction by leveraging the inherent reactivity of the aldehyde products. We envisioned that subsequent reductive amination of the aldehyde could effect formal anti-Markovnikov hydroamination of the olefin starting material. The addition of amines to alkenes has been recognized as an important research topic due to the ubiquity of amines in biologically active small molecules.[21,22] Anti-Markovnikov hydroamination remains a particularly active area of interest since Markovnikov addition is usually favored. While various efforts toward this challenging transformation have been reported, many strategies require air-sensitive transition metal catalysts, harsh conditions, or biased substrates to achieve regioselective hydroamination.[23] Furthermore, in some cases product scope is restricted to tertiary amines,[23h–k] and in other cases the reaction conditions are highly reducing.[23l] Noting these limitations, we anticipated that reductive amination of the aldehyde generated from the aldehyde-selective Tsuji–Wacker oxidation could provide a mild and efficient alternative.

We selected alkene **143a** as the substrate for our formal hydroamination studies due to its excellent performance in the Tsuji–Wacker oxidation. Upon full conversion of the olefin under aldehyde-selective Tsuji–Wacker conditions, filtration through a silica plug and subsequent treatment of the residue with amine and $NaBH(OAc)_3$ at ambient temperature in DCE allowed access to the reductive amination products in good to excellent yields (Table 3.3). Aliphatic (**148a–148c**) and aromatic (**148d**) tertiary amines were prepared in excellent yields through this procedure (Entries 1–4), and electron-rich

(**148e**) and electron-poor (**148f**) anilines were also obtained in high yields (Entries 5–6). Notably, both tertiary and secondary amines are accessible through this operationally simple sequence.

*Table 3.3 Formal anti-Markovnikov hydroamination of **143a** via aldehyde-selective Tsuji–Wacker*

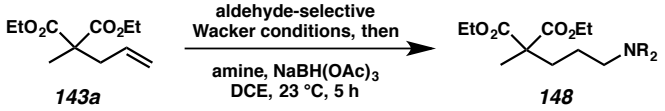

143a ***148***

Entry[a]	Amine	Product	Yield
1	*N*-phenylpiperazine	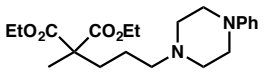 ***148a***	98%
2	morpholine	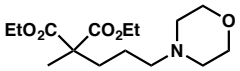 ***148b***	91%
3	dibenzylamine	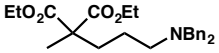 ***148c***	76%
4	indoline	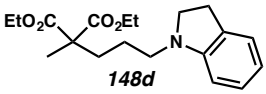 ***148d***	96%
5	4-methoxyaniline	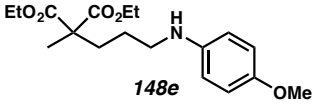 ***148e***	86%
6	4-nitroaniline	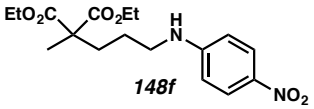 ***148f***	95%

[a]Reactions performed on 0.2 mmol of **143a**. Isolated yields. Conditions for nitrite-Wacker: $PdCl_2(PhCN)_2$ (0.12 equiv), $CuCl_2 \cdot 2H_2O$ (0.12 equiv), $AgNO_2$ (0.06 equiv), 15:1 *t*-BuOH/$MeNO_2$ (0.05 M), 23 °C, 12 h.

3.5 FURTHER SYNTHETIC TRANSFORMATIONS

Encouraged by the success of the formal hydroamination reactions, we sought to extend our two-step procedure to other synthetically useful transformations, enabling

conversion of the alkene starting material to a variety of functional groups. For instance, sodium borohydride reduction of the crude aldehyde afforded formal anti-Markovnikov hydration product **149** in good yield (Scheme 3.3). Likewise, Strecker conditions allowed access to α-aminonitrile **150** while Horner–Wadsworth–Emmons olefination furnished α,β-unsaturated methyl ester **151** in high yield, effecting a two-carbon homologation of alkene **143a**. Fischer indolization also proved successful, affording 3-substituted indole **152** in moderate yield. Further oxidation[24] of the crude aldehyde delivered tris-ethyl ester **153** in high yield whereas treatment with the Ohira–Bestmann reagent enabled conversion of the terminal alkene to a terminal alkyne of one-carbon chain length longer (**154**). Finally, reactivity of alkene **143a** under traditional Tsuji–Wacker conditions was assessed, providing methyl ketone **145a** in good yield.

*Scheme 3.3 Summary of synthetic transformations of alkene **143a***

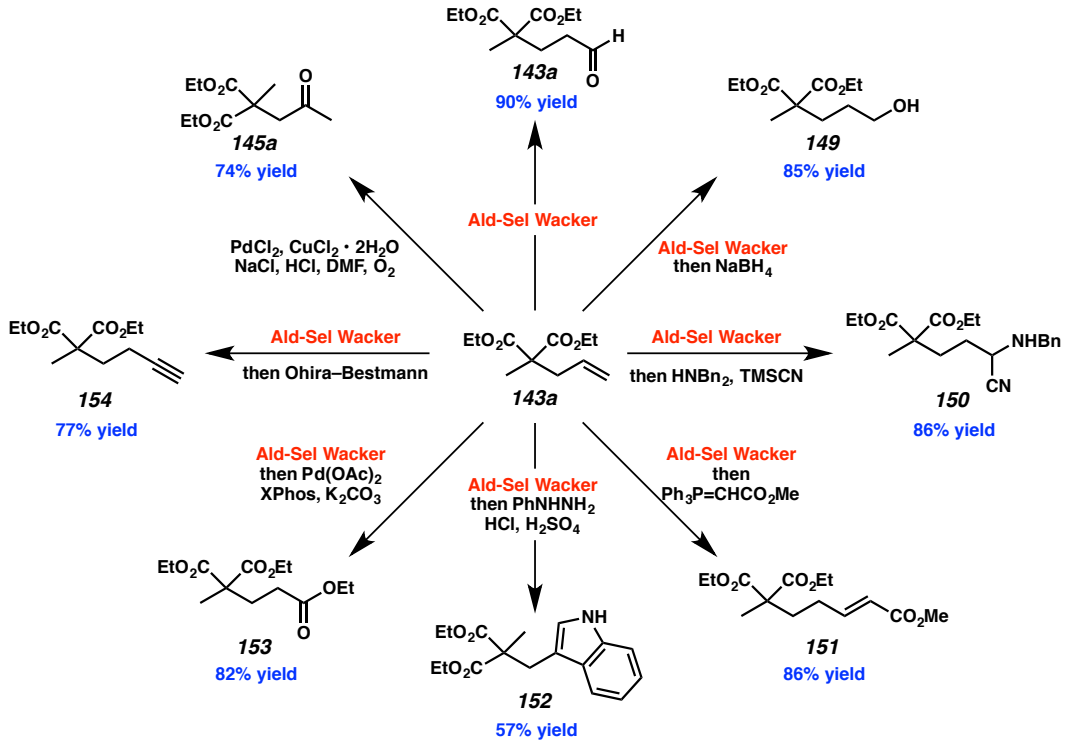

Ald-Sel Wacker = $PdCl_2(PhCN)_2$ (12 mol %), $CuCl_2 \cdot 2H_2O$ (12 mol %), $AgNO_2$ (6 mol %), O_2, 15:1 *t*-BuOH/$MeNO_2$, 23 °C

3.6 CONCLUDING REMARKS

In summary, we have amplified the synthetic impact of the aldehyde-selective Tsuji–Wacker oxidation by demonstrating its efficacy on diversely functionalized terminal alkenes bearing sterically demanding quaternary carbons at the allylic or homoallylic position, common motifs among intermediates in complex molecule synthesis. Moreover, we have illustrated how the aldehyde products of these reactions can be further transformed, enabling direct conversion of the alkene functional handle to a variety of other functional groups.[25] We anticipate that this operationally simple methodology will find many applications in chemical synthesis since several of these overall transformations are unprecedented or require multiple steps. From these studies it is clear that the aldehyde-selective Tsuji-Wacker oxidation is an extremely versatile tool for the facile catalytic functionalization of terminal olefins.

3.7 EXPERIMENTAL SECTION

3.7.1 MATERIALS AND METHODS

Unless noted in the specific procedure, reactions were performed in flame-dried glassware under argon atmosphere. Dried and deoxygenated solvents (Fisher Scientific) were prepared by passage through columns of activated aluminum before use.[26] Methanol (Fisher Scientific) was distilled from magnesium methoxide immediately prior to use. 1,2-dichloroethane (Fisher Scientific) was distilled from calcium hydride immediately prior to use. Anhydrous ethanol, *tert*-butanol, and *N*,*N*-dimethylformamide were purchased from Sigma Aldrich in sure-sealed bottles and used as received unless otherwise noted. Commercial reagents (Sigma Aldrich or Alfa Aesar) were used as received with the exception of palladium(II) acetate (Sigma Aldrich) and XPhos (Sigma Aldrich), which were stored in a nitrogen-filled govebox. The Ohira–Bestmann reagent[27] and carbomethoxy methylene triphenyl phosphorane ($Ph_3P{=}CHCO_2Me$)[28] were prepared according to known procedures. Triethylamine (Oakwood Chemical) and diisopropylethylamine (Oakwood Chemical) were distilled from calcium hydride immediately prior to use. Brine is defined as a saturated aqueous solution of sodium chloride. Reactions requiring external heat were modulated to the specified temperatures using an IKAmag temperature controller. Reaction progress was monitored by thin-layer chromatography (TLC) or Agilent 1290 UHPLC-LCMS. TLC was performed using E. Merck silica gel 60 F254 precoated plates (0.25 mm) and visualized by UV fluorescence quenching, potassium permanganate, or *p*-anisaldehyde staining. Silia*Flash* P60 Academic Silica gel (particle size 0.040–0.063 mm) was used for flash chromatography. NMR spectra were recorded on a Varian Mercury 300 spectrometer (at 300 MHz for ^{1}H

NMR and 75 MHz for ^{13}C NMR), a Varian Inova 500 spectrometer (at 500 MHz for ^{1}H NMR and 126 MHz for ^{13}C NMR), or a Bruker AV III HD spectrometer equipped with a Prodigy liquid nitrogen temperature cryoprobe (at 400 MHz for ^{1}H NMR and 101 MHz for ^{13}C NMR), and are reported relative to residual $CHCl_3$ (δ 7.26 for ^{1}H NMR, δ 77.16 for ^{13}C NMR) or C_6H_6 (δ 7.16 for ^{1}H NMR, δ 128.06 for ^{13}C NMR). Data for ^{1}H NMR spectra are reported as follows: chemical shift (δ ppm) (multiplicity, coupling constant (Hz), integration). Abbreviations are used as follows: s = singlet, bs = broad singlet, d = doublet, t = triplet, q = quartet, m = complex multiplet. Infrared (IR) spectra were recorded on a Perkin Elmer Paragon 1000 spectrometer using thin film samples on KBr plates, and are reported in frequency of absorption (cm^{-1}). High-resolution mass spectra (HRMS) were obtained from the Caltech Mass Spectral Facility using a JEOL JMS-600H High Resolution Mass Spectrometer with fast atom bombardment (FAB+) ionization mode or were acquired using an Agilent 6200 Series TOF with an Agilent G1978A Multimode source in electrospray ionization (ESI+) mode. Optical rotations were measured with a Jasco P-1010 polarimeter at 589 nm using a 100 mm path-length cell.

3.7.2 PREPARATIVE PROCEDURES

3.7.2.1 CATALYST OPTIMIZATION

Table 3.4 Investigation of different nitrite sources in the aldehyde-selective Tsuji–Wacker

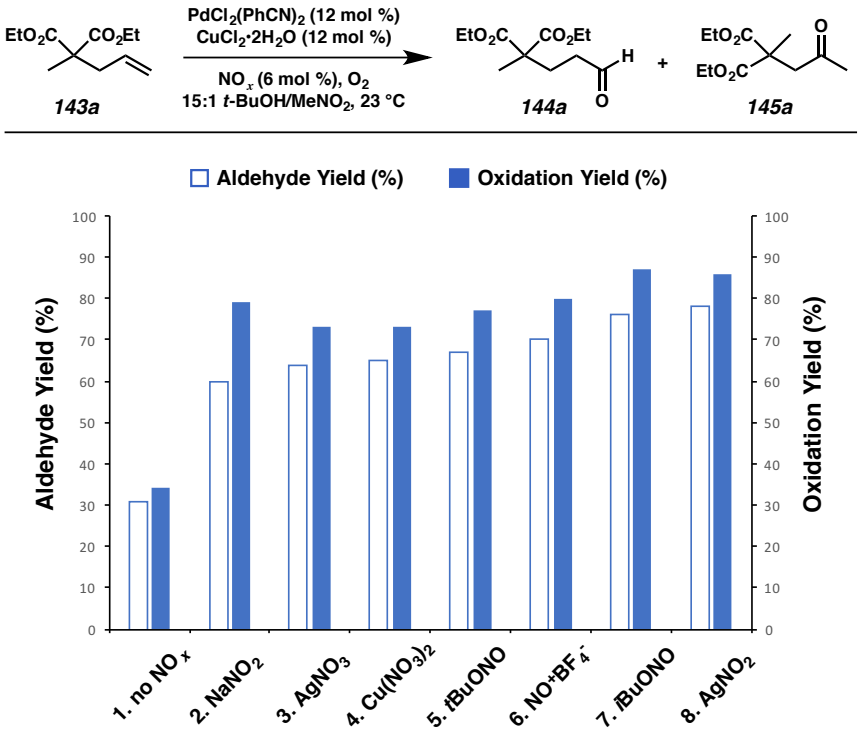

NO_x species	Aldehyde yield (%)[a]	Ketone yield (%)	Oxidation yield (%)[b]	Selectivity (aldehyde:ketone)
$AgNO_2$	78	8	86	10:1
$AgNO_3$	64	9	73	7:1
$NaNO_2$	60	19	79	3:1
$NO^+BF_4^-$	70	10	80	7:1
$Cu(NO_3)_2$	65	8	73	8:1
t-BuONO	67	10	77	7:1
i-BuONO	76	11	87	7:1
no NO_x	31	3	34	10:1

[a] Yields were calculated from the crude ^{1}H NMR spectrum.
[b] Oxidation yield is the sum of the yields of aldehyde **144a** and methyl ketone **145a**.

Procedure for Catalyst Optimization. To a flame-dried 25-mL round-bottom flask with a magnetic stir bar were added bis(benzonitrile)palladium(II) chloride (9.2 mg, 0.024 mmol, 0.12 equiv), copper(II) chloride dihydrate (4.1 mg, 0.024 mmol, 0.12 equiv), and silver nitrite (1.8 mg, 0.012 mmol, 0.06 equiv). The flask was capped with a rubber septum, and *tert*-butyl alcohol (3.75 mL) and nitromethane (0.25 mL) were added sequentially by syringe. The mixture was stirred at 23 °C and sparged with oxygen gas (balloon) for 3 minutes. Alkene **143a** (42.9 mg, 0.20 mmol, 1.00 equiv) was added dropwise by syringe, and the reaction mixture was sparged with oxygen for another minute. The reaction was stirred under oxygen atmosphere at 23 °C for 14 hours, after which the reaction mixture was diluted with water (4 mL) and extracted with dichloromethane (3 x 5 mL). The organic extracts were dried over sodium sulfate, then filtered and concentrated in vacuo. Nitrobenzene (24.6 mg, 0.20 mmol, 1.00 equiv) was added as an internal standard immediately prior to NMR analysis, and the yield and selectivity of the formation of aldehyde **144a** was calculated from the ^{1}H NMR spectrum (d1 = 15s).

3.7.2.2 GENERAL EXPERIMENTAL PROCEDURES

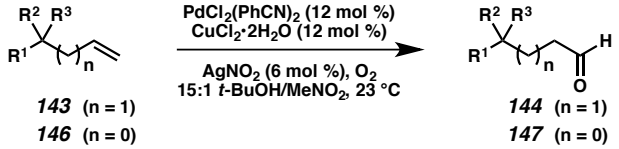

143 **(n = 1)**
146 **(n = 0)**

144 **(n = 1)**
147 **(n = 0)**

General Procedure A. *Aldehyde-selective Wacker-type oxidation of alkenes*.

To a flame-dried 25-mL round-bottom flask with a magnetic stir bar were added bis(benzonitrile)palladium(II) chloride (9.2 mg, 0.024 mmol, 0.12 equiv), copper(II) chloride dihydrate (4.1 mg, 0.024 mmol, 0.12 equiv), and silver nitrite (1.8 mg, 0.012 mmol, 0.06 equiv). The flask was capped with a rubber septum, and *tert*-butyl alcohol (3.75 mL) and nitromethane (0.25 mL) were added sequentially by syringe. The mixture was stirred at 23 °C and sparged with oxygen gas (balloon) for 3 minutes. Alkene **143** or **146** (0.20 mmol, 1.00 equiv) was added dropwise by syringe, and the reaction mixture was sparged with oxygen for another minute. The reaction was stirred under oxygen atmosphere at 23 °C until TLC analysis indicated consumption of starting material. The reaction mixture was diluted with water (4 mL) and extracted with dichloromethane (3 x 5 mL). The organic extracts were dried over sodium sulfate, and then filtered and concentrated in vacuo. The crude residue was purified by silica gel column chromatography, using mixture of hexanes and ethyl acetate as eluent to afford aldehyde **144** or **147**.

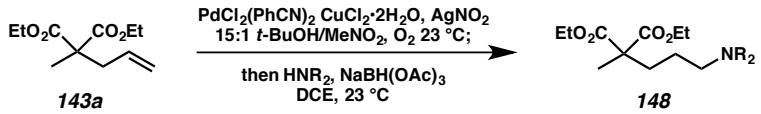

143a *148*

General Procedure B. *Hydroamination of diethyl 2-allyl-2-methylmalonate* ***(143a)***.

To a flame-dried 25-mL round-bottom flask with a magnetic stir bar were added bis(benzonitrile)palladium(II) chloride (9.2 mg, 0.024 mmol, 0.12 equiv), copper(II) chloride dihydrate (4.1 mg, 0.024 mmol, 0.12 equiv), and silver nitrite (1.8 mg, 0.012 mmol, 0.06 equiv). The flask was capped with a rubber septum, and *tert*-butyl alcohol (3.75 mL) and nitromethane (0.25 mL) were added sequentially by syringe. The mixture was stirred at 23 °C and sparged with oxygen gas (balloon) for 3 minutes. Alkene **143a** (42.9 mg, 0.20 mmol, 1.00 equiv) was added dropwise by syringe, and the reaction mixture was sparged with oxygen for another minute. The reaction was stirred under oxygen atmosphere at 23 °C for 12 hours, when TLC analysis indicated consumption of starting material. The solvent was removed under reduced pressure, and the residue was loaded onto a short plug of silica gel, eluting with 30% ethyl acetate in hexanes (100 mL). The oil obtained upon concentration was then redissolved in 1,2-dichloroethane (4 mL) and treated with amine (0.22 mmol, 1.1 equiv) at 23 °C. After one hour, sodium triacetoxyborohydride (63.6 mg, 0.30 mmol, 1.50 equiv) was added in one portion. Stirring was continued at 23 °C for 5 hours, at which time the reaction was diluted with diethyl ether (3 mL), washed with saturated aqueous sodium bicarbonate (5 mL), and extracted with diethyl ether (3 x 5 mL). The organic extracts were dried over sodium sulfate, and then filtered and concentrated under reduced pressure. The crude residue was purified by silica gel column chromatography, using mixture of hexanes and ethyl acetate with 0.5% triethylamine as eluent to afford amine **148**.

3.7.2.3 SUBSTRATE SYNTHESIS AND CHARACTERIZATION DATA

Compounds **143a** and **159,**[16] **143e,**[29] **143g,**[13b] **143h,**[30] **143i,**[13b] **143f,**[30] and **146a–c,**[20] **160**[30] may be prepared as previously reported by our research group.

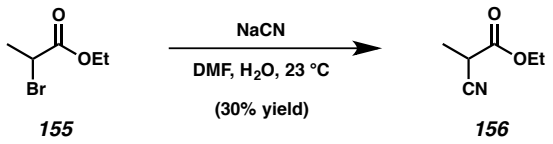

155 *156*

Ethyl-2-cyanopropanoate (156). A round-bottom flask equipped with a magnetic stir bar and thermometer was charged with sodium cyanide (2.44 g, 49.7 mmol, 1.50 equiv), *N*,*N*-dimethylformamide (22 mL), and water (2.2 mL). Alkyl bromide **155** (4.30 mL, 33.1 mmol, 1.00 equiv) was added dropwise over 15 minutes, making sure the internal temperature did not exceed 35 °C throughout addition. After complete addition, the internal thermometer was removed, and the mixture was stirred at 23 °C for 12 hours, at which time the reaction mixture was diluted with diethyl ether and washed sequentially with cold 5% aqueous hydrochloric acid (15 mL) and saturated aqueous sodium bicarbonate (15 mL). The organic layer was dried over sodium sulfate, and then filtered and concentrated under reduced pressure. The crude residue was purified by silica gel column chromatography (10% → 20% ethyl acetate in hexanes), furnishing cyanoester **156** as a colorless oil (1.27 g, 30% yield). Characterization data match those reported in the literature.[31]

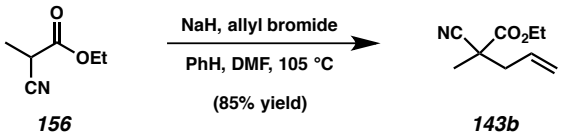

156 ***143b***

Ethyl 2-cyano-2-methylpent-4-enoate (143b). To a suspension of sodium hydride (60% dispersion in mineral oil, 419 mg, 10.5 mmol, 1.05 equiv) in benzene (15 mL) was added a solution of cyanoester **156** (1.27 g, 9.98 mmol, 1.00 equiv) in benzene (12 mL). *N*,*N*-dimethylformamide (8 mL) was added to stabilize the sodium enolate, and the mixture was stirred at 23 °C for 20 minutes before allyl bromide (910 μL mL, 10.5 mmol, 1.05 equiv) was added dropwise. Upon complete addition, the reaction mixture was heated to reflux (105 °C). After 12 hours, the reaction was allowed to cool to room temperature before quenching with water (15 mL) and extracting with diethyl ether (3 x 20 mL). The organic extracts were washed with brine (20 mL) and dried over magnesium sulfate before filtration and concentration under reduced pressure. The crude residue was purified by silica gel column chromatography (11% ethyl acetate in hexanes) to afford alkene **143b** as a colorless oil (1.43 g, 85% yield). R*f* = 0.68 (33% ethyl acetate in hexanes); ^{1}H NMR ($CDCl_3$, 400 MHz) δ 5.81 (ddt, *J* = 16.1, 11.0, 7.3 Hz, 1H), 5.33–5.18 (m, 2H), 4.26 (qd, *J* = 7.1, 1.0 Hz, 2H), 2.67 (ddt, *J* = 13.8, 7.2, 1.2 Hz, 1H), 2.55–2.45 (m, 1H), 1.58 (s, 3H), 1.32 (t, *J* = 7.1 Hz, 3H); ^{13}C NMR ($CDCl_3$, 101 MHz) δ 169.0, 130.7, 121.2, 119.8, 63.0, 43.8, 42.2, 22.8, 14.2; IR (Neat Film, KBr) 3083, 2985, 1744, 1455, 1233, 1174, 1017, 930; HRMS (FAB+) *m/z* calc'd for $C_9H_{14}NO_2$ $[M+H]^+$: 168.1024, found 168.1012.

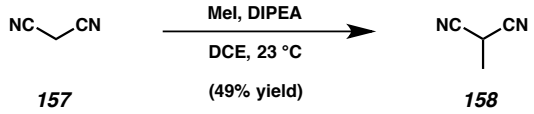

157 ***158***

2-Methylmalononitrile (158). To a flame-dried round-bottom flask were added malononitrile **157** (3.00 g, 45.4 mmol, 1.00 equiv) and 1,2-dichloroethane (90 mL). The suspension was cooled to 0 °C using an ice water bath, and diisopropylethylamine (7.91 mL, 45.4 mmol, 1.00 equiv) and methyl iodide (2.83 mL, 45.4 mmol, 1.00 equiv) were added dropwise sequentially. The resulting mixture was stirred at 23 °C for 24 hours, at which time the reaction was quenched with water and transferred to a separatory funnel. The aqueous layer was extracted with ethyl acetate (5 x 50 mL), and the combined organic extracts were washed with brine (50 mL) and dried over sodium sulfate. After filtration and concentration, the crude residue obtained was purified by silica gel column chromatography (5% → 10% → 15% ethyl acetate in hexanes) to furnish 2-methylmalononitrile (**158**) as a white solid (1.77 g, 49% yield). Characterization data match those reported in the literature.[32]

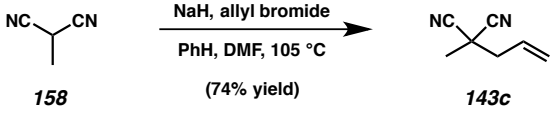

158 ***143c***

2-Allyl-2-methylmalononitrile (143c). To a suspension of sodium hydride (60% dispersion in mineral oil, 309 mg, 7.72 mmol, 1.05 equiv) in benzene (7.1 mL) was added a solution of 2-methylmalononitrile **158** (589 mg, 7.35 mmol, 1.00 equiv) in benzene (7.1 mL). *N*,*N*-dimethylformamide (3.5 mL) was added to stabilize the sodium enolate, and the mixture was stirred at 23 °C for 20 minutes before allyl bromide (670 μL mL, 7.72 mmol, 1.05 equiv) was added dropwise. Upon complete addition, the reaction mixture

was heated to reflux (105 °C). After 12 hours, the reaction was allowed to cool to room temperature before quenching with water (8 mL) and extracting with diethyl ether (3 x 10 mL). The organic extracts were washed with brine (10 mL) and dried over magnesium sulfate before filtration and concentration under reduced pressure. The crude residue was purified by silica gel column chromatography (10% ethyl acetate in hexanes) to afford alkene **143c** as a colorless oil (653 mg, 74% yield). R*f* = 0.52 (33% ethyl acetate in hexanes);^{1}H NMR ($CDCl_3$, 500 MHz) δ 5.89 (ddt, *J* = 16.7, 10.1, 7.3 Hz, 1H), 5.55–5.31 (m, 2H), 2.68 (ddd, *J* = 7.3, 1.3, 0.8 Hz, 2H), 1.79 (s, 3H); ^{13}C NMR ($CDCl_3$, 126 MHz) δ 128.5, 123.6, 115.9, 43.0, 31.7, 24.2; IR (Neat Film, KBr) 3087, 2987, 2927, 1654, 1650, 1454, 1440, 1417, 1276, 1180, 994, 936, 729; HRMS (FAB+) *m/z* calc'd for $C_7H_9N_2$ $[M+H]^+$: 121.0760, found 121.0758.

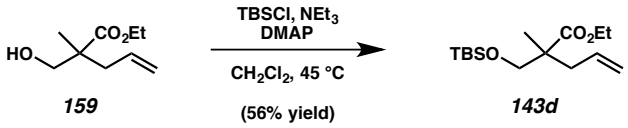

Ethyl 2-(((*tert*-butyldimethylsilyl)oxy)methyl)-2-methylpent-4-enoate (143d). To a flame-dried two-necked round-bottom flask equipped with a reflux condenser and magnetic stir bar were added alcohol **159** (108.2 mg, 0.611 mmol, 1.00 equiv) and dichloromethane (12.2 mL). *tert*-Butyldimethylsilyl chloride (101.2 mg, 0.672 mmol, 1.10 equiv), triethylamine (0.17 mL, 1.22 mmol, 2.00 equiv), and 4-(dimethylamino)pyridine (7.5 mg, 0.0611 mmol, 0.10 equiv) were added at 23 °C, and the mixture was heated to reflux (45 °C). After 42 hours, the reaction was allowed to cool to 23 °C and washed with 2 M aqueous hydrochloric acid (2 x 10 mL) and brine (10 mL), and then dried over sodium sulfate. After filtration and concentration under

reduced pressure, the crude residue was purified by silica gel column chromatography (3% ethyl acetate in hexanes), delivering alkene **143d** as a colorless oil (98.1 mg, 56% yield). R*f* = 0.79 (33% ethyl acetate in hexanes); ^{1}H NMR ($CDCl_3$, 400 MHz) δ 5.72 (ddt, *J* = 16.5, 10.6, 7.4 Hz, 1H), 5.14–4.96 (m, 2H), 4.12 (qd, *J* = 7.2, 0.9 Hz, 2H), 3.70–3.46 (m, 2H), 2.38 (ddt, *J* = 13.6, 7.2, 1.2 Hz, 1H), 2.22 (ddt, *J* = 13.6, 7.7, 1.1 Hz, 1H), 1.24 (t, *J* = 7.1 Hz, 3H), 1.13 (s, 3H), 0.87 (s, 9H), 0.02 (s, 6H); ^{13}C NMR ($CDCl_3$, 101 MHz) δ175.8, 134.1, 118.1, 68.1, 60.4, 48.3, 39.5, 25.9, 19.3, 18.3, 14.4, -5.5; IR (Neat Film, KBr) 2956, 2929, 2857, 1732, 1472, 1386, 1251, 1227, 1101, 837, 776 cm^{-1}; HRMS (ESI+) *m/z* calc'd for $C_{15}H_{31}O_3Si$ $[M+H]^+$: 287.2037, found 287.2040.

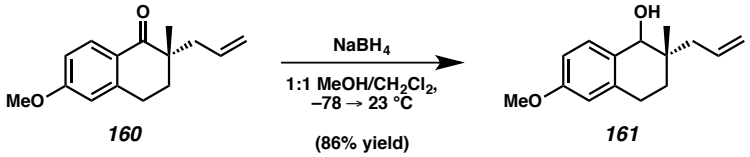

(2*S*)-2-Allyl-6-methoxy-2-methyl-1,2,3,4-tetrahydronaphthalen-1-ol (161). To a solution of ketone **160** (64.9 mg, 0.282 mmol, 1.00 equiv) in dichloromethane (2.8 mL) and methanol (2.8 mL) was added a solution of sodium borohydride (21.3 mg, 0.564 mmol, 2.00 equiv) in dichloromethane (1.2 mL) and methanol (1.2 mL) at –78 °C. The reaction mixture was allowed to warm to 23 °C over the course of six hours. When TLC analysis indicated full consumption of starting material, the reaction was quenched with acetone (2.0 mL) and 2N NaOH (2.0 mL). The phases were separated, and the organic layer was immediately washed with brine (10 mL) and dried over sodium sulfate. After filtration and concentration under reduced pressure, the crude residue was purified by silica gel column chromatography (15% ethyl acetate in hexanes), furnishing alcohol **161** as a 1:1 mixture of diastereomers (56.5 mg, 86% yield). R*f* = 0.26 (20% ethyl acetate in

hexanes); ^{1}H NMR ($CDCl_3$, 500 MHz) δ 7.35 (d, *J* = 8.5 Hz, 1H), 7.28 (d, *J* = 8.5 Hz, 1H), 6.79–6.73 (m, 2H), 6.64 (dt, *J* = 5.1, 1.8 Hz, 2H), 6.04–5.83 (m, 2H), 5.16–5.00 (m, 5H), 4.23 (s, 1H), 3.78 (s, 6H), 2.87–2.65 (m, 5H), 2.28 (ddt, *J* = 13.6, 7.3, 1.2 Hz, 1H), 2.13–2.01 (m, 3H), 1.87 (ddd, *J* = 13.5, 9.4, 6.7 Hz, 1H), 1.78 (ddd, *J* = 13.8, 7.5, 6.3 Hz, 1H), 1.55 (dt, *J* = 13.4, 6.6 Hz, 1H), 1.46 (dddd, *J* = 13.6, 5.9, 4.7, 1.0 Hz, 2H), 0.99 (s, 3H), 0.88 (s, 4H); ^{13}C NMR ($CDCl_3$, 126 MHz) δ 159.0, 158.9, 137.7, 137.4, 135.3, 135.0, 131.0, 130.9, 130.6, 130.2, 117.7, 117.6, 113.3, 113.2, 112.6, 75.1, 74.9, 55.3, 42.6, 41.6, 37.1, 36.9, 29.4, 29.1, 26.1, 26.0, 21.1, 19.9; IR (Neat Film, KBr) 3430 (br), 2928, 1610, 1501, 1456, 1263, 1159, 1104, 1038, 1015, 912, 802 cm^{-1}; HRMS (FAB+) *m/z* calc'd for $C_{15}H_{20}O_2$ $[M\bullet]^+$: 232.1463, found 232.1439.

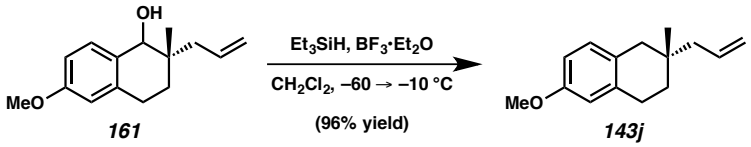

(*S*)-2-Allyl-6-methoxy-2-methyl-1,2,3,4-tetrahydronaphthalene (143j). To a solution of alcohol **161** (56.5 mg, 0.243 mmol, 1.00 equiv) in dichloromethane (5.0 mL) was added triethylsilane (0.12 mL, 0.730 mmol, 3.00 equiv) and boron trifluoride diethyl etherate (60 μL, 0.486 mmol, 2.00 equiv) at –60 °C. After 10 minutes, the reaction mixture was warmed to –10 °C and stirred at this temperature for 7 hours. A saturated aqueous solution of potassium carbonate was added, and the mixture was extracted with dichloromethane (2 x 20 mL). The combined organic extracts were dried over sodium sulfate before filtration and concentration under reduced pressure. The crude residue was purified by silica gel column chromatography (5% ethyl acetate in hexanes), affording tetralin **143j** as a colorless oil (50.3 mg, 96% yield). R*f* = 0.67 (20% ethyl acetate in

hexanes); ^{1}H NMR ($CDCl_3$, 500 MHz) δ 6.97 (d, *J* = 8.3 Hz, 1H), 6.73–6.63 (m, 2H), 5.91 (ddt, *J* = 16.9, 10.2, 7.5 Hz, 1H), 5.14–4.96 (m, 2H), 3.79 (s, 3H), 2.79 (t, *J* = 6.7 Hz, 2H), 2.60–2.39 (m, 2H), 2.06 (qdt, *J* = 13.7, 7.3, 1.2 Hz, 2H), 1.67–1.47 (m, 2H), 0.96 (s, 3H); ^{13}C NMR ($CDCl_3$, 126 MHz) δ 157.5, 137.0, 135.2, 130.5, 128.3, 117.3, 113.4, 112.0, 55.3, 45.4, 41.1, 33.8, 32.6, 26.5, 24.8; IR (Neat Film, KBr) 3073, 2951, 2914, 1611, 1503, 1464, 1267, 1254, 1236, 1153, 1042, 912, 808 cm^{-1}; HRMS (ESI+) *m/z* calc'd for $C_{15}H_{21}O$ $[M+H]^+$: 217.1587, found 217.1584; $[\alpha]^{25}_D$ 6.47 (*c* 1.0, $CHCl_3$).

3.7.2.4 ALDEHYDE CHARACTERIZATION DATA

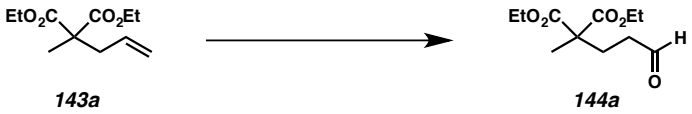

143a ***144a***

Diethyl 2-methyl-2-(3-oxopropyl)malonate (144a). Aldehyde **144a** was prepared from **143a** using General Procedure A, reaction time: 7 h, column eluent: 7% → 10% ethyl acetate in hexanes. 90% isolated yield. R*f* = 0.45 (33% ethyl acetate in hexanes); ^{1}H NMR ($CDCl_3$, 500 MHz) δ 9.76 (t, *J* = 1.3 Hz, 1H), 4.18 (qd, *J* = 7.2, 0.6 Hz, 4H), 2.56–2.47 (m, 2H), 2.22–2.13 (m, 2H), 1.41 (s, 3H), 1.25 (t, *J* = 7.1 Hz, 6H); ^{13}C NMR ($CDCl_3$, 126 MHz) δ 201.1, 171.9, 61.6, 52.9, 39.6, 27.9, 20.5, 14.2; IR (Neat Film, KBr) 2984, 1730, 1465, 1381, 1262, 1110, 1023, 861 cm^{-1}; HRMS (ESI+) *m/z* calc'd for $C_{11}H_{19}O_5$ $[M+H]^+$: 231.1227, found 231.1232.

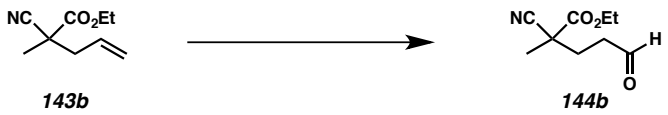

143b ***144b***

Ethyl 2-cyano-2-methyl-5-oxopentanoate (144b). Aldehyde **144b** was prepared from **143b** using General Procedure A, reaction time: 7 h, column eluent: 20% ethyl acetate in hexanes. 81% isolated yield. R*f* = 0.39 (33% ethyl acetate in hexanes); ^{1}H NMR ($CDCl_3$, 400 MHz) δ 9.77 (d, *J* = 0.9 Hz, 1H), 4.25 (qd, *J* = 7.1, 0.7 Hz, 2H), 2.83–2.53 (m, 2H), 2.27 (dddd, *J* = 14.4, 10.0, 5.6, 0.7 Hz, 1H), 2.15–2.02 (m, 1H), 1.61 (d, *J* = 0.7 Hz, 3H), 1.31 (td, *J* = 7.1, 0.7 Hz, 3H); ^{13}C NMR ($CDCl_3$, 101 MHz) δ 199.2, 168.8, 119.5, 63.2, 43.1, 39.9, 30.1, 23.6, 14.1; IR (Neat Film, KBr) 2988, 2944, 1744, 1715, 1453, 1255, 1128, 1017, 857 cm^{-1}; HRMS (FAB+) *m/z* calc'd for $C_9H_{14}NO_3$ $[M+H]^+$: 184.0974, found 184.0976.

143c ***144c***

2-Methyl-2-(3-oxopropyl)malononitrile (144c). Aldehyde **144c** was prepared from **143c** using General Procedure A, reaction time: 17 h, column eluent: 20% ethyl acetate in hexanes. 89% isolated yield. R*f* = 0.25 (33% ethyl acetate in hexanes); ^{1}H NMR ($CDCl_3$, 400 MHz) δ 9.85 (s, 1H), 3.00–2.84 (m, 2H), 2.38–2.21 (m, 2H), 1.84 (s, 3H); ^{13}C NMR ($CDCl_3$, 101 MHz) δ197.7, 115.67, 39.9, 31.6, 31.2, 25.0; IR (Neat Film, KBr) 2848, 1724, 1454, 1389, 1150, 897, 629 cm^{-1}; HRMS (FAB+) *m/z* calc'd for $C_7H_9N_2O$ $[M+H]^+$: 137.0715, found 137.0688.

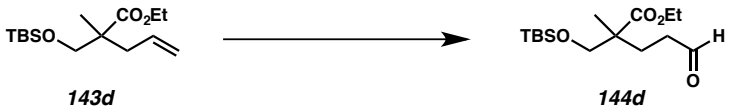

143d ***144d***

Ethyl 2-(((*tert*-butyldimethylsilyl)oxy)methyl)-2-methyl-5-oxopentanoate (144d). Aldehyde **144d** was prepared from **143d** using General Procedure A, reaction time: 15 h, column eluent: 7% ethyl acetate in hexanes. 87% isolated yield. R*f* = 0.70 (33% ethyl acetate in hexanes); ^{1}H NMR ($CDCl_3$, 500 MHz) δ 9.74 (t, *J* = 1.6 Hz, 1H), 4.10 (q, *J* = 7.1 Hz, 2H), 3.64–3.57 (m, 2H), 2.46–2.40 (m, 2H), 1.97 (ddd, *J* = 14.0, 8.7, 7.1 Hz, 1H), 1.82–1.72 (m, 1H), 1.23 (t, *J* = 7.1 Hz, 3H), 1.13 (s, 3H), 0.85 (s, 9H), 0.01 s, 6 H); ^{13}C NMR ($CDCl_3$, 126 MHz) δ 202.1, 175.5, 68.4, 60.7, 47.6, 39.6, 27.2, 25.9, 19.7, 18.3, 14.3, –5.5; IR (Neat Film, KBr) 2955, 2930, 2857, 1728, 1472, 1252, 1184, 1100, 838, 777, 668 cm^{-1}; HRMS (ESI+) *m/z* calc'd for $C_{15}H_{31}O_4Si$ $[M+H]^+$: 303.1986, found 303.1983.

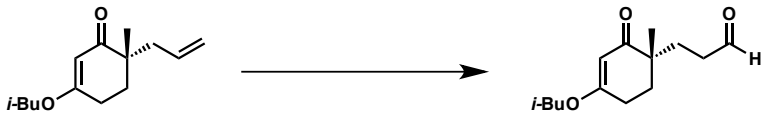

143e ***144e***

(*S*)-3-(4-Isobutoxy-1-methyl-2-oxocyclohex-3-en-1-yl)propanal (144e). Aldehyde **144e** was prepared from **143e** using General Procedure A, reaction time: 14 h, column eluent: 15% ethyl acetate in hexanes. 60% isolated yield. R*f* = 0.34 (33% ethyl acetate in hexanes); ^{1}H NMR ($CDCl_3$, 500 MHz) δ 9.76 (t, *J* = 1.5 Hz, 1H), 5.24 (s, 1H), 3.57 (d, *J* = 6.5 Hz, 2H), 2.53–2.36 (m, 4H), 2.02 (dq, *J* = 13.3, 6.7 Hz, 1H), 1.93–1.69 (m, 4H), 1.10 (s, 3H), 1.00–0.95 (m, 6H); ^{13}C NMR ($CDCl_3$, 126 MHz) δ 203.2, 202.4, 176.3, 101.5, 75.0, 42.7, 39.4, 32.8, 29.1, 27.9, 26.0, 22.6, 19.2; IR (Neat Film, KBr) 2961,

2932, 1724, 1648, 1607, 1384, 1369, 1195, 993, 840 cm^{-1}; HRMS (ESI+) *m/z* calc'd for $C_{14}H_{23}O_3$ $[M+H]^+$: 239.1642, found 239.1638; $[\alpha]^{25}_D$ –5.0 (*c* 0.94, $CHCl_3$).

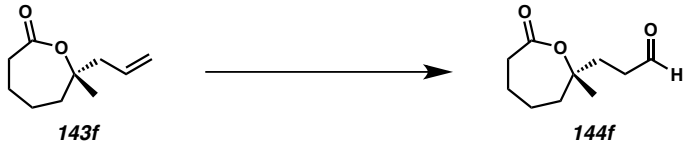

143f ***144f***

(*S*)-3-(2-Methyl-7-oxooxepan-2-yl)propanal (144f). Aldehyde **144f** was prepared from **143f** using General Procedure A, reaction time: 15 h, column eluent: 20% → 40% ethyl acetate in hexanes. 67% isolated yield. R*f* = 0.30 (67% ethyl acetate in hexanes); ^{1}H NMR ($CDCl_3$, 500 MHz) δ 9.82 (d, *J* = 1.2 Hz, 1H), 2.80–2.57 (m, 4H), 2.11 (ddd, *J* = 14.9, 9.0, 6.3 Hz, 1H), 1.96–1.74 (m, 6H), 1.69–1.57 (m, 1H), 1.44 (s, 3H); ^{13}C NMR ($CDCl_3$, 126 MHz) δ 201.8, 174.9, 82.3, 39.4, 38.9, 37.6, 34.9, 24.7, 24.1, 23.7; IR (Neat Film, KBr) 2936, 1720, 1716, 1289, 1185, 1107, 1018, 858 cm^{-1}; HRMS (FAB+) *m/z* calc'd for $C_{10}H_{17}O_3$ $[M+H]^+$: 185.1178, found 185.1177; $[\alpha]^{25}_D$ 1.6 (*c* 2.46, $CHCl_3$).

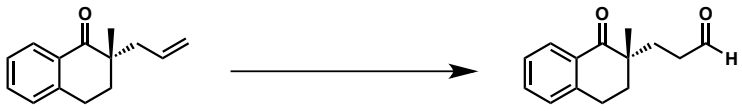

143g ***144g***

(*S*)-3-(2-Methyl-1-oxo-1,2,3,4-tetrahydronaphthalen-2-yl)propanal (144g). Aldehyde **144g** was prepared from **143g** using General Procedure A, reaction time: 12 h, column eluent: 5% ethyl acetate in hexanes. 80% isolated yield. R*f* = 0.15 (20% ethyl acetate in hexanes); ^{1}H NMR ($CDCl_3$, 500 MHz) δ 9.76 (t, *J* = 1.5 Hz, 1H), 8.01 (dd, *J* = 7.9, 1.4 Hz, 1H), 7.49–7.42 (m, 1H), 7.33–7.26 (m, 1H), 7.22 (ddq, *J* = 7.6, 1.5, 0.8 Hz, 1H), 3.01 (t, *J* = 6.3 Hz, 2H), 2.61–2.30 (m, 2H), 2.13–1.82 (m, 4H), 1.21 (s, 3H); ^{13}C

NMR ($CDCl_3$, 126 MHz) δ 202.2, 201.9, 143.1, 133.4, 131.5, 128.9, 128.1, 126.9, 44.1, 39.2, 34.2, 28.8, 25.3, 22.2; IR (Neat Film, KBr) 2929, 1722, 1682, 1600, 1454, 1224, 976, 798, 742 cm^{-1}; HRMS (FAB+) *m/z* calc'd for $C_{14}H_{17}O_2$ $[M+H]^+$: 217.1229, found 217.1258; $[\alpha]^{25}_D$ –1.0 (*c* 1.65, $CHCl_3$).

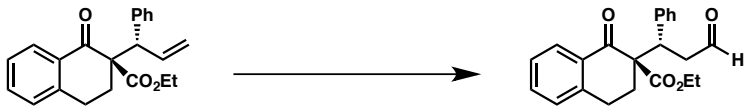

143h ***144h***

Ethyl (*R*)-1-oxo-2-((*S*)-3-oxo-1-phenylpropyl)-1,2,3,4-tetrahydronaphthalene-2-carboxylate (144h). Aldehyde **144h** was prepared from **143h** using General Procedure A, reaction time: 40 h, column eluent: 10% ethyl acetate in hexanes. 75% isolated yield. R*f* = 0.48 (33% ethyl acetate in hexanes); ^{1}H NMR ($CDCl_3$, 400 MHz) δ 9.59 (t, *J* = 1.7 Hz, 1H), 8.00 (dd, *J* = 7.9, 1.5 Hz, 1H), 7.44 (td, *J* = 7.5, 1.5 Hz, 1H), 7.40–7.34 (m, 2H), 7.31–7.24 (m, 2H), 7.24–7.12 (m, 3H), 4.19 (dd, *J* = 8.4, 6.2 Hz, 1H), 4.08 (q, *J* = 7.1 Hz, 2H), 3.13–3.07 (m, 2H), 3.07–2.97 (m, 1H), 2.88 (dt, *J* = 17.8, 4.5 Hz, 1H), 2.34 (ddd, *J* = 13.7, 4.8, 3.7 Hz, 1H), 1.98 (ddd, *J* = 13.8, 11.2, 5.1 Hz, 1H), 1.09 (t, *J* = 7.1 Hz, 3H); ^{13}C NMR ($CDCl_3$, 101 MHz) δ 200.9, 194.7, 170.2, 142.7, 139.1, 133.6, 132.6, 130.5, 128.7, 128.4, 128.3, 127.5, 126.9, 61.8, 60.5, 46.3, 43.0, 30.5, 26.1, 14.0; IR (Neat Film, KBr) 2978, 2725, 1725, 1689, 1600, 1454, 1298, 1235, 1214, 1018, 909, 742, 703, 648 cm^{-1}; HRMS (ESI+) *m/z* calc'd for $C_{22}H_{23}O_5$ $[M+OH]^+$: 367.1540, found 367.1535; $[\alpha]^{25}_D$ 15.7 (*c* 1.52, $CHCl_3$).

143i ***144i***

3-Oxopropyl 2-methyl-1-oxo-1,2,3,4-tetrahydronaphthalene-2-carboxylate (144i). Aldehyde **144i** was prepared from **143i** using General Procedure A, reaction time: 10 h, column eluent: 15% ethyl acetate in hexanes. 74% isolated yield. R*f* = 0.27 (33% ethyl acetate in hexanes); ^{1}H NMR ($CDCl_3$, 500 MHz) δ 9.61 (t, *J* = 1.4 Hz, 1H), 8.02 (dd, *J* = 7.9, 1.4 Hz, 1H), 7.47 (td, *J* = 7.5, 1.5 Hz, 1H), 7.34–7.28 (m, 1H), 7.24–7.19 (m, 1H), 4.54–4.31 (m, 2H), 3.12–2.86 (m, 2H), 2.68 (ddt, *J* = 7.2, 6.0, 1.5 Hz, 2H), 2.58 (ddd, *J* = 13.7, 6.2, 4.9 Hz, 1H), 2.05 (ddt, *J* = 13.8, 9.0, 4.6 Hz, 1H), 1.48 (s, 3H); ^{13}C NMR ($CDCl_3$, 126 MHz) δ 199.0, 196.1, 172.9, 143.1, 133.7, 131.6, 128.9, 128.1, 127.0, 58.9, 54.0, 42.5, 33.7, 25.9, 20.4; IR (Neat Film, KBr) 2936, 1732, 1687, 1682, 1601, 1455, 1308, 1265, 1228, 1189, 1114, 743 cm^{-1}; HRMS (FAB+) *m/z* calc'd for $C_{15}H_{17}O_4$ $[M+H]^+$: 261.1127, found 261.1155.

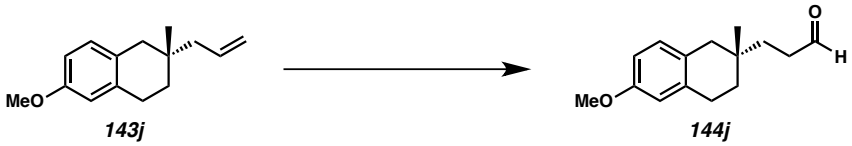

143j ***144j***

(*S*)-3-(6-Methoxy-2-methyl-1,2,3,4-tetrahydronaphthalen-2-yl)propanal (144j). Aldehyde **144j** was prepared from **143j** using General Procedure A, reaction time: 12 h, column eluent: 5% ethyl acetate in hexanes. 63% isolated yield. R*f* = 0.34 (20% ethyl acetate in hexanes); ^{1}H NMR ($CDCl_3$, 500 MHz) δ 9.79 (t, *J* = 1.9 Hz, 1H), 6.95 (d, *J* = 8.4 Hz, 1H), 6.71–6.66 (m, 1H), 6.64 (d, *J* = 2.7 Hz, 1H), 3.77 (s, 3H), 2.77 (td, *J* = 6.7, 4.2 Hz, 2H), 2.56–2.39 (m, 4H), 1.65–1.60 (m, 2H), 1.58 (t, *J* = 6.8 Hz, 2H), 0.93 (s, 3H); ^{13}C NMR ($CDCl_3$, 126 MHz) δ 203.0, 157.7, 136.7, 130.5, 127.7, 113.4, 112.2, 55.4,

41.1, 39.1, 33.9, 32.6, 31.9, 26.4, 24.4; IR (Neat Film, KBr) 2916, 2834, 2719, 1724, 1610, 1503, 1267, 1242, 1040, 808 cm^{-1}; HRMS (FAB+) *m/z* calc'd for $C_{15}H_{20}O_2$ $[M\bullet]^+$: 232.1463, found 232.1473; $[\alpha]^{25}_D$ 85.6 (*c* 1.00, $CHCl_3$).

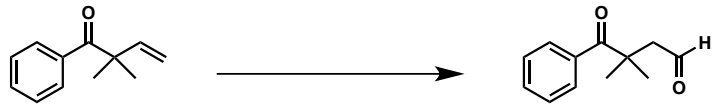

146a ***147a***

3,3-Dimethyl-4-oxo-4-phenylbutanal (147a). Aldehyde **147a** was prepared from **146a** using General Procedure A, reaction time: 20 h, column eluent: 10% ethyl acetate in hexanes. 85% isolated yield. R*f* = 0.30 (33% ethyl acetate in hexanes); ^{1}H NMR ($CDCl_3$, 500 MHz) δ 9.74 (t, *J* = 1.4 Hz, 1H), 7.70–7.64 (m, 2H), 7.50–7.45 (m, 1H), 7.44–7.38 (m, 2H), 2.83 (d, *J* = 1.5 Hz, 2H), 1.46 (s, 6H); ^{13}C NMR ($CDCl_3$, 126 MHz) δ 208.2, 200.6, 138.4, 131.2, 128.3, 127.8, 54.7, 46.1, 26.7; IR (Neat Film, KBr) 2974, 1784, 1712, 1450, 1291, 1114, 967, 714 cm^{-1}; HRMS (ESI+) *m/z* calc'd for $C_{12}H_{15}O_2$ $[M+H]^+$: 191.1067, found 191.1075.

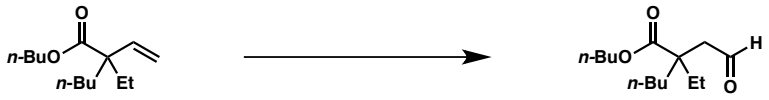

146b ***147b***

Butyl 2-ethyl-2-(2-oxoethyl)hexanoate (147b). Aldehyde **147b** was prepared from **146b** using General Procedure A, reaction time: 45 h, column eluent: 10% ethyl acetate in hexanes. 69% isolated yield. R*f* = 0.36 (10% ethyl acetate in hexanes); ^{1}H NMR ($CDCl_3$, 500 MHz) δ 9.76 (t, *J* = 2.3 Hz, 1H), 4.10 (t, *J* = 6.6 Hz, 2H), 2.62 (d, *J* = 2.3 Hz, 2H), 1.79–1.56 (m, 6H), 1.42–1.32 (m, 2H), 1.31–1.24 (m, 2H), 1.23–1.08 (m, 2H), 0.92 (t, *J* = 7.4 Hz, 3H), 0.87 (t, *J* = 7.2 Hz, 3H), 0.83 (t, *J* = 7.5 Hz, 3H); ^{13}C NMR

($CDCl_3$, 126 MHz) δ 201.7, 176.0, 64.8, 48.1, 47.3, 35.7, 30.7, 29.0, 26.5, 23.2, 19.3, 14.1, 13.8, 8.7; IR (Neat Film, KBr) 2961, 2936, 2874, 1724, 1459, 1383, 1203, 1139, 1022, 737 cm^{-1}; HRMS (ESI+) *m/z* calc'd for $C_{14}H_{26}O_3$ $[M+H]^+$: 243.1955, found 243.1961.

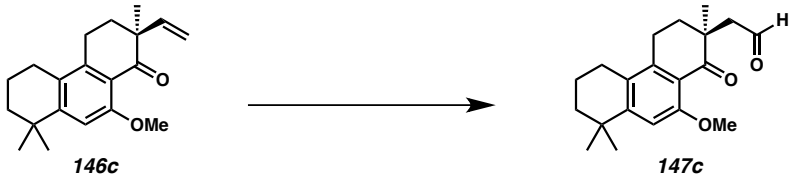

146c ***147c***

(*S*)-2-(10-methoxy-2,8,8-trimethyl-1-oxo-1,2,3,4,5,6,7,8-octahydrophenanthren-2-yl)acetaldehyde (147c). Aldehyde **147c** was prepared from **146c** using General Procedure A, reaction time: 48 h, column eluent: 5% ethyl acetate in hexanes. 64% isolated yield. R*f* = 0.40 (33% ethyl acetate in hexanes); ^1H NMR ($CDCl_3$, 500 MHz) δ 9.89 (t, *J* = 2.5 Hz, 1H), 6.85 (s, 1H), 3.88 (s, 3H), 2.80 (dd, *J* = 8.0, 4.9 Hz, 2H), 2.67 (dd, *J* = 15.5, 2.3 Hz, 1H), 2.60–2.45 (m, 3H), 2.22–2.11 (m, 1H), 1.96 (dt, *J* = 13.6, 4.9 Hz, 1H), 1.89–1.78 (m, 2H), 1.68–1.61 (m, 2H), 1.30 (s, 9H); ^{13}C NMR ($CDCl_3$, 126 MHz) δ 202.3, 200.6, 158.9, 153.1, 143.4, 126.3, 118.9, 108.6, 56.0, 51.3, 45.4, 38.4, 35.0, 33.8, 31.8, 31.7, 27.0, 23.7, 22.0, 19.4; IR (Neat Film, KBr) 2959, 2930, 2866, 1717, 1676, 1591, 1558, 1459, 1401, 1318, 1246, 1227, 1104, 1042, 1013, 972, 850, 734 cm^{-1}; HRMS (ESI+) *m/z* calc'd for $C_{20}H_{26}O_3$ $[M+H]^+$: 315.1955, found 315.1947; $[\alpha]^{25}_D$ 4.03 (*c* 1.00, $CHCl_3$).

3.7.2.5 AMINE CHARACTERIZATION DATA

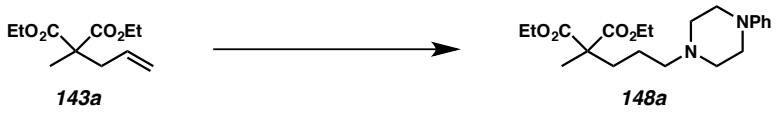

143a ***148a***

Diethyl 2-methyl-2-(3-(4-phenylpiperazin-1-yl)propyl)malonate (148a). Amine **148a** was prepared from **143a** using General Procedure B, column eluent: 25% ethyl acetate in hexanes with 0.5% triethylamine. 98% isolated yield. R*f* = 0.16 (33% ethyl acetate in hexanes); ^{1}H NMR ($CDCl_3$, 400 MHz) δ 7.29–7.18 (m, 2H), 6.92 (dt, *J* = 7.9, 1.0 Hz, 2H), 6.88–6.79 (m, 1H), 4.18 (q, *J* = 7.1 Hz, 4H), 3.26–3.12 (m, 4H), 2.66–2.53 (m, 4H), 2.45–2.33 (m, 2H), 1.94–1.82 (m, 2H), 1.55–1.44 (m, 2H), 1.41 (d, *J* = 4.4 Hz, 3H), 1.25 (t, *J* = 7.1 Hz, 6H); ^{13}C NMR ($CDCl_3$, 101 MHz) δ 172.4, 151.4, 129.2, 119.8, 116.1, 61.3, 58.7, 53.6, 53.3, 49.2, 33.5, 21.9, 20.1, 14.2; IR (Neat Film, KBr) 2816, 1731, 1600, 1502, 1257, 1235, 1110, 759, 692 cm^{-1}; HRMS (ESI+) *m/z* calc'd for $C_{21}H_{33}N_2O_5$ $[M+OH]^+$: 393.2384, found 393.2386.

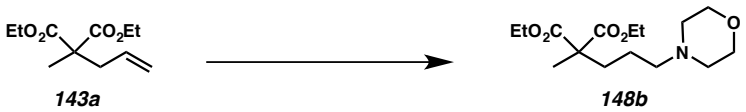

143a ***148b***

Diethyl 2-methyl-2-(3-morpholinopropyl)malonate (148b). Amine **148b** was prepared from **143a** using General Procedure B, column eluent: 8% → 25% ethyl acetate in hexanes with 0.5% triethylamine. 91% isolated yield. ^{1}H NMR ($CDCl_3$, 300 MHz) δ 4.17 (q, *J* = 7.1 Hz, 4H), 3.76–3.65 (m, 4H), 2.41 (dd, *J* = 5.8, 3.6 Hz, 4H), 2.37–2.29 (m, 2H), 1.89–1.81 (m, 2H), 1.52–1.36 (m, 5H), 1.23 (t, *J* = 7.1 Hz, 6H); ^{13}C NMR ($CDCl_3$, 101 MHz) δ 172.4, 66.8, 61.4, 58.9, 53.6, 53.5, 33.4, 21.4, 20.1, 14.2; IR (Neat Film,

KBr) 2958, 1730, 1457, 1256, 1232, 1118, 1023, 862 cm^{-1}; HRMS (ESI+) *m/z* calc'd for $C_{15}H_{28}NO_5$ $[M+H]^+$: 302.1962, found 302.1961.

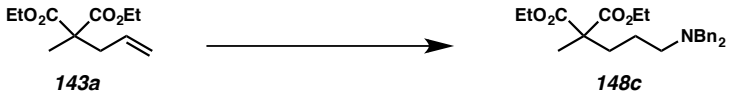

Diethyl 2-(3-(dibenzylamino)propyl)-2-methylmalonate (148c). Amine **148c** was prepared from **143a** using General Procedure B, column eluent: 8% ethyl acetate in hexanes with 0.5% triethylamine. 76% isolated yield. R*f* = 0.72 (33% ethyl acetate in hexanes); ^1H NMR ($CDCl_3$, 500 MHz) δ 7.38–7.27 (m, 8H), 7.25–7.20 (m, 2H), 4.22–4.10 (m, 4H), 3.54 (s, 4H), 2.43 (t, *J* = 7.0 Hz, 2H), 1.88–1.80 (m, 2H), 1.50–1.41 (m, 2H), 1.38 (d, *J* = 0.8 Hz, 3H), 1.22 (td, *J* = 7.1, 0.6 Hz, 6H); ^{13}C NMR ($CDCl_3$, 126 MHz) δ 172.5, 139.8, 128.9, 128.3, 126.9, 61.2, 58.3, 53.6, 53.5, 33.3, 21.9, 20.1, 14.2; IR (Neat Film, KBr) 2981, 2796, 1731, 1453, 1245, 1111, 1028, 746, 699 cm^{-1}; HRMS (ESI+) *m/z* calc'd for $C_{25}H_{34}NO_4$ $[M+H]^+$: 412.2482, found 412.2494.

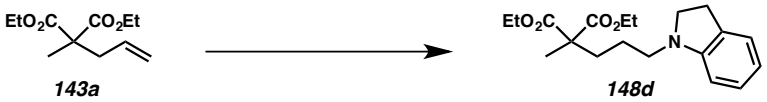

Diethyl 2-(3-(indolin-1-yl)propyl)-2-methylmalonate (148d). Amine **148d** was prepared from **143a** using General Procedure B, column eluent: 6% ethyl acetate in hexanes with 0.5% triethylamine. 96% isolated yield. R*f* = 0.66 (33% ethyl acetate in hexanes); ^1H NMR ($CDCl_3$, 400 MHz) δ 7.12–7.00 (m, 2H), 6.64 (t, *J* = 7.5 Hz, 1H), 6.45 (d, *J* = 7.8 Hz, 1H), 4.18 (q, *J* = 7.1 Hz, 4H), 3.32 (t, *J* = 8.3 Hz, 2H), 3.06 (t, *J* = 7.2 Hz, 2H), 2.95 (t, *J* = 8.2 Hz, 2H), 2.01–1.89 (m, 2H), 1.61–1.54 (m, 2H), 1.43 (s, 3H), 1.25 (t, *J* = 7.1 Hz, 7H); ^{13}C NMR ($CDCl_3$, 101 MHz) δ 172.5, 152.7, 130.2, 127.4,

124.5, 117.5, 107.0, 61.4, 53.6, 53.1, 49.6, 33.3, 28.7, 22.5, 20.2, 14.2; IR (Neat Film, KBr) 2980, 1730, 1607, 1490, 1254, 1232, 1113, 1022, 746 cm^{-1}; HRMS (ESI+) *m/z* calc'd for $C_{19}H_{28}NO_4$ $[M+H]^+$: 334.2013, found 334.2019.

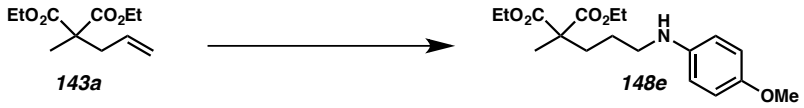

Diethyl 2-(3-((4-methoxyphenyl)amino)propyl)-2-methylmalonate (148e). Amine **148e** was prepared from **143a** using General Procedure B, column eluent: 10% ethyl acetate in hexanes with 0.5% triethylamine. 86% isolated yield. R*f* = 0.45 (33% ethyl acetate in hexanes); ^1H NMR ($CDCl_3$, 400 MHz) δ 6.81–6.71 (m, 2H), 6.60–6.51 (m, 2H), 4.17 (q, *J* = 7.1 Hz, 4H), 3.74 (s, 3H), 3.08 (t, *J* = 6.9 Hz, 2H), 2.00–1.89 (m, 2H), 1.62–1.48 (m, 2H), 1.41 (s, 3H), 1.23 (t, *J* = 7.1 Hz, 7H); ^{13}C NMR ($CDCl_3$, 101 MHz) δ 172.4, 152.2, 142.6, 115.1, 114.2, 61.4, 56.0, 53.6, 45.1, 33.3, 24.7, 20.1, 14.2; IR (Neat Film, KBr) 2982, 1730, 1514, 1235, 1187, 1110, 1037, 820 cm^{-1}; HRMS (ESI+) *m/z* calc'd for $C_{18}H_{28}NO_5$ $[M+H]^+$: 338.1962, found 338.1953.

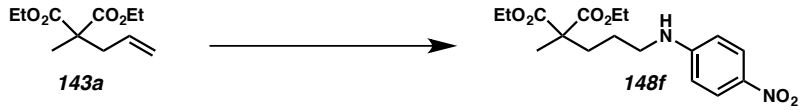

Diethyl 2-methyl-2-(3-((4-nitrophenyl)amino)propyl)malonate (148f). Amine **148f** was prepared from **143a** using General Procedure B, column eluent: 10% → 20% ethyl acetate in hexanes with 0.5% triethylamine. 95% isolated yield. R*f* = 0.31 (33% ethyl acetate in hexanes); ^1H NMR ($CDCl_3$, 500 MHz) δ 8.12–8.04 (m, 2H), 6.54–6.48 (m, 2H), 4.18 (q, *J* = 7.1 Hz, 4H), 3.22 (t, *J* = 6.8 Hz, 2H), 1.98–1.92 (m, 2H), 1.69–1.61

(m, 2H), 1.43 (s, 3H), 1.24 (t, J = 7.1 Hz, 6H); ^{13}C NMR ($CDCl_3$, 126 MHz) δ 172.3, 153.3, 138.1, 126.6, 111.1, 61.6, 53.5, 43.5, 33.1, 24.2, 20.2, 14.2; IR (Neat Film, KBr) 3383, 2836, 1748, 1721, 1610, 1475, 1314, 1328, 1190, 1114, 829 cm^{-1}; HRMS (ESI+) *m/z* calc'd for $C_{17}H_{25}N_2O_6$ $[M+H]^+$: 353.1707, found 353.1707.

3.7.2.6 ALKENE TRANSFORMATION PROCEDURES AND CHARACTERIZATION DATA

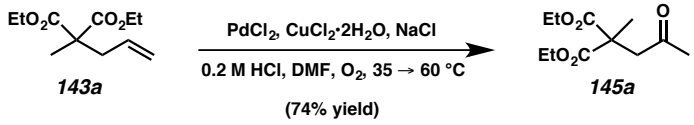

Diethyl 2-methyl-2-(2-oxopropyl)malonate (145a). To a two-necked round-bottom flask were added palladium(II) chloride (10.6 mg, 0.06 mmol, 0.30 equiv), copper(II) chloride dihydrate (20.5 mg, 0.12 mmol, 0.60 equiv), and sodium chloride (15.0 mg, 0.26 mmol, 1.30 equiv). The mixture was diluted with 0.2 M aqueous hydrochloric acid (3.1 mL) and stirred vigorously at 35 °C under oxygen atmosphere (balloon) for 30 minutes. Alkene **143a** (42.9 mg, 0.20 mmol, 1.00 equiv) was added as a solution in *N,N*-dimethylformamide (1.0 mL), and the resulting solution was heated stirred vigorously under oxygen atmosphere at 60 °C for 6 hours. The reaction mixture was allowed to cool to 23 °C and extracted with chloroform (2 x 5 mL). The organic extracts were dried over magnesium sulfate, filtered, and concentrated. The crude residue was purified by silica gel column chromatography (8% ethyl acetate in hexanes) to afford ketone **145a** as a colorless oil (34.3 mg, 74% yield). Rf = 0.24 (33% ethyl acetate in hexanes); ^{1}H NMR ($CDCl_3$, 500 MHz) δ 4.18 (q, J = 7.1 Hz, 4H), 3.08 (s, 2H), 2.15 (s, 3H), 1.51 (s, 3H),

1.24 (t, J = 7.1 Hz, 6H); ^{13}C NMR ($CDCl_3$, 126 MHz) δ 205.1, 171.6, 61.7, 51.6, 48.8, 30.5, 20.6, 14.1; IR (Neat Film, KBr) 2984, 1732, 1463, 1376, 1242, 1109, 1024, 863, 798 cm^{-1}; HRMS (ESI+) *m/z* calc'd for $C_{11}H_{19}O_5$ $[M+H]^+$: 231.1227, found 231.1226.

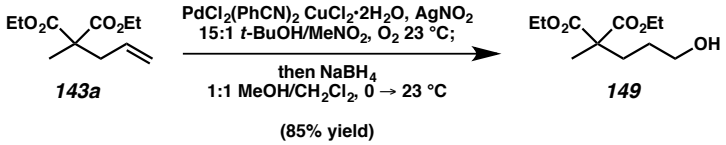

Diethyl 2-(3-hydroxypropyl)-2-methylmalonate (149). To a flame-dried 25-mL round-bottom flask with a magnetic stir bar were added bis(benzonitrile)palladium(II) chloride (9.2 mg, 0.024 mmol, 0.12 equiv), copper(II) chloride dihydrate (4.1 mg, 0.024 mmol, 0.12 equiv), and silver nitrite (1.8 mg, 0.012 mmol, 0.06 equiv). The flask was capped with a rubber septum, and *tert*-butyl alcohol (3.75 mL) and nitromethane (0.25 mL) were added sequentially by syringe. The mixture was stirred at 23 °C and sparged with oxygen gas (balloon) for 3 minutes. Alkene **143a** (42.9 mg, 0.20 mmol, 1.00 equiv) was added dropwise by syringe, and the reaction mixture was sparged with oxygen for another minute. The reaction was stirred under oxygen atmosphere at 23 °C for 12 hours, when TLC analysis indicated consumption of starting material. The solvent was removed under reduced pressure, and the residue was loaded onto a short plug of silica gel, eluting with 30% ethyl acetate in hexanes (100 mL). The oil obtained upon concentration was then redissolved in 1:1 MeOH/CH_2Cl_2 (4 mL total volume) and cooled to 0 °C using an ice water bath. Sodium borohydride (11.3 mg, 0.30 mmol, 1.50 equiv) was added in one portion, and the resulting mixture was stirred at 23 °C for 2 hours, at which time the reaction was quenched with acetone and 2 N aqueous sodium hydroxide (2 mL). The phases were separated, and the organic layer was immediately washed with brine (5 mL)

and dried over sodium sulfate. Filtration and concentration delivered the crude product, which was purified by silica gel column chromatography (35% ethyl acetate in hexanes) to afford alcohol **14** as a colorless oil (39.7 mg, 85% yield). R*f* = 0.18 (33% ethyl acetate in hexanes); ^{1}H NMR ($CDCl_3$, 300 MHz) δ 4.18 (q, *J* = 7.1 Hz, 4H), 3.64 (t, *J* = 6.4 Hz, 2H), 1.98–1.88 (m, 2H), 1.59–1.49 (m, 2H), 1.42 (d, *J* = 2.4 Hz, 3H), 1.24 (t, *J* = 7.1 Hz, 6H); ^{13}C NMR ($CDCl_3$, 75 MHz) δ 172.5, 62.9, 61.4, 53.5, 32.0, 27.8, 20.1, 14.2; IR (Neat Film, KBr) 3469 (br), 2982, 2939, 1730, 1460, 1270, 1119, 1020, 859 cm^{-1}; HRMS (FAB+) *m/z* calc'd for $C_{11}H_{21}O_5$ $[M+H]^+$: 233.1389, found 233.1382.

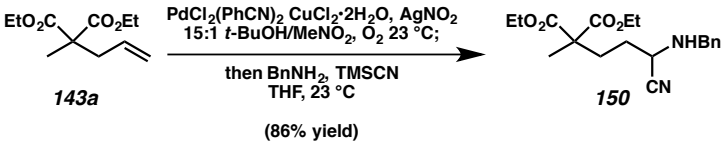

Diethyl 2-(3-(benzylamino)-3-cyanopropyl)-2-methylmalonate (150). To a flame-dried 25-mL round-bottom flask with a magnetic stir bar were added bis(benzonitrile)palladium(II) chloride (9.2 mg, 0.024 mmol, 0.12 equiv), copper(II) chloride dihydrate (4.1 mg, 0.024 mmol, 0.12 equiv), and silver nitrite (1.8 mg, 0.012 mmol, 0.06 equiv). The flask was capped with a rubber septum, and *tert*-butyl alcohol (3.75 mL) and nitromethane (0.25 mL) were added sequentially by syringe. The mixture was stirred at 23 °C and sparged with oxygen gas (balloon) for 3 minutes. Alkene **143a** (42.9 mg, 0.20 mmol, 1.00 equiv) was added dropwise by syringe, and the reaction mixture was sparged with oxygen for another minute. The reaction was stirred under oxygen atmosphere at 23 °C for 12 hours, when TLC analysis indicated consumption of starting material. The solvent was removed under reduced pressure, and the residue was loaded onto a short plug of silica gel, eluting with 30% ethyl acetate in hexanes (100

mL). The oil obtained upon concentration was then redissolved in THF (4 mL total volume) and treated with benzylamine (23 μL, 0.21 mmol, 1.05 equiv) at 23 °C. After one hour, trimethylsilyl cyanide (26 μL, 0.21 mmol, 1.05 equiv) was added, and the resulting mixture was stirred at 23 °C for 7 hours, at which time the volatiles were removed under reduced pressure. The crude residue obtained was purified by silica gel column chromatography (20% ethyl acetate in hexanes) to furnish α-aminonitrile **150** as a colorless oil (59.6 mg, 86% yield). Rf = 0.42 (33% ethyl acetate in hexanes); ^{1}H NMR ($CDCl_3$, 500 MHz) δ 7.37–7.31 (m, 4H), 7.31–7.26 (m, 1H), 4.18 (qd, J = 7.1, 2.2 Hz, 4H), 4.06 (d, J = 12.9 Hz, 1H), 3.82 (d, J = 12.9 Hz, 1H), 3.49 (t, J = 7.0 Hz, 1H), 2.17–2.05 (m, 1H), 2.00 (ddd, J = 13.7, 9.5, 7.4 Hz, 1H), 1.81–1.73 (m, 2H), 1.41 (s, 3H), 1.24 (td, J = 7.1, 2.3 Hz, 6H); ^{13}C NMR ($CDCl_3$, 126 MHz) δ 171.9, 138.2, 128.7, 128.5, 127.7, 119.8, 61.6, 53.2, 51.7, 49.8, 31.8, 28.9, 20.2, 14.2; IR (Neat Film, KBr) 3325, 2983, 1728, 1454, 1261, 1189, 1112, 1027, 738, 700 cm^{-1}; HRMS (ESI+) *m/z* calc'd for $C_{19}H_{27}N_2O_4$ $[M+H]^+$: 347.1965, found 347.1970.

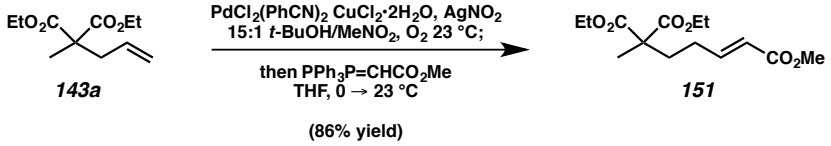

5,5-Diethyl 1-methyl (*E*)-hex-1-ene-1,5,5-tricarboxylate (151). To a flame-dried 25-mL round-bottom flask with a magnetic stir bar were added bis(benzonitrile)palladium(II) chloride (9.2 mg, 0.024 mmol, 0.12 equiv), copper(II) chloride dihydrate (4.1 mg, 0.024 mmol, 0.12 equiv), and silver nitrite (1.8 mg, 0.012 mmol, 0.06 equiv). The flask was capped with a rubber septum, and *tert*-butyl alcohol (3.75 mL) and nitromethane (0.25 mL) were added sequentially by syringe. The mixture

was stirred at 23 °C and sparged with oxygen gas (balloon) for 3 minutes. Alkene **143a** (42.9 mg, 0.20 mmol, 1.00 equiv) was added dropwise by syringe, and the reaction mixture was sparged with oxygen for another minute. The reaction was stirred under oxygen atmosphere at 23 °C for 12 hours, when TLC analysis indicated consumption of starting material. The solvent was removed under reduced pressure, and the residue was loaded onto a short plug of silica gel, eluting with 30% ethyl acetate in hexanes (100 mL). The oil obtained upon concentration was then redissolved in THF (4 mL total volume) and cooled to 0 °C using an ice water bath. Carbomethoxy methylene triphenyl phosphorane (100.3 mg, 0.30 mmol, 1.50 equiv) was added in one portion, and the resulting mixture was stirred at 23 °C for 20 hours, at which time the reaction was transferred to a separatory funnel with diethyl ether and washed sequentially with water (5 mL) and brine (5 mL). The organic layer was dried over sodium sulfate, filtered, and concentrated to a crude yellow oil. Purification by silica gel column chromatography (10% ethyl acetate in hexanes) afforded α,β-unsaturated methyl ester **151** as a colorless oil (49.3 mg, 86% yield). Rf = 0.56 (33% ethyl acetate in hexanes); ^{1}H NMR ($CDCl_3$, 300 MHz) δ 6.93 (dtd, J = 15.3, 6.7, 1.8 Hz, 1H), 5.83 (dt, J = 15.7, 1.7 Hz, 1H), 4.17 (qd, J = 7.2, 1.7 Hz, 4H), 3.71 (d, J = 1.9 Hz, 3H), 2.26–2.10 (m, 2H), 2.04–1.92 (m, 2H), 1.41 (d, J = 1.7 Hz, 3H), 1.24 (td, J = 7.1, 1.7 Hz, 6H); ^{13}C NMR ($CDCl_3$, 126 MHz) δ 172.0, 167.0, 148.1, 121.5, 61.5, 53.4, 51.6, 33.9, 27.3, 20.1, 14.2; IR (Neat Film, KBr) 2984, 2951, 1734, 1730, 1659, 1437, 1268, 1234, 1110, 1024, 858 cm^{-1}; HRMS (FAB+) *m/z* calc'd for $C_{14}H_{23}O_6$ $[M+H]^+$: 287.1489, found 287.1485.

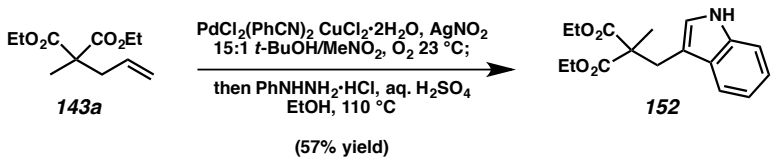

Diethyl 2-((1*H*-indol-3-yl)methyl)-2-methylmalonate (152). To a flame-dried 25-mL round-bottom flask with a magnetic stir bar were added bis(benzonitrile)palladium(II) chloride (23.0 mg, 0.060 mmol, 0.12 equiv), copper(II) chloride dihydrate (10.2 mg, 0.060 mmol, 0.12 equiv), and silver nitrite (4.6 mg, 0.030 mmol, 0.06 equiv). The flask was capped with a rubber septum, and *tert*-butyl alcohol (9.4 mL) and nitromethane (0.60 mL) were added sequentially by syringe. The mixture was stirred at 23 °C and sparged with oxygen gas (balloon) for 3 minutes. Alkene **143a** (107 mg, 0.50 mmol, 1.00 equiv) was added dropwise by syringe, and the reaction mixture was sparged with oxygen for another minute. The reaction was stirred under oxygen atmosphere at 23 °C for 12 hours, when TLC analysis indicated consumption of starting material. The solvent was removed under reduced pressure, and the residue was loaded onto a short plug of silica gel, eluting with 30% ethyl acetate in hexanes (100 mL). The oil obtained upon concentration was then diluted with a pre-heated solution (50 °C) of 4% aqueous sulfuric acid (4.7 mL) and phenyl hydrazine hydrochloride (79.5 mg, 0.550 mmol, 1.10 equiv). After addition of ethanol (3.5 mL), the mixture was heated to reflux at 110 °C for 7 hours. The reaction mixture was cooled to 23 °C and treated with saturated aqueous sodium bicarbonate and ethyl acetate. The phases were separated, and the aqueous layer was extracted with ethyl acetate (2 x 20 mL). The combined organic extracts were dried over sodium sulfate before filtration and concentration under reduced pressure. The crude residue was purified by silica gel column chromatography (20% ethyl acetate in hexanes) to afford indole **152** as yellow oil (86.1 mg, 57% yield).

R*f* = 0.44 (33% ethyl acetate in hexanes); ^{1}H NMR ($CDCl_3$, 500 MHz) δ 8.17 (s, 1H), 7.59 (d, *J* = 7.9 Hz, 1H), 7.32 (dt, *J* = 8.1, 1.0 Hz, 1H), 7.11 (ddd, *J* = 8.0, 7.0, 1.1 Hz, 1H), 6.98 (d, *J* = 2.4 Hz, 1H), 6.98 (d, *J* = 2.4 Hz, 1H), 4.27–4.10 (m, 4H), 3.41 (d, *J* = 0.9 Hz, 2H), 1.44 (s, 3H), 1.24 (t, *J* = 7.1 Hz, 6H); ^{13}C NMR ($CDCl_3$, 126 MHz) δ 172.6, 135.9, 128.5, 123.5, 121.9, 119.5, 111.2, 110.5, 61.4, 55.4, 30.7, 20.4, 14.1; IR (Neat Film, KBr) 3403, 2983, 1728, 1458, 1293, 1254, 1106, 1021, 861, 743 cm^{-1}; HRMS (ESI+) *m/z* calc'd for $C_{17}H_{22}NO_4$ $[M+H]^+$: 304.1543, found 304.1548.

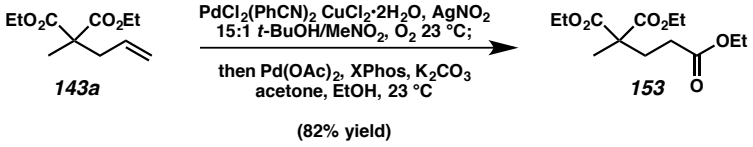

Triethyl butane-1,3,3-tricarboxylate (153). To a flame-dried 25-mL round-bottom flask with a magnetic stir bar were added bis(benzonitrile)palladium(II) chloride (9.2 mg, 0.024 mmol, 0.12 equiv), copper(II) chloride dihydrate (4.1 mg, 0.024 mmol, 0.12 equiv), and silver nitrite (1.8 mg, 0.012 mmol, 0.06 equiv). The flask was capped with a rubber septum, and *tert*-butyl alcohol (3.75 mL) and nitromethane (0.25 mL) were added sequentially by syringe. The mixture was stirred at 23 °C and sparged with oxygen gas (balloon) for 3 minutes. Alkene **143a** (42.9 mg, 0.20 mmol, 1.00 equiv) was added dropwise by syringe, and the reaction mixture was sparged with oxygen for another minute. The reaction was stirred under oxygen atmosphere at 23 °C for 12 hours, when TLC analysis indicated consumption of starting material. The solvent was removed under reduced pressure, and the residue was loaded onto a short plug of silica gel, eluting with 30% ethyl acetate in hexanes (100 mL). The oil obtained upon concentration was then redissolved in degassed ethanol (2 mL), and oven-dried potassium carbonate (10.0

mg, 0.072 mmol, 0.36 equiv) was added. After stirring for 20 minutes, a solution of palladium(II) acetate (2.2 mg, 0.01 mmol, 0.05 equiv) and XPhos (9.5 mg, 0.02 mmol, 0.10 equiv) in acetone (2 mL) that had been stirring at 23 °C for 20 minutes was added via syringe under argon atmosphere. The resulting dark green solution was stirred at 23 °C for 6 hours, at which time the volatiles were removed under reduced pressure. The crude residue obtained was purified by silica gel column chromatography (8% ethyl acetate in hexanes) to furnish tri-ester **153** as a colorless oil (45.0 mg, 82% yield). R*f* = 0.53 (33% ethyl acetate in hexanes); ^{1}H NMR ($CDCl_3$, 500 MHz) δ 4.16 (q, *J* = 7.1, 0.8 Hz, 4H), 4.11 (q, *J* = 7.2, 0.9 Hz, 2H), 2.38–2.27 (m, 2H), 2.23–2.13 (m, 2H), 1.39 (s, 3H), 1.23 (td, *J* = 7.1, 0.8 Hz, 9H); ^{13}C NMR ($CDCl_3$, 126 MHz) δ 173.0, 171.9, 61.5, 60.6, 53.0, 30.7, 29.9, 20.2, 14.3; IR (Neat Film, KBr) 2982, 2941, 1738, 1732, 1466, 1380, 1243, 1185, 1109, 1025, 860 cm^{-1}; HRMS (ESI+) *m/z* calc'd for $C_{13}H_{23}O_6$ $[M+H]^+$: 275.1489, found 275.1483.

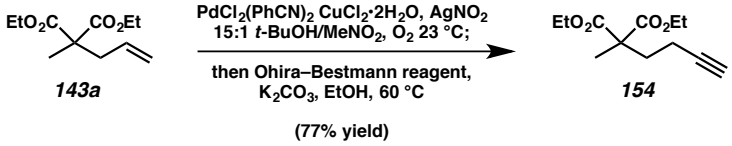

Diethyl 2-(but-3-yn-1-yl)-2-methylmalonate (154). To a flame-dried 25-mL round-bottom flask with a magnetic stir bar were added bis(benzonitrile)palladium(II) chloride (9.2 mg, 0.024 mmol, 0.12 equiv), copper(II) chloride dihydrate (4.1 mg, 0.024 mmol, 0.12 equiv), and silver nitrite (1.8 mg, 0.012 mmol, 0.06 equiv). The flask was capped with a rubber septum, and *tert*-butyl alcohol (3.75 mL) and nitromethane (0.25 mL) were added sequentially by syringe. The mixture was stirred at 23 °C and sparged with oxygen gas (balloon) for 3 minutes. Alkene **143a** (42.9 mg, 0.20 mmol, 1.00 equiv) was

added dropwise by syringe, and the reaction mixture was sparged with oxygen for another minute. The reaction was stirred under oxygen atmosphere at 23 °C for 12 hours, when TLC analysis indicated consumption of starting material. The solvent was removed under reduced pressure, and the residue was loaded onto a short plug of silica gel, eluting with 30% ethyl acetate in hexanes (100 mL). The oil obtained upon concentration was then redissolved in ethanol (4 mL), and potassium carbonate (33.2 mg, 0.24 mmol, 1.20 equiv) and Ohira–Bestmann reagent (46.1 mg, 0.24 mmol, 1.20 equiv) were added. The resulting mixture was stirred at 60 °C for 24 hours, at which time the reaction was quenched with water (4 mL), diluted with diethyl ether (2 mL), and washed with 5% aqueous sodium bicarbonate. The organic layer was dried over magnesium sulfate, filtered, and concentrated. The crude residue obtained was purified by silica gel column chromatography (8% ethyl acetate in hexanes) to furnish alkyne **154** as a colorless oil (35.0 mg, 77% yield). R*f* = 0.72 (33% ethyl acetate in hexanes); ^{1}H NMR ($CDCl_3$, 300 MHz) δ 4.18 (q, *J* = 7.1 Hz, 4H), 2.28–2.06 (m, 4H), 1.95 (t, *J* = 2.5 Hz, 1H), 1.42 (s, 3H), 1.25 (t, *J* = 7.1 Hz, 7H); ^{13}C NMR ($CDCl_3$, 75 MHz) δ 171.9, 83.5, 68.8, 61.5, 53.2, 34.6, 20.0, 14.3, 14.2; IR (Neat Film, KBr) 3291, 2983, 1731, 1465, 1381, 1265, 1189, 1109, 1025, 861, 659 cm^{-1}; HRMS (FAB+) *m/z* calc'd for $C_{12}H_{20}O_4$ $[M+H]^+$: 227.1283, found 227.1287.

3.8 NOTES AND REFERENCES

(1) Bäckvall, J.-E. *Acc. Chem. Res.* **1983**, *16*, 335–342.

(2) Smidt, J.; Hafner, W.; Jira, R.; Sedlmeier, J.; Sieber, R.; Rüttinger, R.; Kojer, H. *Angew. Chem.* **1959**, *71*, 176–182.

(3) (a) Tsuji, J. *Synthesis* **1984**, *1984*, 369–384; (b) Takacs, J.M.; Jiang, X.-T. *Curr. Org. Chem.* **2003**, 7, 369–396; (c) Tsuji, J. *Palladium Reagents and Catalysts: New Perspectives for the 21st Century*, 2nd ed. Wiley, Hoboken, **2004**; (d) Jira, R. *Angew. Chem., Int. Ed.* **2009**, 48, 9034–9037.

(4) Stahl, S. S. *Angew. Chem., Int. Ed.* **2004**, *43*, 3400–3420.

(5) Muzart, J. *Tetrahedron* **2007**, *63*, 7505–7521.

(6) For Wacker oxidation of internal alkenes, see: (a) Mitsudome, T.; Mizumoto, K; Mizugaki, T; Jitsukawa, K; Kaneda, K. *Angew. Chem., Int. Ed.* **2010**, *49*, 1238–1240; (b) Morandi, B.; Wickens, Z. K.; Grubbs, R. H. *Angew. Chem., Int. Ed.* **2013**, *52*, 2944–2948; (c) DeLuca, R. J.; Edwards, J. L.; Steffens, L. D.; Michel, B. W.; Qiao, X.; Zhu, C.; Cook, S. P.; Sigman, M. S. *J. Org. Chem.* **2013**, *78*, 1682–1686; (d) Mitsudome, T.; Yoshida, S; Mizugaki, T.; Jitsukawa, K.; Kaneda, K. *Angew. Chem., Int. Ed.* **2013**, *52*, 5961–5964; (e) Mitsudome, T.; Yoshida, S.; Tsubomoto, Y; Mizugaki, T.; Jitsukawa, K.; Kaneda, K. *Tetrahedron Lett.* **2013**,

54, 1596–1598; (f) Darabi, H. R.; Mirzakhani, M.; Aghapoor, K.; Jadidi, K.; Faraji, L; Sakhaee, N. *J. Organomet. Chem.* **2013**, *740*, 131–134; (g) Morandi, B.; Wickens, Z. K.; Grubbs, R. H. *Angew. Chem., Int. Ed.* **2013**, *52*, 9751–9754.

(7) For studies using dioxygen as the sole oxidant, see: (a) Mitsudome, T.; Umetani, T; Nosaka, N.; Mori, K.; Mizugaki, T.; Ebitani, K.; Kaneda, K. *Angew. Chem., Int. Ed.* **2006**, *45*, 481–485; (b) Cornell, C. N.; Sigman, M. S. *Inorg. Chem.* **2007**, *46*, 1903–1909; (c) Gligorich, K. M.; Sigman, M. S. *Chem. Commun.* **2009**, 3854–3867; (d) Campbell, A. N.; Stahl, S. S. *Acc. Chem. Res.* **2012**, *45*, 851–863.

(8) For catalyst-controlled Wacker oxidation with Markovnikov selectivity, see: (a) Michel, B. W.; Camelio, A. M.; Cornell, C. N.; Sigman, M. S. *J. Am. Chem. Soc.* **2009**, *131*, 6076–6077; (b) Michel, B. W.; McCombs, J. R.; Winkler, A.; Sigman, M. S. *Angew. Chem., Int. Ed.* **2010**, *49*, 7312–7315; (c) Sigman, M. S.; Werner, E. W. *Acc. Chem. Res.* **2012**, *45*, 874–884.

(9) Wickens, Z. K.; Morandi, B.; Grubbs, R. H. *Angew. Chem., Int. Ed.* **2013**, *52*, 11257–11260. An alternative method has recently been reported by the Kang group: Ning, X.-S.; Wang, M.-M.; Yao, C.-Z.; Chen, X.-M.; Kang, Y.-B. *Org. Lett.* **2016**, *18*, 2700–2703.

(10) (a) Weiner, B.; Baeza, A.; Jerphagnon, T.; Feringa, B. L. *J. Am. Chem. Soc.* **2009**, *131*, 9473–9474; (b) Dong, J. J.; Fañanás-Mastral, M.; Alsters, P. L.; Browne, W.

R.; Feringa, B. L. *Angew. Chem., Int. Ed.* **2013**, *52*, 5561–5565; (c) Wright, J. A.; Gaunt, M. J.; Spencer, J. B. *Chem.–Eur. J.* **2006**, *12*, 949–955; (d) Teo, P.; Wickens, Z. K.; Dong, G.; Grubbs, R. H. *Org. Lett.* **2012**, *14*, 3237–3239; (e) Yamamoto, M.; Nakaoka, S.; Ura, Y.; Kataoka, Y. *Chem. Commun.* **2012**, *48*, 1165–1167.

(11) While investigations into the complex mechanism of this transformation are still ongoing, evidence suggests that a *t*-BuOH-ligated nitrite Pd–Cu species promotes selective formation of the aldehyde. For detailed mechanistic analysis, see: (a) Jiang, Y.-Y.; Zhang, Q.; Yu, H.-Z.; Fu, Y. *ACS Catal.* **2015**, *5*, 1414–1423; b) Anderson, B. J.; Keith, J. A.; Sigman, M. S. *J. Am. Chem. Soc.* **2010**, *132*, 11872–11874; (c) Keith, J. A.; Nielsen, R. J.; Oxgaard, J.; Goddard, W. A., III *J. Am. Chem. Soc.* **2007**, *129*, 12342–12343.

(12) Wickens, Z. K.; Skakuj, K.; Morandi, B.; Grubbs, R. H. *J. Am. Chem. Soc.* **2014**, *136*, 890–893.

(13) (a) Behenna, D. C.; Stoltz, B. M. *J. Am. Chem. Soc.* **2004**, *126*, 15044–15045; (b) Behenna, D. C.; Mohr, J. T.; Sherden, N. H.; Marinescu, S. C.; Harned, A. M.; Tani, K.; Seto, M.; Ma, S.; Novák, Z.; Krout, M. R.; McFadden, R. M.; Roizen, J. L.; Enquist, J. A. Jr.; White, D. E.; Levine, S. R.; Petrova, K. V.; Iwashita, A.; Virgil, S. C.; Stoltz, B. M. *Chem.–Eur. J.* **2011**, *17*, 14199–14223; (c) Behenna, D. C.; Liu, Y.; Yurino, T.; Kim, J.; White, D. E.; Virgil, S. C.; Stoltz, B. M. *Nat.*

Chem. **2012**, *4*, 130–133; (d) Reeves, C. M.; Eidamshaus, C.; Kim, J.; Stoltz, B. M. *Angew*. *Chem., Int*. *Ed*. **2013**, *52*, 6718–6721; (e) Liu, Y.; Han, S.-J.; Liu, W.-B.; Stoltz, B. M. *Acc*. *Chem*. *Res*. **2015**, *48*, 740–751; (f) Craig, R. A., II; Loskot, S. A.; Mohr, J. T.; Behenna, D. C.; Harned, A. M.; Stoltz, B. M. *Org*. *Lett*. **2015**, *17*, 5160–5163.

(14) For reviews on the use of enantioselective decarboxylative allylic alkylations in total synthesis, see: Hong, A. Y.; Stoltz, B. M. *Eur*. *J*. *Org*. *Chem*. **2013**, 2745–2759.

(15) For selected examples of total syntheses using enantioselective decarboxylative allylic alkylation, see: (a) Trost, B. M.; Pissot-Soldermann, C.; Chen, I.; Schroeder, G. M. *J*. *Am*. *Chem*. *Soc*. **2004**, *126*, 4480–4481; (b) McFadden, R. M.; Stoltz, B. M. *J*. *Am*. *Chem*. *Soc*. **2006**, *128,* 7738–7739; (c) Varseev, G. N.; Maier, M. E. *Angew*. *Chem., Int*. *Ed*. **2009**, *48*, 3685–3688; (d) Enquist, J. A. Jr.; Stoltz, B. M. *Nature*, **2008**, *453*, 1228–1231; (e) Enquist, J. A., Jr.; Virgil, S. C.; Stoltz, B. M. *Chem.–Eur*. *J*. **2011**, *17*, 9957–9969; (f) Hong, A. Y.; Stoltz, B. M. *Angew*. *Chem., Int*. *Ed*. **2012**, *51*, 9674–9678.

(16) Xing, X.; O'Connor, N. R.; Stoltz, B. M. *Angew*. *Chem., Int*. *Ed*. **2015**, *54*, 11186–11190.

(17) Anhydrous CuCl and $CuCl_2$ were also examined as copper sources, but use of $CuCl_2 \bullet 2H_2O$ resulted in the highest yields.

(18) When unprotected **143d** was subjected to the aldehyde-selective Wacker conditions, mixtures containing several inseparable compounds were obtained after purification.

(19) Lactams bearing quaternary carbons at the homoallylic position were also investigated as substrates. These compounds reacted sluggishly, and only low yields (32–37%) of the aldehyde product were obtained, often contaminated by enal side product.

(20) Liu, Y.; Virgil, S. C.; Grubbs, R. H.; Stoltz, B. M. *Angew. Chem., Int. Ed.* **2015**, *54*, 11800–11803.

(21) For general reviews on hydroamination, see: (a) Müller, T. E.; Hultzsch, K. C.; Yus, M.; Foubelo, F.; Tada, M. *Chem. Rev.* **2008**, *108*, 3795–3892; (b) Hultzsch, K. C. *Adv. Synth. Catal.* **2005**, *347*, 367–391; (c) Beller, M.; Seayad, J.; Tillack, A.; Jiao, H. *Angew. Chem., Int. Ed.* **2004**, *43*, 3368–3398.

(22) (a) Henkel, T.; Brunne, R. M.; Müller, H.; Reichel, F. *Angew. Chem., Int. Ed.* **1999**, *38*, 643–647; (b) Hili, R.; Yudin, A. K. *Nat. Chem. Biol.* **2006**, *2*, 284–287.

(23) (a) Beller, M.; Trauthwein, H.; Eichberger, M.; Breindl, C.; Herwig, J.; Müller, T. E.; Thiel, O. R. *Chem.–Eur. J.* , **1999**, *5*, 1306–1319; (b) Horrillo-Martínez, P.; Hultzsch, K. C.; Gil, A.; Branchadell, V. *Eur. J. Org. Chem.* **2007**, *2007*, 3311–3325; (c) Kumar, K.; Michalik, D.; Castro, I. G.; Tillack, A.; Zapf, A.; Arlt, M.; Heinrich, T.; Böttcher, H.; Beller, M. *Chem.–Eur. J.* **2004**, *10*, 746–757; (d) Ryu, J.-S.; Li, G. Y.; Marks, T. J. *J. Am. Chem. Soc.* **2003**, *125*, 12584–12605; (e) Barrett, A. G. M.; Brinkmann, C.; Crimmin, M. R.; Hill, M. S.; Hunt, P.; Procopiou, P. A. *J. Am. Chem. Soc.* **2009**, *131*, 12906–12907; (f) Bronner, S. M.; Grubbs, R. H. *Chem. Sci.* **2014**, *5*, 101–106; (g) Crimmin, M. R.; Casely, I. J.; Hill, M. S. *J. Am. Chem. Soc.* **2005**, *127*, 2042–2043; (h) Utsunomiya, M.; Kuwano, R.; Kawatsura, M.; Hartwig, J. F. *J. Am. Chem. Soc.* **2003**, *125*, 5608–5609; (i) Utsunomiya, M.; Hartwig, J. F. *J. Am. Chem. Soc.* **2004**, *126*, 2702–2703; (j) Rucker, R. P.; Whittaker, A. M.; Dang, H.; Lalic, G. *J. Am. Chem. Soc.* **2012**, *134*, 6571–6574; (k) Zhu, S.; Niljianskul, N.; Buchwald, S. L. *J. Am. Chem. Soc.* **2013**, *135*, 15746–15749; (l) Strom, A. E.; Hartwig, J. F. *J. Org. Chem.* **2013**, *78*, 8909–8914.

(24) Tschaen, B. A.; Schmink, J. R.; Molander, G. A. *Org. Lett.* **2013**, *15*, 500–503.

(25) Kim, K. E.; Li, J.; Grubbs, R. H.; Stoltz, B. M. *J. Am. Chem. Soc.* **2016**, *138*, 13179–13182.

(26) Pangborn, A. B.; Giardello, M. A.; Grubbs, R. H.; Rosen, R. K.; Timmers, F. J. *Organometallics* **1996**, *15*, 1518–1520.

(27) Pietruszka, J.; Witt, A. *Synthesis* **2006**, *24*, 4266–4268.

(28) Boers, R. B.; Randulfe, Y. P.; van der Haas, H. N. S.; van Rossum-Baan, M.; Lugtenburg, J. *Eur. J. Org. Chem.* **2002**, *2002*, 2094–2108.

(29) Hong, A. Y.; Krout, M. R.; Jensen, T.; Bennett, N. B.; Harned, A. M.; Stoltz, B. M. *Angew. Chem., Int. Ed.* **2011**, *50*, 2756–2760.

(30) Liu, W.-B.; Reeves, C. M.; Virgil, S. C.; Stoltz, B. M. *J. Am. Chem. Soc.* **2013**, *135*, 10626–10629.

(31) Zhang, X.; Jia, X.; Fang, L.; Liu, N.; Wang, J.; Fan, X. *Org. Lett.* **2011**, *13*, 5024–5027.

(32) Ghorai, M. K.; Talukdar, R.; Tiwari, D. P. *Org. Lett.* **2014**, *16*, 2204–2207.

APPENDIX 4

Supplementary Synthetic Information Relevant to Chapter 3

A4.1 INTRODUCTION

This section presents alkenes that were poor substrates for the nitrite-modified Tsuji–Wacker described in Chapter 3. These substrates were either unreactive, formed a complex mixture of products, generated only trace amounts of product, or supplied low yields of the desired aldehyde product.

A4.2 PRODUCTS FORMED IN LOW YIELD

Some substrates underwent oxidation under nitrite-modified Tsuji–Wacker conditions but generated aldehyde product in low yield. For instance, aldehydes **162–165** (Figure A4.1A) were isolated in low yields. Certain aldehyde products were formed as inseparable mixtures with ketone side products (**166–167**, Figure A4.1B). Notably, lactam substrates generally produced low yields of aldehyde product that were often contaminated by ketone side-product (**168–169**). Aldehydes **170** and **171** were formed in trace amounts, and aldehyde **172** was observed in situ (via disappearance of substrate by

TLC) but was difficult to isolate (Figure A4.1C). Similarly, aldehyde **176** was generated readily from oxindole substrate **175** but contained inseparable impurities (Scheme A4.1).

Figure A4.1 Aldehyde products formed in low yield under nitrite-modified Tsuji–Wacker conditions

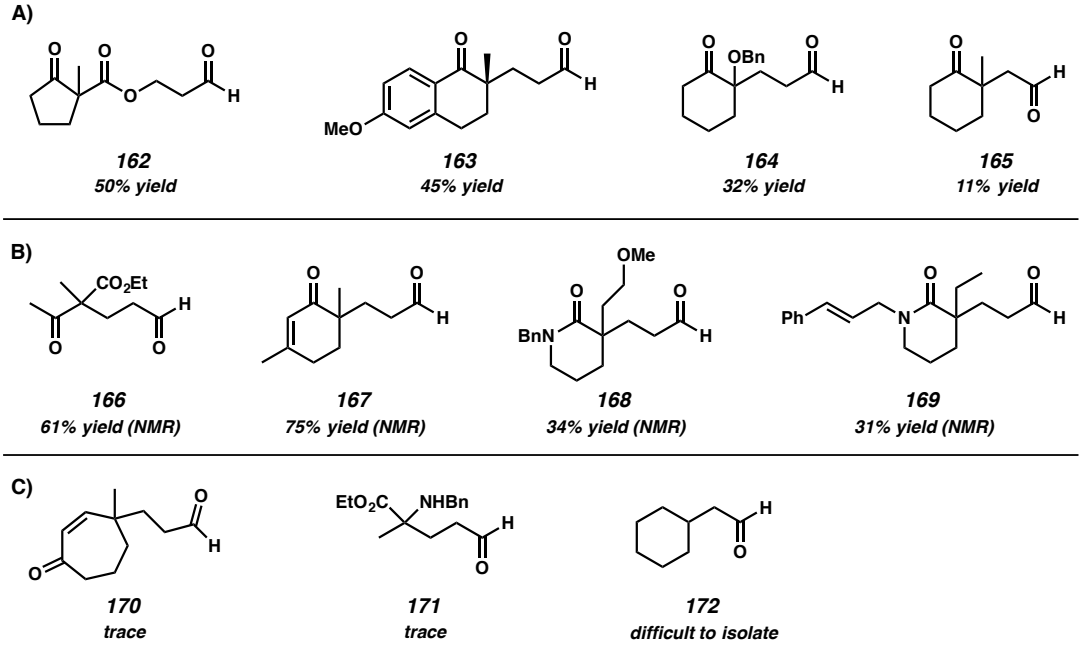

*Scheme A4.1 A) Synthesis of oxindole substrate **175** and B) subjection of **175** to nitite-modified Tsuji–Wacker conditions*

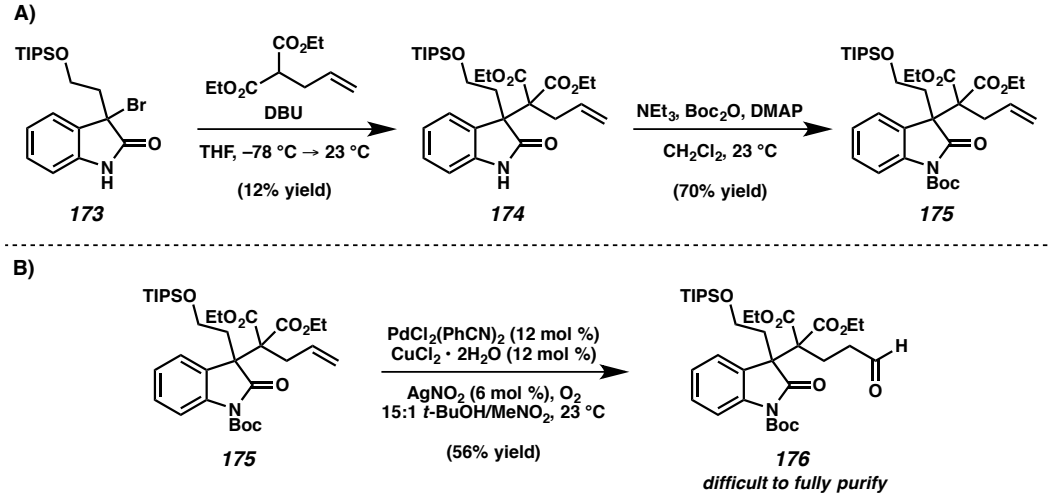

A4.3 SUBSTRATES THAT FORM A COMPLEX MIXTURE OF PRODUCTS

Figure A4.2 Substrates that form a mixture of inseparable products under nitrite-modified Tsuji–Wacker conditions

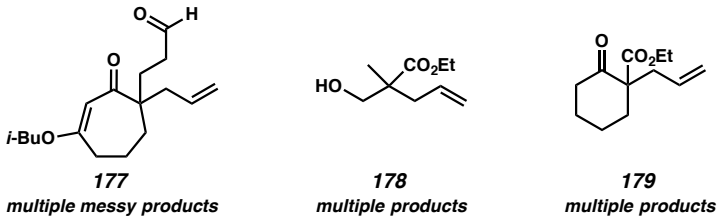

A4.4 UNREACTIVE SUBSTRATES

Some substrates were unreactive under the conditions for aldehyde-selective Tsuji–Wacker oxidation. These substrates include disubstituted olefins **180**–**181** (Figure A4.3A), dienes **182**–**183**, and enynes **184**–**185** (Figure A4.3B). We hypothesize that compounds **182**–**183** are unsuitable substrates for oxidation due to deactivation of the Pd catalyst through coordination to the second site of unsaturation in the substrate.

Figure A4.3 Substrates that do not react under nitrite-modified Tsuji–Wacker conditions

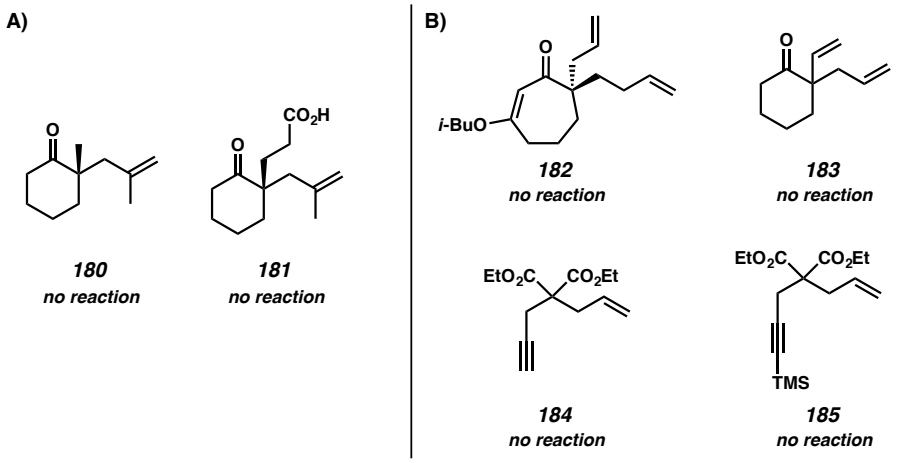

A4.5 FUTURE DIRECTIONS

These uncooperative substrates outline the limitations of the otherwise robust aldehyde-selective Tsuji–Wacker oxidation. A potential avenue for future exploration in this area is the addition of co-catalysts (i.e., Co) to pre-bind the alkyne moieties (e.g. in **184**–**185**) and thereby enable oxidation to proceed at the alkene. Issues in catalyst compatibility and side reactivity initiated by the co-catalyst may arise, however, and would need to be addressed.

APPENDIX 5

Spectra Relevant to Chapter 3:

The Aldehyde-Selective Tsuji–Wacker Oxidation, A Tool

for Facile Catalytic Transformations of Hindered Terminal Olefins

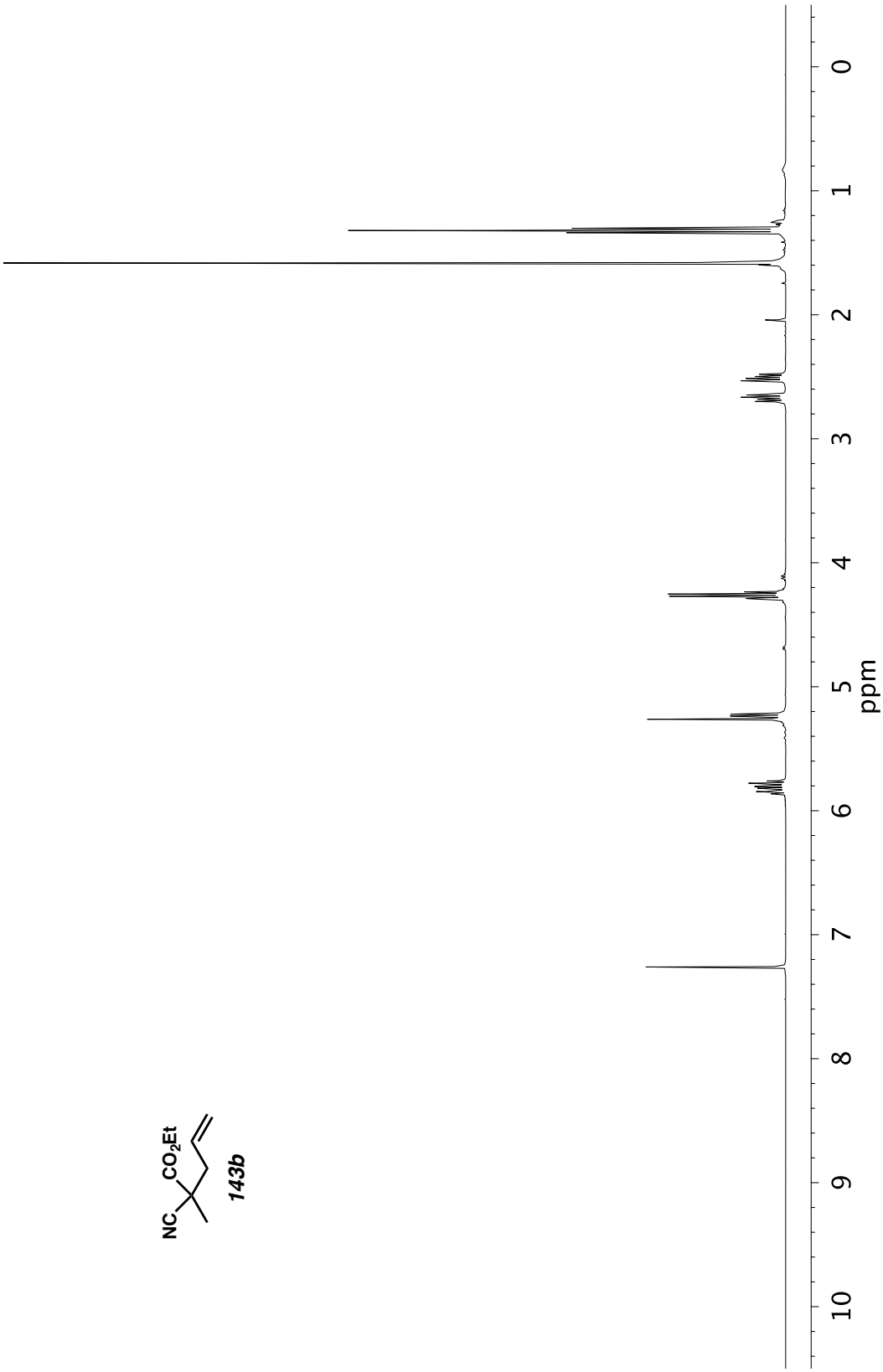

Figure A5.1. ^{1}H NMR (400 MHz, $CDCl_3$) of compound **143b**.

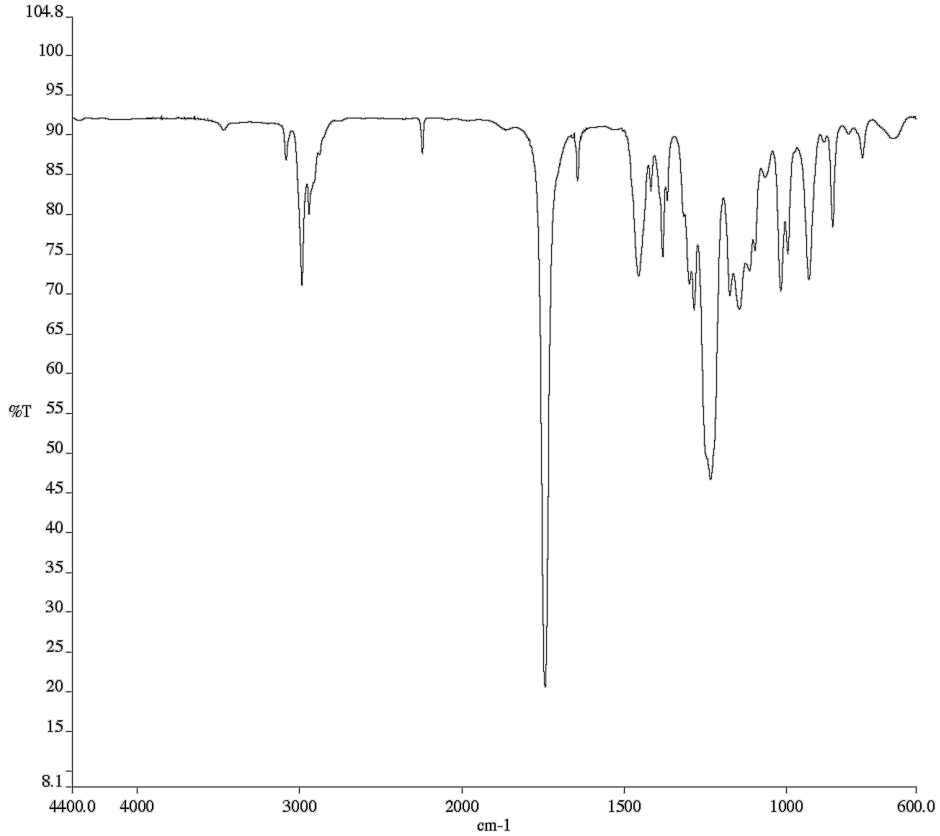

Figure A5.2. Infrared spectrum (Thin Film, KBr) of compound **143b**.

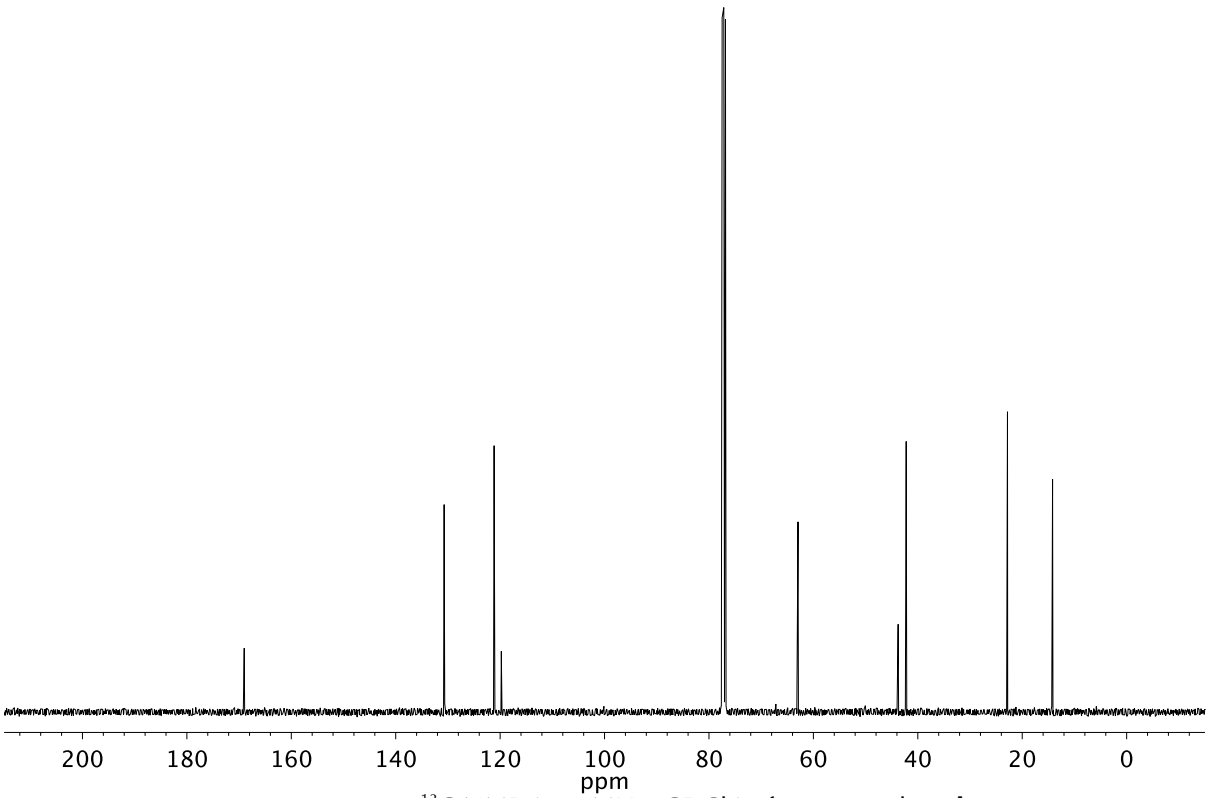

Figure A5.3. ^{13}C NMR (101 MHz, $CDCl_3$) of compound **143b**.

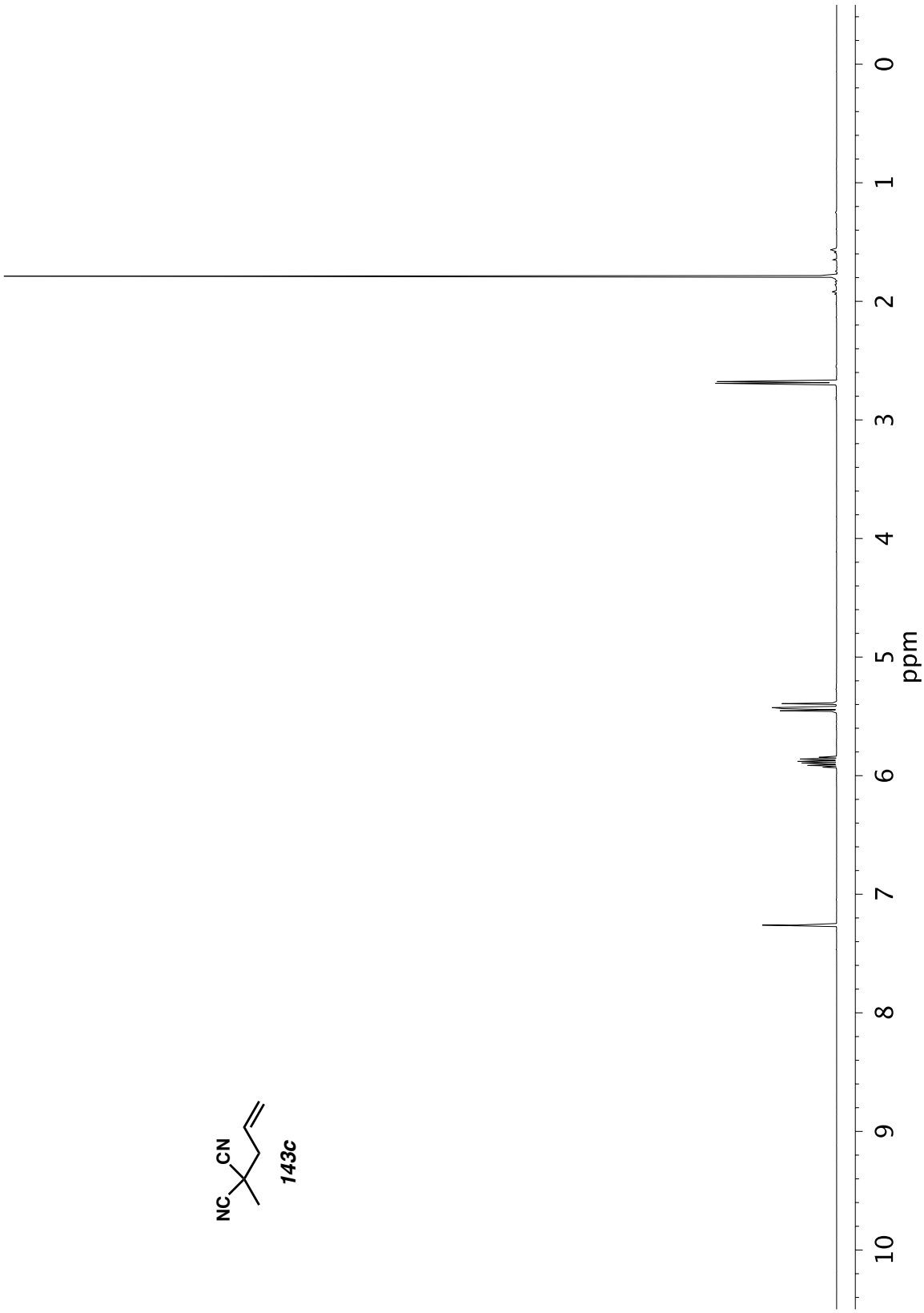

Figure A5.4. ^{1}H NMR (500 MHz, $CDCl_3$) of compound **143c**.

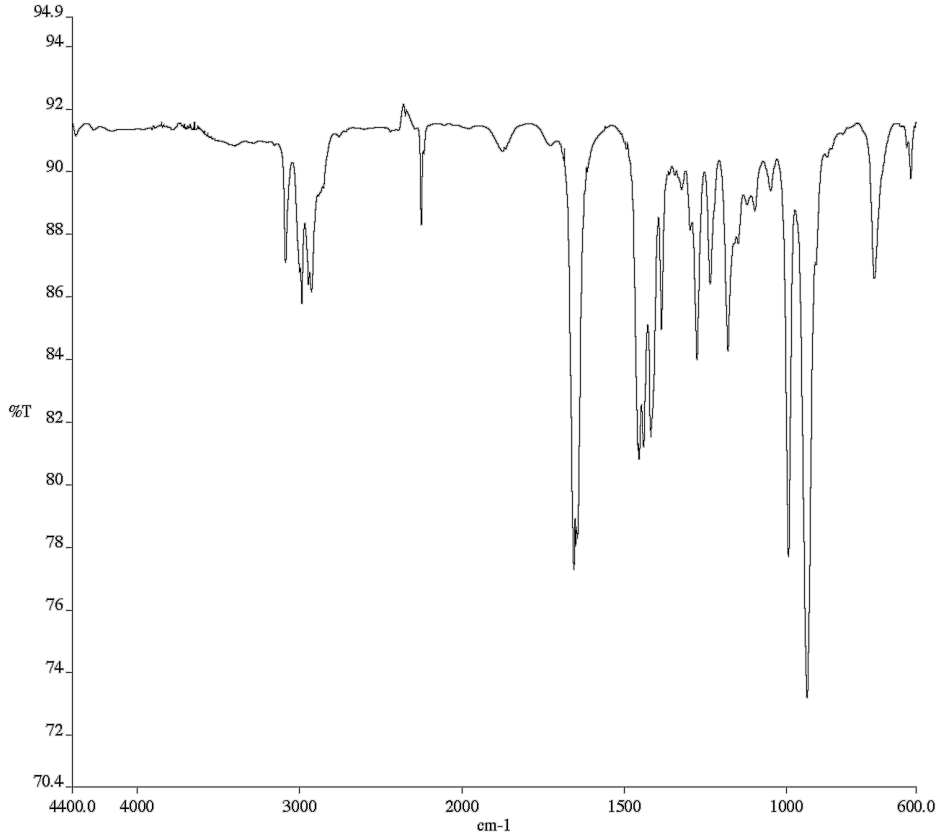

Figure A5.5. Infrared spectrum (Thin Film, KBr) of compound **143c**.

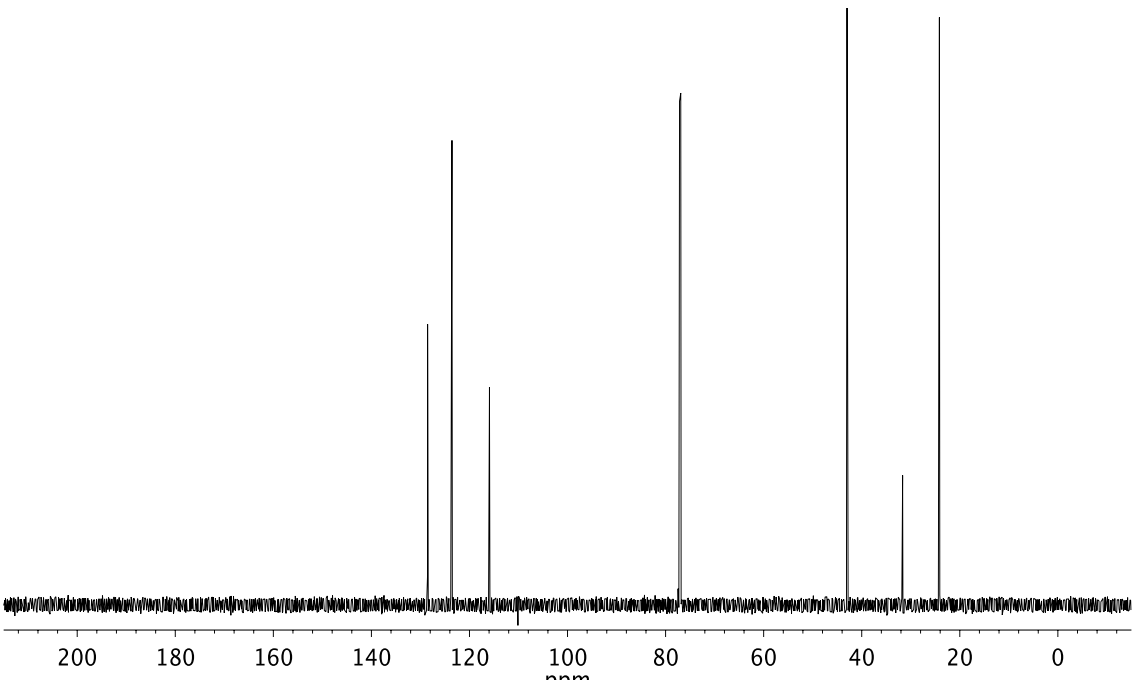

Figure A5.6. ^{13}C NMR (126 MHz, $CDCl_3$) of compound **143c**.

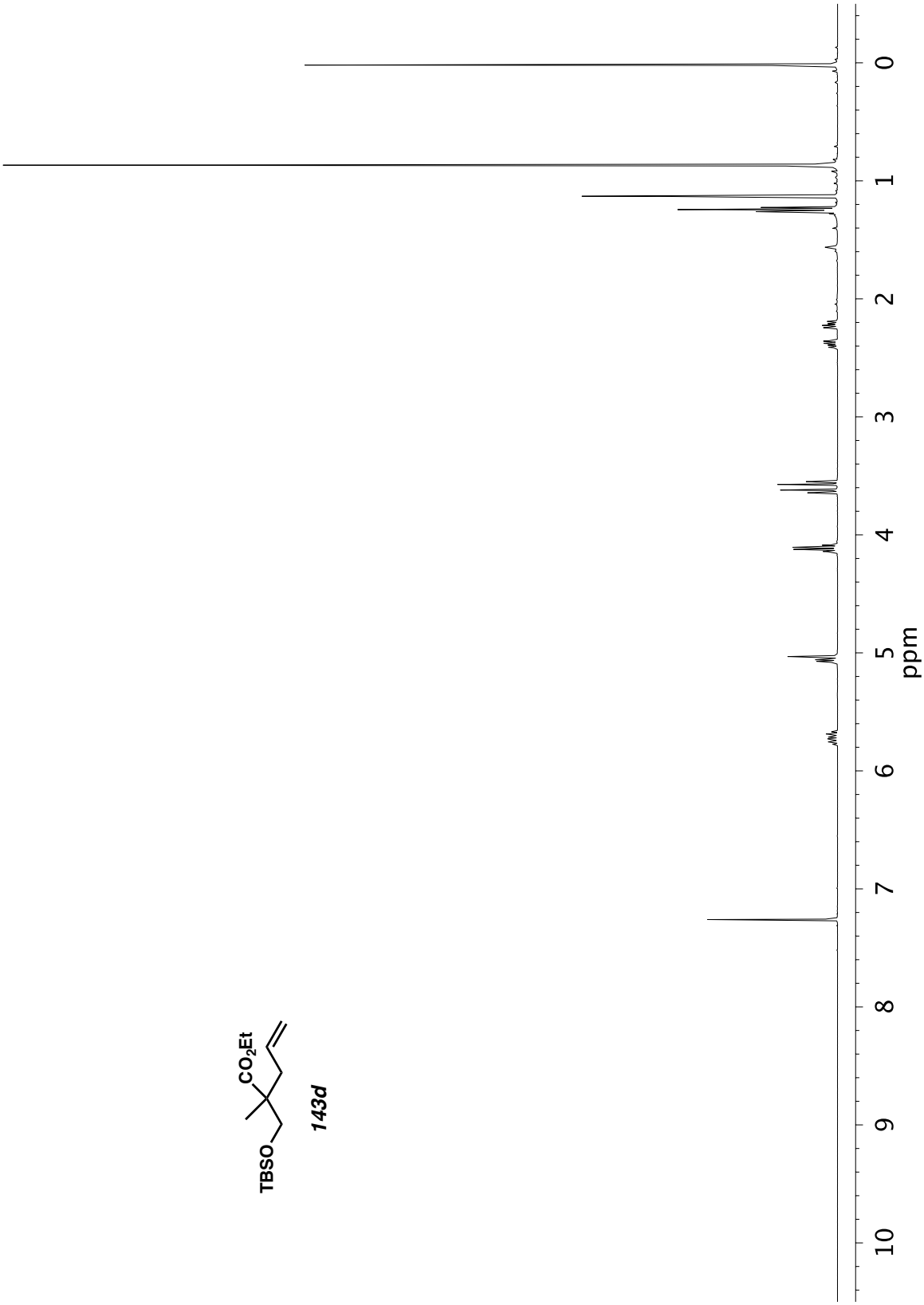

Figure A5.7. ^{1}H NMR (400 MHz, $CDCl_3$) of compound **143d**.

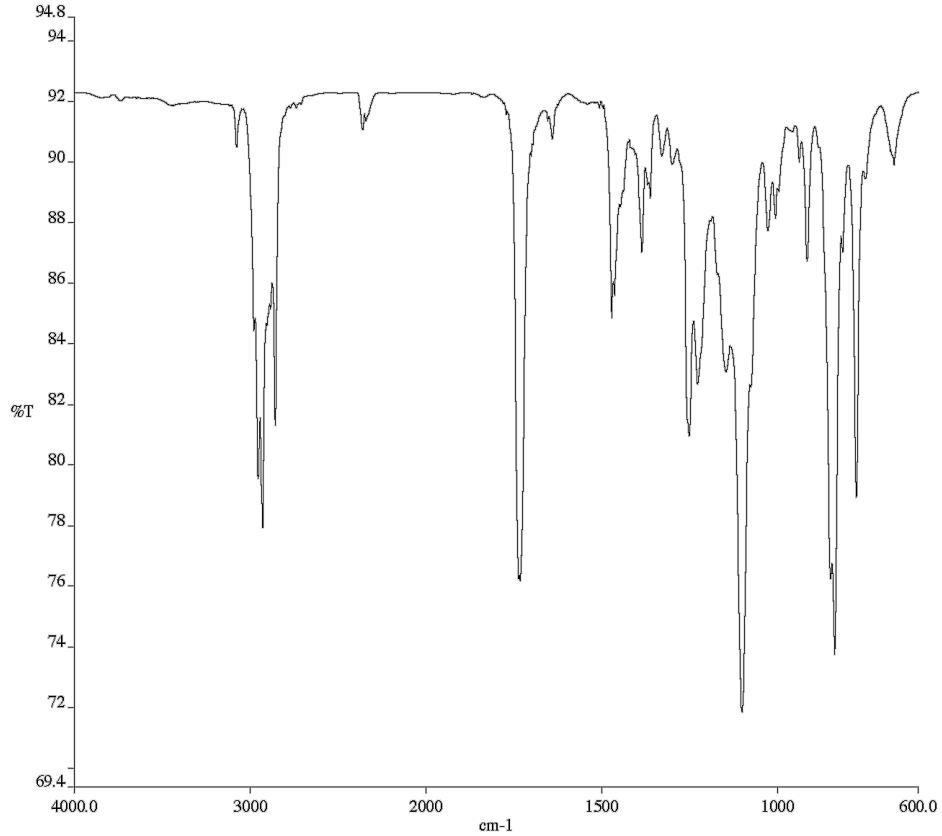

Figure A5.8. Infrared spectrum (Thin Film, KBr) of compound **143d**.

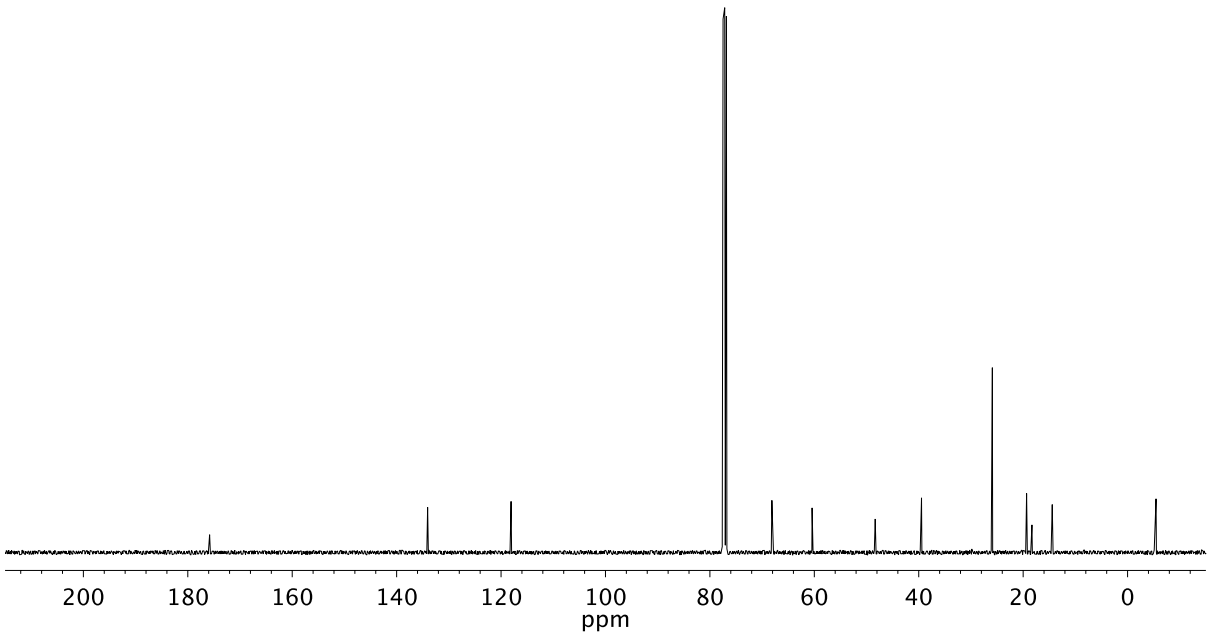

Figure A5.9. ^{13}C NMR (101 MHz, $CDCl_3$) of compound **143d**.

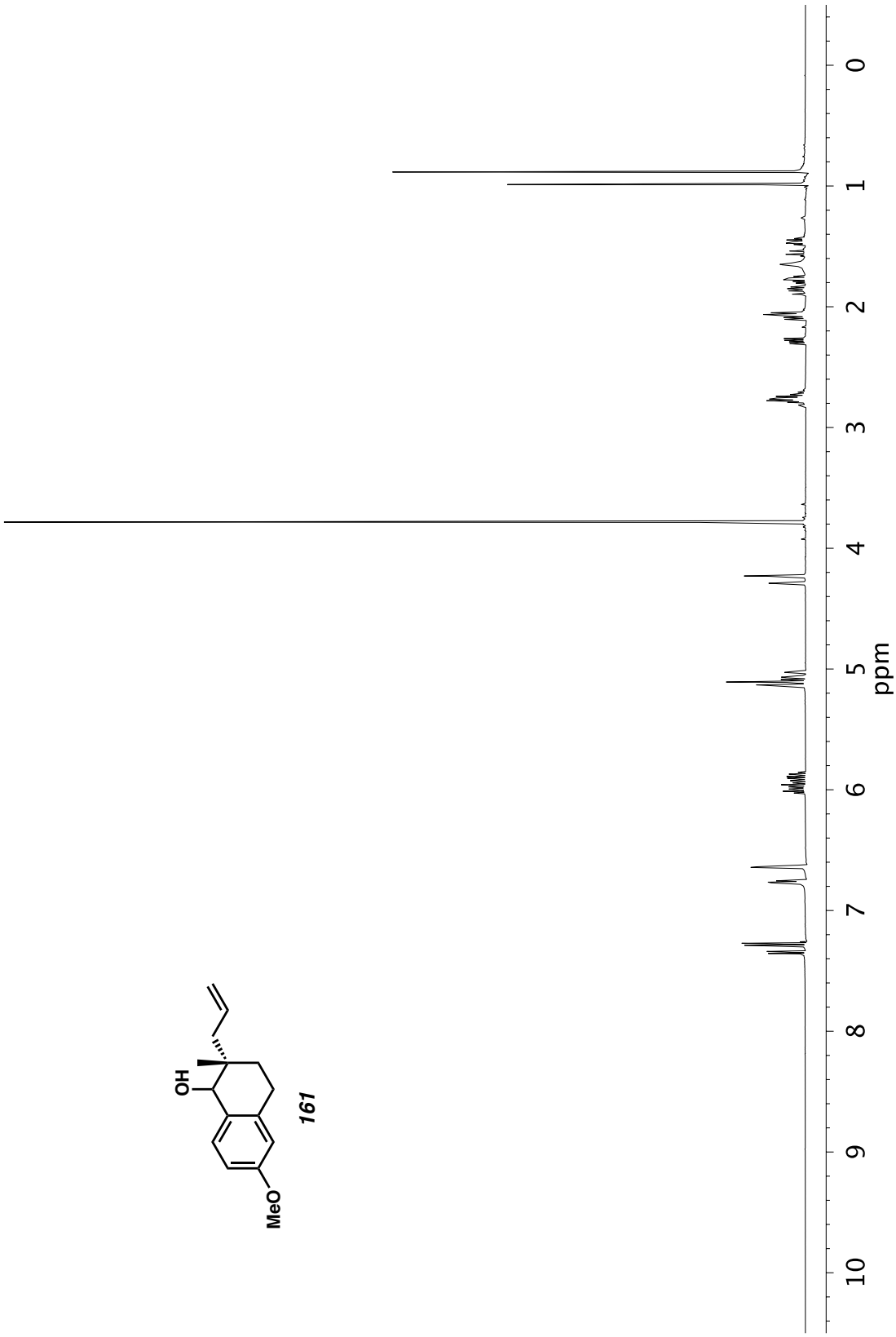

Figure A5.10. ^{1}H NMR (500 MHz, $CDCl_3$) of compound **161**.

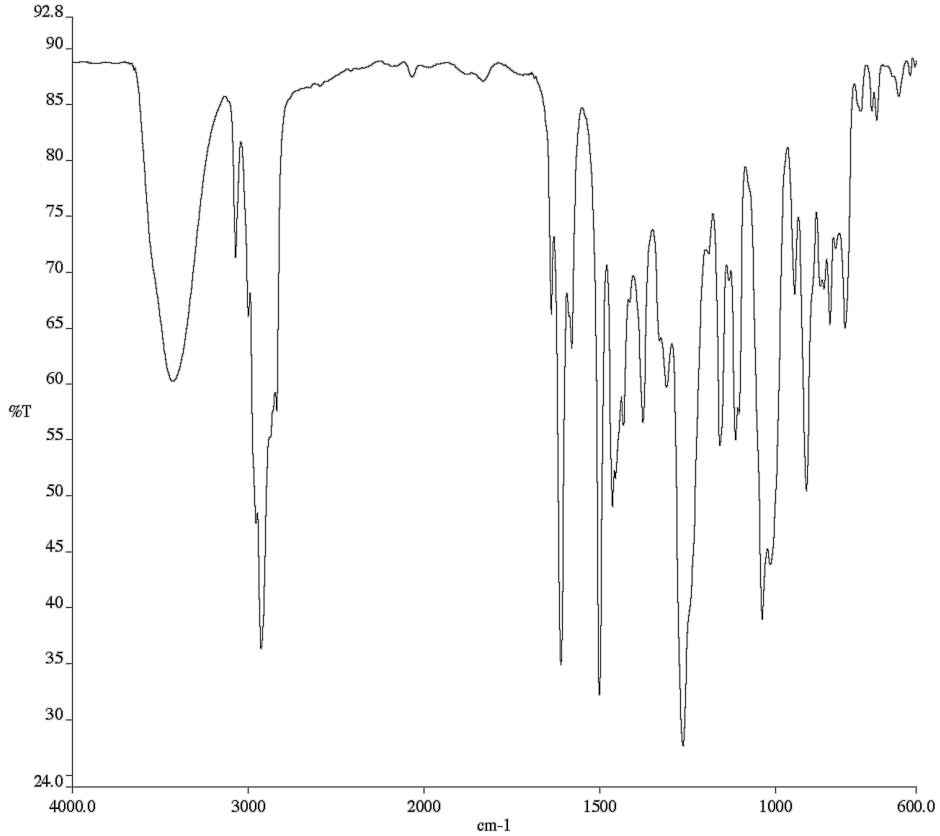

Figure A5.11. Infrared spectrum (Thin Film, KBr) of compound **161**.

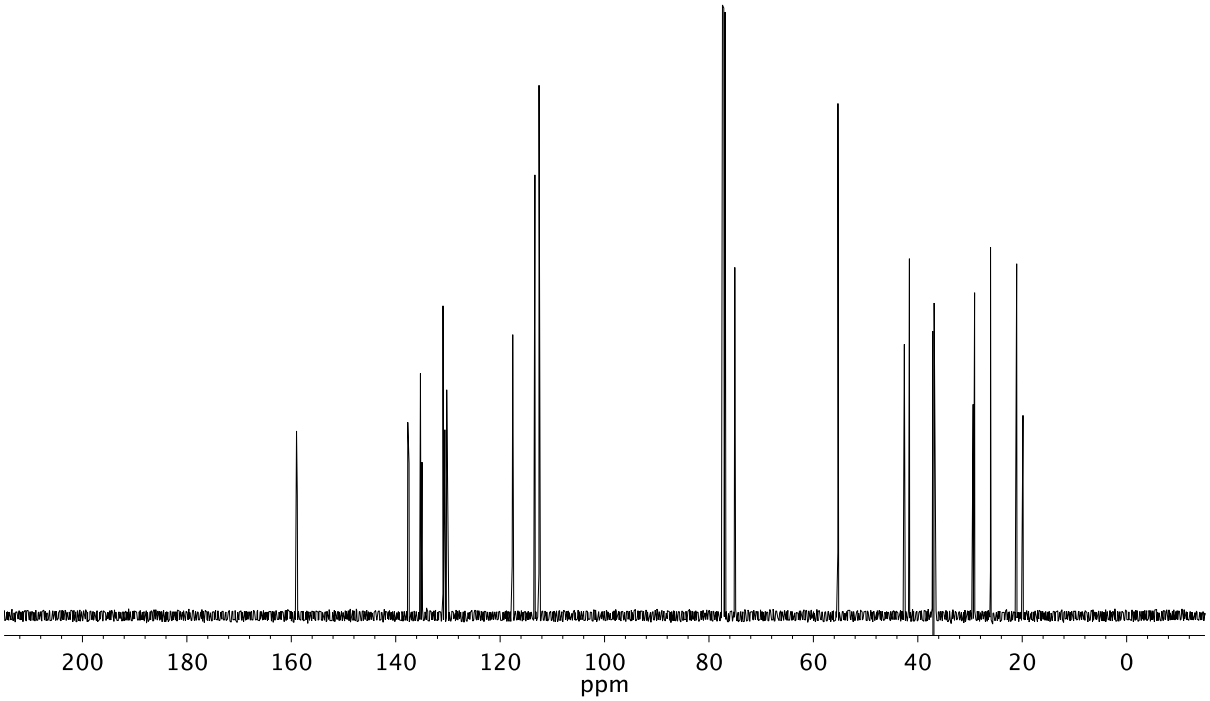

Figure A5.12. ^{13}C NMR (126 MHz, $CDCl_3$) of compound **161**.

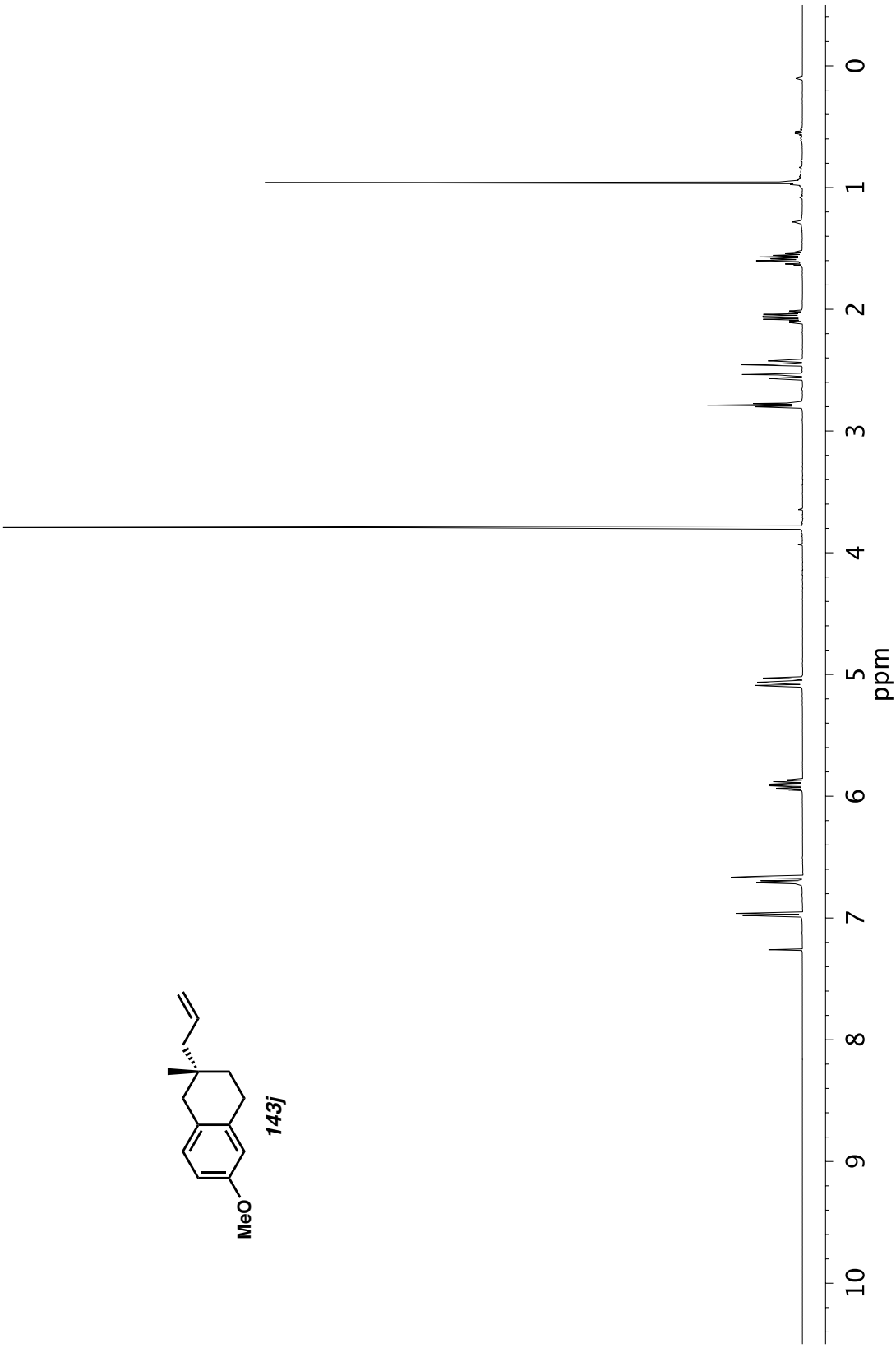

Figure A5.13. ^{1}H NMR (500 MHz, $CDCl_3$) of compound **143j**..

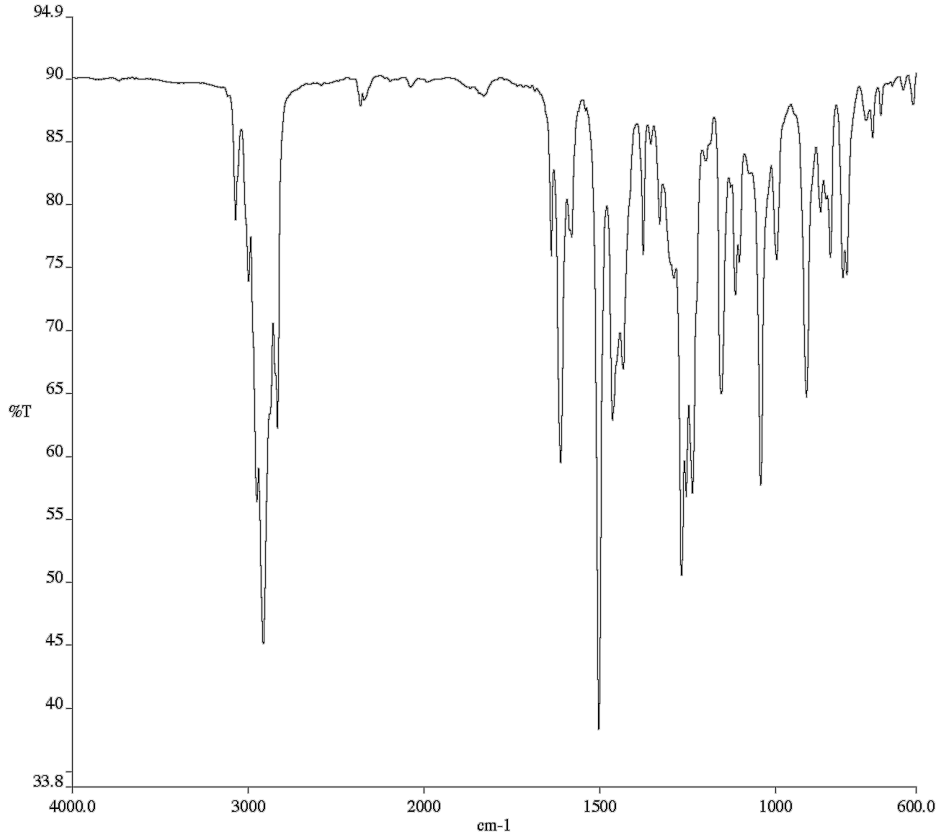

Figure A5.14. Infrared spectrum (Thin Film, KBr) of compound **143j**.

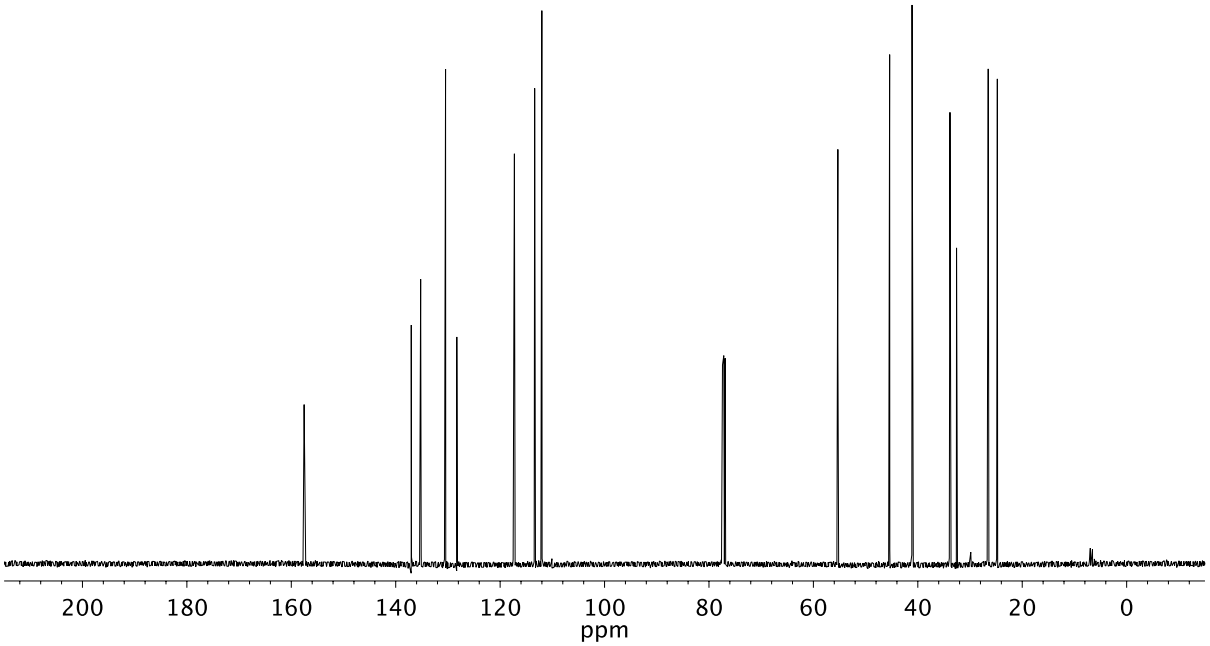

Figure A5.15. ^{13}C NMR (126 MHz, $CDCl_3$) of compound **143j**.

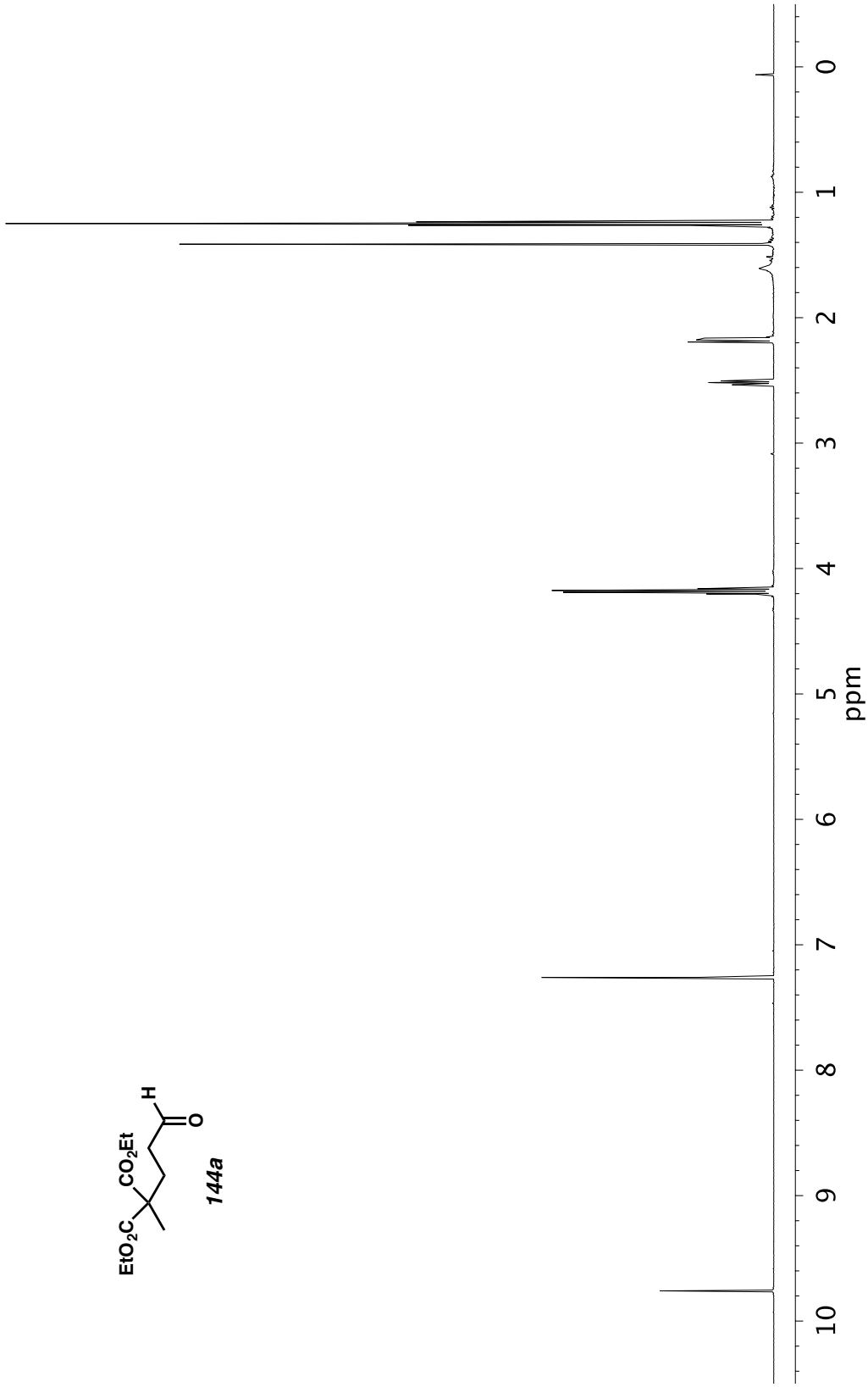

Figure A5.16. ^{1}H NMR (500 MHz, $CDCl_3$) of compound **144a**.

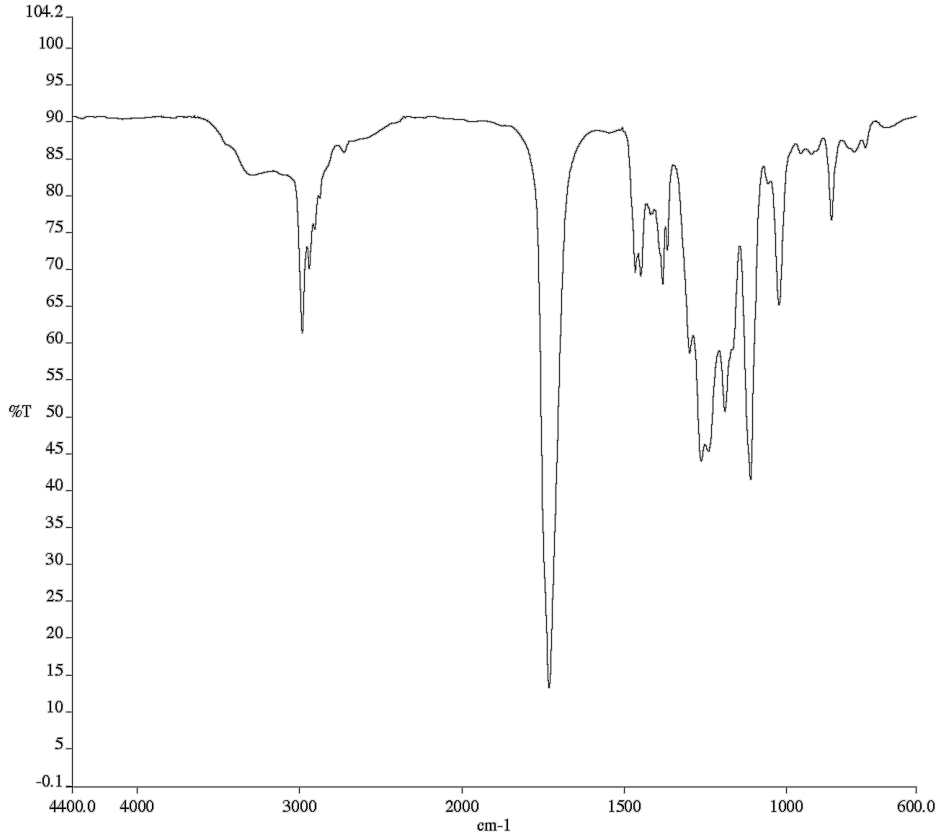

Figure A5.17. Infrared spectrum (Thin Film, KBr of compound **144a**.

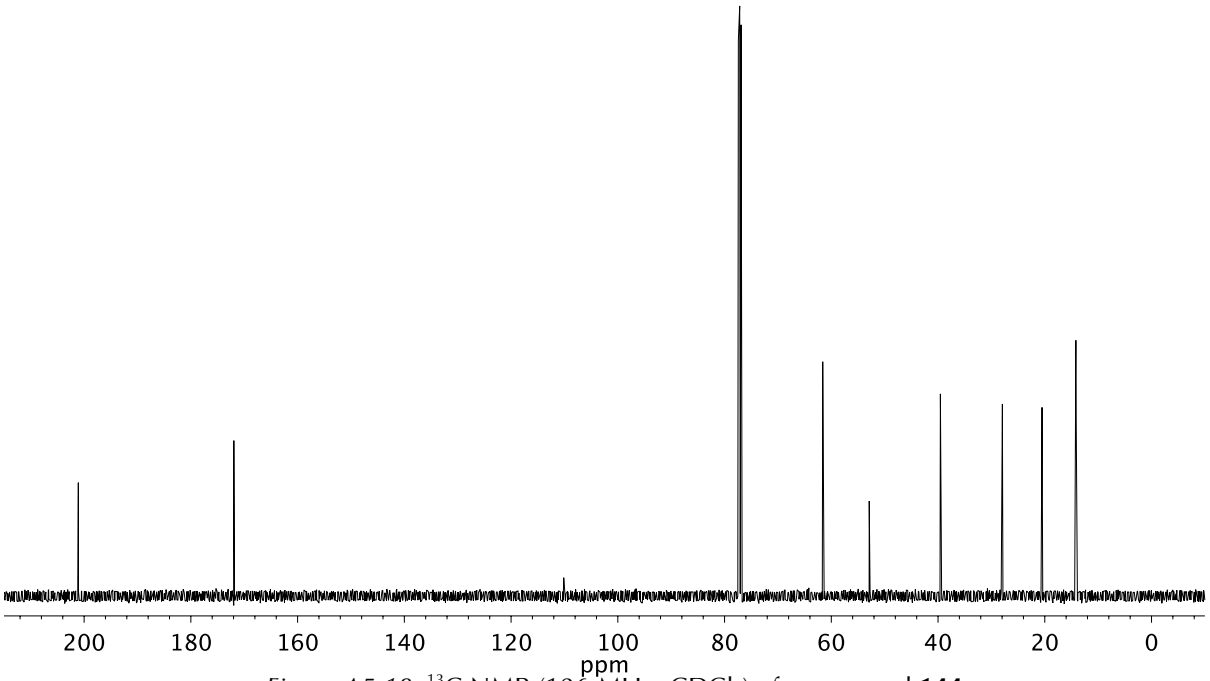

Figure A5.18. ^{13}C NMR (126 MHz, $CDCl_3$) of compound **144a**.

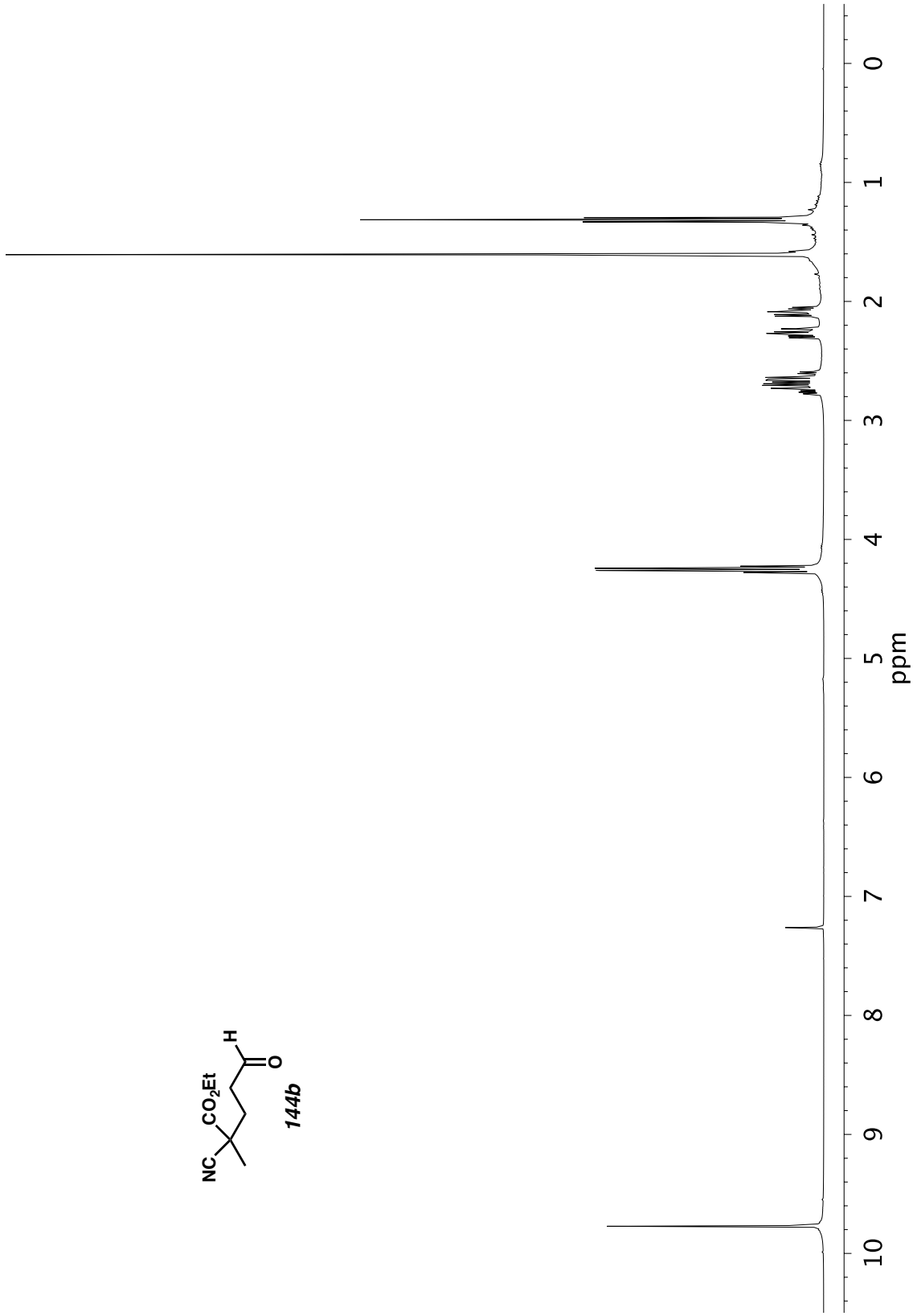

Figure A5.19. ^{1}H NMR (400 MHz, $CDCl_3$) of compound **144b**.

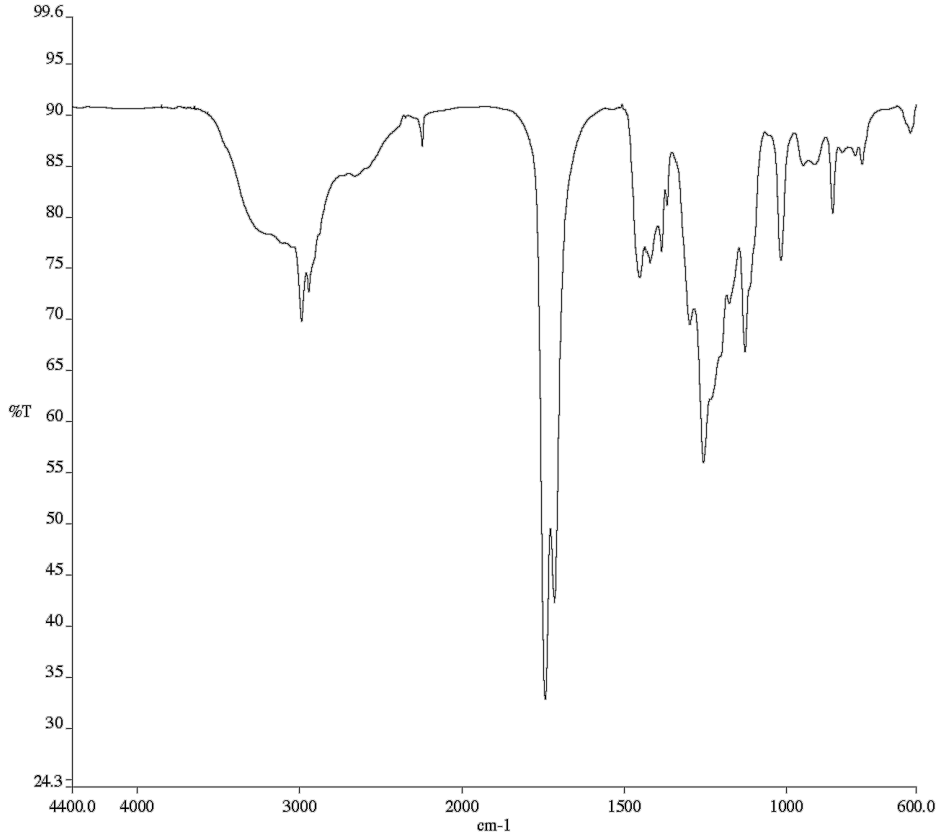

Figure A5.20. Infrared spectrum (Thin Film, KBr) of compound **144b**.

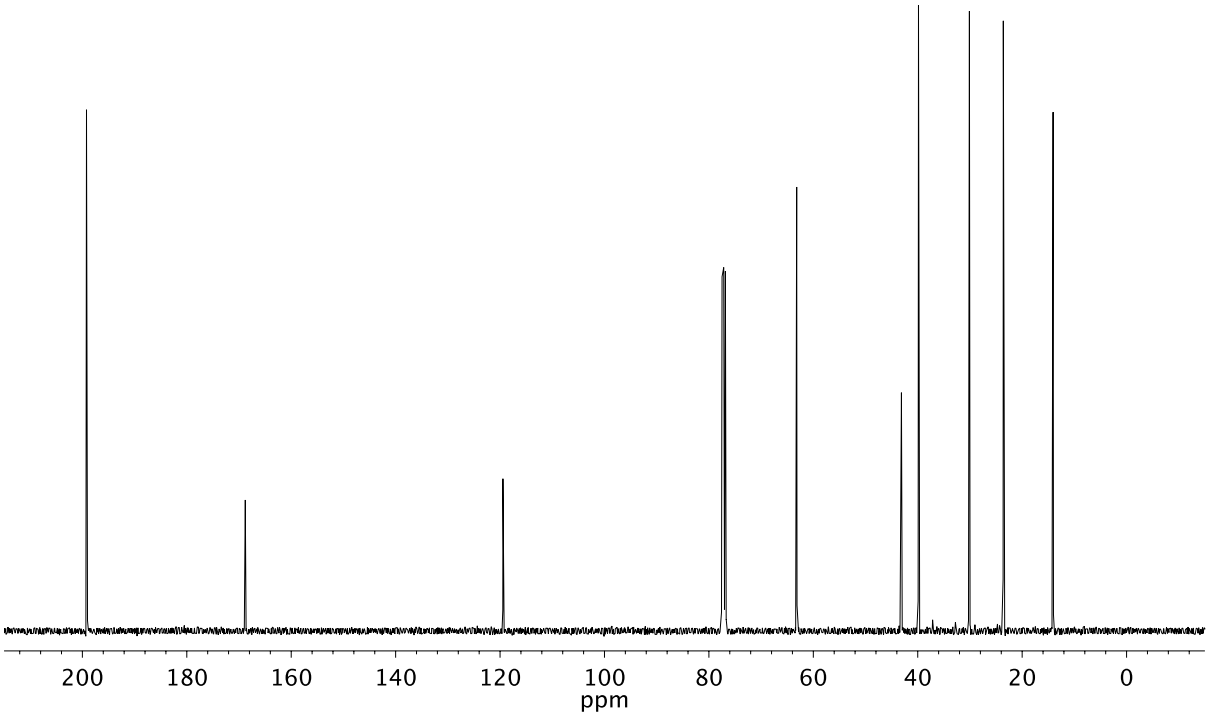

Figure A5.21. ^{13}C NMR (101 MHz, $CDCl_3$) of compound **144b**.

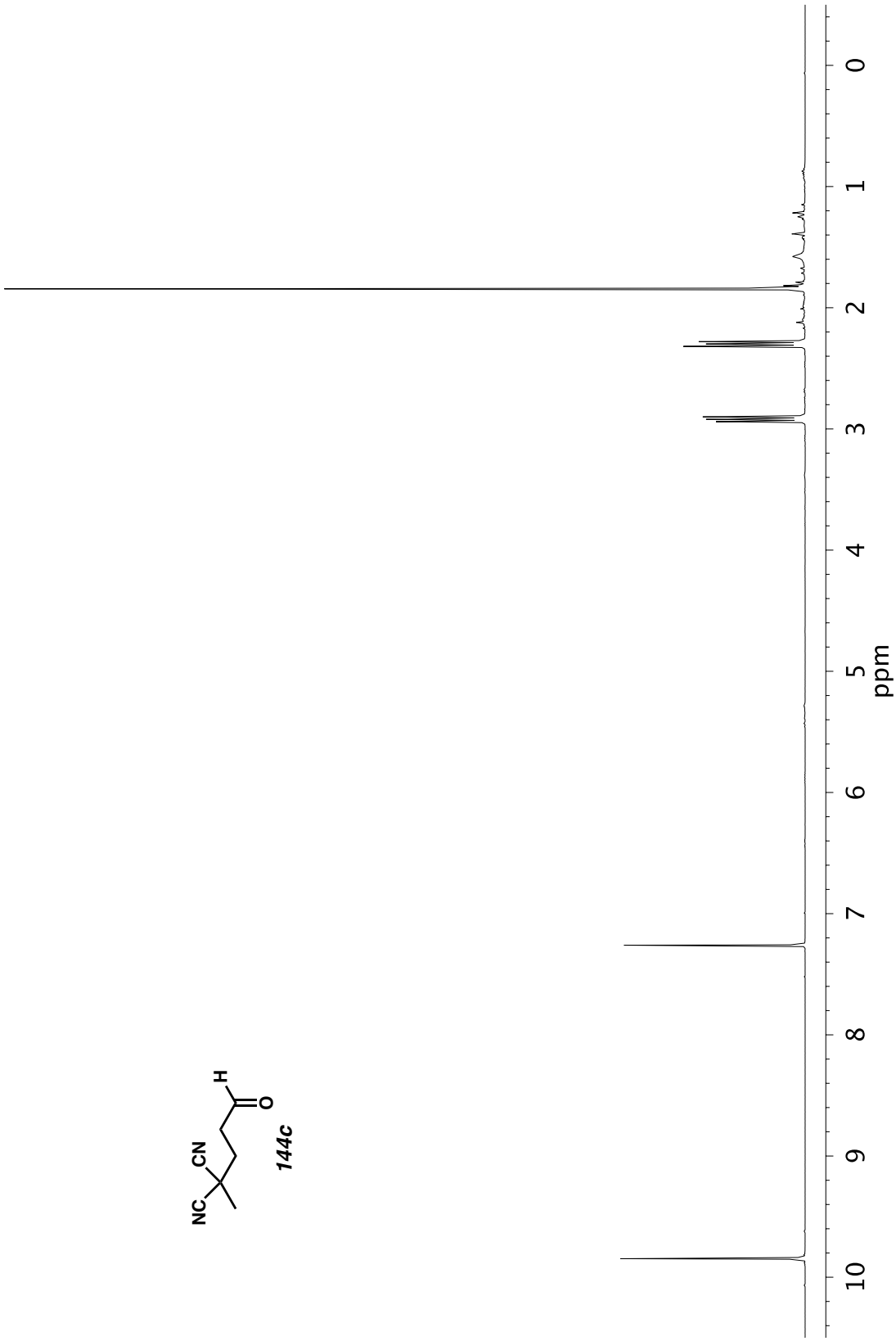

Figure A5.22. ^{1}H NMR (400 MHz, $CDCl_3$) of compound **144c**.

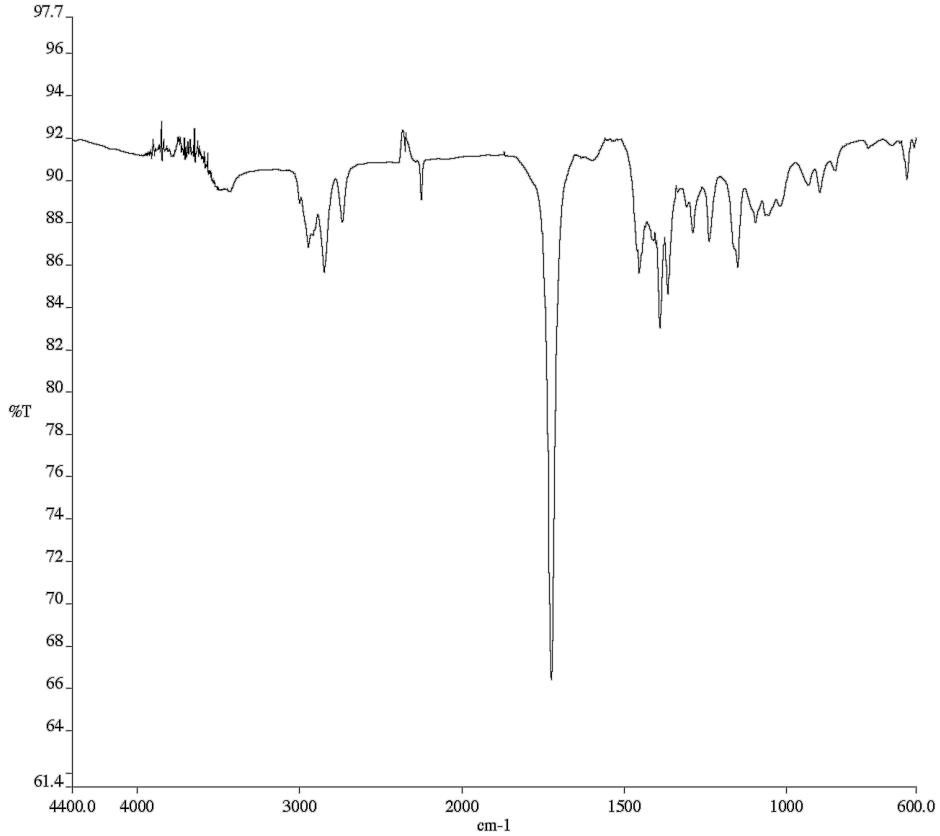

Figure A5.23. Infrared spectrum (Thin Film, KBr) of compound **144c**.

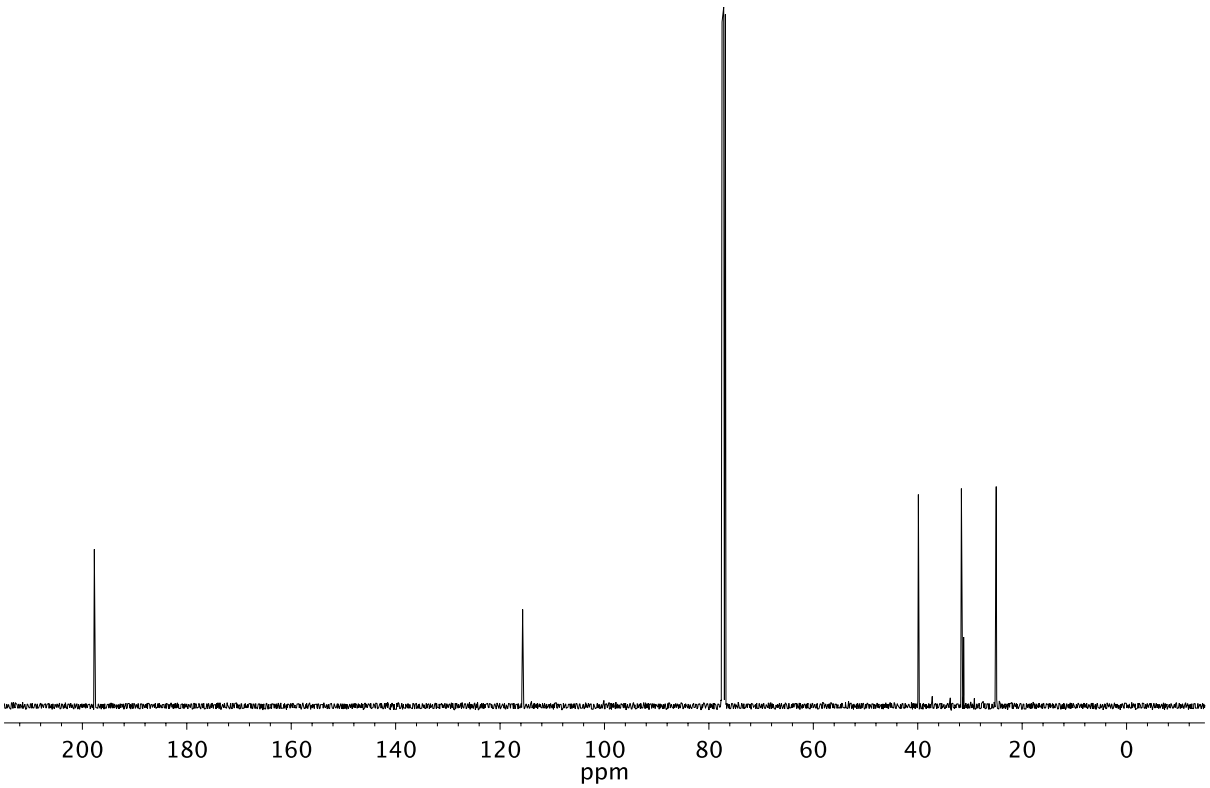

Figure A5.24. ^{13}C NMR (101 MHz, $CDCl_3$) of compound **144c**.

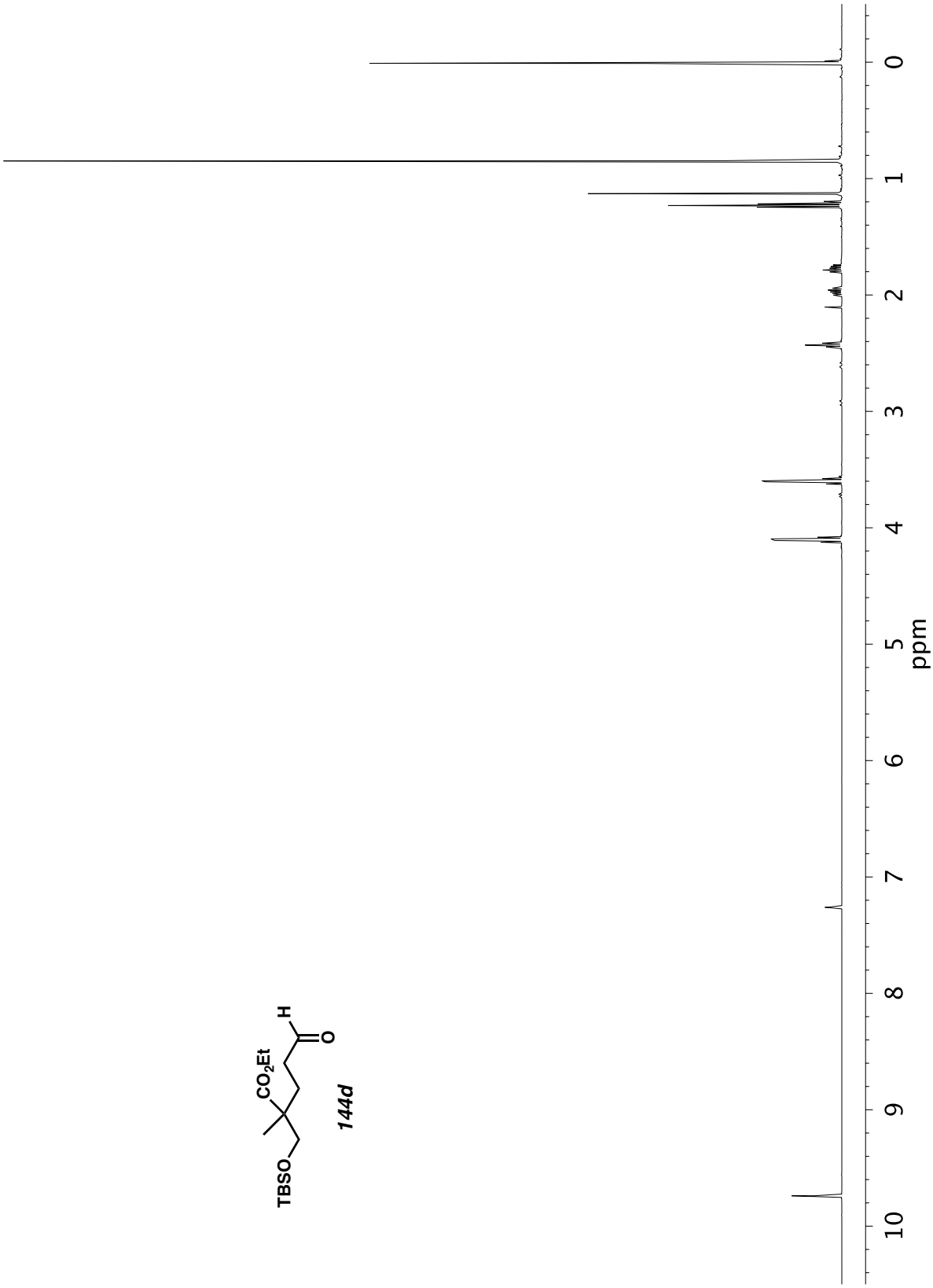

Figure A5.25. ^{1}H NMR (500 MHz, $CDCl_3$) of compound **144d**.

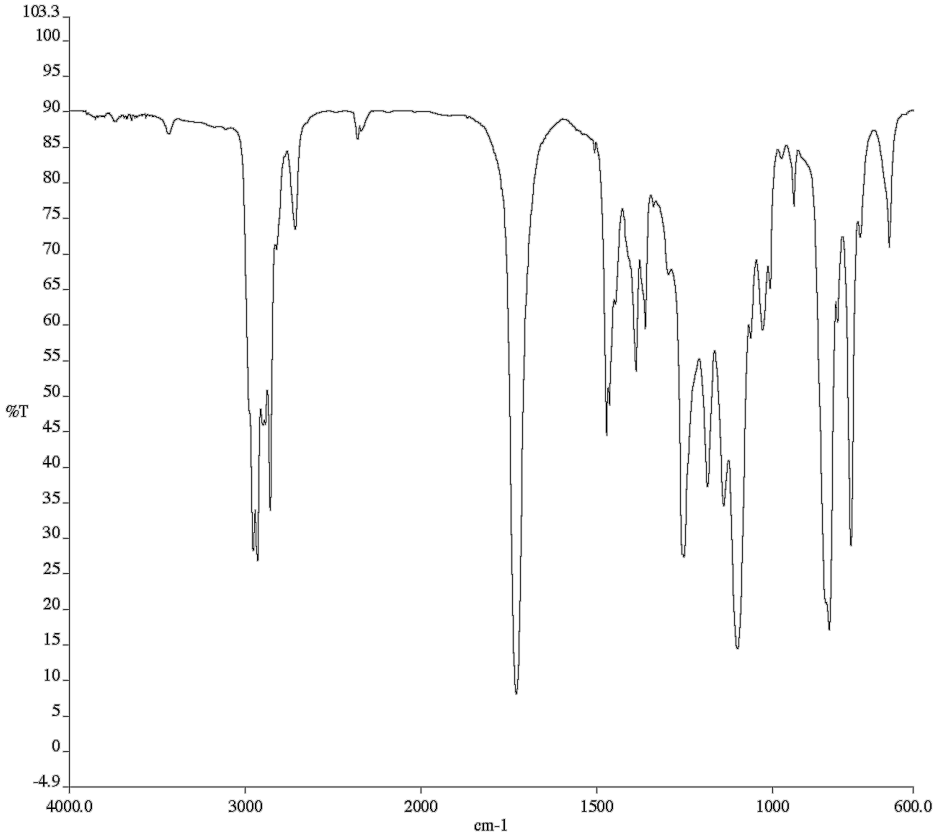

Figure A5.26. Infrared spectrum (Thin Film, KBr) of compound **144d**.

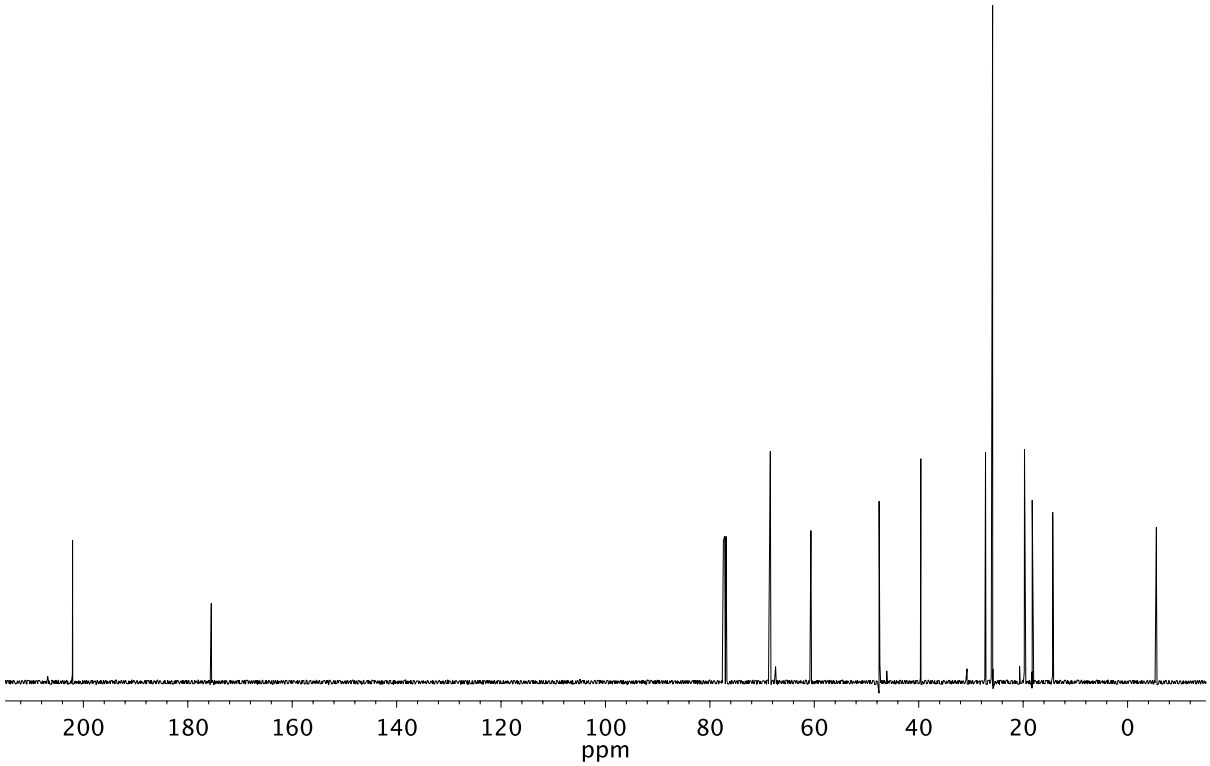

Figure A5.27. ^{13}C NMR (126 MHz, $CDCl_3$) of compound **144d**.

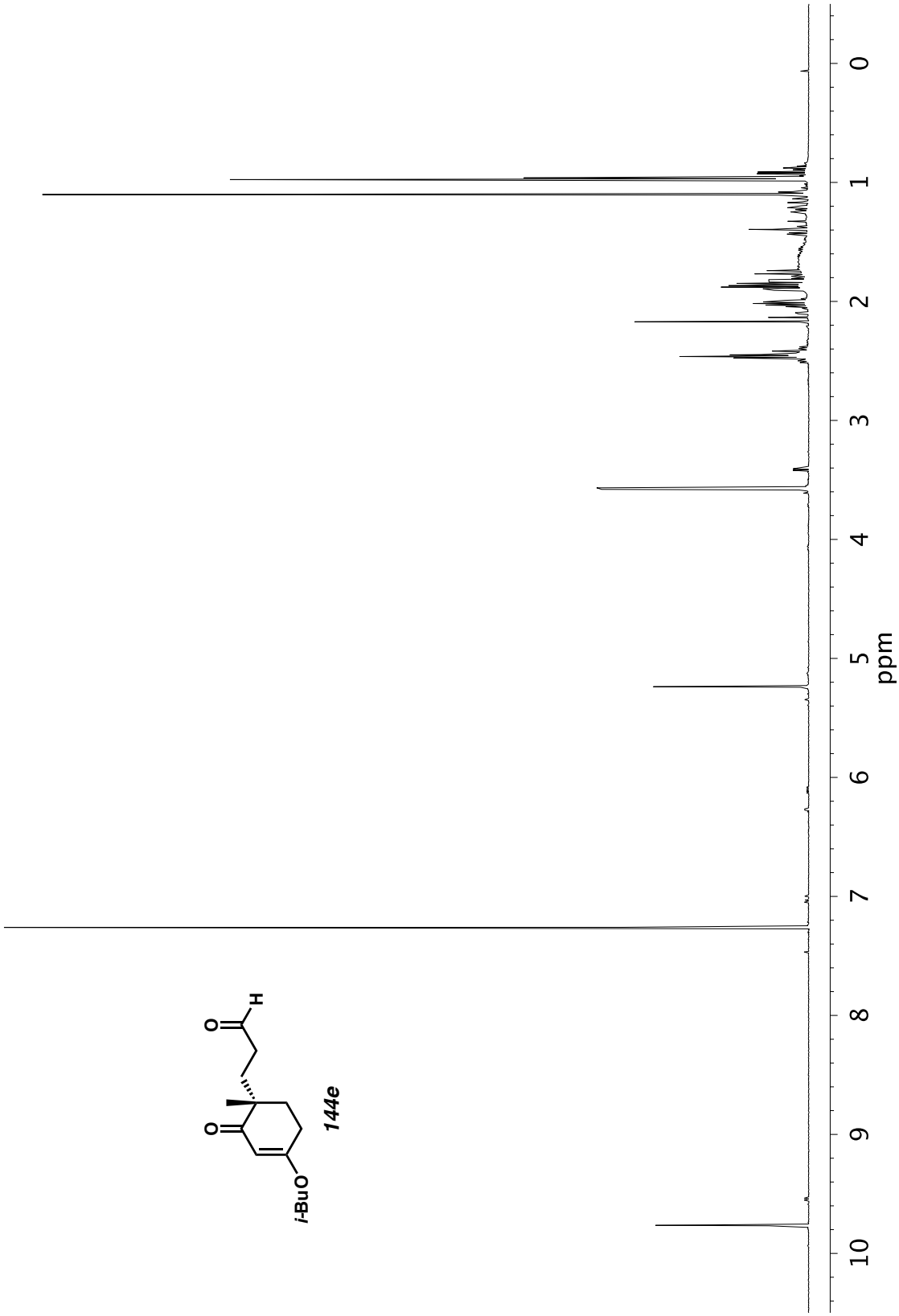

Figure A5.28. ^{1}H NMR (500 MHz, $CDCl_3$) of compound **144e**.

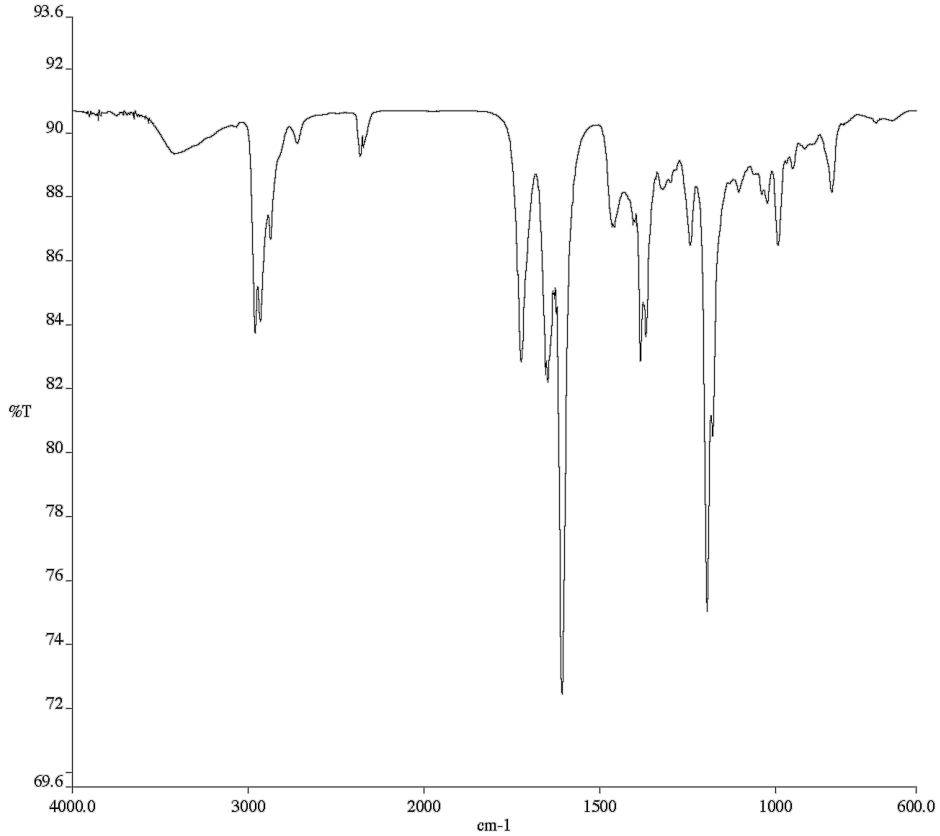

Figure A5.29. Infrared spectrum (Thin Film, KBr) of compound **144e**.

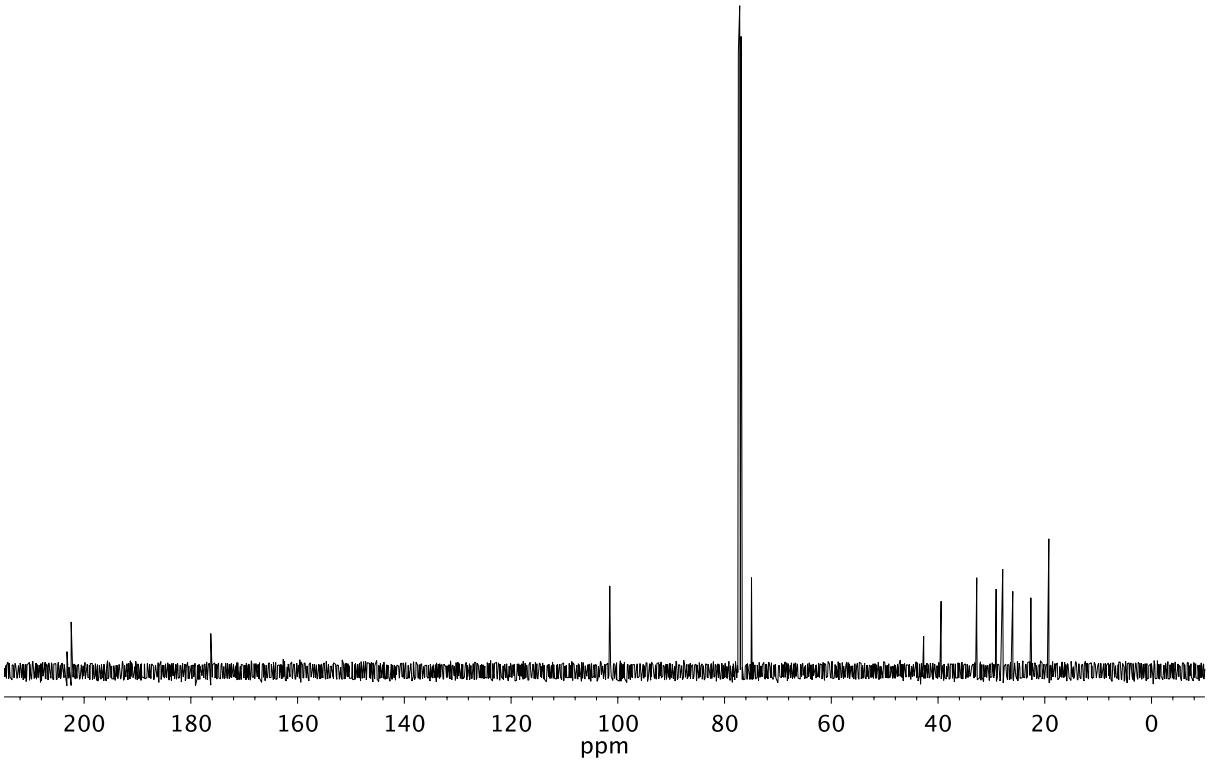

Figure A5.30. ^{13}C NMR (126 MHz, $CDCl_3$) of compound **144e**.

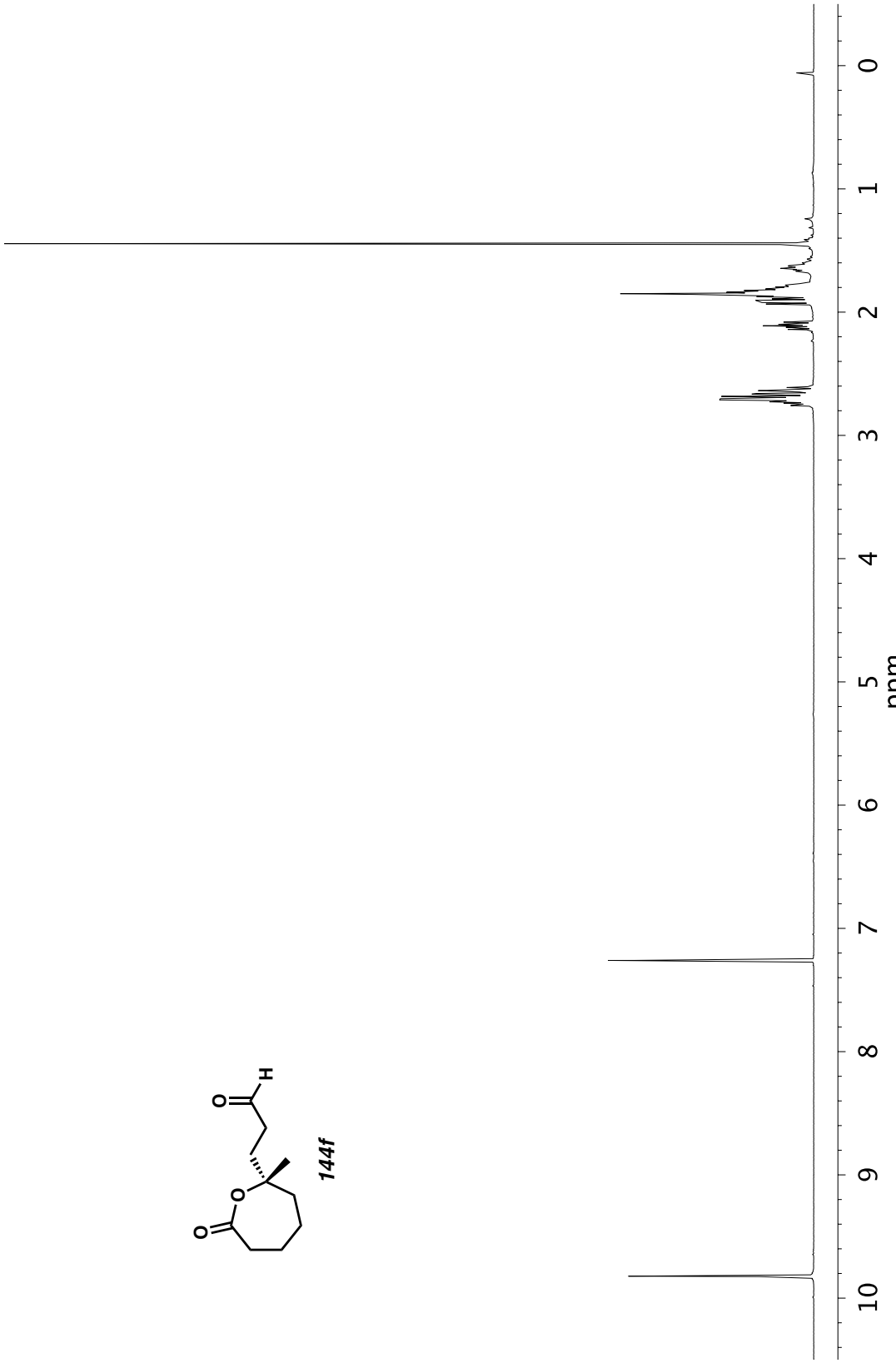

Figure A5.31. ^{1}H NMR (500 MHz, $CDCl_3$) of compound **144f**.

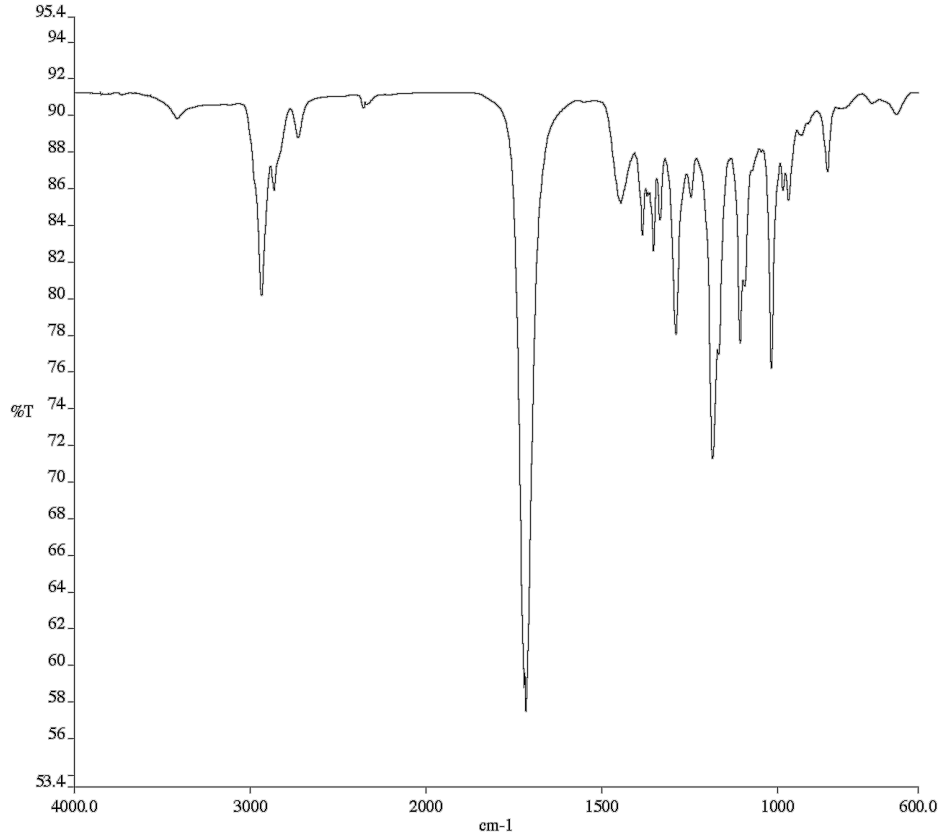

Figure A5.32. Infrared spectrum (Thin Film, KBr) of compound **144f**.

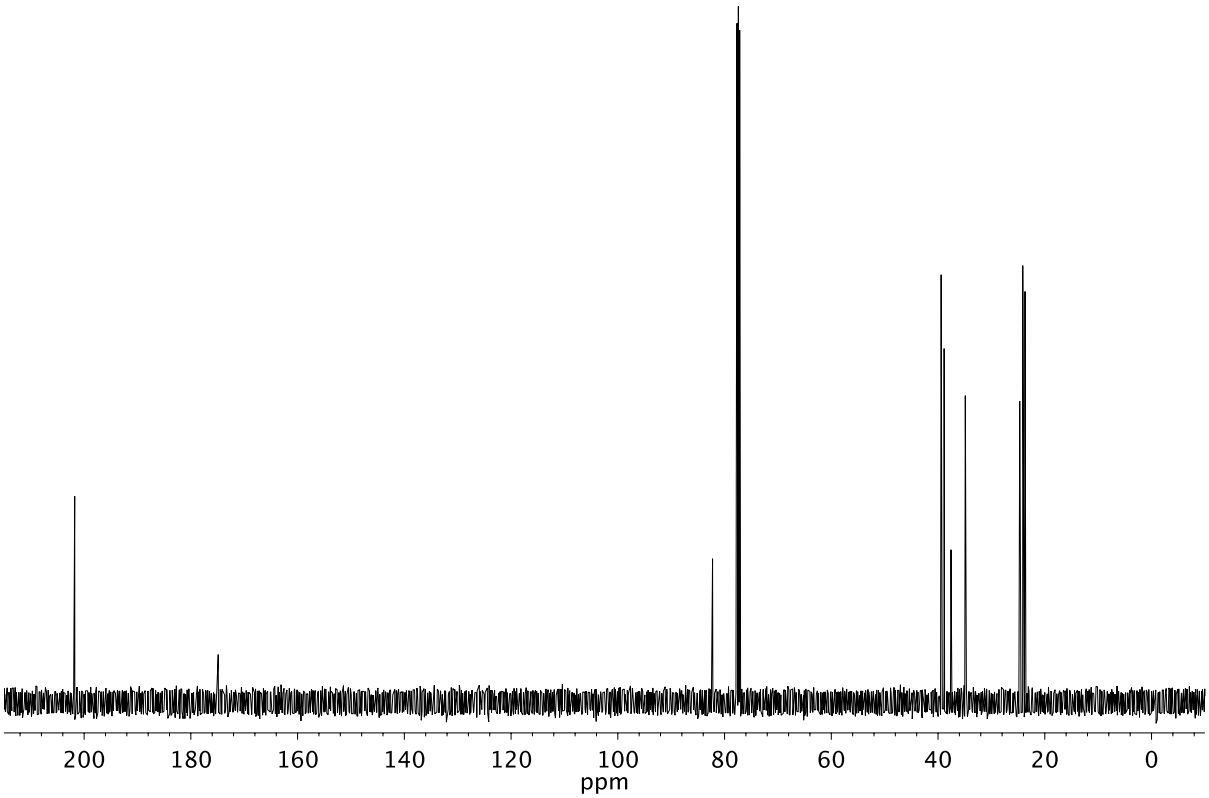

Figure A5.33. ^{13}C NMR (126 MHz, $CDCl_3$) of compound **144f**.

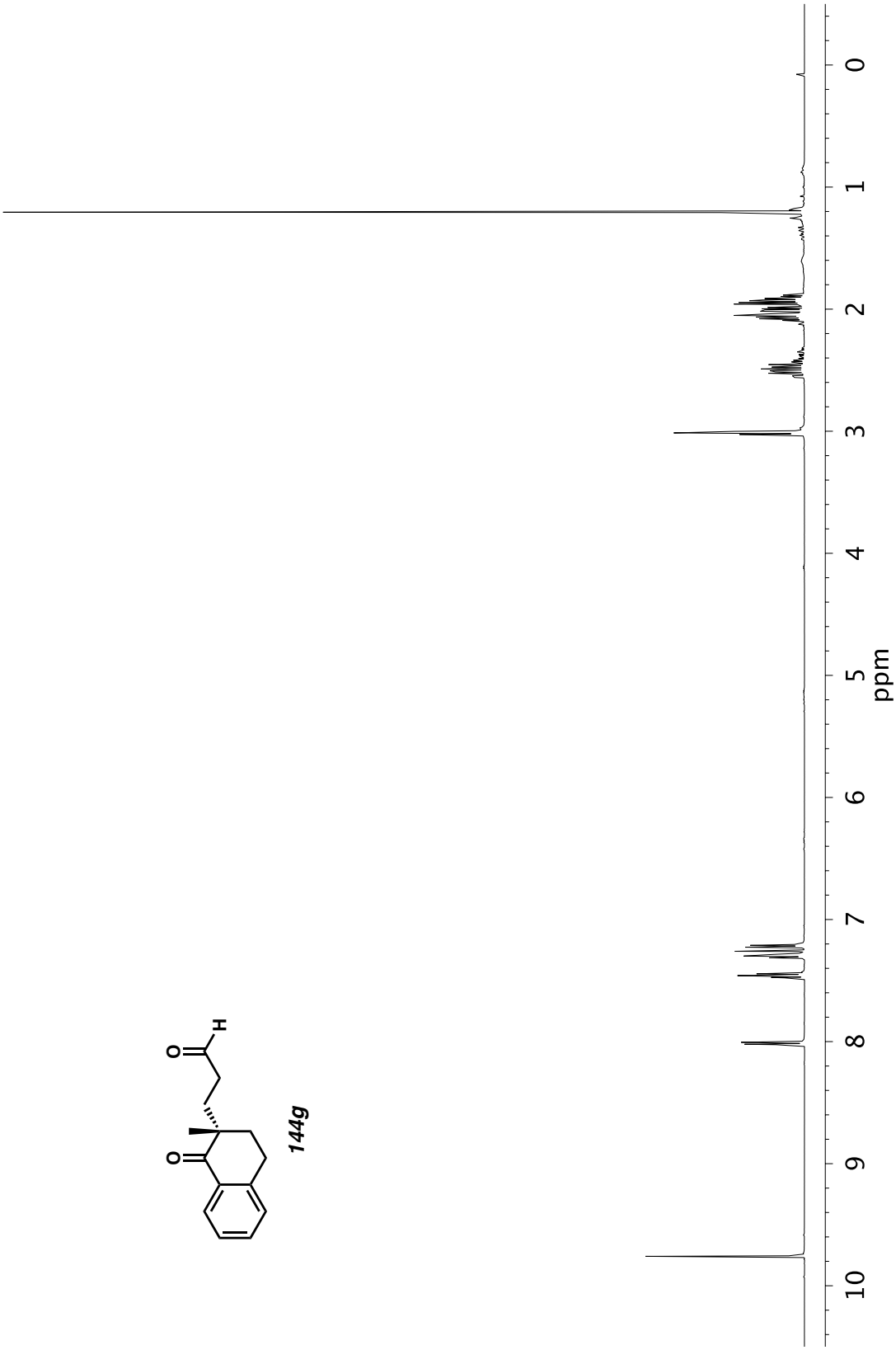

Figure A5.34. ^{1}H NMR (500 MHz, $CDCl_3$) of compound **144g**.

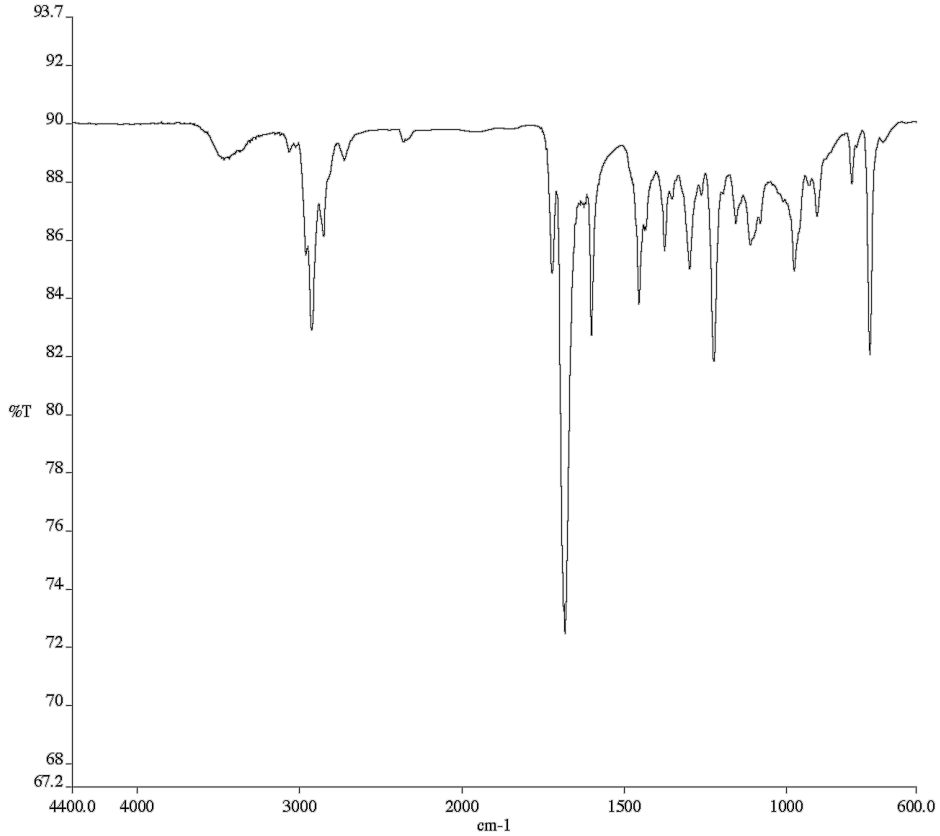

Figure A5.35. Infrared spectrum (Thin Film, KBr) of compound **144g**.

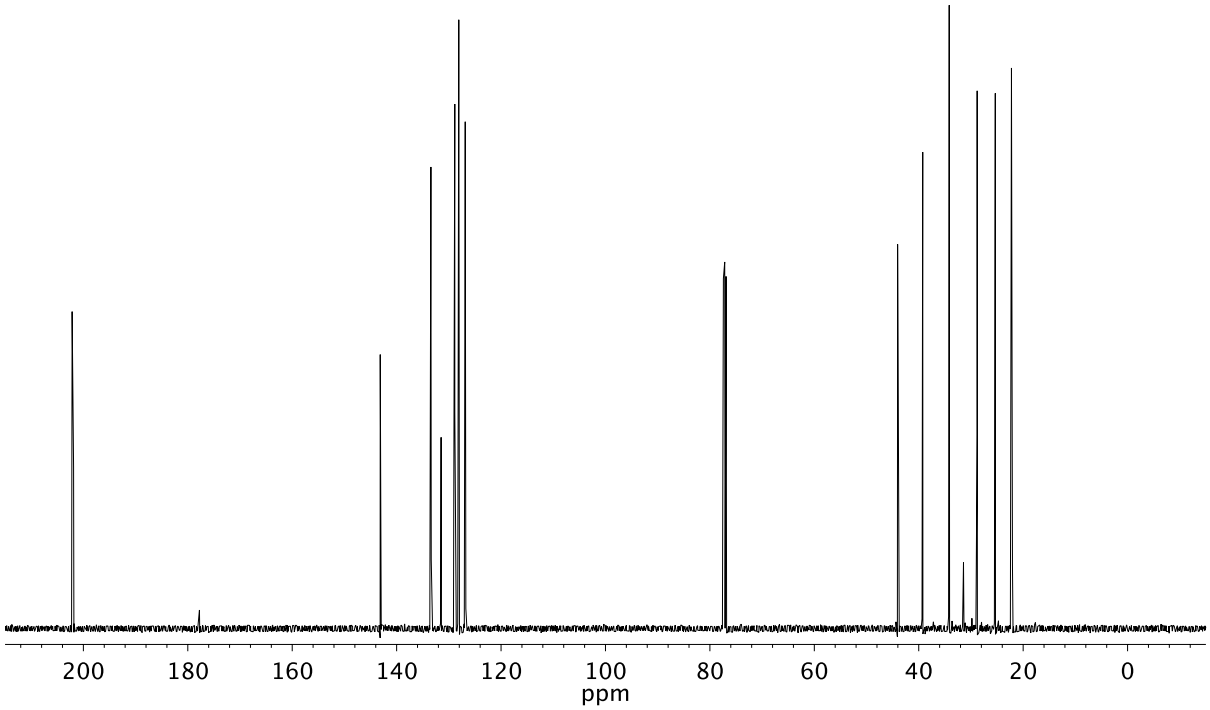

Figure A5.36. ^{13}C NMR (126 MHz, $CDCl_3$) of compound **144g**.

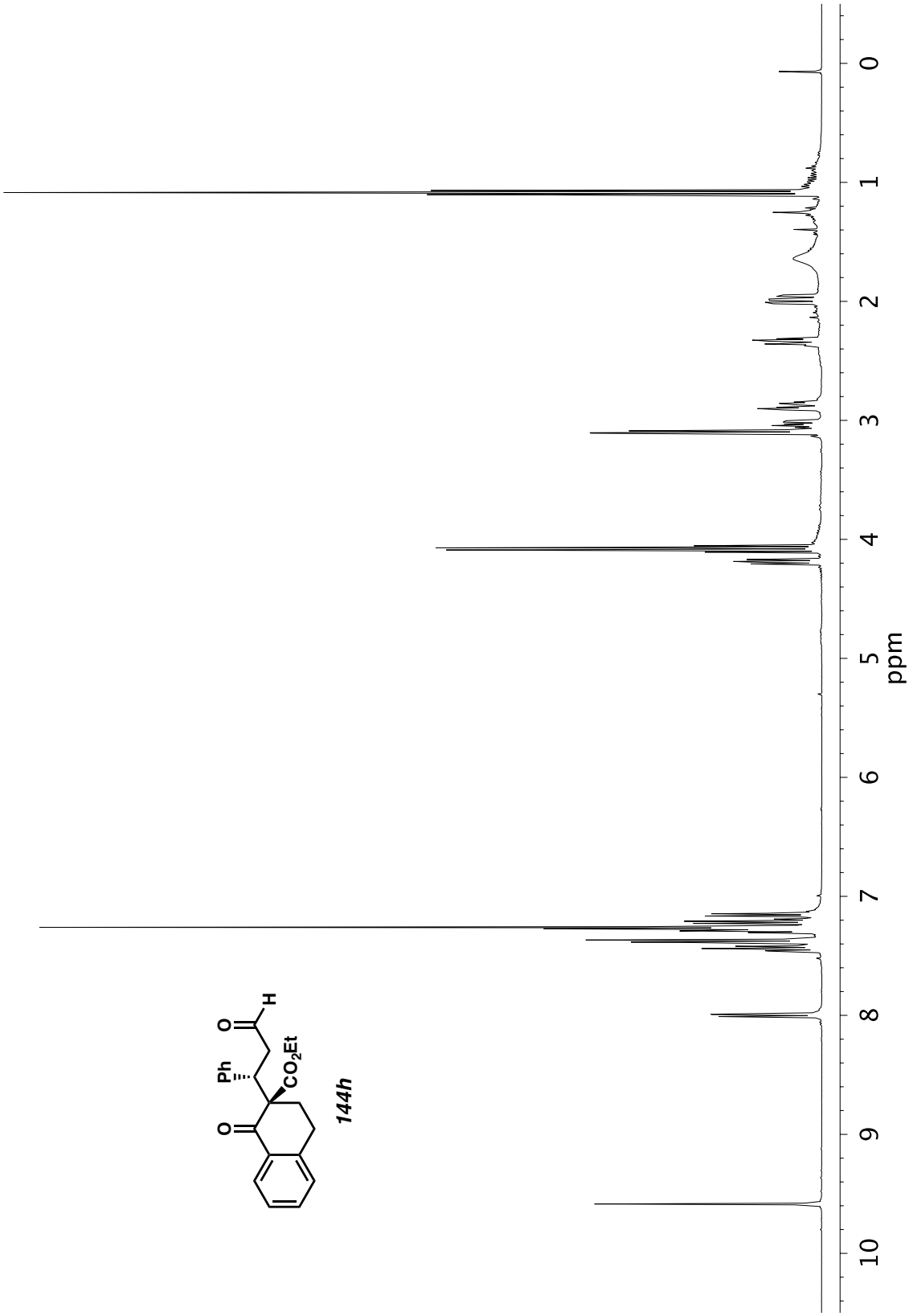

Figure A5.37. ^{1}H NMR (400 MHz, $CDCl_3$) of compound **144h**.

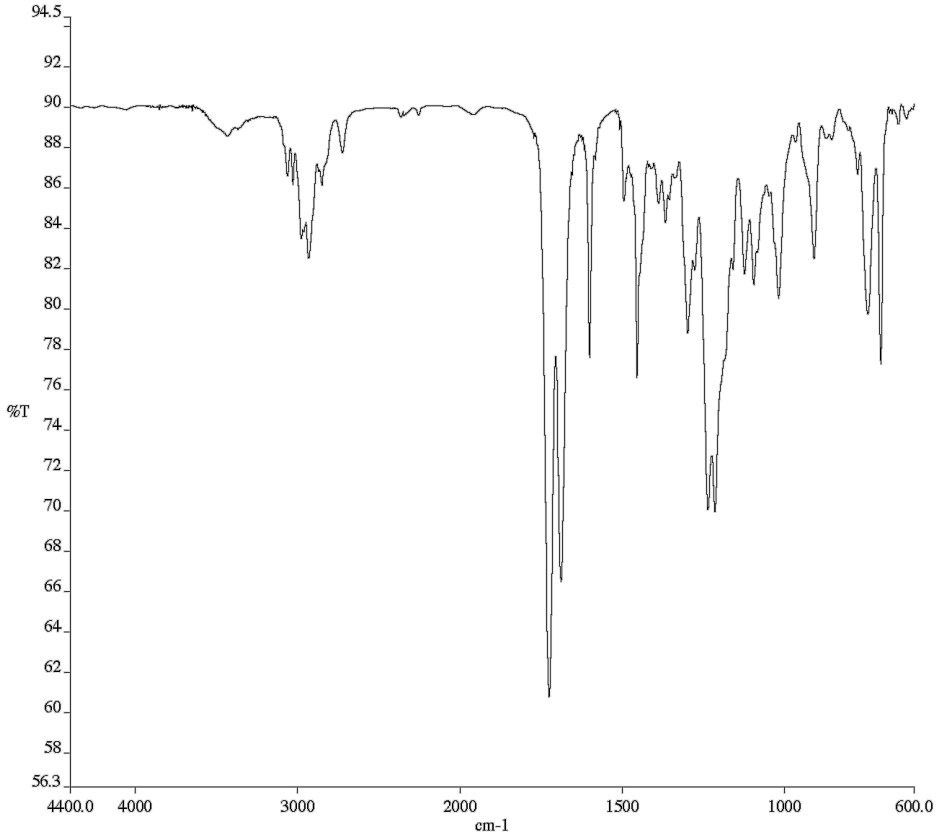

Figure A5.38. Infrared spectrum (Thin Film, KBr) of compound **144h**.

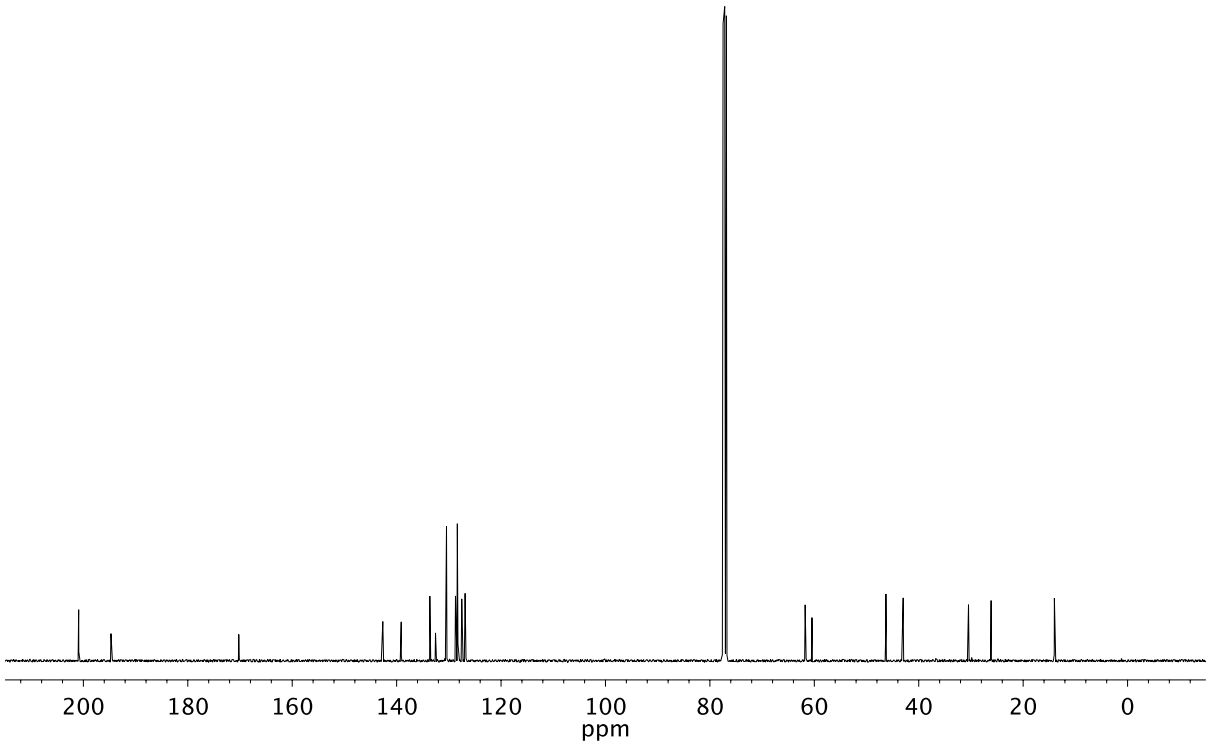

Figure A5.39. ^{13}C NMR (101 MHz, $CDCl_3$) of compound **144h**.

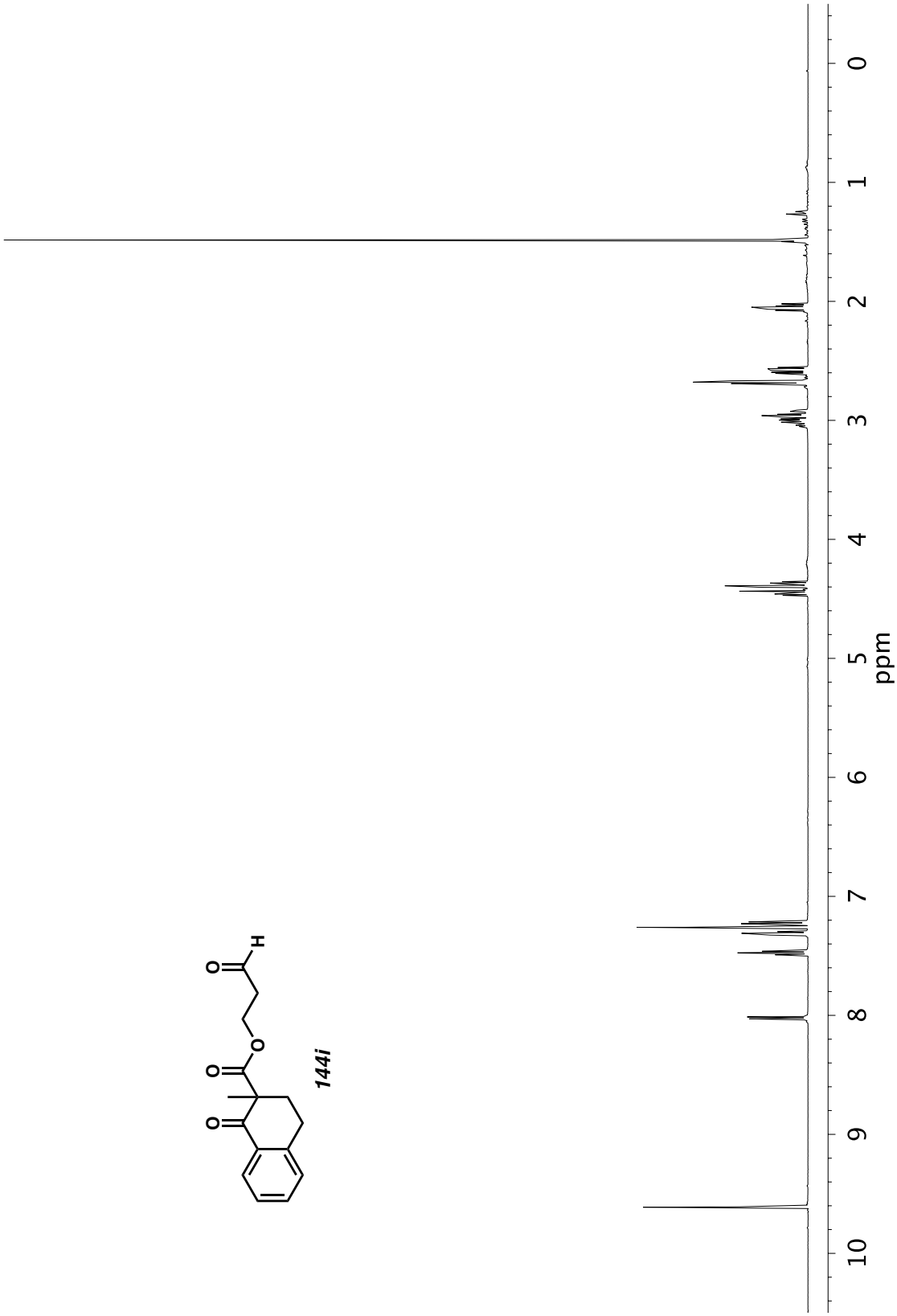

Figure A5.40. ^{1}H NMR (500 MHz, $CDCl_3$) of compound **144i**.

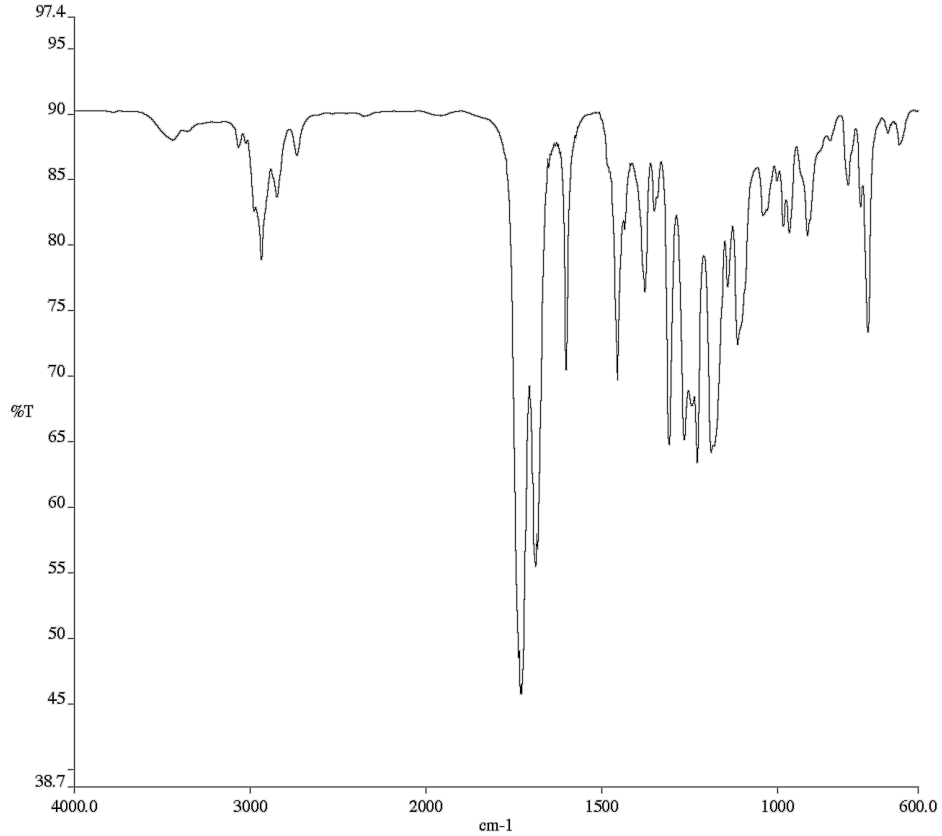

Figure A5.41. Infrared spectrum (Thin Film, KBr) of compound **144i**.

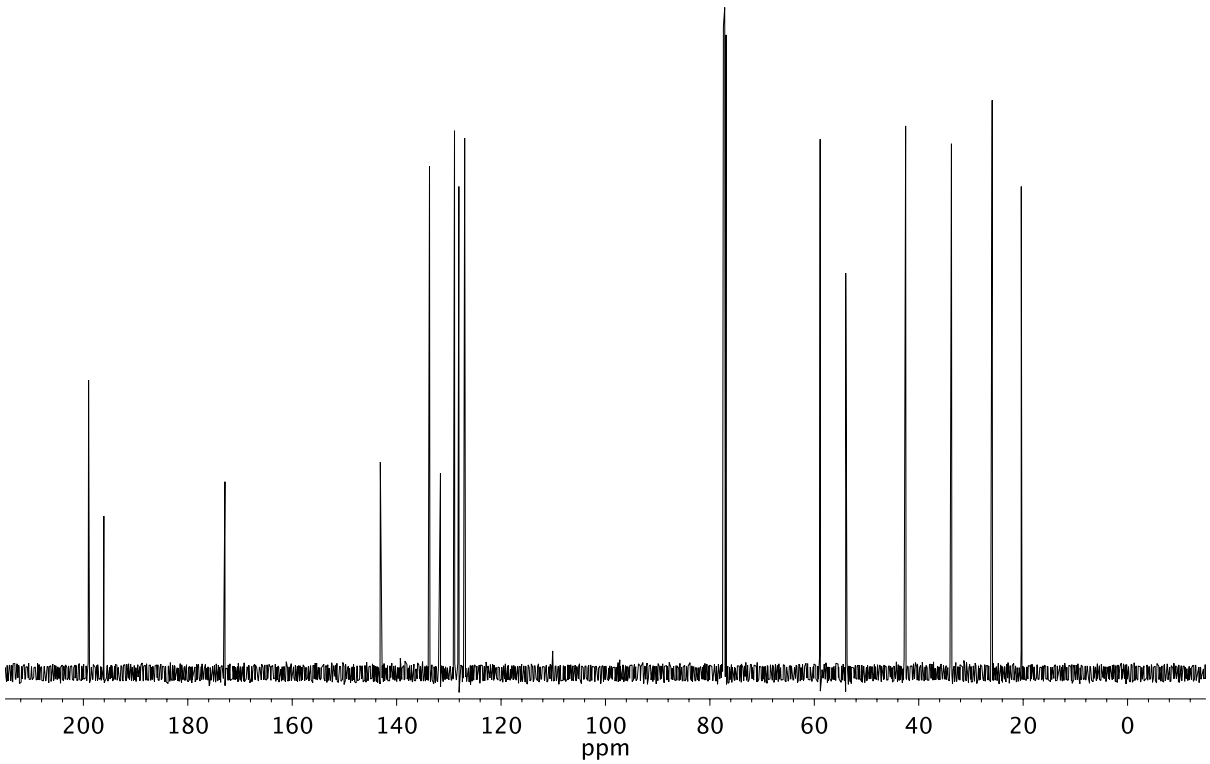

Figure A5.42. ^{13}C NMR (126 MHz, $CDCl_3$) of compound **144i**.

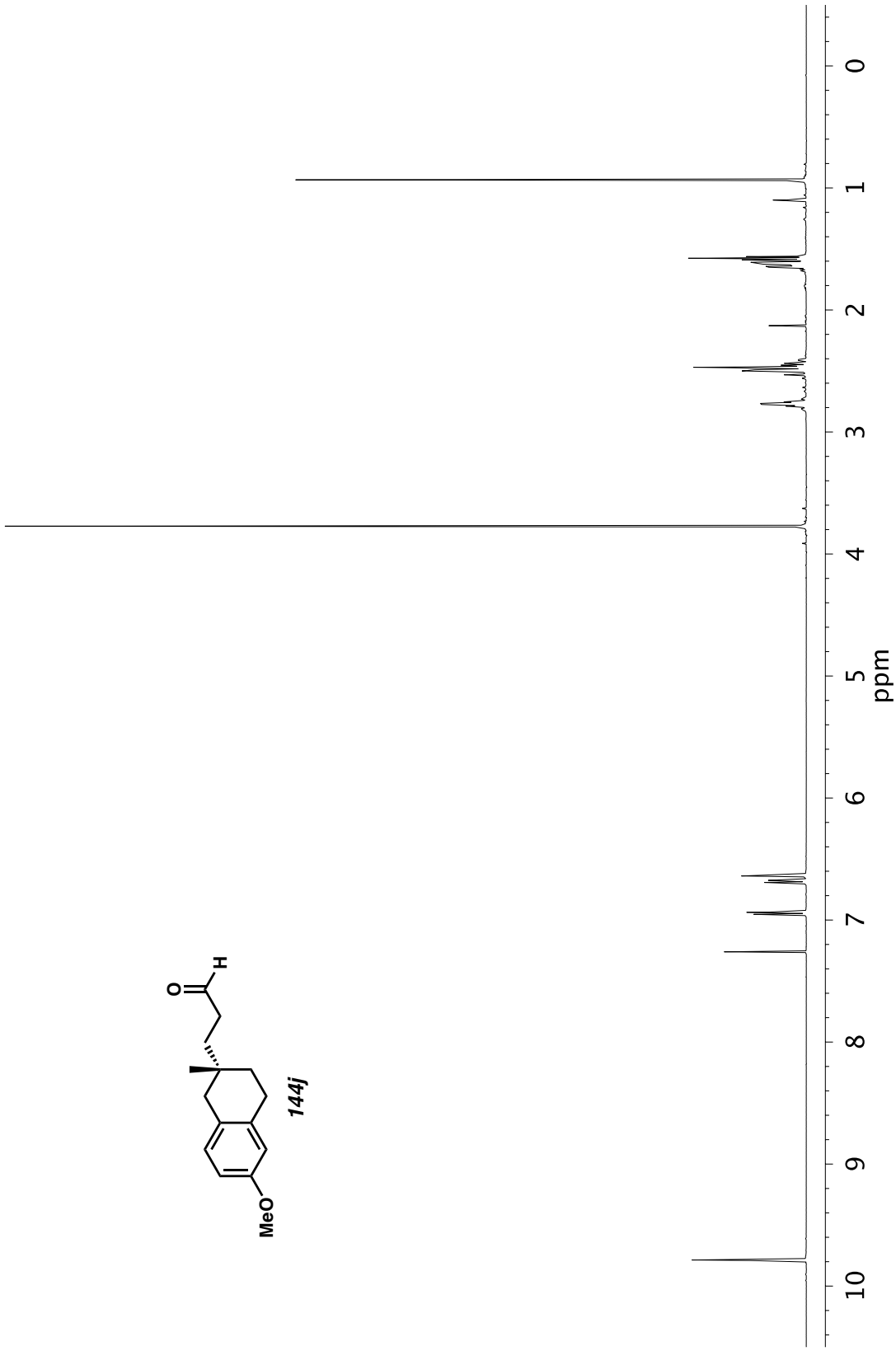

Figure A5.43. ^{1}H NMR (500 MHz, $CDCl_3$) of compound **144j**.

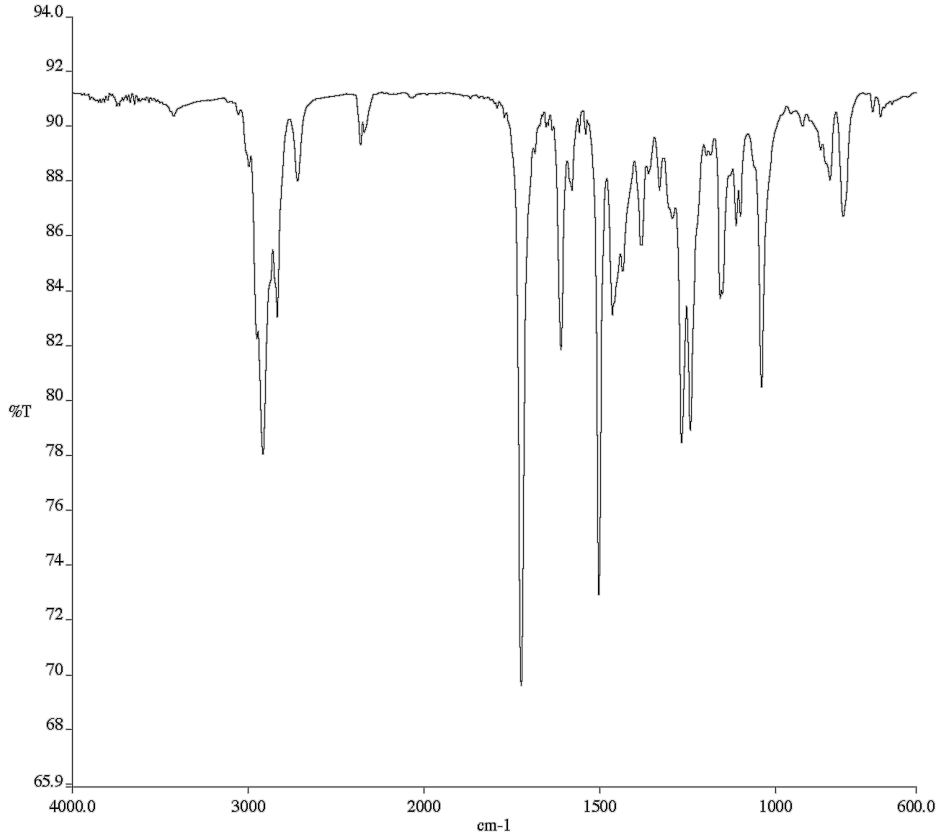

Figure A5.44. Infrared spectrum (Thin Film, KBr) of compound **144j**.

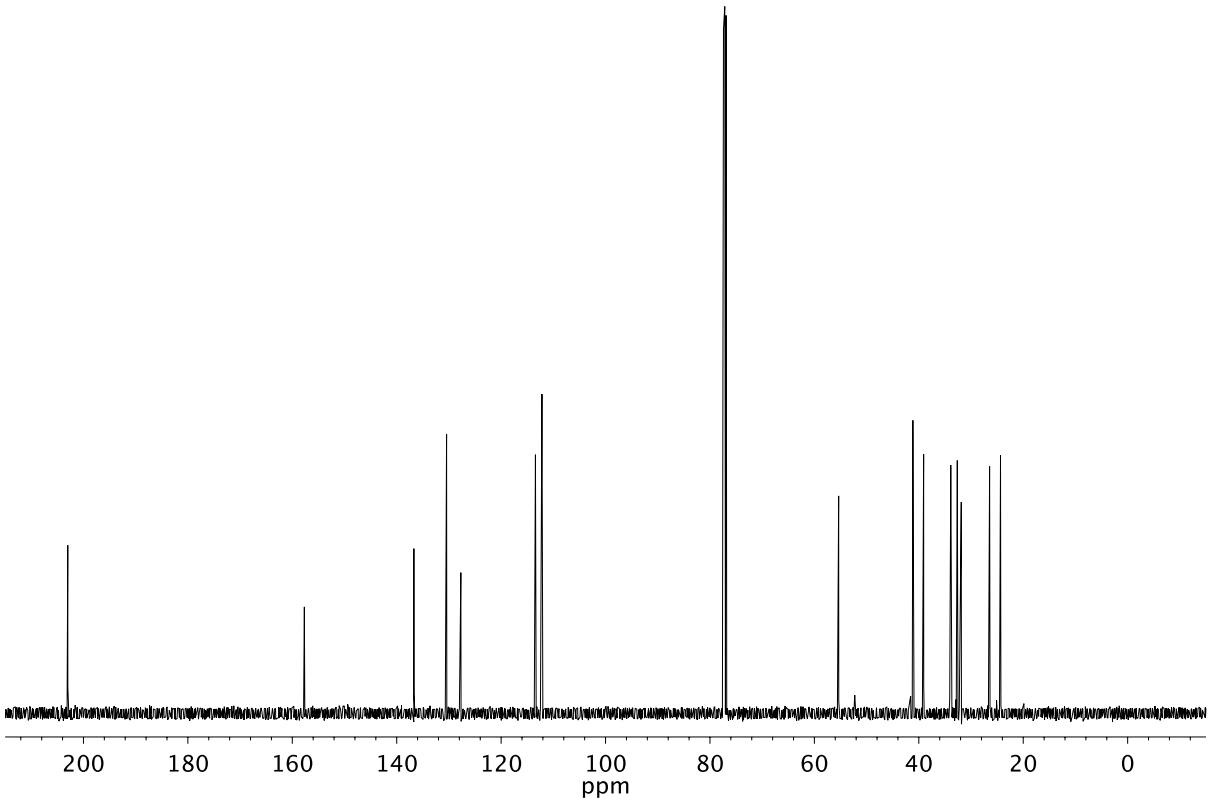

Figure A5.45. ^{13}C NMR (126 MHz, $CDCl_3$) of compound **144j**.

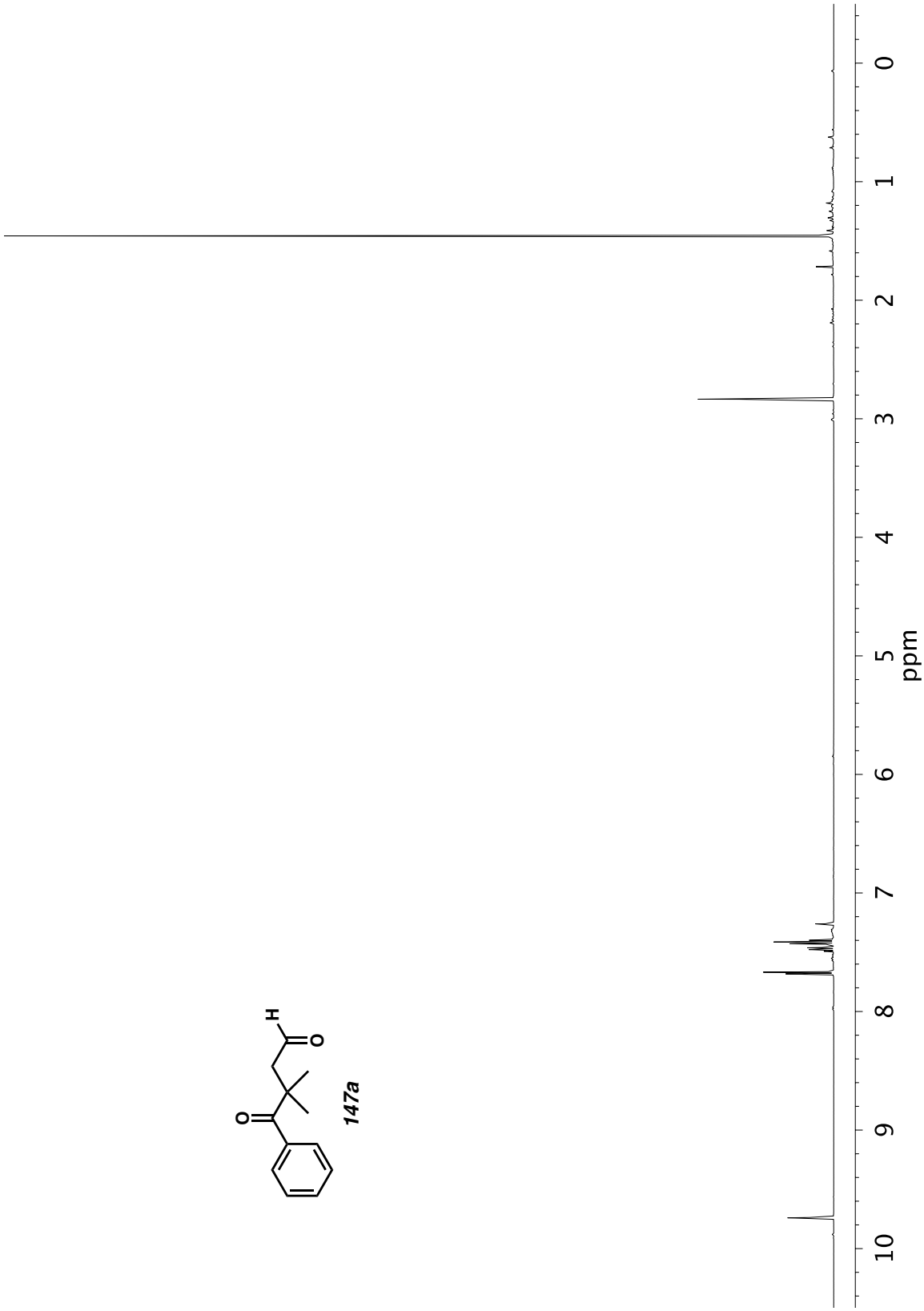

Figure A5.46. ^{1}H NMR (500 MHz, $CDCl_3$) of compound **147a**.

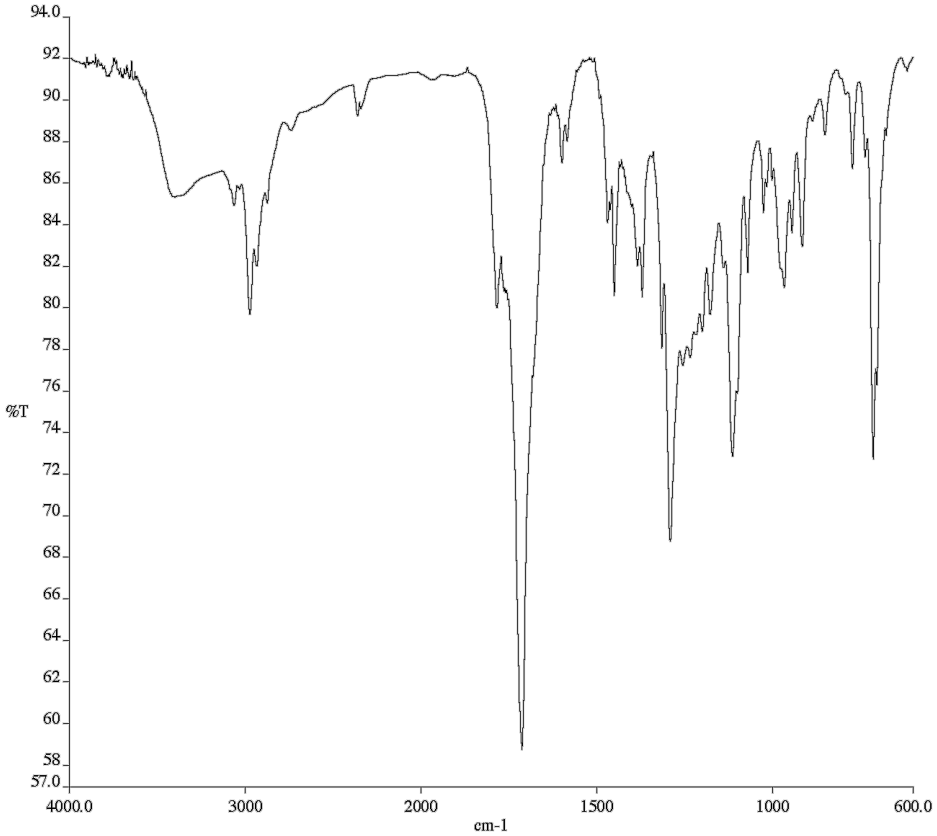

Figure A5.47. Infrared spectrum (Thin Film, KBr) of compound **147a**.

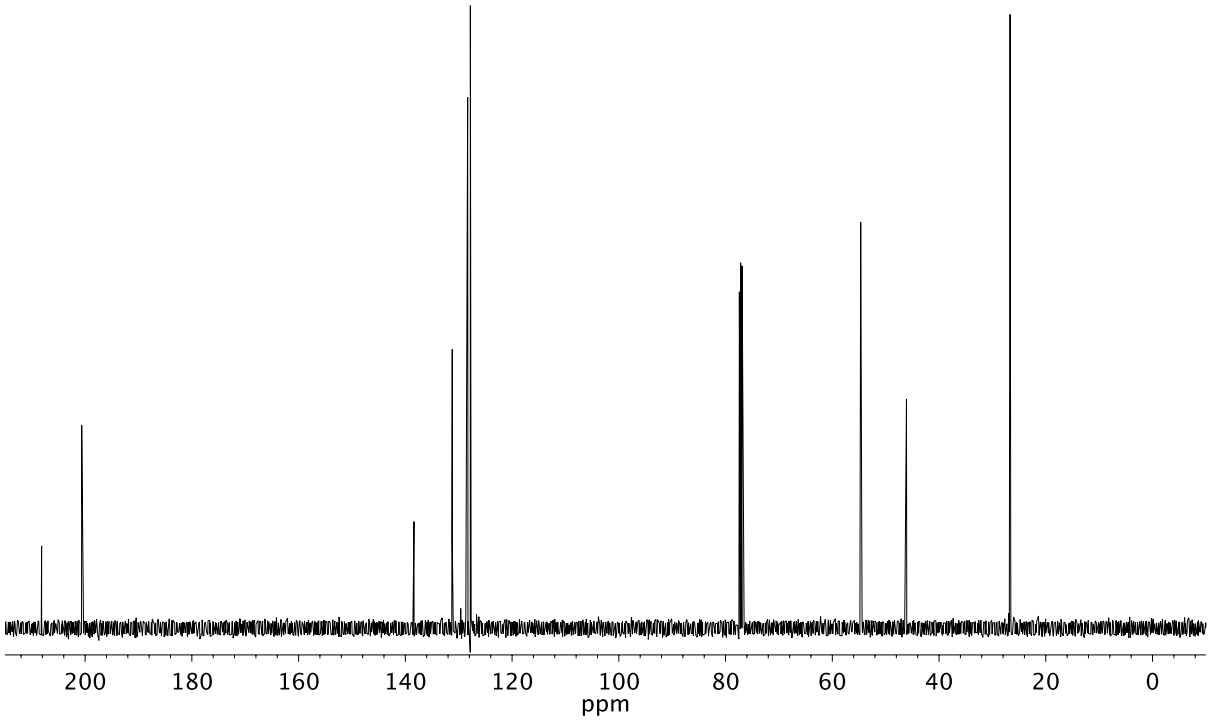

Figure A5.48. ^{13}C NMR (126 MHz, $CDCl_3$) of compound **147a**.

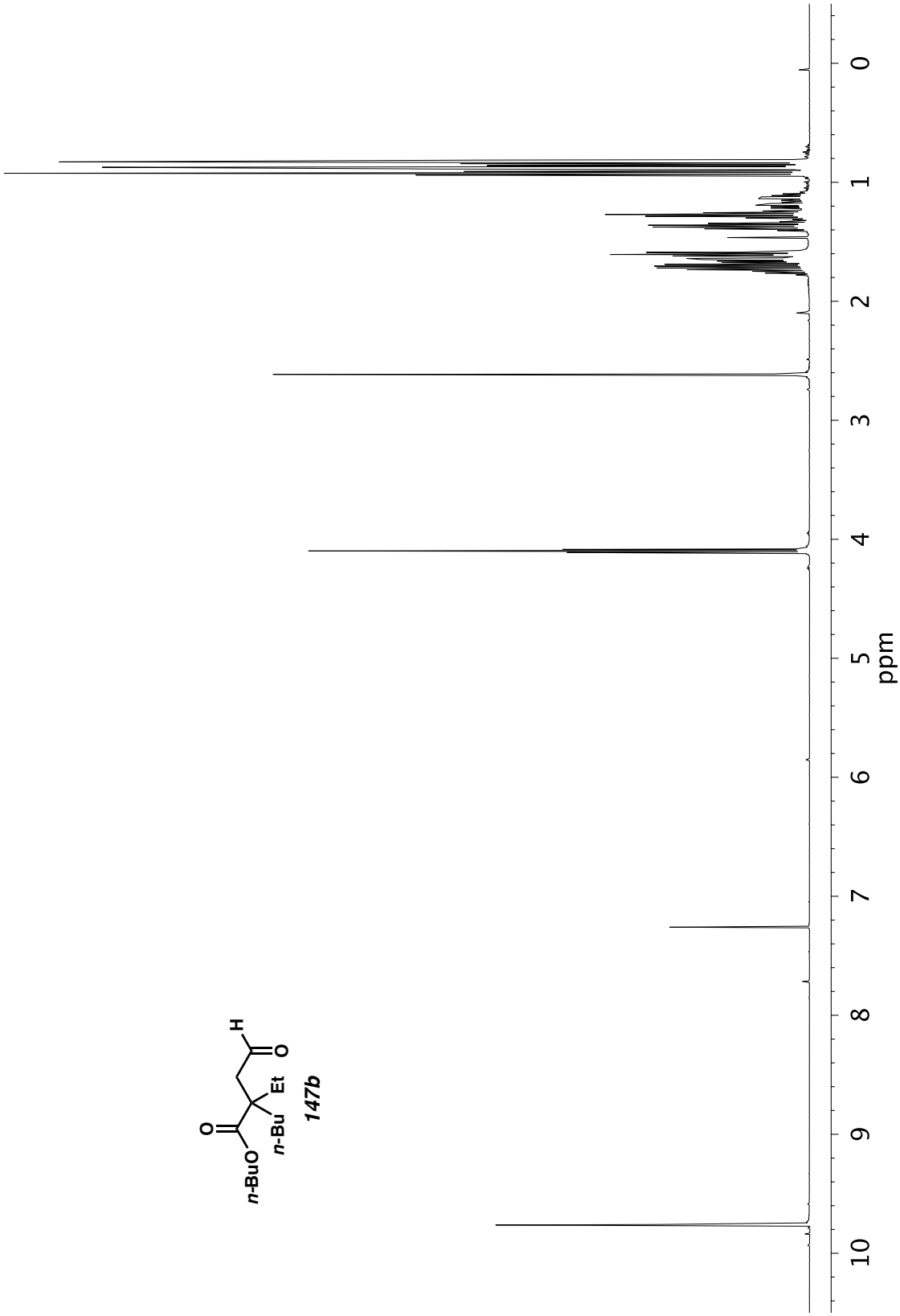

Figure A5.49. ^{1}H NMR (500 MHz, $CDCl_3$) of compound **147b**.

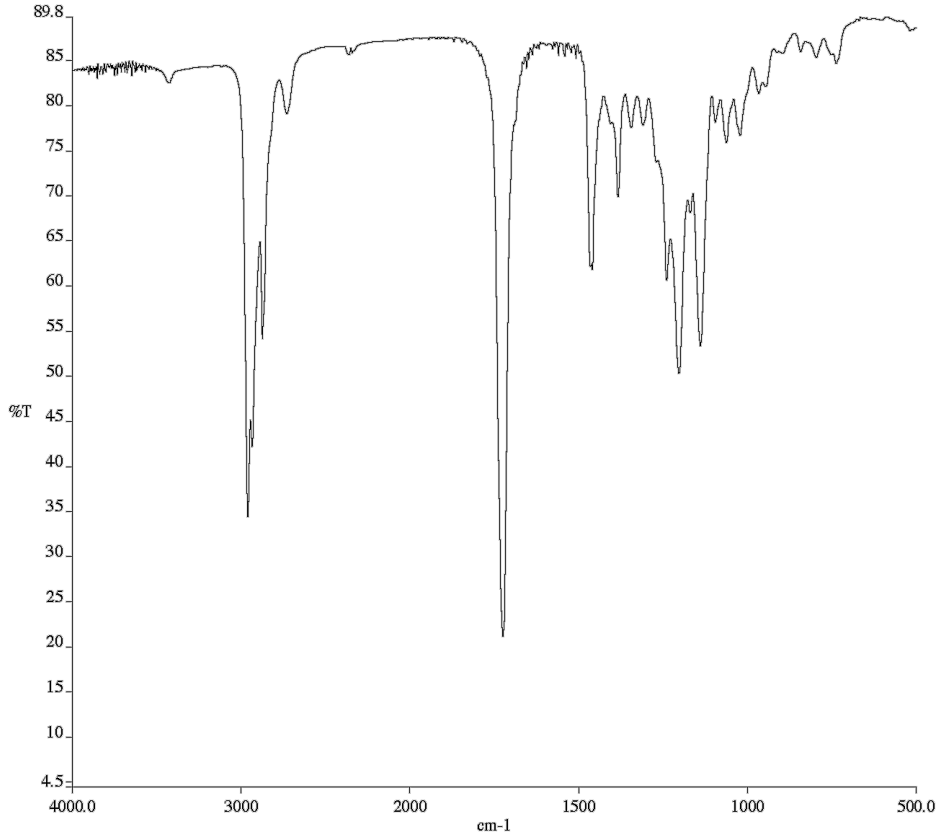

Figure A5.50. Infrared spectrum (Thin Film, KBr) of compound **147b**.

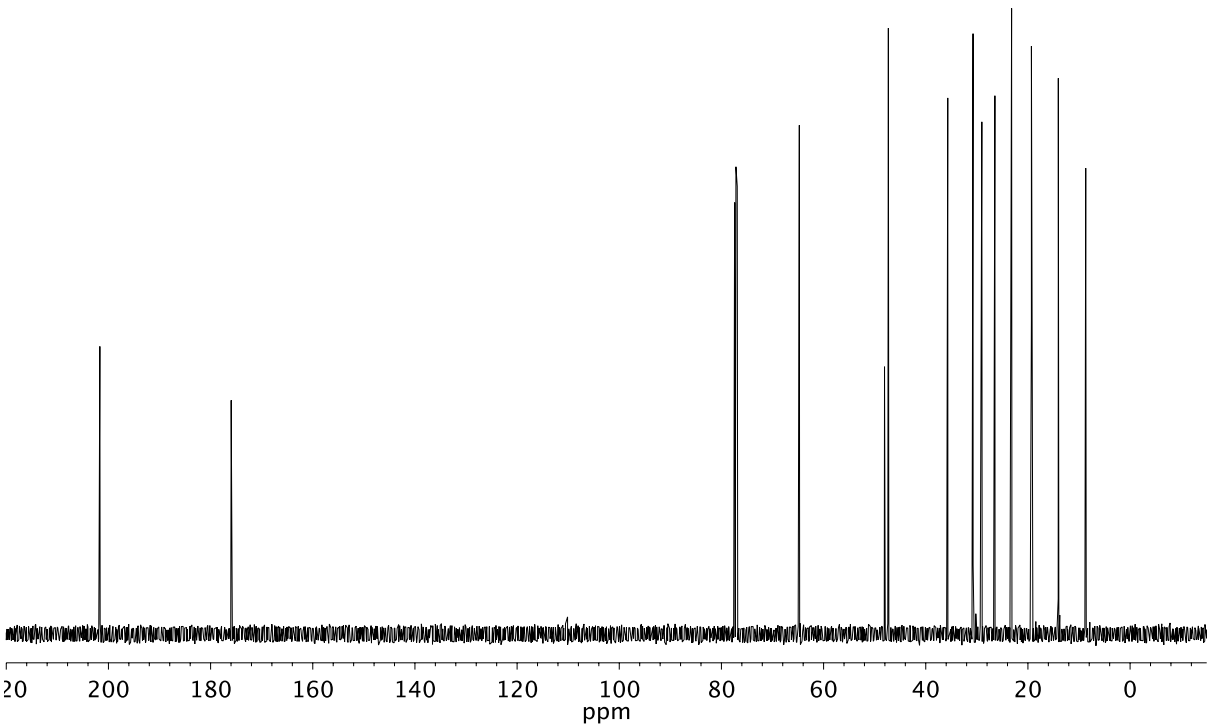

Figure A5.51. ^{13}C NMR (126 MHz, $CDCl_3$) of compound **147b**.

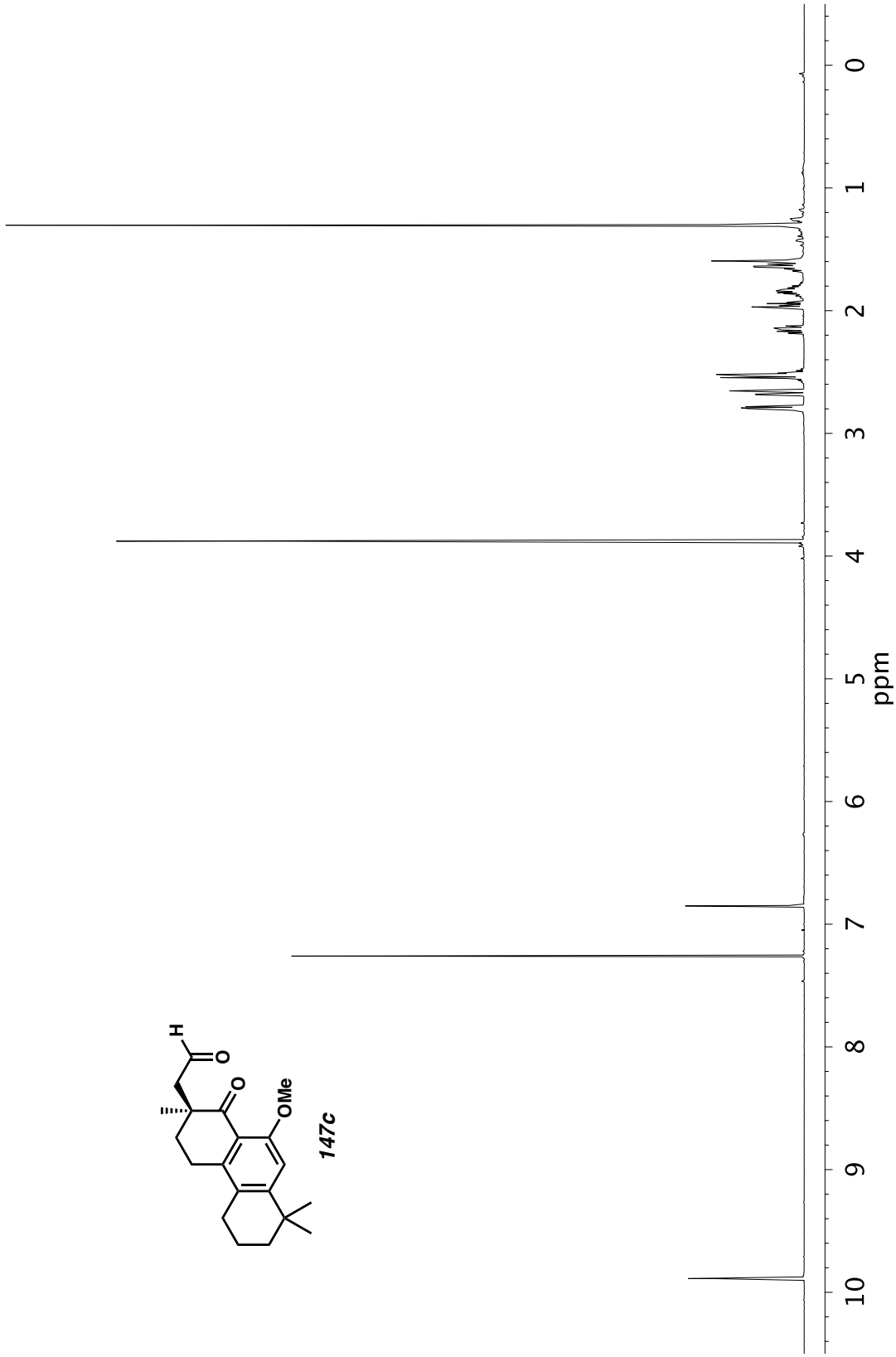

Figure A5.52. ^{1}H NMR (500 MHz, $CDCl_3$) of compound **147c**.

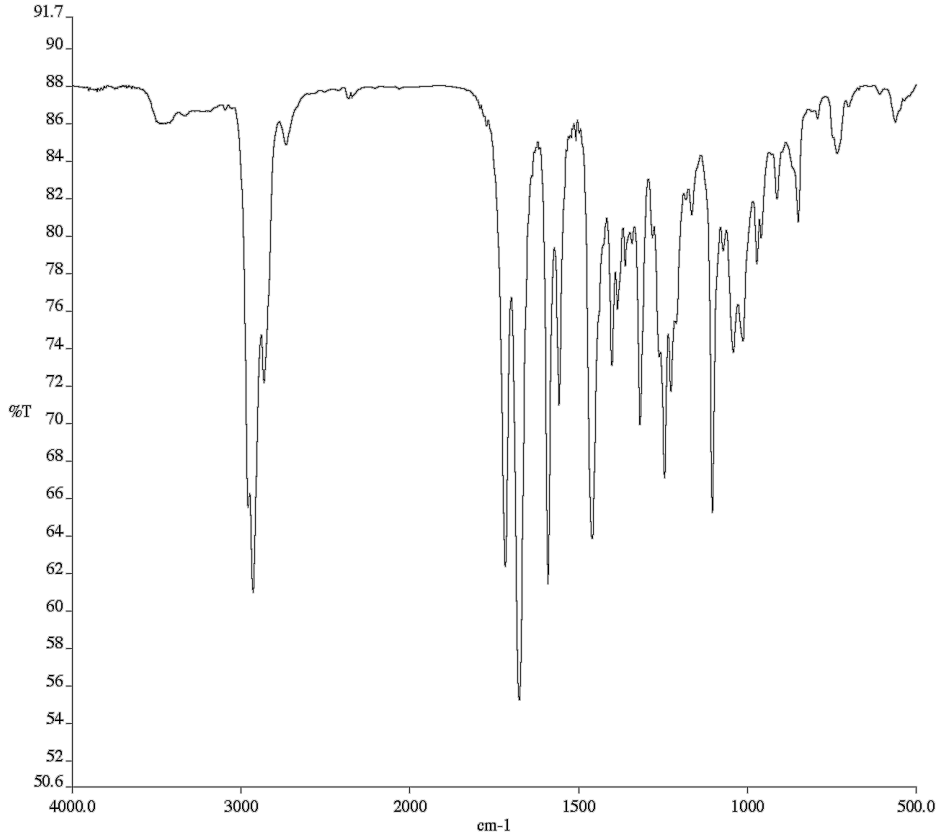

Figure A5.53. Infrared spectrum (Thin Film, KBr) of compound **147c**.

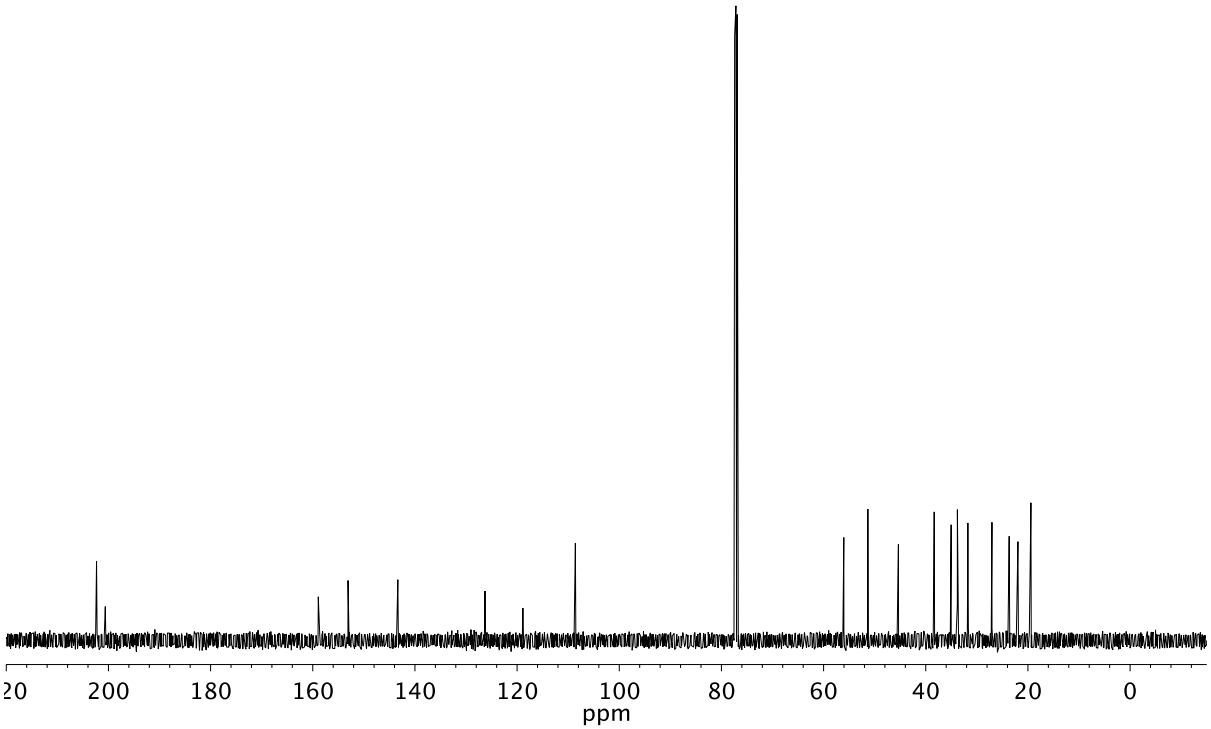

Figure A5.54. ^{13}C NMR (126 MHz, $CDCl_3$) of compound **147c**.

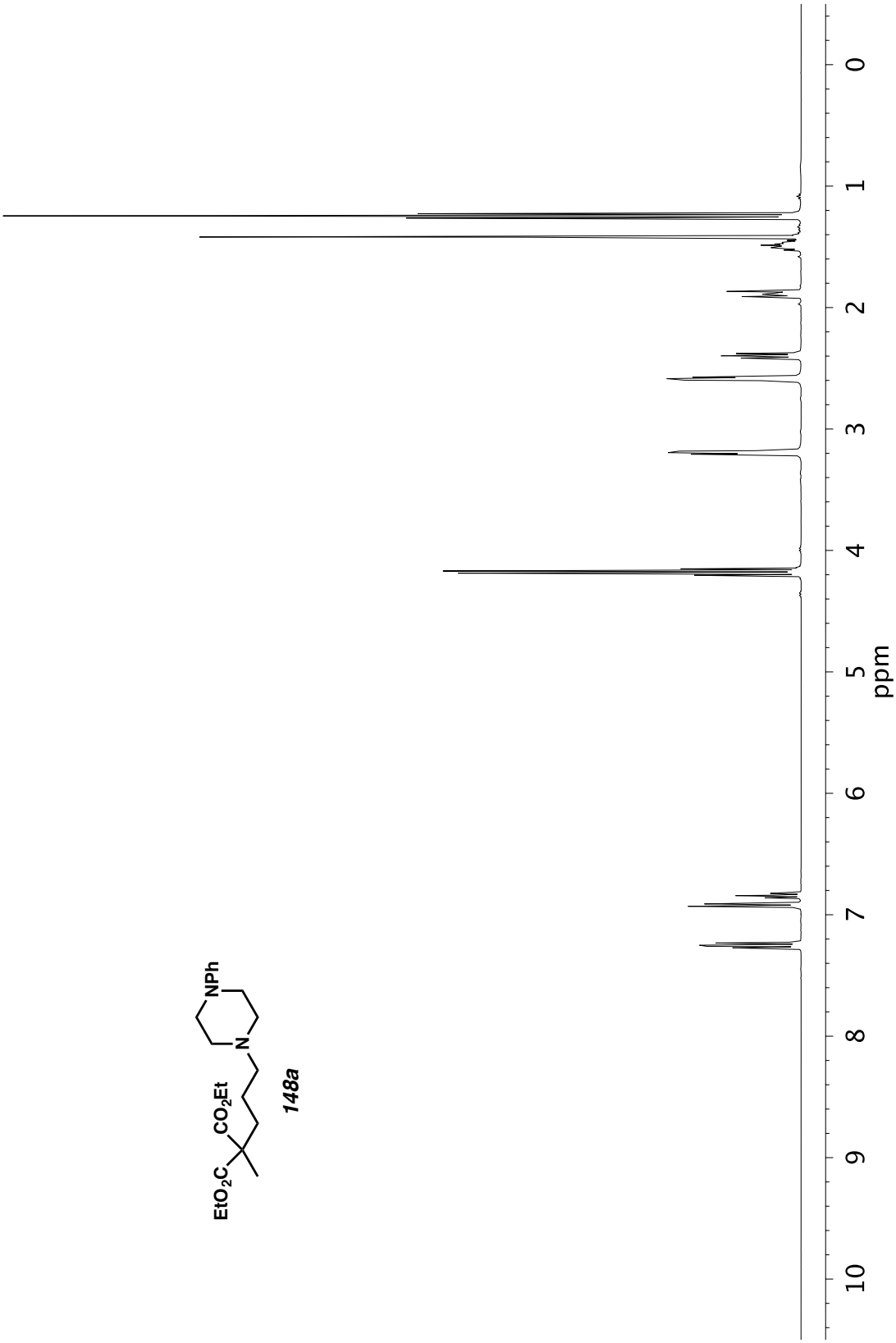

Figure A5.55. ^{1}H NMR (400 MHz, $CDCl_3$) of compound **148a**.

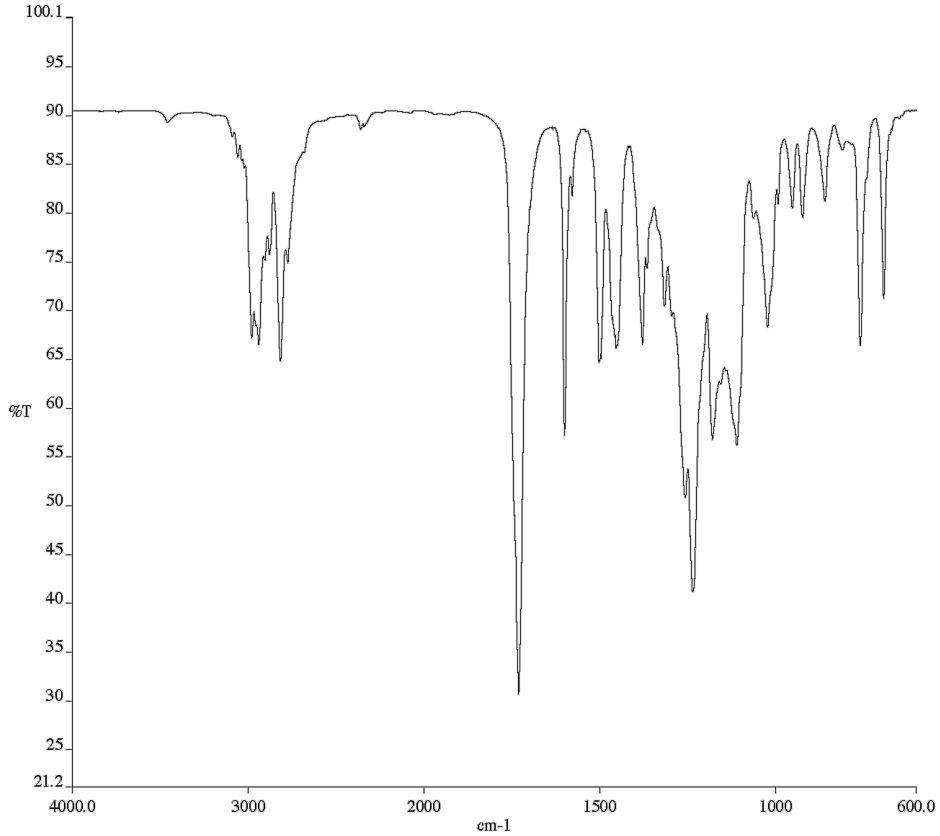

Figure A5.56. Infrared spectrum (Thin Film, KBr) of compound **148a**.

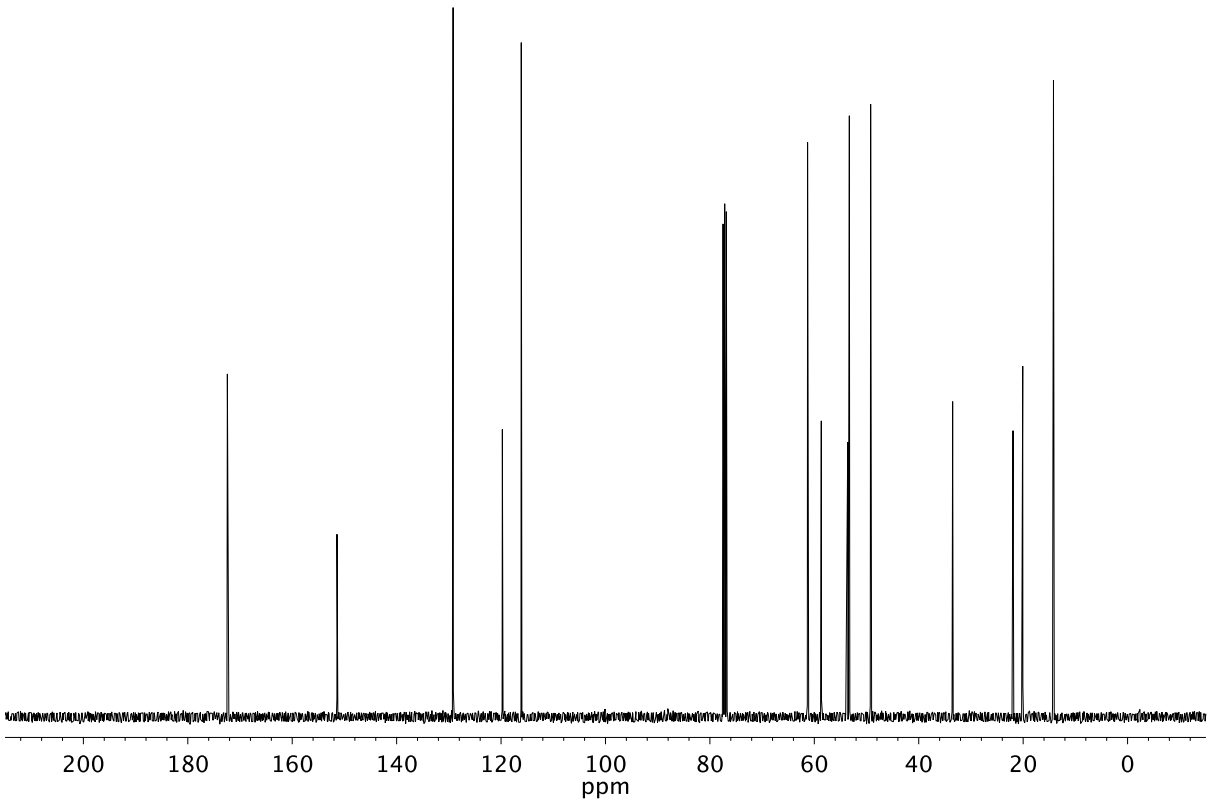

Figure A5.57. ^{13}C NMR (101 MHz, $CDCl_3$) of compound **148a**.

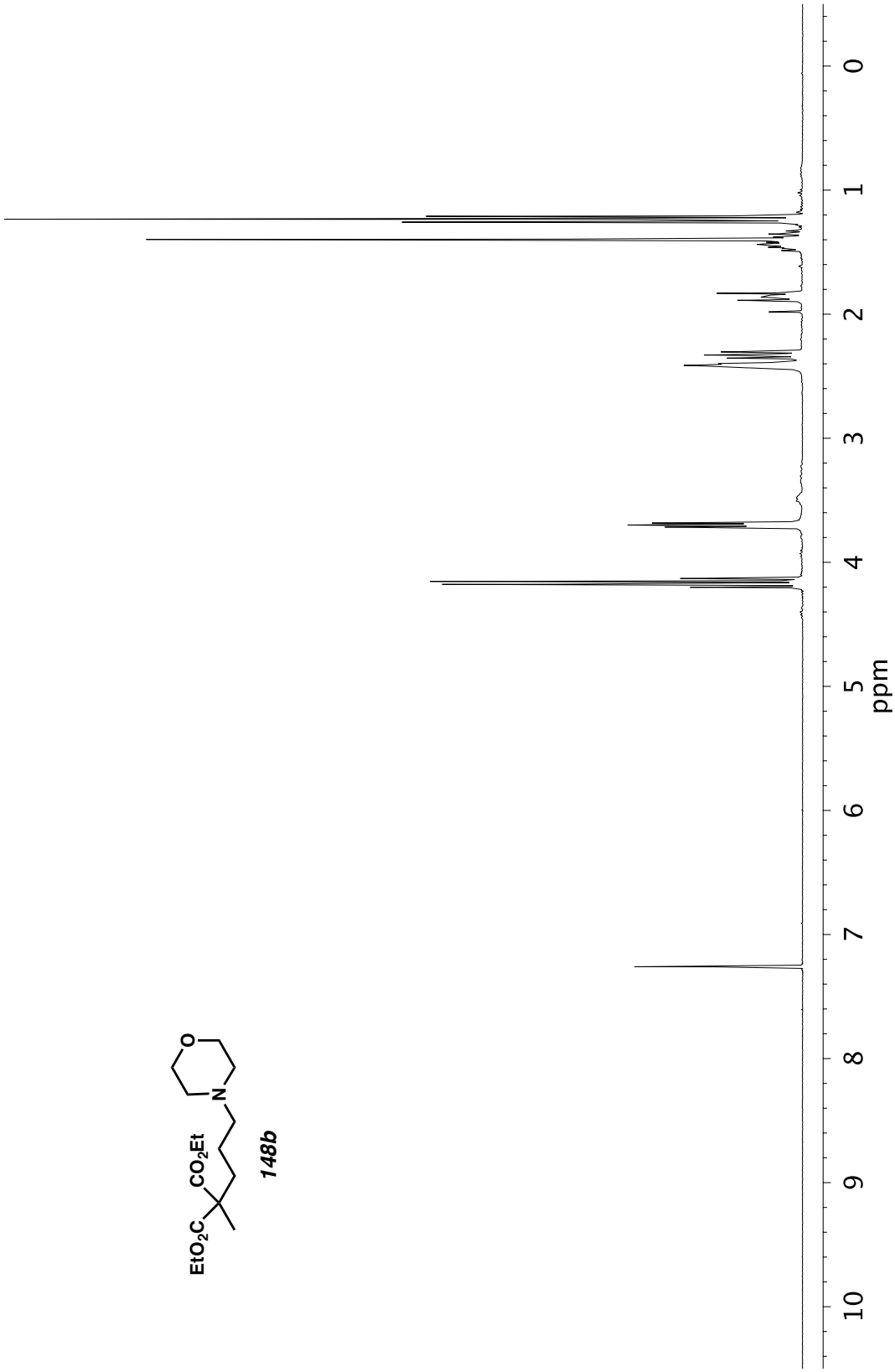

Figure A5.58. ^{1}H NMR (300 MHz, $CDCl_3$) of compound **148b**.

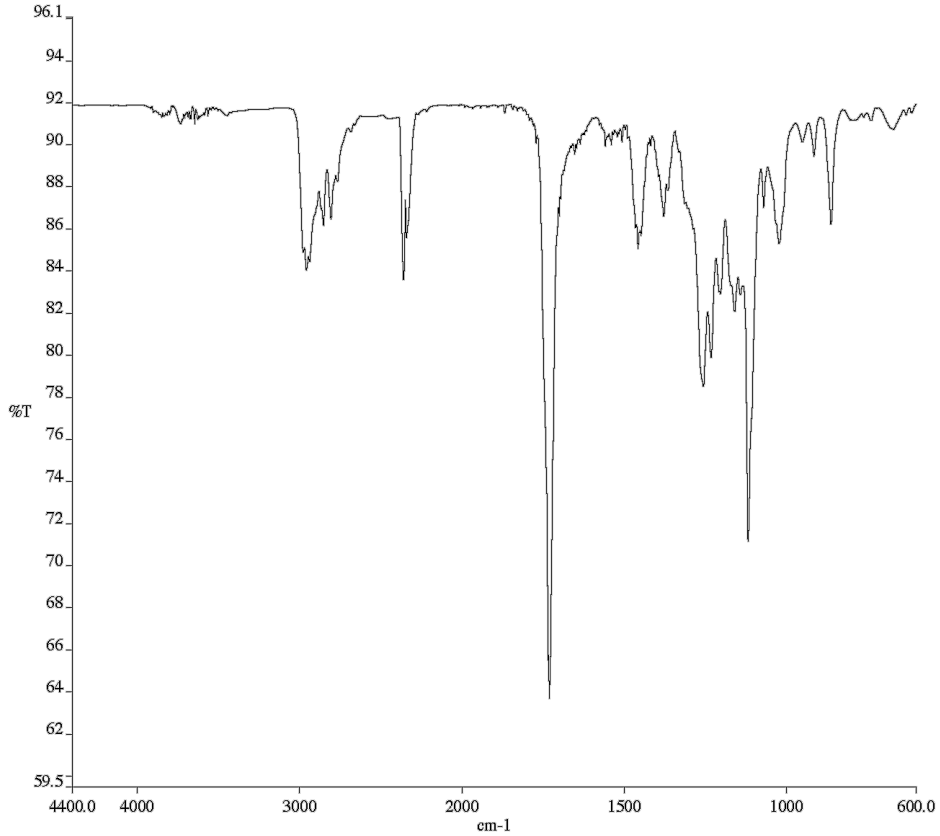

Figure A5.59. Infrared spectrum (Thin Film, KBr) of compound **148b**.

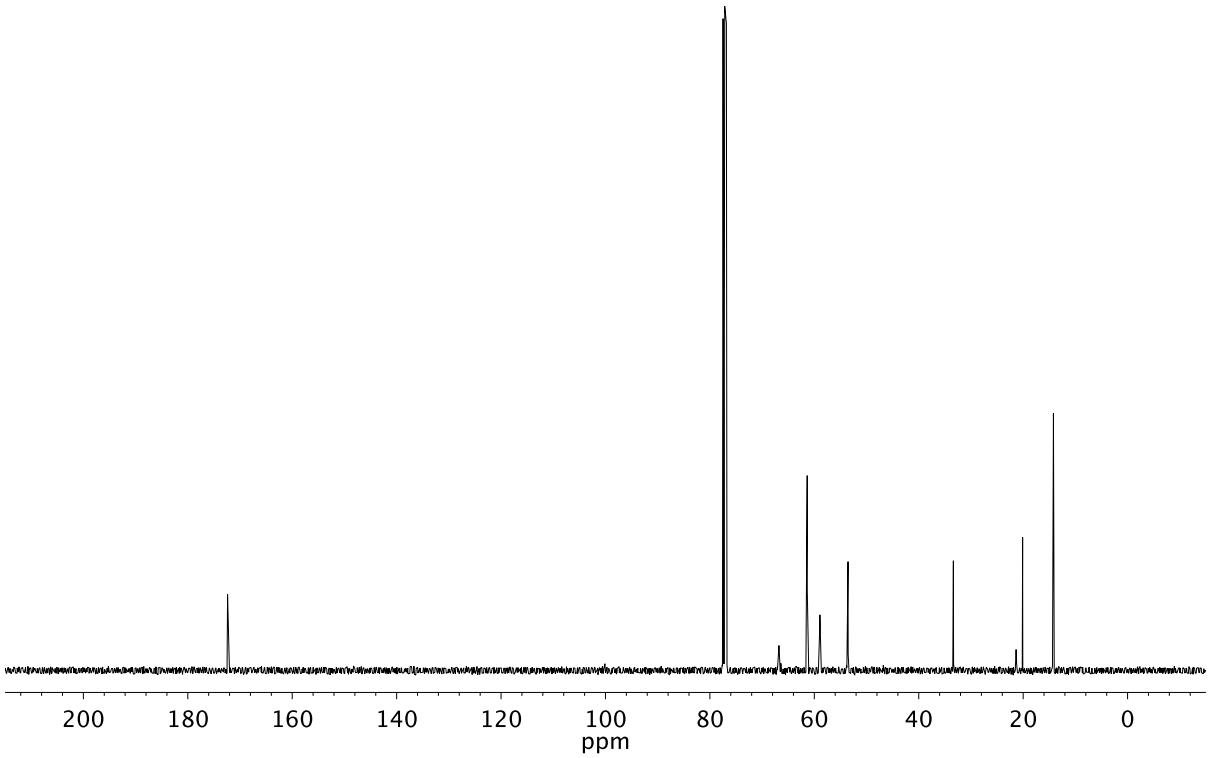

Figure A5.60. ^{13}C NMR (101 MHz, $CDCl_3$) of compound **148b**.

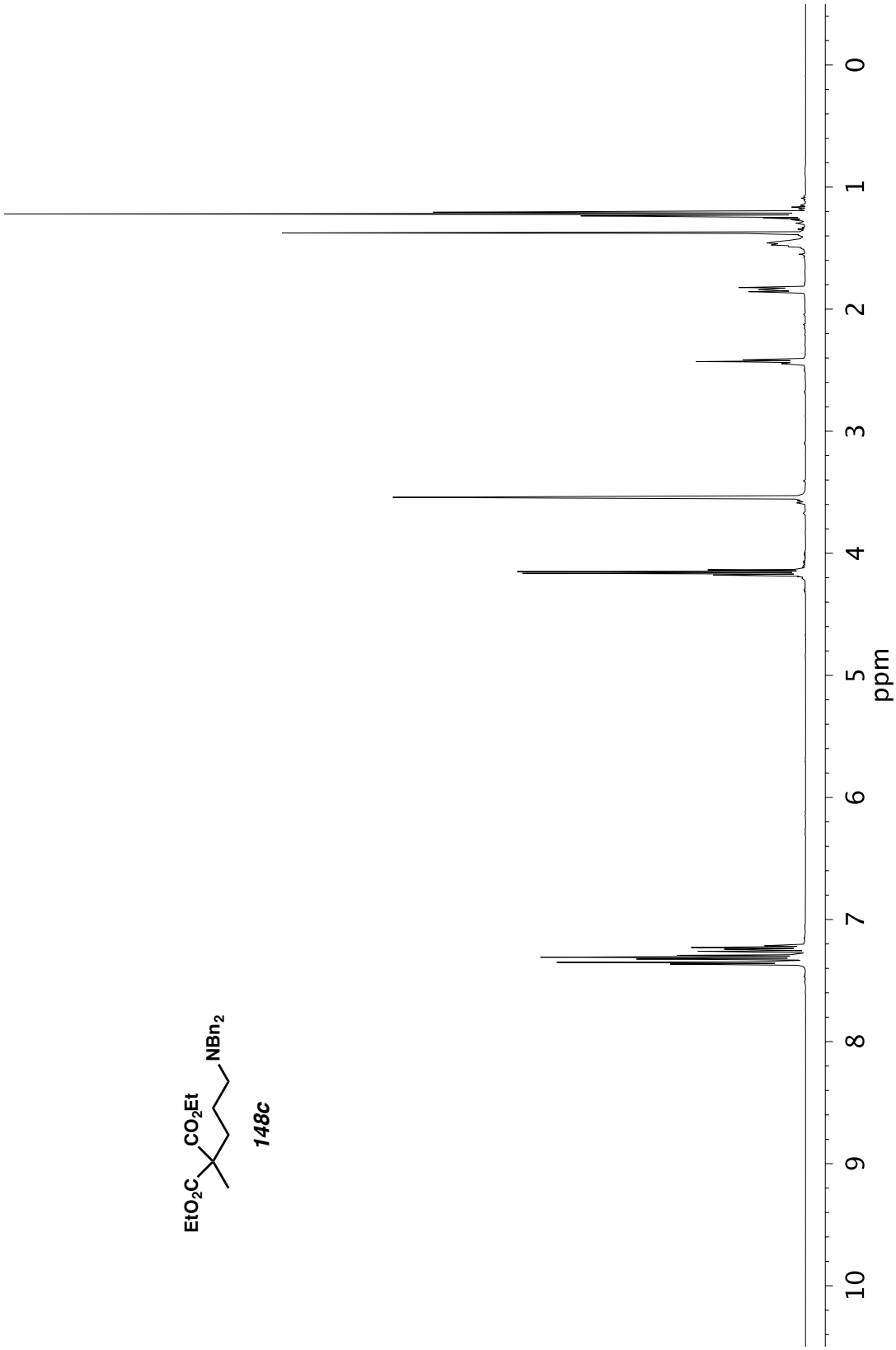

Figure A5.61. ^{1}H NMR (500 MHz, $CDCl_3$) of compound **148c**.

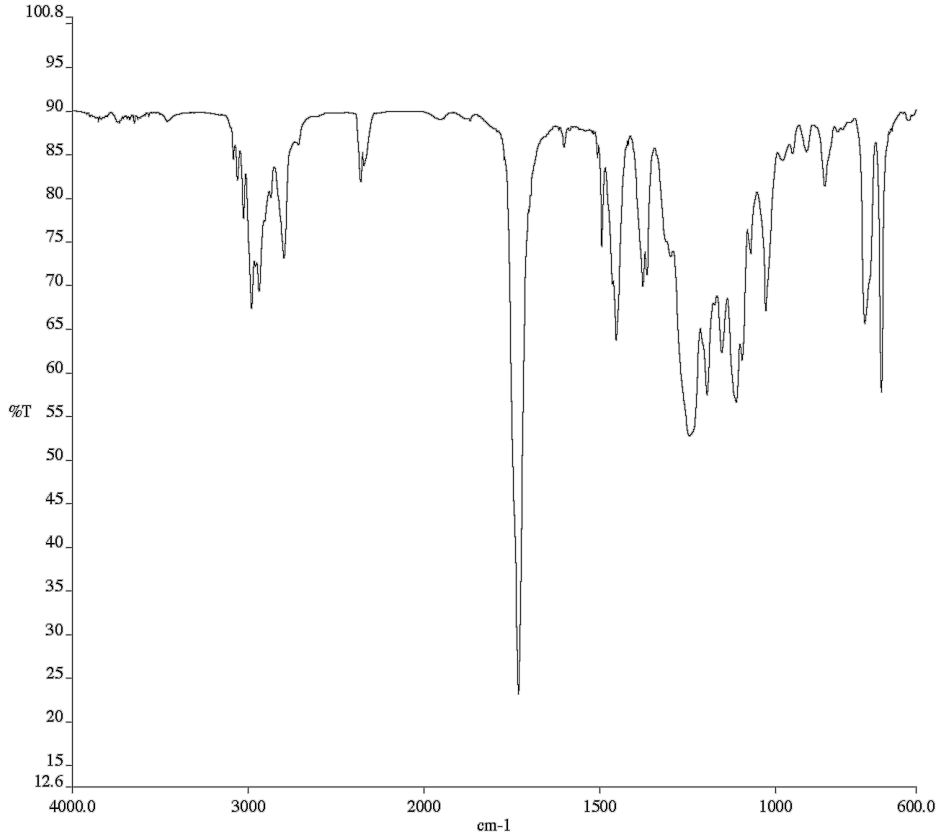

Figure A5.62. Infrared spectrum (Thin Film, KBr) of compound **148c**.

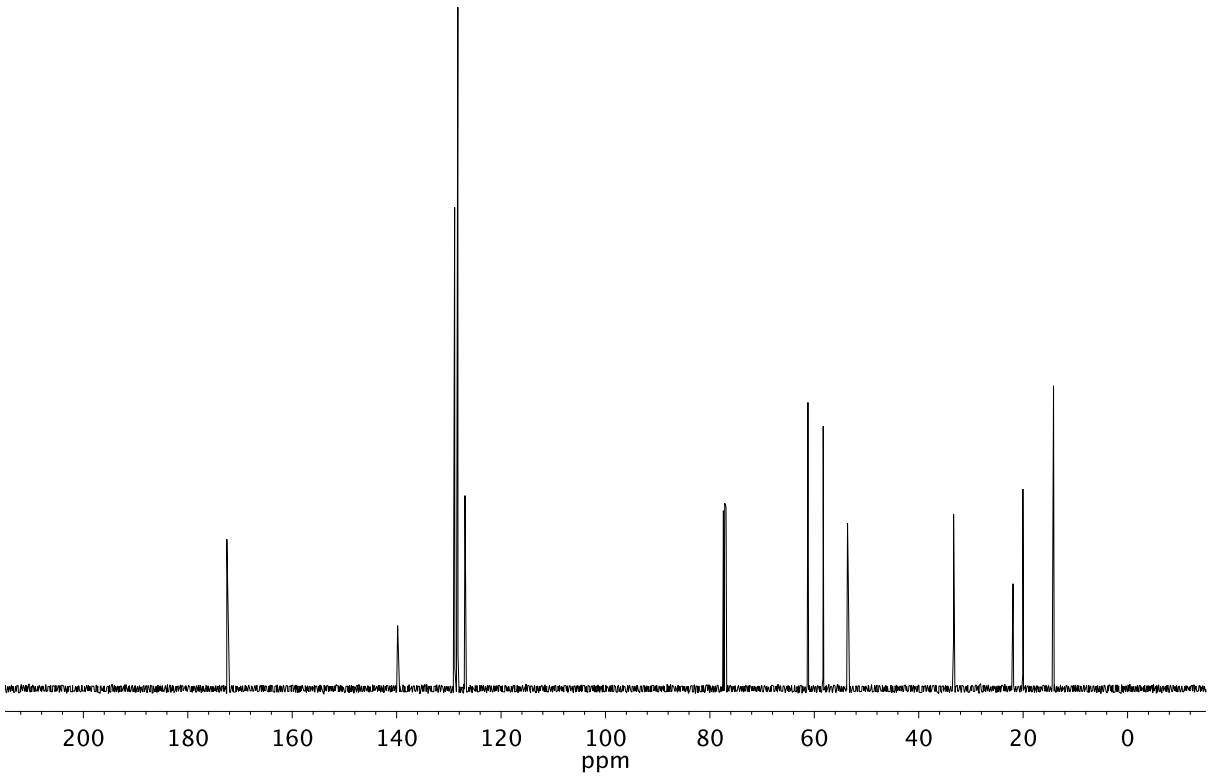

Figure A5.63. ^{13}C NMR (126 MHz, $CDCl_3$) of compound **148c.**

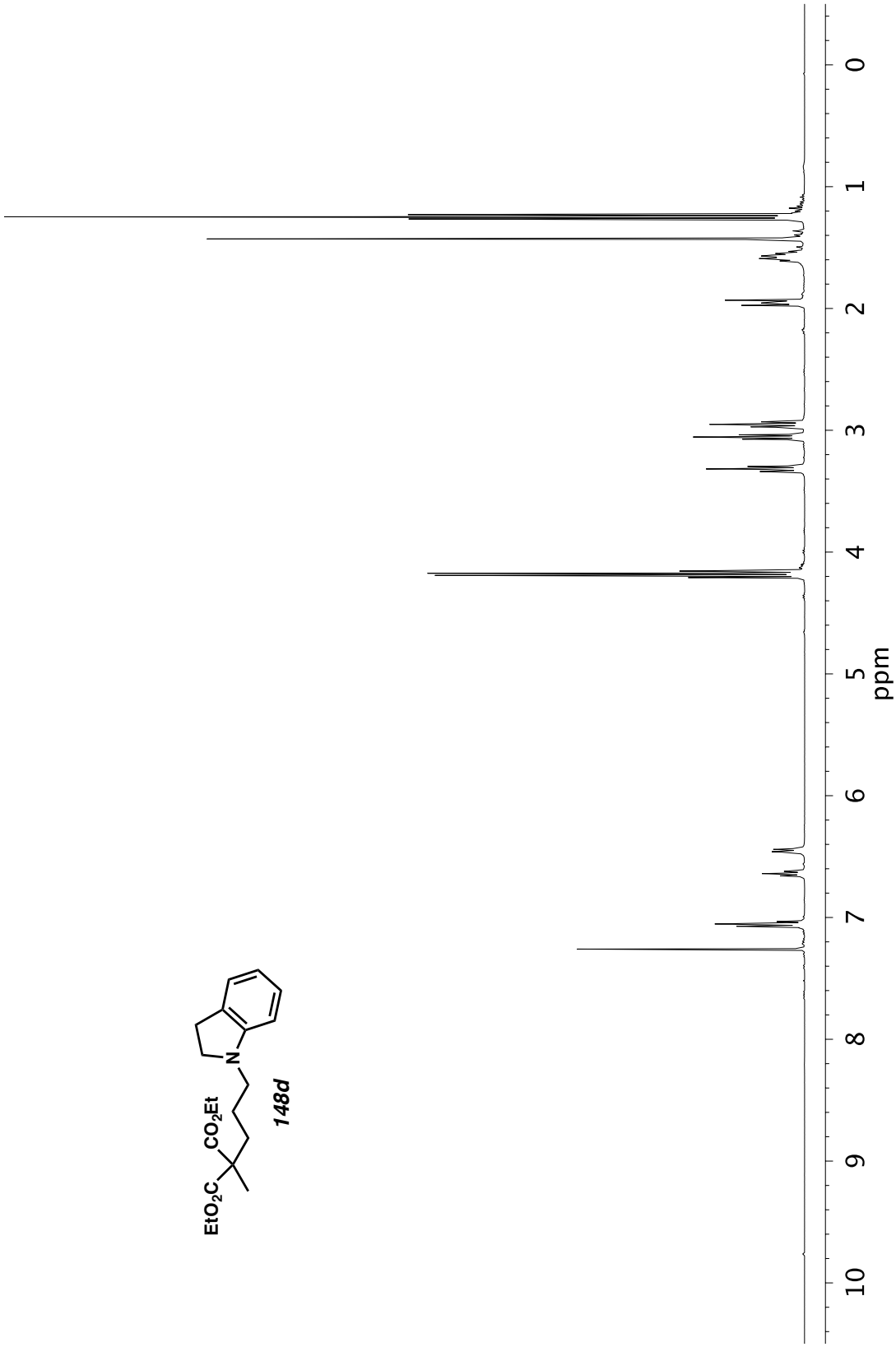

Figure A5.64. ^{1}H NMR (400 MHz, $CDCl_3$) of compound **148d**.

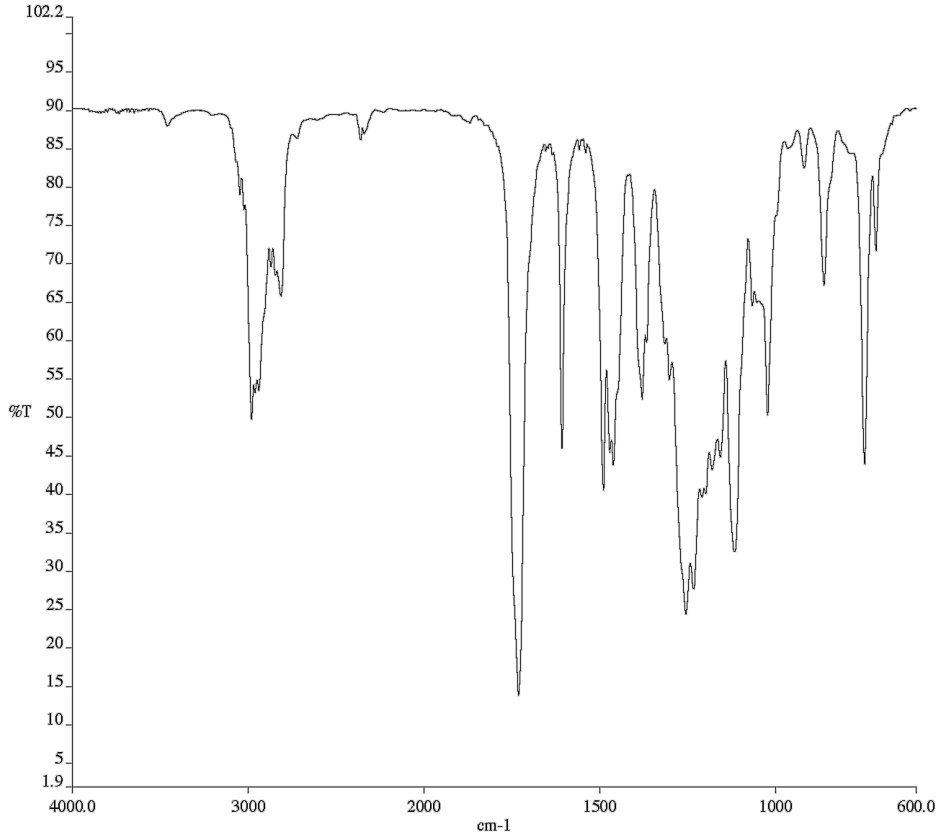

Figure A5.65. Infrared spectrum (Thin Film, KBr) of compound **148d**.

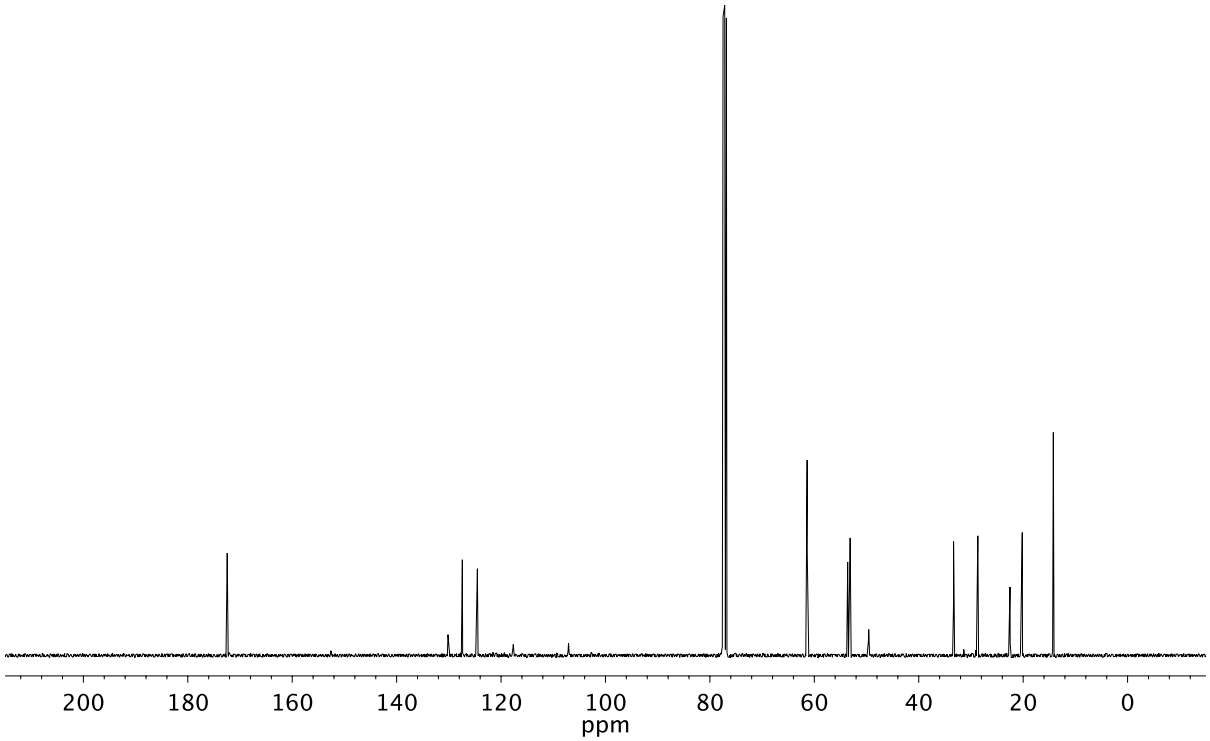

Figure A5.66. ^{13}C NMR (101 MHz, $CDCl_3$) of compound **148d**.

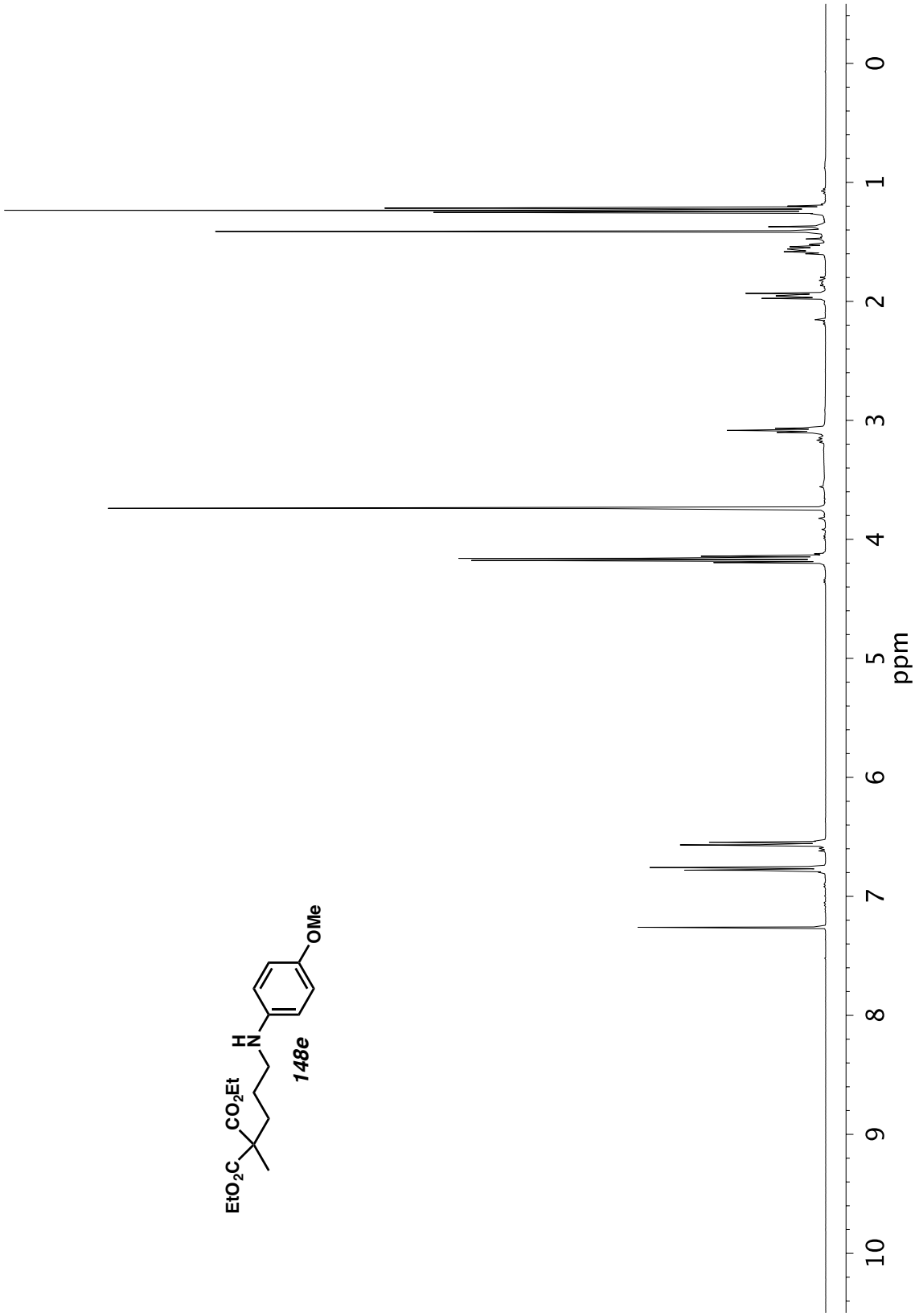

Figure A5.67. ^{1}H NMR (400 MHz, $CDCl_3$) of compound **148e**.

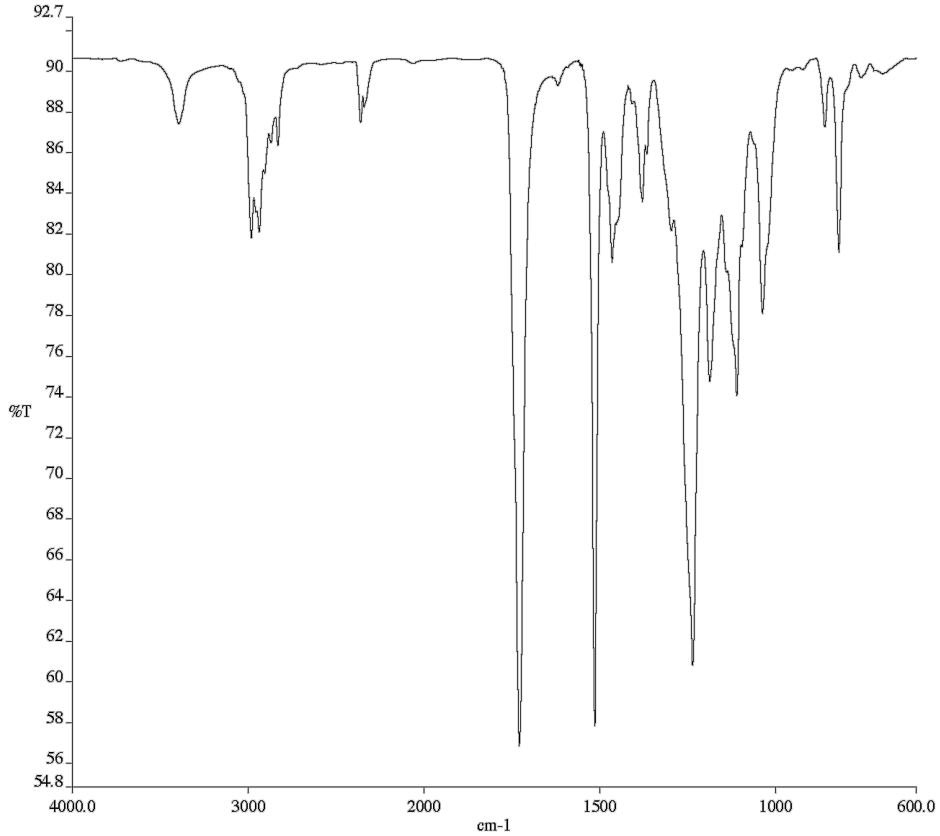

Figure A5.68. Infrared spectrum (Thin Film, KBr) of compound **148e**.

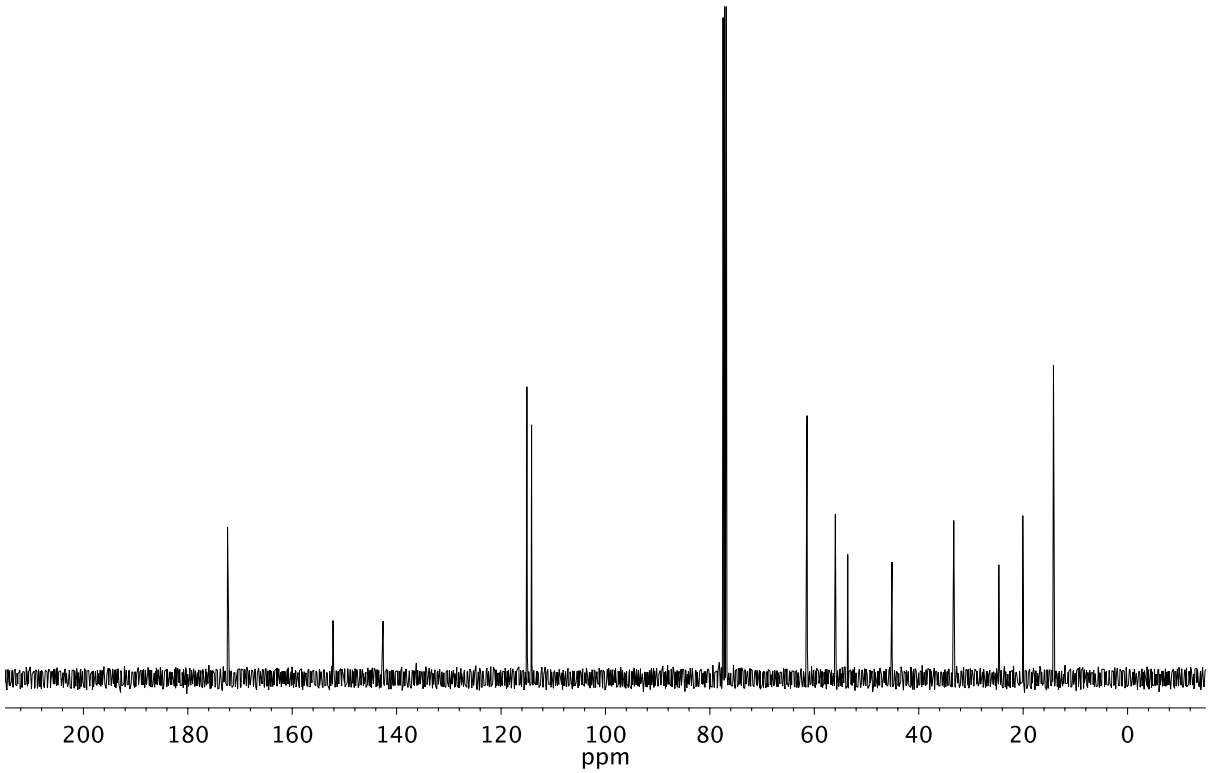

Figure A5.69. ^{13}C NMR (101 MHz, $CDCl_3$) of compound **148e**.

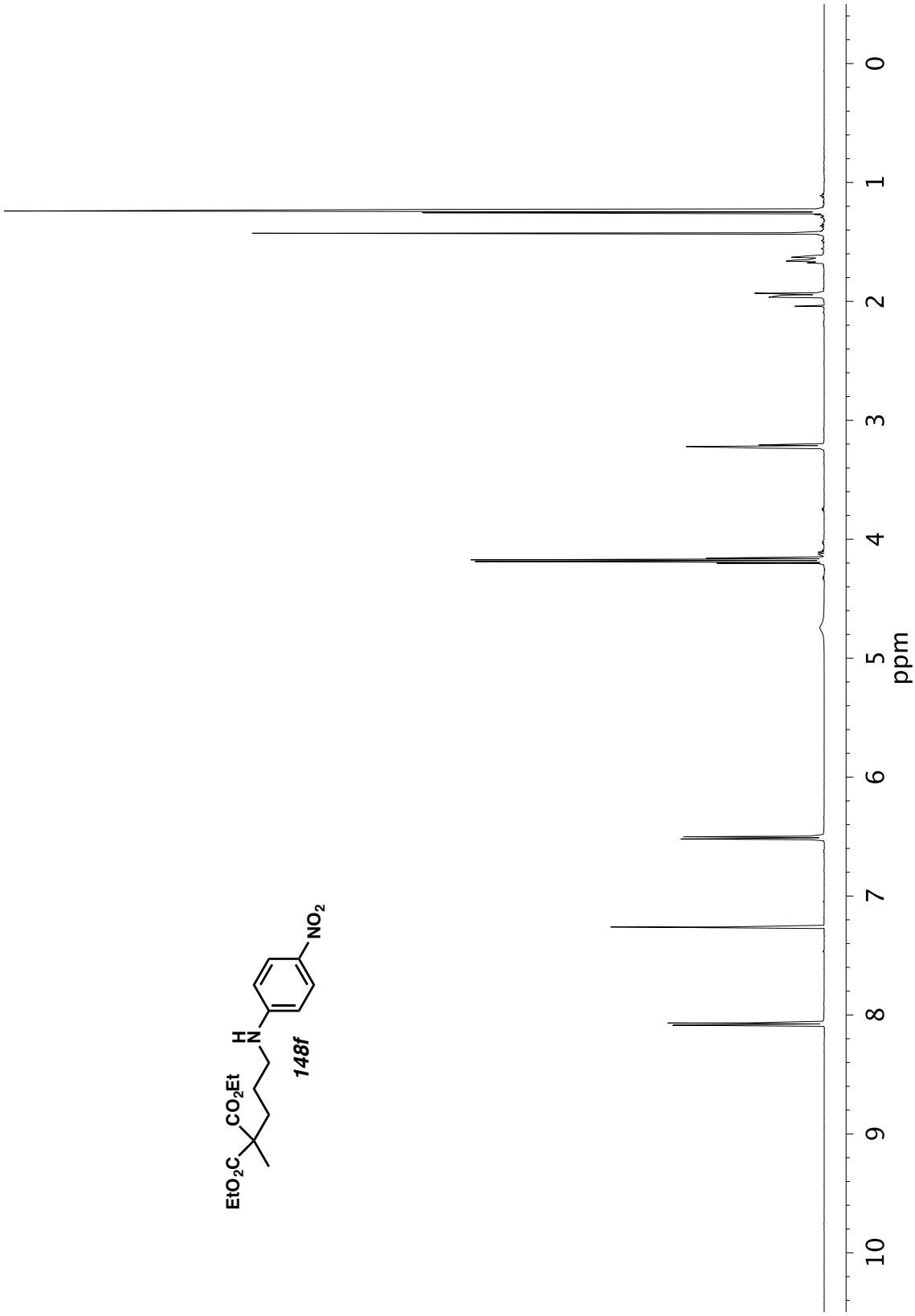

Figure A5.70. ^{1}H NMR (500 MHz, $CDCl_3$) of compound **148f**.

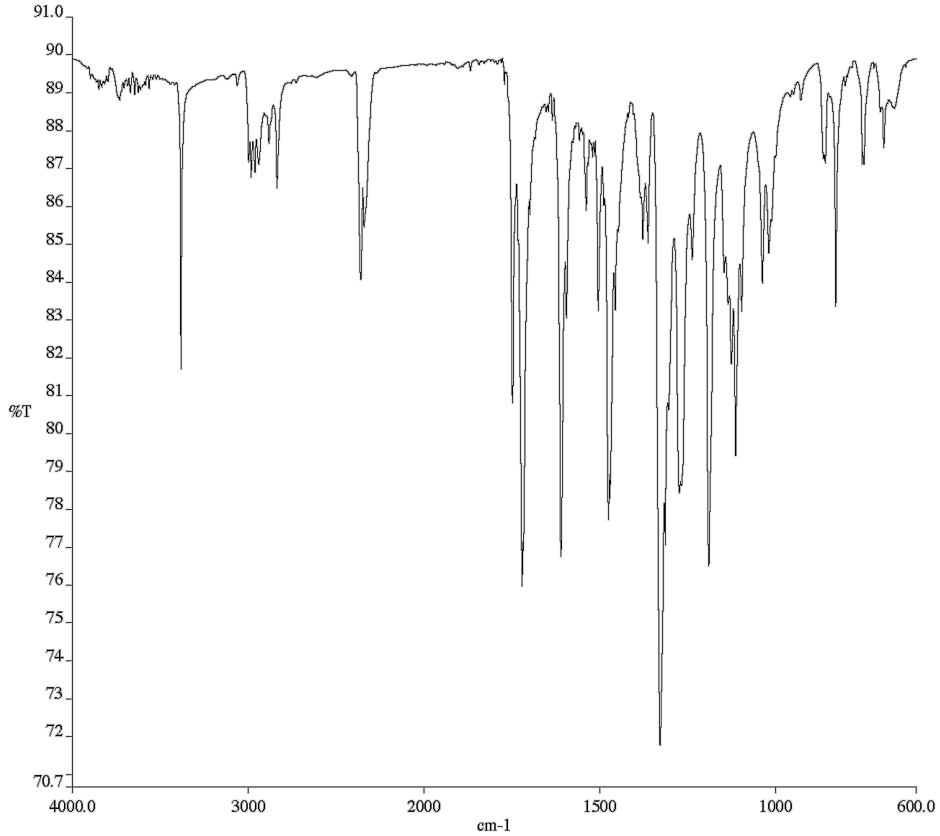

Figure A5.71. Infrared spectrum (Thin Film, KBr) of compound **148f**.

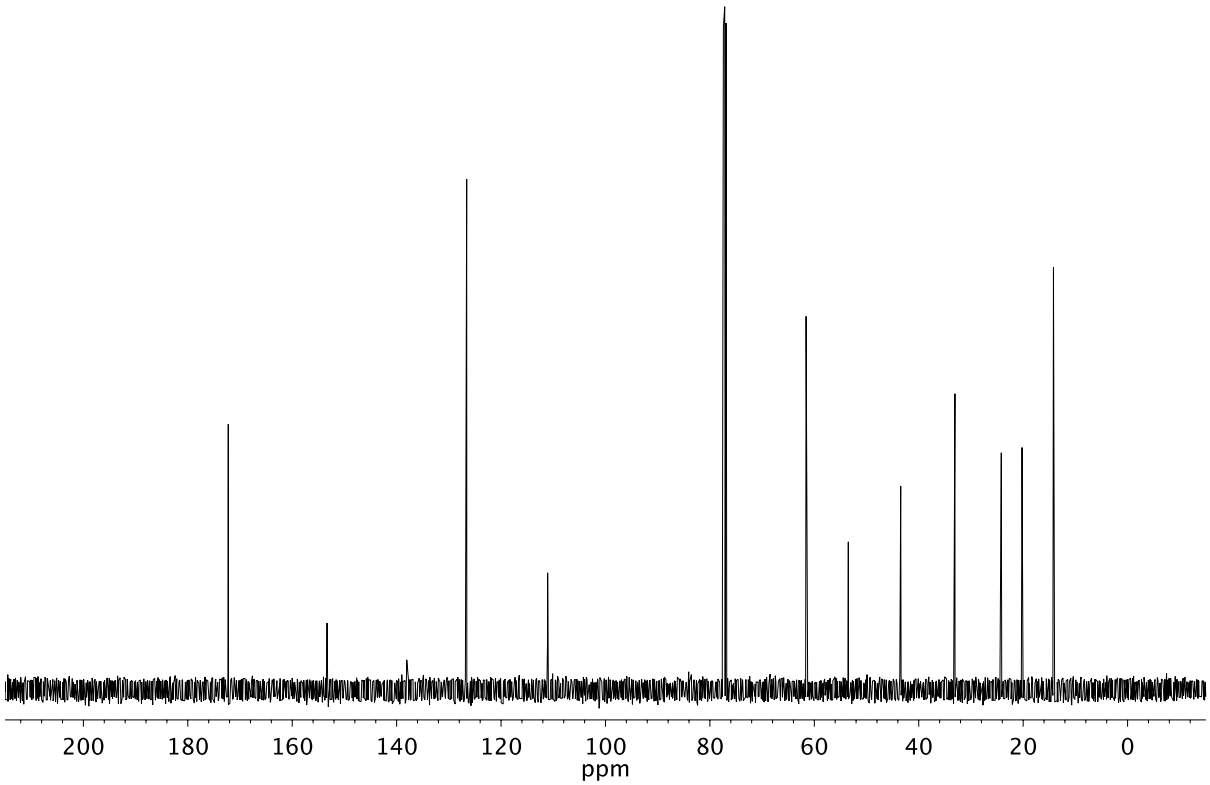

Figure A5.72. ^{13}C NMR (126 MHz, $CDCl_3$) of compound **148f**.

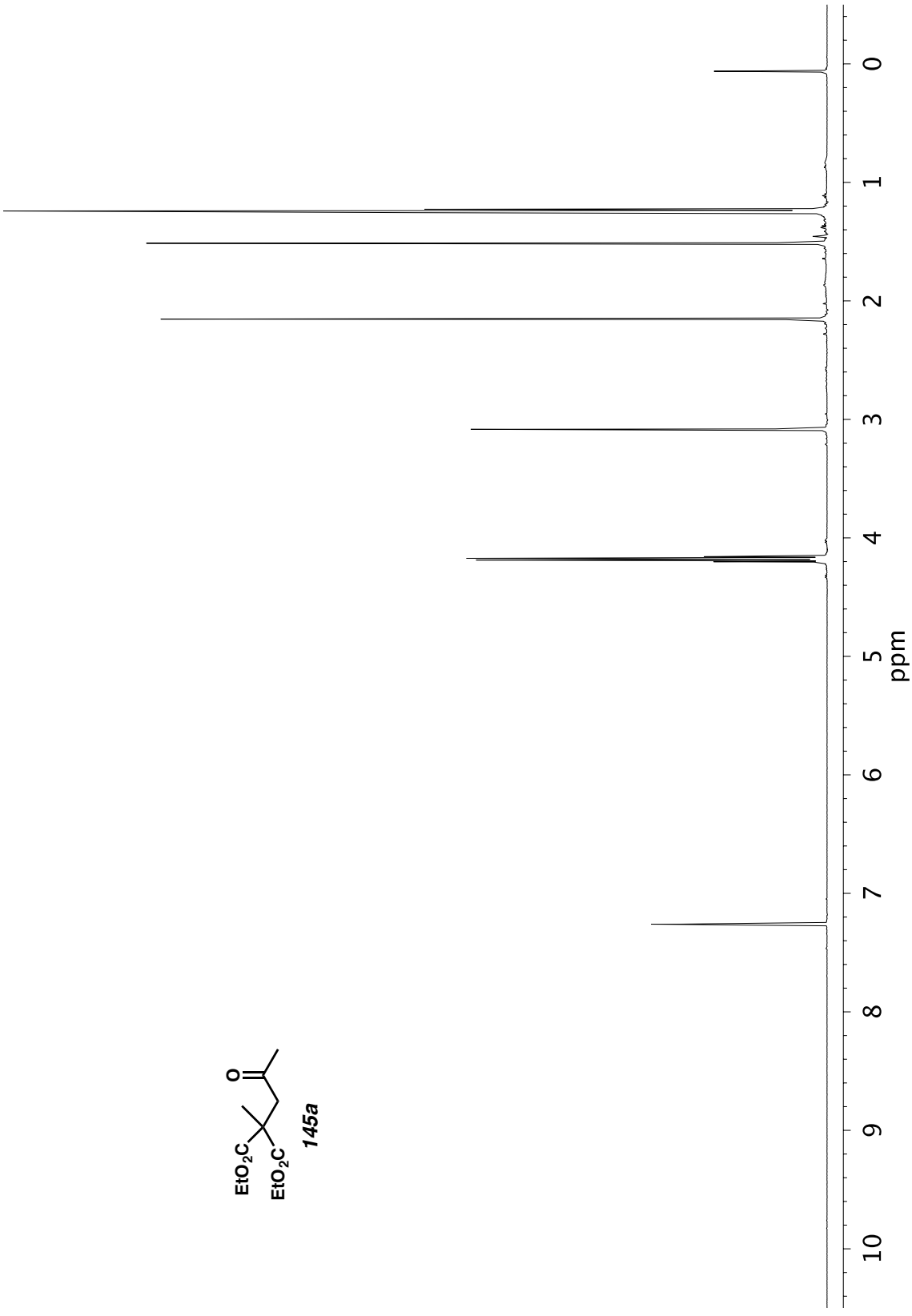

Figure A5.73. ^{1}H NMR (500 MHz, $CDCl_3$) of compound **145a**.

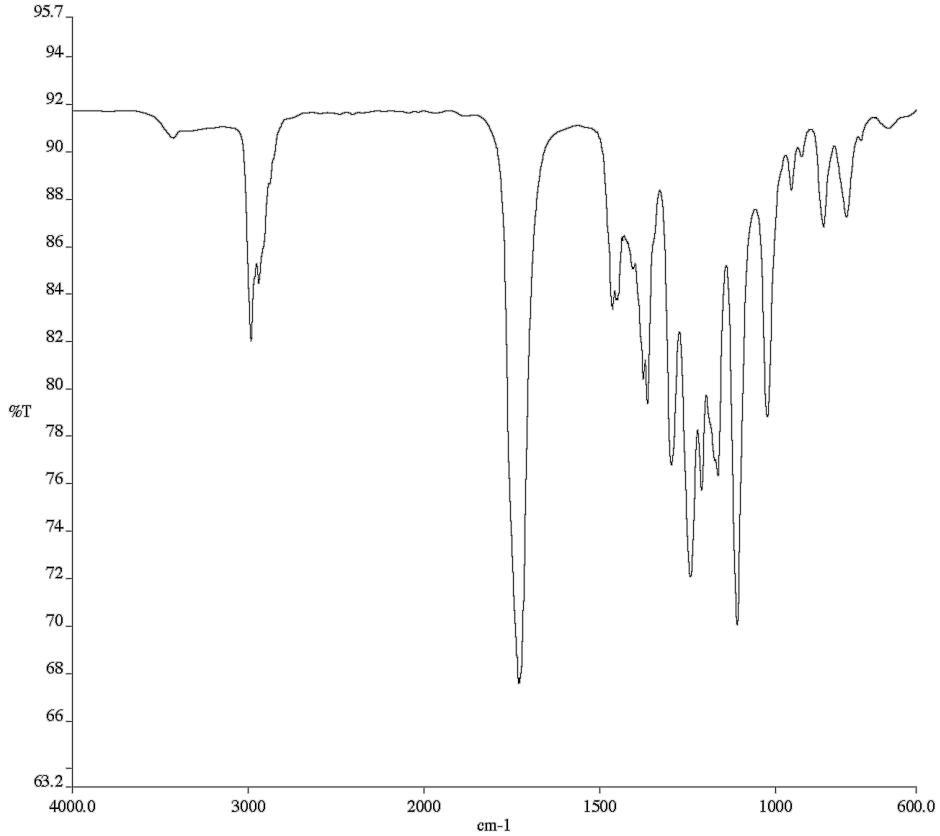

Figure A5.74. Infrared spectrum (Thin Film, KBr) of compound **145a**.

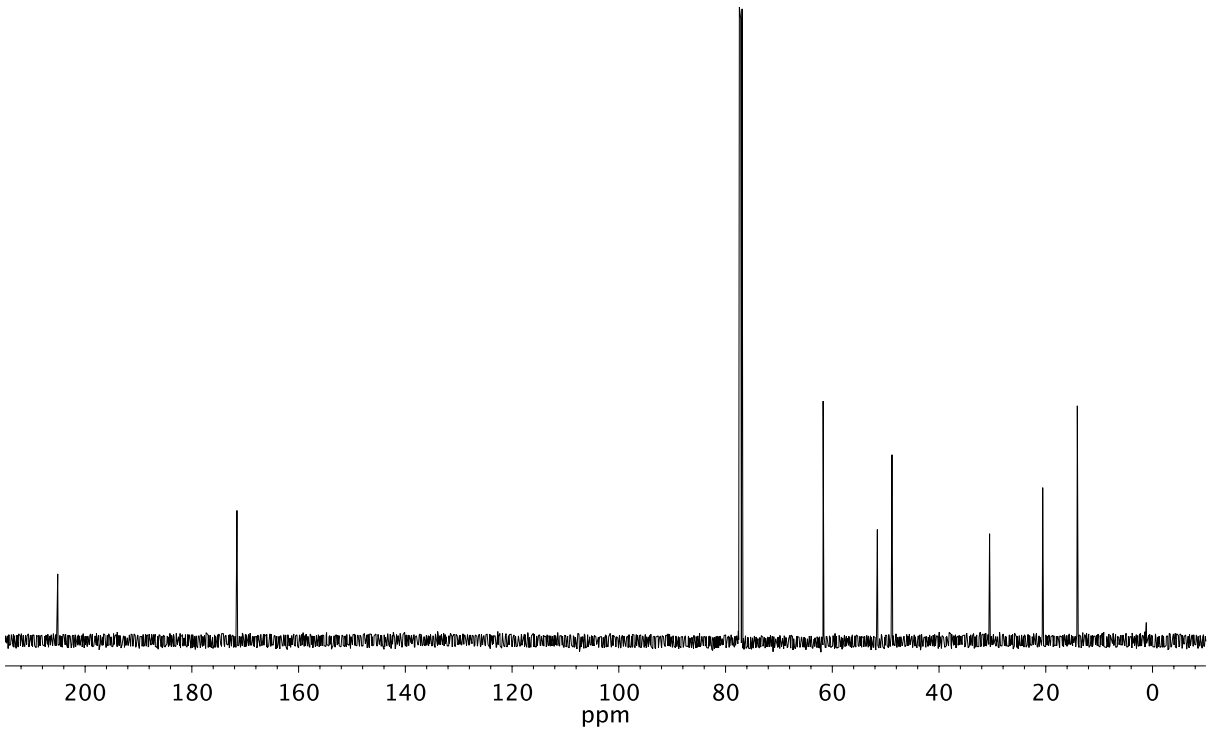

Figure A5.75. ^{13}C NMR (126 MHz, $CDCl_3$) of compound **145a**.

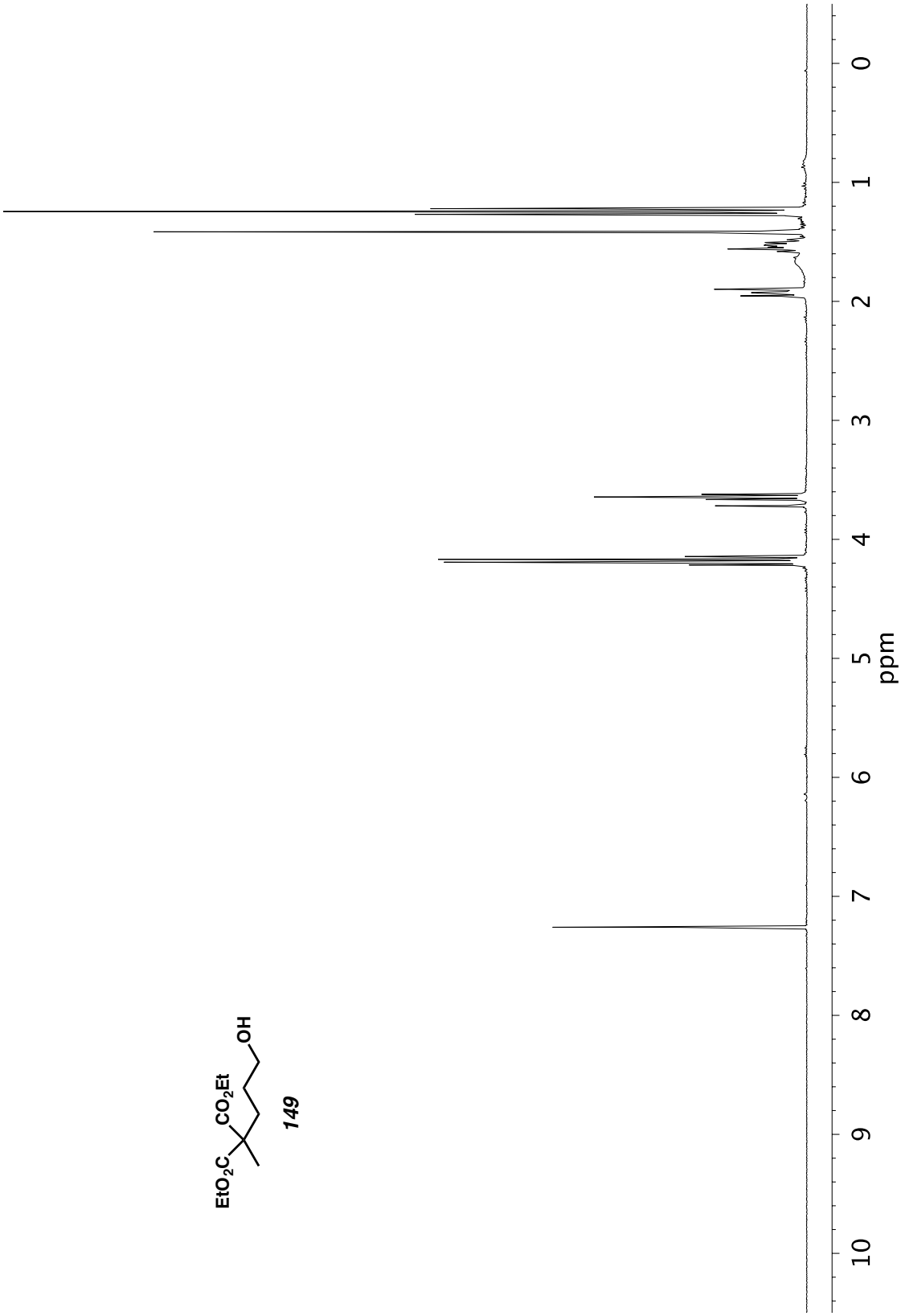

Figure A5.76. ^{1}H NMR (300 MHz, $CDCl_3$) of compound **149**.

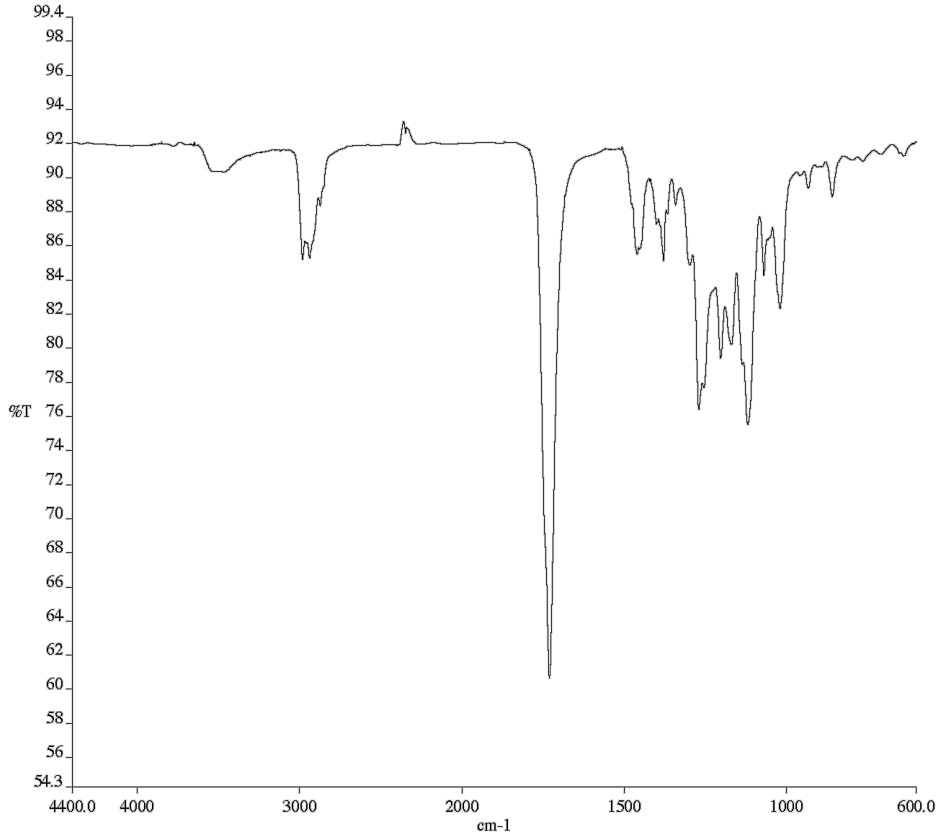

Figure A5.77. Infrared spectrum (Thin Film, KBr) of compound **149**.

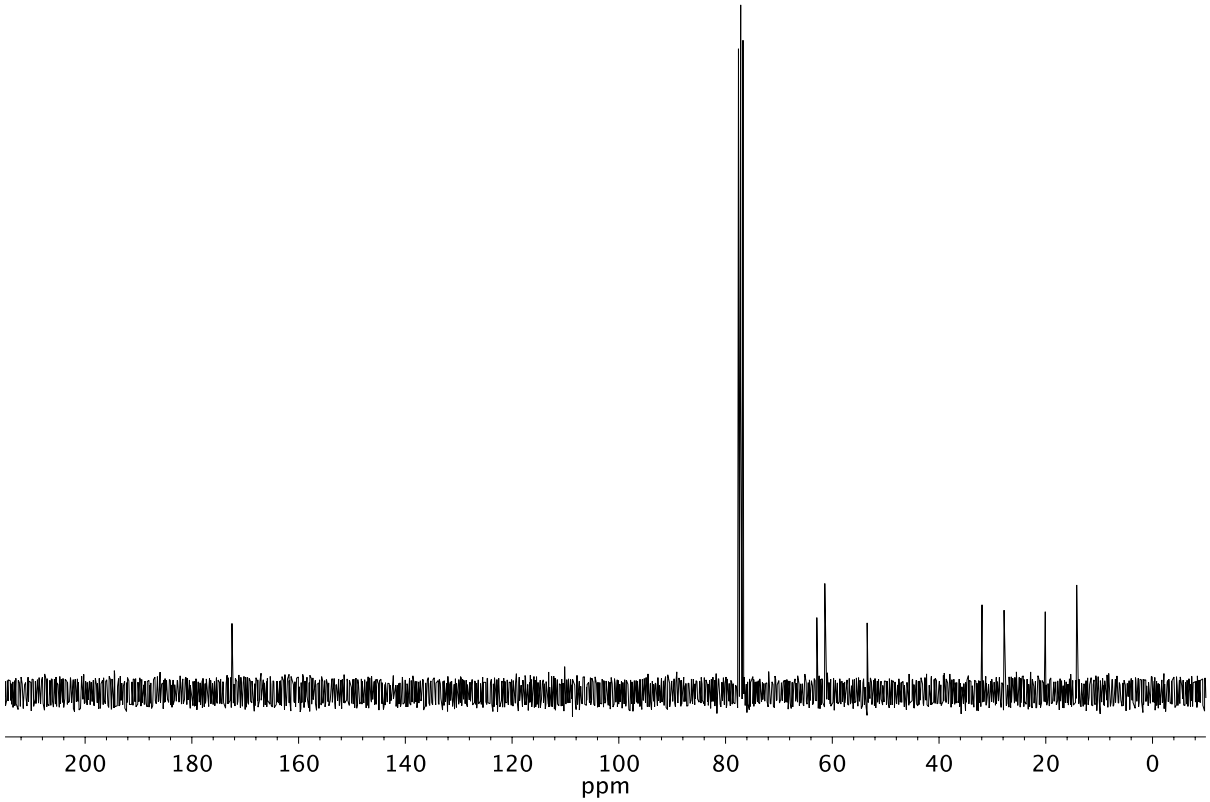

Figure A5.78. ^{13}C NMR (75 MHz, $CDCl_3$) of compound **149**.

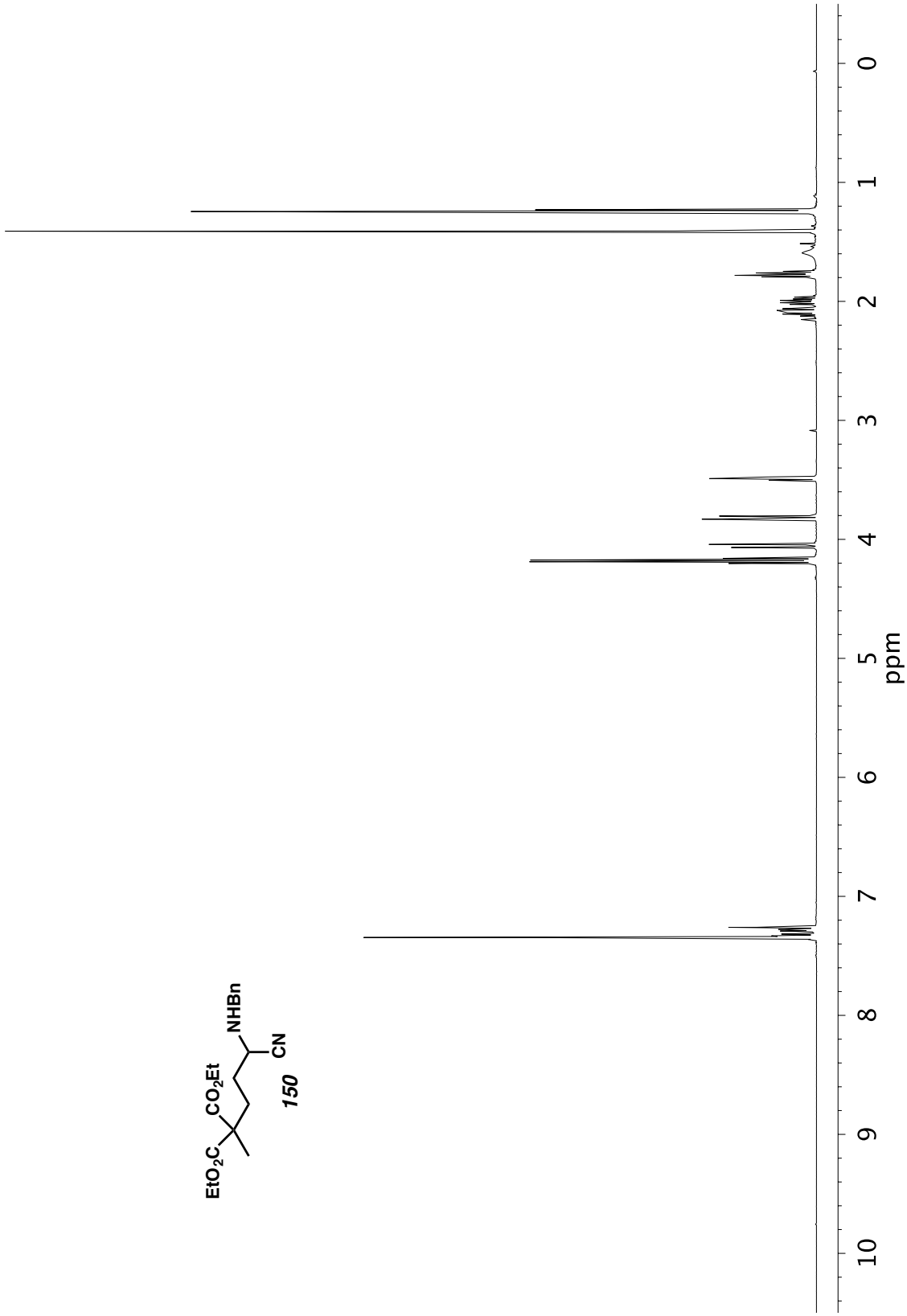

Figure A5.79. ^{1}H NMR (500 MHz, $CDCl_3$) of compound **150**.

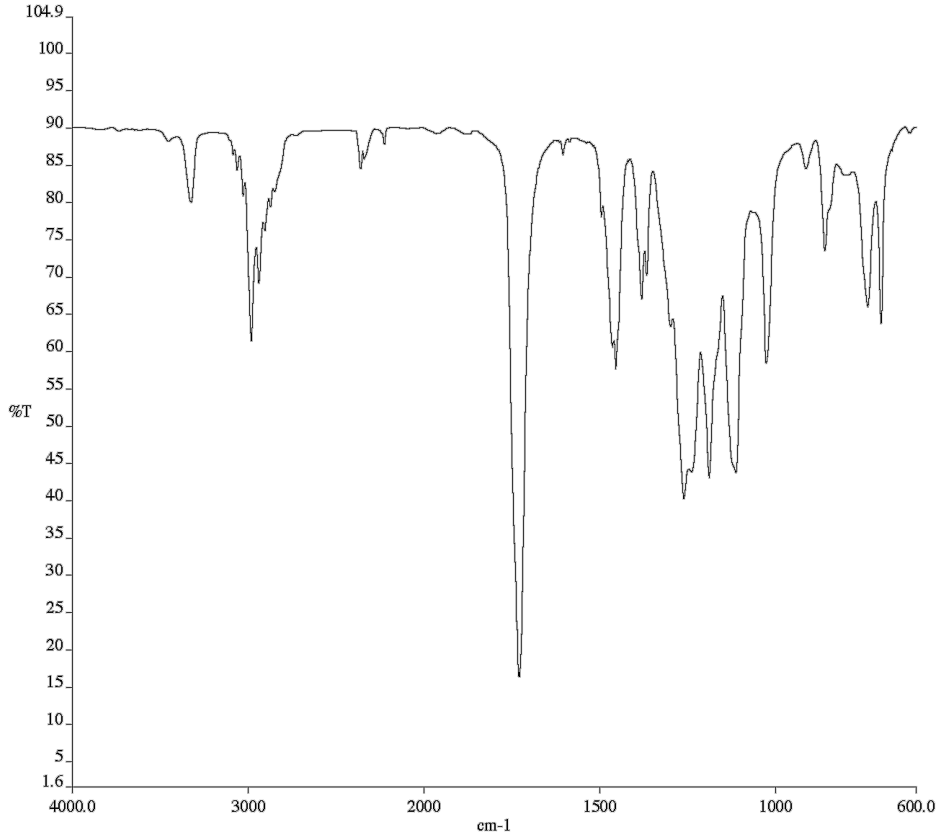

Figure A5.80. Infrared spectrum (Thin Film, KBr) of compound **150**.

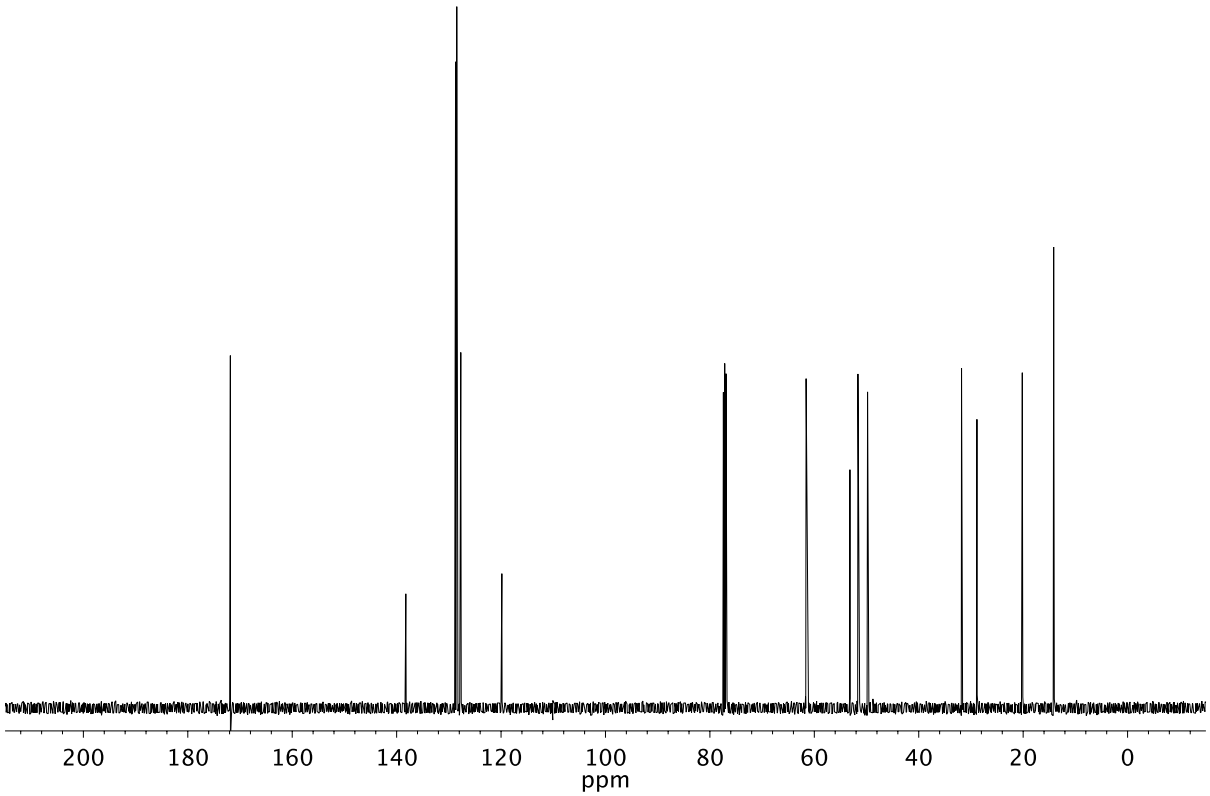

Figure A5.81. ^{13}C NMR (126 MHz, $CDCl_3$) of compound **150**.

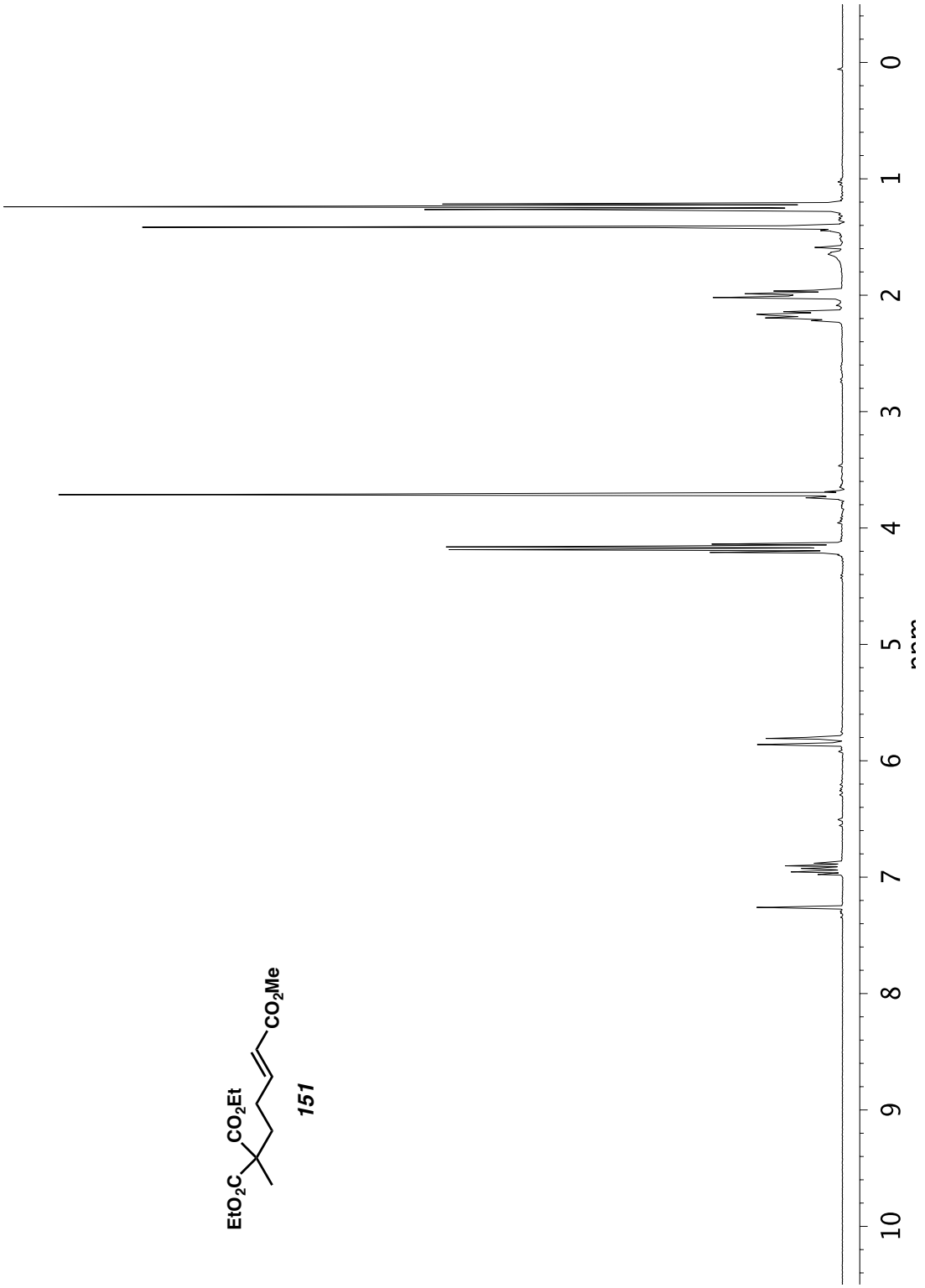

Figure A5.82. ^{1}H NMR (300 MHz, $CDCl_3$) of compound **151**.

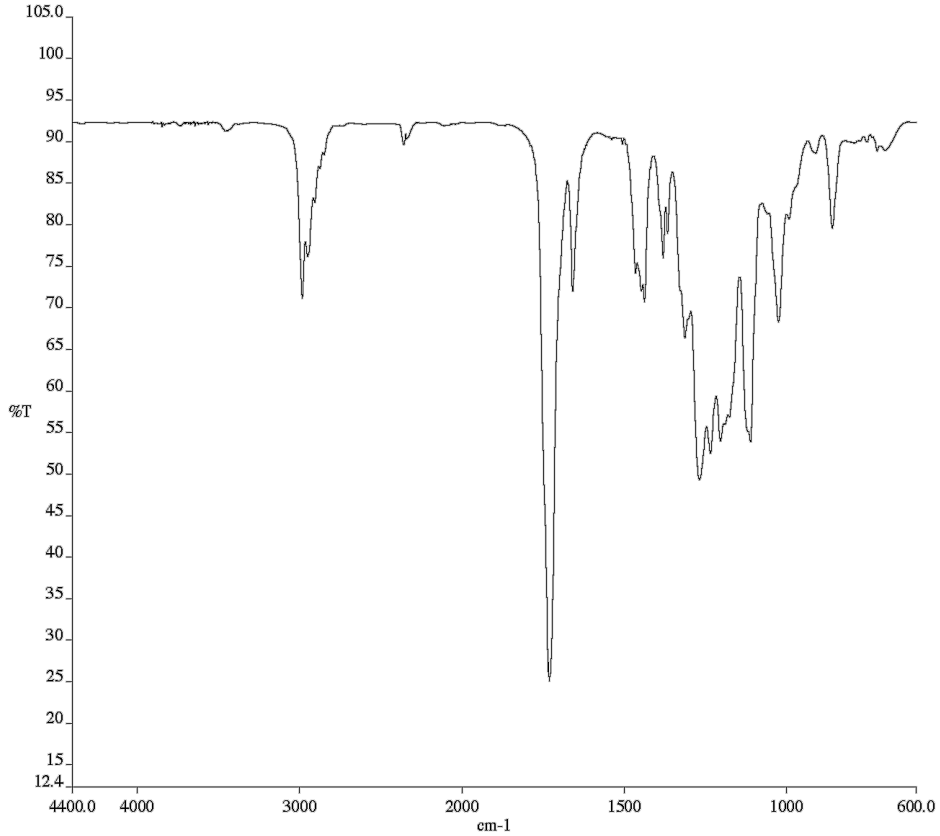

Figure A5.83. Infrared spectrum (Thin Film, KBr) of compound **151**.

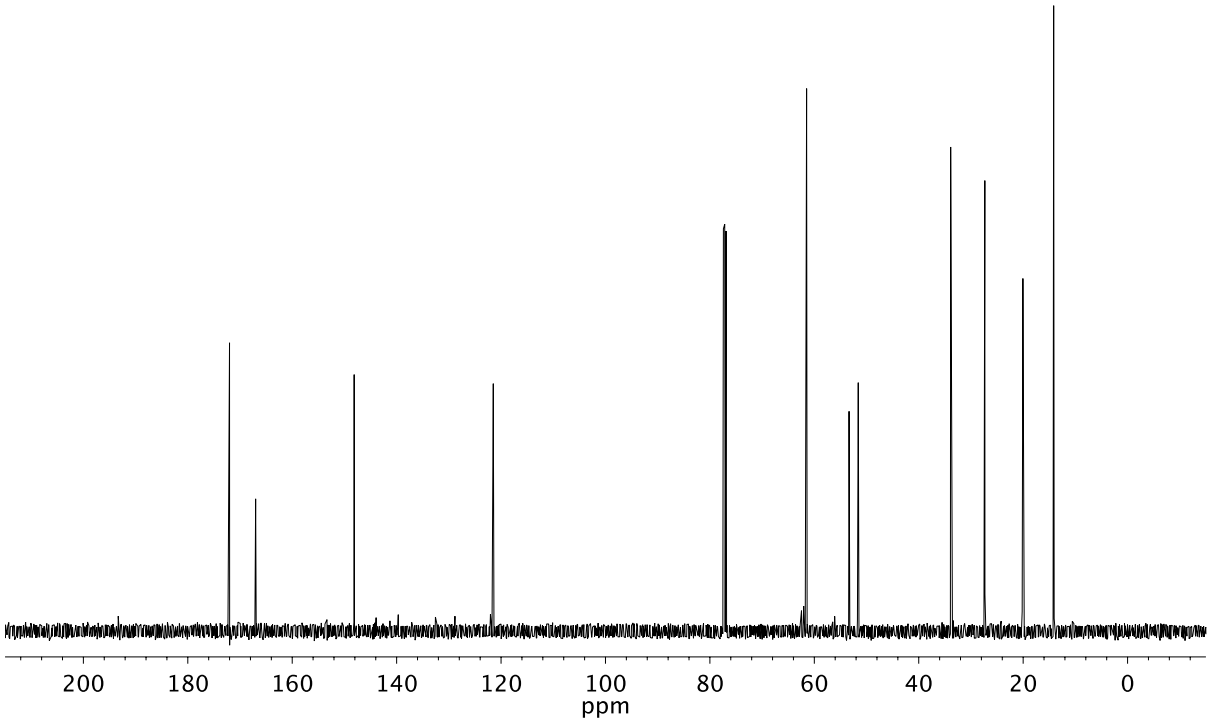

Figure A5.84. ^{13}C NMR (126 MHz, $CDCl_3$) of compound **151**.

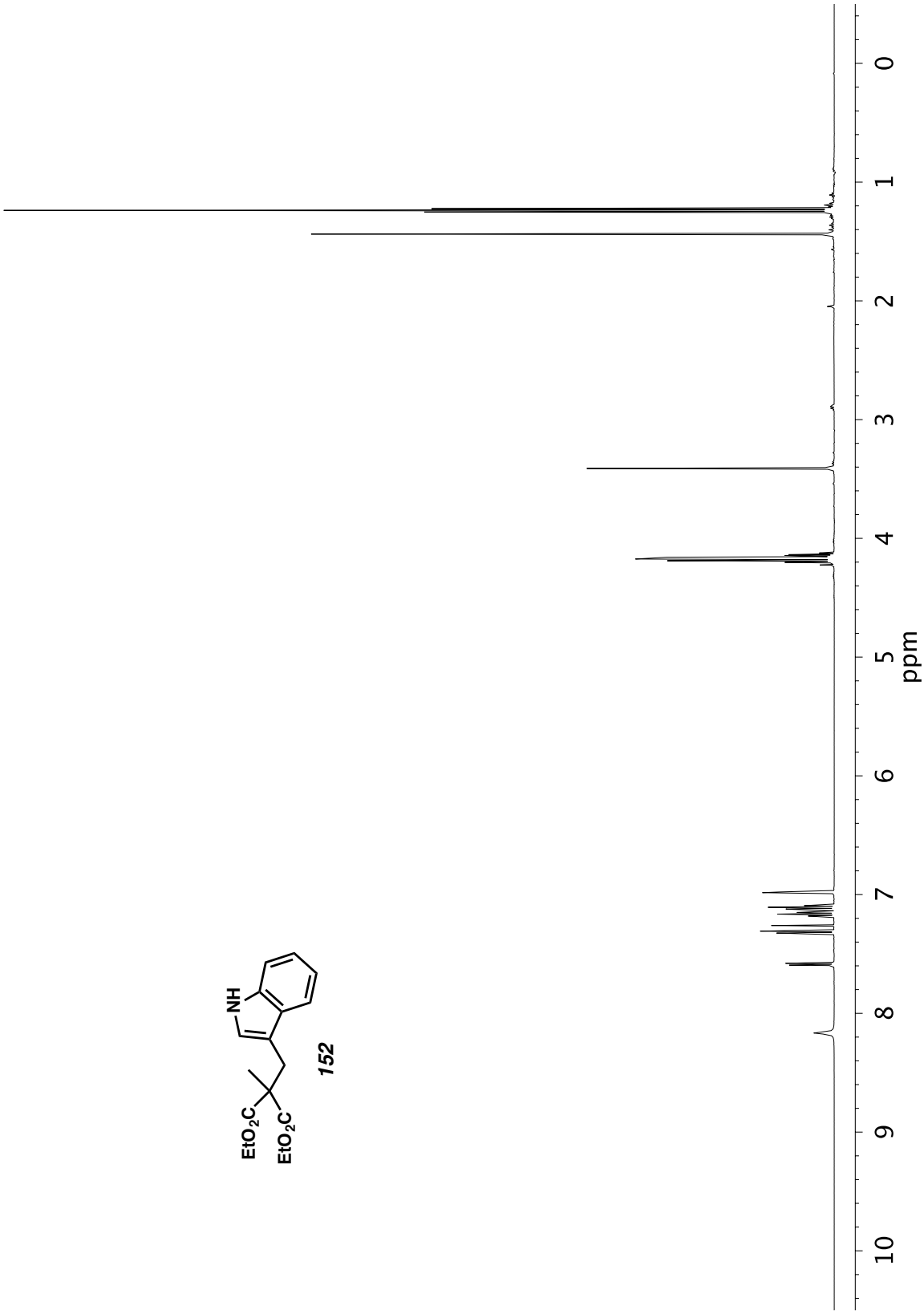

Figure A5.85. ^{1}H NMR (500 MHz, $CDCl_3$) of compound **152**.

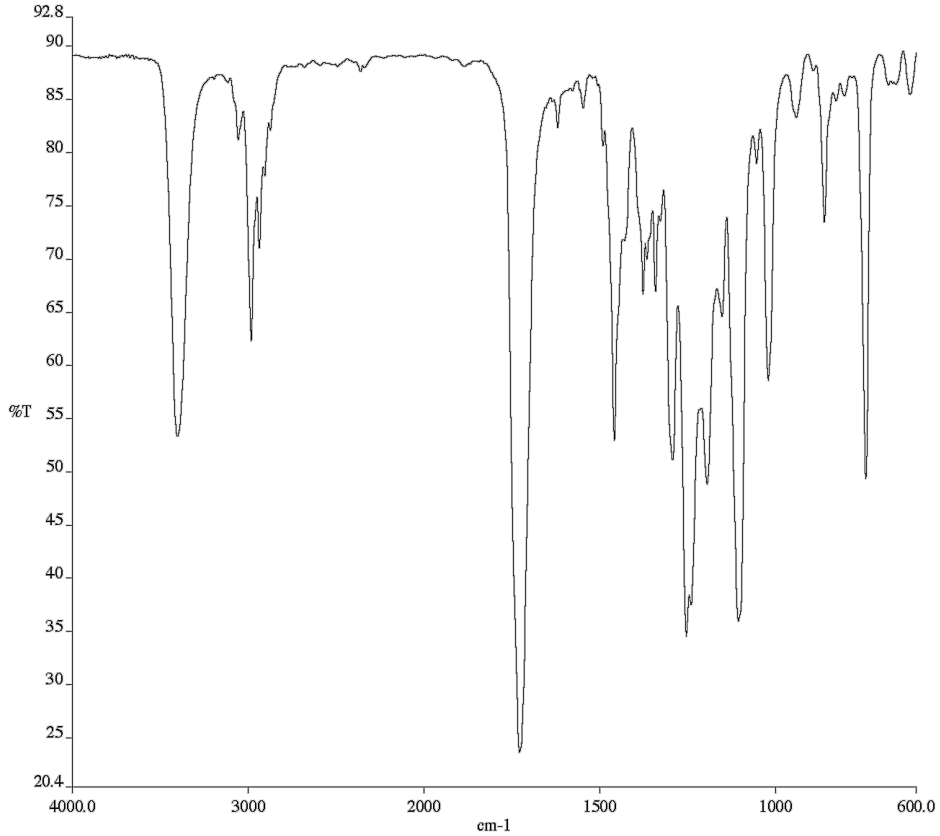

Figure A5.86. Infrared spectrum (Thin Film, KBr) of compound **152**.

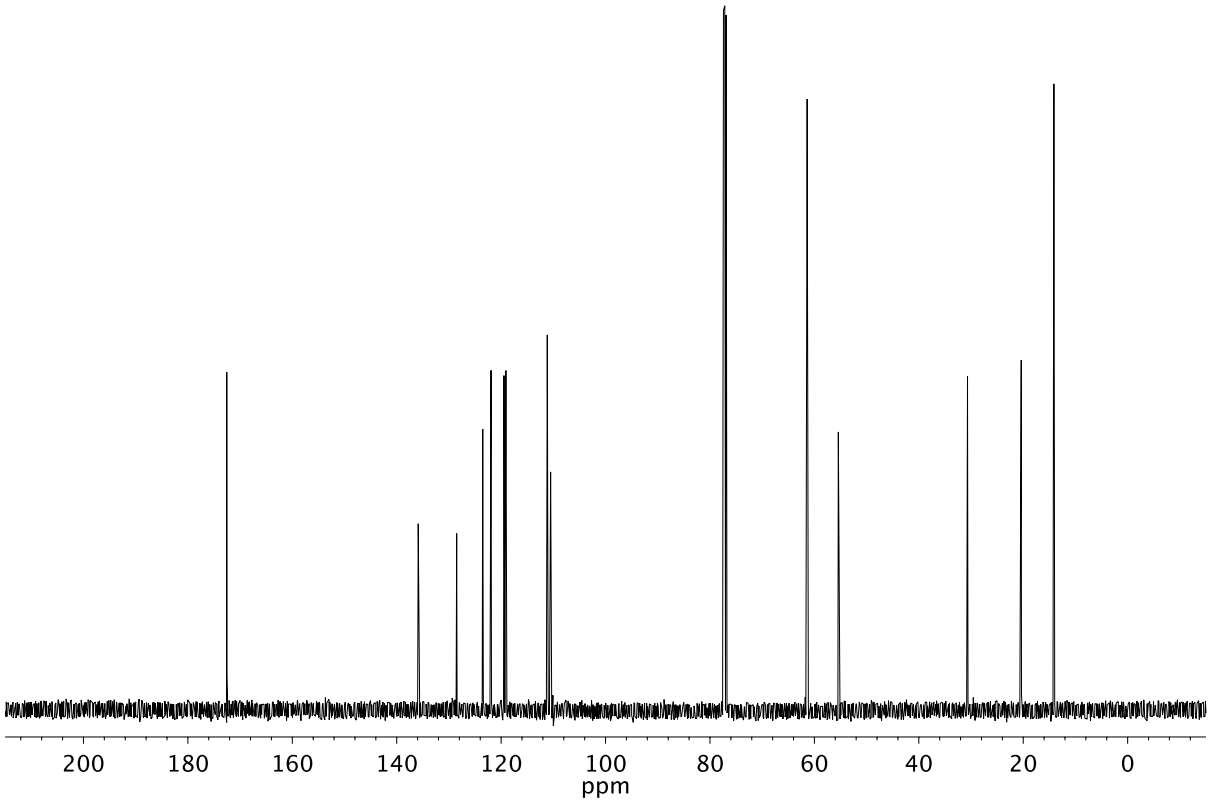

Figure A5.87. ^{13}C NMR (126 MHz, $CDCl_3$) of compound **152**.

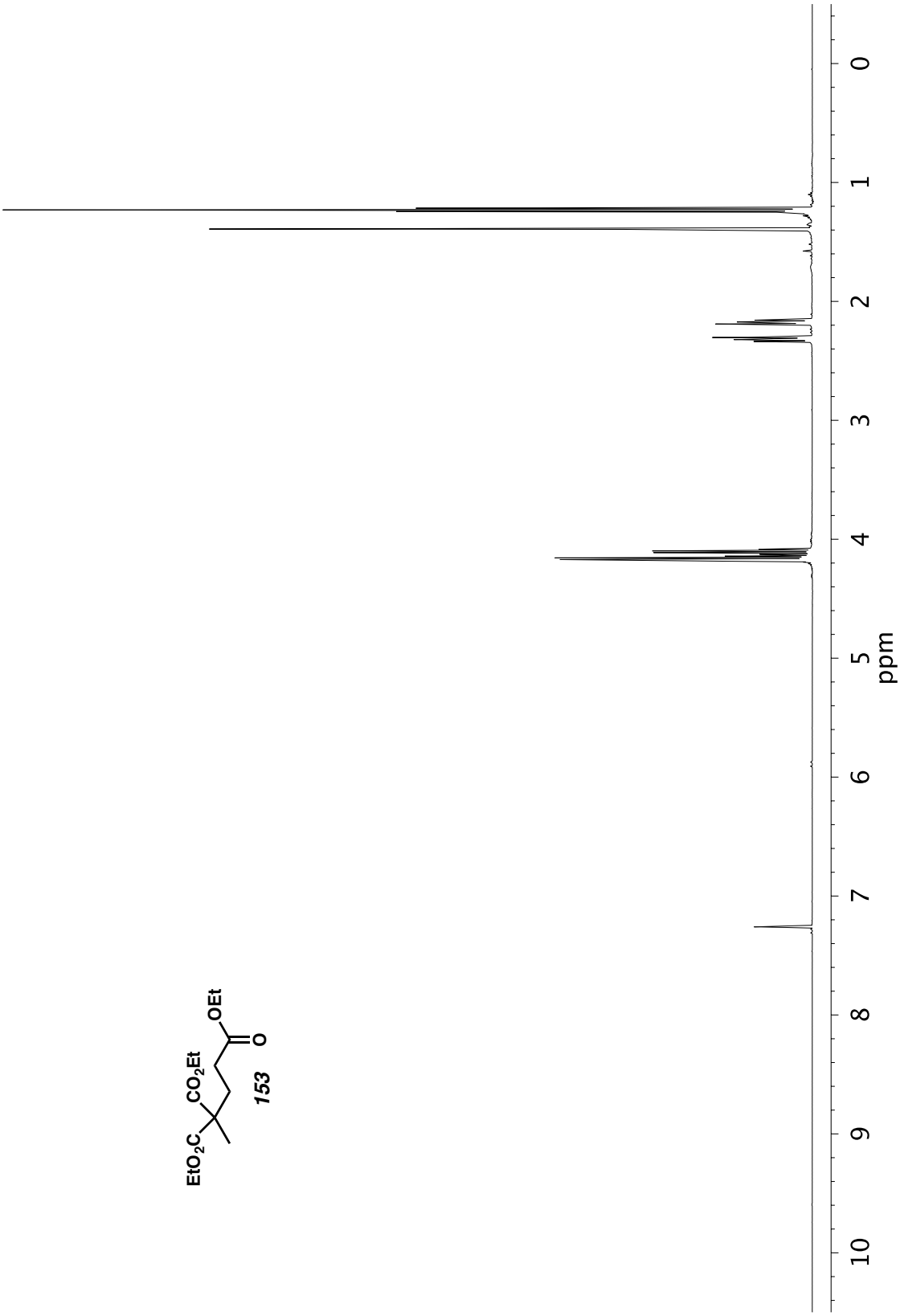

Figure A5.88. ^{1}H NMR (500 MHz, $CDCl_3$) of compound **153**.

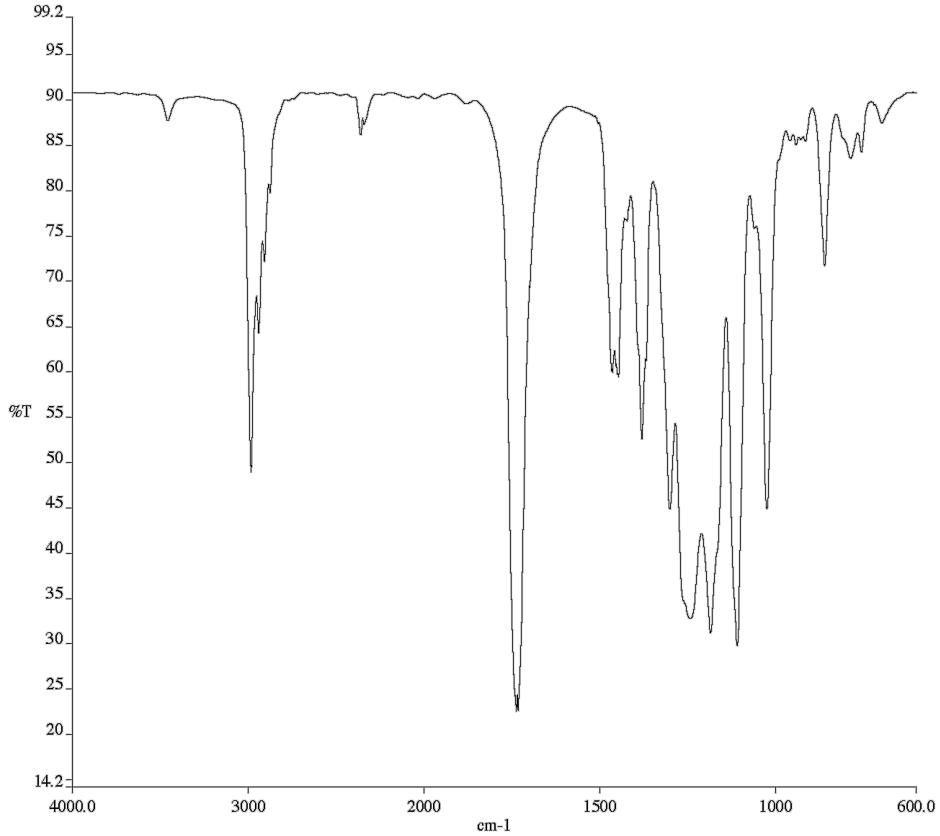

Figure A5.89. Infrared spectrum (Thin Film, KBr) of compound **153**.

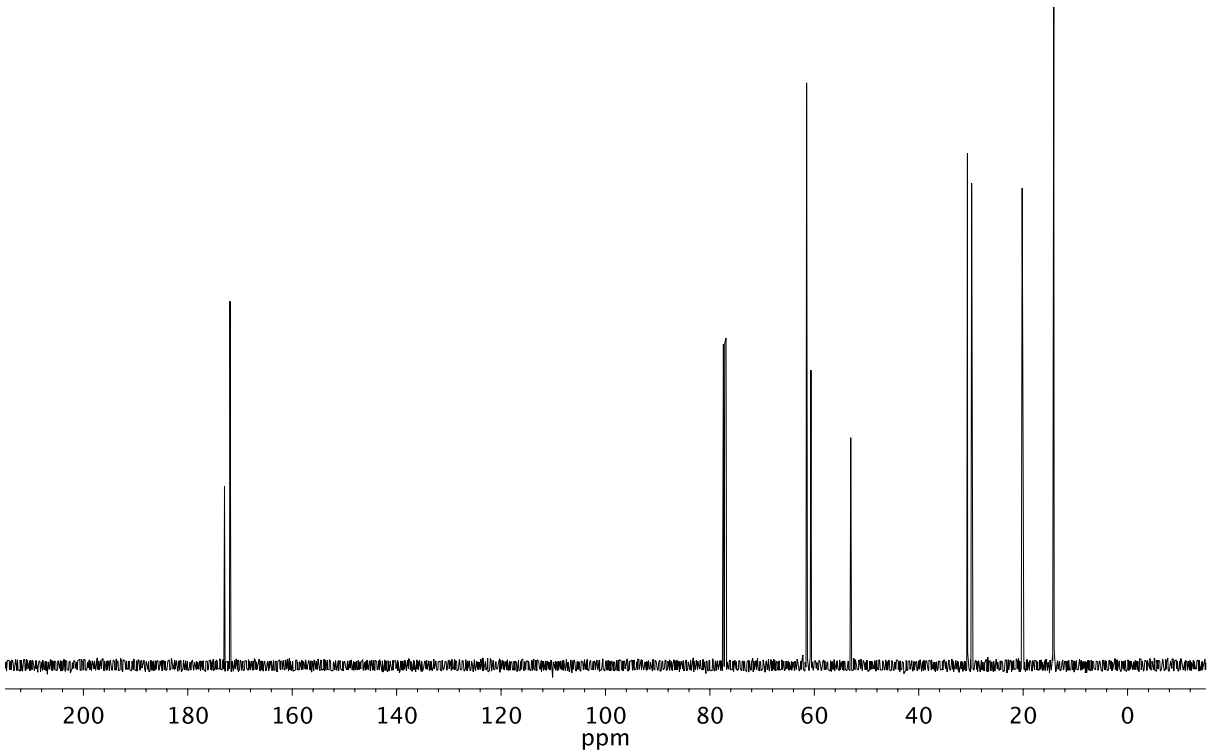

Figure A5.90. ^{13}C NMR (126 MHz, $CDCl_3$) of compound **153**.

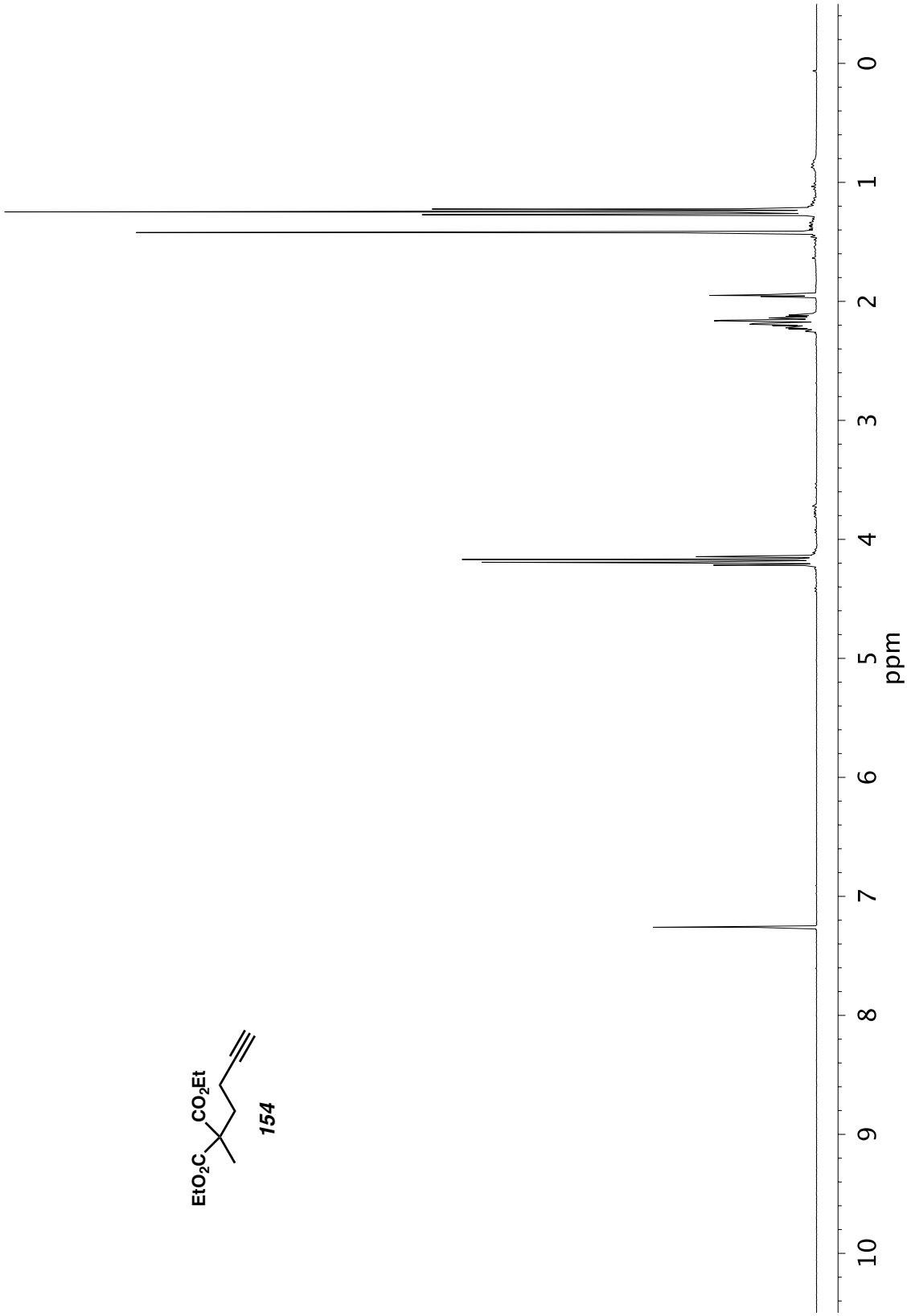

Figure A5.91. ^{1}H NMR (300 MHz, $CDCl_3$) of compound **154**.

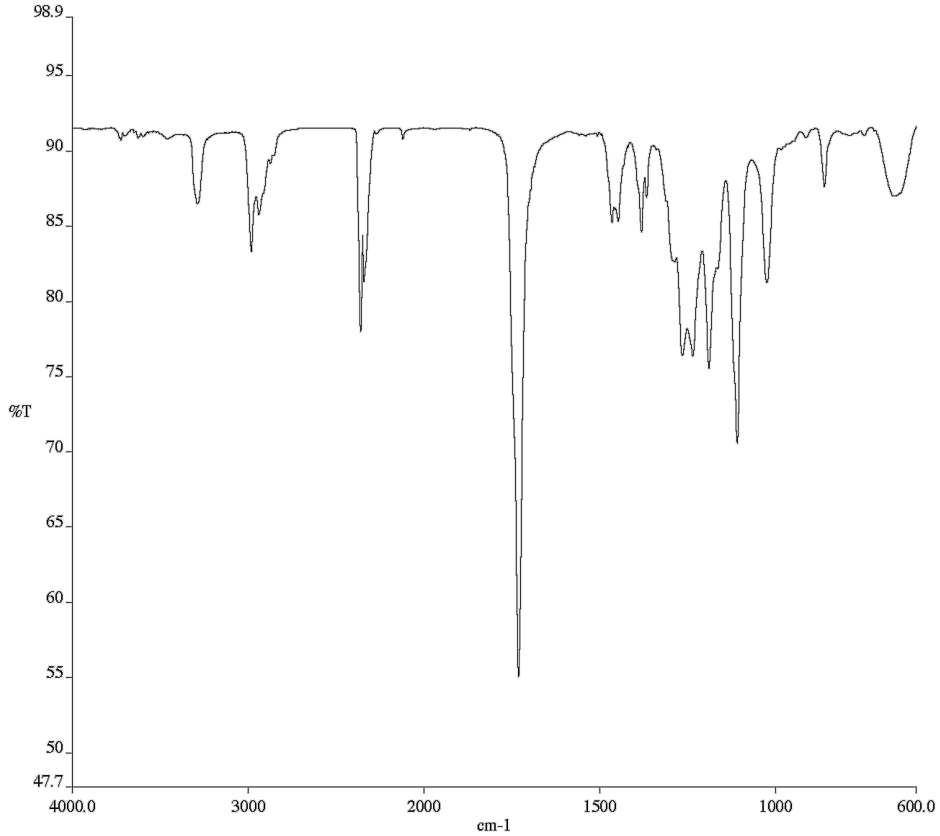

Figure A5.92. Infrared spectrum (Thin Film, KBr) of compound **154**.

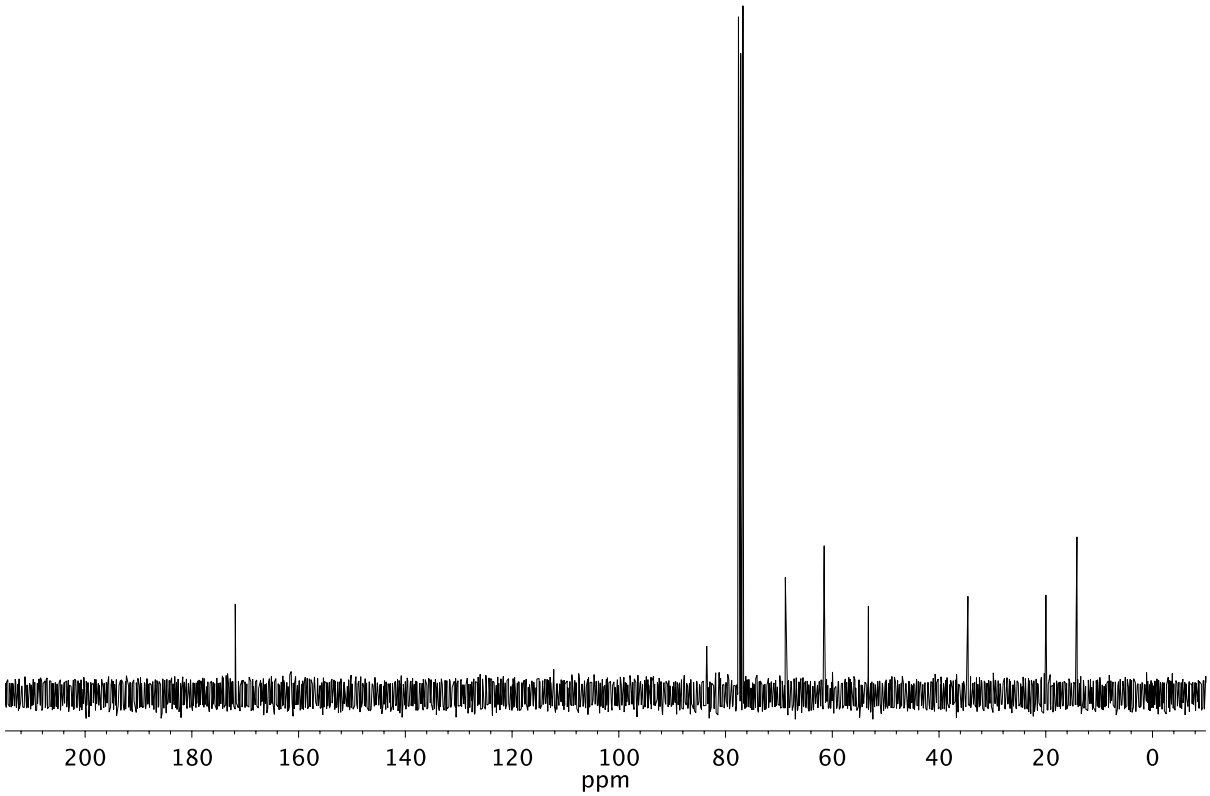

Figure A5.93. ^{13}C NMR (75 MHz, $CDCl_3$) of compound **154**.

CHAPTER 4[†]

The Cyanthiwigin Natural Product Core as a Complex Molecular Scaffold

for Comparative Late-Stage C–H Functionalization Studies

4.1 INTRODUCTION

With access to large quantities of the cyanthiwigin natural product core, we were ready to undertake studies in late-stage diversification. As active participants in the NSF Center for Selective C–H Functionalization (CCHF), we envisioned that the tricyclic compound could serve as a scaffold from which to probe the reactivity of complex molecules under various conditions for C–H functionalization. To this end, we carried out a comparative study of late-stage C–H oxidation methodologies. The results of these investigations are described herein.

[†] This work was performed in collaboration with the Du Bois group at Stanford University through the NSF Center for Selective C–H Functionalization. Portions of this chapter have been reproduced from a manuscript and supporting information intended for submission at *J. Am. Chem. Soc.*

4.1.1 BACKGROUND

The selective functionalization of unactivated C–H bonds has long fascinated the chemical community, having even been referred to as a "Holy Grail" of synthetic chemistry.[1] C–H bonds are ubiquitous in organic molecules, and the direct conversion of these traditionally inert moieties to other functional groups has the potential to streamline synthetic strategies while reducing waste generation. Recognizing this potential, developers of C–H functionalization methodologies often include in their reports examples of commercially available complex substrates such as sclareolide (**1**) or artemisinin (**186**) (Figure 4.1). While wisdom gained from this practice has contributed to the successful application of C–H functionalization in total synthesis,[2] a complementary approach involving comparison of many different methodologies on a single complex scaffold would greatly improve understanding of the fate of complex molecules under conditions for C–H functionalization. Furthermore, the direct comparison of various protocols for the same transformation on a single substrate would be a good indicator of how practical a method might be in the synthesis of a complex molecule.

Figure 4.1 Commercially available complex molecules employed in previous C–H functionalization studies

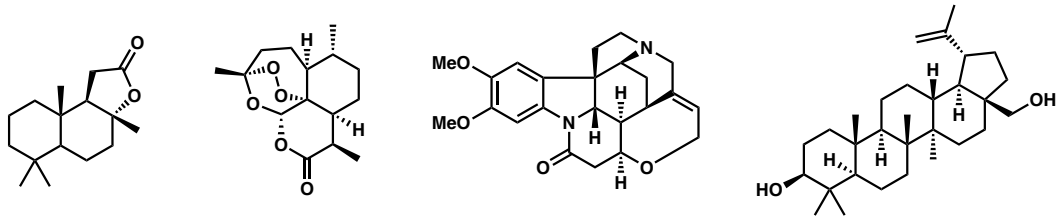

The concept of diversifying complex scaffolds using C–H functionalization has gained much traction within the last decade,[3] with various research groups communicating derivatizations of molecules as diverse as drug candidates,[4] organic light-emitting diodes (OLEDs),[5] metal–organic frameworks (MOFs),[6] and polymers, most commonly by way of $C(_{sp^2})$–H functionalization.[7] However, few reports exist detailing comparative studies of methodologies for $C(_{sp^3})$–H oxidation on a single complex scaffold. An account by Davies and Beckwith explores various conditions and catalysts for C–C bond formation on the complex alkaloid brucine (**187**, Figure 4.1)[8] while a report by Du Bois and Malik compares the efficacies of various C–O bond-forming methods on relatively simple substrates.[9] However, so far the only comparative study involving C–O bond formation on a complex scaffold was disclosed by Baran and co-workers in 2014,[10] outlining the oxidation of betulin (**188**) in conjunction with the optimization of physicochemical properties relevant to drug discovery.[11,12]

With this in mind, we envisioned that the tricyclic carbon framework of the cyanthiwigin natural product family (**109**) could serve as a complex scaffold on which to conduct a comparative study of C–H oxidation methodologies. Tricycle **109** is readily available from succinic acid (**114**) in an efficient 7-step sequence previously developed by our group[13] and features an A–B–C tricyclic fused carbon skeleton containing a variety of C–H bonds. Additionally, the presence of two quaternary stereocenters allows for assessment of steric influences while the two carbonyl moieties enable examination of electronic factors (Figure 4.2). Elucidating the behavior of tricycle **109** under various conditions for C–H oxidation would provide insights into the reactivity of complex molecules complementary to the previously reported findings on commercially available

scaffolds. This report is not intended as an exhaustive survey of all known strategies for C–H oxidation but rather as a sampling of a balanced cross-section of the C–H oxidation literature. We have chosen to focus on intermolecular strategies, which do not require the installation and removal of directing functionalities as most intramolecular methods do.[14]

*Figure 4.2 Availability of the cyanthiwigin core (**109**) from succinic acid (**114**) and features relevant to reactivity under common conditions for C–H oxidation*

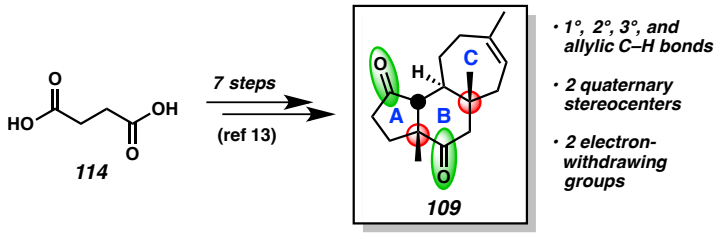

4.2 OXYGENATION VIA C–H FUNCTIONALIZATION

The introduction of oxygen atoms into carbon frameworks has been shown to significantly influence aqueous solubility and other physicochemical properties of complex molecules,[10] resulting in important implications for biological activity.[15] As such, various oxygen transfer reagents exist for the oxygenation of functionalized substrates.[16] In constrast, the oxidation of unactivated C–H bonds, such as those present in many natural products and other complex molecules, is a more recent field of study. Interest in C–H oxygenation has grown rapidly over the past two decades due to the potential for introducing oxygen atoms at sites inaccessible under conventional oxidation conditions. To this end, we began our investigations into the reactivity of the cyanthiwigin core by examining the formation of C–O bonds.

4.2.1 ALLYLIC C–H ACETOXYLATION

We first targeted the most activated C–H bonds in the cyanthiwigin framework, those at allylic positions. Treatment of **109** with stoichiometric quantities of selenium dioxide in refluxing ethanol[17] afforded enal **189** in moderate yield (42%) along with allylic alcohol **190** (22%) (Table 4.1, Entry 1). In contrast, the use of catalytic selenium with stoichiometric *tert*-butyl hydroperoxide (TBHP) at room temperature[18] enabled formation of **190** as the major product, with only trace amounts of enal **189** observed in the crude reaction mixture (Entry 2). Interestingly, in both of these experiments, oxidation was observed only at the C15 methyl despite a priori assumptions that the endocyclic C11 position would be favored.[19]

*Table 4.1 Allylic oxidation of the cyanthiwigin core (**109**) using selenium dioxide*

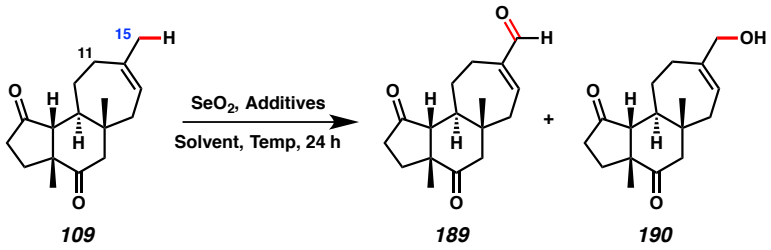

109 **189** **190**

Entry	SeO_2 loading	Additives	Solvent	Temp.	Yield[c]	***189*** : ***190***
1[a]	1.0 equiv	none	25:1 EtOH/H_2O	95 °C	64%	1.8 : 1.0
2[b]	10 mol %	TBHP, AcOH	CH_2Cl_2	23 °C	53%	0 : 1.0[d]

[a] Conditions adapted from ref 17. [b] Conditions adapted from ref 18. [c] Combined isolated yields of **189** and **190**. [d] Trace amount of enal **189** was observed in the crude reaction mixture.

Table 4.2 Comparison of Pd-catalyzed allylic C–H acetoxylation methods on tricycle ***109***

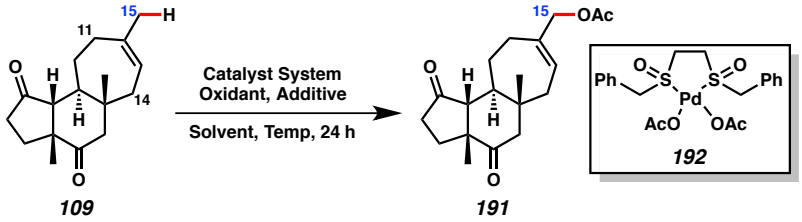

Entry	Cat. System (mol %)	Oxidant	Additive	Solvent	Temp.	Yield[e]
1[b]	$Pd(OAc)_2$ (5) 4,5-diazafluorenone (5)	O_2	NaOAc, AcOH	1,4-dioxane	60 °C	trace[f]
2[c]	$Pd(OAc)_2$ (10)	BQ	4Å MS	1:1 DMSO/AcOH	40 °C	0[f]
3[c]	Pd cat ***192*** (10)	BQ	none	1:1 CH_2Cl_2/AcOH	40 °C	trace[f]
4[d]	$Pd(hfacac)_2$ (7.5)	Oxone	4Å MS	5:1:1 MeCN/AcOH/Ac_2O	60 °C	0[f]
5	$Pd(OAc)_2$ (10)	Oxone	none	1:1 AcOH/$CH_3CH_2NO_2$	95 °C	31%

[a] Conditions adapted from: [b] ref 20, [c] ref 21, [d] ref 22. [e] Isolated yield. [f] Starting material was recovered (>90%).

Shifting our attention to more recently developed procedures for allylic oxidation, we investigated the efficacies of various conditions employing Pd catalysis (Table 4.2). Efforts to effect allylic C–H acetoxylation using catalytic $Pd(OAc)_2$ with either O_2 or benzoquinone (BQ) as the oxidant, strategies reported previously by Stahl[20] and White,[21] respectively, resulted in little to no conversion of tricycle **109** (Entries 1–2). Employing Pd^{II} complex **192** as the catalyst and changing the solvent system improved conversion only slightly (Entry 3). Interestingly, although conditions developed previously by our group for allylic acetoxylation using Oxone as the terminal oxidant[22] were ineffective for the oxidation of **109** (Entry 4), modification of the conditions resulted in the formation of C15 acetoxylation product **191** in modest yield (Entry 5). The temperature of these modified conditions was significantly higher than those of the previous experiments, suggesting that oxidation of the C15 allylic C–H bonds is an energy-intensive process.

Notably, no oxidation was observed at the C11 and C14 positions, likely due to steric factors.[23]

4.2.2 HYDROGENATION OF THE CYANTHIWIGIN CORE

While the alkene functionality was instrumental in the allylic oxidation studies, it proved to be a liability in the exploration of methods for C–H hydroxylation,[24] an important strategy in the modulation of physicochemical properties of lead candidates in drug discovery.[10] To render the cyanthiwigin framework compatible with common C–H hydroxylation conditions, we sought to remove the C-ring olefin through hydrogenation (Table 4.3). After unsuccessful attempts using catalytic (Entry 1) or superstoichiometric Pd/C in various solvent systems (Entries 2–5), we were delighted to find that PtO_2 catalyzed the transformation smoothly with 100% conversion of **109** (Entry 6).

*Table 4.3 Catalyst and solvent optimization for hydrogenation of the cyanthiwigin core (**109**)*

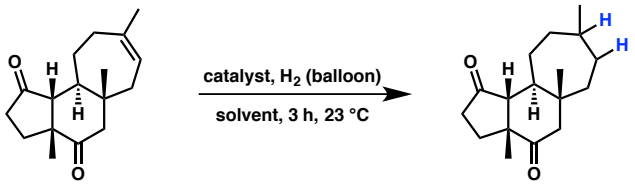

109 ***193***

Entry	Catalyst	Cat. Loading	Solvent	Conversion
1	Pd/C	3 mol %	EtOAc	0
2	Pd/C	2.3 equiv	EtOAc	0
3	Pd/C	3.5 equiv	AcOH/EtOAc (2:1)	0
4	Pd/C	3.0 equiv	AcOH/EtOAc (5:2)	0
5	Pd/C	3.0 equiv	TFA/EtOAc (3:1)	0
6	PtO_2	20 mol %	EtOAc	100%

When hydrogenation was carried out at ambient temperature, saturated tricycle **193** was obtained in 6:1 dr, whereas when the temperature was lowered to 0 °C, the dr increased to 9:1 (Scheme 4.1).[25] To facilitate structural determination of the major diastereomer, deuterium-labeled compound **194** was prepared, enabling stereochemical elucidation by nOe analysis. This assignment was further substantiated by an X-ray crystal structure of compound **193**. The stereoselectivity of the reaction likely arises from steric constraints, with hydrogenation occurring preferentially on the more accessible α-face of **109**.

*Scheme 4.1 Structural determination for saturated tricycle **193** facilitated by NMR analysis of deuterated tricycle **194** and X-ray crystallography*

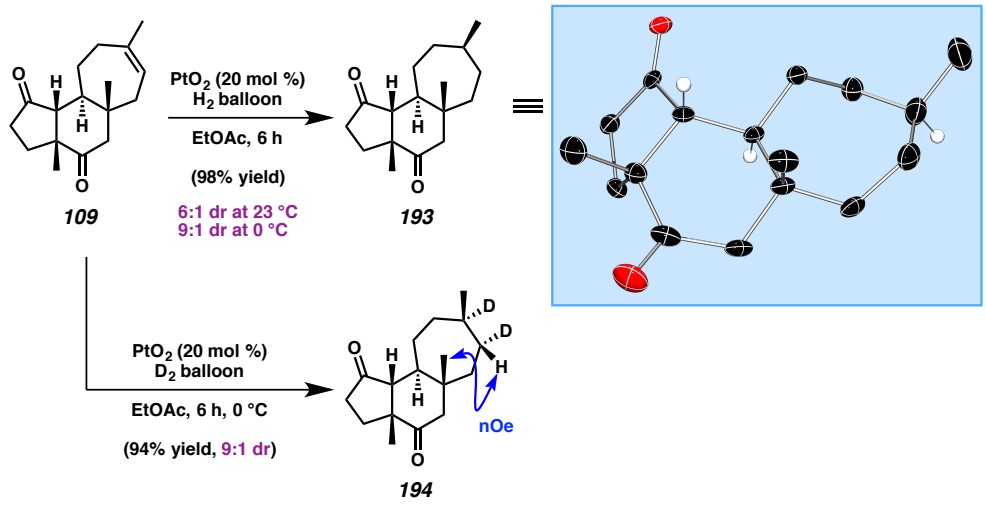

4.2.3 TERTIARY C–H HYDROXYLATION

With saturated tricycle **193** in hand, we proceeded to conduct a comparative study of 3° C–H bond hydroxylation (Table 4.4). Initial investigations using catalytic $RuCl_3 \bullet xH_2O$ supplied tertiary alcohol **195** in moderate yield (Entry 1),[26] and the milder

(Me_3tacn)$RuCl_3$ system proved even more effective (Entry 2).[27] Unfortunately, metal-free conditions catalyzed by oxaziridine **196** resulted in significantly lower yields of **195**, suffering from low conversion and epimerization at the C12 position, presumably through ionization of the tertiary alcohol in situ (Entry 3).[28] Likewise, the use of excess dimethyldioxirane (DMDO) provided only small quantities of **195**, returning primarily unreacted **193** (Entry 4).[29] Fe-catalyzed[30] and Mn-catalyzed[9] protocols were similarly inefficient, although starting material was consumed in both cases (Entries 5–6). Formation of smaller quantities of another product suspected to arise from C13 oxidation was also observed.

*Table 4.4 Comparison of tertiary C–H hydroxylation methods on saturated tricycle **193***

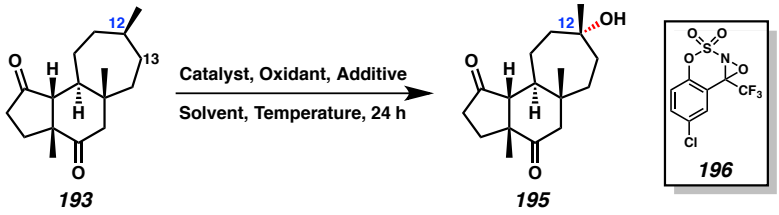

Entry	Catalyst (mol %)	Oxidant	Additive	Solvent	Temp.	Yield[h]
1[b]	$RuCl_3$•xH_2O (5)	$KBrO_3$	pyridine	MeCN	60 °C	42%[i,m]
2[c]	(Me_3tacn)$RuCl_3$ (2)	CAN	$AgClO_4$	*t*-BuOH/H_2O	23 °C	64%[i,m]
3[d]	oxaziridine ***196*** (20)	Oxone	none	HFIP/H_2O	70 °C	21%[i,m]
4[e]	none	DMDO	none	acetone	23 °C	15%[i]
5[f]	Fe(*S,S*-PDP) (15)[j]	H_2O_2	AcOH	MeCN	23 °C	22%[k,n]
6[g]	$Mn(OTf)_2$ (0.1)	AcOOH	bipy	AcOH/H_2O	23 °C	20%[l,n]

[a] Conditions adapted from: [b] ref 26, [c] ref 27, [d] ref 28, [e] ref 29b, [f] ref 30, [g] ref 9. [h] Isolated yield. [i] Starting material was recovered. [j] Iterative protocol was employed (3 x 5 mol %). [k] Reaction time = 30 min. [l] Reaction time = 90 s. [m] Minor product with opposite stereochemistry at C12 was also observed. [n] Ketone product **197** derived from 2° C–H oxidation at C13 was also observed.

4.2.4 SECONDARY C–H OXIDATION

To elucidate the structure of the presumed C13 oxidation product, tricycle **193** was subjected to oxidation by Fe(*R*,*R*-CF_3-PDP), a modified Fe-PDP catalyst known to prefer oxidation of 2° over 3° C–H bonds.[31] Indeed, ketone **197** was formed as the major product, with a smaller amount of C12 oxidation product **195** also isolated (Scheme 4.2). In this experiment as well as the tertiary C–H hydroxylation studies, oxidation was not observed at the C4 or C5 positions, likely due to deactivation by the nearby carbonyls and torsional strain associated with the axial configuration of those C–H bonds.[32] Although the yields of product formation in this system vary, it is interesting that all of the C–H hydroxylation conditions studied oxidized the same region of **193** and, with one exception (cf. Scheme 4.2), stereoselective C–H hydroxylation of C12 is observed as the major oxidation product. In terms of synthetic design, this points to electronically remote 3° C–H bonds as the most likely to be oxidized and could provide enough confidence to the practitioner to incorporate this design feature into a complex plan.

*Scheme 4.2 Secondary C–H oxidation of saturated tricycle **193***

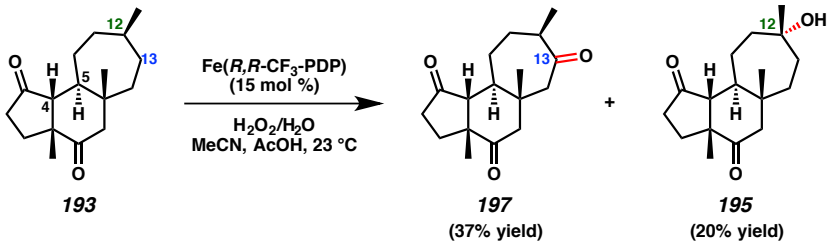

4.3 NITROGENATION VIA C–H FUNCTIONALIZATION

We next turned our attention to the formation of C–N bonds, an important research area due to the ubiquity of nitrogen-containing bioactive molecules.[33] Nitrogen atoms influence biological activity through the basicity of the nitrogen lone pair and the capacity for hydrogen bonding, which can also be modulated through substitution. Despite the vital roles nitrogen atoms play in bioactive molecules, however, nitrogenation in nature is generally not accomplished through direct C–N bond formation. Instead, most nitrogen atoms are introduced downstream of C–O bonds, often through condensation reactions.[34] As such, direct C–N bond formation via synthetic catalysis represents an especially significant accomplishment because such strategies can effectively access nitrogenated molecules for which no biosynthetic pathways exist.[35]

4.3.1 TERTIARY C–H AMINATION

Noting these considerations, we commenced our investigations into nitrogenation with C–H amination. Application of Du Bois's Rh-catalyzed methodology[36] enabled formation of C12 amination product **198a** in modest yield (Table 4.5, Entry 1). Pleasingly, a revised set of conditions featuring fewer additives furnished C–H amination product **198b** in greatly improved yield, with the remaining mass balance composed of unreacted **193** (Entry 2). Access to fluorine-containing product **198c** was also achieved in good yield through the modified protocol (Entry 3). In all cases, C–H functionalization occurred selectively at C12 with retention of stereochemistry.

Table 4.5 Tertiary C–H amination of saturated tricycle ***193***

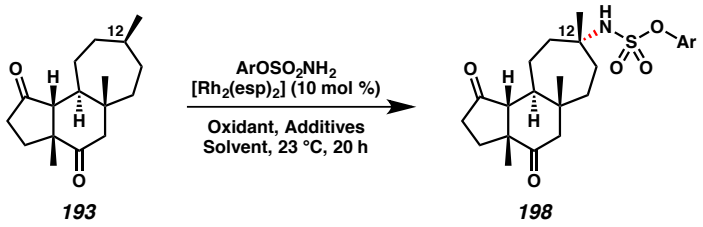

193 ***198***

Entry	Ar	Oxidant	Additives	Solvent	Product	Yield[b]
1[a]	2,6-FC_6H_3	$PhI(OAc)_2$	$PhMe_2CCO_2H$ MgO, 5Å MS	*i*-PrOAc	***198a***	30%[c]
2	C_6H_5	$PhI(OPiv)_2$	Al_2O_3	*t*-BuCN	***198b***	70%[c]
3	4-FC_6H_4	$PhI(OPiv)_2$	Al_2O_3	*t*-BuCN	***198c***	72%[c]

[a] Conditions were adapted from ref 36. [b] Isolated yield. [c] Starting material was recovered.

4.3.2 TERTIARY C–H AZIDATION

Encouraged by the success of the C–H amination reactions, we next examined various conditions for C–H azidation. Organic azides are readily reduced to primary amines and can be useful intermediates in the preparation of a variety of nitrogen-containing compounds.[37] A metal-free protocol reported by Tang and co-workers[38] effected C–N bond formation smoothly at the C12 position (Table 4.6, Entry 1). Likewise, Hartwig's Fe-catalyzed strategy afforded comparably high conversion of **193** (Entry 2).[39] In both cases two products were isolated and characterized as diastereomers **199a** and **199b**.

The lack of stereoselectivity matches results from the methodological reports and indicates a loss of stereochemical information at the reactive site during the reaction mechanism, which both Tang and Hartwig propose as proceeding through a radical intermediate. Also in agreement with Hartwig's findings, efforts to initiate azidation using benzoyl peroxide resulted in poor yields and substrate decomposition (Entry 3). As

was observed in the 3° C–H amination and 3° C–H hydroxylation studies, azidation of **193** occurred exclusively at the C12 position. Overall, the high conversions and regioselectivities of the C–H azidation reactions indicate good potential for synthetic applications, although more development in stereochemical control is needed for more universal utility in chemical synthesis.

*Table 4.6 Tertiary C–H azidation of saturated tricycle **193***

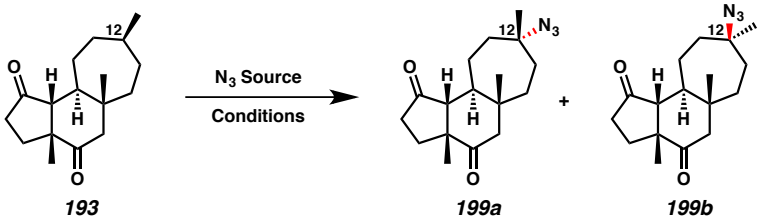

193 ***199a*** ***199b***

Entry	N_3 Source	Conditions	Yield[c]	***199a*** : ***199b***
1[a]	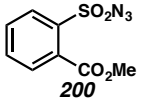 ***200***	$K_2S_2O_8$, $NaHCO_3$ MeCN/H_2O, 85 °C, 24 h	90%[d]	1.0 : 1.9
2[b]	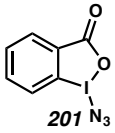 ***201*** N_3	$Fe(OAc)_2$, *i*-Pr-pybox MeCN, 35 → 50 °C, 24 h	86%[d]	1.2 : 1.0
3[b]	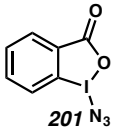 ***201*** N_3	BzOOBz, ABCN DCE, 84 °C, 24 h	13%	0 : 1.0

[a] Conditions adapted from ref 38. [b] Conditions adapted from ref 39. [c] Combined isolated yields of **199a** and **199b**. [d] Starting material was recovered.

4.4 SECONDARY C–H CHLORINATION

Having successfully effected C–O and C–N bond formation on saturated tricycle **193**, we rounded out our studies with C–X bond formation. Site-selective halogenation is an important aim in chemical synthesis due to the versatility of alkyl halides as synthetic

building blocks.[40] Noting the existence of over 2000 chlorine-containing natural products,[41] Alexanian and co-workers developed a protocol for site-selective C–H chlorination enabled by visible light and an *N*-chloroamide reagent.[42] Significantly, in contrast to previously reported methodologies, the Alexanian procedure avoids the use of strong acid solvents[43] and superstoichiometric substrate,[44] two major synthetic limitations, especially in the context of late-stage functionalization using precious materials.

After efforts to fluorinate the hydrogenated cyanthiwigin core (**193**) proved challenging,[45] we turned to Alexanian's procedure for C–H chlorination and were pleased to find that irradiation of **193** with visible light (23W CFL) in the presence of *N*-chloroamide **203** effected 2° C–H chlorination at C13, generating chloride **202** in modest yield (Scheme 4.3). The remaining mass balance consisted of recovered starting material in addition to small quantities of unassigned dichlorinated products.[46]

Scheme 4.3 Secondary C–H chlorination of saturated tricycle ***193***

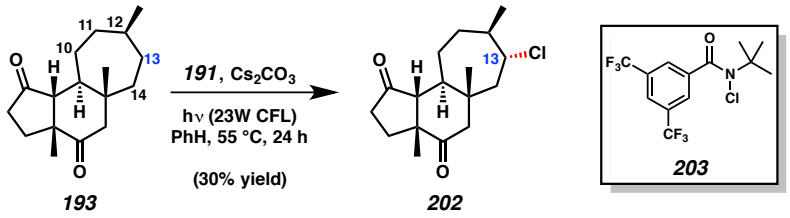

With the A- and B-rings deactivated by the electron-withdrawing carbonyls, the C-ring remains the most viable location for oxidation. As discussed in Alexanian's original report, the regioselectivity of this reaction is strongly influenced by steric constraints due to the bulkiness of the chlorinating reagent, *N*-chloroamide **203**. Accordingly, chlorination occurs primarily at the C13 position, the least sterically encumbered site in

the C-ring. Although the C11 position appears relatively unhindered as well, it is possible that anisotropic effects from the A-ring ketone cause electronic deactivation since the cupped conformation of the tricyclic system brings the A-ring carbonyl in proximity to the C10 and C11 positions on the C-ring. Finally, the stereoselectivity of the C13 oxidation can also be explained by sterics, as chlorination occurs preferentially on the less sterically burdened α-face of **193**, resembling the facial selectivity observed in the hydrogenation of **109** (cf. Scheme 4.1).

4.5 CONCLUDING REMARKS

Through these investigations, we have examined the reactivity of a complex natural product core in a comparative study of various known methods for C–H oxidation. Having observed that selenium dioxide is the most effective catalyst for selective allylic oxidation of **109**, we conclude that the direct allylic C–H acetoxylation of trisubstituted olefins in complex scaffolds remains a challenging transformation that could benefit from further methodological development, although the use of catalytic selenium dioxide is a significant advance. Additionally, while many methods for 3° C–H hydroxylation and amination proceed with good conversion and stereoselectivity, protocols for 3° C–H azidation tend to permit epimerization at the site of oxidation, limiting applications in chemical synthesis despite overall high conversion. Finally, there remains much room for growth in the area of C–Cl bond formation by C–H functionalization, although the ability to isolate a single enantiopure product in serviceable, albeit suboptimal, yield is an impressive feat and a convenient resource for the chlorination of organic compounds.

To conclude, the results of these experiments indicate that electronic and steric factors play significant roles in the regio- and stereoselectivity of most C–H oxidation reactions of complex molecules, corroborating previous accounts by other research groups. Furthermore, the tendency for functionalization to occur at just one site (C12) in the 17-carbon saturated cyanthiwigin core (**193**) under vastly differing conditions for C–H oxidation lends credence to the concept of "innate" functionalizations guided by the intrinsic reactivities of C–H bonds within the substrate.[47] This finding also highlights the importance of methodologies exhibiting alternative regioselectivities (e.g. C13-selective oxidations) since they enable chemists to target less inherently reactive C–H bonds as desired. We anticipate the insights derived from these investigations will enhance understanding of complex molecules with respect to predicting sites of reactivity in C–H oxidation reactions, thereby amplifying the applicability of C–H functionalization as a tool in chemical synthesis.

4.6 EXPERIMENTAL SECTION

4.6.1 MATERIALS AND METHODS

Unless noted in the specific procedure, reactions were performed in flame-dried glassware under argon atmosphere. Dried and deoxygenated solvents (Fisher Scientific) were prepared by passage through columns of activated aluminum before use.[48] Methanol (Fisher Scientific) was distilled from magnesium methoxide immediately prior to use. 1,2-dichloroethane (Fisher Scientific) and hexafluoroisopropanol (Matrix Scientific) were distilled from calcium hydride immediately prior to use. Isopropyl acetate was distilled and stored over activated molecular sieves (5Å) immediately prior to use. Anhydrous ethanol, *tert*-butanol, and dimethylsulfoxide (DMSO) were purchased from Sigma Aldrich in sure-sealed bottles and used as received unless otherwise noted. Commercial reagents (Sigma Aldrich or Alfa Aesar) were used as received. Catalysts $(Me_3tacn)RuCl_3$, benzoxathiazine **204**, $Mn(OTf)_2$, and $Rh_2(esp)_2$ were donated by the Du Bois group (Stanford) and used without further purification. The Fe(*S*,*S*-PDP) catalyst was donated by the Sarpong group (UC Berkeley) and used without further purification. The Fe(*R*,*R*-CF_3-PDP) catalyst was donated by the White group (UIUC) and used without further purification. Dimethyldioxirane (DMDO),[49] 2,6-difluorophenyl sulfamate,[36] sulfonyl azide **200**,[50] hypervalent iodine reagent **201**,[51] and *N*-chloroamide **203**[42] were prepared according to known procedures. *p*-Benzoquinone was recrystallized from petroleum ether prior to use. Brine is defined as a saturated aqueous solution of sodium chloride. Reactions requiring external heat were modulated to the specified temperatures using an IKAmag temperature controller. Reaction progress was monitored by thin-layer chromatography (TLC) or Agilent 1290 UHPLC-LCMS. TLC was performed using E.

Merck silica gel 60 F254 precoated plates (0.25 mm) and visualized by UV fluorescence quenching, potassium permanganate, or *p*-anisaldehyde staining. Silia*Flash* P60 Academic Silica gel (particle size 0.040–0.063 mm) was used for flash chromatography. NMR spectra were recorded on a Varian Mercury 300 spectrometer (at 300 MHz for ^{1}H NMR and 75 MHz for ^{13}C NMR), a Varian Inova 500 spectrometer (at 500 MHz for ^{1}H NMR and 126 MHz for ^{13}C NMR), or a Bruker AV III HD spectrometer equipped with a Prodigy liquid nitrogen temperature cryoprobe (at 400 MHz for ^{1}H NMR and 101 MHz for ^{13}C NMR), and are reported in terms of chemical shift relative to residual $CHCl_3$ (δ 7.26 and δ 77.16 ppm, respectively). Data for ^{1}H NMR spectra are reported as follows: chemical shift (δ ppm) (multiplicity, coupling constant (Hz), integration). Abbreviations are used as follows: s = singlet, bs = broad singlet, d = doublet, t = triplet, q = quartet, m = complex multiplet. Infrared (IR) spectra were recorded on a Perkin Elmer Paragon 1000 spectrometer using thin film samples on KBr plates, and are reported in frequency of absorption (cm^{-1}). High-resolution mass spectra (HRMS) were obtained from the Caltech Mass Spectral Facility using a JEOL JMS-600H High Resolution Mass Spectrometer with fast atom bombardment (FAB+) ionization mode or were acquired using an Agilent 6200 Series TOF with an Agilent G1978A Multimode source in electrospray ionization (ESI+) mode. Optical rotations were measured with a Jasco P-1010 polarimeter at 589 nm using a 100 mm path-length cell.

4.6.2 PREPARATIVE PROCEDURES

4.6.2.1 ALLYLIC C–H OXIDATION OF 109 BY SELENIUM DIOXIDE

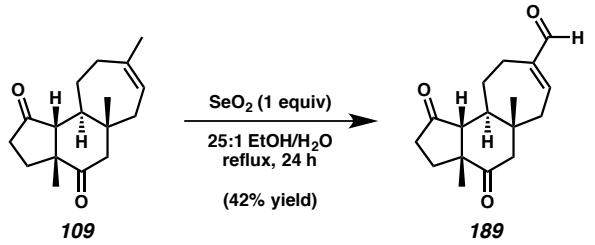

109 *189*

Tricyclic Enal 189. A solution of selenium dioxide (5.5 mg, 50 μmol, 1.00 equiv) in 25:1 ethanol/water (1.0 mL) was added dropwise to a solution of tricyclic diketone **109** (13.0 mg, 49.9 μmol, 1.00 equiv) in absolute ethanol (2.5 mL), and the resulting mixture was heated to reflux (95 °C). After 24 hours, the reaction was allowed to cool to 23 °C and extracted with diethyl ether (2 x 5 mL). The combined organic extracts were washed with water (10 mL) and dried over sodium sulfate. Filtration followed by concentration in vacuo afforded the crude residue, which was purified by silica gel column chromatography (10% → 20% → 40% → 60% ethyl acetate in hexanes), furnishing enal **189** as a colorless oil (5.7 mg, 42% yield). R*f* = 0.25 (50% ethyl acetate in hexanes); ^{1}H NMR ($CDCl_3$, 500 MHz) δ 9.39 (s, 1H), 6.67 (dddd, *J* = 8.8, 5.0, 2.5, 1.4 Hz, 1H), 3.02 (ddt, *J* = 15.4, 6.6, 1.6 Hz, 1H), 2.78 (d, *J* = 14.5 Hz, 1H), 2.62–2.53 (m, 2H), 2.45–2.37 (m, 1H), 2.36–2.30 (m, 1H), 2.27 (dd, *J* = 14.4, 8.8 Hz, 1H), 2.20 (ddt, *J* = 15.4, 6.6, 1.6 Hz, 1H), 2.15 (d, *J* = 14.4 Hz, 1H), 1.96–1.78 (m, 4H), 1.12 (s, 3H), 1.09–1.00 (m, 1H), 0.76 (s, 3H); ^{13}C NMR ($CDCl_3$, 126 MHz) δ 217.1, 211.6, 193.0, 150.9, 148.2, 62.7, 52.4, 51.1, 47.5, 43.3, 40.4, 34.4, 31.5, 23.9, 22.5, 21.7, 17.6; IR (Neat Film, KBr) 2927, 1732,

1704, 1682, 1456, 1384, 1262, 1178, 1155, 915, 732 cm^{-1}; HRMS (EI+) *m/z* calc'd for $C_{17}H_{22}O_3$ $[M\bullet]^+$: 274.1569, found 274.1558; $[\alpha]^{25}_D$ –71.5 (*c* 0.57, $CHCl_3$).

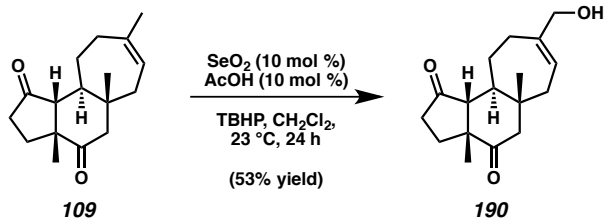

Allylic Alcohol 190. A round-bottom flask was charged with selenium dioxide (0.3 mg, 2.5 μmol, 0.10 equiv), *tert*-butyl hydroperoxide (5.5 M solution in decane, 12 μmol, 6.3 μmol, 2.50 equiv), and acetic acid (1 drop), and the resulting mixture was diluted with dichloromethane (0.50 mL) and stirred at 23 °C. After 30 minutes, a solution of tricyclic diketone **109** (6.6 mg, 25.3 μmol, 1.00 equiv) in dichloromethane (1.5 mL) was added, and stirring was continued over the next 24 hours. After this time, the reaction mixture was filtered over Celite, and the filtrate was concentrated. The resulting residue was diluted with diethyl ether (5 mL) and washed with 10% aq. potassium hydroxide solution (5 mL), water (5 mL), and brine (5 mL). The organic layer was separated and dried over sodium sulfate before filtration and concentration. The crude residue was purified by silica gel column chromatography (10% → 20% → 35% → 40% → 50% ethyl acetate in hexanes), affording allylic alcohol **190** as a colorless oil (7.0 mg, 53% yield). R*f* = 0.16 (50% ethyl acetate in hexanes); ^{1}H NMR ($CDCl_3$, 500 MHz) δ 5.61 (t, *J* = 6.7, 13.6, 1H), 4.04 (s, 2H), 2.68 (d, *J* = 14.7 Hz, 1H), 2.59–2.51 (m, 1H), 2.42–2.30 (m, 3H), 2.17–2.04 (m, 3H), 2.06 (d, *J* = 14.7 Hz, 1H), 1.92–1.82 (m, 3H), 1.81–1.74 (m, 1H), 1.17–1.11 (m, 1H), 1.11 (s, 3H), 0.72 (s, 3H); ^{13}C NMR ($CDCl_3$, 101 MHz) δ 217.8,

212.5, 145.4, 121.9, 67.5, 63.1, 52.5, 51.0, 47.8, 42.0, 40.0, 34.4, 31.4, 28.7, 24.6, 21.8, 17.3; IR (Neat Film, KBr) 3446 (br), 2925, 2853, 1733, 1704, 1456, 1384, 1178, 1149, 1024, 732 cm^{-1}; HRMS (EI+) *m/z* calc'd for $C_{17}H_{24}O_3$ $[M\bullet]^+$: 276.1726, found 276.1716; $[\alpha]^{25}_D$ –68.0 (*c* 0.31, $CHCl_3$).

4.6.2.2 PALLADIUM-CATALYZED ALLYLIC C–H ACETOXYLATION

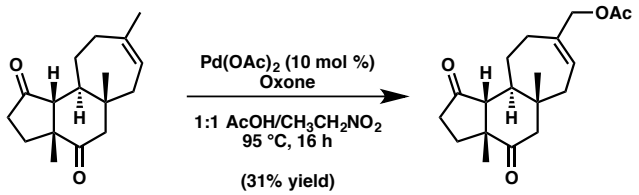

Allylic Acetate 191. A flame-dried 1-dram vial was charged with tricyclic diketone **109** (10.0 mg, 38.1 μmol, 1.00 equiv), palladium(II) acetate (0.9 mg, 3.8 μmol, 0.10 equiv), and Oxone (13 mg, 42 μmol, 1.10 equiv), and the resulting mixture was diluted with 1:1 acetic acid/nitroethane (0.30 mL total). The vial was sealed with a Teflon-lined cap and heated to 95 °C. After 24 hours, heating was discontinued, and the reaction mixture was quenched with aq. sodium bicarbonate (1.0 mL) and extracted with ethyl acetate (3 x 5 mL). The combined organic extracts were dried over sodium sulfate, filtered, and concentrated. The resulting crude residue was purified by silica gel column chromatography (10% → 30% ethyl acetate in hexanes), delivering allylic acetate **191** as a colorless oil (3.9 mg, 31% yield). R*f* = 0.14 (33% ethyl acetate in hexanes); ^{1}H NMR ($CDCl_3$, 400 MHz) δ 5.66 (dd, *J* = 8.8, 5.3 Hz, 1H), 4.47 (s, 2H), 2.68 (d, *J* = 14.6 Hz, 1H), 2.60–2.50 (m, 1H), 2.40–2.29 (m, 3H), 2.16–2.12 (m, 2H), 2.10–2.05 (m, 1H), 2.07

(s, 3H), 2.04–2.01 (m, 1H), 1.92–1.77 (m, 4H), 1.11 (s, 4H), 0.72 (s, 3H); ^{13}C NMR ($CDCl_3$, 101 MHz) δ 217.8, 212.3, 171.1, 140.6, 125.8, 68.8, 63.0, 52.5, 51.0, 47.8, 42.0, 39.9, 34.4, 31.4, 28.8, 24.4, 21.8, 21.2, 17.3; IR (Neat Film, KBr) 2919, 2850, 1736, 1703, 1458, 1384, 1227, 1025, 959 cm^{-1}; HRMS (FAB+) *m/z* calc'd for $C_{19}H_{26}O_4$ $[M\bullet]^+$: 318.1831, found 318.1823; $[\alpha]^{25}_D$ –58.2 (*c* 0.25, $CHCl_3$).

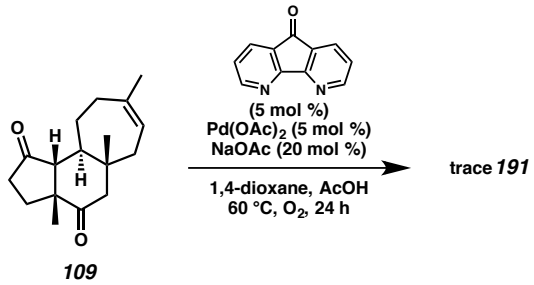

Unsuccessful Procedure 1. A flame-dried round-bottom flask was charged with tricycle **109** (10.0 mg, 38.1 μmol, 1.00 equiv), sodium acetate (0.6 mg, 7.7 μmol, 0.20 equiv), palladium(II) acetate (0.4 mg, 1.9 μmol, 0.050 equiv), and 4,5-diazafluorenone (0.4 mg, 1.9 μmol, 0.050 equiv). This mixture was diluted with 1,4-dioxane (0.70 mL) and acetic acid (0.20 mL), and oxygen gas (balloon) was bubbled through the resulting solution for 10 minutes. The reaction mixture was then heated to 60 °C while being stirred vigorously. After 24 hours, heating was discontinued, and the solvent was removed under reduced pressure. The crude residue was purified by silica gel column chromatography (5% ethyl acetate in hexanes), returning predominantly unreacted **109** (9.1 mg, 91% recovery).

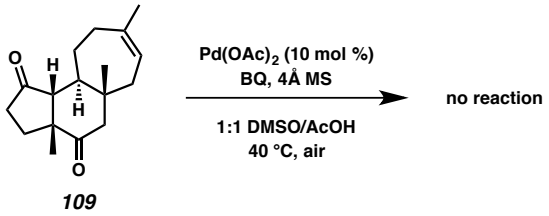

Unsuccessful Procedure 2. A flame-dried 1-dram vial was charged with palladium(II) acetate (0.3 mg, 1.46 μmol, 0.10 equiv), *p*-benzoquinone (3.2 mg, 29.2 μmol, 2.00 equiv), and activated 4Å molecular sieves (10 mg). To this mixture was added a solution of tricyclic diketone **109** (3.8 mg, 14.6 μmol, 1.00 equiv) in DMSO (1.0 mL). Acetic acid (1.0 mL) was added, and the vial was sealed with a Teflon-lined cap and heated to 40 °C. After 24 hours, heating was discontinued, and the reaction mixture was quenched with aq. saturated ammonium chloride (2.0 mL) and extracted with dichloromethane (3 x 5 mL). The combined organic extracts were washed with water (2 x 10 mL) and dried over magnesium sulfate. After filtration and concentration, the crude residue was purified by silica gel column chromatography (5% ethyl acetate in hexanes), returning predominantly unreacted **109** (3.5 mg, 92% recovery).

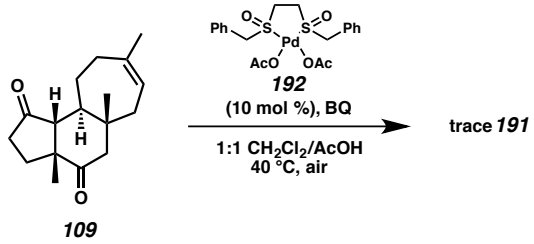

Unsuccessful Procedure 3. A flame-dried 1-dram vial was charged with palladium catalyst **192** (0.7 mg, 1.46 μmol, 0.10 equiv) and *p*-benzoquinone (3.2 mg, 29.2 μmol, 2.00 equiv), and activated 4Å molecular sieves (10 mg). To this mixture was added a solution of tricyclic diketone **109** (3.8 mg, 14.6 μmol, 1.00 equiv) in dichloromethane

(1.0 mL). Acetic acid (1.0 mL) was added, and the vial was sealed with a Teflon-lined cap and heated to 40 °C. After 24 hours, heating was discontinued, and the reaction mixture was quenched with aq. saturated ammonium chloride (2.0 mL) and extracted with dichloromethane (3 x 5 mL). The combined organic extracts were washed with water (2 x 10 mL) and dried over magnesium sulfate. After filtration and concentration, the crude residue was purified by silica gel column chromatography (5% ethyl acetate in hexanes), returning predominantly unreacted **109** (3.4 mg, 90% recovery).

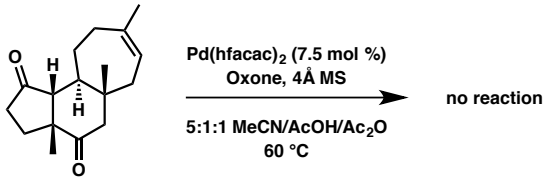

109

Unsuccessful Procedure 4. A flame-dried 1-dram vial was charged with tricyclic diketone **109** (7.3 mg, 28.0 μmol, 1.00 equiv), palladium(II) hexafluoroacetylacetonate (1.1 mg, 2.10 μmol, 0.075 equiv), and Oxone (21.5 mg, 70.1 μmol, 2.50 equiv). Activated 4Å molecular sieves (20 mg) were added, and the reaction vessel was evacuated and backfilled with argon twice before addition of acetonitrile (0.50 mL) and 1:1 acetic acid/acetic anhydride (0.20 mL) which had been pre-dried over 4Å molecular sieves. The vial was sealed with a Teflon-lined cap, and the reaction mixture was stirred at 23 °C for 5 minutes before heating to 60 °C. After 8 hours, the reaction was removed from heat and filtered over a pad a silica gel, eluting with ethyl acetate. The filtrate was concentrated, and the resulting residue was purified by silica gel column chromatography (5% ethyl acetate in hexanes), returning predominantly unreacted **109** (6.9 mg, 95% recovery).

4.6.2.3 HYDROGENATION AND DEUTERATION OF TRICYCLE 109

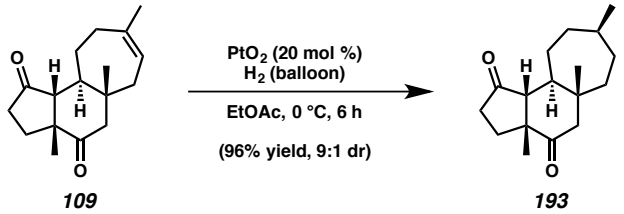

109 *193*

Saturated Tricycle 193. To a solution of tricyclic diketone **109** (15.0 mg, 57.6 μmol, 1.00 equiv) in ethyl acetate (10 mL) was added platinum dioxide (2.6 mg, 11.4 μmol, 0.20 equiv), and the resulting suspension was cooled in an ice/water bath. A hydrogen balloon connected to a three-way adapter was fitted to the flask, and the headspace was evacuated for 3 minutes (~400 Torr) and backfilled with hydrogen gas. This process was repeated twice more, after which the reaction mixture was allowed to stir at 0 °C under hydrogen atmosphere. Within a few minutes, the color of the reaction mixture changed from brown to black. After 6 hours, the solvent was removed in vacuo, and the resulting residue was passed through a pad of silica gel, eluting with 20% ethyl acetate in hexanes (150 mL). Concentration of the filtrate afforded saturated tricycle **193** as a colorless oil which required no further purification (14.5 mg, 96% yield). Crystals for X-ray diffraction were grown using slow evaporation of trace amounts of dichloromethane and d_3-chloroform at –20 °C over a 5-month period. R*f* = 0.43 (25% ethyl acetate in hexanes); ^{1}H NMR ($CDCl_3$, 300 MHz) δ 2.59 (d, *J* = 15.2 Hz, 1H), 2.55–2.44 (m, 1H), 2.43–2.21 (m, 2H), 2.05 (d, *J* = 14.8 Hz, 1H), 1.90 (d, *J* = 12.6, Hz, 1H), 1.86–1.73 (m, 2H), 1.55–1.48 (m, 2H), 1.47–1.38 (m, 3H), 1.38–1.21 (m, 4H), 1.11 (s, 3H), 0.89 (d, *J* = 6.8 Hz, 3H), 0.77 (s, 3H); ^{13}C NMR ($CDCl_3$, 101 MHz) δ 218.2, 213.1,

62.3, 52.8, 51.0, 45.0, 42.0, 41.8, 34.4, 34.3, 31.5, 31.1, 29.3, 23.4, 21.8, 21.4, 19.1; IR (Neat Film, KBr) 2952, 2919, 1737, 1705, 1458, 1384, 1172, 1124, 1052 cm^{-1}; HRMS (FAB+) *m/z* calc'd for $C_{17}H_{27}O_2$ $[M+H]^+$: 263.2011, found 263.2020; $[\alpha]^{25}_D$ –61.3 (*c* 0.31, $CHCl_3$).

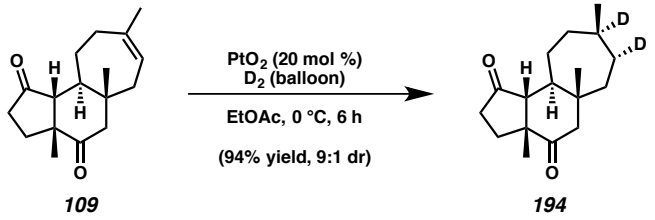

109 ***194***

Deuterated Tricycle 194. To a solution of tricyclic diketone **109** (11.7 mg, 44.9 μmol, 1.00 equiv) in ethyl acetate (8.0 mL) was added platinum dioxide (2.1 mg, 9.2 μmol, 0.20 equiv), and the resulting suspension was cooled in an ice/water bath. A deuterium balloon connected to a three-way adapter was fitted to the flask, and the headspace was evacuated for 3 minutes (~400 Torr) and backfilled with deuterium gas. This process was repeated twice more, after which the reaction mixture was allowed to stir at 0 °C under deuterium atmosphere. Within a few minutes, the color of the reaction mixture changed from brown to black. After 6 hours, the solvent was removed in vacuo, and the resulting residue was passed through a pad of silica gel, eluting with 20% ethyl acetate in hexanes (150 mL). Concentration of the filtrate afforded deuterated tricycle **194** as a colorless oil which required no further purification (11.2 mg, 94% yield). R*f* = 0.43 (25% ethyl acetate in hexanes); ^{1}H NMR ($CDCl_3$, 400 MHz) δ 2.59 (d, *J* = 14.8 Hz, 1H), 2.55–2.47 (m, 1H), 2.40–2.31 (m, 1H), 2.31–2.24 (m, 1H), 2.04 (d, *J* = 14.7 Hz, 1H), 1.89 (d, *J* = 12.5 Hz 1H), 1.87–1.82 (m, 1H), 1.77–1.71 (m, 1H), 1.64 (ddd, *J* = 12.5, 9.8, 1.5 Hz, 1H), 1.56–1.51 (m, 1H), 1.43–1.36 (m, 3H), 1.32–1.28 (m, 1H), 1.25

(m, 1H), 1.10 (s, 3H), 0.90–0.85 (m, 3H), 0.77 (s, 3H); ^{13}C NMR ($CDCl_3$, 101 MHz) δ 218.2, 213.1, 62.3, 52.8, 51.0, 45.0, 41.9, 41.8, 34.3, 34.2, 31.1, 30.8, 28.8 (t, J = 18.2, 36.5 Hz), 23.3, 21.8, 21.4, 19.0; IR (Neat Film, KBr) 2953, 2924, 1736, 1702, 1458, 1384, 1173, 1144, 1052, 804 cm^{-1}; HRMS (FAB+) *m/z* calc'd for $C_{17}H_{24}O_2{}^2H_2$ $[M\bullet]^+$: 264.2058, found 264.2047; $[\alpha]^{25}_D$ –77.7 (*c* 1.12, $CHCl_3$).

4.6.2.4 TERTIARY C–H HYDROXYLATION OF SATURATED TRICYCLE 193

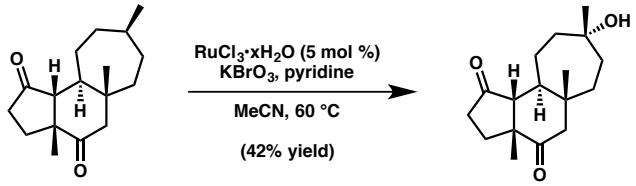

193 *195*

Tertiary C–H Hydroxylation Catalyzed by $RuCl_3$•xH_2O. A 1-dram vial was charged with ruthenium(III) trichloride hydrate (1.0 mg, 0.95 μmol, 0.05 equiv) and potassium bromate (9.6 mg, 57.3 μmol, 3.00 equiv), and water (0.2 mL) and pyridine (0.20 μL, 1.91 μmol, 0.10 equiv) were added sequentially. A solution of tricyclic diketone **193** (5.0 mg, 19.1 μmol, 1.00 equiv) was added, and the vial was sealed with a Teflon-lined cap and heated to 60 °C with vigorous stirring. After 24 hours, heating was discontinued, and the reaction mixture was quenched with saturated aq. sodium sulfite solution (1.0 mL), diluted with water (1.0 mL), and extracted with ethyl acetate (3 x 5 mL). The combined organics were dried over sodium sulfate, filtered, and concentrated. The crude residue was purified by silica gel column chromatography (10% → 40% → 50% ethyl acetate in hexanes), furnishing tertiary alcohol **195** as a white amorphous solid

(2.2 mg, 42% yield). R*f* = 0.15 (50% ethyl acetate in hexanes); ^{1}H NMR ($CDCl_3$, 400 MHz) δ 2.63 (d, *J* = 15.0 Hz, 1H), 2.59–2.45 (m, 1H), 2.42–2.32 (m, 1H), 2.26 (dt, *J* = 13.3, 10.3 Hz, 1H), 2.08 (d, *J* = 15.1 Hz, 1H), 1.96–1.85 (m, 3H), 1.80–1.71 (m, 3H), 1.71–1.63 (m, 2H), 1.53 (s, 1H), 1.24 (s, 3H), 1.13 (s, 3H), 1.11–1.04 (m, 1H), 0.75 (s, 3H); ^{13}C NMR ($CDCl_3$, 101 MHz) δ 218.2, 212.6, 73.8, 61.5, 52.7, 51.0, 46.9, 42.9, 40.9, 37.1, 36.2, 34.3, 31.2, 31.0, 21.8, 21.2, 19.0; IR (Neat Film, KBr) 3417 (br), 2958, 2925, 2853, 1738, 1704, 1463, 1384, 1261, 1126, 1052, 803 cm^{-1}; HRMS (EI+) *m/z* calc'd for $C_{17}H_{24}O_2$ [M–H_2O]: 260.1776, found 260.1769; $[\alpha]^{25}_{D}$ –9.5 (*c* 0.28, $CHCl_3$).

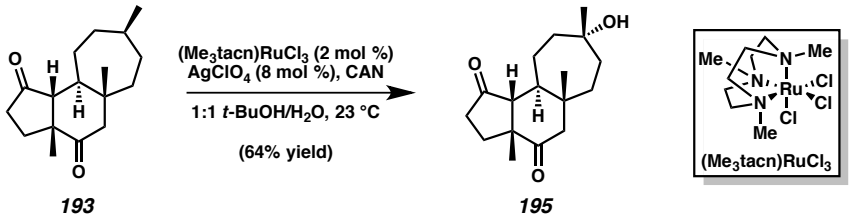

Tertiary C–H Hydroxylation Catalyzed by (Me_3tacn)$RuCl_3$. A 1-dram vial was charged with (1,4,7-trimethyl-1,4,7-triazacyclononane)ruthenium(III) trichloride (0.2 mg, 0.63 μmol, 0.020 equiv), silver perchlorate (0.5 mg, 2.50 μmol, 0.080 equiv), and water (0.5 mL). The vial was sealed with a Teflon-lined cap and heated to 80 °C with vigorous stirring for 5 minutes. The reaction mixture was then allowed to cool to 23 °C, and a solution of saturated tricycle **193** (8.2 mg, 31.2 μmol, 1.00 equiv) in *tert*-butanol (0.50 mL) was added, followed by ceric(IV) ammonium nitrate (51.4 mg, 93.7 μmol, 3.00 equiv). The resulting mixture suspension was stirred at 23 °C for 25 minutes, at which time a second portion of ceric(IV) ammonium nitrate (51.4 mg, 93.7 μmol, 3.00 equiv) was added. After 24 hours, the reaction was quenched with methanol (2 mL), diluted

with water (5 mL), and extracted with ethyl acetate (3 x 5 mL). The combined organic extracts were dried over magnesium sulfate, filtered, and concentrated. The crude residue was purified by silica gel column chromatography (10% → 40% → 50% ethyl acetate in hexanes), furnishing tertiary alcohol **195** as a white amorphous solid (5.6 mg, 64% yield).

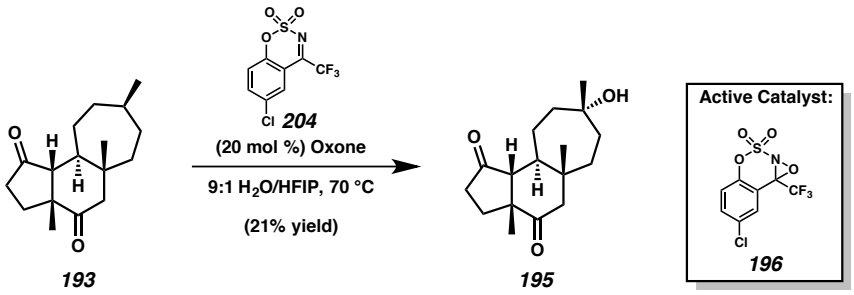

Tertiary C–H Hydroxylation Catalyzed by Benzoxaziridine 196. A 1-dram vial was charged with saturated tricycle **193** (10.0 mg, 38.1 μmol, 1.00 equiv), benzoxathiazine **204** (2.2 mg, 7.62 μmol, 0.20 equiv), and Oxone (29.3 mg, 95.3 μmol, 2.50 equiv), and this mixture was diluted with 9:1 water/hexafluoroisopropanol (1.0 mL total volume). The vial was sealed with a Teflon-lined cap and heated to 70 °C with vigorous stirring, forming the active catalyst **196** in situ. After 24 hours, the reaction was allowed to cool to 23 °C, diluted with water (5 mL), and extracted with ethyl acetate (3 x 5 mL). The combined organic extracts were dried over sodium sulfate, filtered, and concentrated. The crude residue was purified by silica gel column chromatography (10% → 20% → 50% → 80% ethyl acetate in hexanes), affording tertiary alcohol **195** as a white amorphous solid (2.2 mg, 21% yield).

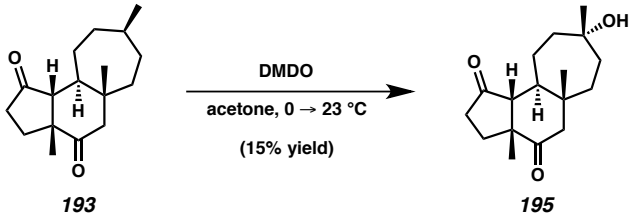

Tertiary C–H Hydroxylation Mediated by DMDO. A solution of dimethyldioxirane in acetone (0.0125 M, 24.4 mL, 0.305 mmol, 8.00 equiv) was added slowly to a solution of saturated tricycle **193** (10.0 mg, 38.1 μmol, 1.00 equiv) in acetone at 0 °C. The resulting mixture was stirred at this temperature for 6 hours before being allowed to gradually warm to 23 °C over 2 hours. After 16 hours at this temperature, the volatiles were removed under reduced pressure, and the crude residue was purified by silica gel column chromatography (10% → 20% → 50% → 80% ethyl acetate in hexanes), affording tertiary alcohol **195** as a white amorphous solid (1.6 mg, 15% yield).

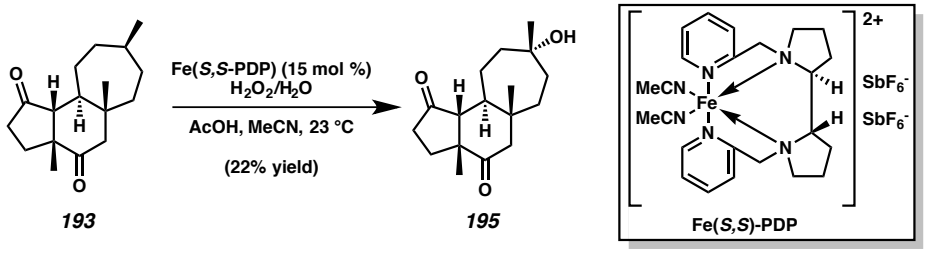

Tertiary C–H Hydroxylation Catalyzed by Fe(*S*,*S*-PDP). To a solution of tricyclic diketone **193** (10.0 mg, 38.1 μmol, 1.00 equiv) and Fe(*S*,*S*-PDP) (1.8 mg, 1.91 μmol, 0.050 equiv) in acetonitrile (1.0 mL) was added acetic acid (1 drop). In a separate vial, a solution of hydrogen peroxide (50 wt % solution in water, 3.0 μL, 45.7 μmol, 1.20 equiv) was diluted with acetonitrile (0.30 mL). This solution was added dropwise very slowly to the solution of **193** and Fe catalyst while stirring. After 10 minutes had elapsed, another solution of Fe(*S*,*S*-PDP) (1.8 mg) in acetonitrile (0.30 mL) was added to the reaction

mixture, followed by acetic acid (1 drop) and dropwise addition of another portion of hydrogen peroxide (3.0 μL) in acetonitrile (0.30 mL). After 10 minutes, this process was repeated once more. Ten minutes after the final addition (total reaction time of 30 minutes), the volatiles were removed in vacuo, and the residue was diluted with diethyl ether (3 mL) and filtered through a pad of silica gel. The filtrate was dried over magnesium sulfate, filtered, and concentrated in vacuo, and the crude residue was purified by silica gel column chromatography (20% → 40% → 60% → 80% ethyl acetate in hexanes) to furnish tertiary alcohol **195** as an amorphous white solid (2.3 mg, 22% yield).

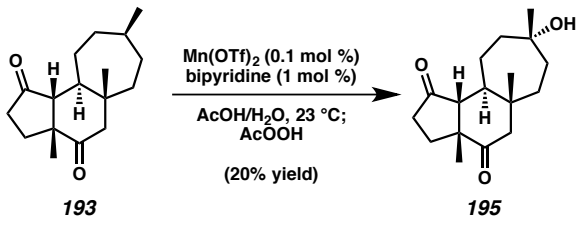

193 ***195***

Tertiary C–H Hydroxylation Catalyzed by $Mn(OTf)_2$. Stock solutions were prepared as follows: manganese(II) triflate (4.4 mg) was dissolved in 9:1 acetic acid/water (1.0 mL) to afford a 0.0125 M solution. 2,2-bipyridine (3.9 mg) was dissolved in acetic acid (1.0 mL) to generate a 0.025 M solution. Commercial peracetic acid was modified by adding 10% aq. potassium hydroxide solution (0.30 mL) to a 35 wt % solution of peracetic acid in acetic acid (1.0 mL).

To a solution of tricyclic diketone **193** (7.0 mg, 26.7 μmol, 1.00 equiv) in acetic acid (0.13 mL) and water (5.3 μL) were added sequentially solutions of manganese(II) triflate (2.1 μL) and 2,2-bipyridine (10.7 μL). The resulting mixture was stirred for 10 minutes,

and then a solution of modified peracetic acid (23.5 μL) was added very slowly in a dropwise fashion. After 90 seconds, the reaction mixture was diluted with acetone (2.7 mL) and stirred for an additional 30 seconds before filtration through a small pad of Celite, rinsing with acetone (5 mL). The filtrate was concentrated under reduced pressure, and the resulting crude residue was purified by silica gel column chromatography (10% → 20% → 50% → 80% ethyl acetate in hexanes) to afford tertiary alcohol **195** as a white amorphous solid (1.5 mg, 20% yield).

4.6.2.5 SECONDARY C–H OXIDATION OF SATURATED TRICYCLE 193

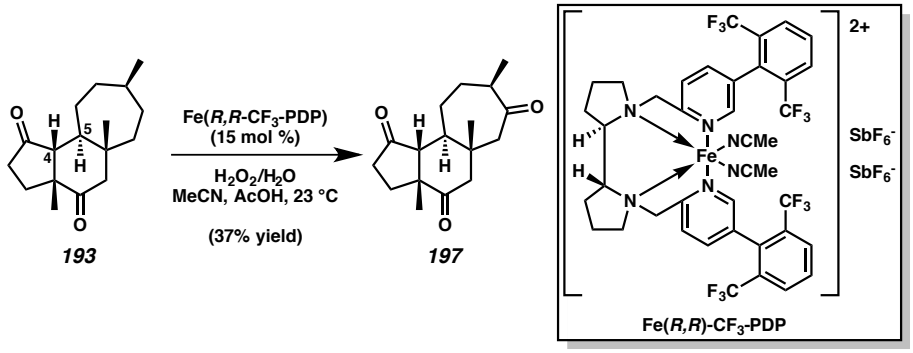

Triketone 197. To a solution of tricyclic diketone **193** (10.0 mg, 38.1 μmol, 1.00 equiv) and Fe(*R*,*R*-CF_3-PDP) (2.6 mg, 1.91 μmol, 0.050 equiv) in acetonitrile (1.0 mL) was added acetic acid (1 drop). In a separate vial, a solution of hydrogen peroxide (50 wt % solution in water, 3.0 μL, 45.7 μmol, 1.20 equiv) was diluted with acetonitrile (0.30 mL). This solution was added dropwise very slowly to the solution of **193** and Fe catalyst while stirring. After 10 minutes had elapsed, another solution of Fe(*R*,*R*-CF_3-PDP) (2.6 mg) in acetonitrile (0.30 mL) was added to the reaction mixture, followed by

acetic acid (1 drop) and dropwise addition of another portion of hydrogen peroxide (3.0 μL) in acetonitrile (0.30 mL). After 10 minutes, this process was repeated once more. Ten minutes after the final addition (total reaction time of 30 minutes), the volatiles were removed in vacuo, and the residue was diluted with ethyl acetate (3 mL) and filtered through a pad of silica gel. After concentration of the filtrate, the crude residue was purified by silica gel column chromatography (20% → 30% → 50% → 80% ethyl acetate in hexanes) to furnish major product triketone **197** as a colorless oil (3.9 mg, 37% yield). R*f* = 0.40 (50% ethyl acetate in hexanes); ^{1}H NMR ($CDCl_3$, 400 MHz) δ 2.70 (d, *J* = 14.2 Hz, 1H), 2.60–2.46 (m, 4H), 2.44–2.36 (m, 1H), 2.27 (m, 1H), 2.12 (d, *J* = 14.7 Hz, 1H), 2.04–1.97 (m, 1H), 1.94 (m, 1H), 1.83–1.75 (m, 2H), 1.62–1.58 (m, 1H), 1.53–1.48 (m, 1H), 1.47–1.41 (m, 1H), 1.15 (s, 3H), 1.08 (d, *J* = 7.0 Hz, 3H), 0.87 (s, 3H); ^{13}C NMR ($CDCl_3$, 101 MHz) δ 217.0, 214.6, 211.8, 61.0, 52.2, 51.2, 47.2, 42.6, 41.4, 40.7, 39.3, 34.4, 31.2, 26.8, 21.9, 18.1, 18.1; IR (Neat Film, KBr) 2960, 2927, 1738 (overlapping peaks), 1704, 1456, 1384, 1261, 1172, 1108, 802 cm^{-1}; HRMS (ESI+) *m/z* calc'd for $C_{17}H_{25}O_3$ $[M+H]^+$: 277.1804, found 277.1819; $[\alpha]^{25}_D$ –6.9 (*c* 0.39, $CHCl_3$). Tertiary alcohol **195** was also isolated (2.1 mg, 20% yield).

4.6.2.6 TERTIARY C–H AMINATION OF SATURATED TRICYCLE 193

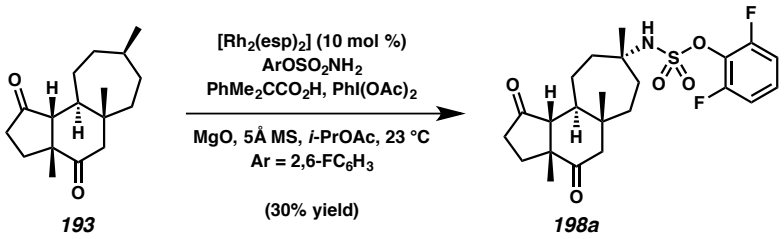

Sulfamate Ester 198a. A 1-dram vial was charged with 5Å molecular sieves (30 mg) and magnesium oxide (2.9 mg, 71.6 μmol, 4.00 equiv) and flame dried under vacuum. Upon cooling, the reaction vessel was charged with 2,6-difluorophenyl sulfamate (4.9 mg, 23.3 μmol, 1.30 equiv), 2-phenylisobutyric acid (1.5 mg, 8.95 μmol, 0.50 equiv), and $Rh_2(esp)_2$ (0.2 mg, 0.18μmol, 0.010 equiv), followed by a solution of tricyclic diketone **193** (4.7 mg, 17.9 μmol, 1.00 equiv) in isopropyl acetate (1.0 mL). The resulting green mixture was stirred for 5 minutes before the addition of (diacetoxyiodo)benzene (11.5 mg, 35.8 μmol, 2.00 equiv). The vial was then sealed with a Teflon-lined cap and stirred at 23 °C. After 20 hours, the mixture was filtered through Celite and rinsed with ethyl acetate (15 mL). Concentration of the filtrate and purification of the crude residue by silica gel column chromatography (2% methanol in dichloromethane) afforded pure sulfamate ester **198a** as a colorless oil (2.5 mg, 30% yield). R_f = 0.18 (2% methanol in dichloromethane); ^{1}H NMR ($CDCl_3$, 500 MHz) δ 7.21 (td, *J* = 6.1, 3.1 Hz, 1H), 7.02–6.99 (m, 2H), 4.72 (s, 1H), 2.64 (d, *J* = 15.1 Hz, 1H), 2.58–2.48 (m, 1H), 2.45–2.35 (m, 1H), 2.31–2.25 (m, 1H), 2.20–2.13 (m, 2H), 2.10 (d, *J* = 15.2 Hz, 1H), 2.03–1.98 (m, 1H), 1.91 (d, *J* = 12.8 Hz, 1H), 1.81–1.71 (m, 5H), 1.50 (s, 3H), 1.37–1.33 (m, 1H), 1.15 (s, 3H), 1.12 (m, 1H), 0.78 (s, 3H); ^{13}C NMR ($CDCl_3$, 101

MHz) δ 218.1, 212.3, 156.2 (dd, *J* = 253.2, 4.0 Hz) 130.0 (d, *J* = 29.5 Hz), 127.5 (t, *J* = 18.5, 9.1 Hz), 112.7 (m), 62.1, 61.1, 52.4, 51.0, 46.9, 41.2, 40.7. 36.7, 34.3, 33.5, 31.0, 28.0, 21.8, 20.3, 19.0; ^{19}F NMR ($CDCl_3$, 300 MHz) δ –124.0; IR (Neat Film, KBr) 3261 (br), 2957, 2933, 1737, 1704, 1605, 1497, 1480, 1384, 1300, 1208, 1178, 1012, 861, 745, 734 cm^{-1}; HRMS (ESI+) *m/z* calc'd for $C_{23}H_{30}NO_5F_2S$ $[M+H]^+$: 470.1813, found 470.1828; $[\alpha]^{25}_D$ –36.4 (*c* 0.23, $CHCl_3$).

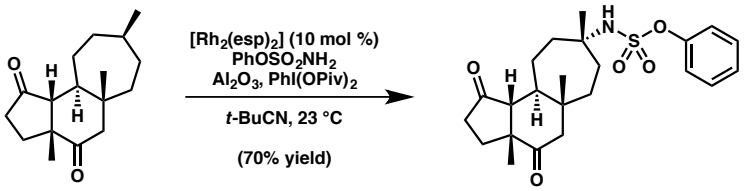

193 ***198b***

Sulfamate Ester 198b. A 1-dram vial was charged with aluminum oxide (15.5 mg, 0.152 mmol, 4.00 equiv, Brockmann grade 1, neutral) and flame dried under vacuum. Upon cooling, the reaction vessel was charged with tricyclic diketone **193** (10.0 mg, 38.1 μmol, 1.00 equiv), $Rh_2(esp)_2$ (3.0 mg, 3.81 μmol, 0.10 equiv), and phenyl sulfamate (8.6 mg, 49.5 μmol, 1.30 equiv). The mixture was diluted with pivalonitrile (1.0 mL) and stirred at room temperature. After five minutes, the green reaction mixture had turned navy blue, and di-(pivaloyloxy)iodobenzene (23.2 mg, 57.2 μmol, 1.5 equiv) was added in a single portion. The reaction was stirred at 23 °C for 24 hours, developing a grayish hue during that time. The mixture was filtered through Celite and rinsed with ethyl acetate (15 mL). The filtrate was concentrated, and the crude residue was purified by column chromatography (5% → 15% → 50% ethyl acetate in hexanes) to furnish pure sulfamate ester **198b** as a colorless oil (11.6 mg, 70% yield). R*f* = 0.22 (33% ethyl

acetate in hexanes); ^{1}H NMR ($CDCl_3$, 400 MHz) δ 7.40–7.37 (m, 2H), 7.30–7.27 (m, 3H), 4.67 (s, 1H), 2.59 (d, *J* = 15.1 Hz, 1H), 2.54–2.45 (m, 1H), 2.42–2.32 (m, 1H), 2.28–2.20 (m, 1H), 2.11–2.04 (m, 3H), 2.00–1.94 (m, 1H), 1.87 (d, *J* = 8.0 Hz, 1H), 1.79–1.75 (m, 1H), 1.74–1.71 (m, 1H), 1.70–1.64 (m, 4H), 1.45 (s, 3H), 1.31–1.29 (m, 1H), 1.13 (s, 3H), 0.75 (s, 3H); ^{13}C NMR ($CDCl_3$, 101 MHz) δ 218.1, 212.2, 150.4, 129.9, 126.9, 121.8, 61.4, 61.1, 52.5, 51.0, 47.0, 41.4, 40.7, 36.7, 34.3, 33.7, 31.0, 28.3, 21.8, 20.3, 18.9; IR (Neat Film, KBr) 3285 (br), 2958, 2927, 2254, 1736, 1702, 1588, 1488, 1459, 1376, 1194, 1171, 1150, 1054, 913, 859, 782, 731, 691, 647 cm^{-1}; HRMS (FAB+) *m/z* calc'd for $C_{23}H_{32}NO_5S$ $[M+H]^+$: 434.2001, found 434.1999; $[\alpha]^{25}_D$ –33.5 (*c* 1.16, $CHCl_3$).

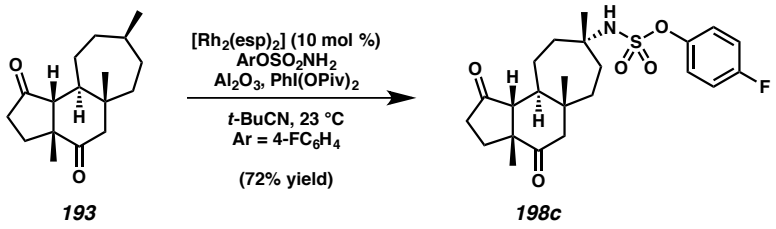

Sulfamate Ester 198c. A 1-dram vial was charged with aluminum oxide (15.5 mg, 0.152 mmol, 4.00 equiv, Brockmann grade 1, neutral) and flame dried under vacuum. Upon cooling, the reaction vessel was charged with tricyclic diketone **193** (10.0 mg, 38.1 μmol, 1.00 equiv), $Rh_2(esp)_2$ (3.0 mg, 3.81 μmol, 0.10 equiv), and 4-fluorophenyl sulfamate (9.5 mg, 49.5 μmol, 1.30 equiv). The mixture was diluted with pivalonitrile (1.0 mL) and stirred at room temperature. After five minutes, the green reaction mixture had turned navy blue, and di-(pivaloyloxy)iodobenzene (23.2 mg, 57.2 μmol, 1.50 equiv) was added in a single portion. The reaction was stirred at 23 °C for 24 hours, developing a grayish hue during that time. The mixture was filtered through Celite and rinsed with ethyl acetate (15 mL). The filtrate was concentrated, and the crude residue was purified

by column chromatography (10% → 20% → 25% ethyl acetate in hexanes) to furnish pure sulfamate ester **198c** as a colorless oil (12.4 mg, 72% yield). R*f* = 0.20 (33% ethyl acetate in hexanes); ^{1}H NMR ($CDCl_3$, 500 MHz) δ 7.40–7.37 (m, 2H), 7.30–7.27 (m, 3H), 4.67 (s, 1H), 2.59 (d, *J* = 15.1 Hz, 1H), 2.54–2.45 (m, 1H), 2.42–2.32 (m, 1H), 2.28–2.20 (m, 1H), 2.11–2.04 (m, 3H), 2.00–1.94 (m, 1H), 1.87 (d, *J* = 8.0 Hz, 1H), 1.79–1.75 (m, 1H), 1.74–1.71 (m, 1H), 1.70–1.64 (m, 4H), 1.45 (s, 3H), 1.31–1.29 (m, 1H), 1.13 (s, 3H), 0.75 (s, 3H); ^{13}C NMR ($CDCl_3$, 101 MHz) δ 218.1, 212.1, 161.0 (d, *J* = 246.3 Hz), 146.1 (d, *J* = 3.0 Hz), 123.6, (d, *J* = 8.8 Hz), 116.6 (d, *J* = 23.8 Hz), 61.6, 61.1, 52.4, 51.0, 47.0, 41.4, 40.7, 36.7, 34.3, 33.7, 31.0, 28.2, 21.8, 20.3, 18.9; ^{19}F NMR ($CDCl_3$, 300 MHz) δ –115.0; IR (Neat Film, KBr) 3286 (br), 2959, 2927, 1737, 1704, 1500, 1464, 1384, 1360, 1191, 1162, 1010, 987, 870, 849, 803, 736, 639 cm^{-1}; HRMS (ESI+) *m/z* calc'd for $C_{23}H_{31}NO_5FS$ $[M+H]^+$: 452.1907, found 452.1920; $[\alpha]^{25}_D$ –32.0 (*c* 1.24, $CHCl_3$).

4.6.2.7 TERTIARY C–H AZIDATION OF SATURATED TRICYCLE 193

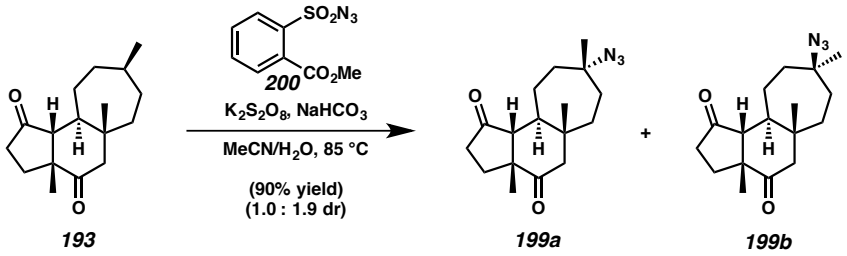

Tertiary C–H Azidation Mediated by Sulfonyl Azide 200. A flame-dried 1-dram vial was charged with sulfonyl azide **200** (10.6 mg, 44.0 μmol, 1.50 equiv), potassium

persulfate (23.8 mg, 88.0 μmol, 3.00 equiv), and sodium bicarbonate (2.5 mg, 29.3 μmol, 1.00 equiv). To this mixture was added water (0.4 mL) and a solution of tricyclic diketone **193** (11.2 mg, 42.5 μmol, 1.00 equiv) in acetonitrile (0.6 mL). The reaction vial was sealed with a Teflon-line cap and heated to 85 °C with vigorous stirring. After 24 hours, heating was discontinued, and the reaction mixture was diluted with ethyl acetate (3 mL) and water (3 mL) and extracted with ethyl acetate (3 x 5 mL). The combined organic extracts were dried over magnesium sulfate, and the crude residue obtained after filtration and concentration was purified by silica gel column chromatography (10% → 15% → 40% ethyl acetate in hexanes) to afford diastereomers **199a** and **199b** as amorphous solids (4.1 mg **199a** and 7.6 mg **199b**, combined 11.7 mg, 90% yield). **Diastereomer 199a**: R*f* = 0.28 (20% ethyl acetate in hexanes); ^{1}H NMR ($CDCl_3$, 500 MHz) δ 2.61 (d, *J* = 15.1 Hz, 1H), 2.55–2.47 (m, 1H), 2.42–2.33 (m, 1H), 2.30–2.22 (m, 1H), 2.08 (d, *J* = 15.1 Hz, 1H), 2.01–1.94 (m, 1H), 1.94–1.85 (m, 2H), 1.80–1.74 (m, 1H), 1.73–1.70 (m, 1H), 1.70–1.64 (m, 3H), 1.54 (m, 1H), 1.29 (s, 3H), 1.28–1.24 (m, 1H), 1.13 (s, 3H), 1.12–1.07 (m, 1H), 0.75 (s, 3H); ^{13}C NMR ($CDCl_3$, 101 MHz) δ 218.0, 212.2, 64.4, 61.3, 52.6, 51.0, 47.0, 40.8, 39.8, 37.2, 34.3, 33.2, 31.0, 27.2, 21.8, 20.7, 18.8; IR (Neat Film, KBr) 2960, 2923, 2097, 1732, 1704, 1464, 1384, 1260, 1142, 1108, 1052, 802, 641 cm^{-1}; HRMS (FAB+) *m/z* calc'd for $C_{17}H_{25}O_2$ $[M–N_3]^+$: 261.1855, found 261.1860; $[\alpha]^{25}_D$ –59.5 (*c* 0.31, $CHCl_3$). **Diastereomer 199b**: R*f* = 0.13 (20% ethyl acetate in hexanes); ^{1}H NMR ($CDCl_3$, 500 MHz) δ 2.64 (d, *J* = 15.2 Hz, 1H), 2.53–2.44 (m, 1H), 2.43–2.33 (m, 1H), 2.27–2.18 (m, 1H), 2.05 (d, *J* = 15.1 Hz, 1H), 1.97–1.84 (m, 3H), 1.80–1.73 (m, 1H), 1.73–1.64 (m, 3H), 1.64–1.60 (m, 1H), 1.41–1.34 (m, 2H), 1.32 (s, 3H), 1.28–1.23 (m, 1H), 1.14 (s, 3H), 0.78 (s, 3H); ^{13}C NMR ($CDCl_3$, 101 MHz) δ

218.1, 212.6, 64.4, 60.7, 51.9, 51.1, 45.6, 40.9, 40.6, 36.3, 34.4, 33.0, 30.9, 28.4, 21.8, 20.6, 19.9; IR (Neat Film, KBr) 2959, 2928, 2101, 1736, 1703, 1458, 1384, 1259, 1147, 824 cm^{-1}; HRMS (FAB+) *m/z* calc'd for $C_{17}H_{26}O_2N_3$ $[M+H]^+$: 304.2025, found 304.2027; $[\alpha]^{25}_D$ –16.6 (*c* 0.75, $CHCl_3$).

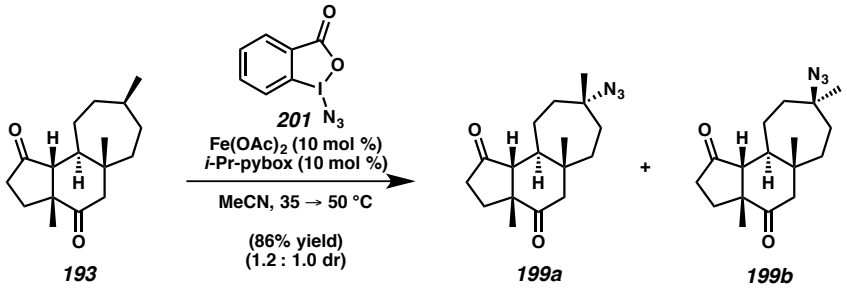

Tertiary C–H Azidation Catalyzed by Iron(II) Acetate. In a nitrogen-filled glovebox, iron(II) acetate (0.4 mg, 2.13 μmol, 0.10 equiv) and *i*-Pr-pybox ligand (0.6 mg, 2.13 μmol, 0.10 equiv) were combined in a flame-dried 1-dram vial and diluted with acetonitrile (0.5 mL) and stirred for 40 minutes at 23 °C, generating a blue solution. After this time, a solution of tricyclic diketone **193** (5.6 mg, 21.3 μmol, 1.00 equiv) was added, followed by hypervalent iodine reagent **201** (12.3 mg, 42.7 μmol, 2.00 equiv). The vial was sealed with a Teflon-lined cap, and the orange mixture was stirred at 35 °C for 4 hours, after which time the temperature was increased to 50 °C. After 20 hours at this temperature, the reaction vial was removed from the glovebox and diluted with diethyl ether (3 mL) and filtered through a pad of basic alumina, rinsing the filter cake with diethyl ether. The filtrate was concentrated, and the crude residue was purified by silica gel column chromatography (10% → 20% → 30% ethyl acetate in hexanes),

furnishing diastereomers **199a** and **199b** as amorphous solids (3.1 mg **199a** and 2.5 mg **199b**, combined 5.6 mg, 86% yield).

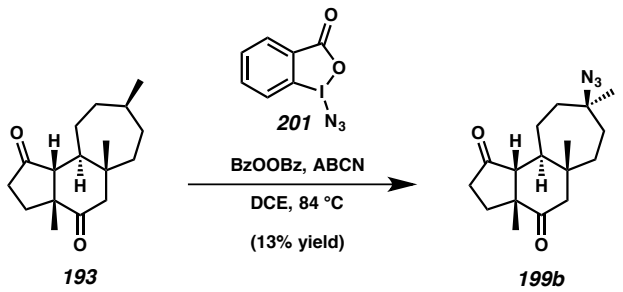

Tertiary C–H Azidation Mediated by Benzoyl Peroxide. In a nitrogen-filled glovebox, benzoyl peroxide (0.5 mg, 2.21 μmol, 0.10 equiv) and 1,1'-azobis(cyclohexanecarbonitrile) (0.3 mg, 1.11 μmol, 0.05 equiv) were combined in a flame-dried 1-dram vial and diluted with 1,2-dichloroethane (0.5 mL). A solution of tricyclic diketone **193** (5.8 mg, 22.1 μmol, 1.00 equiv) in 1,2-dichloroethane (0.6 mL) was added, followed by hypervalent iodine reagent **201** (12.8 mg, 44.2 μmol, 2.00 equiv), and the vial was sealed with a Teflon-lined cap and heated to 84 °C. After 24 hours, the reaction vial was removed from the glovebox, and the reaction mixture was filtered through a pad a basic alumina, rinsing with diethyl ether, and the filtrate was concentrated. The resulting crude residue was purified by silica gel column chromatography (10% → 15% → 40% ethyl acetate in hexanes), delivering tricyclic azide **199b** as an amorphous solid (0.9 mg, 13% yield).

4.6.2.8 SECONDARY C–H CHLORINATION OF TRICYCLE 193

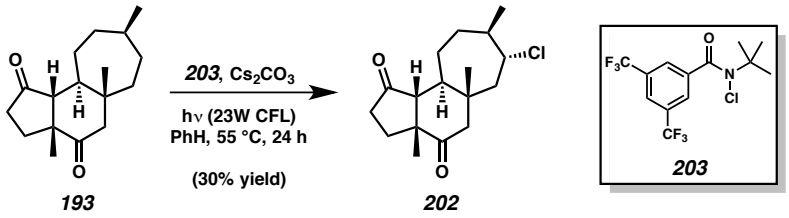

Tricyclic Chloride 202. In a flame-dried 1-dram vial, tricyclic diketone **193** (5.0 mg, 19.1 μmol, 1.00 equiv) was diluted with dry benzene (0.50 mL) and concentrated under reduced pressure. This azeotropic drying procedure was repeated twice more before drying under high vacuum (0.65 Torr) for 10 minutes. The vial was wrapped with foil and brought into a nitrogen-filled glovebox, and a solution of *N*-chloroamide **203** (6.6 mg, 19.1 μmol, 1.00 equiv) in benzene (0.30 mL) was added, followed by cesium carbonate (6.2 mg, 19.1 μmol, 1.00 equiv). The vial was sealed with a Teflon-lined cap, removed from the glovebox, and heated to 55 °C in heating block after removing the foil from the reaction vial (note: fume hood lights turned off). Once this temperature had been reached, the reaction vial was irradiated with two 23W CFL bulbs positioned 5 cm from either side of the heating block. After 24 hours, the reaction was removed from heat and immediately diluted with dichloromethane (2 mL) and filtered over a plug of silica gel, rinsing with dichloromethane. Concentration of the filtrate and purification of the crude residue by silica gel column chromatography (7% → 10% → 20% ethyl acetate in hexanes) afforded chlorinated tricycle **202** as a colorless oil (1.7 mg, 30% yield). R*f* = 0.25 (20% ethyl acetate in hexanes); ^{1}H NMR ($CDCl_3$, 500 MHz) δ 3.84 (t, *J* = 9.5, 19.1 Hz, 1H), 2.67 (d, *J* = 15.1 Hz, 1H), 2.55–2.47 (m, 1H), 2.42–2.33 (m, 1H), 2.31–2.23 (m, 1H), 2.22–2.11 (m, 3H), 1.97–1.89 (m, 1H), 1.89–1.83 (m, 2H), 1.81–1.74 (m, 1H), 1.74–

1.62 (m, 3H), 1.15 (m, 1H), 1.14 (s, 3H), 1.12 (d, J = 6.9 Hz, 3H), 0.85 (s, 3H); ^{13}C NMR ($CDCl_3$, 101 MHz) δ 217.9, 211.9, 63.9, 61.3, 52.7, 50.9, 50.8, 46.6, 41.3, 41.0, 34.3, 32.8, 31.1, 21.7, 21.3, 20.2, 18.5; IR (Neat Film, KBr) 3361, 3194, 2922, 2960, 2853, 1732, 1738, 1704, 1469, 1456, 1384, 1261, 1106, 1052, 1023, 800, 764, 705 cm^{-1}; HRMS (EI+) *m/z* calc'd for $C_{17}H_{25}ClO_2$ $[M\bullet]^+$: 296.1543, found 296.1550; $[\alpha]^{25}_D$ –24.6 (*c* 0.17, $CHCl_3$).

4.8 NOTES AND REFERENCES

(1) Arndtsen, B. A.; Bergman, R. G.; Mobley, T. A.; Peterson, T. H. *Acc. Chem. Res.* **1995**, *28*, 154–162.

(2) For reviews on C–H functionalization in natural product synthesis, see: (a) Newhouse, T.; Baran, P. S. *Angew. Chem., Int. Ed.* **2011**, *50*, 3362–3374; (b) Gutekunst, W. R.; Baran, P. S. *Chem. Soc. Rev.* **2011**, *40*, 1976–1991; (c) McMurray, L.; O'Hara, F.; Gaunt, M. J. *Chem. Soc. Rev.* **2011**, *40*, 1885–1898; (d) Chen, D. Y.-K.; Youn, S. W. *Chem.–Eur. J.* **2012**, *18*, 9452–9474; (e) Kuttruff, C. A.; Eastgate, M. D.; Baran, P. S. *Nat. Prod. Rep.* **2014**, *31*, 419–432; (f) Noisier, A. F. M.; Brimble, M. A. *Chem. Rev.* **2014**, *114*, 8775–8806; (g) Qiu, Y.; Gao, S. *Nat. Prod. Rep.* **2016**, *33,* 562–581.

(3) (a) Wencel-Delord, J.; Glorius, F. *Nat. Chem.* **2013**, *5*, 369–375; (b) Cernak, T.; Dykstra, K. D.; Tyagarajan, S.; Vachal, P.; Krska, S. W. *Chem. Soc. Rev.* **2016**, *45*, 546–576.

(4) (a) Dai, H.-X.; Stepan, A. F.; Plummer, M. S.; Zhang, Y.-H.; Yu, J.-Q. *J. Am. Chem. Soc.* **2011**, *133*, 7222–7228; (b) Meyer, C.; Schepmann, D.; Yanagisawa, S.; Yamaguchi, J.; Itami, K.; Wünsch, B. *Eur. J. Org. Chem.* **2012**, *2012*, 5972–5979.

(5) Beydoun, K.; Zaarour, M.; Williams, J. A. G.; Doucet, H.; Guerchais, V. *Chem. Commun*. **2012**, *48*, 1260–1262.

(6) Dröge, T.; Notzon, A.; Fröhlich, R.; Glorius, F. *Chem.–Eur. J*. **2011**, *17*, 11974–11977.

(7) (a) Kondo, Y.; García-Cuadrado, D.; Hartwig, J. F.; Boaen, N. K.; Wagner, N. L.; Hillmyer, M. A. *J. Am. Chem. Soc*. **2002**, *124*, 1164–1165; (b) Jo, T. S.; Kim, S. H.; Shin, J.; Bae, C. *J. Am. Chem. Soc*. **2009**, *131*, 1656–1657.

(8) He, J.; Hamann, L. G.; Davies, H. M. L.; Beckwith, R. E. J. *Nat. Comms*. **2015**, *6*, 5943.

(9) Adams, A. M.; Du Bois, J.; Malik, H. A. *Org. Lett*. **2015**, *17*, 6066–6069.

(10) Michaudel, Q.; Journot, G.; Regueiro-Ren, A.; Goswami, A.; Guo, Z.; Tully, T. P.; Zou, L.; Ramabhadran, R. O.; Houk, K. N.; Baran, P. S. *Angew. Chem., Int. Ed*. **2014**, *53*, 12091–12096.

(11) For a report on the diversity-oriented synthesis of benzanilides via $C(sp^2)$–H oxidation, see: Sun, Y.-H.; Sun, T.-Y.; Wu, Y.-D.; Zhang, X.; Rao, Y. *Chem. Sci*. **2016**, *7*, 2229–2238.

(12) For a study of the biological properties of ingenol derivatives accessed via C(sp^3)–H oxidation see: Jin, Y.; Yeh, C.-H.; Kuttruff, C. A.; Jørgensen, L.; Dünstl, G.; Felding, J.; Natarajan, S. R.; Baran, P. S. *Angew. Chem., Int. Ed.* **2015**, *54*, 14044–14048.

(13) (a) Enquist, J. A., Jr.; Stoltz, B. M. *Nature* **2008**, *453*, 1228–1231; (b) Enquist, J. A., Jr.; Virgil, S. C.; Stoltz, B. M. *Chem.–Eur. J.* **2011**, *17*, 9957–9969; (c) Kim, K. E.; Stoltz, B. M. *Org. Lett.* **2016**, *18*, 5720–5723.

(14) (a) Lyons, T. W.; Sanford, M. S. *Chem. Rev.* **2010**, *110*, 1147–1169; (b) Zhang, M.; Zhang, Y.; Jie, X.; Zhao, H.; Li, G.; Su, W. *Org. Chem. Front.* **2014**, *1*, 843–895.

(15) Fatta-Kassinos, D.; Vasquez, M. I.; Kümmerer, K. *Chemosphere* **2011**, *85*, 693–709.

(16) For leading references, see: (a) *Oxygenases and Model Systems* (Ed.: Funabiki, T.), Kluwer, Boston, **1997**; (b) Groves, J. T.; Quinn, R. *J. Am. Chem. Soc.* **1985**, *107*, 5790–5792; (c) Neumann, R.; Dahan, M. *Nature* **1997**, *388*, 353–355; (d) Döbler, C.; Mehltretter, G. M.; Sundermeier, U.; Beller, M. *J. Am. Chem. Soc.* **2000**, *122*, 10289–10297.

(17) Sakuda, Y. *Bull. Chem. Soc. Jpn.* **1969**, *42*, 3348–3349.

(18) (a) Ernet, T.; Haufe, G. *Synthesis* **1997**, *1997*, 953–956; (b) Umbreit, M. A.; Sharpless, K. B. *J. Am. Chem. Soc.* **1977**, *99*, 5526–5528.

(19) Młochowski, J.; Wójtowicz-Młochowska, H. *Molecules* **2015**, *20*, 10205–10243.

(20) Campbell, A. N.; White, P. B.; Guzei, I. A.; Stahl, S. S. *J. Am. Chem. Soc.* **2010**, *132*, 15116–15119.

(21) Chen, M. S.; White, M. C. *J. Am. Chem. Soc.* **2004**, *126*, 1346–1347.

(22) Xing, X.; O'Connor, N. R.; Stoltz, B. M. *Angew. Chem., Int. Ed.* **2015**, *54*, 11186–11190.

(23) Efforts to effect Pd-catalyzed allylic C–H azidation using conditions developed by Jiang and co-workers proved unsuccessful, returning unreacted **109**. For the methodology report, see: Chen, H.; Yang, W.; Wu, W.; Jiang, H. *Org. Biomol. Chem.* **2014**, *12*, 3340–3343.

(24) Application of Ru-catalyzed conditions for C–H hydroxylation to **109** resulted in epoxidation of the olefin.

(25) Lowering the temperature below 0 °C did not yield further increases in dr.

(26) McNeill, E.; Du Bois, J. *J. Am. Chem. Soc.* **2010**, *132*, 10202–10204.

(27) McNeill, E.; Du Bois, J. *Chem. Sci.* **2012**, *3*, 1810–1813.

(28) Adams, A. M.; Du Bois, J. *Chem. Sci.* **2014**, *5*, 656–659.

(29) For selected examples of dioxiranes as reagents for C–H hydroxylation, see: (a) Curci, R.; D'Accolti, L.; Fusco, C. *Acc. Chem. Res.* **2006**, *39*, 1–9; (b) Chen, K.; Baran, P. S. *Nature* **2009**, *459*, 824–828. For a study of the molecular dynamics of DMDO C–H oxidation, see: Yang, Z.; Yu, P.; Houk, K. N. *J. Am. Chem. Soc.* **2016**, *138*, 4237–4242.

(30) Chen, M. S.; White, M. C. *Science* **2007**, *318*, 783–787.

(31) Gormisky, P. E.; White, M. C. *J. Am. Chem. Soc.* **2013**, *135*, 14052–14055.

(32) Salamone, M.; Ortega, V. B.; Bietti, M. *J. Org. Chem.* **2015**, *80*, 4710–4715.

(33) (a) Henkel, T.; Brunne, R. M.; Müller, H.; Reichel, F. *Angew. Chem., Int. Ed.* **1999**, *38*, 643–647; (b) Hili, R.; Yudin, A. K. *Nat. Chem. Biol.* **2006**, *2*, 284–287.

(34) For an example, see: Grue-Sorensen, G.; Spenser, I. D. *J. Am. Chem. Soc.* **1983**, *105*, 7401–7404.

(35) (a) Nicolaou, K. C.; Pfefferkorn, J. A.; Barluenga, S.; Mitchell, H. J.; Roecker, A. J.; Cao, G.-Q. *J. Am. Chem. Soc.* **2000**, *122*, 9968–9976; (b) Walsh, C. T. *Science* **2004**, *303*, 1805–1810.

(36) Roizen, J. L.; Zalatan, D. N.; Du Bois, J. *Angew. Chem., Int. Ed.* **2013**, *52*, 11343–11346.

(37) (a) Gaoni, Y. *J. Org. Chem.* **1994**, *59*, 6853–6855; (b) Scriven, E. F. V.; Turnbull, K. *Chem. Rev.* **1988**, *88*, 297–368.

(38) Zhang, X.; Yang, H.; Tang, P. *Org. Lett.* **2015**, *17*, 5828–5831.

(39) Sharma, A.; Hartwig, J. F. *Nature* **2015**, *517*, 600–604.

(40) Gutekunst, W. R.; Baran, P. S. *Chem. Soc. Rev.* **2011**, *40*, 1976–1991.

(41) Gribble, G. W. *Naturally Occurring Organohalogen Compounds: A Comprehensive Update*; Springer-Verlag: Weinheim Germany, **2010**.

(42) Quinn, R. K.; Könst, Z. A.; Michalak, S. E.; Schmidt, Y.; Szklarski, A. R.; Flores, A. R.; Nam, S.; Horne, D. A.; Vanderwal, C. D.; Alexanian, E. J. *J. Am. Chem. Soc.* **2016**, *138*, 696–702.

(43) Minisci, F.; Galli, R.; Galli, A.; Bernardi, R. *Tetrahedron Lett.* **1967**, *8*, 2207–2209.

(44) (a) Davies, H. M. L.; Hansen, T.; Churchill, M. R. *J. Am. Chem. Soc.* **2000**, *122*, 3063–3070; (b) Ochiai, M.; Miyamoto, K.; Kaneaki, T.; Hayashi, S.; Nakanishi, W. *Science* **2011**, *332*, 448–451; (c) Tran, B. L.; Li, B.; Driess, M.; Hartwig, J. F. *J. Am. Chem. Soc.* **2014**, *136*, 2555–2563; (d) Michaudel, Q.; Thevenet, D.; Baran, P. S. *J. Am. Chem. Soc.* **2012**, *134*, 2547–2550.

(45) Protocols for C–H fluorination yielded either irreproducible results or extremely low conversion of **193**.

(46) Indicated by mass-spectrometry.

(47) Brückl, T.; Baxter, R. D.; Ishihara, Y.; Baran, P. S. *Acc. Chem. Res.* **2012**, *45*, 826–839.

(48) Pangborn, A. B.; Giardello, M. A.; Grubbs, R. H.; Rosen, R. K.; Timmers, F. J. *Organometallics* **1996**, *15*, 1518–1520.

(49) Taber, D. F.; DeMatteo, P. W.; Hassan, R. A. *Org. Synth.* **2013**, *90*, 350–357.

(50) Waser, J.; Gaspar, B.; Nambu, H.; Carreira, E. M. *J. Am. Chem. Soc.* **2006**, *128*, 11693–11712.

(51) Vita, M. V.; Waser, J. *Org. Lett.* **2013**, *15*, 3246–3249.

APPENDIX 6[†]

Synthetic Summary for Chapter 4

and Further C–H Functionalization Studies

A6.1 INTRODUCTION

This Appendix summarizes the transformations of the cyanthiwigin core (**109**) and its hydrogenated counterpart (**193**) under the various conditions for intermolecular C–H functionalization detailed in Chapter 4. Additionally, efforts toward intramolecular C–H amination are presented, along with preliminary data from enzymatic oxidation studies.

A6.2 SUMMARY OF INTERMOLECULAR C–H FUNCTIONALIZATION

Overall, our investigations into the reactivity of the cyanthiwigin core (**109**) involved the formation of three allylic oxidation products over seven different conditions for oxidation examined. A summary of product formation from our allylic oxidation studies is presented in Scheme A6.1

[†] The enzymatic oxidations described in this appendix were performed in collaboration with Dr. David Romney in the Arnold research group at Caltech.

*Scheme A6.1 Summary of the allylic C–H acetoxylation reactions of the cyanthiwigin core (**109**)*

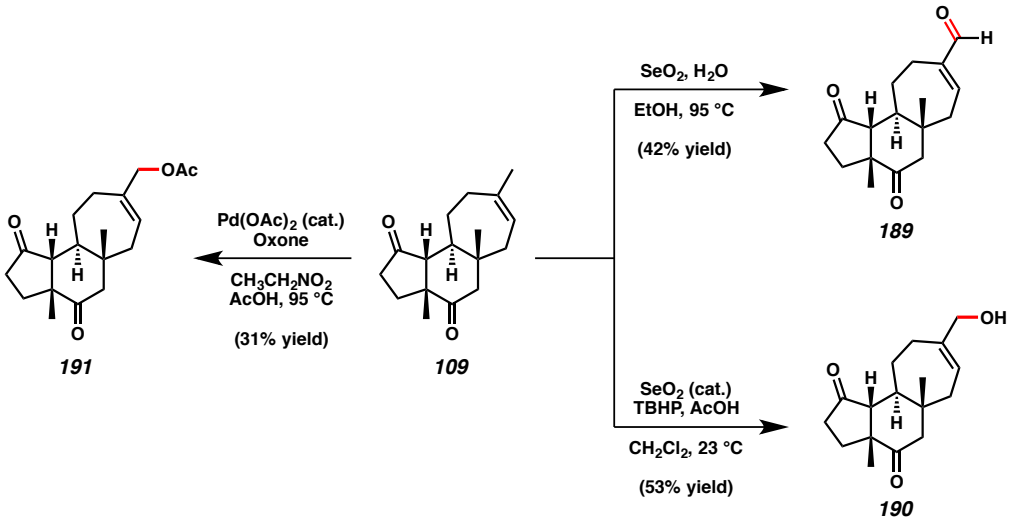

Explorations into the reactivity of the hydrogenated cyanthiwigin core (**193**) supplied six products resulting from tertiary C–H oxidation: hydroxylation (6 methods), amination (2 methods), and azidation (3 methods), which are depicted in Scheme A6.2. Efforts to apply the conditions for tertiary C–H azidation developed by Groves and co-workers proved inconclusive due to uncertainties about catalyst efficacy and purity.

*Scheme A6.2 Summary of the tertiary C–H oxidation reactions of saturated tricycle **193***

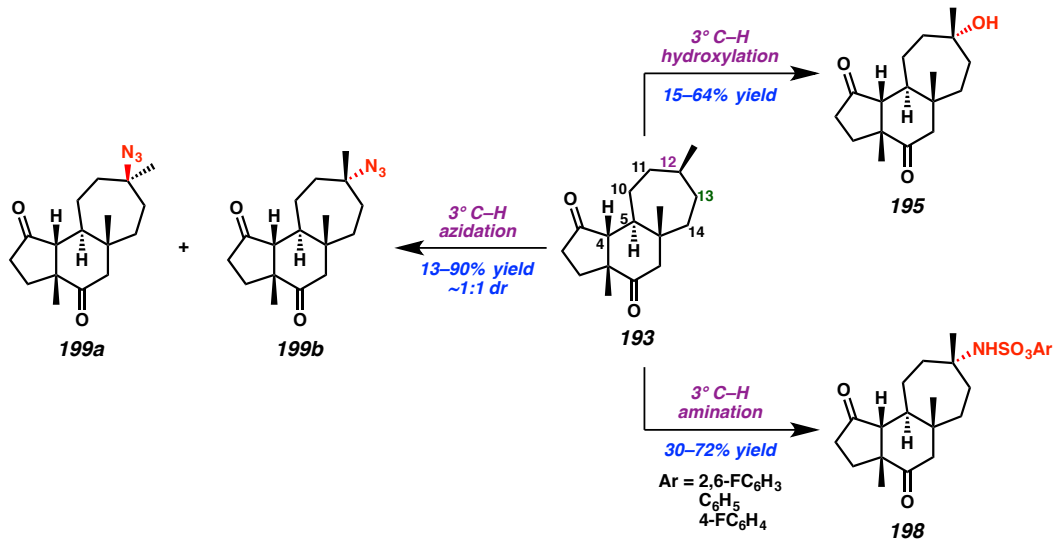

Finally, while secondary C–H oxidation was observed far less frequently than tertiary oxidation, the regioselectivity and stereoselectivity of the two methodologies examined provided unique insights into the reactivity of the hydrogenated cyanthiwigin core (**193**). The products generated from these studies are summarized in Scheme A6.3

Scheme A6.3 Summary of the secondary C–H oxidation reactions of saturated tricycle ***193***

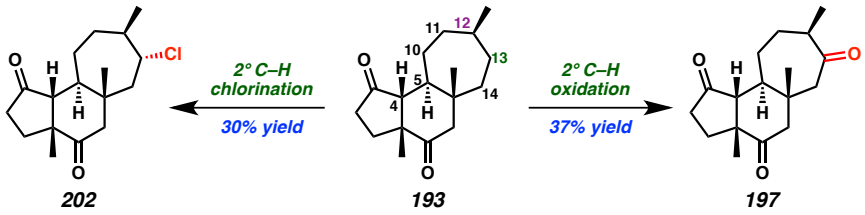

A6.3 EFFORTS TOWARD INTRAMOLECULAR C–H AMINATION

Having gained insight into the reactivity of the cyanthiwigin framework under various conditions for intermolecular C–H functionalization, we turned our attention to strategies for intramolecular C–H functionalization. In 2001, the Du Bois laboratory reported the conversion of carbamates (**205**) to oxazolidinones (**206**) via Rh-catalyzed intramolecular C–H amination (Scheme A6.4A).[1] To apply this approach to the cyanthiwigin core, we would first need to install the carbamate handle to generate a suitable substrate such as **207** for the Du Bois amination. Successful execution of the intramolecular C–H amination would subsequently furnish oxazolidinone **208** (Scheme A6.4B).

Scheme A6.4 Plan for intramolecular C–H amination

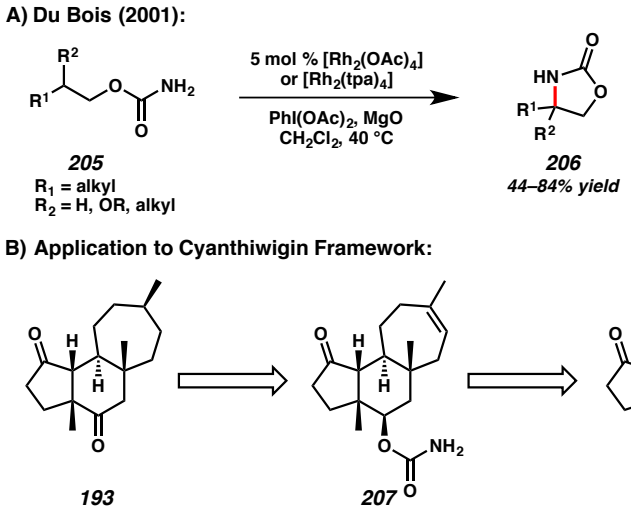

*Scheme A6.5 Unexpected reactivity of the cyanthiwigin core (**109**) with CSI*

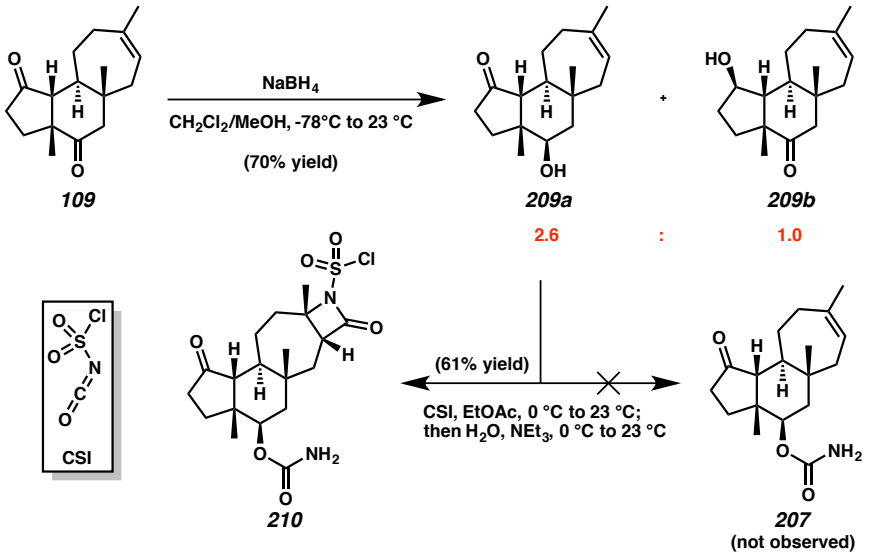

Treatment of tricycle **109** with $NaBH_4$ afforded a mixture of isomers **209a** and **209b** which were separable by column chromatography. We were surprised to find that the reaction of major product **209a** with chlorosulfonyl isocyanate (CSI) did not form the

expected carbamate (**207**). Instead, β-lactam **210** was isolated in 61% yield, indicating that CSI had undergone cycloaddition with the olefin moiety[2] in addition to installing the carbamate group at the secondary alcohol (Scheme A6.5).

Since tetracycle **210** was unreactive under Du Bois's conditions for C–H amination, we prepared a carbamate substrate that would preclude the possibility of cycloaddition with CSI. Treatment of hydrogenated tricycle **193** with $NaBH_4$ at –78 °C effected regioselective carbonyl reduction, furnishing C8 alcohol **211** as a single diastereomer in excellent yield (Scheme A6.6). Reaction of **211** with CSI afforded carbamate **212** which was unreactive under various C–H amination conditions employing different Rh catalysts, solvents, and temperatures. Efforts to effect intramolecular C–H amination using conditions reported by He and co-workers[3] were also unsuccessful, as were procedures employing elevated levels (up to 50 mol %) of Rh catalyst.

*Scheme A6.6 Efforts toward intramolecular C–H amination of carbamate **212***

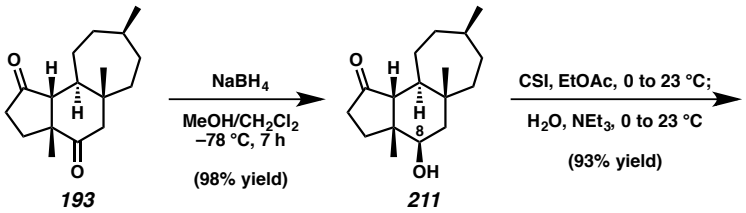

Rh cat.	Solvent	Temperature
$Rh_2(OAc)_4$	CH_2Cl_2	40 °C
$Rh_2(tfa)_4$	CH_2Cl_2	40 °C
$Rh_2(esp)_2$	CH_2Cl_2	40 °C
$Rh_2(cap)_4$	CH_2Cl_2	40 °C
$Rh_2(tpa)_4$	CH_2Cl_2	40 °C
$Rh_2(esp)_2$	DCE	85 °C
$Rh_2(tpa)_4$	DCE	85 °C

We hypothesized that the apparent lack of reactivity of carbamate **212** under intramolecular C–H amination conditions could be due to the stereochemical configuration of the molecule. Namely, the axial positioning of the C8 carbamate functionality in the six-membered B-ring of **212** could be hindering reactivity. To test this hypothesis, we designed a synthesis of a carbmate with the opposite stereochemistry at C8. After repeated efforts to effect carbonyl reduction from the β-face of **193** using L-selectride, K-selectride, and SmI_2 yielded exclusively α-face reduction, we finally discovered that treatment of tricycle **193** with a large excess (70 equiv) of sodium metal in boiling ethanol induced rapid reduction of both ketones from the β-face, generating diol **214** with the desired stereochemistry at C3 and C8. Subsequent reaction with CSI furnished bis-carbamate **215**, which, disappointingly, was also unreactive under Du Bois's conditions for Rh-catalyzed intramolecular C–H amination (Scheme A6.7).

*Scheme A6.7 Efforts toward intramolecular C–H amination of bis-carbamate **215***

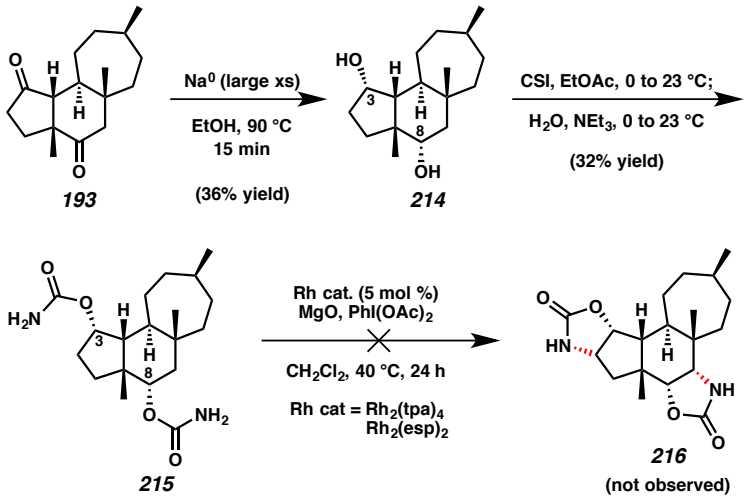

Considering the lack of reactivity of both **212** and **215**, we surmised that the difficulty may be arising from the fact that in both cases a secondary C–H bond was targeted. As such, we reasoned that bis-carbamate **218** could undergo tertiary C–H activation at C4 to generate oxazolidinone **219**. Unfortunately, after preparation of **218** via borohydride reduction of **193** and subsequent carbamate formation, we found that bis-carbamate **218** was also unreactive under conditions for Rh-catalyzed C–H amination, returning unreacted starting material as was observed in all previous cases (Scheme A6.8).

*Scheme A6.8 Efforts toward intramolecular C–H amination of bis-carbamate **218***

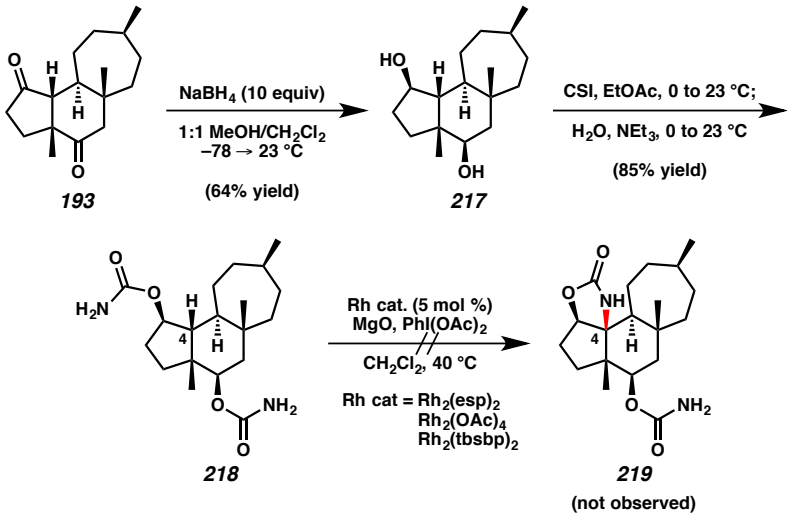

Subjection of diol **217** to Du Bois's Ru-catalyzed conditions for intermolecular tertiary C–H hydroxylation[4] resulted in re-oxidation of the secondary alcohols, furnishing alcohol **220** and diketone **193** (Scheme A6.9). The product distribution of this reaction indicates that the C8 hydroxyl is more readily oxidized than the C3 hydroxyl in diol **217**. Significantly, this transformation enables access to the C3-hydroxylated tricycle, which is

generally inaccessible from hydride reduction of diketone **193**, which tends to produce the C8-reduced alcohol product **211** (cf. Scheme A6.6).

*Scheme A6.9 Re-oxidation of diol **217** using Du Bois's Ru-catalyzed C–H hydroxylation conditions*

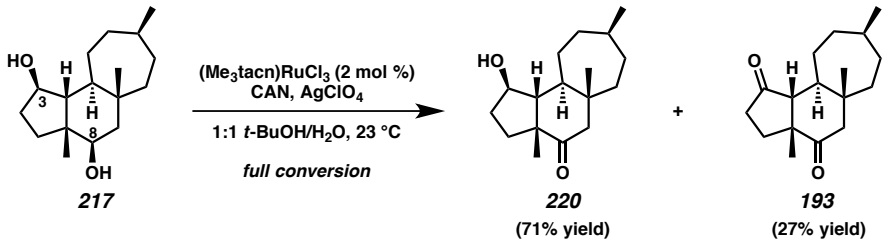

217 ***220*** (71% yield) ***193*** (27% yield)

A6.4 FUTURE DIRECTIONS

These investigations into intramolecular C–H amination of the cyanthiwigin core demonstrate that C–H functionalization of molecules with complex three-dimensional architectures remains a challenging research goal. We believe that much of the difficulties encountered in our studies toward intramolecular C–H amination can be attributed to steric factors, given the compactness of the cyanthiwigin core and the density of tertiary and quaternary stereocenters around the potential sites of reactivity. The two methyl substiuents at the A–B and B–C ring junctures contribute significantly to steric deactivation of the β-face of the cyanthwigin core, as observed in the facial selectivity exhibited by carbonyl reduction reactions.

A6.4.1 INTRAMOLECULAR C–H AMINATION

We anticipate that a potential future direction for this project could entail intramolecular C–H amination at the C5 tertiary C–H bond on the α-face of the molecule, thereby avoiding the steric influence of the β-face methyls. This reactivity could be studied using bis-sulfamate **221**, which would be accessible from diol **214** (Scheme A6.10). The Du Bois group showed previously that sulfamates could undergo intramolecular C–H amination in the presence of a Rh catalyst, oxidant, and additive, generating a six-membered ring in the product which could be hydrolyzed to generate a 1,3-functionalized amine derivative.[5] This is a critical difference from the carbamate reactivity because the formation of a six-membered cycle enables access to sites in the cyanthiwigin core previously unreachable using the carbamate handles at C3 and C8.

Scheme A6.10 Future directions toward intramolecular C–H amination

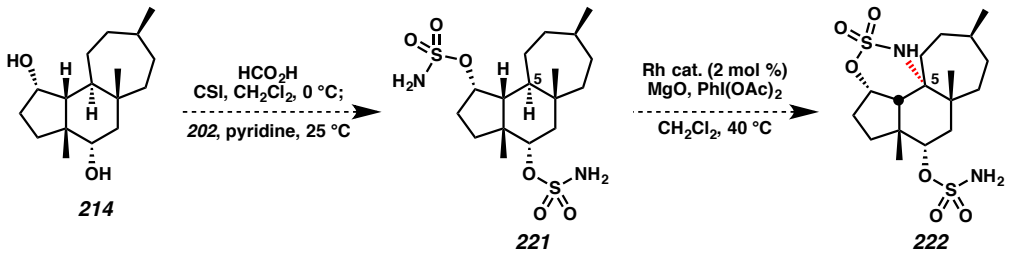

A6.4.2 ENYZMATIC C–H OXIDATION

Another frontier for C–H oxidation includes hydroxylation by enzymatic catalysts. Preliminary studies show that treatment of the cyanthiwigin core (**109**) with a mutated P450 enzyme catalyst[6] results in allylic oxidation at the C15 position, as was observed in the selenium dioxide studies, along with multiple other unidentified products (Scheme

A6.11A). Likewise, hydrogenated tricycle **193** reacts in a familiar fashion with the enzyme catalyst, furnishing the C12 alcohol **195** under the reaction conditions (Scheme A6.11B), the same product as was observed in methods employing synthetic catalysts for C–H hydroxylation (see Chapter 4). Future studies in this research area would involve exploring the reactivity of these two scaffolds with various other enzyme catalysts that have been prepared out of directed evolution studies.

*Scheme A6.11 Preliminary data toward enzymatic oxidation of tricycles **109** and **193***

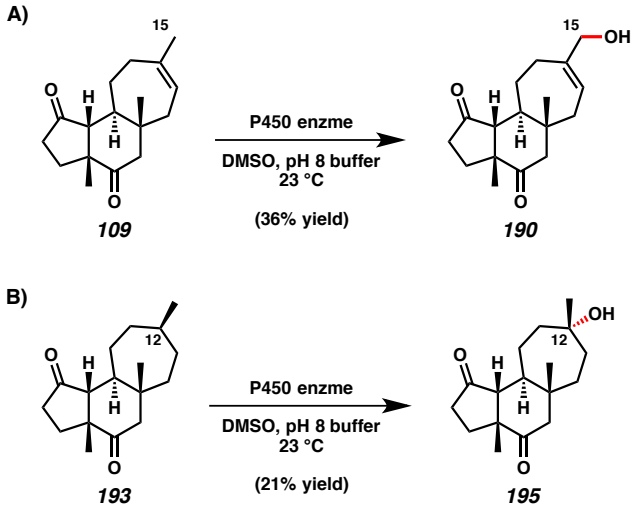

A6.5 EXPERIMENTAL SECTION

A6.5.1 MATERIALS AND METHODS

Unless noted in the specific procedure, reactions were performed in flame-dried glassware under argon atmosphere. Dried and deoxygenated solvents (Fisher Scientific) were prepared by passage through columns of activated aluminum before use.[7] Methanol (Fisher Scientific) was distilled from magnesium methoxide immediately prior to use. Triethylamine (Oakwood Chemicals) was distilled from calcium hydride immediately prior to use. Anhydrous ethanol, *tert*-butanol, and dimethylsulfoxide (DMSO) were purchased from Sigma Aldrich in sure-sealed bottles and used as received unless otherwise noted. Commercial reagents (Sigma Aldrich, Alfa Aesar, or Oakwood Chemicals) were used as received. Catalysts $(Me_3tacn)RuCl_3$ and $Rh_2(esp)_2$ were donated by the Du Bois group (Stanford) and used without further purification. The $Rh_2(tbsbp)_2$ was donated by the Davies group (Emory) and used without further purification. Brine is defined as a saturated aqueous solution of sodium chloride. Reactions requiring external heat were modulated to the specified temperatures using an IKAmag temperature controller. Reaction progress was monitored by thin-layer chromatography (TLC) or Agilent 1290 UHPLC-LCMS. TLC was performed using E. Merck silica gel 60 F254 precoated plates (0.25 mm) and visualized by UV fluorescence quenching, potassium permanganate, or *p*-anisaldehyde staining. Silia*Flash* P60 Academic Silica gel (particle size 0.040–0.063 mm) was used for flash chromatography. NMR spectra were recorded on a Varian Mercury 300 spectrometer (at 300 MHz for ^{1}H NMR and 75 MHz for ^{13}C NMR), a Varian Inova 500 spectrometer (at 500 MHz for ^{1}H NMR and 126 MHz for ^{13}C NMR), or a Bruker AV III HD spectrometer equipped with a Prodigy liquid nitrogen

temperature cryoprobe (at 400 MHz for ^{1}H NMR and 101 MHz for ^{13}C NMR), and are reported in terms of chemical shift relative to residual $CHCl_3$ (δ 7.26 and δ 77.16 ppm, respectively). Data for ^{1}H NMR spectra are reported as follows: chemical shift (δ ppm) (multiplicity, coupling constant (Hz), integration). Abbreviations are used as follows: s = singlet, bs = broad singlet, d = doublet, t = triplet, q = quartet, m = complex multiplet. Infrared (IR) spectra were recorded on a Perkin Elmer Paragon 1000 spectrometer using thin film samples on KBr plates, and are reported in frequency of absorption (cm^{-1}). High-resolution mass spectra (HRMS) were obtained from the Caltech Mass Spectral Facility using a JEOL JMS-600H High Resolution Mass Spectrometer with fast atom bombardment (FAB+) ionization mode or were acquired using an Agilent 6200 Series TOF with an Agilent G1978A Multimode source in electrospray ionization (ESI+) mode. Optical rotations were measured with a Jasco P-1010 polarimeter at 589 nm using a 100 mm path-length cell.

A6.5.2 PREPARATIVE PROCEDURES

A6.5.2.1 GENERAL PROCEDURES

General Procedure A. *Sodium borohydride reduction*. To a solution of tricyclic diketone **109** or saturated tricyclic diketone **193** (1.0 equiv) in 1:1 CH_2Cl_2/MeOH (0.02 M) was added a solution of sodium borohydride (5.0 equiv for mono-reduction, 10 equiv for bis-reduction) in 1:1 CH_2Cl_2/MeOH (0.02 M) at –78 °C. The reaction mixture was allowed to warm to 23 °C over the course of six hours. When TLC analysis indicated full consumption of starting material, the reaction was quenched with acetone and 2N NaOH.

The phases were separated, and the organic layer was immediately washed with brine and dried over sodium sulfate. After filtration and concentration under reduced pressure, the crude residue was purified by silica gel column chromatography (ethyl acetate/hexanes).

General Procedre B. *Reaction with CSI*. To a solution of alcohol **209a** or **211** or diol **214** or **217** (1.0 equiv) in ethyl acetate (0.31 M) at 0 °C was added dropwise chlorosulfonyl isocyanate (1.33 equiv for **209a** or **211**, 2.66 equiv for **214** or **217**). The resulting mixture was stirred at 0 °C for 10 minutes, after which time the ice/water bath was removed, and the reaction allowed to warm to 23 °C. After 10 hours, the reaction mixture was cooled to 0 °C once more, and water (3 mL) was added dropwise, followed by dropwise addition of triethylamine (2.03 equiv for **209a** or **211**, 4.06 equiv for **214** or **217**). The resulting mixture was stirred at 23 °C for 24 hours, after which time the phases were separated, and the aqueous phase was extracted with ethyl acetate (2x). The combined organic layers were washed with brine and dried over Na_2SO_4, filtered, and concentrated. The crude residue was purified by silica gel column chromatography, (ethyl acetate/hexanes).

General Procedure C. *Rh-catalyzed intramolecular C–H amination*. A flame-dried 1-dram vial under argon was charged with carbamate **212** or bis-carbamates **215** or **218** (1.0 equiv), magnesium oxide (2.3 equiv), (diacetoxyiodo)benzene (1.4 equiv), and Rh catalyst (0.05 equiv), and the resulting mixture was diluted with dichloromethane (0.02 M in substrate). The vial was sealed with a Teflon-lined cap and heated to 40 °C. After 24 hours, heating was discontinued, and the reaction mixture was diluted with

dichloromethane (2 mL) and filtered through a pad of Celite, rinsing the filter cake with dichloromethane (2x). The filtrate was concnetrated in vacuo, and the crude residue was purified by silica gel column chromatography (ethyl acetate/hexanes).

A6.5.2.2 SUBSTRATE PREPARATION FOR INTRAMOLECULAR C–H AMINATION STUDIES

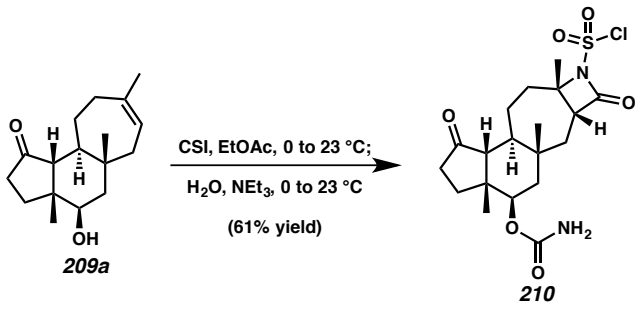

***β*-Lactam 210.** Prepared using General Procedure B (3.0 mg, 61% yield). Column eluent: 20% to 30% to 40% to 75% ethyl acetate in hexanes. Partial characterization data is as follows: R*f* = 0.20 (75% ethyl acetate in hexanes); ^{1}H NMR ($CDCl_3$, 400 MHz) δ 4.82 (dd, *J* = 3.9, 2.3 Hz, 1H), 4.56 (br s, 2H), 3.20 (dd, *J* = 10.9, 7.7 Hz, 1H), 2.44–2.32 (m, 3H), 2.07–2.00 (m, 2H), 1.96 (m, 1H), 1.84 (d, *J* = 4.1 Hz, 1H), 1.82 (s, 3H), 1.79 (d, *J* = 3.3 Hz, 2H), 1.74–1.67 (m, 3H), 1.23–1.17 (m, 2H), 0.97 (s, 3H), 0.90 (s, 3H); ^{13}C NMR ($CDCl_3$, 101 MHz) δ 219.0, 164.6, 155.9, 74.1, 72.6, 57.8, 57.3, 46.4, 41.9, 41.3, 39.4, 35.5, 35.1, 33.3, 30.3, 23.8, 23.3, 22.6, 17.3; HRMS (EI+) *m/z* calc'd for $C_{19}H_{28}N_2O_6SCl$ $[M+H]^+$: 447.1357, found 447.1353; $[a]^{25}_D$ –13.3 (*c* 0.20, $CHCl_3$).

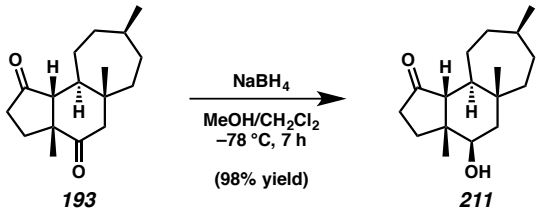

Tricyclic Alcohol 211. Prepared using General Procedure A (10.9 mg, 98% yield). Column eluent: 10% to 20% ethyl acetate in hexanes. Full characterization data is as follows: R*f* = 0.24 (25% ethyl acetate in hexanes); ^{1}H NMR ($CDCl_3$, 500 MHz) δ 3.69 (t, *J* = 3.4 Hz, 1H), 2.37 (dddd, *J* = 19.6, 10.8, 2.3, 0.8 Hz, 1H), 2.32–2.22 (m, 1H), 2.02–1.94 (m, 1H), 1.75–1.67 (m, 3H), 1.62 (dd, *J* = 14.8, 3.2 Hz, 1H), 1.58 (m, 2H), 1.57–1.49 (m, 3H), 1.42–1.35 (m, 3H), 1.27–1.19 (m, 3H), 1.01 (s, 6H), 0.88 (d, *J* = 6.6 Hz, 3H); ^{13}C NMR ($CDCl_3$, 126 MHz) δ 220.3, 72.6, 57.7, 45.9, 45.4, 43.4, 41.1, 35.2, 34.9, 33.7, 32.8, 30.9, 30.4, 24.5, 23.5, 23.2, 20.4; IR (Neat Film, KBr) 3462, 2950, 2925, 2867, 1715, 1468, 1385, 1180, 734 cm^{-1}; HRMS (FAB+) *m/z* calc'd for $C_{17}H_{29}O_2$ $[M+H]^+$: 265.2168, found 265.2178; $[a]^{25}_D$ –11.3 (*c* 0.35, $CHCl_3$).

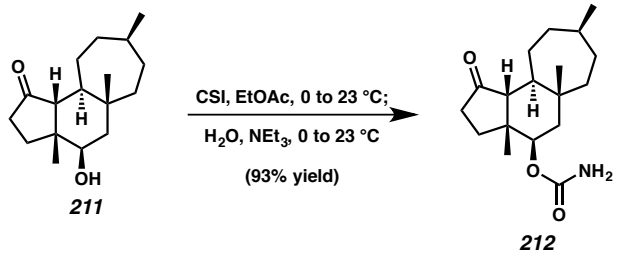

Carbamate 212. Prepared using General Procedure B (2.7 mg, 93% yield). Column eluent: 30% to 50% to 70% ethyl acetate in hexanes. Partial characterization data is as follows: R*f* = 0.34 (50% ethyl acetate in hexanes); ^{1}H NMR ($CDCl_3$, 500 MHz) δ 4.75 (t, *J* = 3.2 Hz, 1H), 4.54 (br s, 2H), 2.44–2.35 (m, 1H), 2.33–2.23 (m, 1H), 2.10–2.00 (m,

1H), 1.76–1.73 (m, 1H), 1.71 (m, 2H), 1.66–1.61 (m, 2H), 1.54–1.48 (m, 2H), 1.43–1.39 (m, 1H), 1.39–1.35 (m, 2H), 1.34 (m, 1H), 1.25–1.17 (m, 3H), 0.94 (s, 3H), 0.93 (s, 3H), 0.88 (d, J = 6.7 Hz, 3H); ^{13}C NMR ($CDCl_3$, 101 MHz) δ 215.4, 156.3, 74.8, 57.8, 45.5, 42.1, 40.8, 34.8, 34.7, 33.3, 32.7, 30.6, 29.9, 29.7, 24.3, 23.3, 23.0, 19.7; HRMS (EI+) *m/z* calc'd for $C_{18}H_{30}NO_3$ $[M+H]^+$: 308.2226, found 308.2210; $[a]^{25}_D$ –14.5 (*c* 0.27, $CHCl_3$).

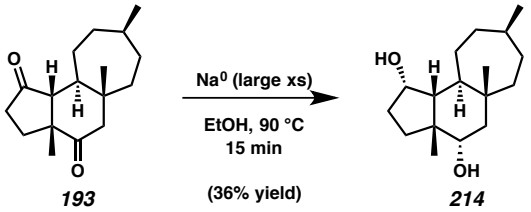

Tricyclic Diol 214. A flame-dried two-necked round-bottom flasked fitted with a reflux condenser and magnetic stir bar was charged with a solution of tricyclic diketone **193** (15 mg, 0.0572, 1.0 equiv) in absolute ethanol (6 mL) and heated to reflux. Once the solution had reached reflux (90 °C), small chunks (~10 mg) of freshly cut sodium metal (90 mg total, 3.94 mmol, 69.0 equiv) were added carefully through the open second neck of the flask. Pieces were added one at a time, waiting for each chunk to dissolve fully before addition of the next. After the last piece of sodium metal had dissolved, the reaction was removed from heat, quenched with ice water (10 mL), and extracted with Et_2O (2 x 10 mL). The combined organic layers were washed with brine and dried over $MgSO_4$, filtered, and concentrated. The crude residue was purified by silica gel column chromatography (10% to 20% ethyl acetate in hexanes) to afford diol **214** as a white amorphous solid (5.5 mg, 36% yield). Characterization was hampered by persisting impurities.

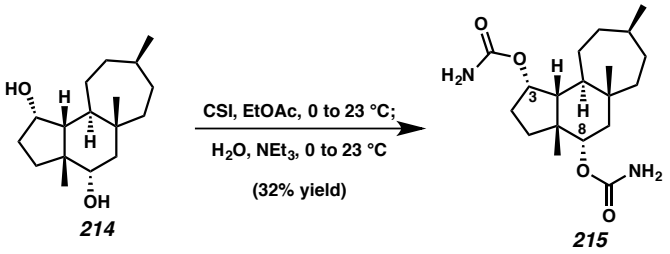

Bis-carbamate 215. Prepared using General Procedure B (2.1 mg, 32% yield). Column eluent: 40% ethyl acetate in hexanes. Characterization was hampered by persisting impurities.

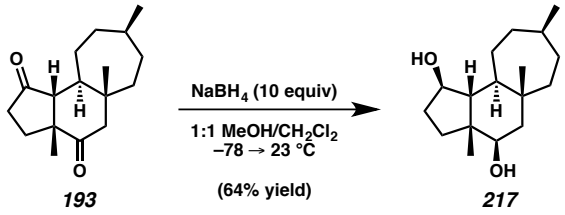

Tricyclic Diol 217. Prepared using General Procedure A (11.8 mg, 64% yield). Column eluent: 25% ethyl acetate in hexanes. Full characterization data is as follows: R*f* = 0.43 (50% ethyl acetate in hexanes); ^{1}H NMR ($CDCl_3$, 500 MHz) δ 3.97 (td, *J* = 6.3, 3.0 Hz, 1H), 3.64 (dd, *J* = 10.0, 4.1 Hz, 1H), 2.06–1.96 (m, 1H), 1.70–1.64 (m, 3H), 1.64–1.60 (m, 2H), 1.59–1.55 (m, 2H), 1.50 (d, *J* = 10.0 Hz, 1H), 1.48–1.43 (m, 2H), 1.43–1.38 (m, 3H), 1.34–1.29 (m, 1H), 1.29–1.25 (m, 2H), 1.24–1.20 (m, 1H), 1.18–1.13 (m, 1H), 1.11 (s, 3H), 0.95 (s, 3H), 0.88 (d, *J* = 6.7 Hz, 3H); ^{13}C NMR ($CDCl_3$, 126 MHz) δ 80.8, 73.2, 58.7, 46.9, 46.2, 45.5, 42.8, 37.0, 36.7, 35.7, 33.6, 33.4, 32.5, 25.6, 24.9, 22.3, 22.2; IR (Neat Film, KBr) 3338 (br), 2909, 1458, 1376, 1026, 758 cm^{-1}; HRMS

(FAB+) *m/z* calc'd for $C_{17}H_{31}O_2$ $[M+H]^+$: 267.2324, found 267.2336; $[a]^{25}_D$ 7.57 (*c* 1.2, $CHCl_3$).

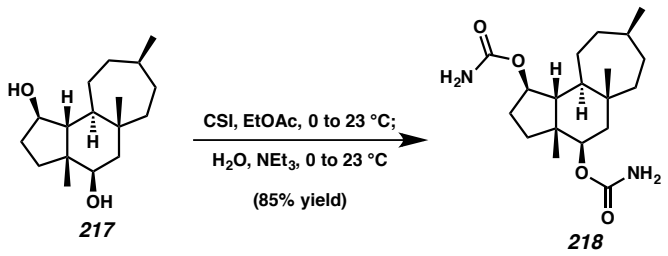

Bis-carbamate 218. Prepared using General Procedure B (11.8 mg, 85% yield). Column eluent: 50% ethyl acetate in hexanes. Partial characterization data is as follows: R*f* = 0.17 (50% ethyl acetate in hexanes); ^{1}H NMR ($CDCl_3$, 400 MHz) δ 4.91–4.85 (m, 1H), 4.72 (dd, *J* = 5.6, 3.7 Hz, 1H), 4.66 (br s, 4H), 2.27–2.18 (m, 1H), 1.75 (m, 1H), 1.72–1.67 (m, 2H), 1.60 (dd, *J* = 14.6, 5.5 Hz, 3H), 1.53–1.48 (m, 3H), 1.47–1.41 (m, 2H), 1.33 (td, *J* = 7.5, 4.2 Hz, 2H), 1.28–1.23 (m, 2H), 1.07 (s, 3H), 0.99 (ddd, *J* = 12.5, 9.1, 1.7 Hz, 1H), 0.92 (s, 3H), 0.87 (d, *J* = 6.6 Hz, 3H); ^{13}C NMR ($CDCl_3$, 101 MHz) δ 157.0, 156.6, 83.2, 75.8, 54.3, 46.5, 44.4, 42.6, 42.2, 36.0, 35.8, 35.6, 32.9, 31.8, 30.1, 25.3, 24.6, 23.6, 21.0.

A6.5.2.3 RE-OXIDATION OF DIOL 217 UNDER Ru CATALYSIS

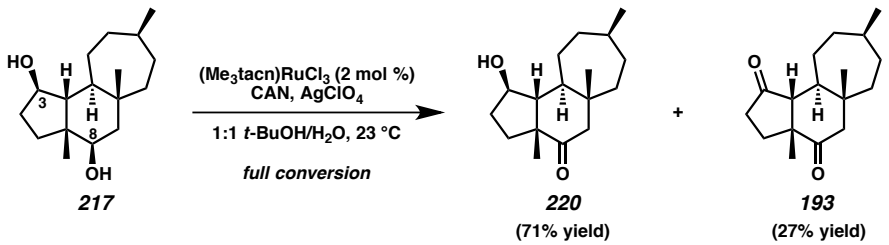

Tricyclic Alcohol 220. A 1-dram vial was charged with (1,4,7-trimethyl-1,4,7-triazacyclononane)ruthenium(III) trichloride (0.2 mg, 0.63 μmol, 0.020 equiv), silver perchlorate (0.3 mg, 1.5 μmol, 0.080 equiv), and water (0.5 mL). The vial was sealed with a Teflon-lined cap and heated to 80 °C with vigorous stirring for 5 minutes. The reaction mixture was then allowed to cool to 23 °C, and a solution of diol **217** (5.0 mg, 18.8 μmmol, 1.0 equiv) in *tert*-butanol (0.50 mL) was added, followed by ceric(IV) ammonium nitrate (30.9 mg, 56.4 μmol, 3.0 equiv). The resulting mixture suspension was stirred at 23 °C for 25 minutes, at which time a second portion of ceric(IV) ammonium nitrate (30.9 mg, 56.4 μmol, 3.0 equiv) was added. After 24 hours, the reaction was quenched with methanol (2 mL), diluted with water (5 mL), and extracted with ethyl acetate (3 x 5 mL). The combined organic extracts were dried over magnesium sulfate, filtered, and concentrated. The crude residue was purified by silica gel column chromatography (10% to 20% to 50% ethyl acetate in hexanes), furnishing tricyclic alcohol **220** (3.6 mg, 71% yield) and tricyclic diketone (1.7 mg, 27% yield). Full characterization data for **220** is as follows: R*f* = 0.59 (50% ethyl acetate in hexanes); ^{1}H NMR ($CDCl_3$, 400 MHz) δ 4.20 (ddd, *J* = 7.0, 4.8, 1.5 Hz, 1H), 2.35 (d, *J* = 14.6 Hz, 1H), 2.32–2.25 (m, 1H), 1.99 (d, *J* = 14.7 Hz, 1H), 1.92–1.84 (m, 1H), 1.85–1.77 (m, 2H), 1.71–1.65 (m, 1H), 1.65–1.59 (m, 2H), 1.52–1.40 (m, 5H), 1.35–1.30 (m, 2H), 1.29 (s, 3H), 1.26–1.21 (m, 1H), 0.91 (d, *J* = 6.8 Hz, 3H), 0.77 (s, 3H); ^{13}C NMR ($CDCl_3$, 126 MHz) δ 215.7, 80.7, 62.9, 53.7, 53.3, 48.9, 42.6, 40.0, 37.3, 35.3, 34.4, 32.0, 29.5, 24.5, 23.6 (x2), 19.1; IR (Neat Film, KBr) 3419 (br), 2918, 2869, 1697, 1456, 1384, 1269, 1021, 974 cm^{-1}; HRMS (EI+) *m/z* calc'd for $C_{17}H_{29}O_2$ $[M+H]^+$: 265.2168, found 265.2171; $[a]^{25}_D$ –58.6 (*c* 0.36, $CHCl_3$).

A6.5.2.4 ENZYMATIC C–H OXIDATION PROCEDURES

Protein Expression:

E. coli DH5α cells that harbored a pCWori plasmid encoding variant 8C7 under the control of the Plac promoter were stored as a glycerol stock. These cells were streaked onto a plate of LB_{amp}/agar, which was incubated at 37 °C. After 12 h, the plate was stored at 4 °C until further use.

A 5-mL culture of LB_{amp} was inoculated with a single colony from the aforementioned agar plate, then shaken at 37 °C (220 RPM). After 12 hours, the culture was poured into a 1-L Erlenmeyer flask that contained 500 mL of TB_{amp} with 500 μL of trace metals mix. This new culture was shaken at 37 °C (220 RPM). After 3 hours, the culture was chilled in ice. After 20 minutes, 250 μL of IPTG and 500 μL of ALA were added to the culture, which was shaken at 220 RPM at 25 °C. After 17 hours, the culture was transferred into plastic bottles, then subjected to centrifugation at 5000×*g* at 4 °C for 10 minutes. The supernatant was discarded, and the combined cell pellet was stored at –30 °C.

Lysis:

After thawing, the cell pellet (2.6 g) was suspended in a lysis cocktail consisting of hen egg-white lysozyme (10.2 mg), bovine pancreas DNase (1 mg), BugBuster (1 mL) and potassium phosphate buffer (10 mL, pH 8, 100 mM phosphate). The cell pellet was suspended through vortexing, then the suspension was shaken at 37 °C (220 RPM). After 15 min, the culture was cooled on ice, and then subjected to centrifugation at 5000×*g* at 4 °C for 10 min. The supernatant was used directly in the biocatalytic transformation.

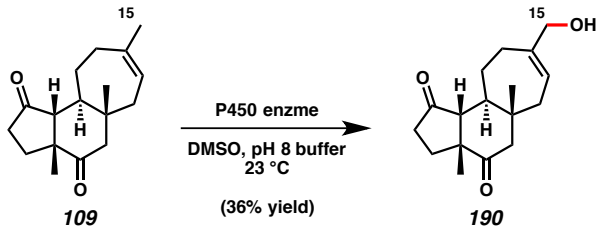

Enzymatic Oxidation of Tricycle 109. A 20-mL vial was charged with a solution of tricyclic diketone **109** (5.0 mg, 0.0192 mmol, 1.0 equiv) in DMSO (111 μL), followed by β-NADP disodium salt (1.8 mg, 0.1 equiv) and potassium phosphate buffer (3.4 mL, pH 8, 100 mM). The cell lysate (891 μL) was added, followed by *E. coli* alcohol dehydrogenase (17.8 μL). After addition of isopropanol (34.1 μL), the reaction vessel was wrapped in aluminum foil and shaken at 23 °C (230 RPM). After 14 hours, the product was extracted from the reaction mixture with ethyl acetate (3x). (If an emulsion formed, then the mixture was subjected to centrifugation at 4000×*g* for 2 minutes to separate the layers.) The combined organic portions were dried over Na_2SO_4, filtered, and concentrated in vacuo. The crude residue was purified by silica gel column chromatography (10% to 25% to 40% to 50% ethyl acetate in hexanes), affording unreacted starting material (2.1 mg, 42% recovery), a mixture of unidentified oxidation products (1.0 mg), and allylic alcohol **190** (1.9 mg, 36% yield), which matched previously reported characterization data (see Chapter 4).

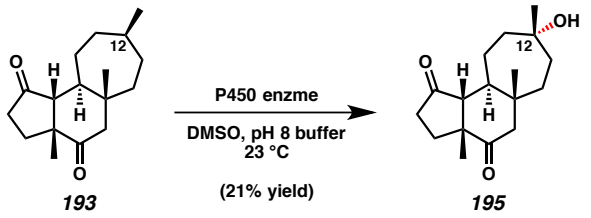

Enzymatic Oxidation of Hydrogenated Tricycle 193. A 20-mL vial was charged with a solution of tricyclic diketone **193** (4.5 mg, 0.0171 mmol, 1.0 equiv) in DMSO (111 μL), followed by β-NADP disodium salt (1.8 mg, 0.1 equiv) and potassium phosphate buffer (3.4 mL, pH 8, 100 mM). The cell lysate (891 μL) was added, followed by *E. coli* alcohol dehydrogenase (17.8 μL). After addition of isopropanol (34.1 μL), the reaction vessel was wrapped in aluminum foil and shaken at 23 °C (230 RPM). After 14 hours, the product was extracted from the reaction mixture with ethyl acetate (3x). (If an emulsion formed, then the mixture was subjected to centrifugation at 4000×*g* for 2 minutes to separate the layers.) The combined organic portions were dried over Na_2SO_4, filtered, and concentrated in vacuo. The crude residue was purified by silica gel column chromatography (10% to 25% to 35% to 50% ethyl acetate in hexanes), affording unreacted starting material (2.5 mg, 56% recovery), a mixture of unidentified oxidation products (0.7 mg), and tertiary alcohol **195** (1.0 mg, 21% yield), which matched previously reported characterization data (see Chapter 4).

A6.6 NOTES AND REFERENCES

(1) Espino, C. G.; Du Bois, J. *Angew. Chem., Int. Ed.* **2001**, *40*, 598–600.

(2) A literature search on the reactivity of CSI shows that examples of cycloaddition with alkenes are known. For a review on CSI, see: Dhar, D. N.; Murthy, K. S. K. *Synthesis* **1986**, *1986*, 437–449.

(3) Cui, Y.; He, C. *Angew. Chem., Int. Ed.* **2004**, *43*, 4210–4212.

(4) McNeill, E.; Du Bois, J. *Chem. Sci.* **2012**, *3*, 1810–1813.

(5) Espino, C. G.; Wehn, P. M.; Chow, J.; Du Bois, J. *J. Am. Chem. Soc.* **2001**, *123*, 6935–6936.

(6) Lewis, J. C.; Mantovani, S. M.; Fu, Y.; Snow, C. D.; Komor, R. S.; Wong, C.-H.; Arnold, F. H. *Chembiochem* **2010**, *11*, 2502–2505.

(7) Pangborn, A. B.; Giardello, M. A.; Grubbs, R. H.; Rosen, R. K.; Timmers, F. J. *Organometallics* **1996**, *15*, 1518–1520.

APPENDIX 7

Spectra Relevant to Chapter 4:

The Cyanthiwigin Natural Product Core as a Complex Molecular Scaffold for Comparative Late-Stage C–H Functionalization Studies

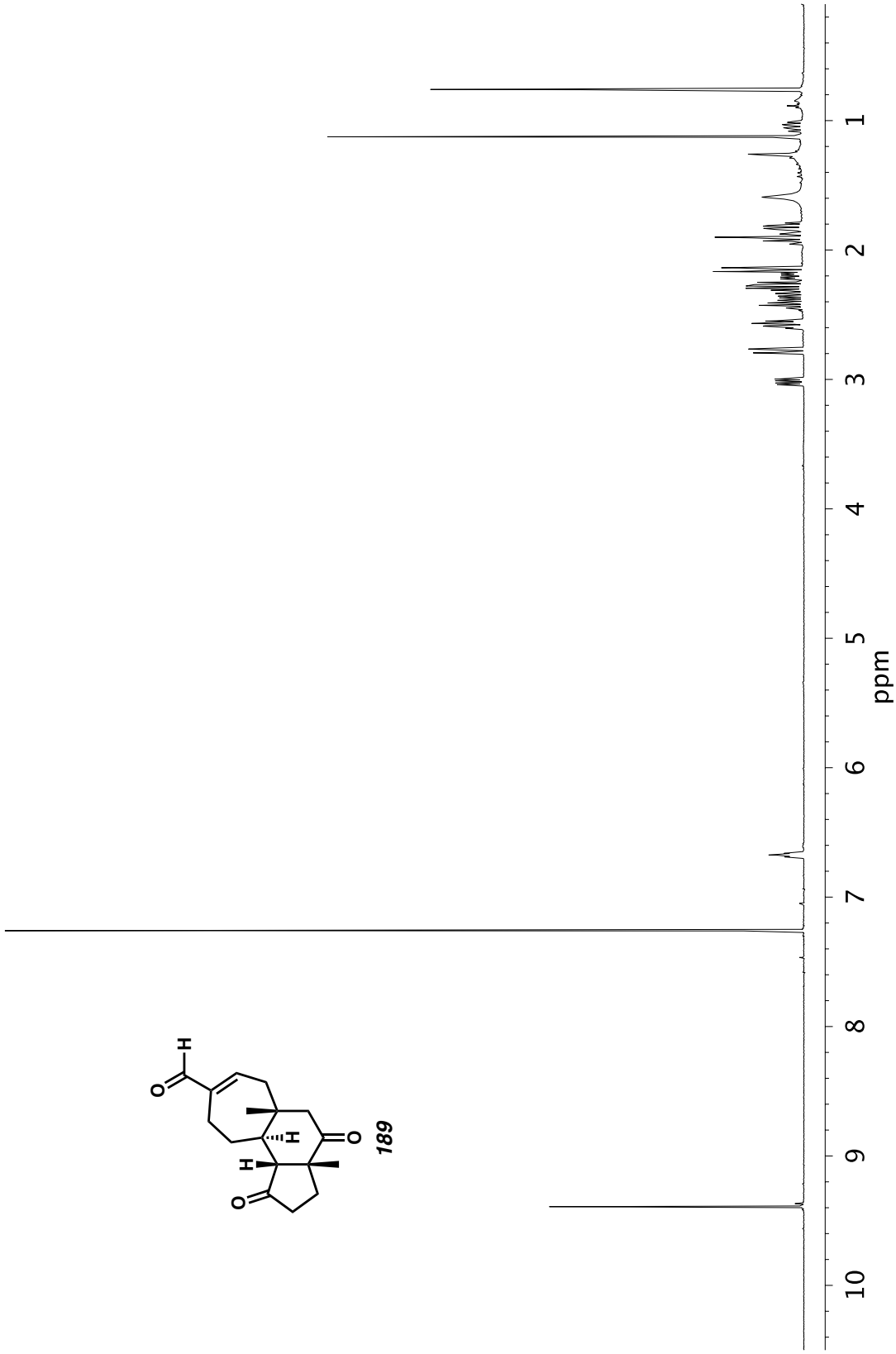

Figure A7.1. ^{1}H NMR (500 MHz, $CDCl_3$) of compound **189**.

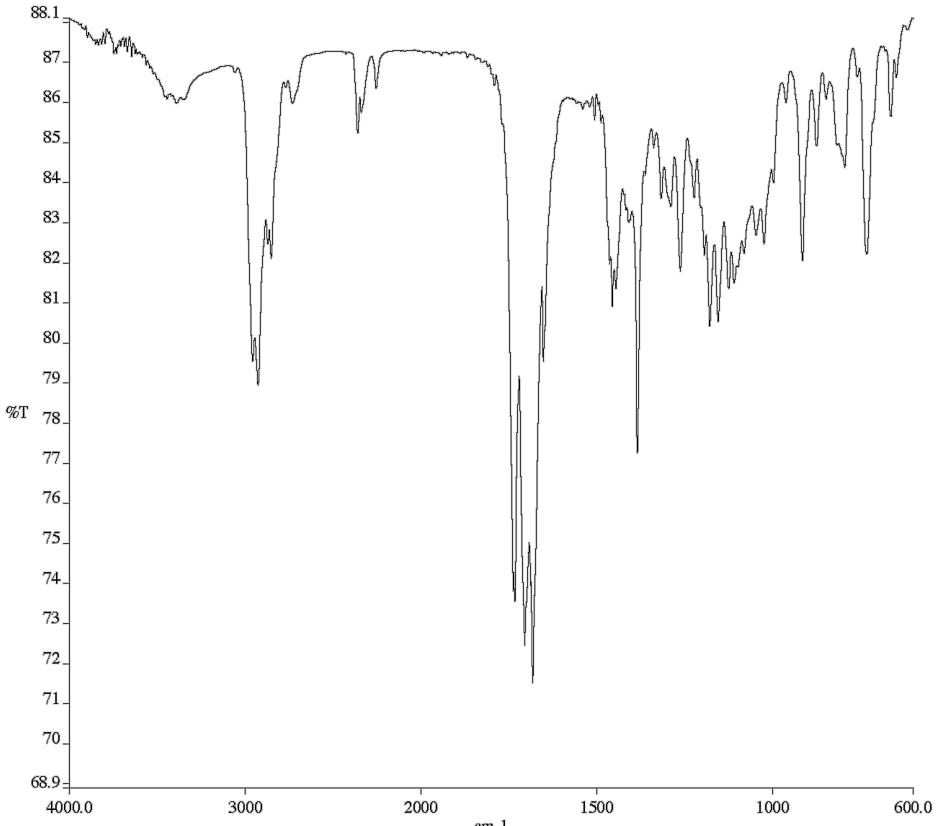

Figure A7.2. Infrared spectrum (Thin Film, KBr) of compound **189**.

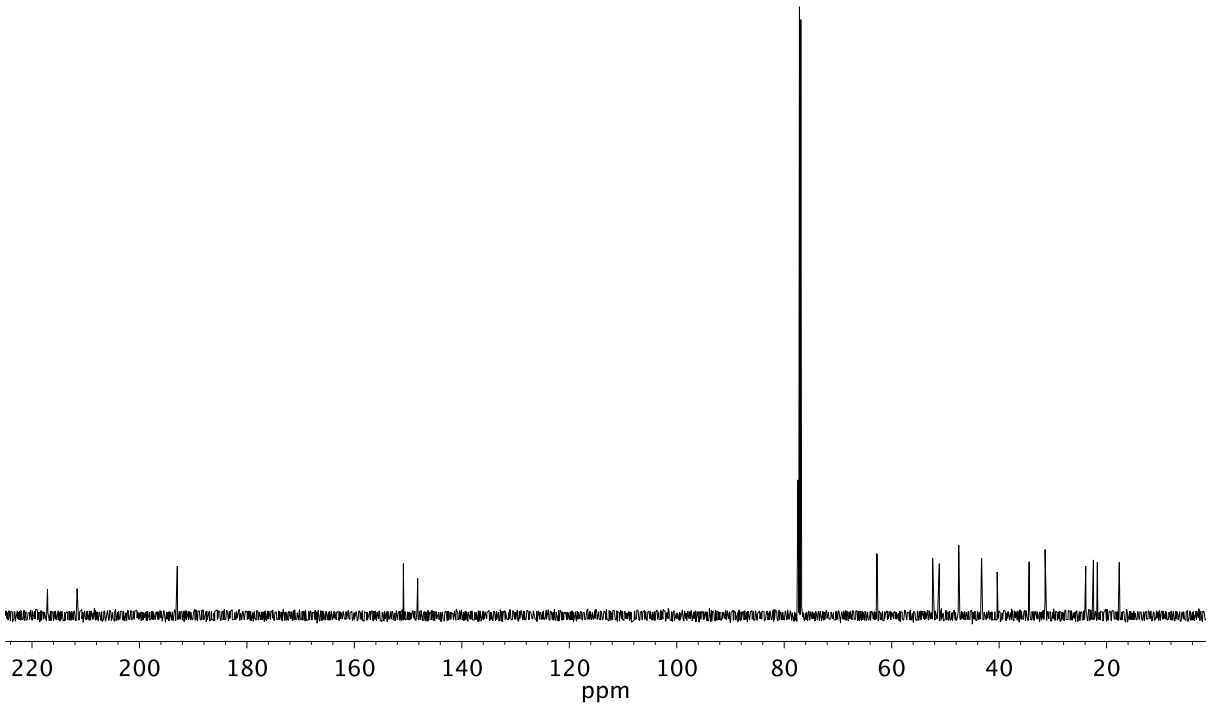

Figure A7.3. ^{13}C NMR (126 MHz, $CDCl_3$) of compound **189**.

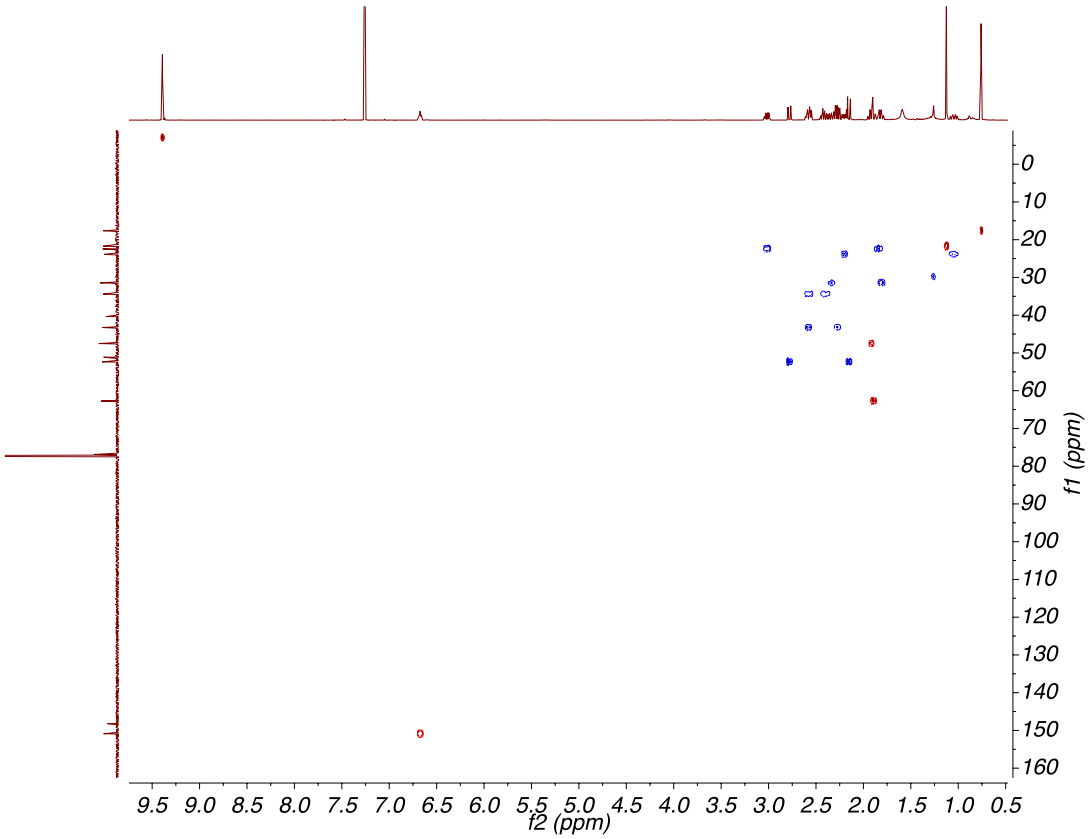

Figure A7.4. HSQC (500, 126 MHz, $CDCl_3$) of compound **189**.

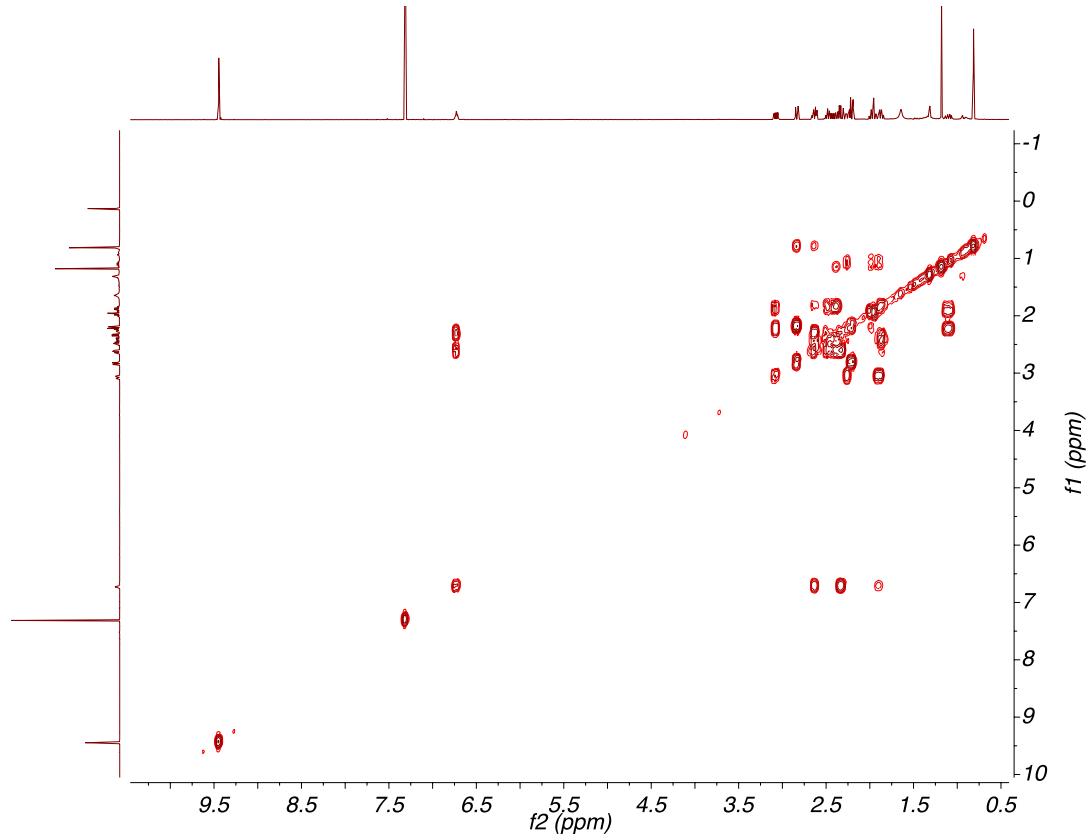

Figure A7.5. COSY (500 MHz, $CDCl_3$) of compound **189**.

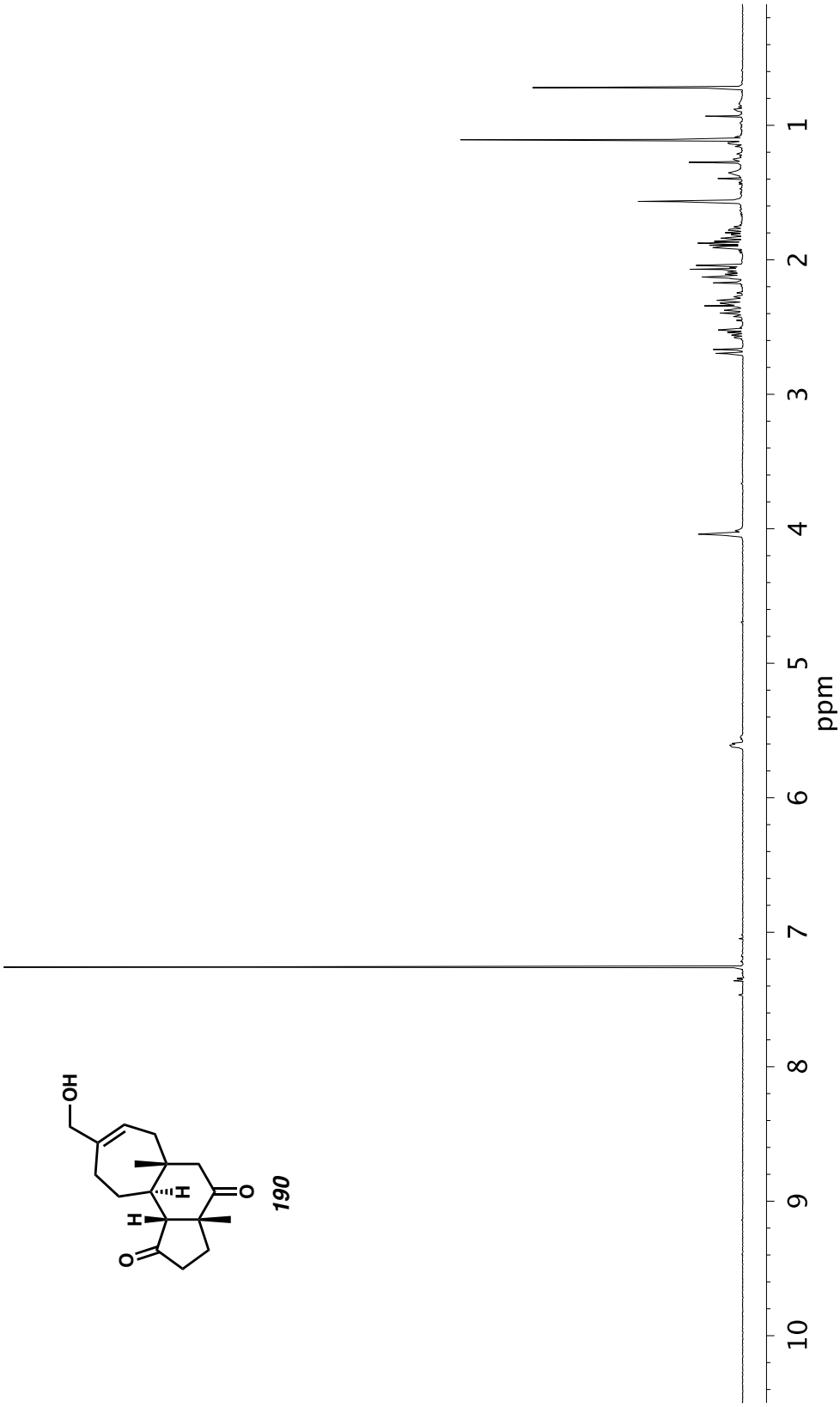

Figure A7.6. ^{1}H NMR (500 MHz, $CDCl_3$) of compound **190**.

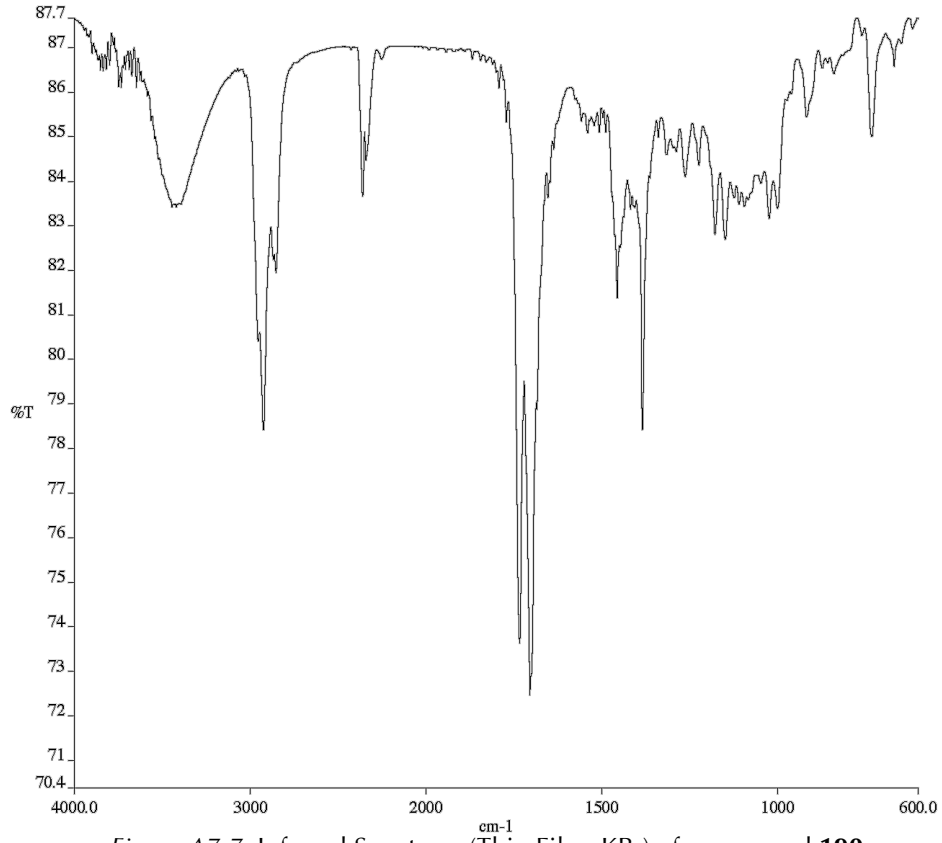

Figure A7.7. Infrared Spectrum (Thin Film, KBr) of compound **190**.

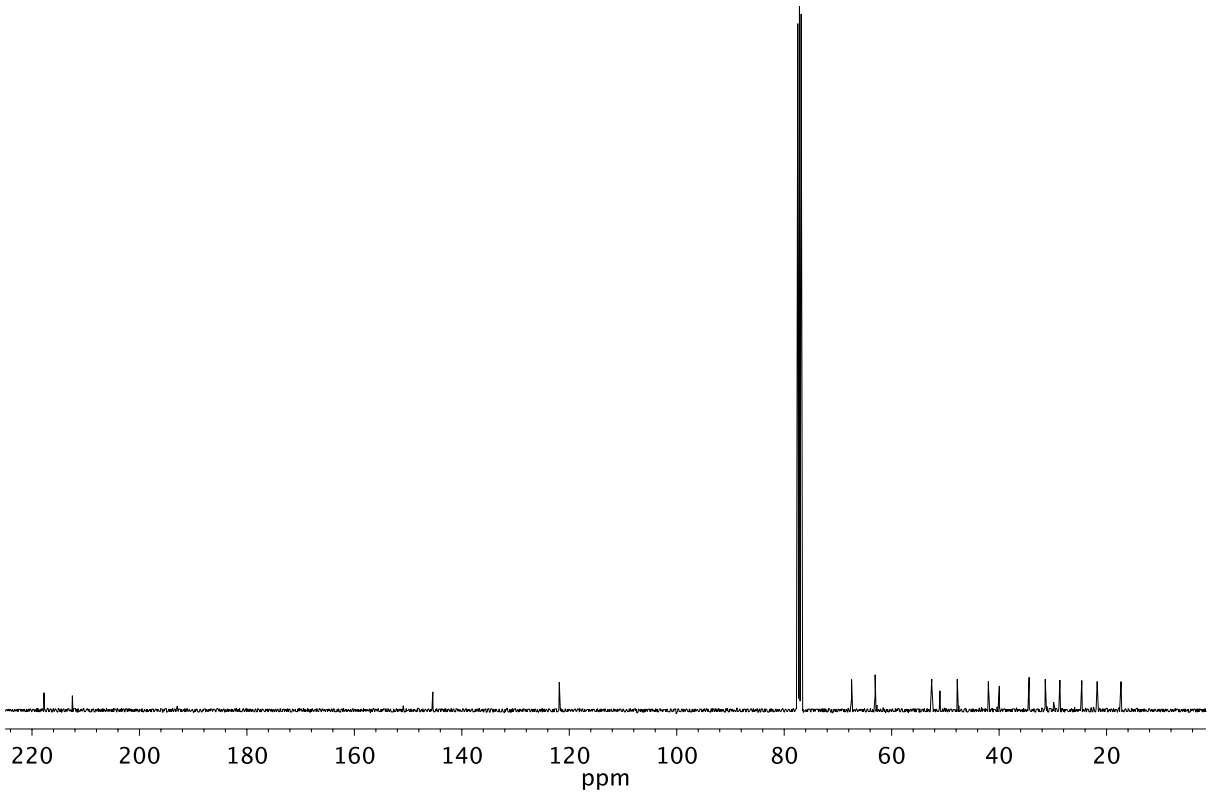

Figure A7.8. ^{13}C NMR (101 MHz, $CDCl_3$) of compound **190**.

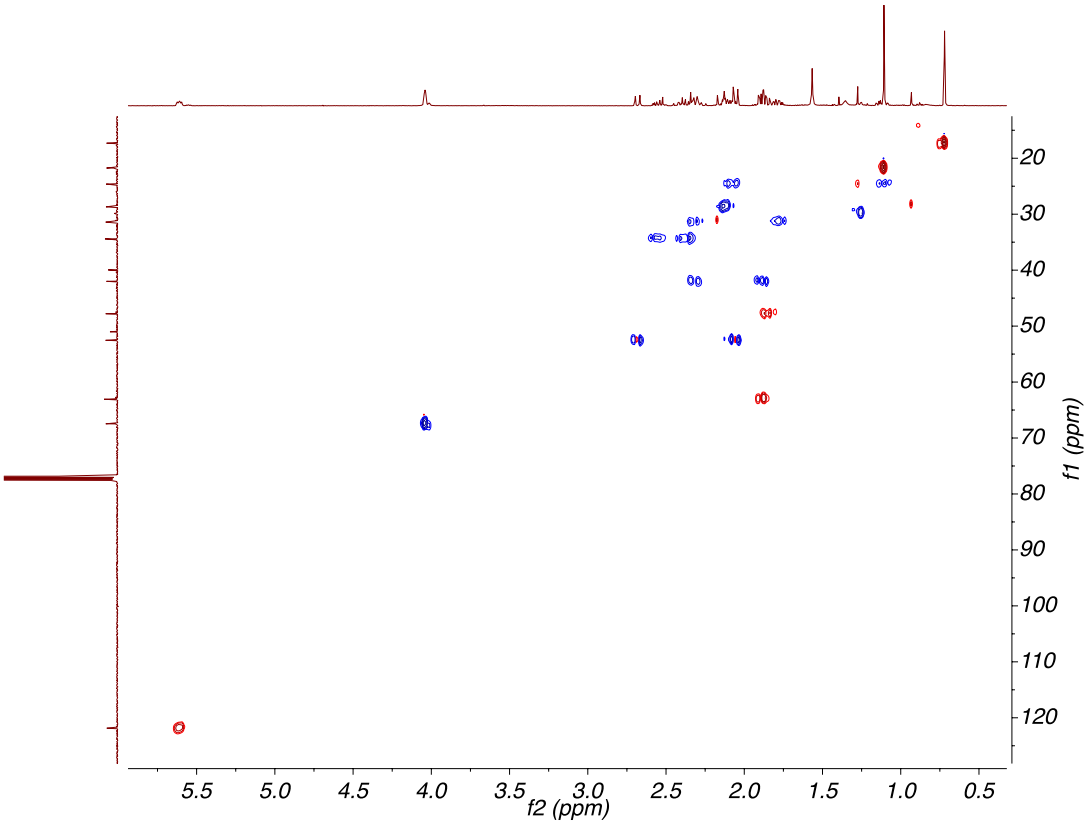

Figure A7.9. HSQC (400, 101 MHz, $CDCl_3$) of compound **190**.

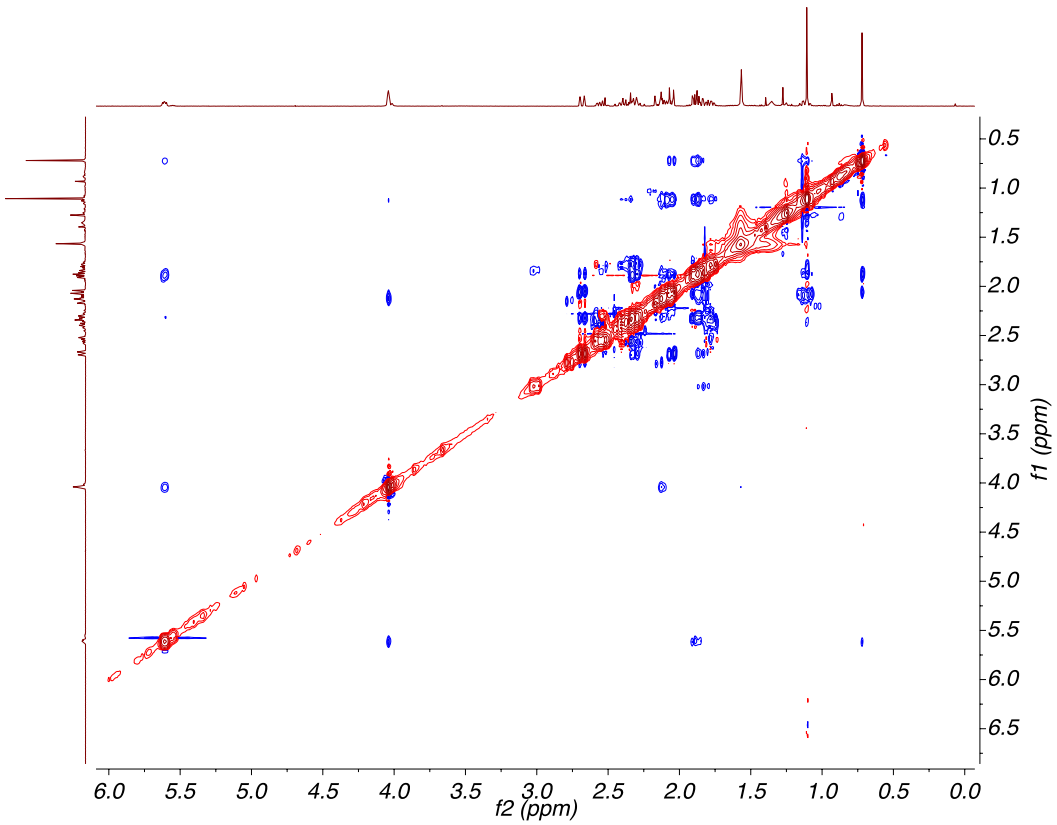

Figure A7.10. NOESY (400 MHz, $CDCl_3$) of compound **190**.

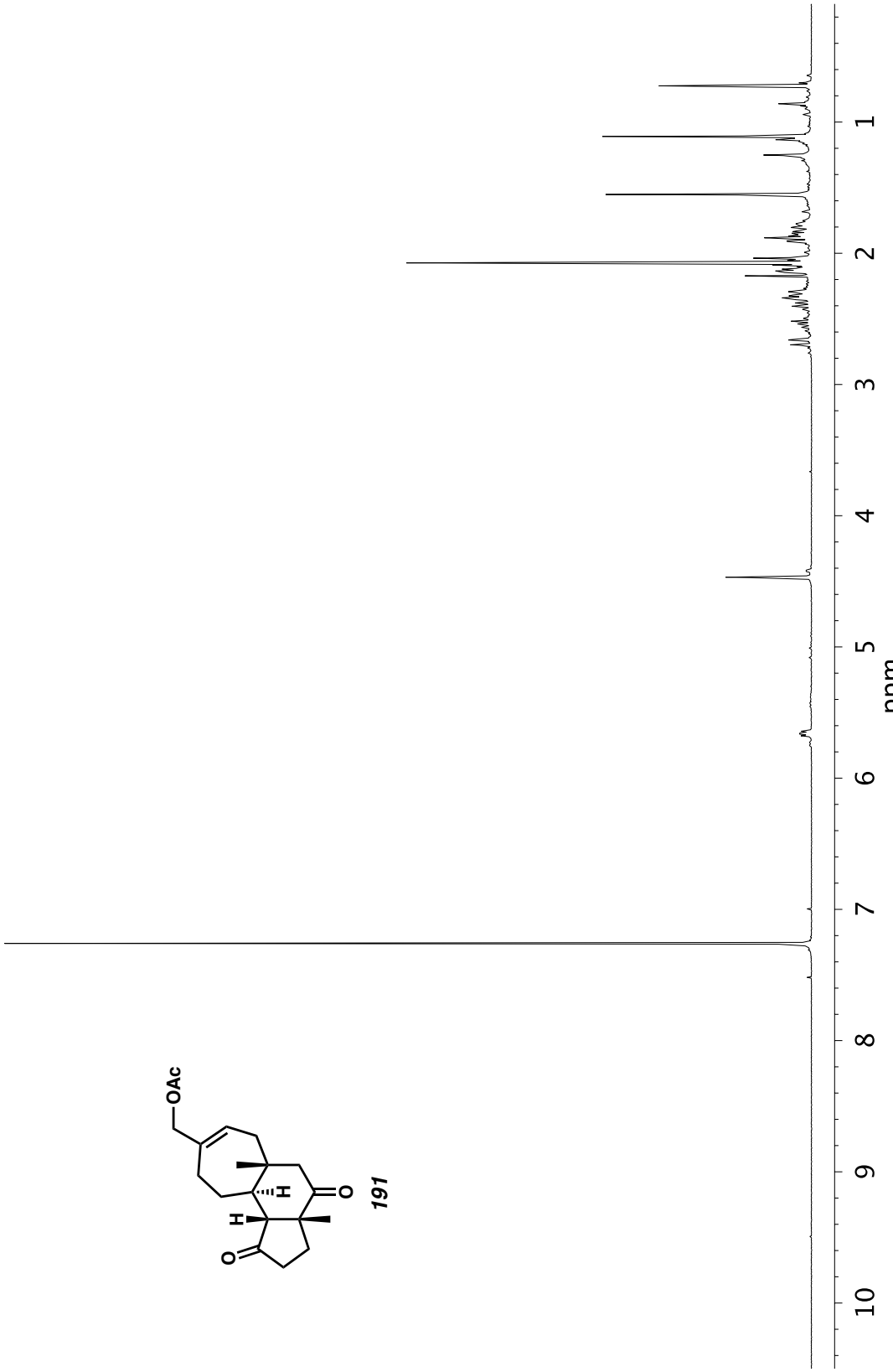

Figure A7.11. ^{1}H NMR (400 MHz, $CDCl_3$) of compound **191**.

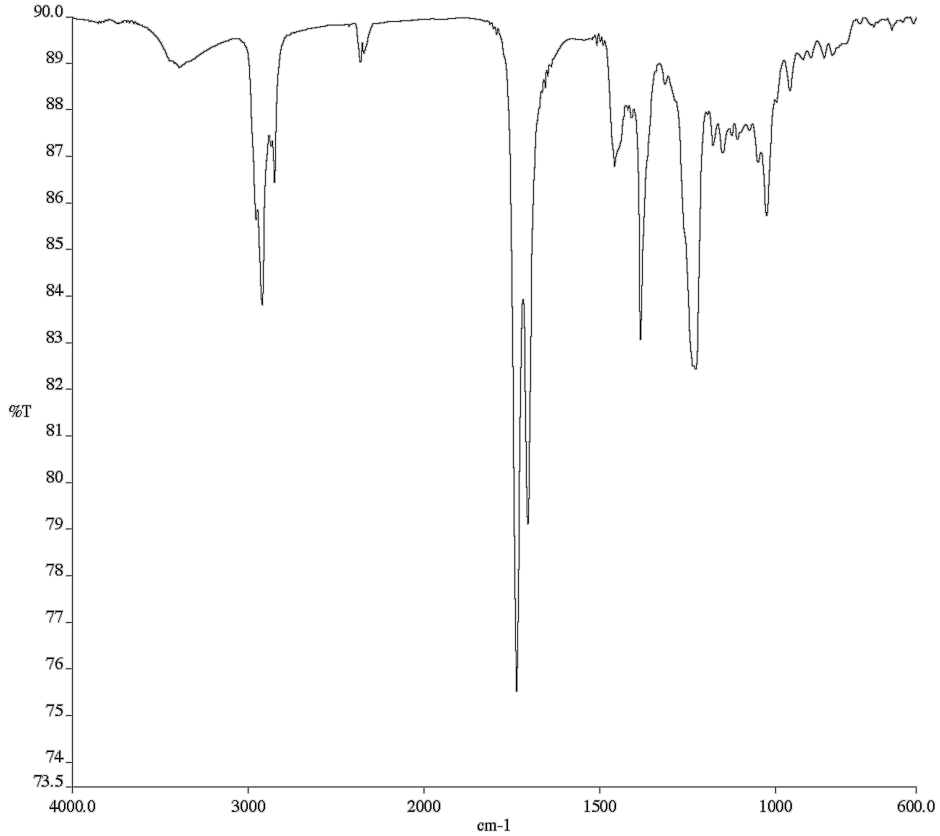

Figure A7.12. Infrared Spectrum (Thin Film, KBr) of compound **191**.

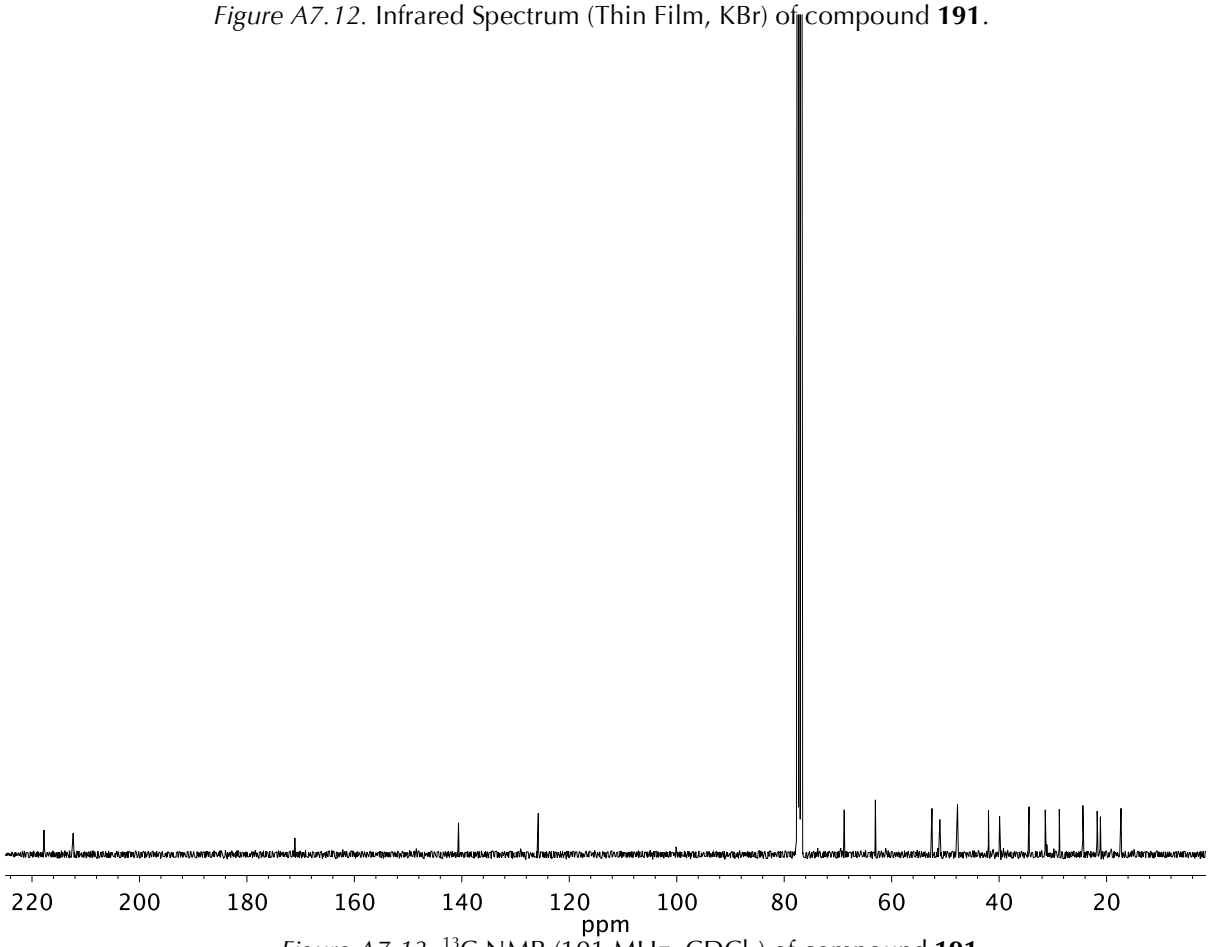

Figure A7.13. ^{13}C NMR (101 MHz, $CDCl_3$) of compound **191**.

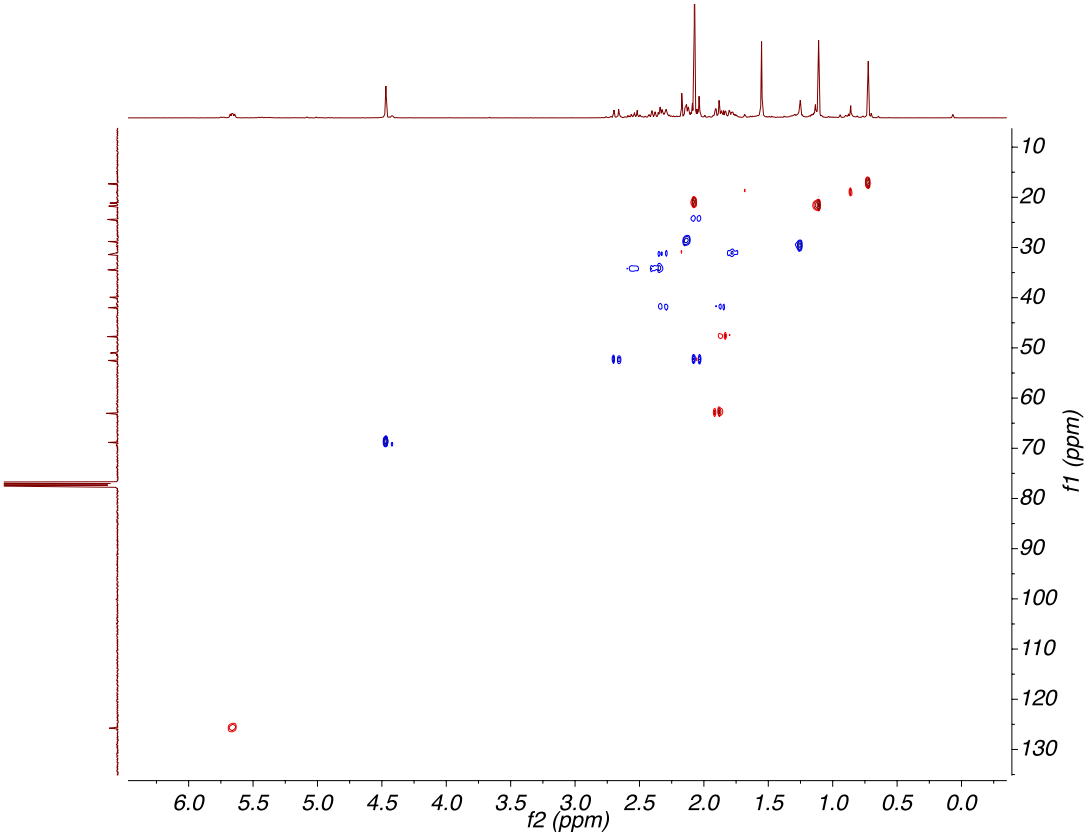

Figure A7.14. HSQC (400, 101 MHz, $CDCl_3$) of compound **191**.

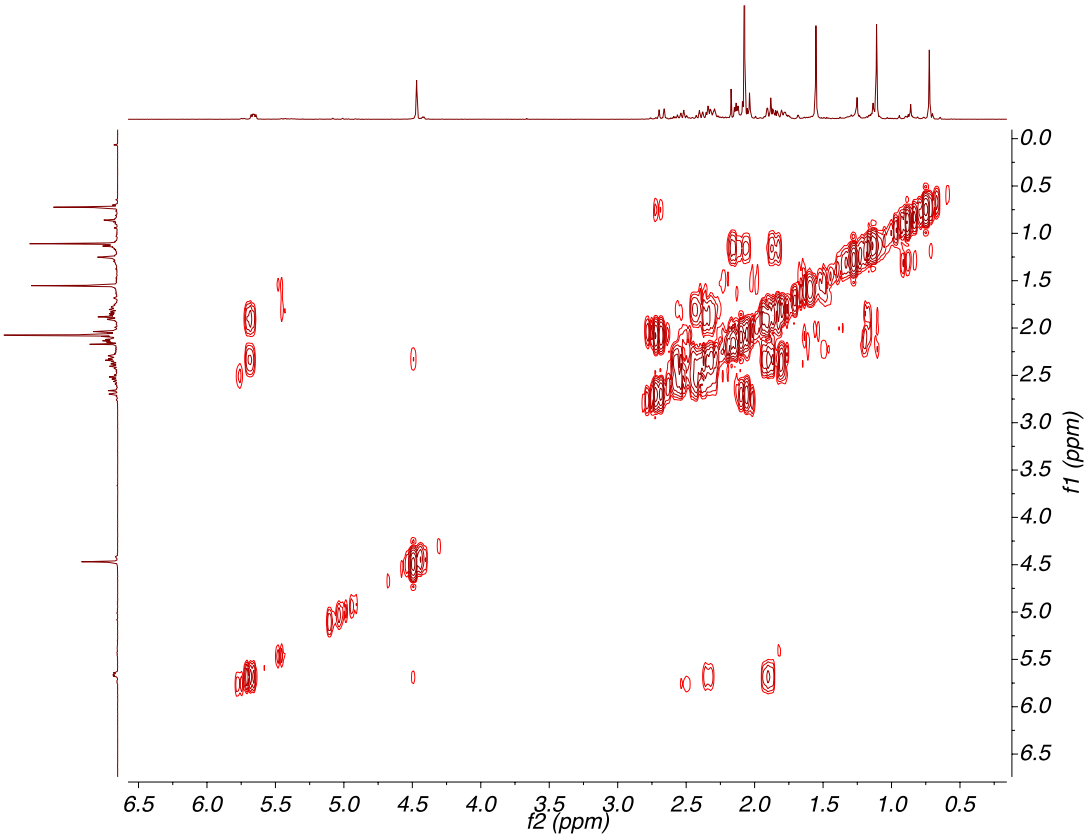

Figure A7.15. COSY (400 MHz, $CDCl_3$) of compound **191**.

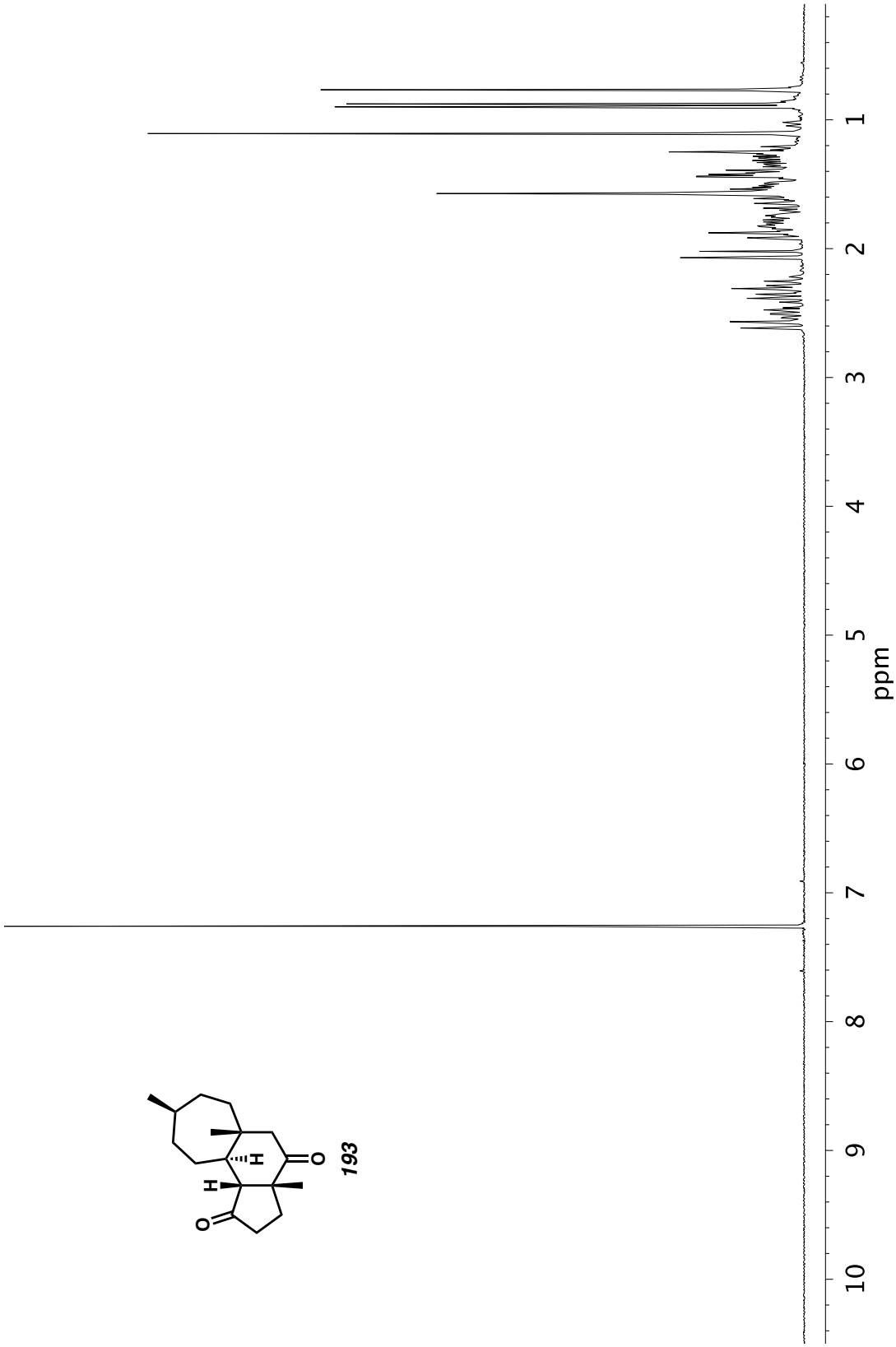

Figure A7.16. ^{1}H NMR (300 MHz, $CDCl_3$) of compound **193**.

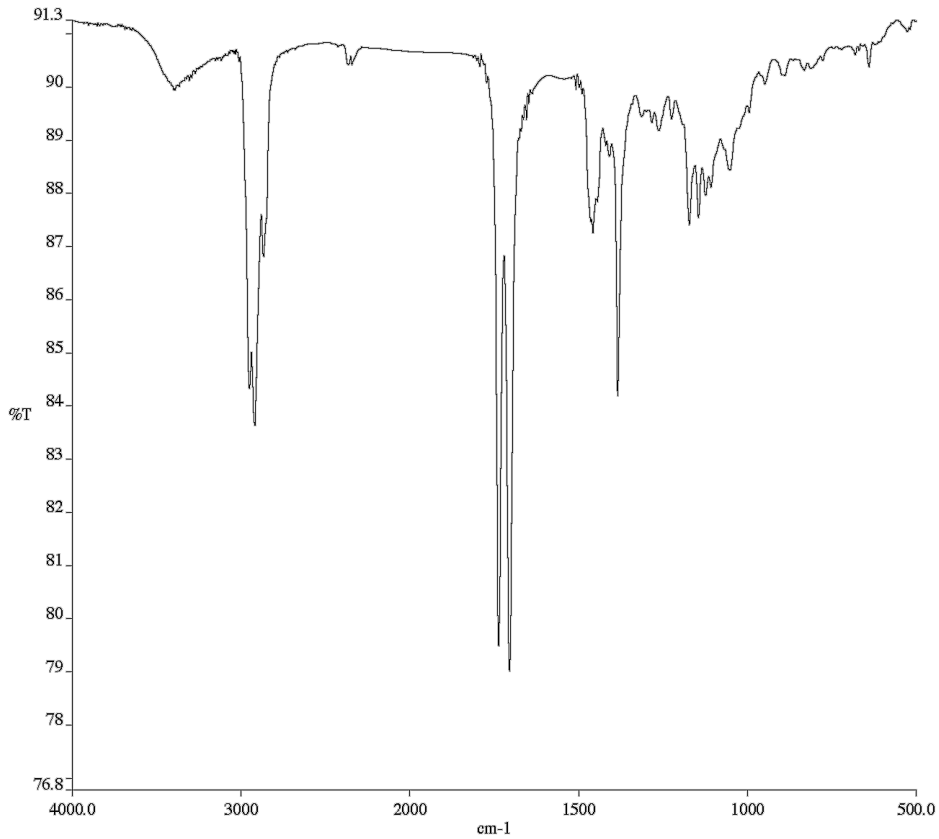

Figure A7.17. Infrared Spectrum (Thin Film, KBr) of compound **193**.

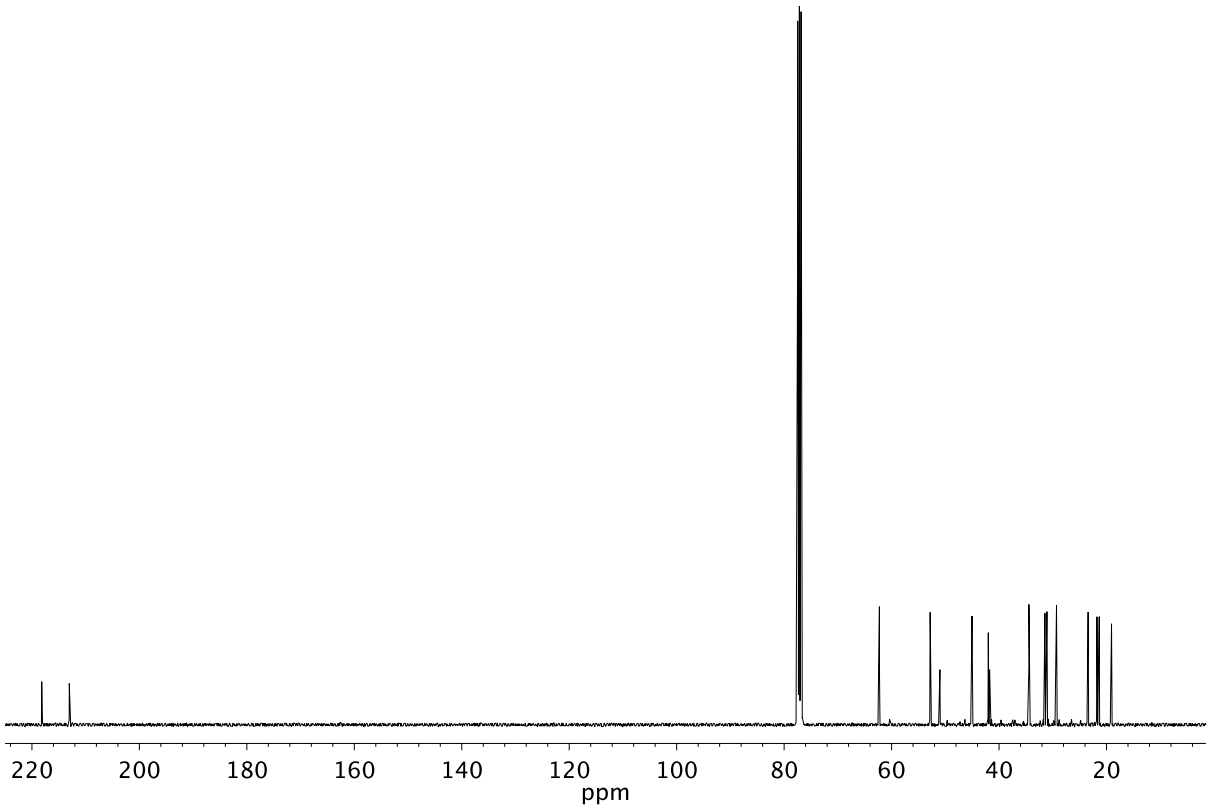

Figure A7.18. ^{13}C NMR (101 MHz, $CDCl_3$) of compound **193**.

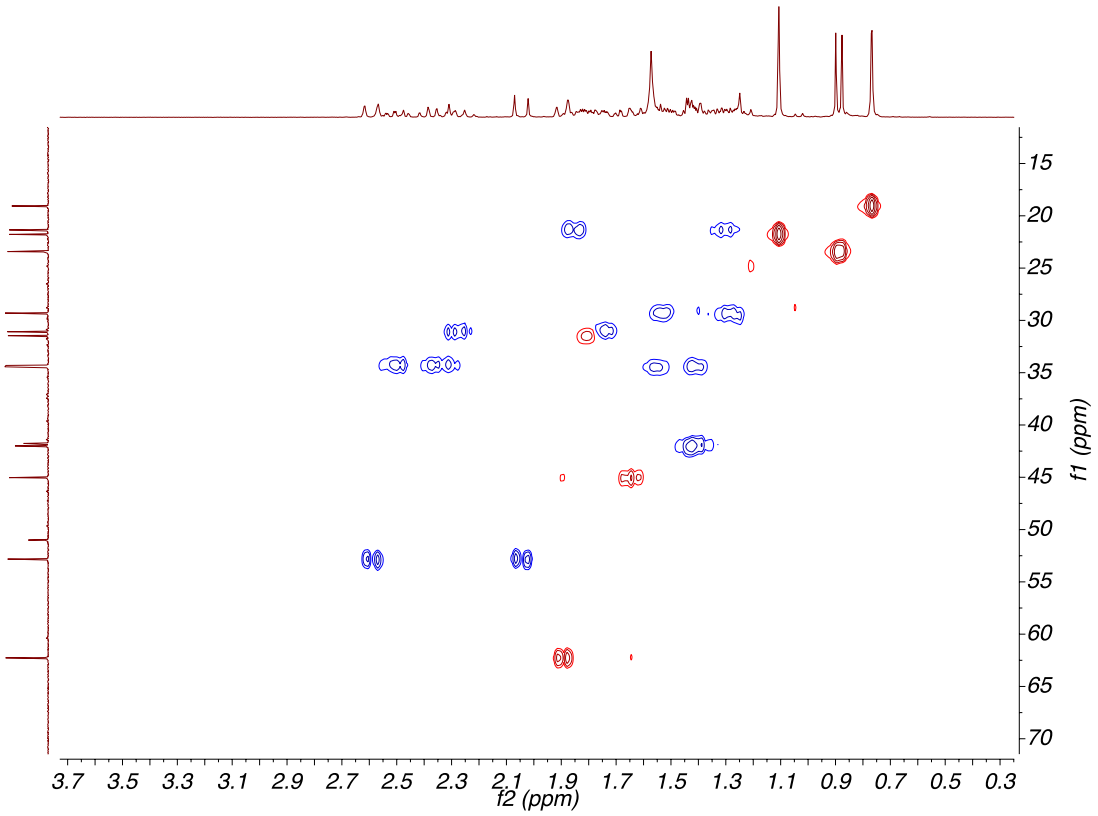

Figure A7.19. HSQC (400, 101 MHz, $CDCl_3$) of compound **193**.

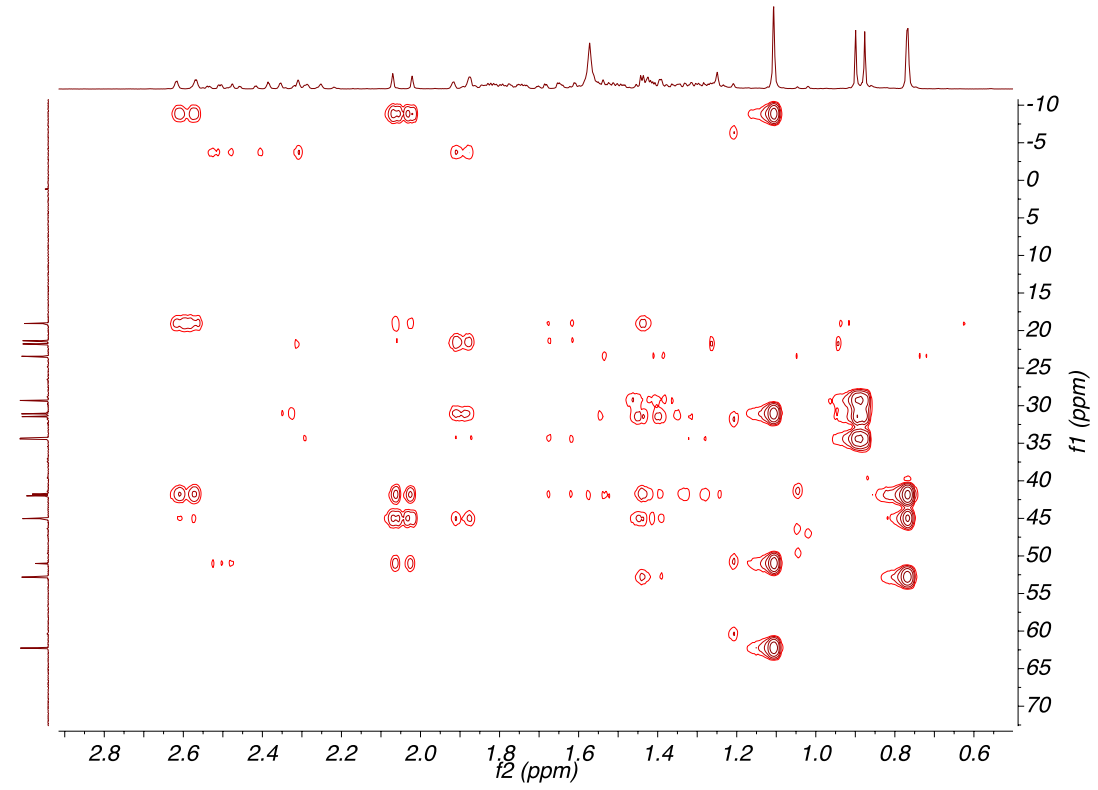

Figure A7.20. HMBC (400, 101 MHz, $CDCl_3$) of compound **193**.

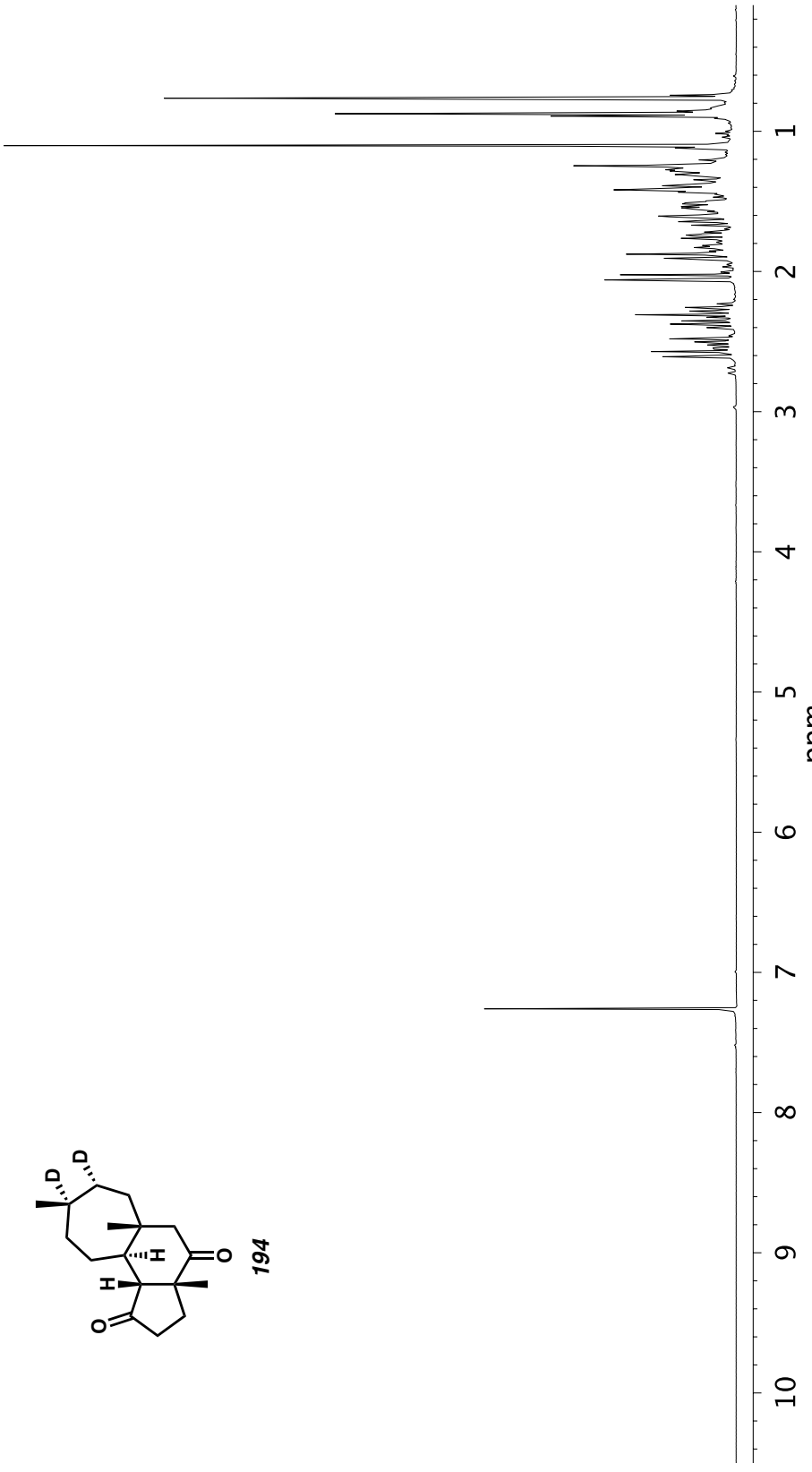

Figure A7.21. ^{1}H NMR (400 MHz, $CDCl_3$) of compound **194**.

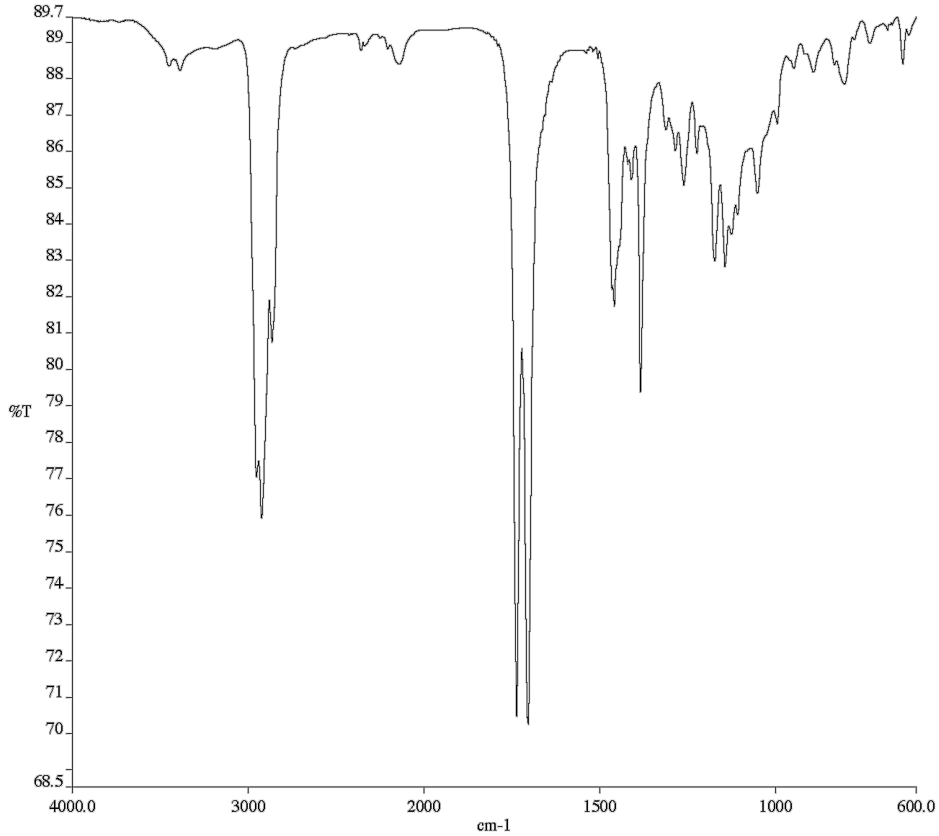

Figure A7.22. Infrared Spectrum (Thin Film, KBr) of compound **194**.

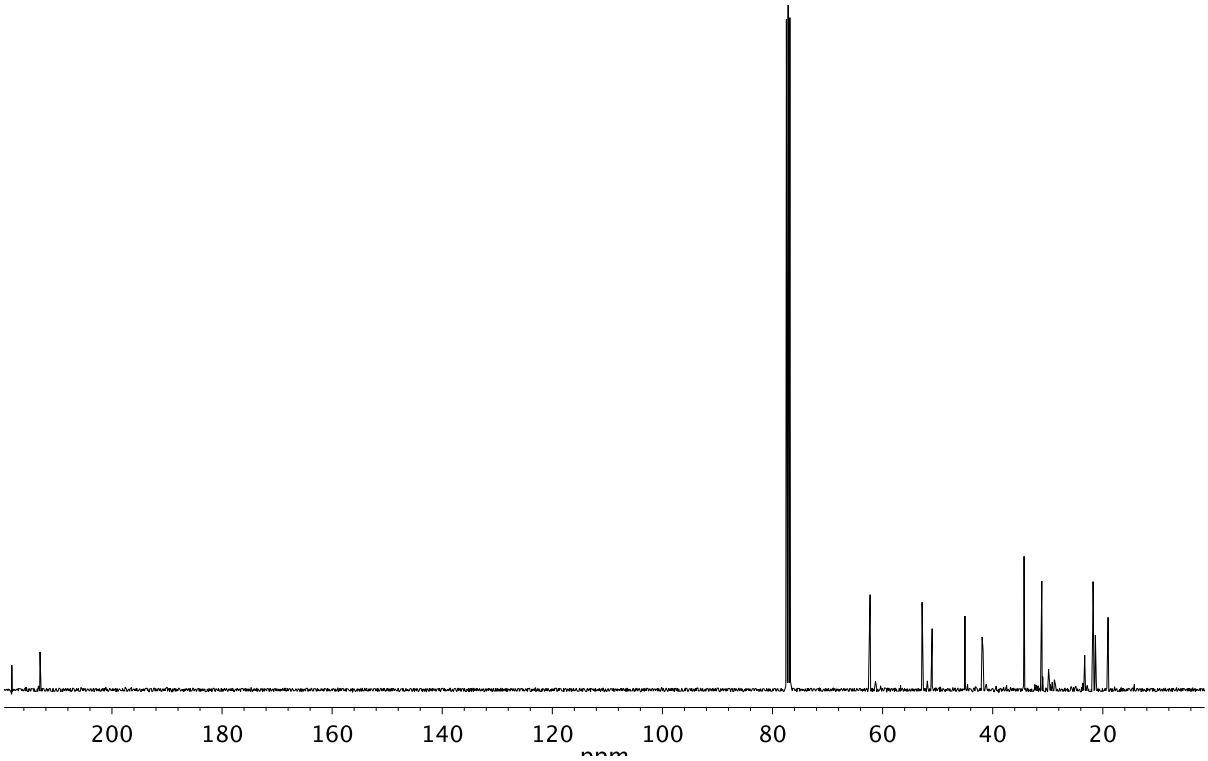

Figure A7.23. ^{13}C NMR (101 MHz, $CDCl_3$) of compound **194**.

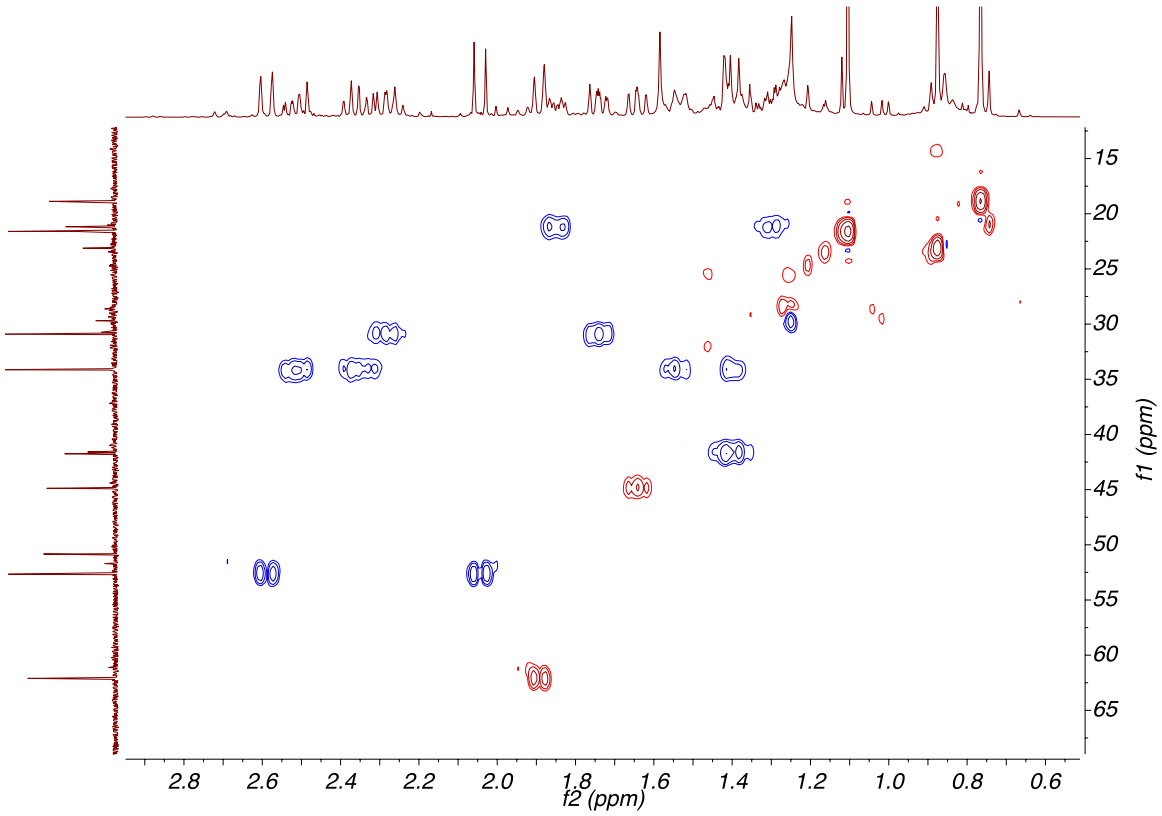

Figure A7.24. HSQC (500, 126 MHz, $CDCl_3$) of compound **194**.

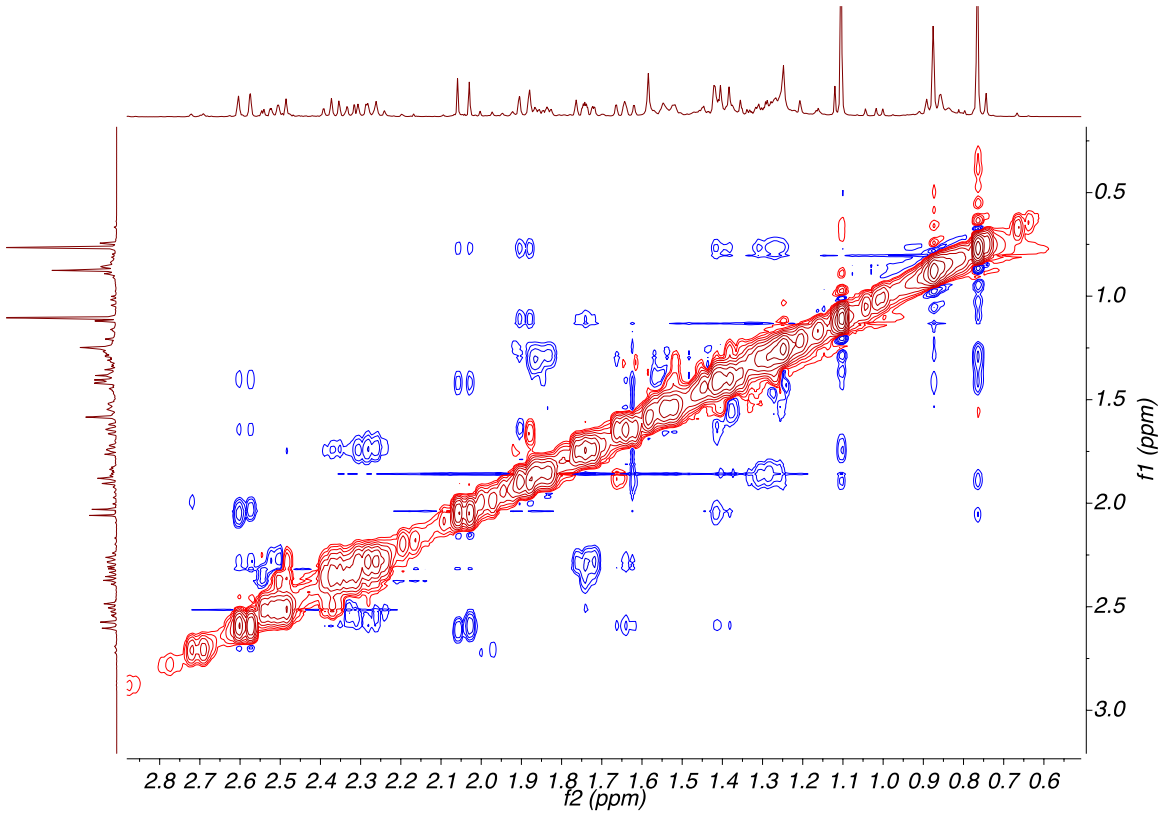

Figure A7.25. NOESY (500 MHz, $CDCl_3$) of compound **194**.

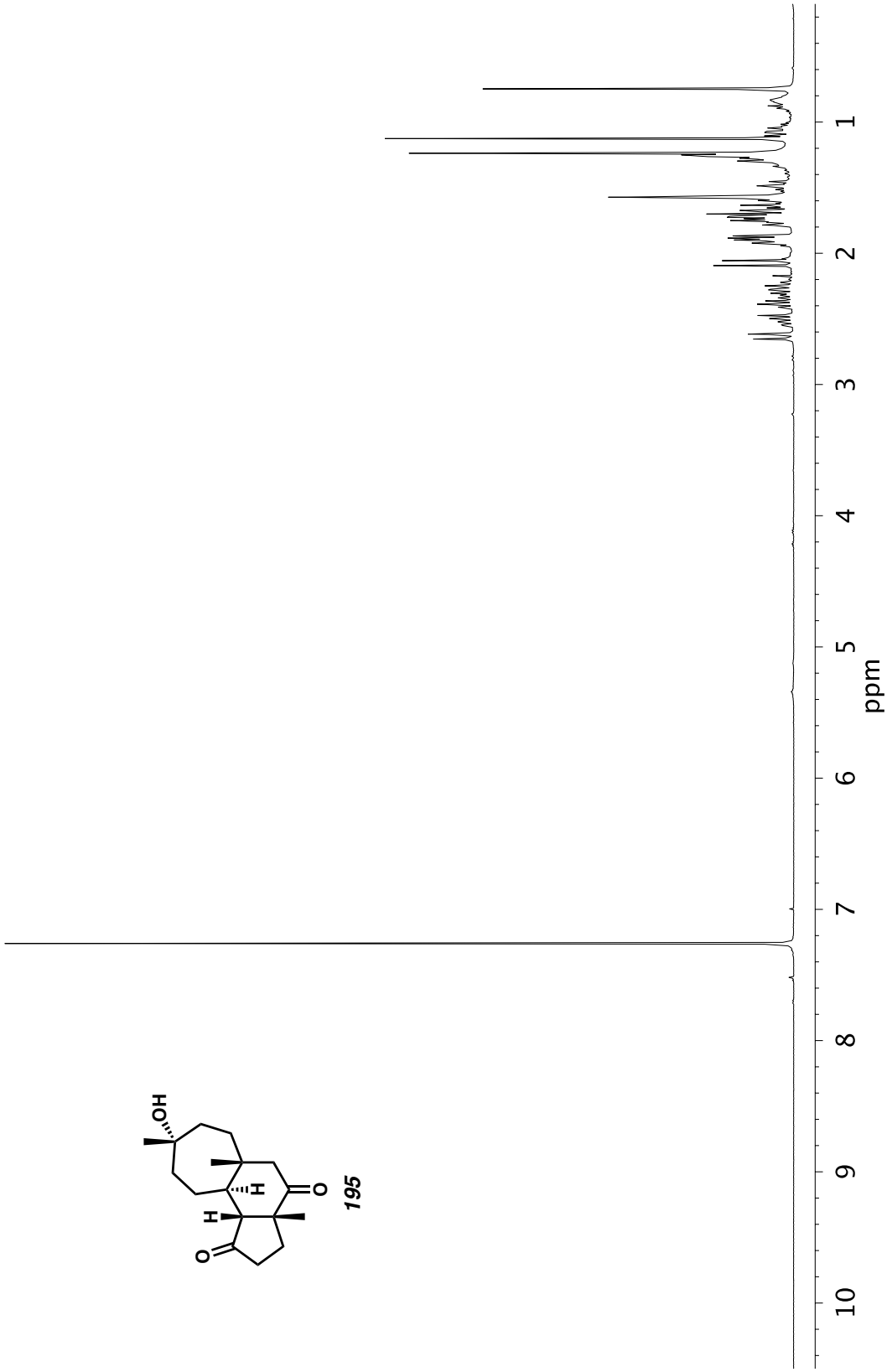

Figure A7.26. ^{1}H NMR (400 MHz, $CDCl_3$) of compound **195**.

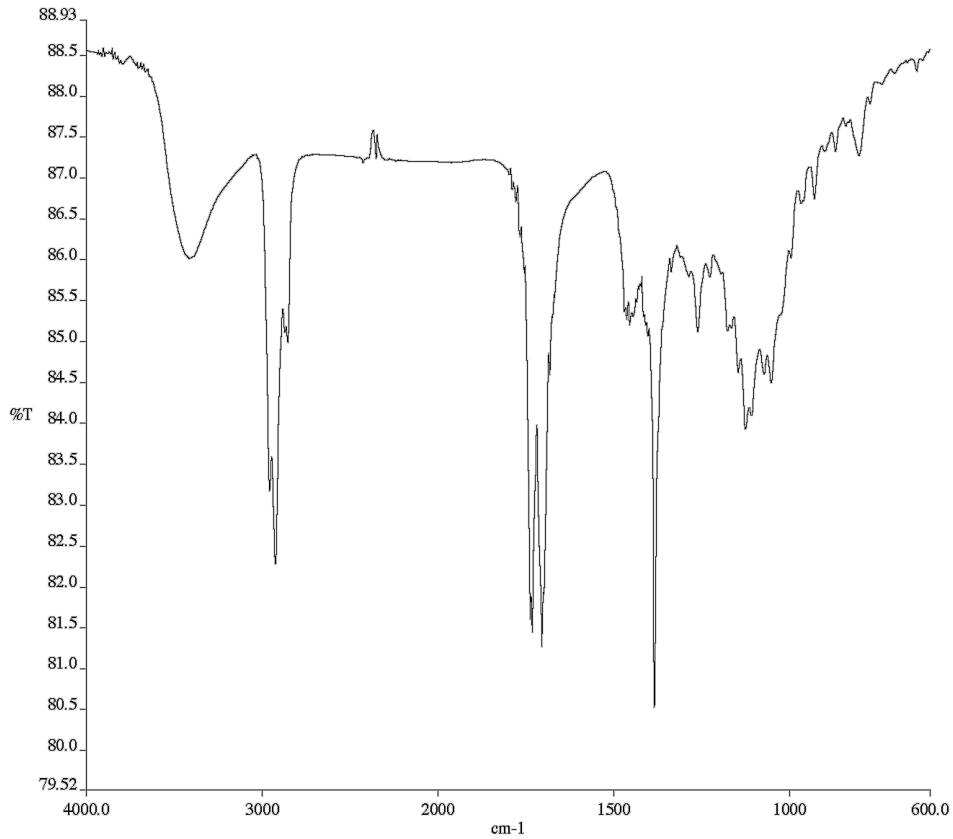

Figure A7.27. Infrared Spectrum (Thin Film, KBr) of compound **195**.

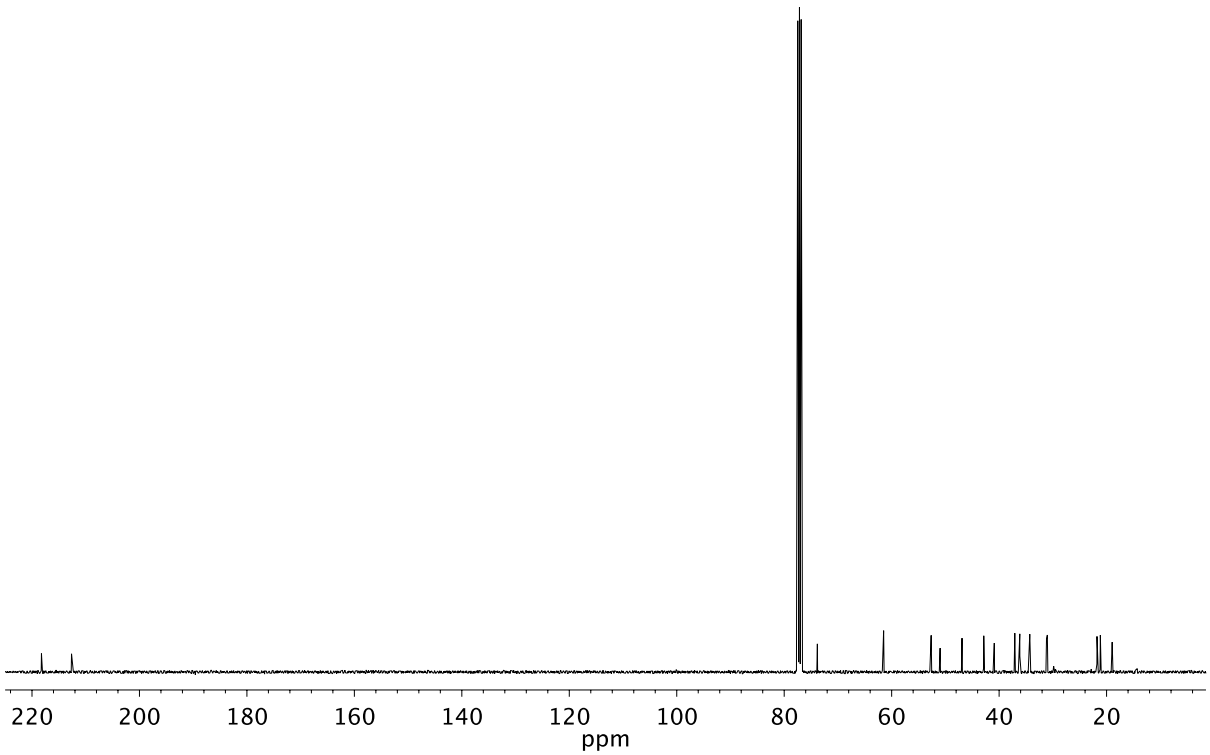

Figure A7.28. ^{13}C NMR (101 MHz, $CDCl_3$) of compound **195**.

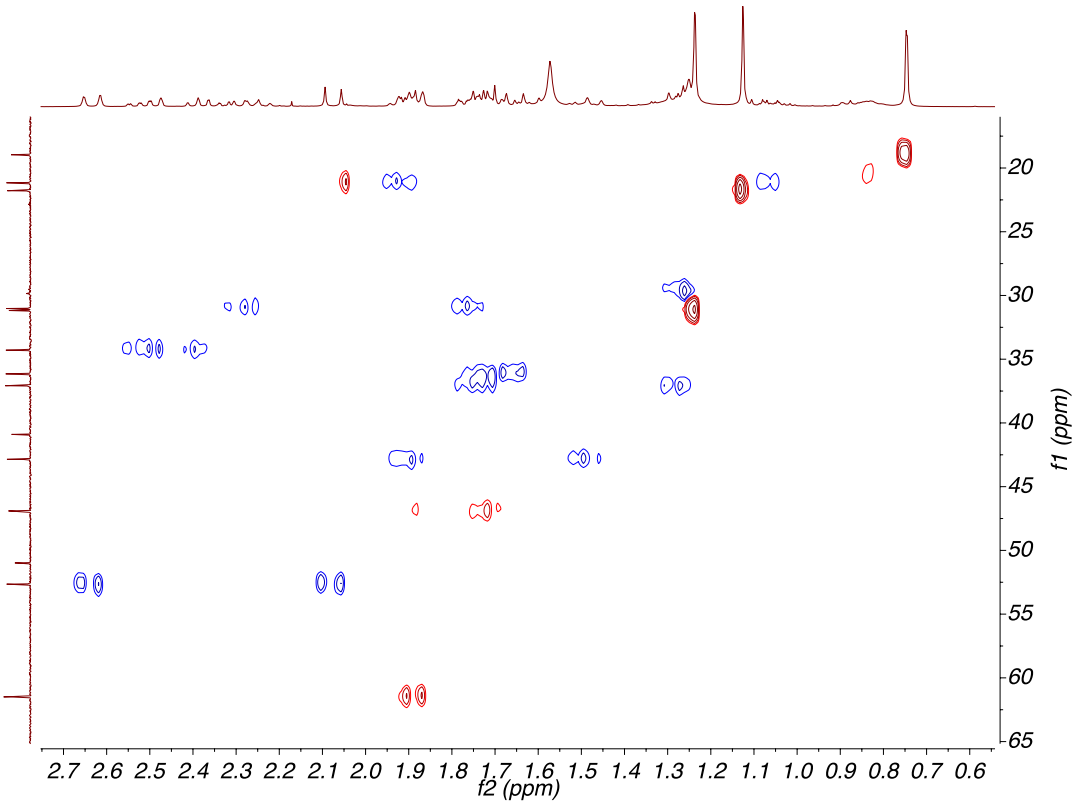

Figure A7.29. HSQC (400, 101 MHz, $CDCl_3$) of compound **195**.

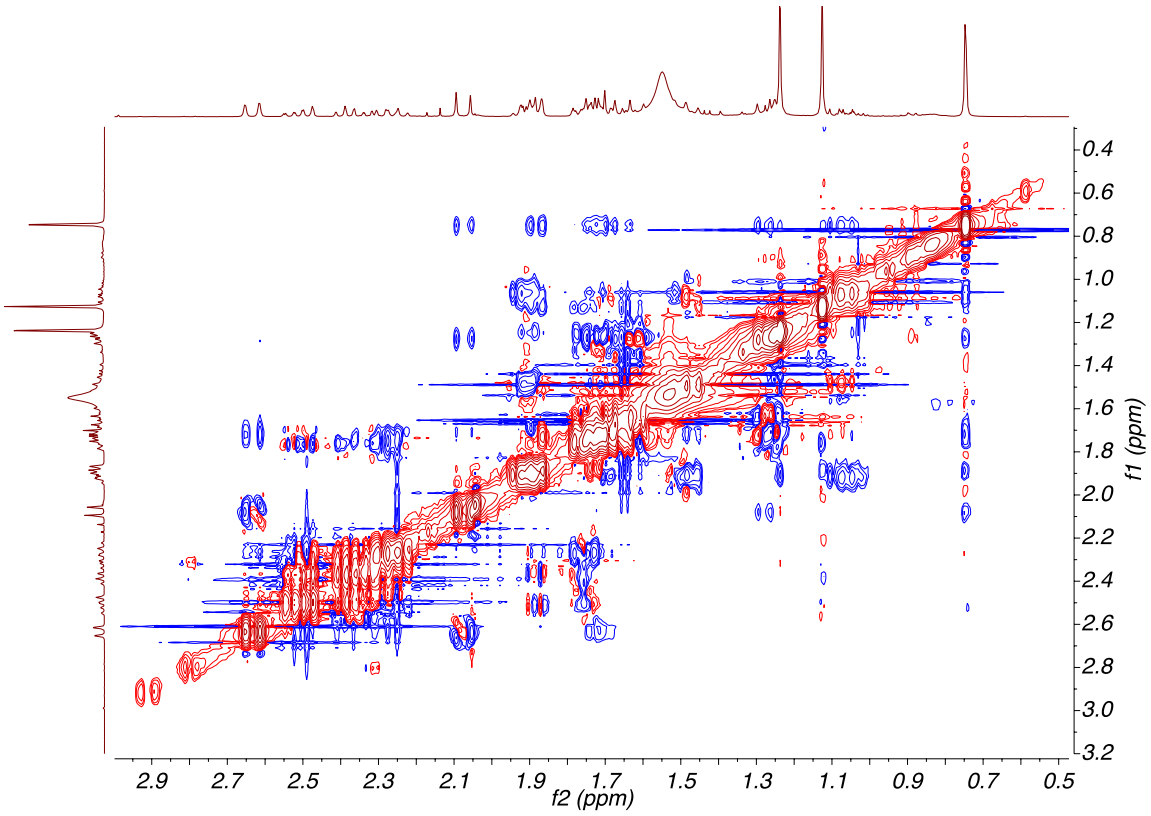

Figure A7.30. NOESY (400 MHz, $CDCl_3$) of compound **195**.

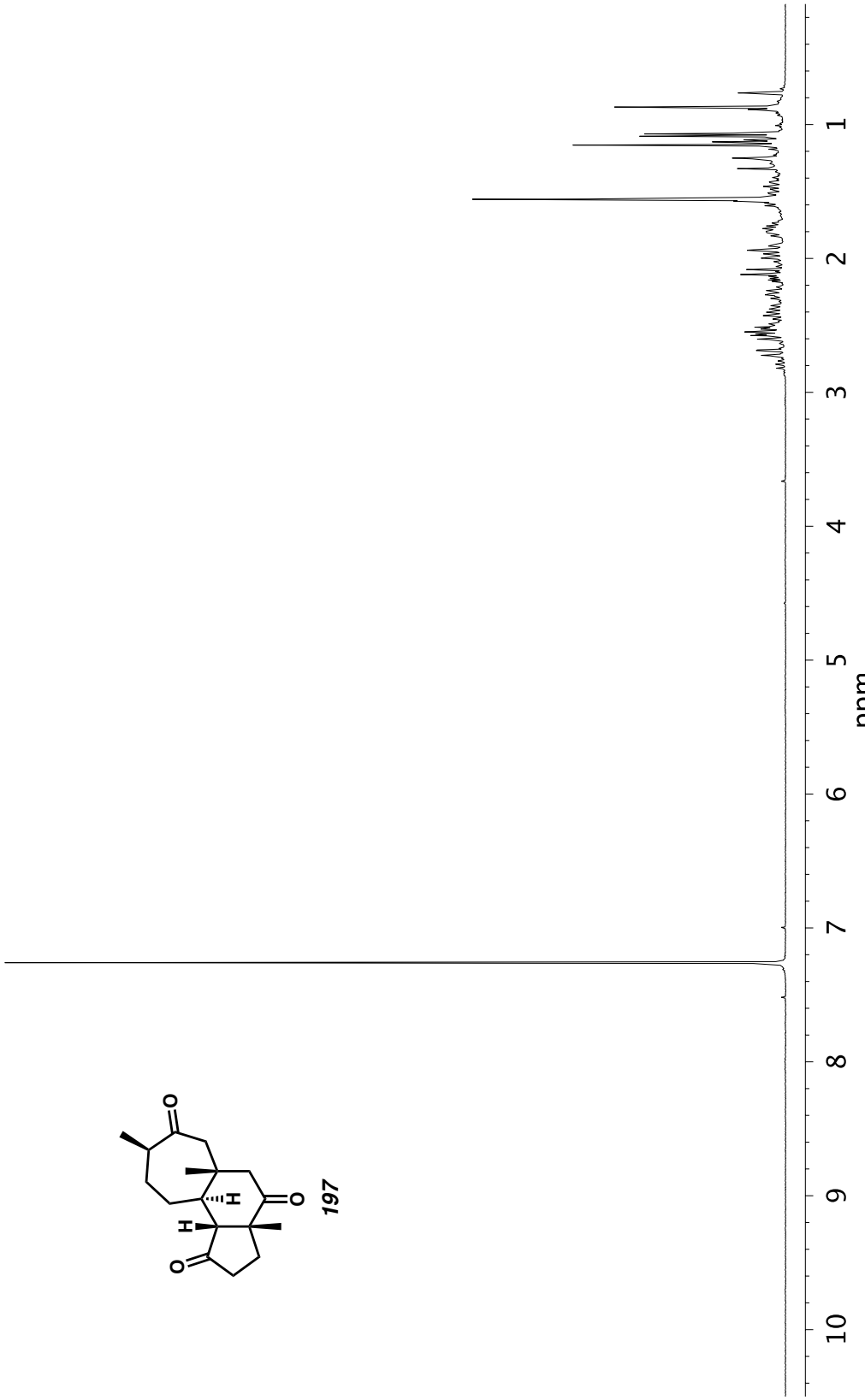

Figure A7.31. ^{1}H NMR (400 MHz, $CDCl_3$) of compound **197**.

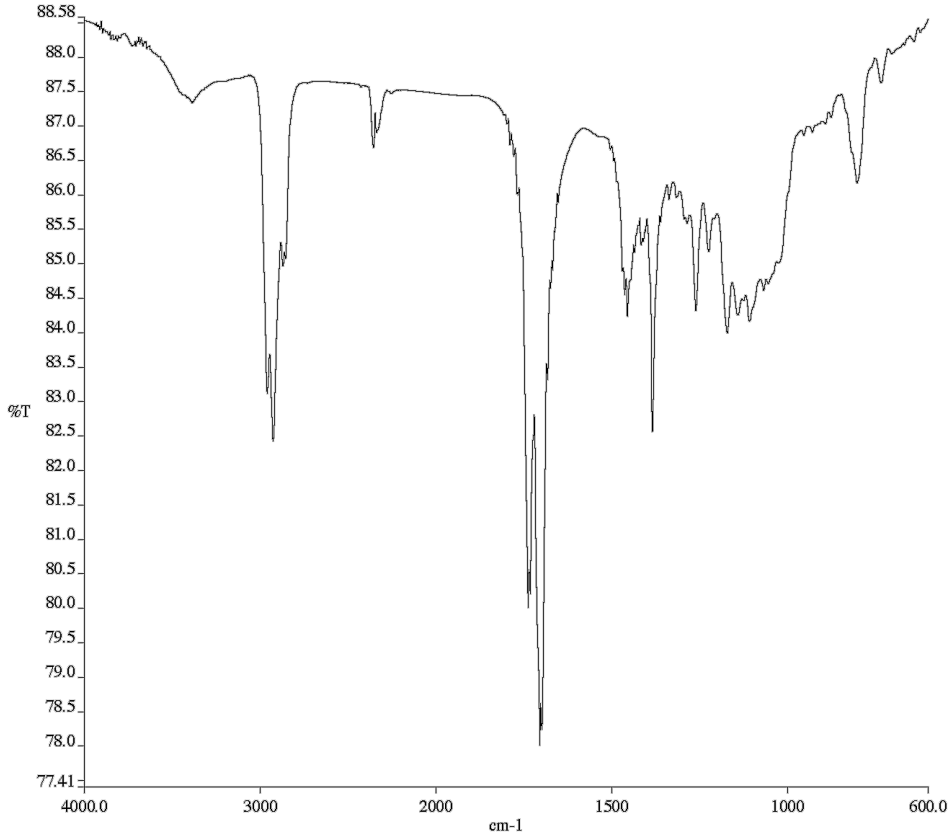

Figure A7.32. Infrared Spectrum (Thin Film, KBr) of compound **197**.

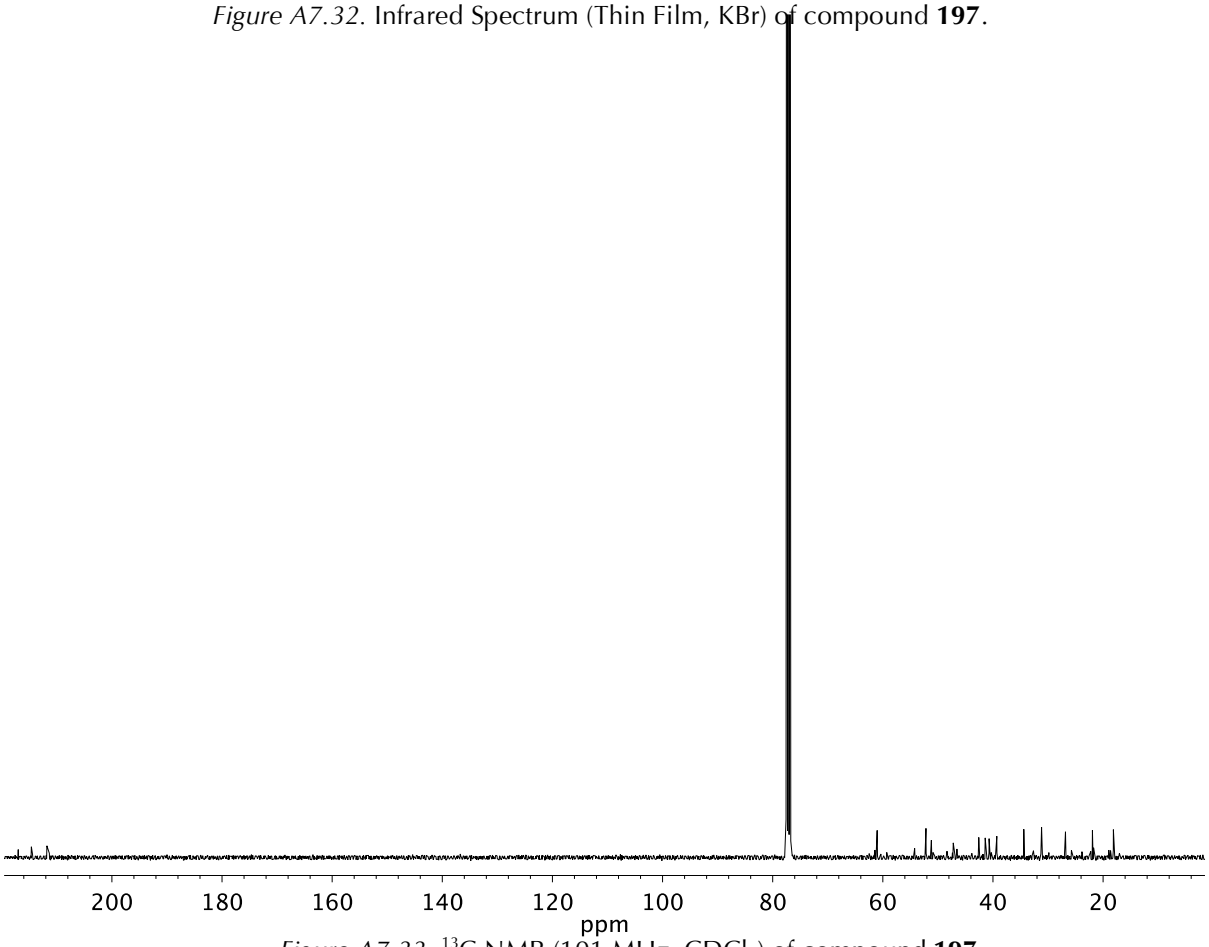

Figure A7.33. ^{13}C NMR (101 MHz, $CDCl_3$) of compound **197**.

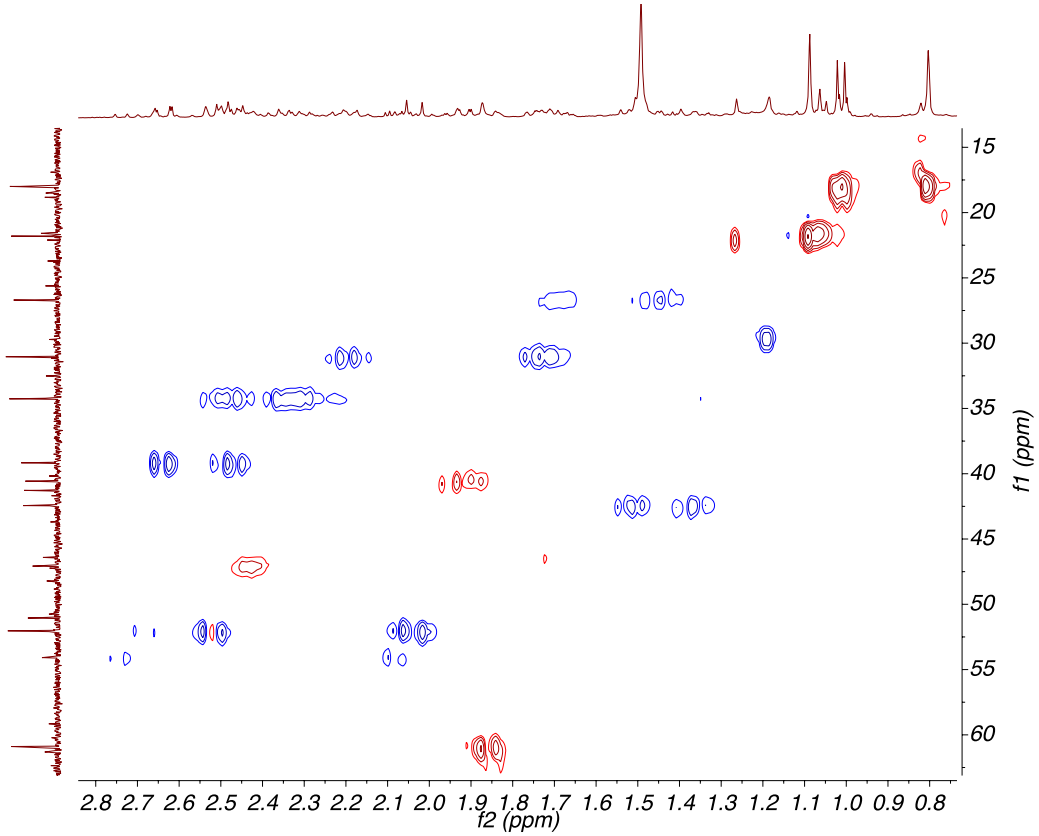

Figure A7.34. HSQC (400, 101 MHz, $CDCl_3$) of compound **197**.

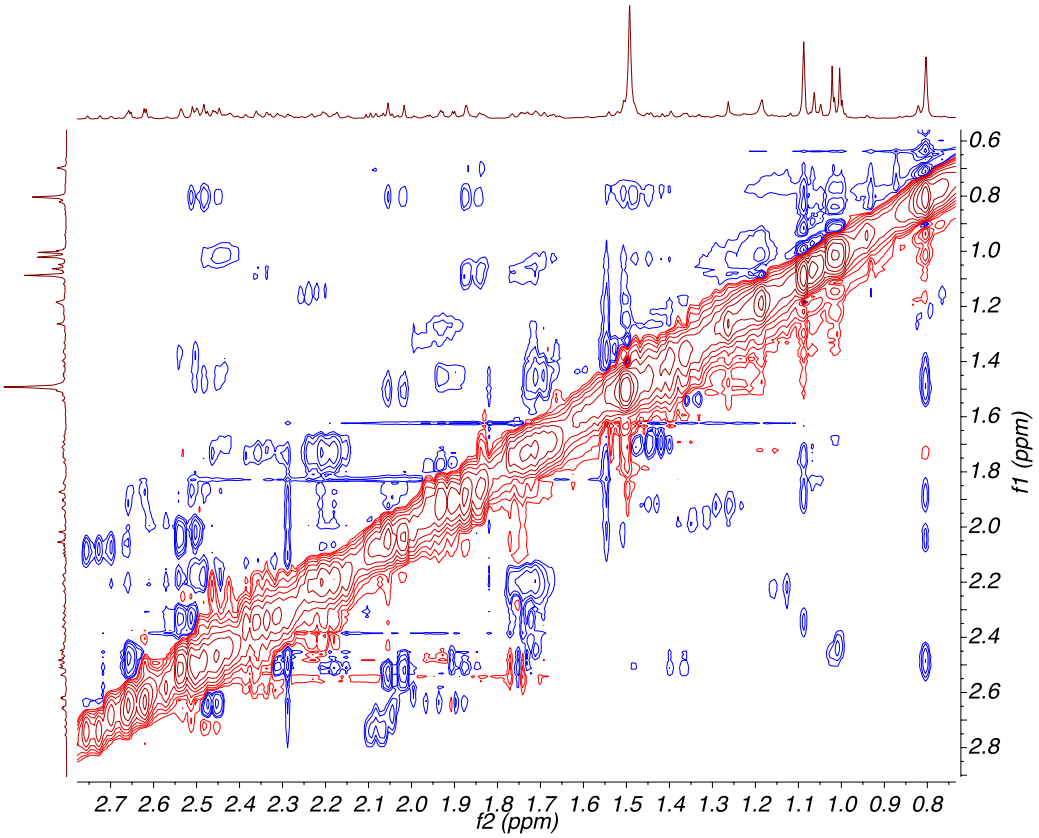

Figure A7.35. NOESY (400 MHz, $CDCl_3$) of compound **197**.

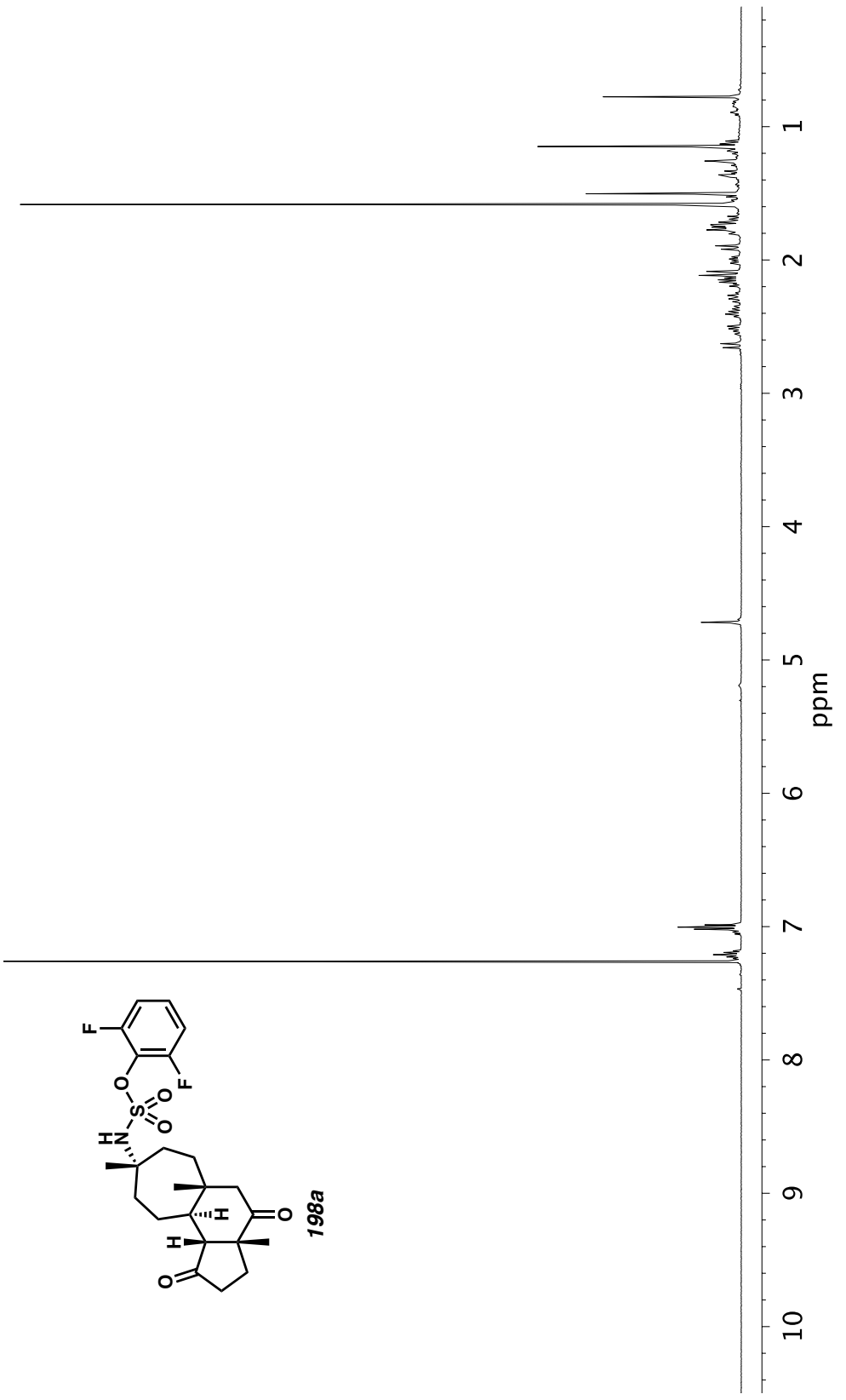

Figure A7.36. ^{1}H NMR (500 MHz, $CDCl_3$) of compound **198a**.

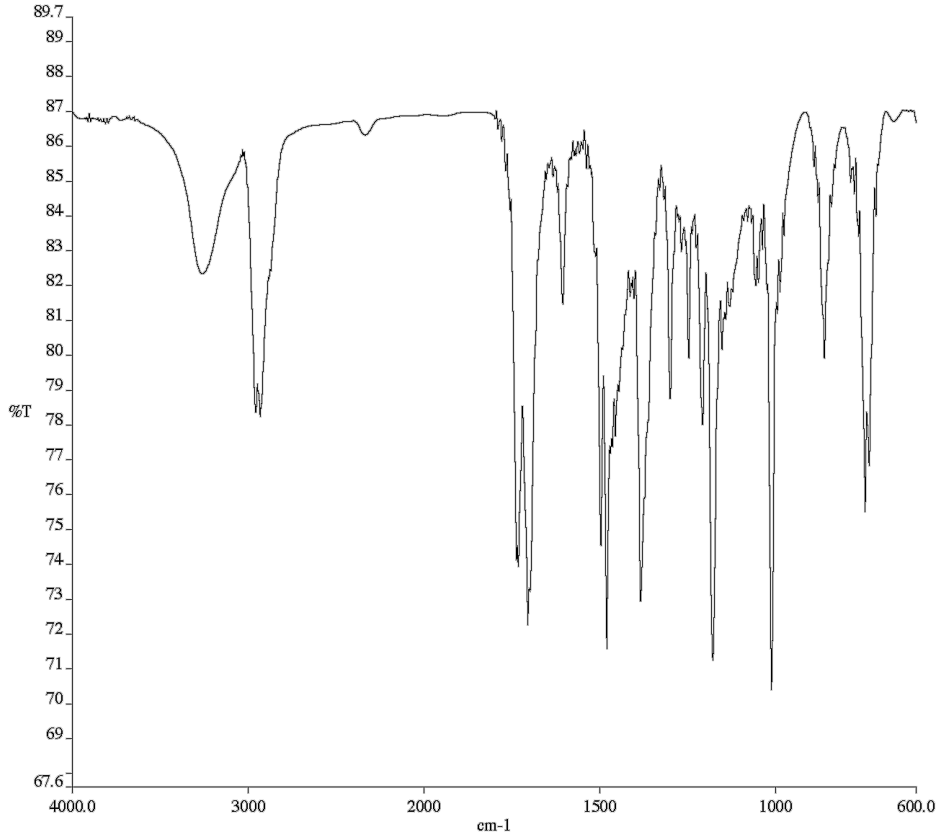

Figure A7.37. Infrared Spectrum (Thin Film, KBr) of compound **198a**.

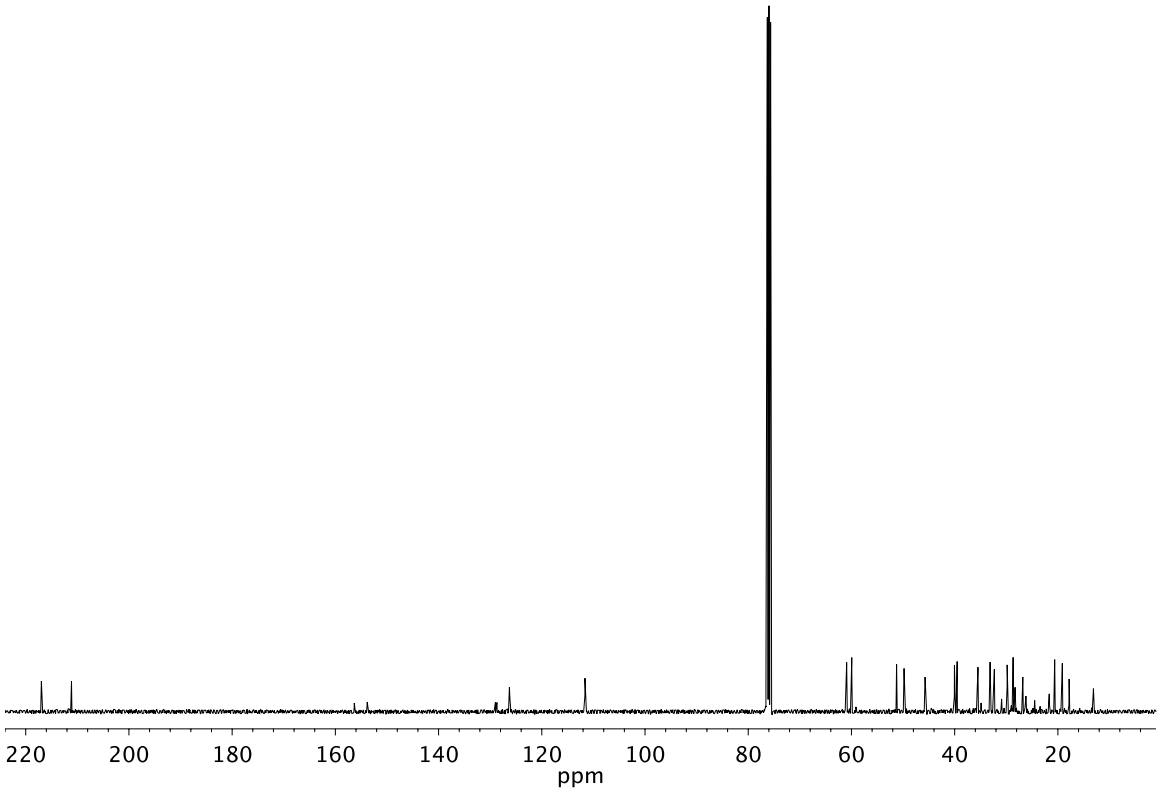

Figure A7.38. ^{13}C NMR (101 MHz, $CDCl_3$) of compound **198a**.

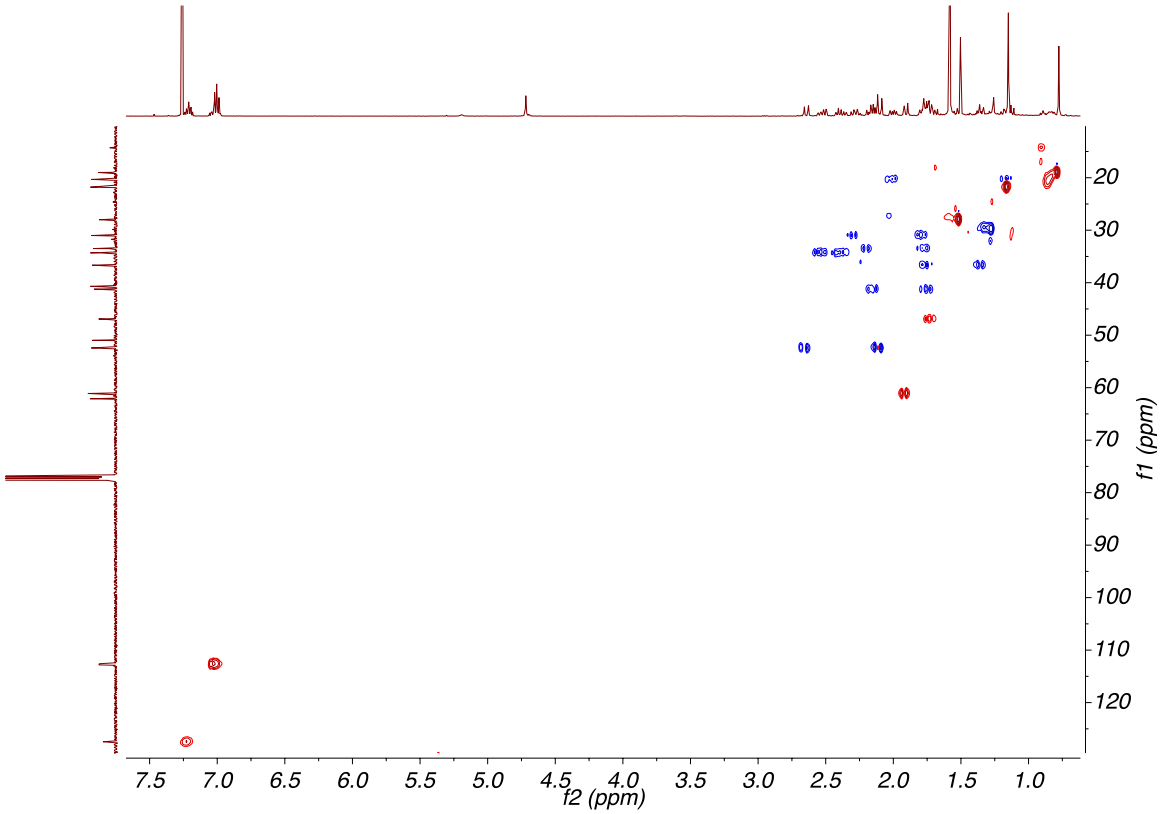

Figure A7.39. HSQC (400, 101 MHz, $CDCl_3$) of compound **198a**.

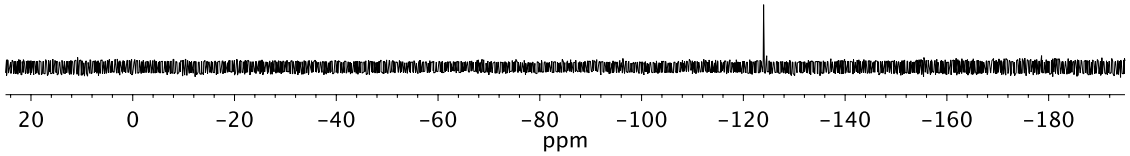

Figure A7.40. ^{19}F NMR (300 MHz, $CDCl_3$) of compound **198a**.

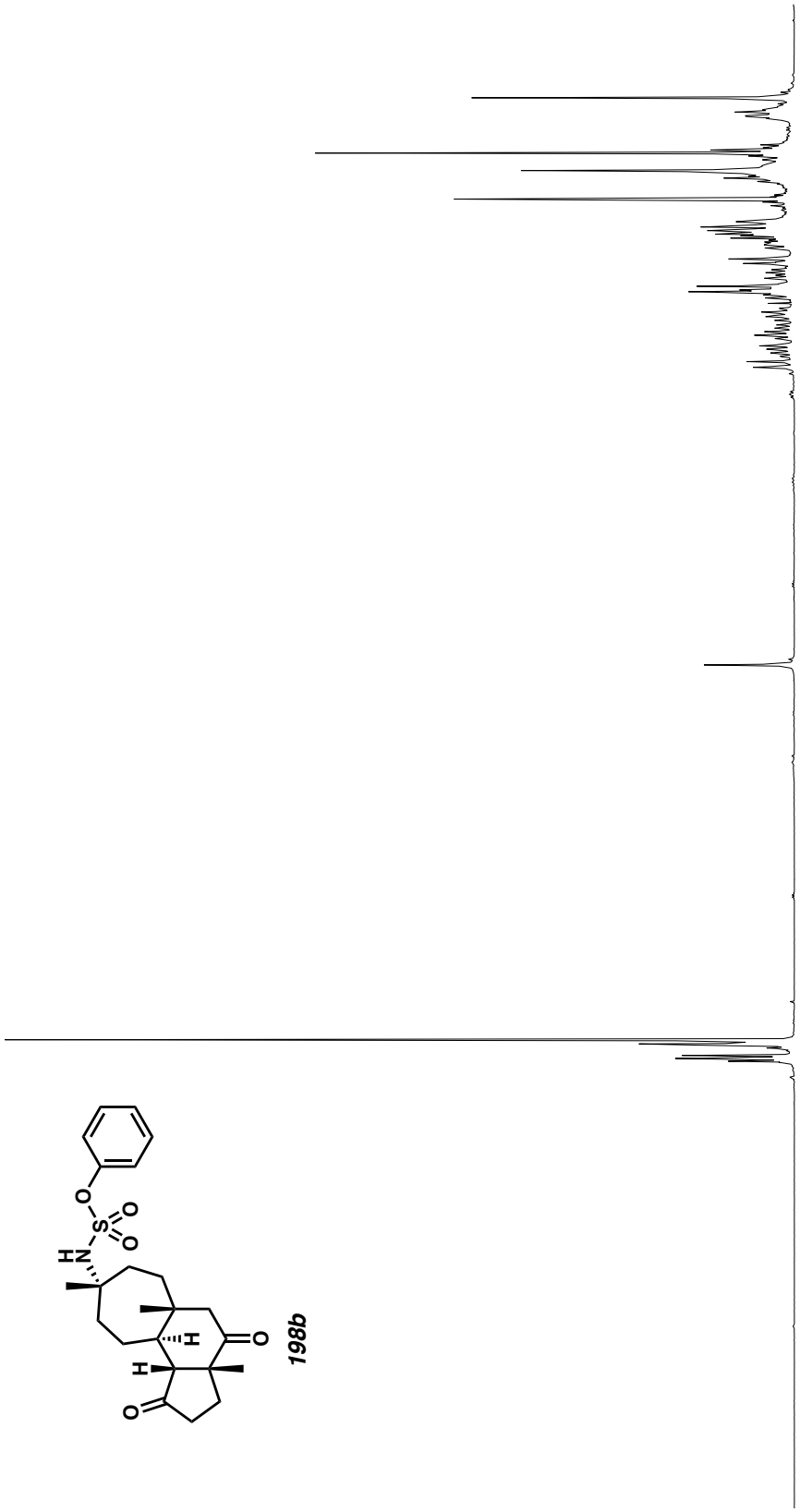

Figure A7.41. ^{1}H NMR (400 MHz, $CDCl_3$) of compound **198b**.

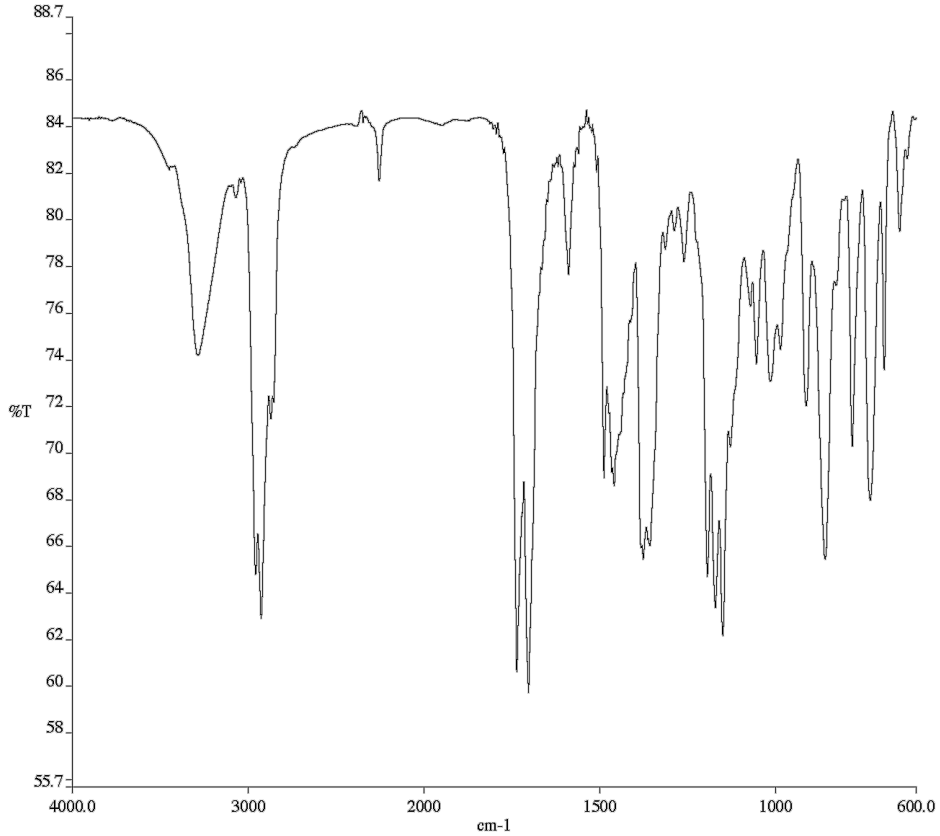

Figure A7.42. Infrared Spectrum (Thin Film, KBr) of compound **198b**.

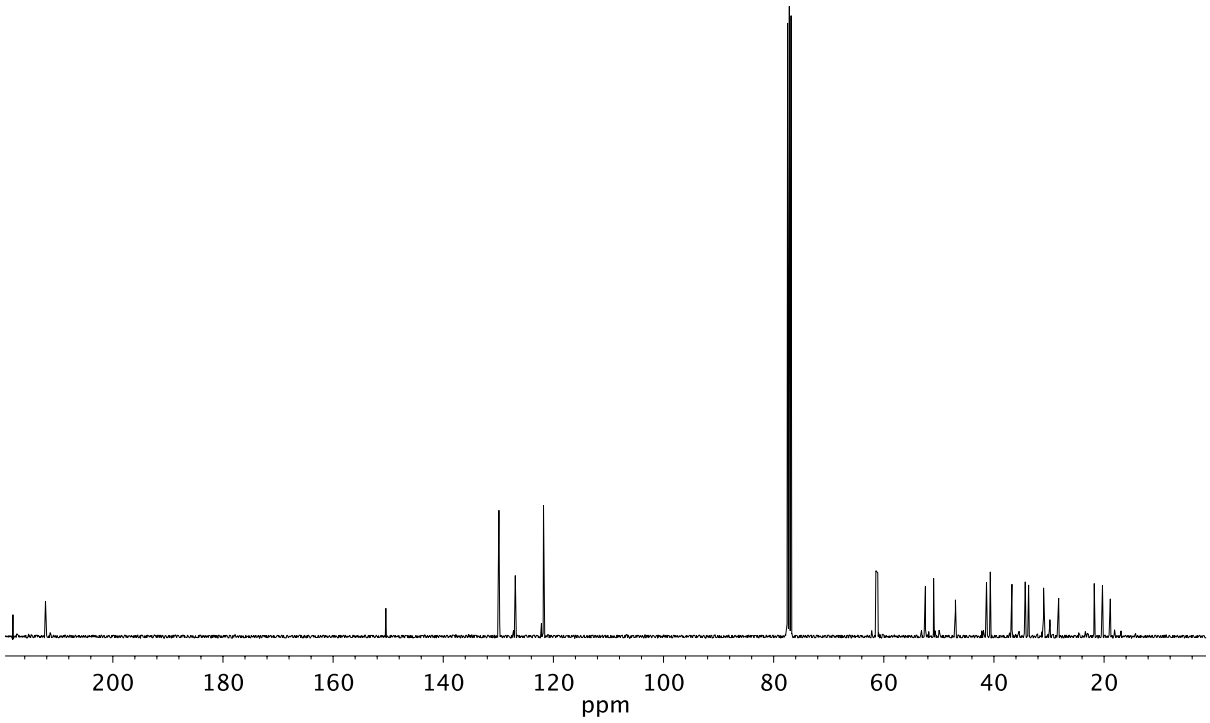

Figure A7.43. ^{13}C NMR (101 MHz, $CDCl_3$) of compound **198b**.

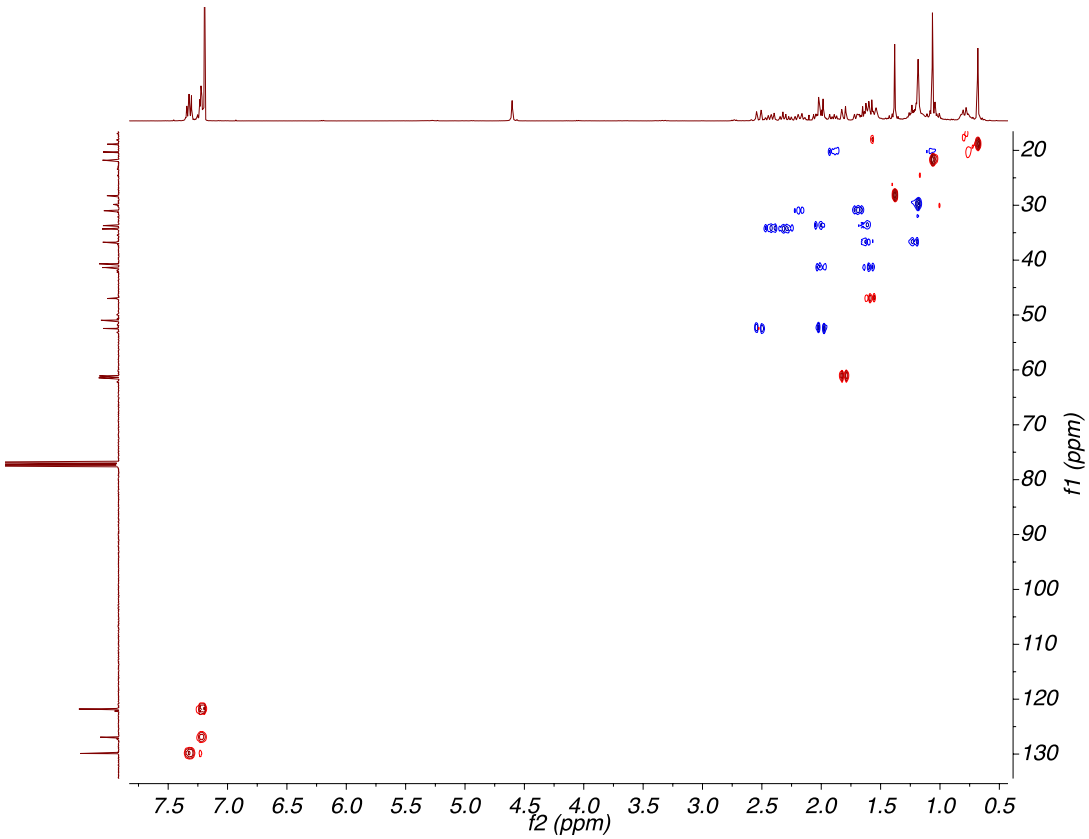

Figure A7.44. HSQC (400, 101 MHz, $CDCl_3$) of compound **198b**.

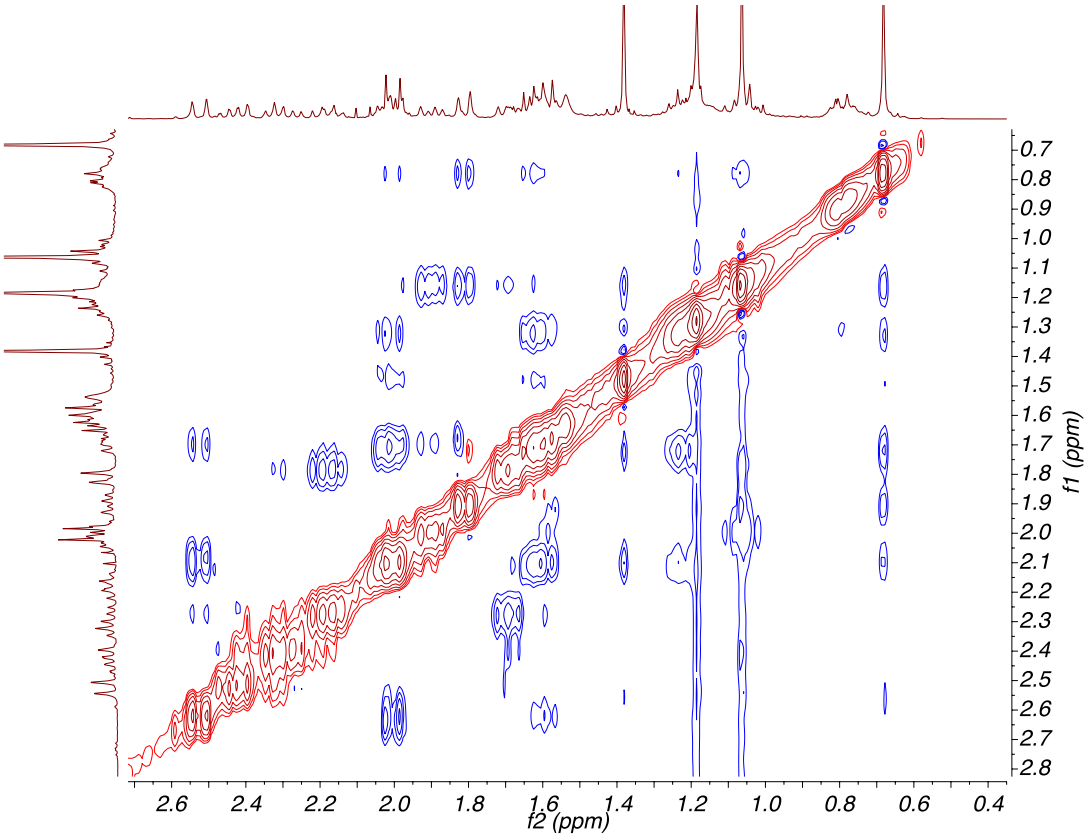

Figure A7.45. NOESY (400 MHz, $CDCl_3$) of compound **198b**.

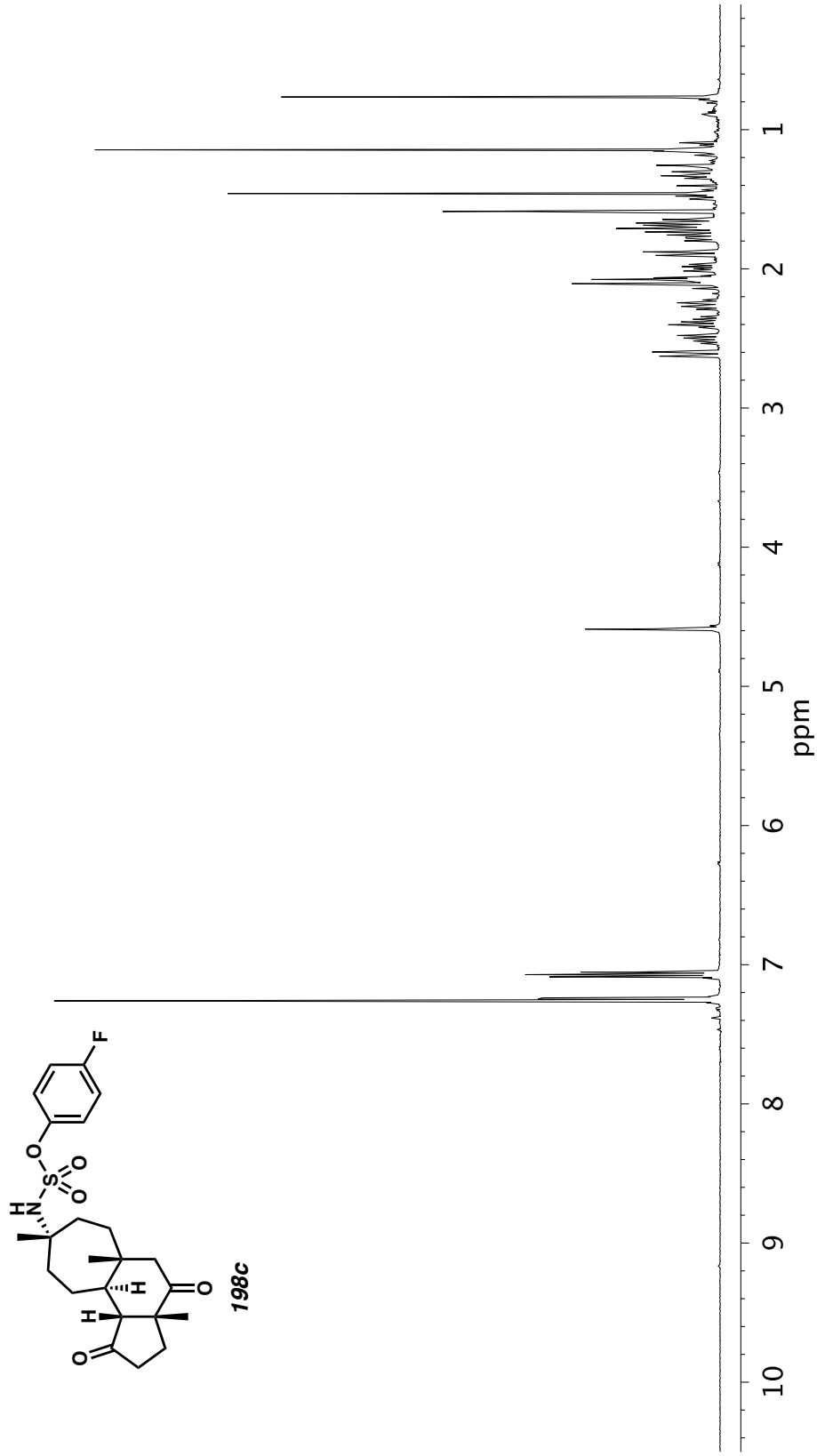

Figure A7.46. ^{1}H NMR (500 MHz, $CDCl_3$) of compound **198c**.

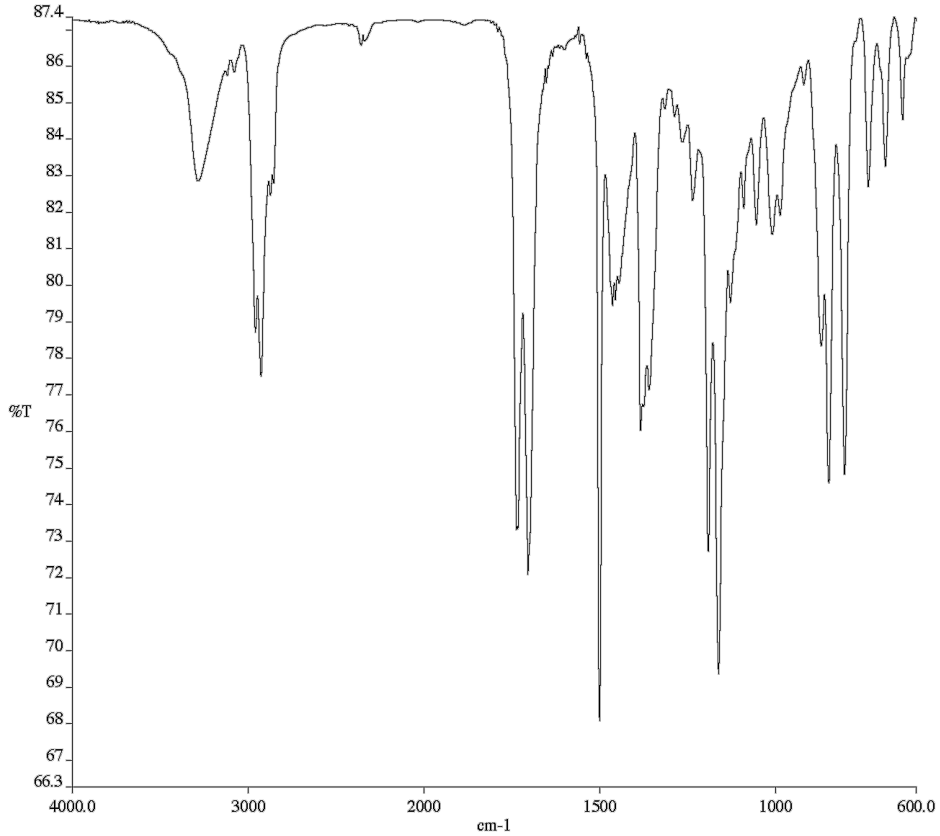

Figure A7.47. Infrared Spectrum (Thin Film, KBr) of compound **198c**.

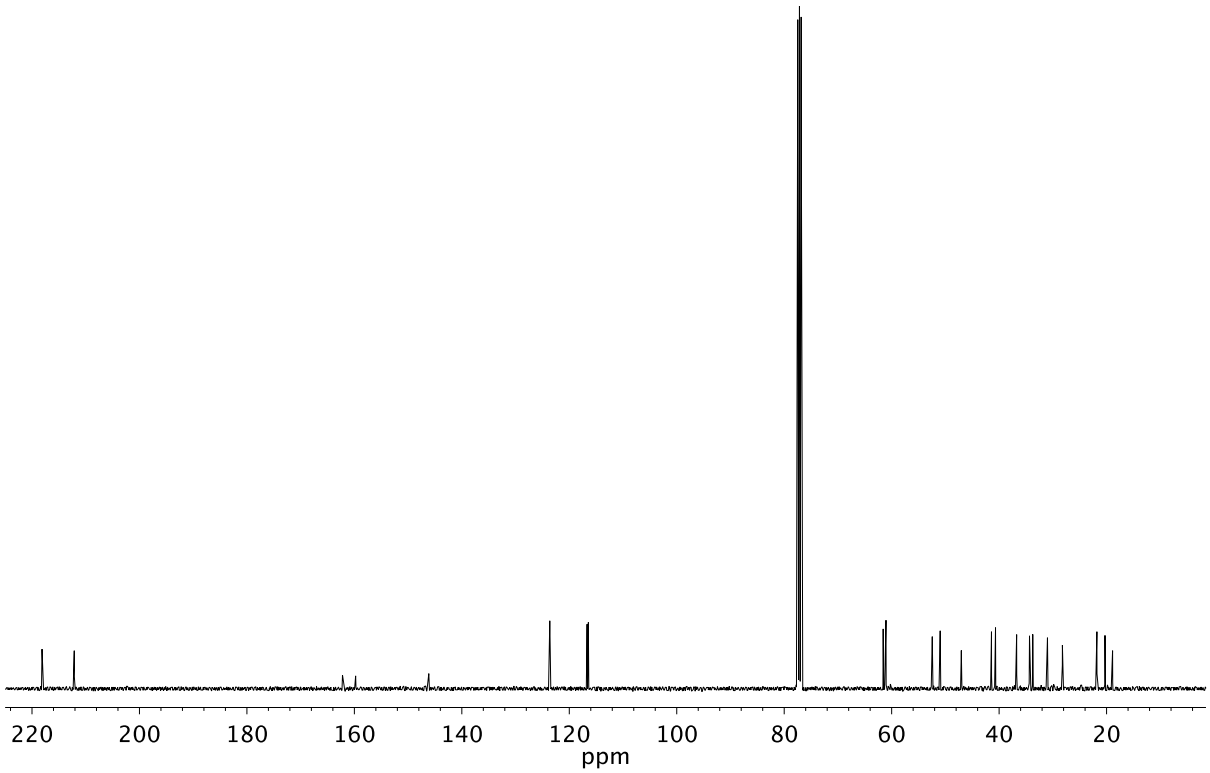

Figure A7.48. ^{13}C NMR (101 MHz, $CDCl_3$) of compound **198c.**

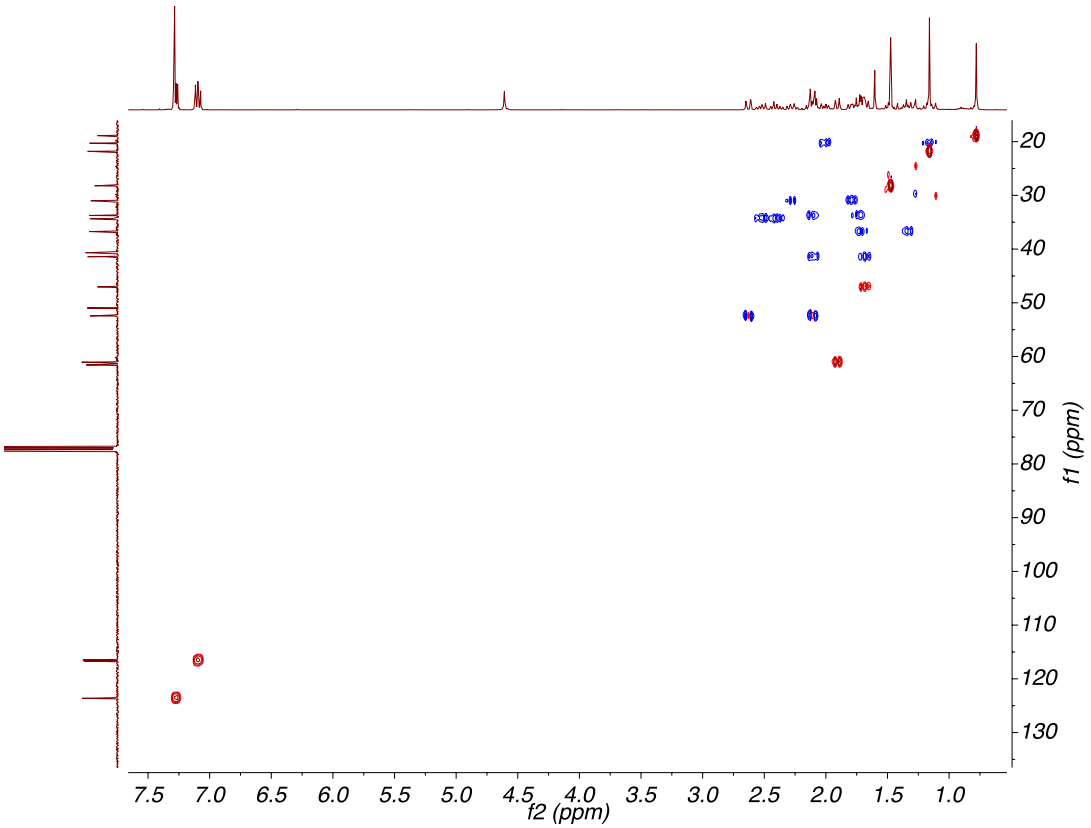

Figure A7.49. HSQC (400, 101 MHz, $CDCl_3$) of compound **198c**.

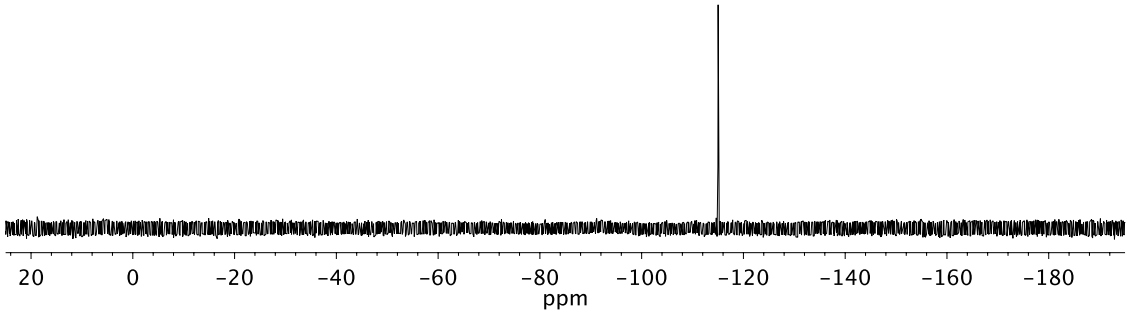

Figure A7.50. ^{19}F NMR (300 MHz, $CDCl_3$) of compound **198c**.

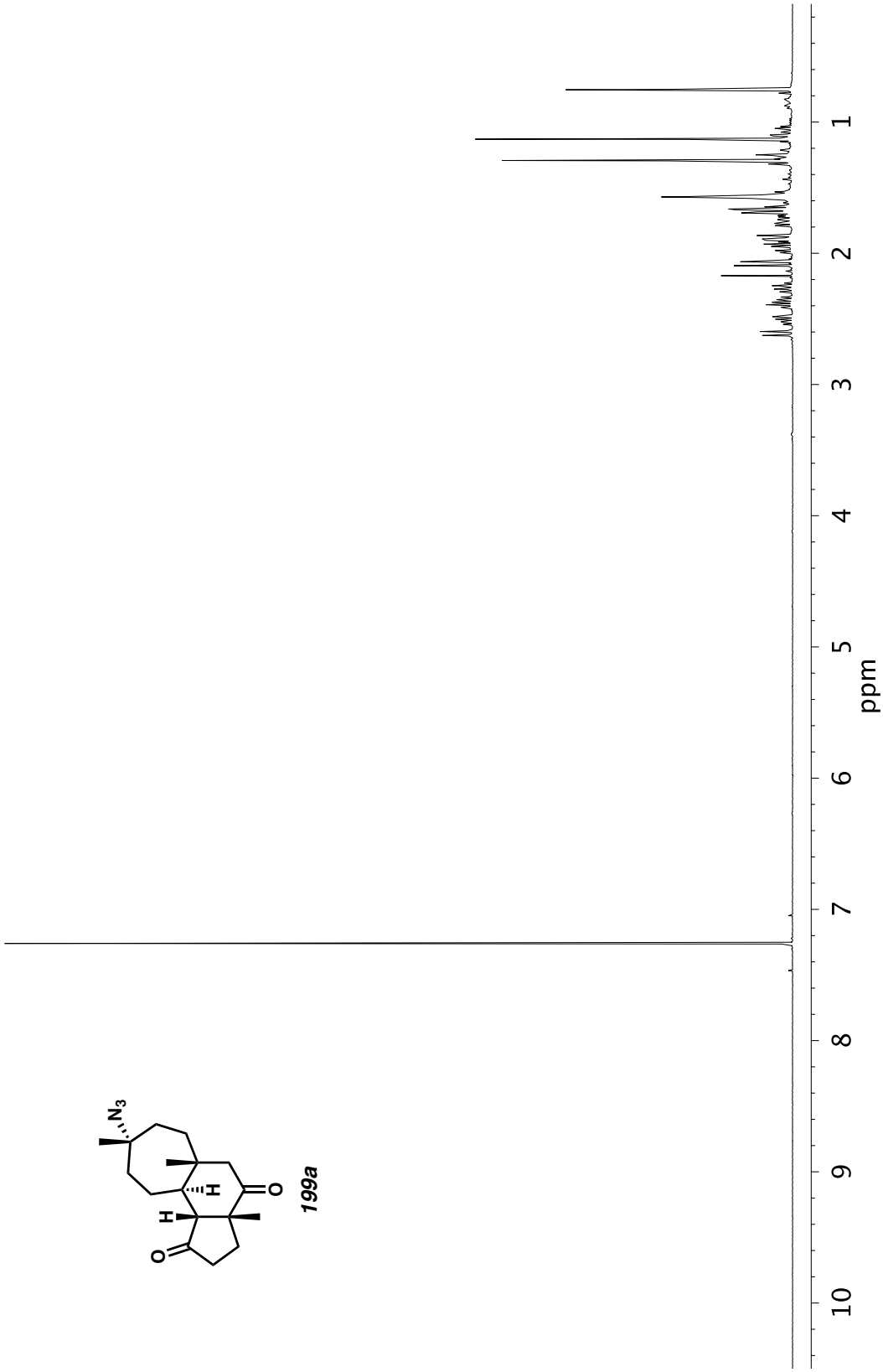

Figure A7.51. ^{1}H NMR (500 MHz, $CDCl_3$) of compound **199a**.

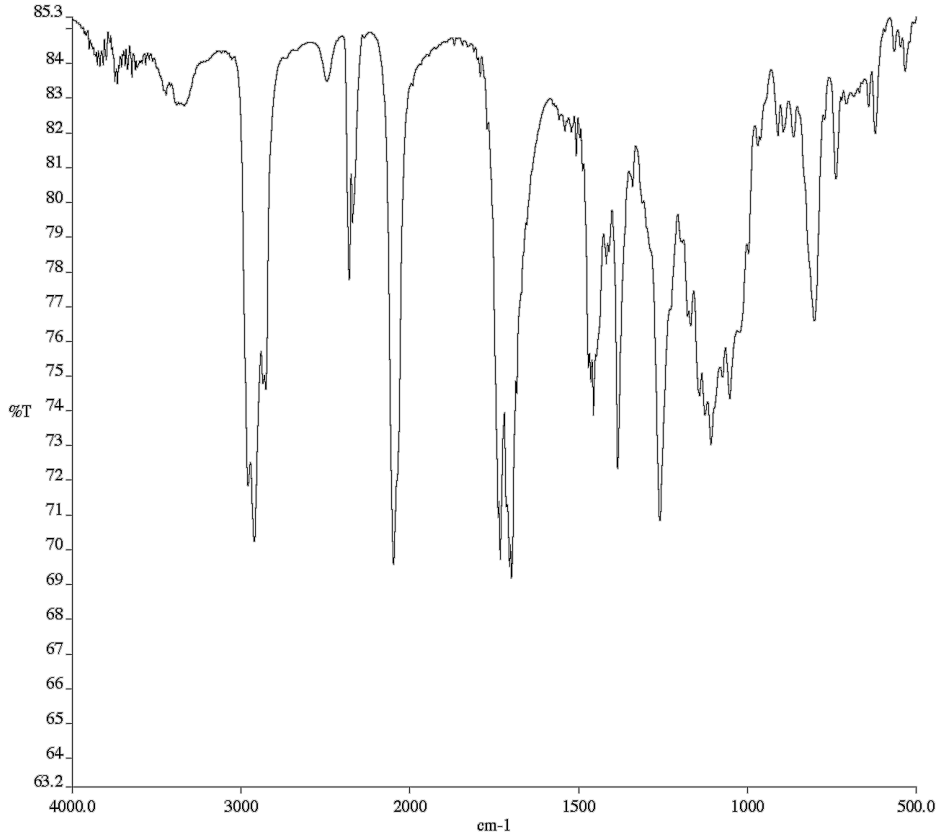

Figure A7.52. Infrared Spectrum (Thin Film, KBr) of compound **199a.**

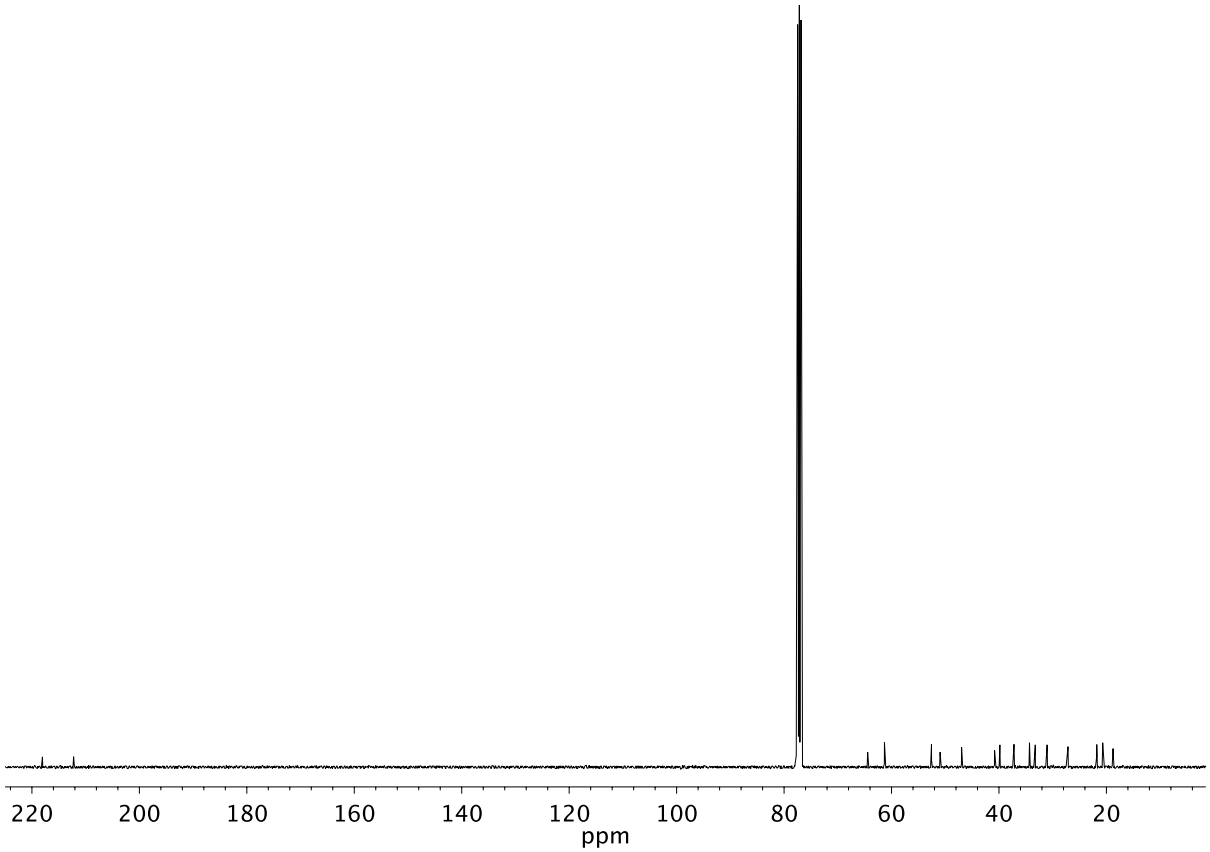

Figure A7.53. ^{13}C NMR (101 MHz, $CDCl_3$) of compound **199a.**

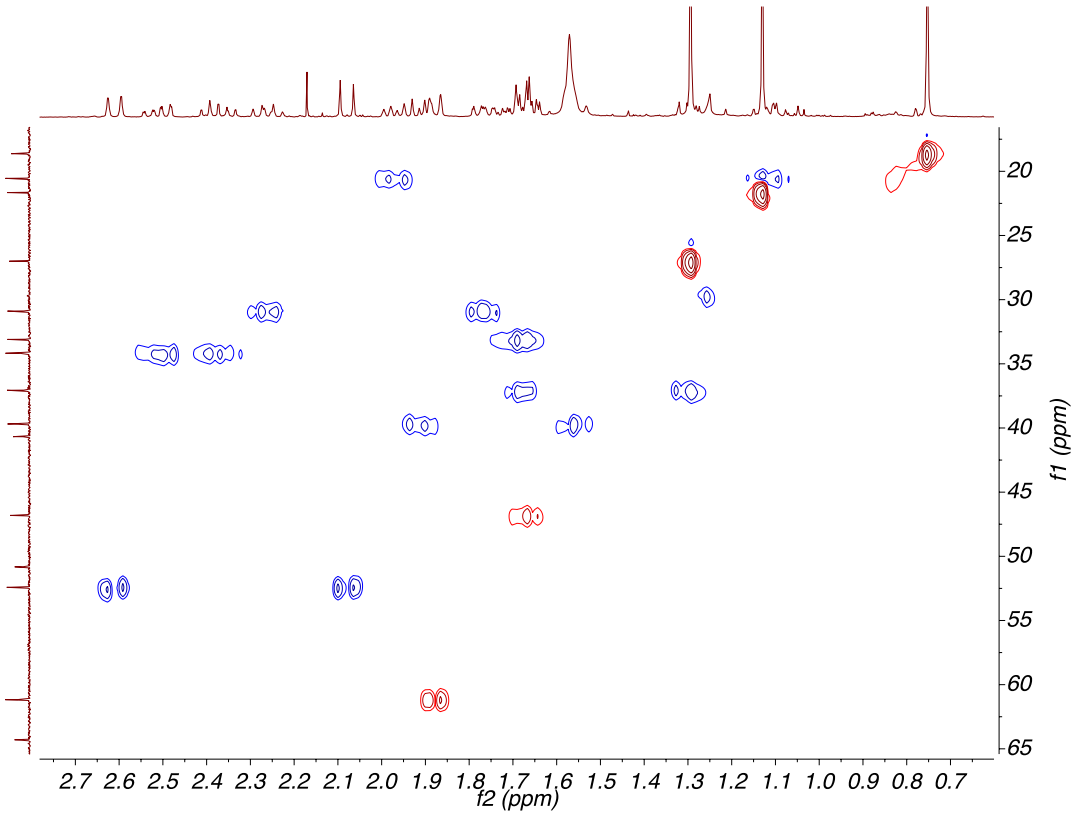

Figure A7.54. HSQC (400, 101 MHz, $CDCl_3$) of compound **199a**.

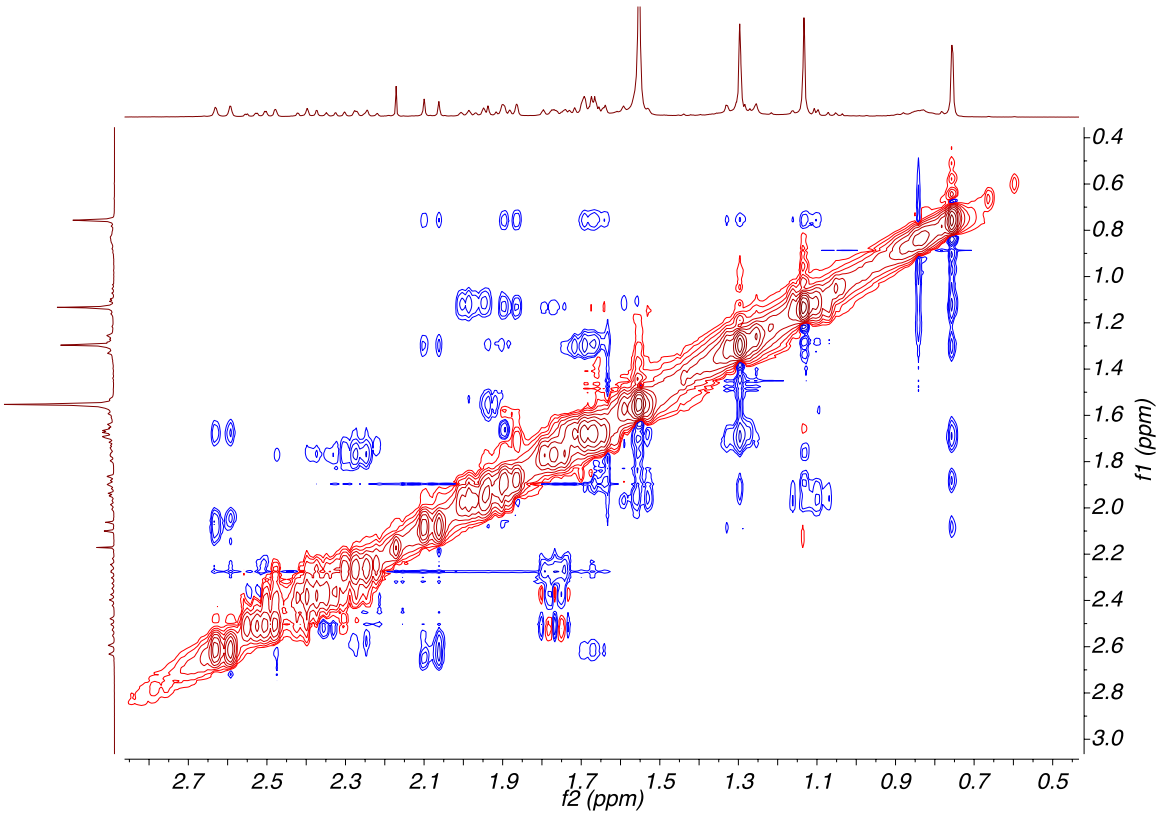

Figure A7.55. NOESY (400 MHz, $CDCl_3$) of compound **199a**.

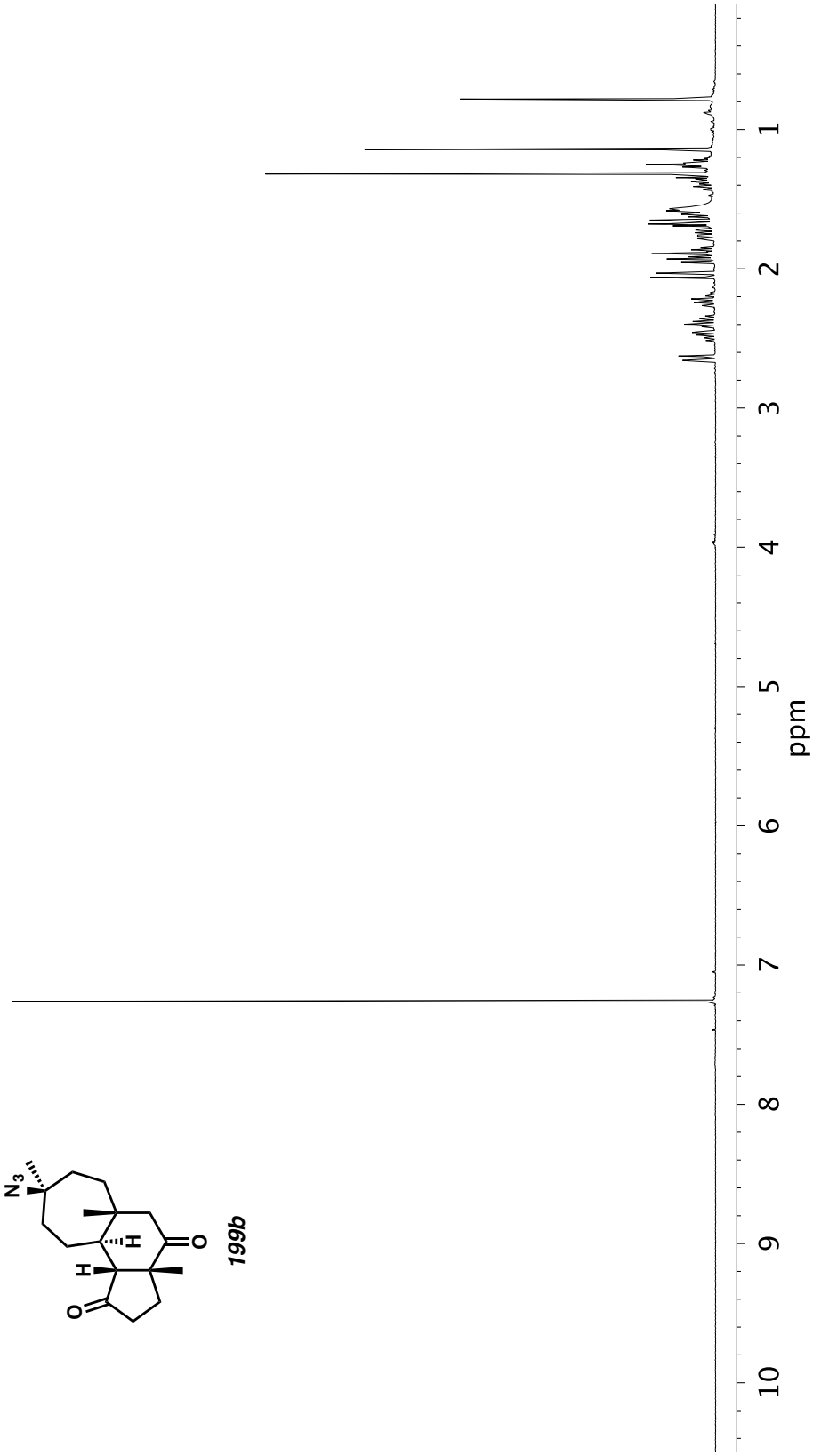

Figure A7.56. ^{1}H NMR (500 MHz, $CDCl_3$) of compound **199b**.

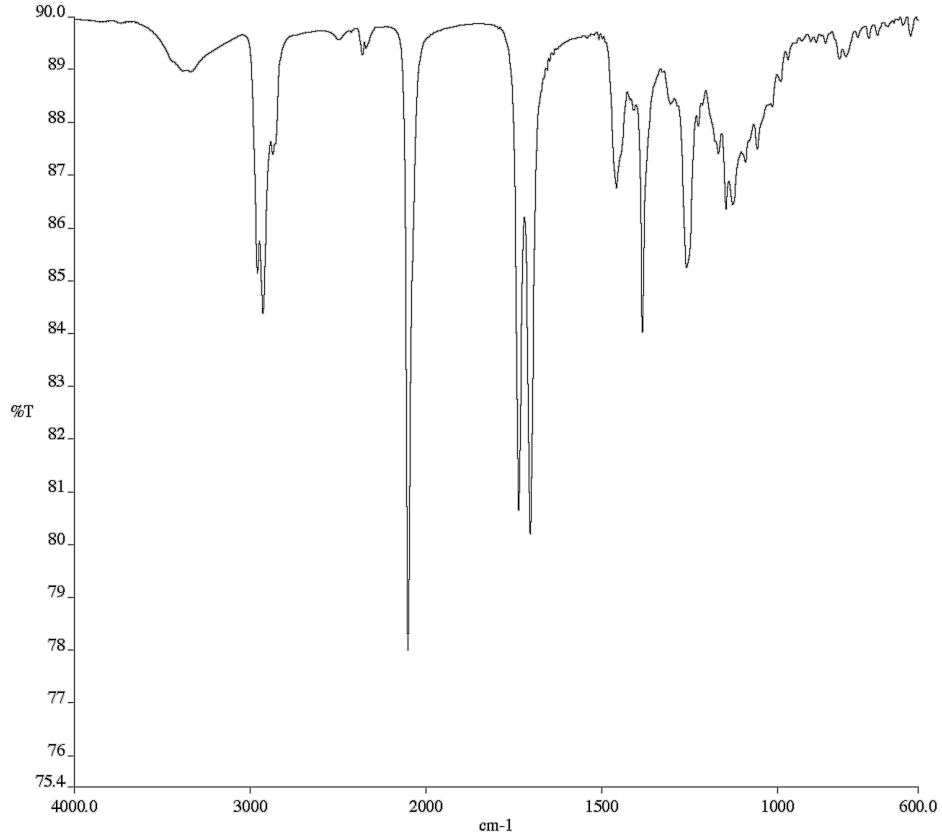

Figure A7.57. Infrared Spectrum (Thin Film, KBr) of compound **199b.**

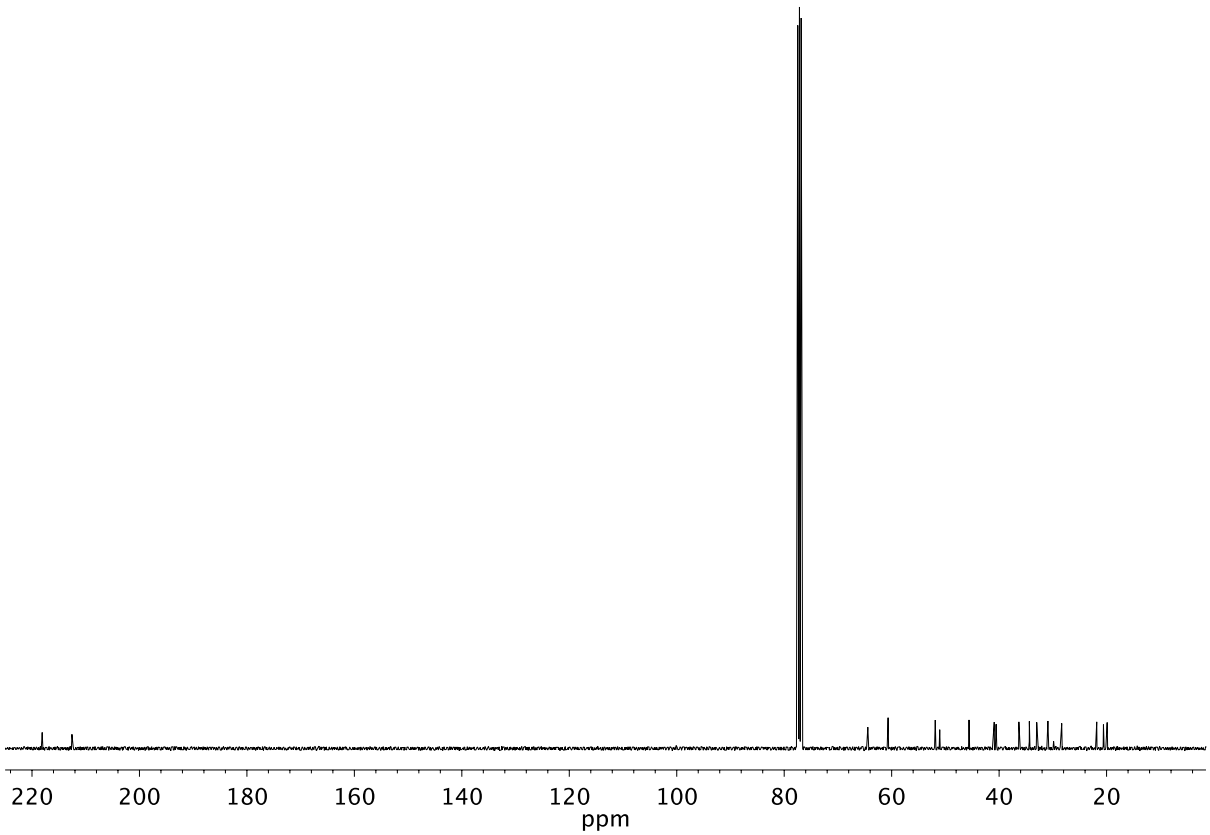

Figure A7.58. ^{13}C NMR (101 MHz, $CDCl_3$) of compound **199b.**

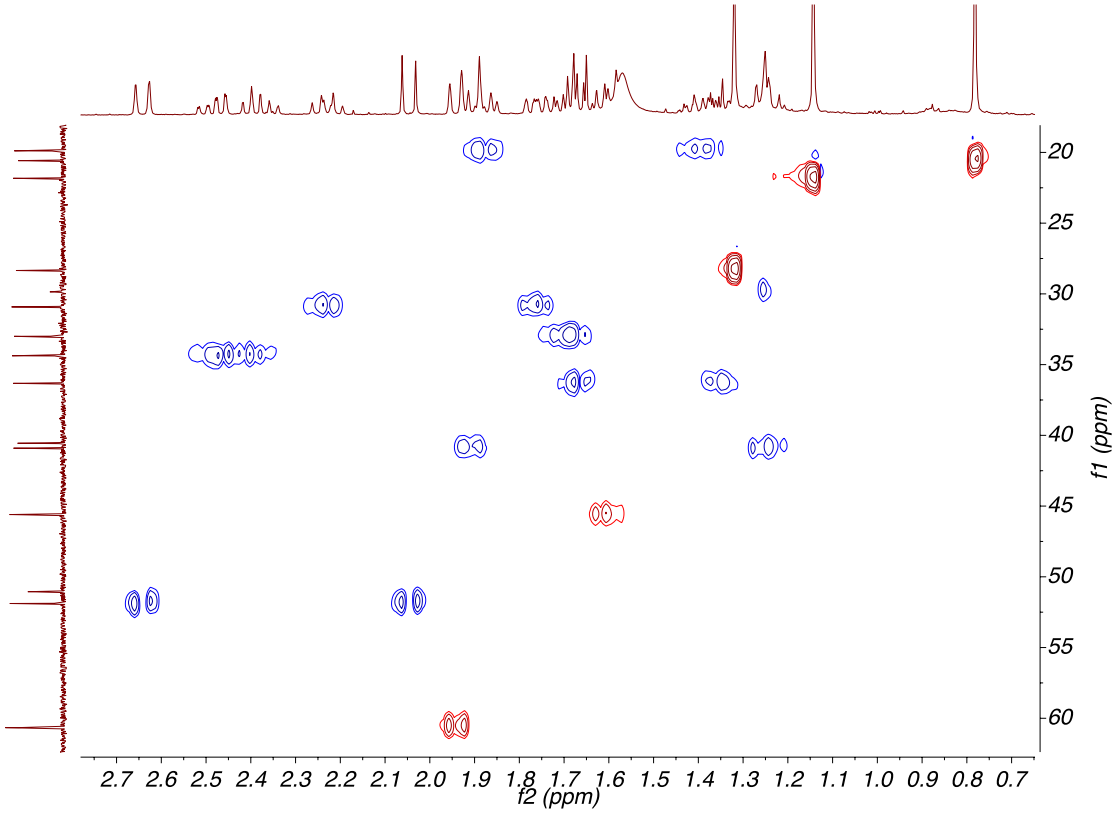

Figure A7.59. HSQC (400, 101 MHz, $CDCl_3$) of compound **199b.**

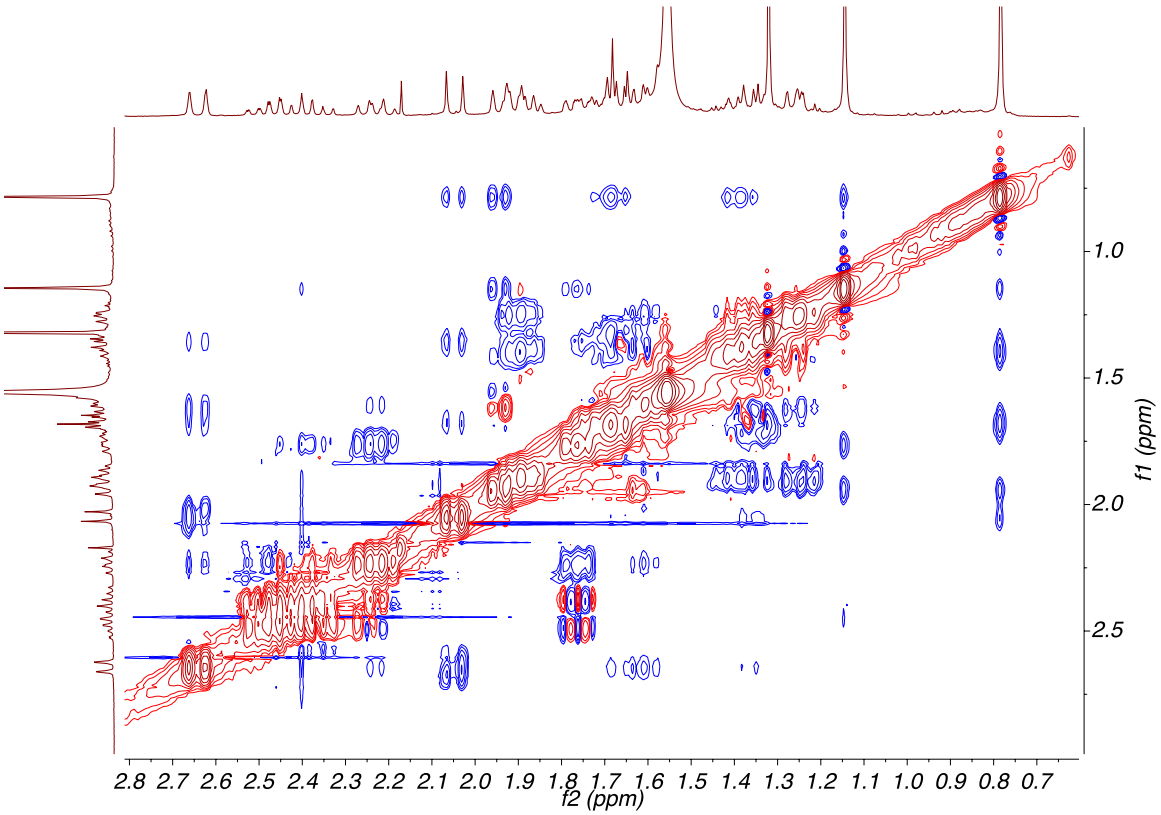

Figure A7.60. NOESY (400 MHz, $CDCl_3$) of compound **199b.**

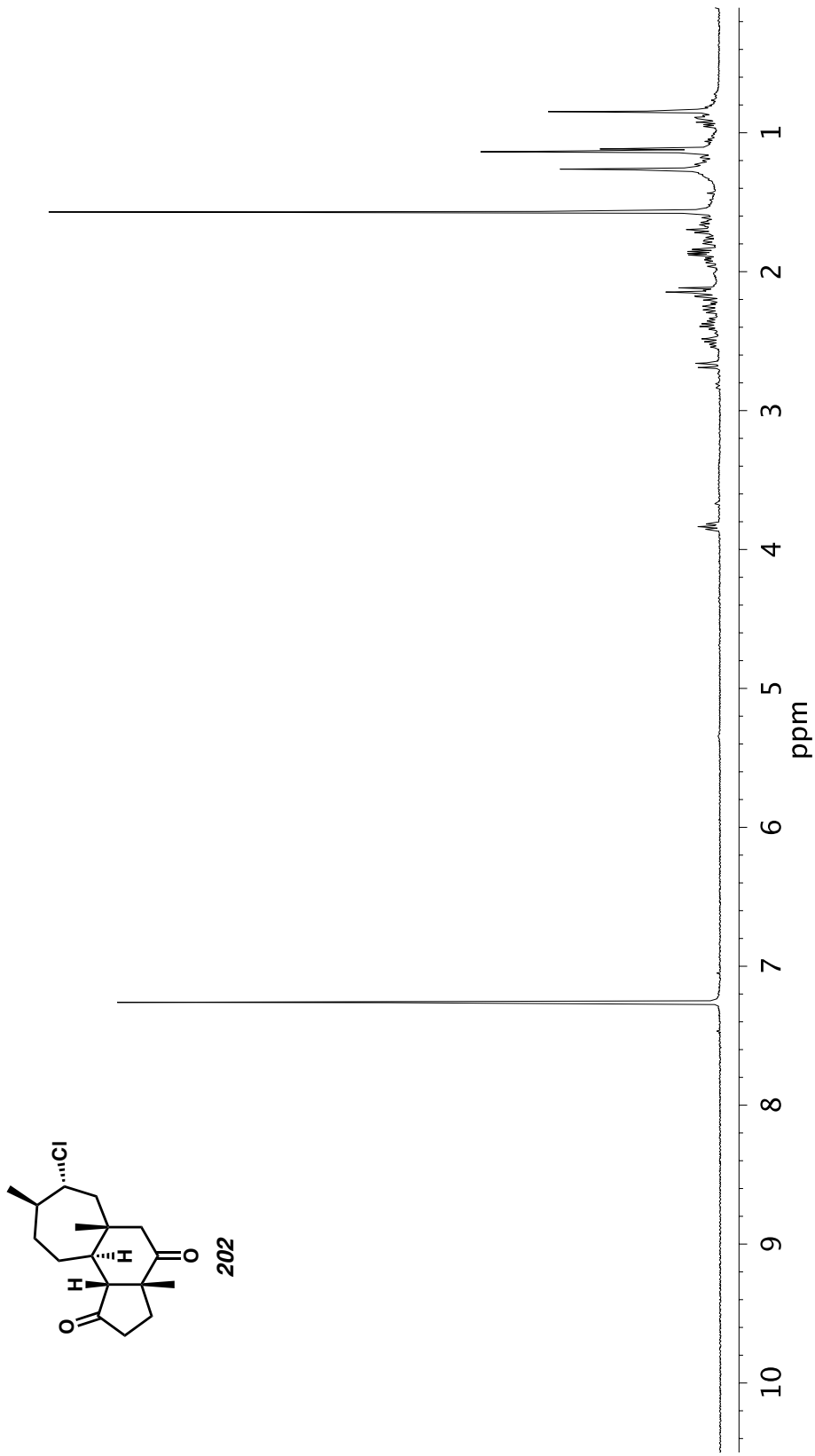

Figure A7.61. ^{1}H NMR (500 MHz, $CDCl_3$) of compound **202**.

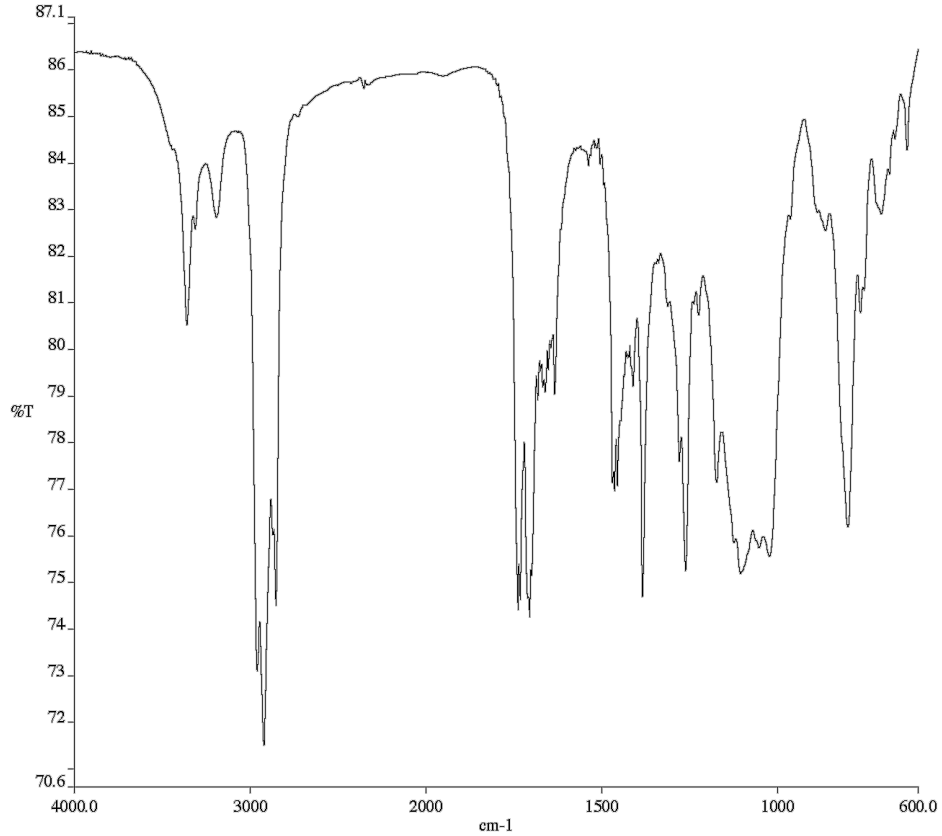

Figure A7.62. Infrared Spectrum (Thin Film, KBr) of compound **202.**

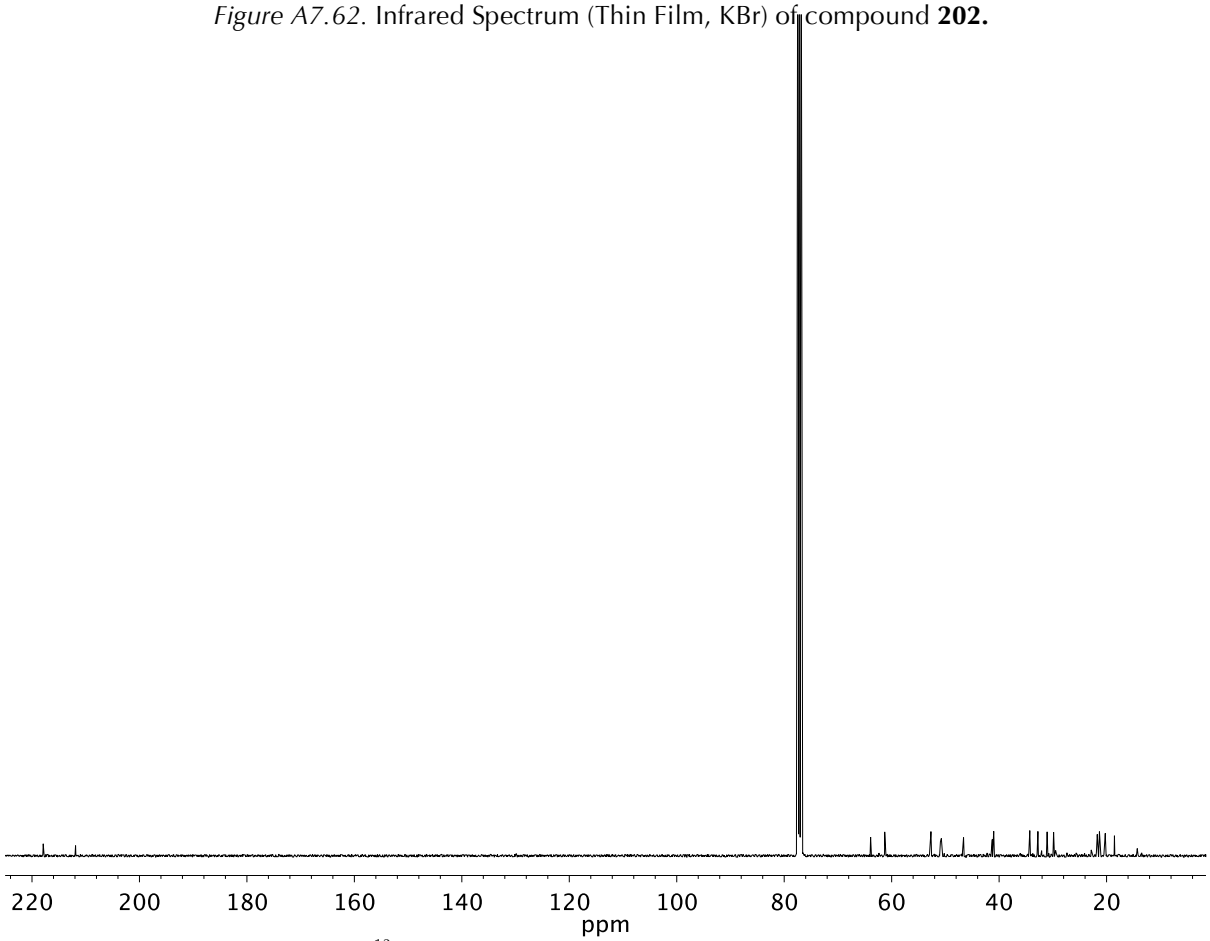

Figure A7.63. ^{13}C NMR (101 MHz, $CDCl_3$) of compound **202.**

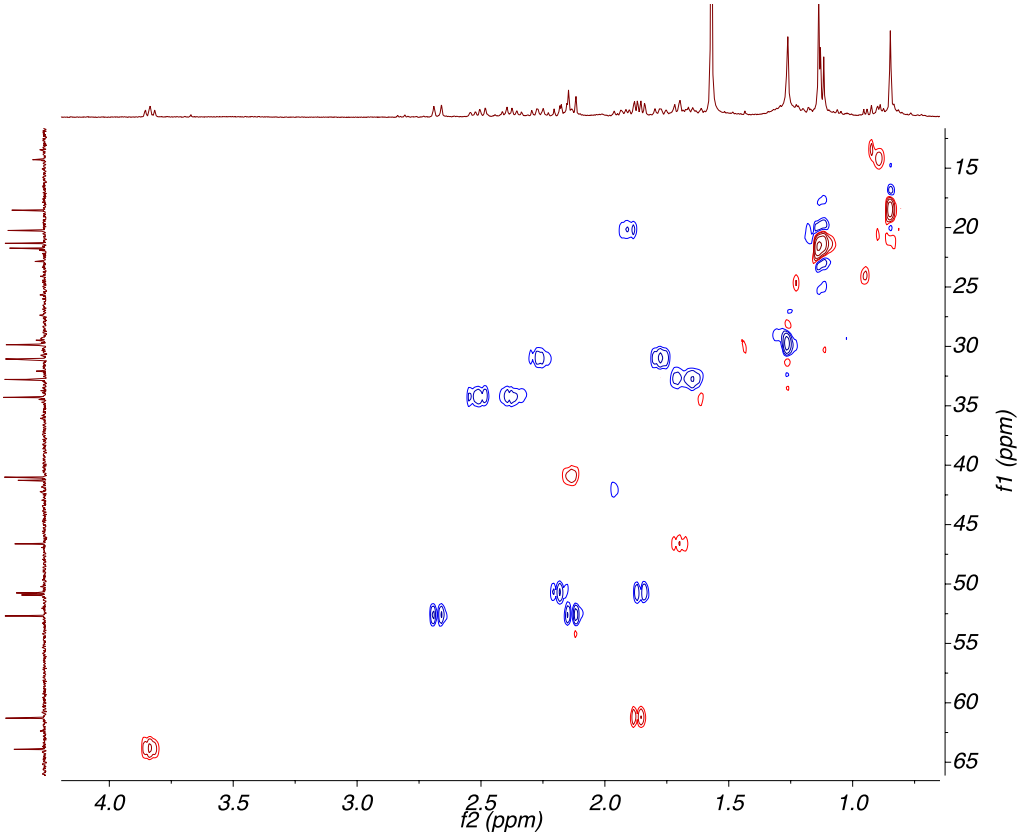

Figure A7.64. HSQC (500, 101 MHz, $CDCl_3$) of compound **202.**

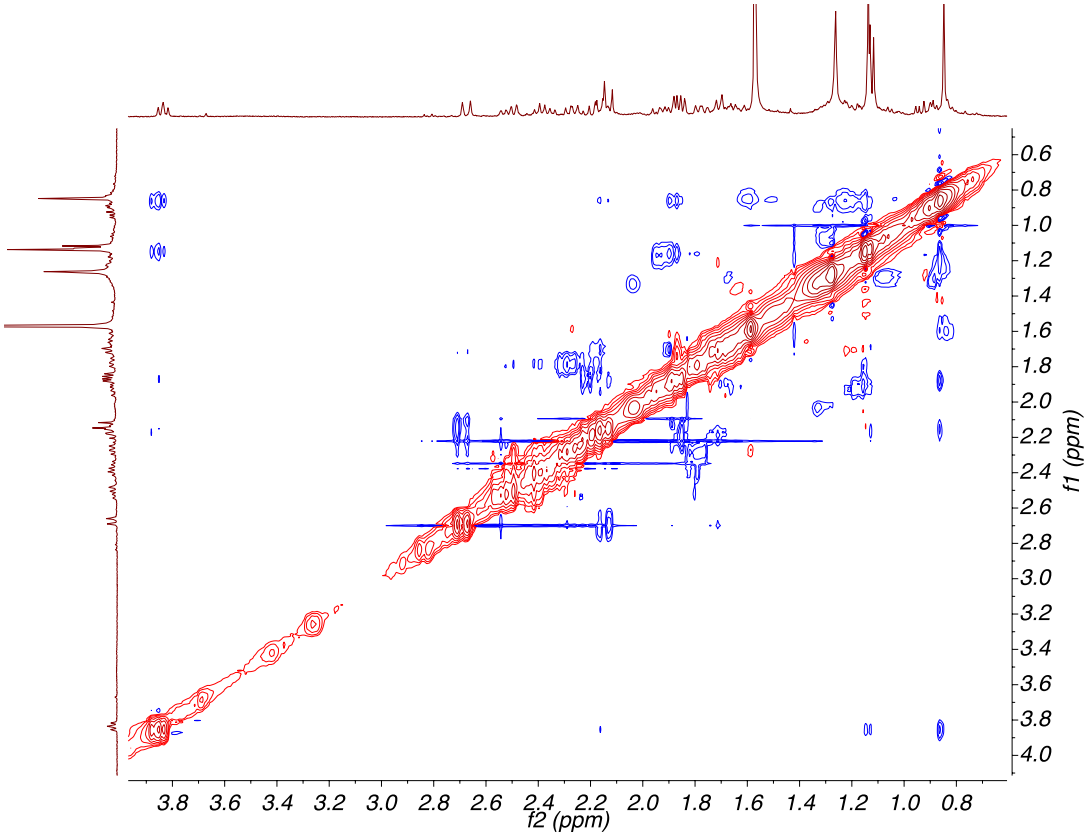

Figure A7.65. NOESY (400 MHz, $CDCl_3$) of compound **202.**

APPENDIX 8

X-Ray Crystallography Reports Relevant to Chapter 4

A8.1 CRYSTAL STRUCTURE ANALYSIS OF DIKETONE 193

Low-temperature diffraction data (ϕ-and ω-scans) were collected on a Bruker AXS D8 VENTURE KAPPA diffractometer coupled to a PHOTON 100 CMOS detector with Cu K_α radiation (λ = 1.54178 Å) from an IμS micro-source for the structure of compound P16423. The structure was solved by direct methods using SHELXS[1] and refined against F^2 on all data by full-matrix least squares with SHELXL-2014[2] using established refinement techniques.[3] All non-hydrogen atoms were refined anisotropically. All hydrogen atoms were included into the model at geometrically calculated positions and refined using a riding model. The isotropic displacement parameters of all hydrogen atoms were fixed to 1.2 times the U value of the atoms they are linked to (1.5 times for methyl groups).

Tricyclic diketone **193** (P16423) crystallizes in the monoclinic space group $P2_1$ with one molecule in the asymmetric unit.

*Table A8.1 Crystal data and structure refinement for tricyclic diketone **193** (P16423).*

Identification code	P16423	
Empirical formula	$C_{17} H_{26} O_2$	
Formula weight	262.38	
Temperature	100(2) K	
Wavelength	1.54178 Å	
Crystal system	Monoclinic	
Space group	$P2_1$	
Unit cell dimensions	a = 9.4497(4) Å	a= 90°.
	b = 6.4699(3) Å	b= 99.507(2)°.
	c = 12.5564(6) Å	g = 90°.
Volume	757.14(6) $Å^3$	
Z	2	
Density (calculated)	1.151 Mg/m^3	
Absorption coefficient	0.569 mm^{-1}	
F(000)	288	
Crystal size	0.350 x 0.050 x 0.050 mm^3	
θ range for data collection	3.569 to 74.508°.	
Index ranges	$-11 \le h \le 11, -8 \le k \le 7, -14 \le l \le 15$	
Reflections collected	8282	
Independent reflections	3039 [$R_{int} = 0.0473$]	
Completeness to θ = 67.679°	99.9 %	
Absorption correction	Semi-empirical from equivalents	
Max. and min. transmission	0.7538 and 0.5623	
Refinement method	Full-matrix least-squares on F^2	
Data / restraints / parameters	3039 / 1 / 175	
Goodness-of-fit on F^2	1.062	
Final R indices [$I>2\sigma(I)$]	R1 = 0.0380, *w*R2 = 0.0898	
R indices (all data)	R1 = 0.0422, *w*R2 = 0.0924	
Absolute structure parameter	-0.23(15)	
Extinction coefficient	n/a	
Largest diff. peak and hole	0.196 and -0.190 $e.Å^{-3}$	

Figure A8.1 ORTEP drawing of tricyclic diketone ***193*** *(P16423) (shown with 50% probability ellipsoids).*

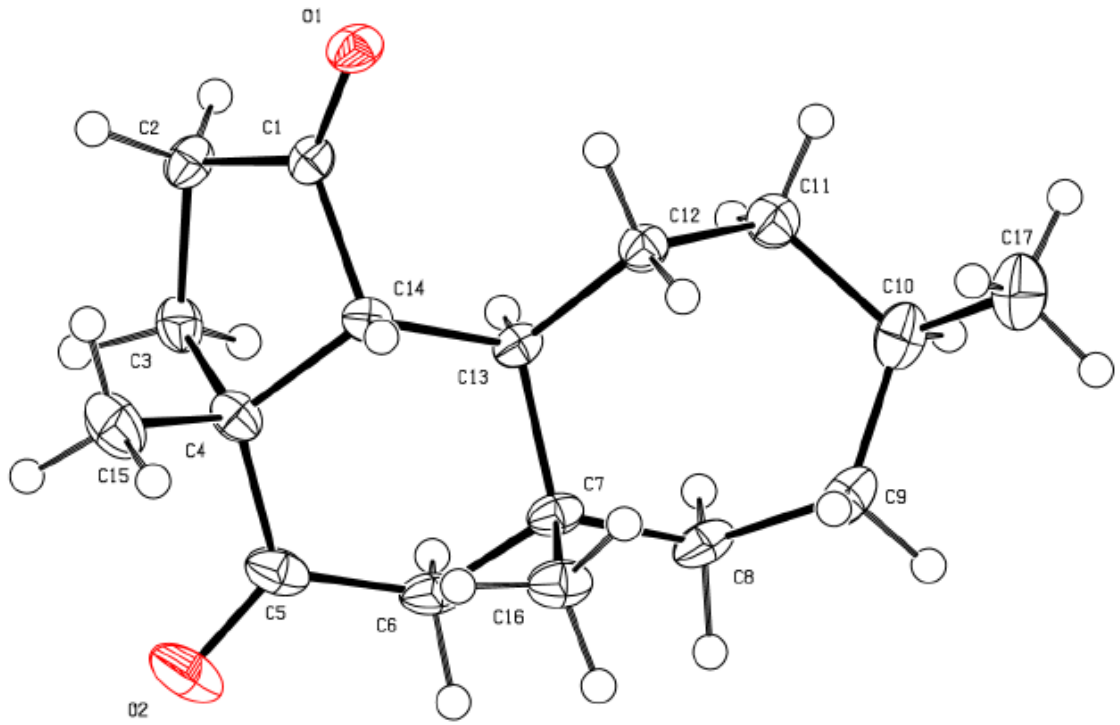

Table A8.2 Atomic coordinates (x 10^4) and equivalent isotropic displacement parameters ($Å^2$x 10^3) for ***193*** *(P16423). U(eq) is defined as one third of the trace of the orthogonalized U^{ij} tensor.*

	x	y	z	U(eq)
C(1)	6553(2)	6937(3)	4492(2)	17(1)
O(1)	6064(2)	8638(2)	4601(1)	23(1)
C(2)	7176(2)	5540(3)	5423(2)	21(1)
C(3)	7566(2)	3544(3)	4893(2)	22(1)
C(4)	7846(2)	4238(3)	3754(2)	21(1)
C(15)	9315(2)	5285(4)	3839(2)	33(1)
C(5)	7780(3)	2338(3)	3043(2)	26(1)
O(2)	8861(2)	1348(3)	2975(2)	46(1)
C(6)	6324(3)	1641(3)	2478(2)	24(1)

C(7)	5353(2)	3429(3)	1991(2)	20(1)
C(16)	6076(3)	4467(3)	1121(2)	25(1)
C(8)	3900(3)	2462(3)	1487(2)	24(1)
C(9)	2816(3)	3881(4)	797(2)	30(1)
C(10)	1790(3)	5062(4)	1403(2)	31(1)
C(17)	1056(3)	6798(5)	691(2)	44(1)
C(11)	2499(2)	5896(4)	2510(2)	25(1)
C(12)	4053(2)	6648(3)	2589(2)	19(1)
C(13)	5175(2)	4943(3)	2917(2)	17(1)
C(14)	6655(2)	5873(3)	3416(2)	17(1)

*Table A8.3 Bond lengths [Å] and angles [°] for **193** (P16423).*

C(1)-O(1)	1.210(3)
C(1)-C(2)	1.517(3)
C(1)-C(14)	1.534(3)
C(2)-C(3)	1.526(3)
C(2)-H(2A)	0.9900
C(2)-H(2B)	0.9900
C(3)-C(4)	1.562(3)
C(3)-H(3A)	0.9900
C(3)-H(3B)	0.9900
C(4)-C(5)	1.514(3)
C(4)-C(15)	1.533(3)
C(4)-C(14)	1.551(3)
C(15)-H(15A)	0.9800
C(15)-H(15B)	0.9800
C(15)-H(15C)	0.9800
C(5)-O(2)	1.221(3)
C(5)-C(6)	1.510(3)
C(6)-C(7)	1.539(3)
C(6)-H(6A)	0.9900
C(6)-H(6B)	0.9900
C(7)-C(16)	1.536(3)

C(7)-C(8)	1.546(3)
C(7)-C(13)	1.550(3)
C(16)-H(16A)	0.9800
C(16)-H(16B)	0.9800
C(16)-H(16C)	0.9800
C(8)-C(9)	1.532(3)
C(8)-H(8A)	0.9900
C(8)-H(8B)	0.9900
C(9)-C(10)	1.532(4)
C(9)-H(9A)	0.9900
C(9)-H(9B)	0.9900
C(10)-C(17)	1.529(4)
C(10)-C(11)	1.537(3)
C(10)-H(10)	1.0000
C(17)-H(17A)	0.9800
C(17)-H(17B)	0.9800
C(17)-H(17C)	0.9800
C(11)-C(12)	1.535(3)
C(11)-H(11A)	0.9900
C(11)-H(11B)	0.9900
C(12)-C(13)	1.538(3)
C(12)-H(12A)	0.9900
C(12)-H(12B)	0.9900
C(13)-C(14)	1.556(3)
C(13)-H(13)	1.0000
C(14)-H(14)	1.0000

O(1)-C(1)-C(2)	124.14(19)
O(1)-C(1)-C(14)	126.07(19)
C(2)-C(1)-C(14)	109.78(16)
C(1)-C(2)-C(3)	104.98(17)
C(1)-C(2)-H(2A)	110.7
C(3)-C(2)-H(2A)	110.7
C(1)-C(2)-H(2B)	110.7
C(3)-C(2)-H(2B)	110.7
H(2A)-C(2)-H(2B)	108.8

C(2)-C(3)-C(4)	104.26(17)
C(2)-C(3)-H(3A)	110.9
C(4)-C(3)-H(3A)	110.9
C(2)-C(3)-H(3B)	110.9
C(4)-C(3)-H(3B)	110.9
H(3A)-C(3)-H(3B)	108.9
C(5)-C(4)-C(15)	110.38(18)
C(5)-C(4)-C(14)	115.78(18)
C(15)-C(4)-C(14)	109.01(17)
C(5)-C(4)-C(3)	108.03(17)
C(15)-C(4)-C(3)	110.57(19)
C(14)-C(4)-C(3)	102.79(16)
C(4)-C(15)-H(15A)	109.5
C(4)-C(15)-H(15B)	109.5
H(15A)-C(15)-H(15B)	109.5
C(4)-C(15)-H(15C)	109.5
H(15A)-C(15)-H(15C)	109.5
H(15B)-C(15)-H(15C)	109.5
O(2)-C(5)-C(6)	121.2(2)
O(2)-C(5)-C(4)	121.0(2)
C(6)-C(5)-C(4)	117.72(18)
C(5)-C(6)-C(7)	113.55(18)
C(5)-C(6)-H(6A)	108.9
C(7)-C(6)-H(6A)	108.9
C(5)-C(6)-H(6B)	108.9
C(7)-C(6)-H(6B)	108.9
H(6A)-C(6)-H(6B)	107.7
C(16)-C(7)-C(6)	107.78(17)
C(16)-C(7)-C(8)	110.77(18)
C(6)-C(7)-C(8)	106.84(17)
C(16)-C(7)-C(13)	111.89(16)
C(6)-C(7)-C(13)	107.98(16)
C(8)-C(7)-C(13)	111.35(17)
C(7)-C(16)-H(16A)	109.5
C(7)-C(16)-H(16B)	109.5
H(16A)-C(16)-H(16B)	109.5

C(7)-C(16)-H(16C)	109.5
H(16A)-C(16)-H(16C)	109.5
H(16B)-C(16)-H(16C)	109.5
C(9)-C(8)-C(7)	117.05(18)
C(9)-C(8)-H(8A)	108.0
C(7)-C(8)-H(8A)	108.0
C(9)-C(8)-H(8B)	108.0
C(7)-C(8)-H(8B)	108.0
H(8A)-C(8)-H(8B)	107.3
C(10)-C(9)-C(8)	115.9(2)
C(10)-C(9)-H(9A)	108.3
C(8)-C(9)-H(9A)	108.3
C(10)-C(9)-H(9B)	108.3
C(8)-C(9)-H(9B)	108.3
H(9A)-C(9)-H(9B)	107.4
C(17)-C(10)-C(9)	109.8(2)
C(17)-C(10)-C(11)	111.0(2)
C(9)-C(10)-C(11)	114.03(19)
C(17)-C(10)-H(10)	107.2
C(9)-C(10)-H(10)	107.2
C(11)-C(10)-H(10)	107.2
C(10)-C(17)-H(17A)	109.5
C(10)-C(17)-H(17B)	109.5
H(17A)-C(17)-H(17B)	109.5
C(10)-C(17)-H(17C)	109.5
H(17A)-C(17)-H(17C)	109.5
H(17B)-C(17)-H(17C)	109.5
C(12)-C(11)-C(10)	116.08(19)
C(12)-C(11)-H(11A)	108.3
C(10)-C(11)-H(11A)	108.3
C(12)-C(11)-H(11B)	108.3
C(10)-C(11)-H(11B)	108.3
H(11A)-C(11)-H(11B)	107.4
C(11)-C(12)-C(13)	113.59(17)
C(11)-C(12)-H(12A)	108.8
C(13)-C(12)-H(12A)	108.8

C(11)-C(12)-H(12B)	108.8
C(13)-C(12)-H(12B)	108.8
H(12A)-C(12)-H(12B)	107.7
C(12)-C(13)-C(7)	114.06(17)
C(12)-C(13)-C(14)	111.38(15)
C(7)-C(13)-C(14)	110.18(16)
C(12)-C(13)-H(13)	106.9
C(7)-C(13)-H(13)	106.9
C(14)-C(13)-H(13)	106.9
C(1)-C(14)-C(4)	102.32(16)
C(1)-C(14)-C(13)	110.22(15)
C(4)-C(14)-C(13)	114.19(16)
C(1)-C(14)-H(14)	110.0
C(4)-C(14)-H(14)	110.0
C(13)-C(14)-H(14)	110.0

Symmetry transformations used to generate equivalent atoms:

*Table A8.4 Anisotropic displacement parameters ($Å^2 x\ 10^3$) for **193** (P16423). The anisotropic displacement factor exponent takes the form: $-2p^2[\ h^2\ a^{*2}U^{11} + \ldots + 2\ h\ k\ a^*\ b^*\ U^{12}\ ]$*

	U^{11}	U^{22}	U^{33}	U^{23}	U^{13}	U^{12}
C(1)	16(1)	15(1)	19(1)	-1(1)	3(1)	-6(1)
O(1)	30(1)	14(1)	23(1)	-2(1)	3(1)	-1(1)
C(2)	24(1)	19(1)	18(1)	0(1)	1(1)	-4(1)
C(3)	21(1)	19(1)	24(1)	4(1)	0(1)	2(1)
C(4)	18(1)	20(1)	26(1)	2(1)	6(1)	1(1)
C(15)	20(1)	33(1)	47(2)	2(1)	10(1)	-1(1)
C(5)	33(1)	21(1)	27(1)	4(1)	12(1)	8(1)
O(2)	37(1)	43(1)	60(1)	-8(1)	12(1)	19(1)
C(6)	38(1)	13(1)	21(1)	-1(1)	8(1)	4(1)
C(7)	31(1)	13(1)	15(1)	0(1)	6(1)	0(1)
C(16)	38(1)	21(1)	20(1)	2(1)	11(1)	2(1)
C(8)	36(1)	18(1)	18(1)	-4(1)	4(1)	-4(1)
C(9)	36(1)	32(1)	19(1)	-2(1)	-2(1)	-4(1)
C(10)	26(1)	35(1)	30(1)	-1(1)	-2(1)	-6(1)

C(17)	38(1)	52(2)	37(2)	2(1)	-8(1)	8(1)
C(11)	24(1)	28(1)	24(1)	-1(1)	4(1)	0(1)
C(12)	22(1)	17(1)	19(1)	0(1)	3(1)	-1(1)
C(13)	23(1)	13(1)	14(1)	0(1)	3(1)	-2(1)
C(14)	21(1)	11(1)	18(1)	2(1)	6(1)	0(1)

*Table A8.5 Hydrogen coordinates (x 10^4) and isotropic displacement parameters (Å^{2}x 10^3) for **193** (P16423).*

	x	y	z	U(eq)
H(2A)	6460	5271	5900	25
H(2B)	8037	6175	5856	25
H(3A)	6769	2536	4829	26
H(3B)	8437	2911	5314	26
H(15A)	10069	4302	4132	49
H(15B)	9353	6485	4319	49
H(15C)	9464	5737	3121	49
H(6A)	5838	884	3000	28
H(6B)	6454	667	1894	28
H(16A)	7081	4766	1417	38
H(16B)	5576	5759	891	38
H(16C)	6032	3539	500	38
H(8A)	4097	1280	1033	29
H(8B)	3441	1901	2079	29
H(9A)	3354	4899	432	35
H(9B)	2237	3034	229	35
H(10)	1024	4071	1534	37
H(17A)	1759	7878	613	66
H(17B)	281	7386	1025	66
H(17C)	660	6243	-22	66
H(11A)	1911	7058	2706	30
H(11B)	2476	4793	3053	30
H(12A)	4221	7781	3125	23

H(12B)	4188	7219	1881	23
H(13)	4835	4109	3496	20
H(14)	6974	6887	2904	20

*Table A8.6 Torsion angles [°] for **193** (P16423).*

O(1)-C(1)-C(2)-C(3)	176.75(19)
C(14)-C(1)-C(2)-C(3)	-3.7(2)
C(1)-C(2)-C(3)-C(4)	26.6(2)
C(2)-C(3)-C(4)-C(5)	-162.43(17)
C(2)-C(3)-C(4)-C(15)	76.7(2)
C(2)-C(3)-C(4)-C(14)	-39.6(2)
C(15)-C(4)-C(5)-O(2)	29.3(3)
C(14)-C(4)-C(5)-O(2)	153.7(2)
C(3)-C(4)-C(5)-O(2)	-91.7(3)
C(15)-C(4)-C(5)-C(6)	-154.3(2)
C(14)-C(4)-C(5)-C(6)	-29.9(3)
C(3)-C(4)-C(5)-C(6)	84.7(2)
O(2)-C(5)-C(6)-C(7)	-141.1(2)
C(4)-C(5)-C(6)-C(7)	42.5(3)
C(5)-C(6)-C(7)-C(16)	63.0(2)
C(5)-C(6)-C(7)-C(8)	-177.92(18)
C(5)-C(6)-C(7)-C(13)	-58.0(2)
C(16)-C(7)-C(8)-C(9)	-53.9(3)
C(6)-C(7)-C(8)-C(9)	-171.00(19)
C(13)-C(7)-C(8)-C(9)	71.3(2)
C(7)-C(8)-C(9)-C(10)	-89.1(3)
C(8)-C(9)-C(10)-C(17)	165.3(2)
C(8)-C(9)-C(10)-C(11)	40.1(3)
C(17)-C(10)-C(11)-C(12)	-88.9(3)
C(9)-C(10)-C(11)-C(12)	35.7(3)
C(10)-C(11)-C(12)-C(13)	-89.5(2)
C(11)-C(12)-C(13)-C(7)	76.8(2)
C(11)-C(12)-C(13)-C(14)	-157.72(17)
C(16)-C(7)-C(13)-C(12)	70.1(2)

C(6)-C(7)-C(13)-C(12)	-171.45(17)
C(8)-C(7)-C(13)-C(12)	-54.5(2)
C(16)-C(7)-C(13)-C(14)	-56.0(2)
C(6)-C(7)-C(13)-C(14)	62.4(2)
C(8)-C(7)-C(13)-C(14)	179.42(16)
O(1)-C(1)-C(14)-C(4)	158.91(19)
C(2)-C(1)-C(14)-C(4)	-20.66(19)
O(1)-C(1)-C(14)-C(13)	-79.3(2)
C(2)-C(1)-C(14)-C(13)	101.17(18)
C(5)-C(4)-C(14)-C(1)	153.68(17)
C(15)-C(4)-C(14)-C(1)	-81.2(2)
C(3)-C(4)-C(14)-C(1)	36.16(18)
C(5)-C(4)-C(14)-C(13)	34.6(2)
C(15)-C(4)-C(14)-C(13)	159.74(18)
C(3)-C(4)-C(14)-C(13)	-82.9(2)
C(12)-C(13)-C(14)-C(1)	66.2(2)
C(7)-C(13)-C(14)-C(1)	-166.21(15)
C(12)-C(13)-C(14)-C(4)	-179.32(17)
C(7)-C(13)-C(14)-C(4)	-51.7(2)

A8.2 NOTES AND REFERENCES

(1) Sheldrick, G. M. *Acta. Cryst.* **1990**, A46, 467–473.

(2) Sheldrick, G. M. *Acta Cryst.* **2008**, A64, 112–122.

(3) Müller, P. *Crystallography Reviews* **2009**, *15*, 57–83.

APPENDIX 9

Spectra Relevant to Appendix 6:

Synthetic Summary for Chapter 4

and Further C–H Functionalization Studies

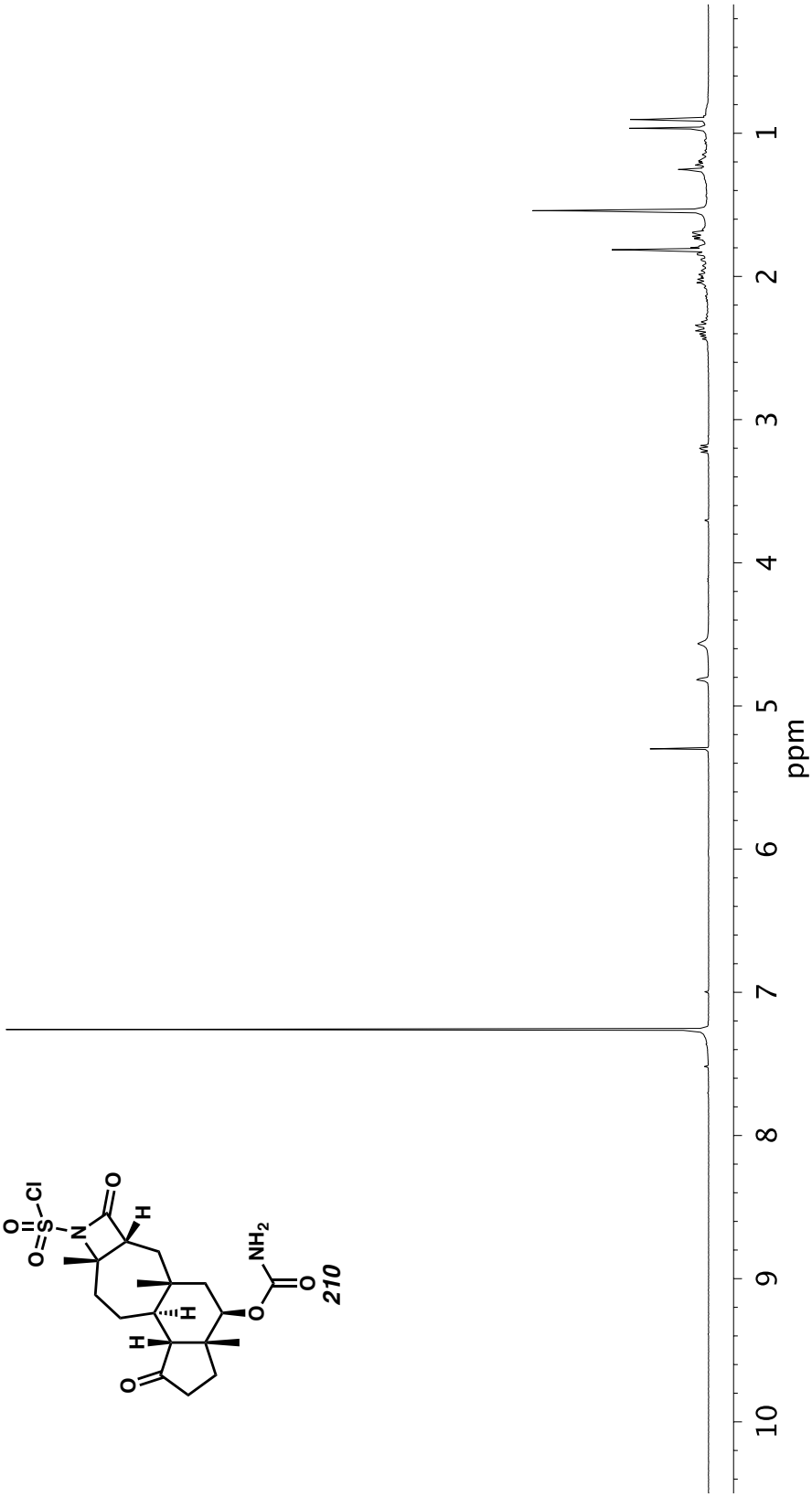

Figure A9.1. ^{1}H NMR (400 MHz, $CDCl_3$) of compound **210**.

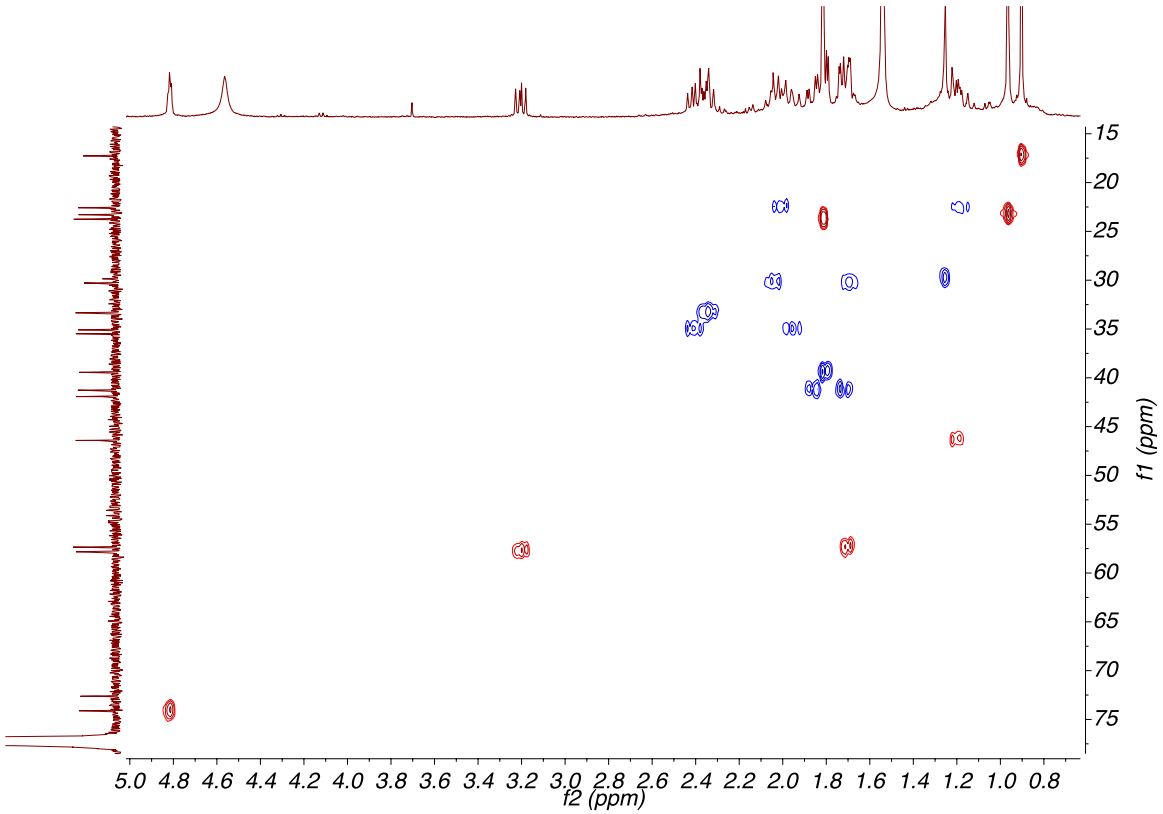

Figure A9.2. HSQC (400, 101 MHz, $CDCl_3$) of compound **210**.

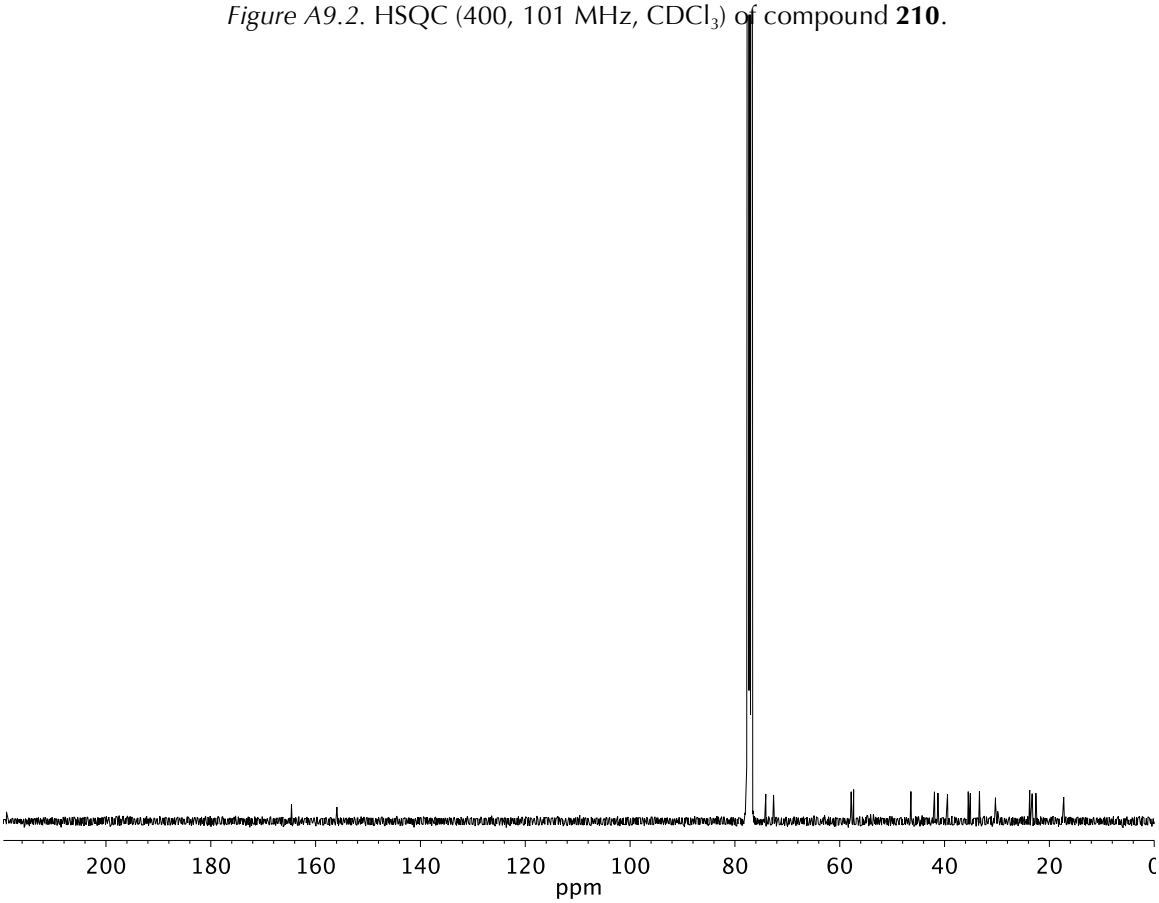

Figure A9.3. ^{13}C NMR (101 MHz, $CDCl_3$) of compound **210**.

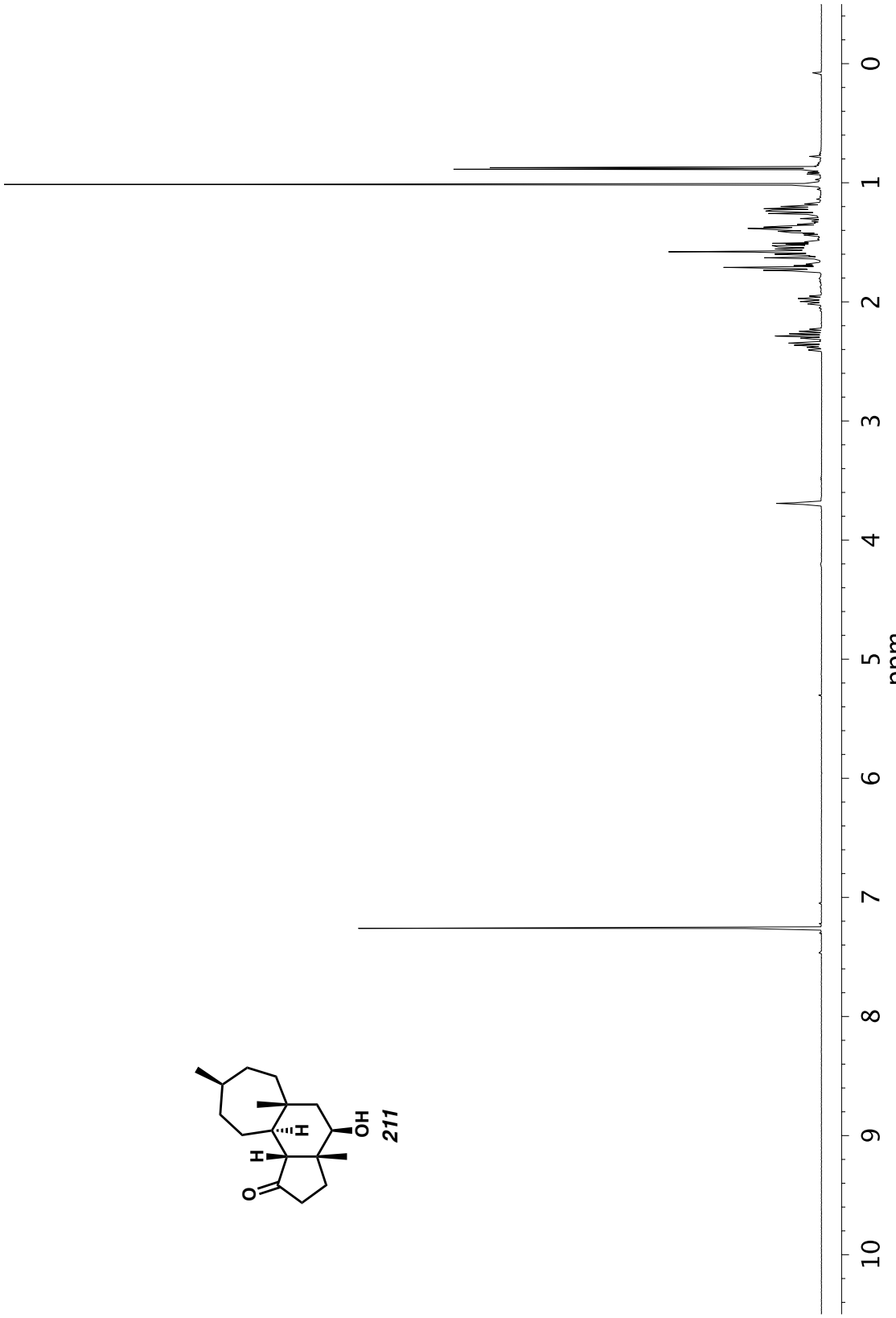

Figure A9.4. ^{1}H NMR (500 MHz, $CDCl_3$) of compound **211**.

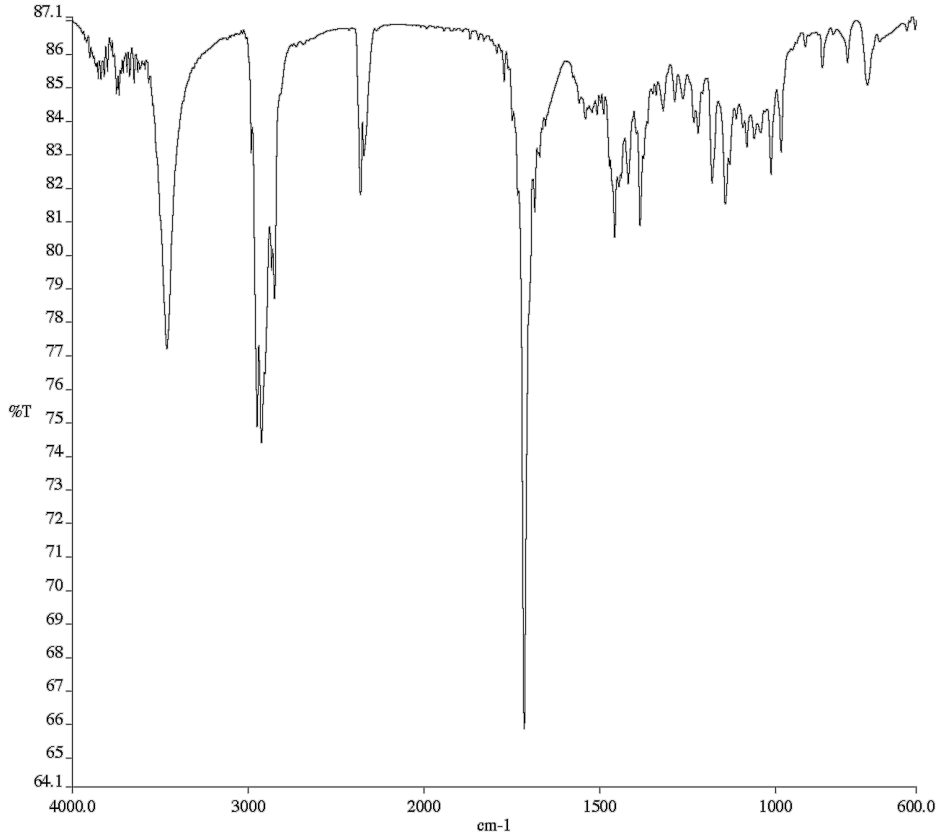

Figure A9.5. Infrared Spectrum (Thin Film, KBr) of compound **211**.

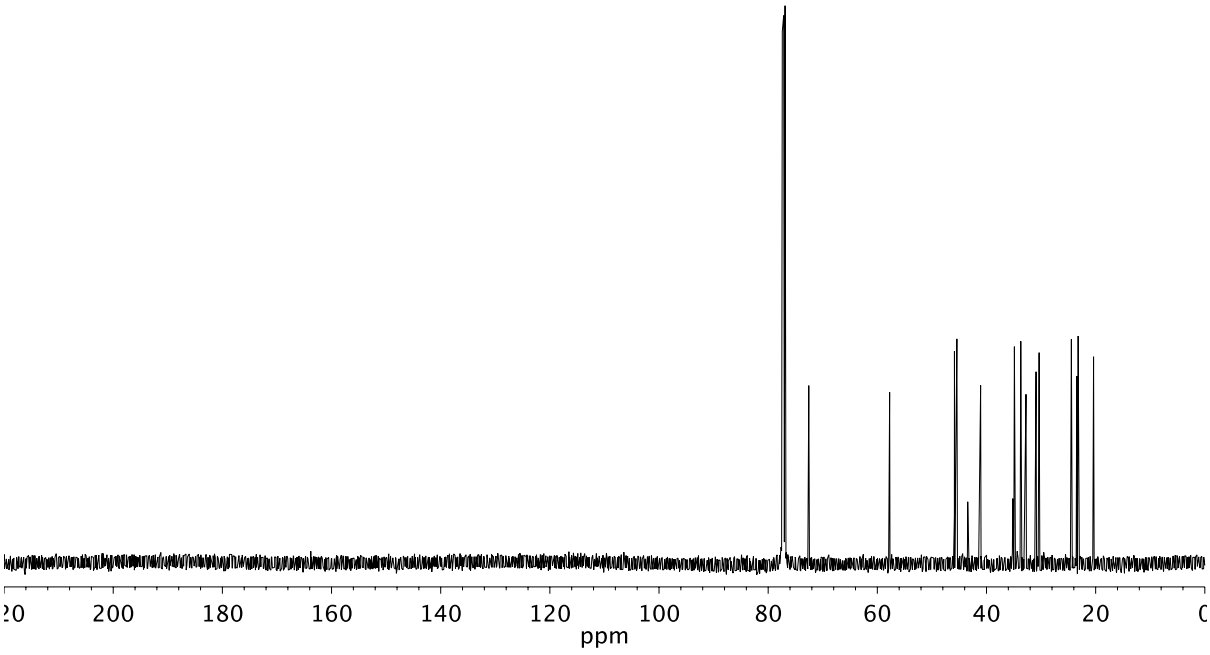

Figure A9.6. ^{13}C NMR (101 MHz, $CDCl_3$) of compound **211**.

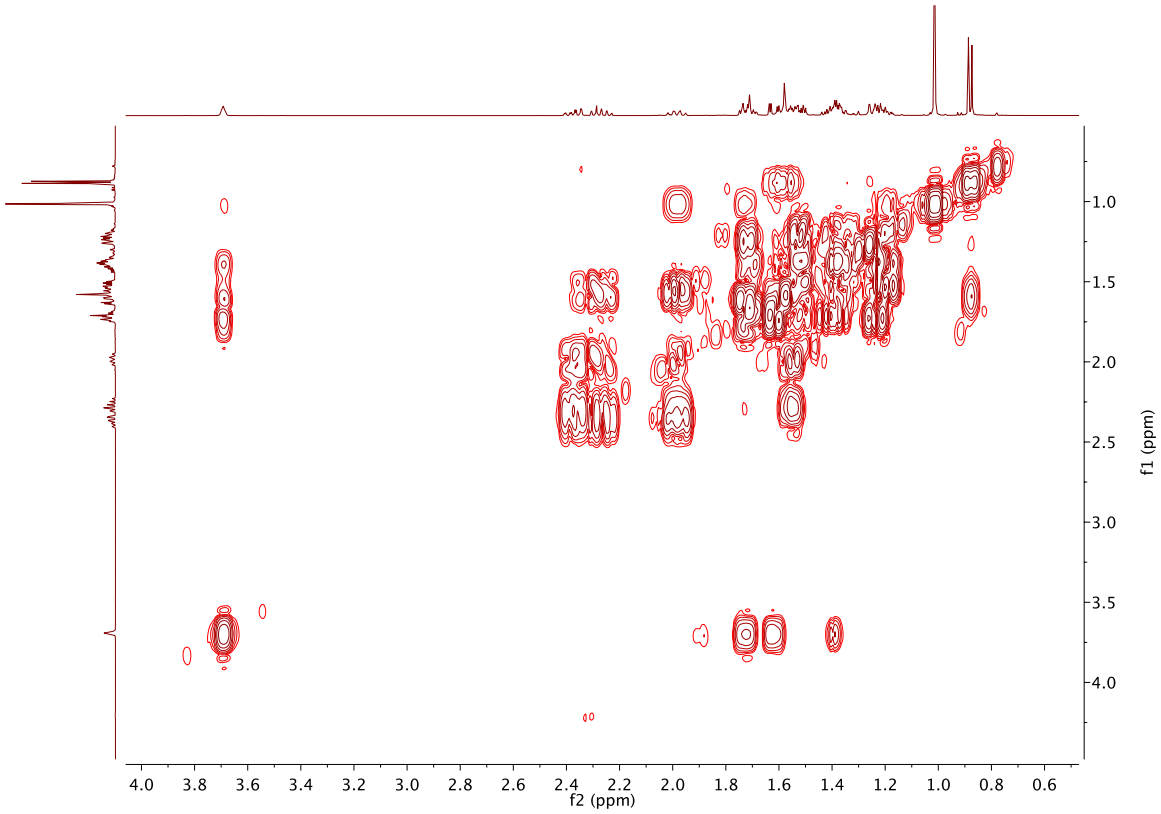

Figure A9.7. COSY (500 MHz, $CDCl_3$) of compound **211**.

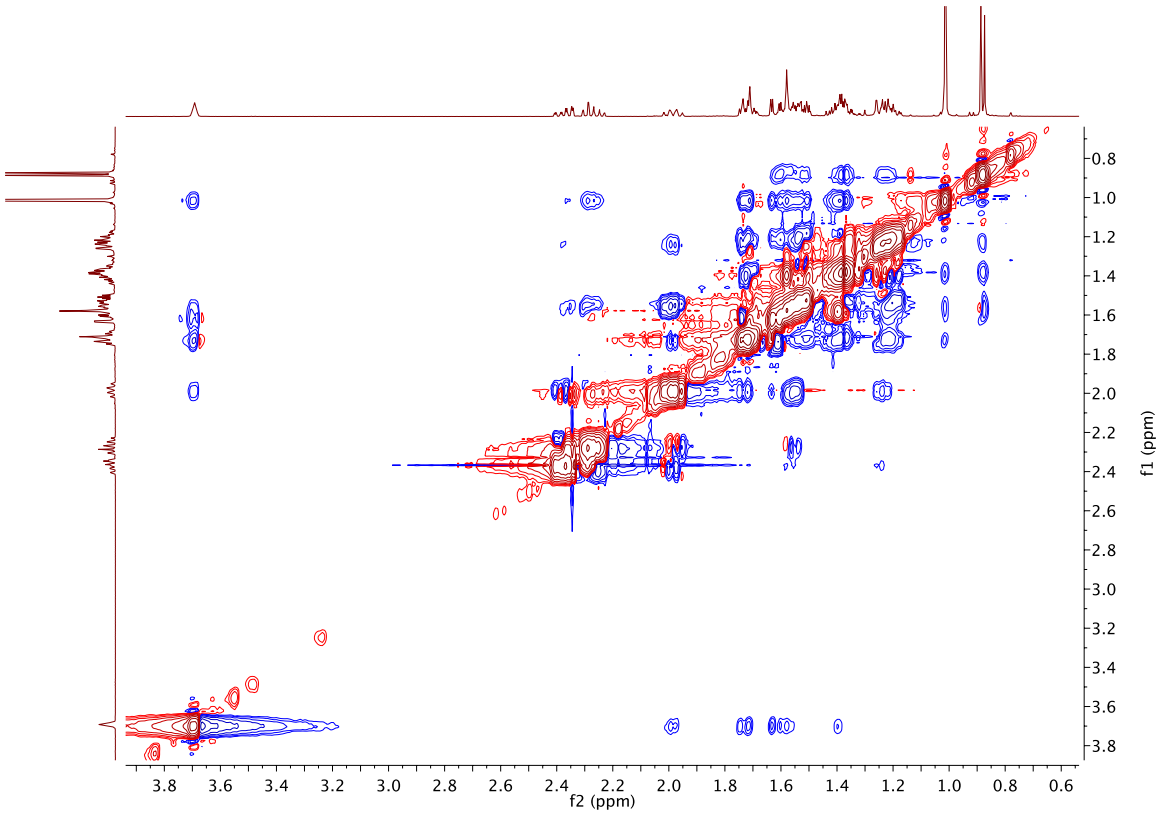

Figure A9.8. NOESY (500 MHz, $CDCl_3$) of compound **211**.

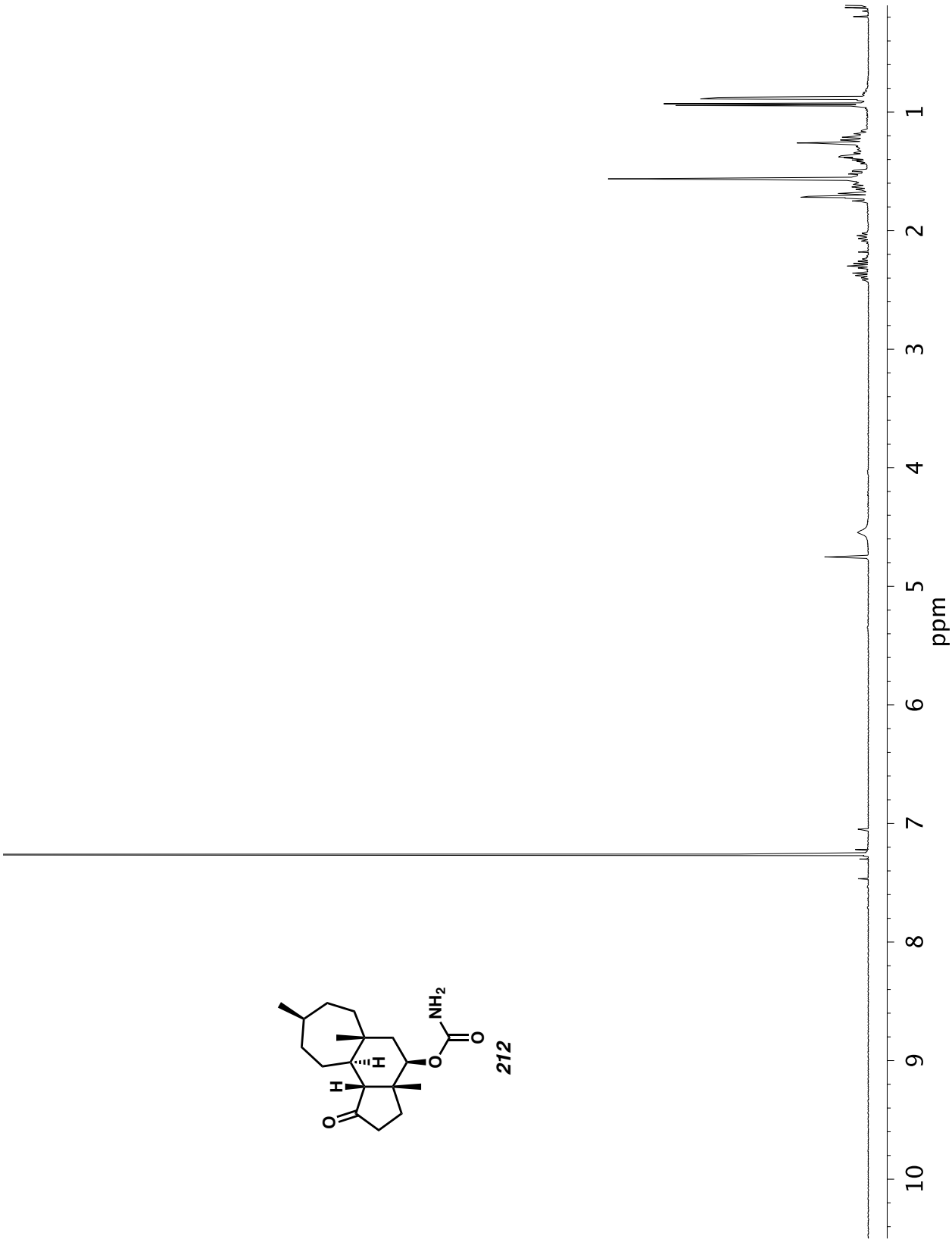

Figure A9.9. ^{1}H NMR (500 MHz, $CDCl_3$) of compound **212**.

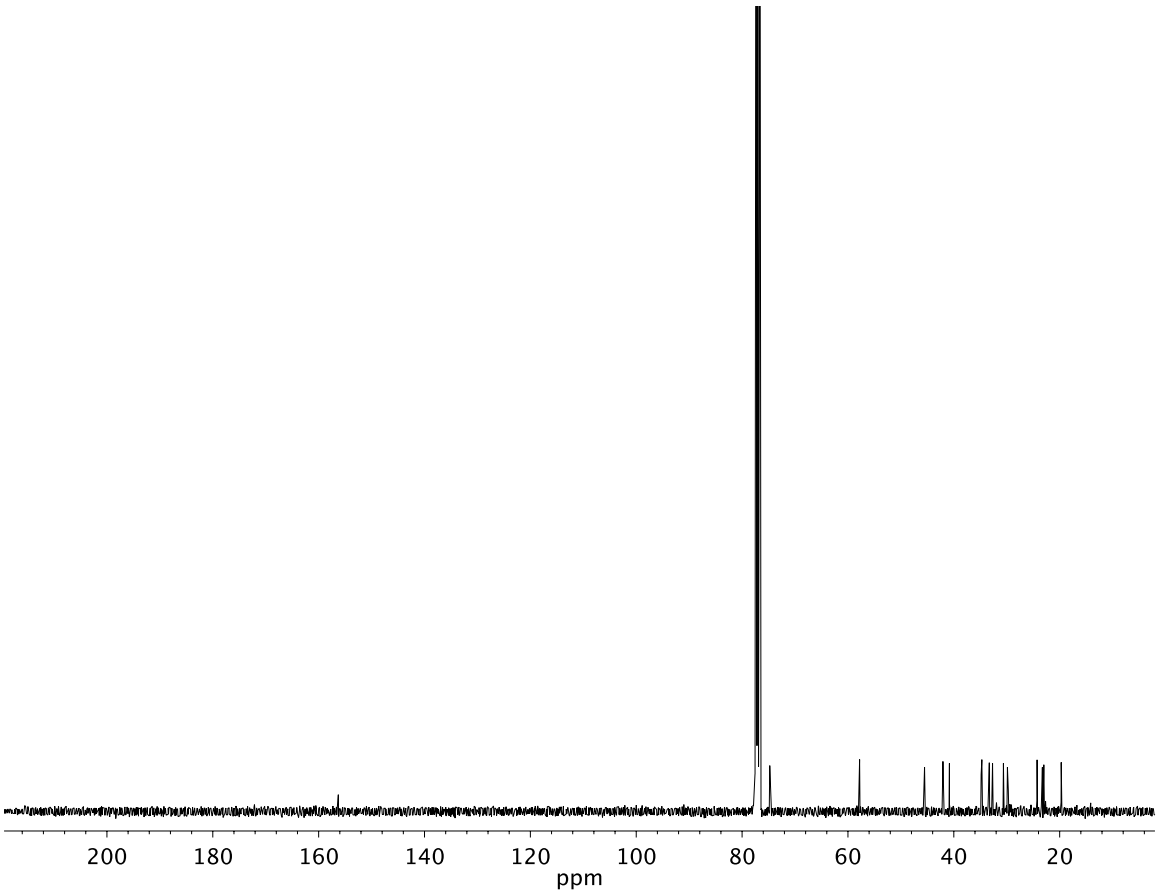

Figure A9.10. ^{13}C NMR (101 MHz, $CDCl_3$) of compound **212**.

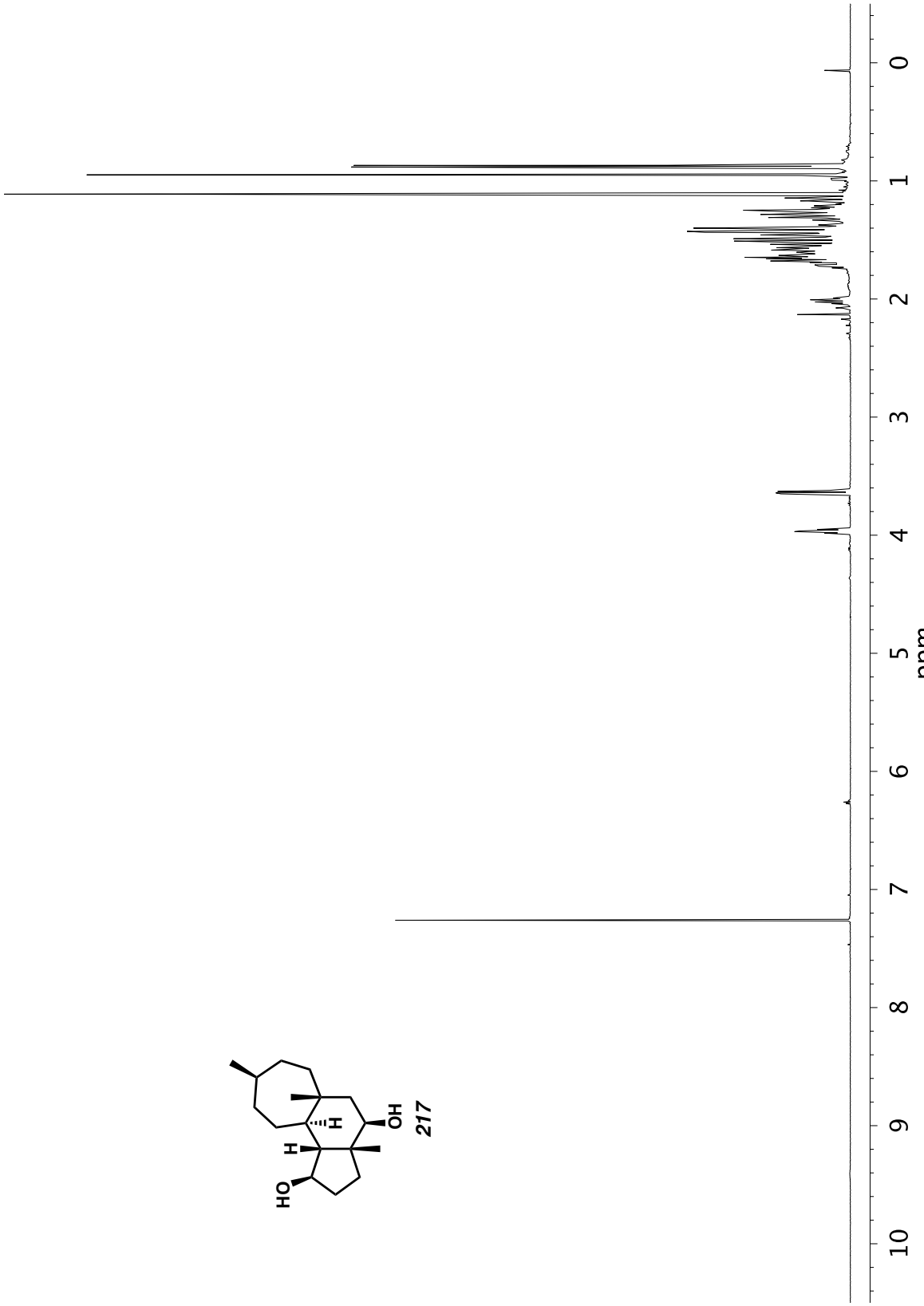

Figure A9.11. ^{1}H NMR (500 MHz, $CDCl_3$) of compound **217**.

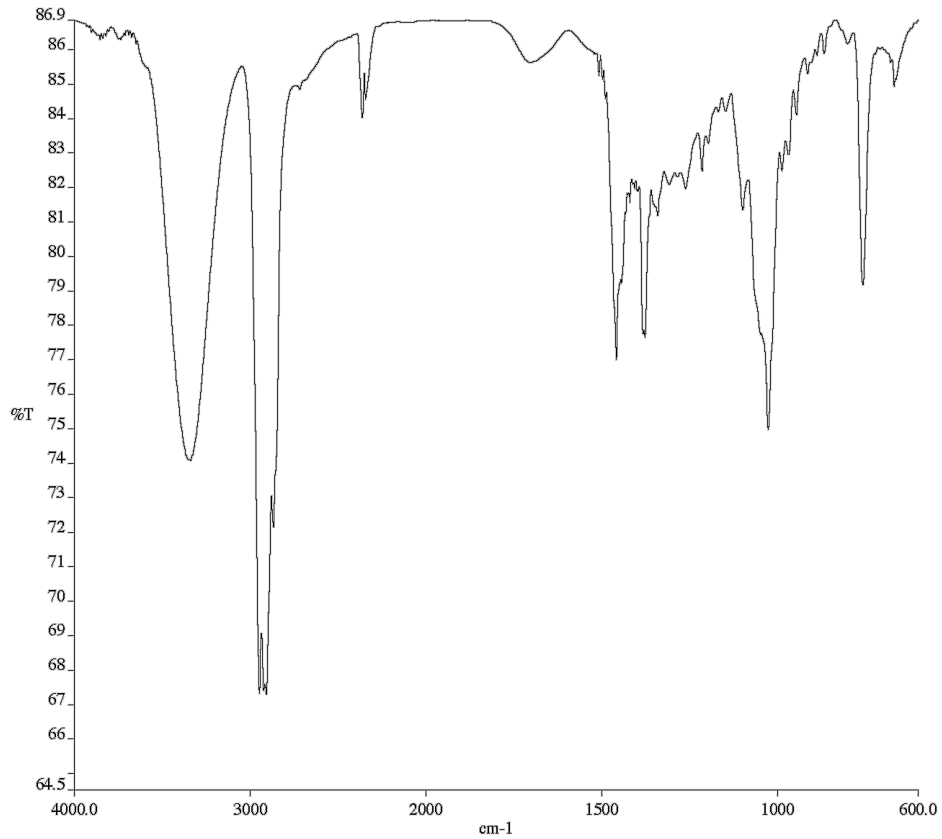

Figure A9.12. Infrared Spectrum (Thin Film, KBr) of compound **217**.

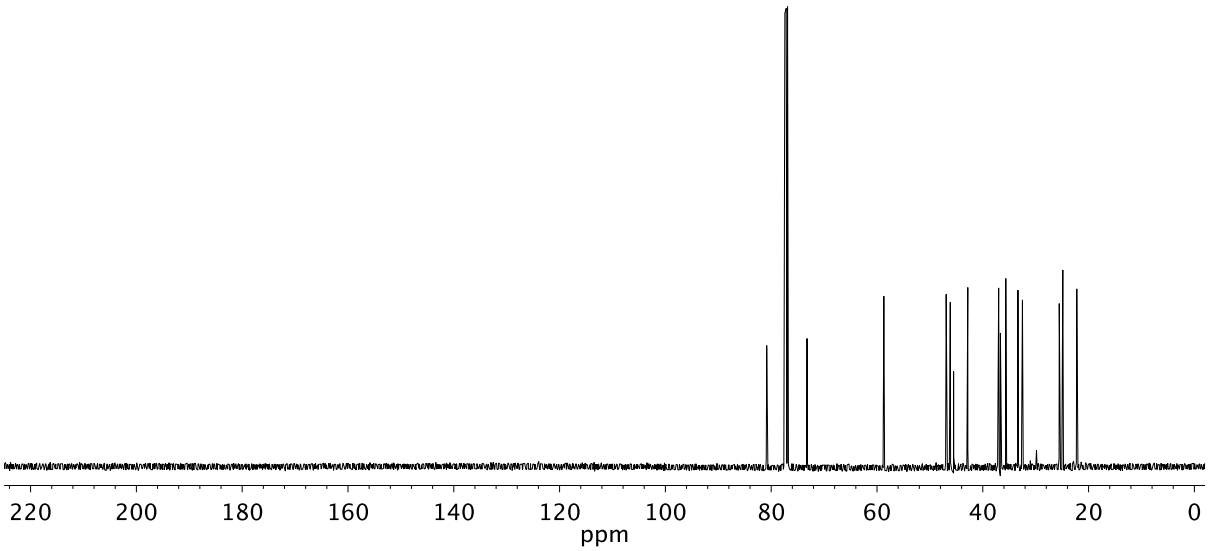

Figure A9.13. ^{13}C NMR (101 MHz, $CDCl_3$) of compound **217**.

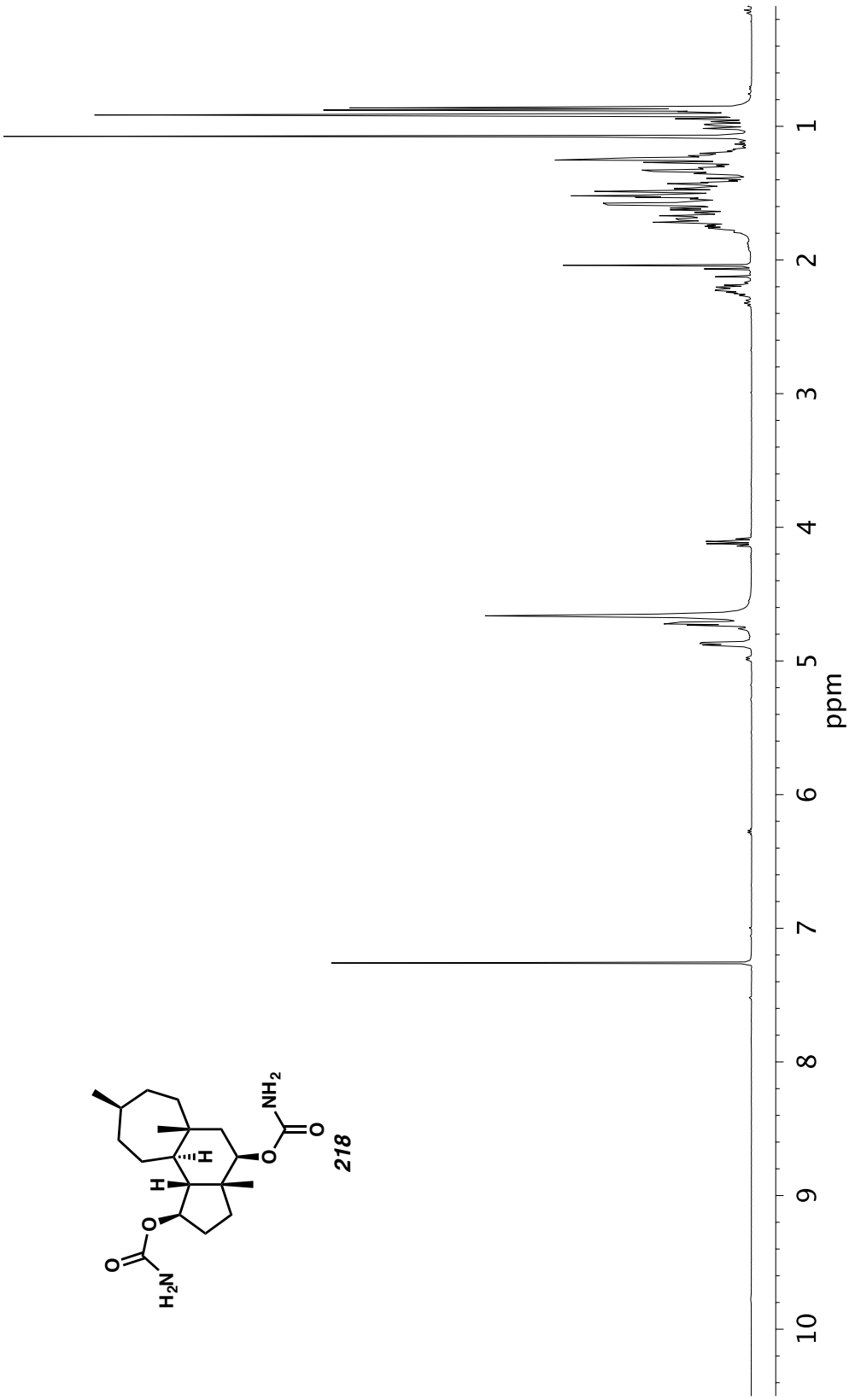

Figure A9.14. ^{1}H NMR (400 MHz, $CDCl_3$) of compound **218**.

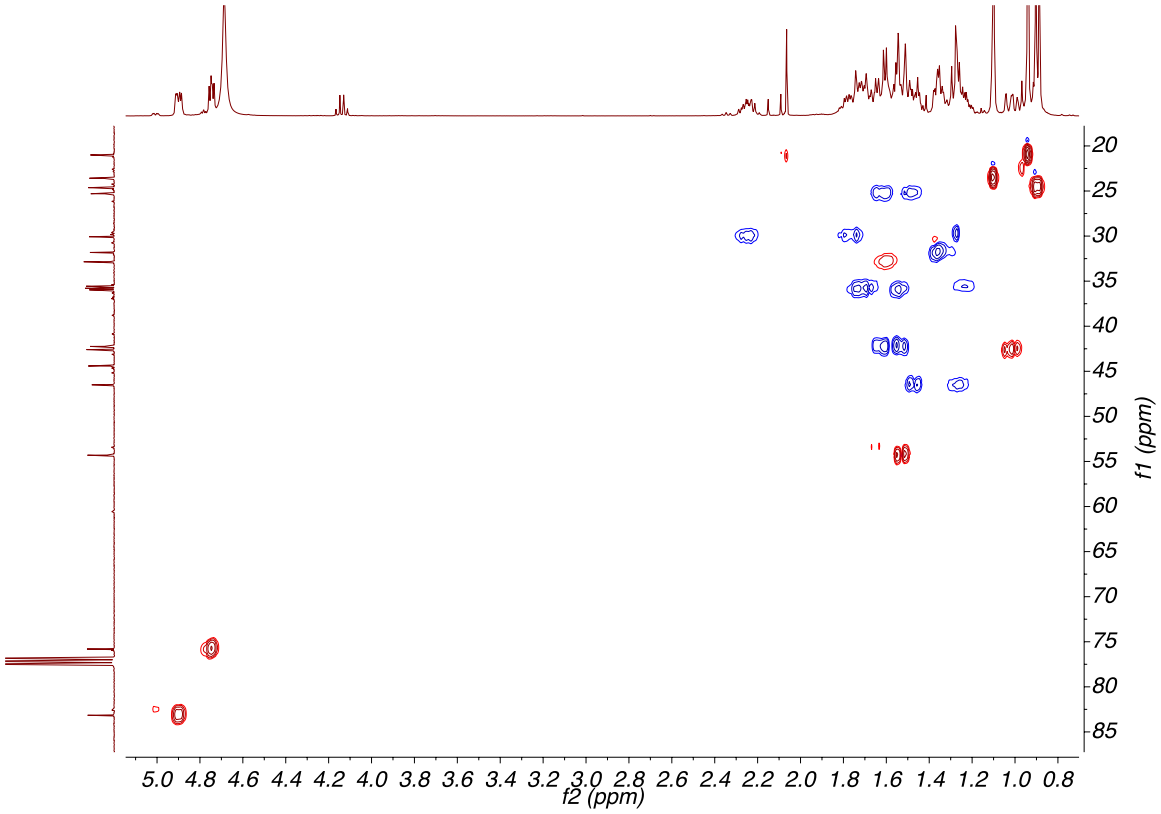

Figure A9.15. HSQC (400, 101 MHz, $CDCl_3$) of compound **218**.

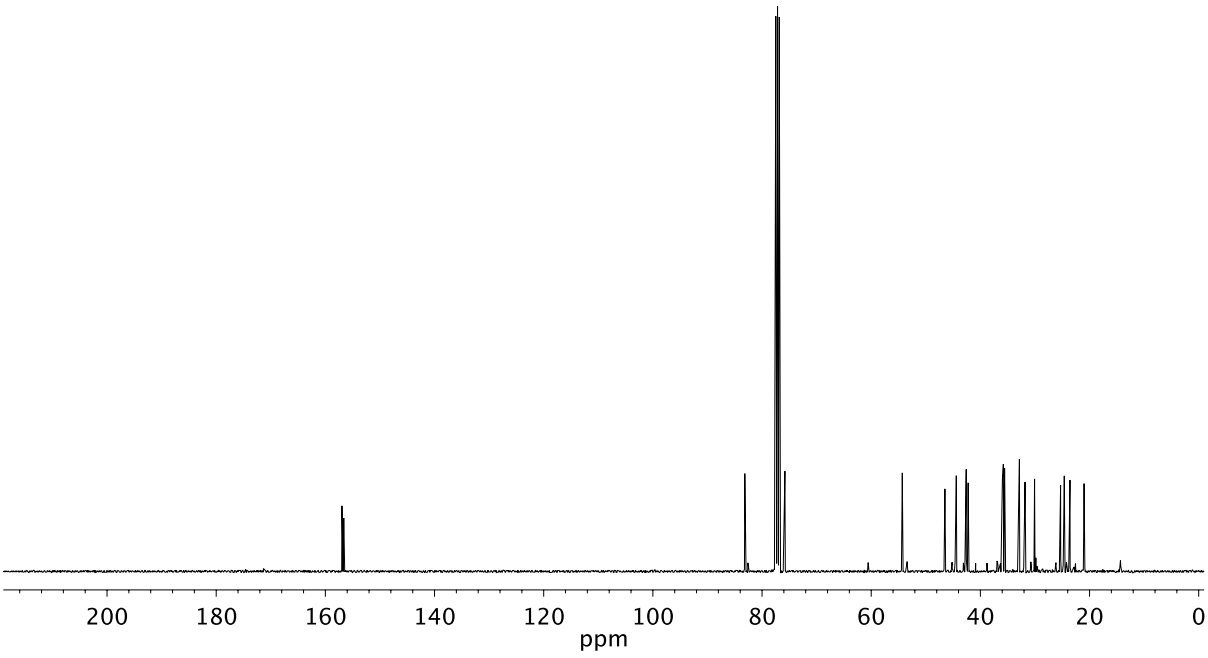

Figure A9.16. ^{13}C NMR (101 MHz, $CDCl_3$) of compound **218**.

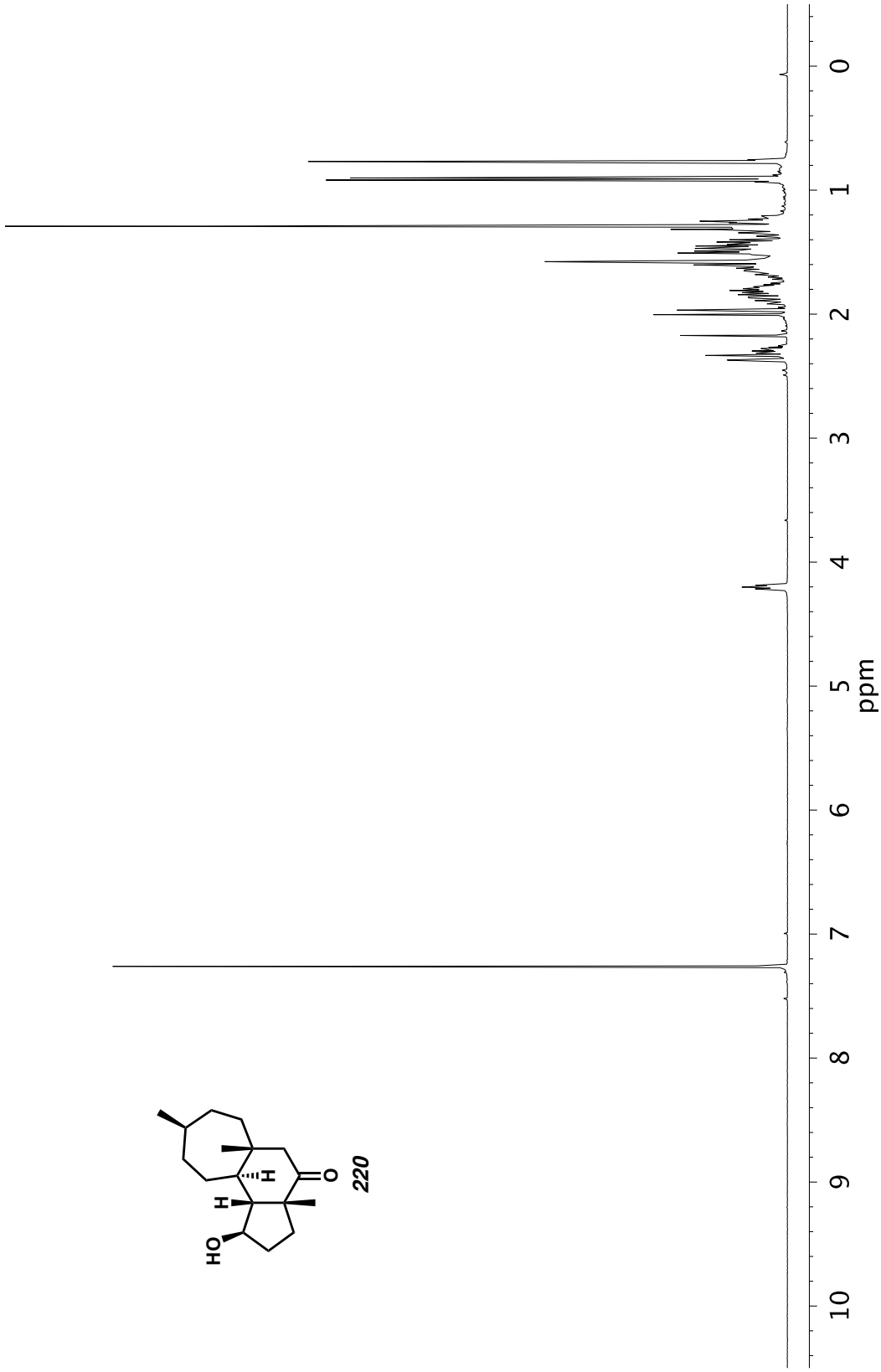

Figure A9.17. ^{1}H NMR (400 MHz, $CDCl_3$) of compound **220**.

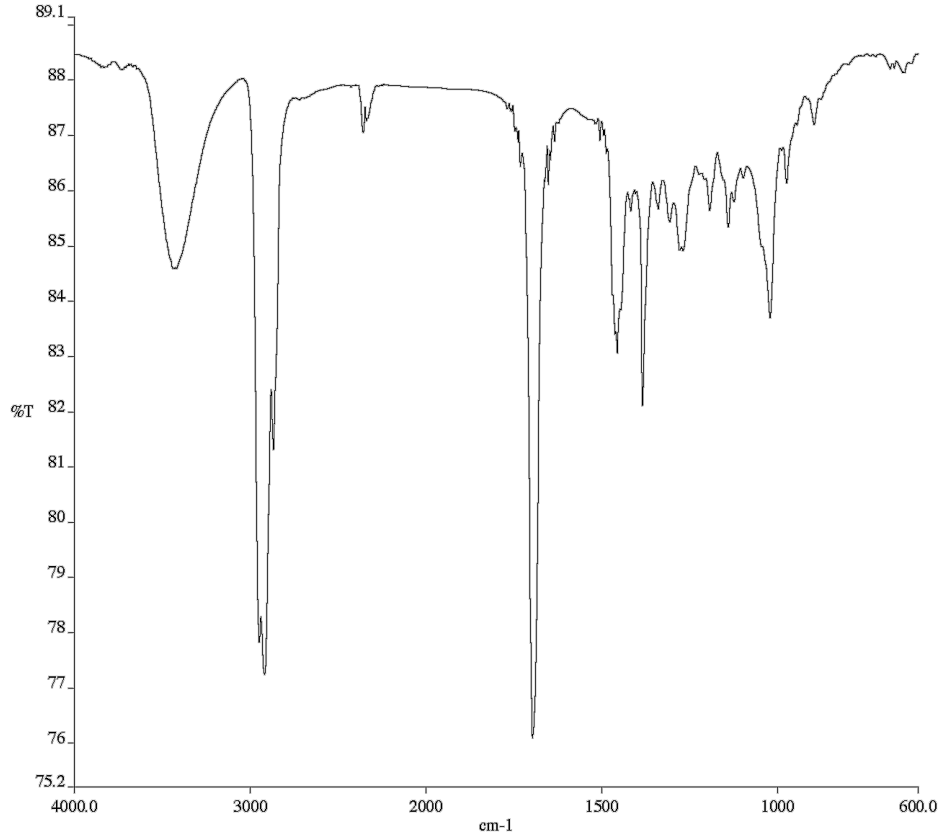

Figure A9.18. Infrared Spectrum (Thin Film, KBr) of compound **220**.

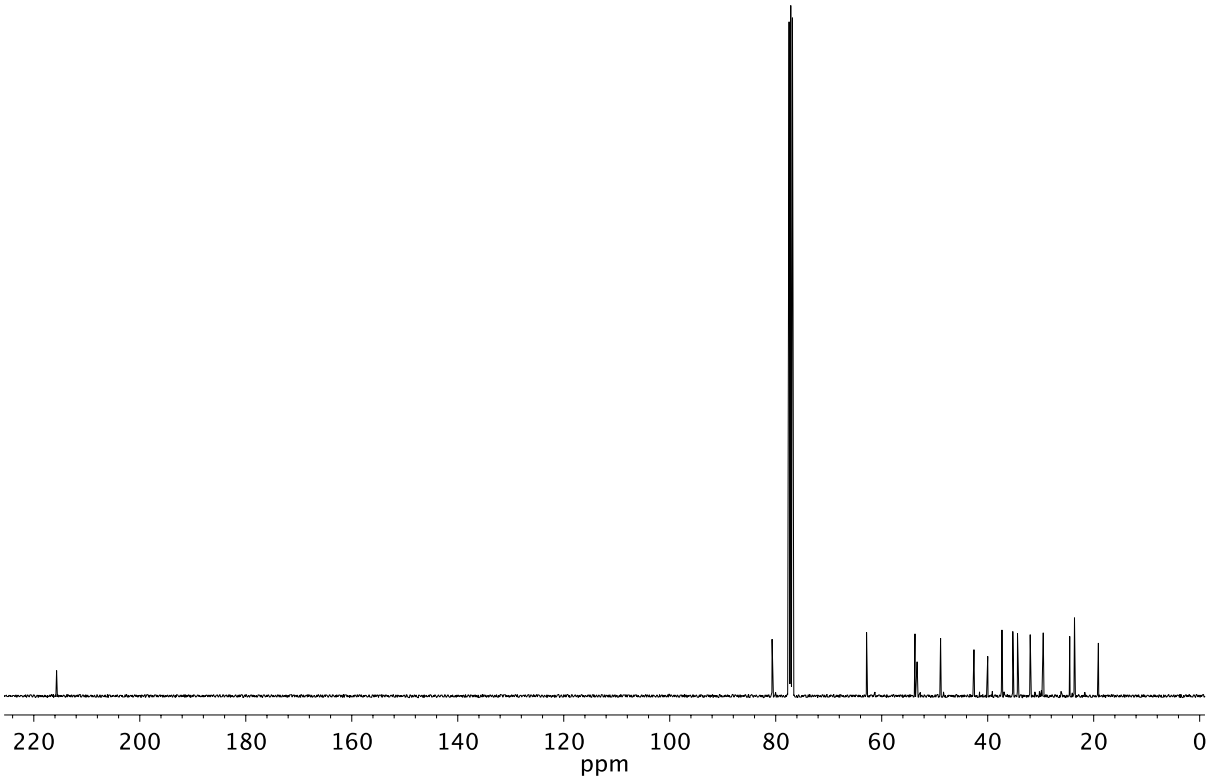

Figure A9.19. ^{13}C NMR (101 MHz, $CDCl_3$) of compound **220**.

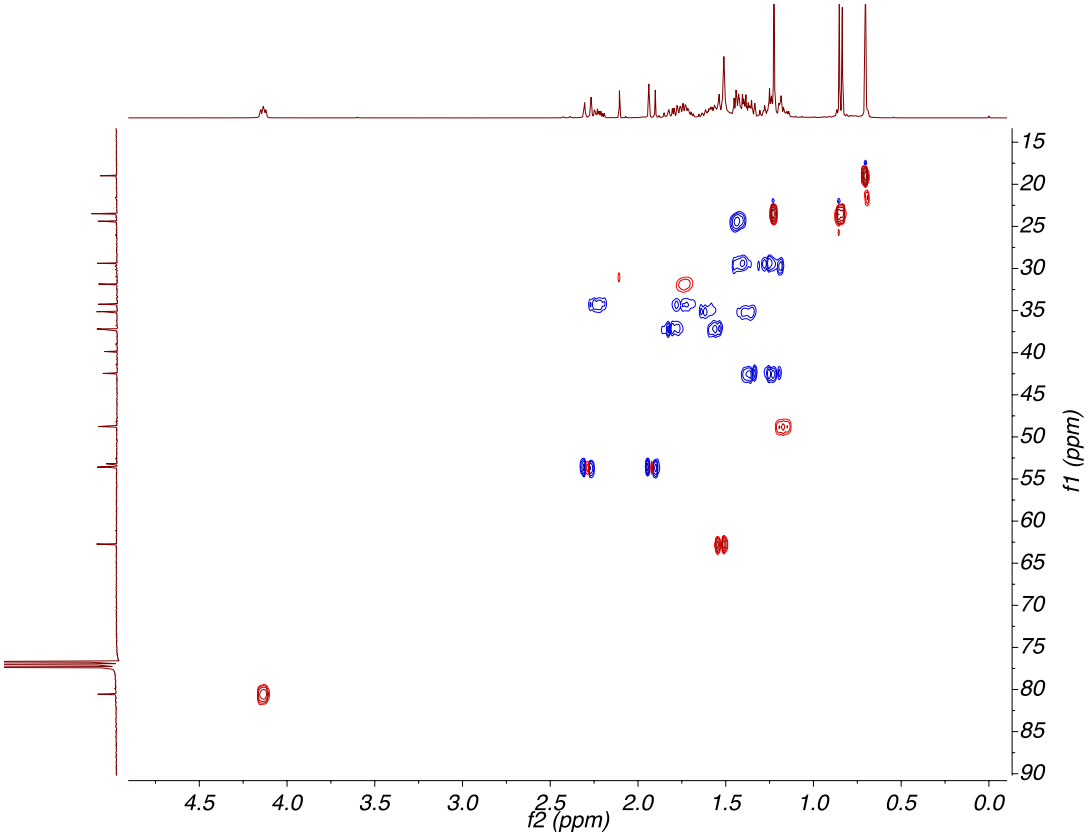

Figure A9.20. HSQC (400, 101 MHz, $CDCl_3$) of compound **220**.

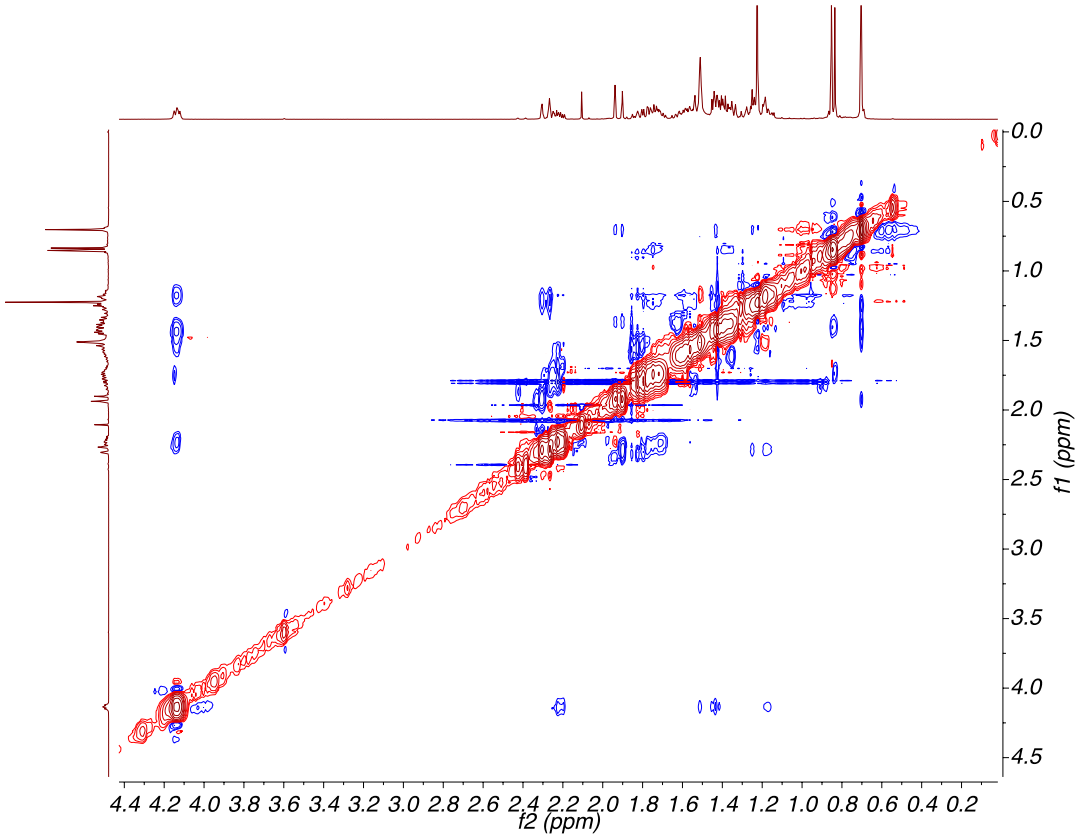

Figure A9.21. NOESY (400 MHz, $CDCl_3$) of compound **220**.

CHAPTER 5[†]

Synthesis of Non-natural Cyanthiwigin–Gagunin Hybrids

through Late-Stage Diversification of the Cyanthiwigin Natural Product Core

5.1 INTRODUCTION

As described in Chapter 1, the derivatization of an easily accessible complex molecular scaffold offers many opportunities for synthetic and biological insight. Having probed the reactivity of the cyanthiwigin natural product core as a scaffold for the study of C–H functionalization, we sought to use the tricyclic framework as a starting point for accessing non-natural cyanthiwigin derivatives and assessing their biological activities. Taking our structural inspiration from the gagunin natural product family, we designed and executed the synthesis of several non-natural cyanthiwigin–gagunin "hybrid" molecules. The results of these investigations are described herein.

[†] The biological evaluations described in this chapter were performed in collaboration with Dr. Sangkil Nam and Dr. David Horne at the City of Hope.

5.1.1 THE CYANTHIWIGIN NATURAL PRODUCTS

Comprising a subset of a large class of bioactive natural products known as the cyathins, the cyanthiwigins are a family of diterpenoid natural products isolated from the marine sponges *Epipolasis reiswigi*[1] and *Myrmekioderma styx*.[2] Their complex architectures and interesting biological properties have attracted much attention in the chemical community. Of the 30 known cyanthiwigins, all except cyanthiwigin AC (**105**, Figure 5.2) possess 5–6–7 fused tricyclic carbon skeletons (**101**) featuring four contiguous stereocenters, two of which are quaternary. Additionally, many of these compounds display noteworthy biological activity against such disease agents as HIV-1 (cyanthiwigin B, **107**),[2] lung cancer and leukemia cells (cyanthiwigin C, **223**),[3] and primary tumor cells (cyanthiwigin F, **106**).[2]

*Figure 5.1 The cyathane skeleton (**101**) and biological properties of selected cyanthiwigins*

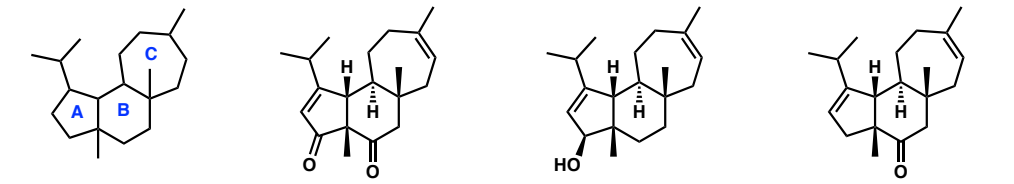

cyathane skeleton (101) ***cyanthiwigin B (107)*** anti-HIV ***cyanthiwigin C (223)*** anti-leukemia ***cyanthiwigin F (106)*** anti-tumor

Since not all of the cyanthiwigins have been isolated in large enough quantities for biological evaluation, exhaustive exploration of the medicinal properties of all 30 of the cyanthiwigins has remained elusive. Noting this along with the structural challenges presented by the molecules, chemists have targeted several members of the cyanthiwigin family for total synthesis efforts.[4] To date, seven cyanthiwigins have been prepared synthetically, including cyanthiwigins U (**102**),[5] W (**103**),[6] and Z (**104**)[6] by Phillips and

co-workers, cyanthiwigin AC (**105**) by Reddy and co-workers,[7] and cyanthiwigins F (**106**),[8] B (**107**),[9] and G (**108**)[9] by Stoltz and co-workers (Figure 5.2).

Figure 5.2 Cyanthiwigins prepared by total synthesis to date

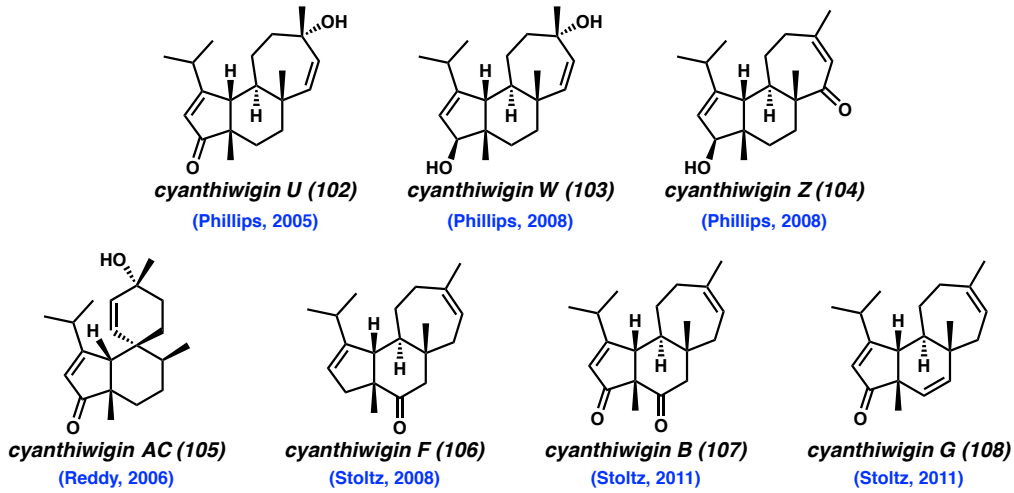

5.1.2 THE GAGUNIN NATURAL PRODUCTS

Isolated from the sponge *Phorbas* sp. by Shin and co-workers off the coast of South Korea,[10] the gagunins are a family of diterpenoid natural products featuring the same 5–6–7 fused tricyclic core as the cyanthiwigins along with a range of biological activities. The main structural differences between the gagunins and the cyanthiwigins are the placement of the methyl substituent in the seven-membered C-ring and the degree of oxidation surrounding the carbocyclic framework. The density of functionalization and presence of numerous contiguous stereocenters (up to 11) make the gagunins challenging targets for total synthesis, and as such, only a partial synthesis of any gagunin has been completed to date.[11]

Figure 5.3 Structures and anti-leukemia activities of selected gagunins

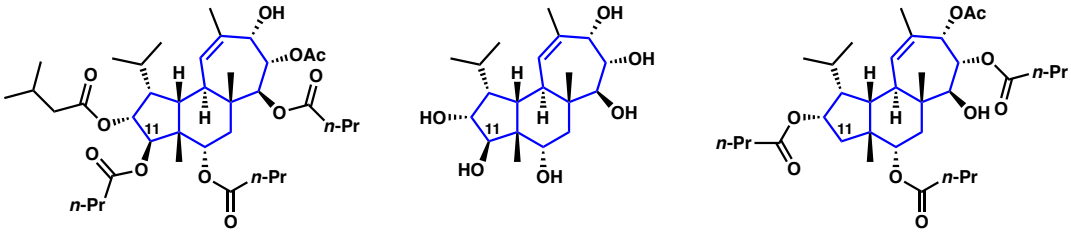

The gagunins exhibit cytotoxic activity against the human leukemia cell line K562, with gagunin E (**226**) displaying the most potent activity (LC_{50} = 0.03 μg/mL) out of all 17 known members of the natural product family.[10] Gagunin E (**226**) is over one thousand times more potent than the least biologically active member of the family, gagunin A (**224**) (Figure 5.3). Interestingly, these two compounds differ only in the placement and identity of the ester substituents surrounding the carbocyclic framework, an observation that led Shin and co-workers to propose that the biological properties of the gagunins are highly sensitive to the ester functionalities, especially at the C11 position. Indeed, evaluation of perhydroxylated gagunin A (**225**), in which all of the esters are hydrolyzed, revealed no appreciable biological activity, lending credence to Shin's hypothesis.

5.1.3 APPROACH TO HYBRID SYNTHESIS

With this in mind, we envisioned that the cyanthiwigin natural product core (**109**), for which we had previously established an efficient synthetic route,[8,9,12] could serve as a scaffold from which to access non-natural compounds combining structural features from both the cyanthiwigin and gagunin natural products (Scheme 5.1). Specifically, we

anticipated that the two carbonyl moieties and olefin in **109** could serve as functional handles for facile installation of ester functionalities, generating poly-esterified compounds (**227**) reminiscent of the densely oxygenated gagunins. Given the diverse biological activities displayed by the parent cyanthiwigins and gagunins, we hypothesized that some of these cyanthiwigin–gagunin "hybrid" molecules might exhibit interesting biological properties that could be correlated to structure through systematic fine-tuning of the ester functionalities. Overall, these efforts could enable the identification of exceptionally potent non-natural complex molecules[13] while providing insight into the reactivity of the cyanthiwigin core and the relationship between framework substitution and biological activity.

Scheme 5.1 Approach toward cyanthiwigin–gagunin hybrid synthesis

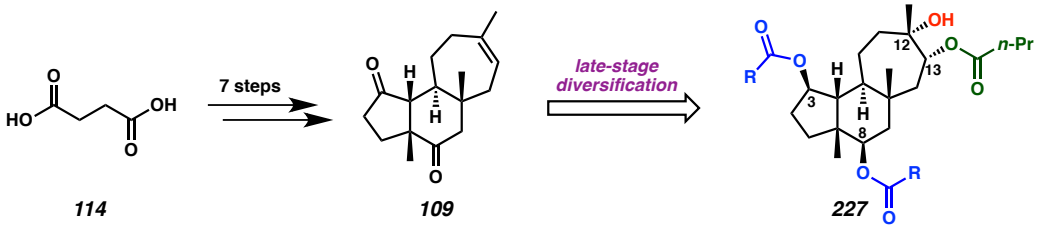

5.2 SYNTHESIS OF CYANTHIWIGIN–GAGUNIN HYBRIDS

At the outset of our efforts, we identified the C-ring olefin in **109** as a key starting point for diversification. Namely, oxygenation could be achieved through di-hydroxylation of the olefin with either *syn* or *anti* relative stereochemistry, ultimately giving rise to diastereomeric cyanthiwigin–gagunin hybrids.

5.2.1 SYN DIOL ROUTE

We began our studies targeting hybrid molecules derived from the *syn*-dihydroxylation pathway. Retrosynthetically, we envisioned that polyesterified hybrids **227** could arise through diversification of tris-hydroxylated compound **228**, which itself would be accessed through reduction of the A- and B-ring ketones in **229**. Mono-esterified compound **229** could be traced back to *syn*-diol **230**, which would result from *syn*-dihydroxylation of the cyanthiwigin core (**109**) (Scheme 5.2).

Scheme 5.2 Retrosynthetic analysis of cyanthiwigin–gagunin hybrid(s) ***227***

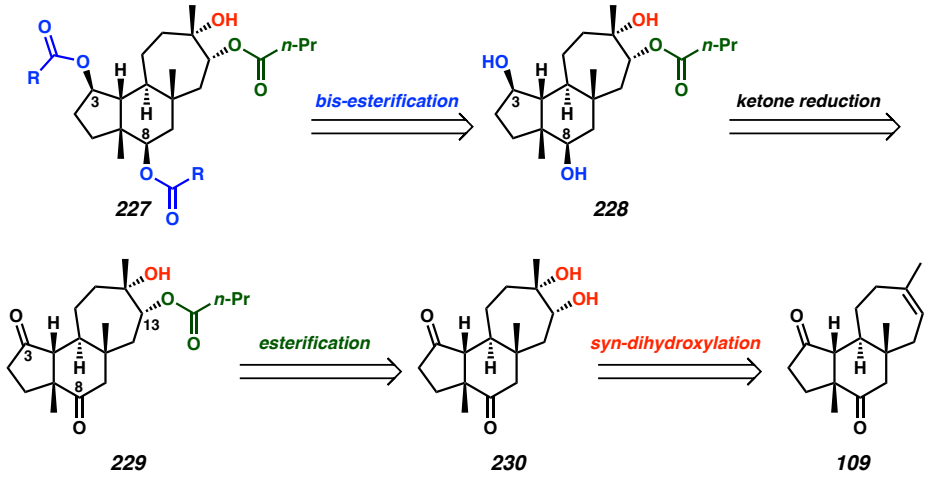

Preparation of the *syn*-diol-derived hybrids commenced with dihydroxylation of **109** using osmium tetroxide and NMO. We were pleased to find that *syn*-diol **230** was formed in good yield as a single diastereomer under these conditions. As observed in our previous studies on the hydrogenation and C–H functionalization of the cyanthiwigin core,[14] oxygenation occurred selectively from the α-face of the molecule, likely due to steric shielding of the β-face by the methyl substituent at the B–C ring juncture. Diol **230**

was subsequently treated with butyric acid, EDCI, and DMAP to effect selective esterification of the secondary C13 hydroxyl, furnishing tricyclic mono-ester **229** in moderate yield. Treatment of **229** with excess sodium borohydride resulted in the formation of triol **228** along with smaller quantities of mono-reduction product **231**, which were separable by column chromatography.

*Scheme 5.3 Preparation of key tris-hydroxylated intermediate **228** in the syn-diol route*

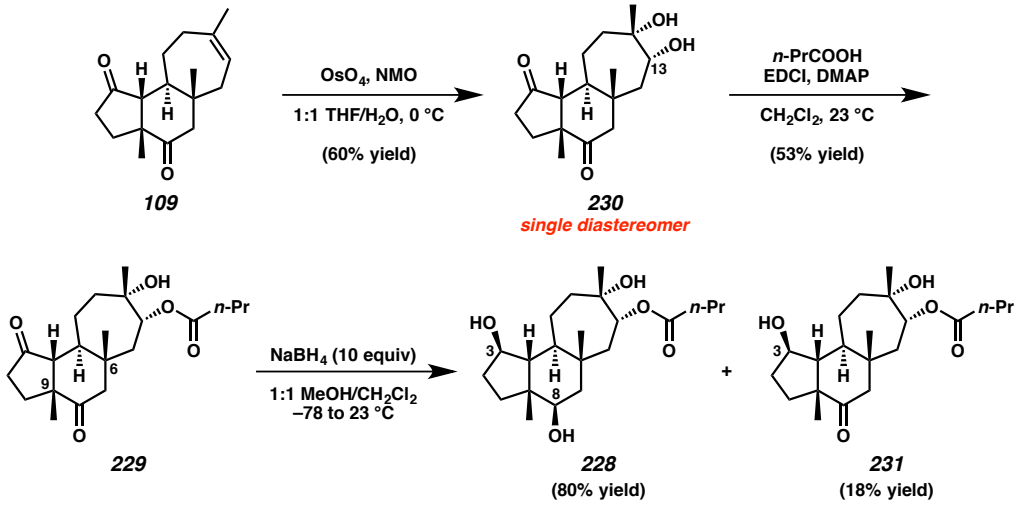

Notably, hydride reduction occurred selectively from the α-face of diketone **229**, presumably due to steric factors as in previous cases. The spatial relationship of the C9 and C6 methyl substituents to the C3 and C8 ketones in the cyanthiwigin core can be observed in an X-ray crystal structure of hydrogenated tricycle **193** (Figure 5.4). We propose that the C9 and C6 methyls are instrumental in controlling the facial selectivity of reduction. Specifically, the C9 methyl effectively blocks approach of the hydride from the Burgi–Dunitz angle[15] on the β-face, necessitating attack from the more accessible α-face despite the concavity of the three-dimensional architecture of **229**. Likewise,

hydride approach toward the B-ring ketone from the β-face is rendered highly unfavorable by the C9 and C6 methyl substituents, giving rise to the observed stereochemistry at C3 and C8 in the product (**228**).

*Figure 5.4 Steric shielding of the β-face of the cyanthiwigin core caused by the C9 and C6 methyls, as illustrated by a crystal structure of hydrogenated tricycle **193***

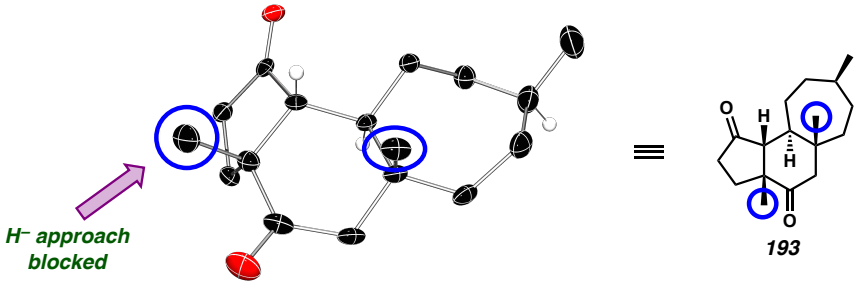

With tris-hydroxylated intermediate **228** in hand, we proceeded to the final transformation in generating cyanthiwigin–gagunin hybrids (**227**). Initial efforts at bis-esterification employing the same conditions used previously (butyric acid, EDCI, and DMAP) proved unsuccessful, returning large quantities of unreacted **228** (Table 5.1, Entry 1). Further attempts to access tri-ester **227a** using butyryl chloride and DMAP were also ineffective, instead converting **228** to a complex mixture of unidentified compounds (Entry 2). Finally, we discovered that the combination of butyric anhydride, triethylamine, and DMAP provided the optimal balance in reactivity, supplying cyanthiwigin–gagunin hybrid **227a** in high yield (Entry 3). Gratifyingly, application of these conditions to **228** using isovaleric anhydride or acetic anhydride enabled access to hybrids **227b** or **227c**, respectively (Scheme 5.4).

Table 5.1 Optimization of final esterification conditions for synthesis of hybrid ***227a***

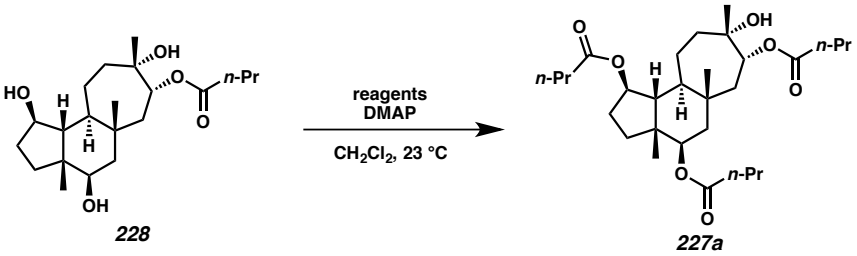

Entry	Reagents	Result
1	*n*-PrCOOH, EDCI	low conversion
2	*n*-PrCOCl	messy mixture
3	$(n\text{-PrCO})_2O$, NEt_3	81% yield of ***227a***

Scheme 5.4 Preparation of cyanthiwigin–gagunin hybrids ***227a–c*** *from common intermediate* ***228***

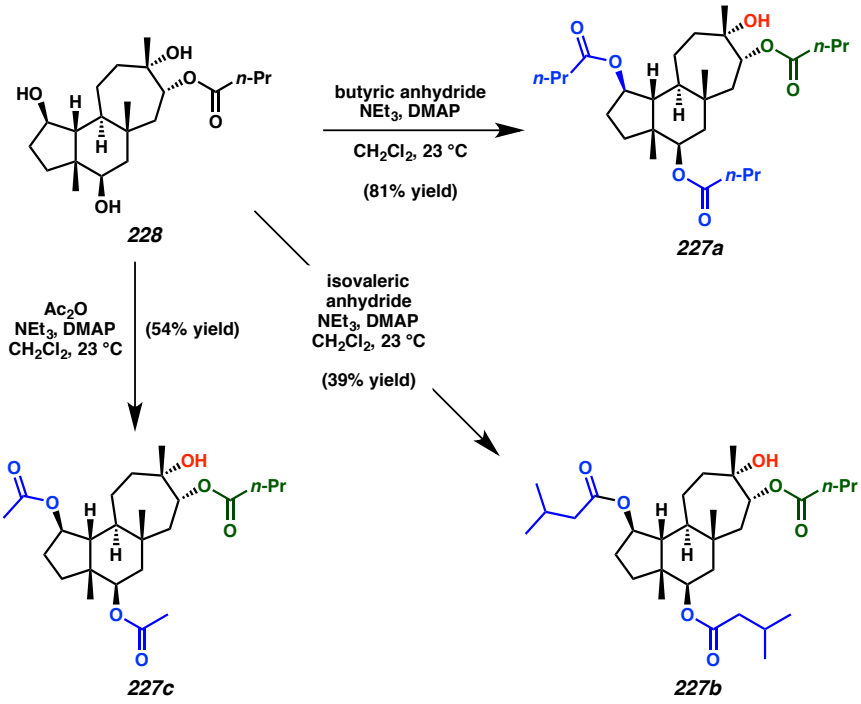

5.2.1.1 FURTHER SYNTHETIC CONSIDERATIONS

Having observed the discrepancies in efficacy between the three sets of esterification conditions employed in the preparation of **227a**, we re-examined the esterification of diol **230**. Comparison of the three different sets of conditions when applied to **230** revealed that, although the desired ester (**229**) was generated in serviceable quantities in every case, use of butyric anhydride and triethylamine in the presence of DMAP resulted in significantly higher yields (Table 5.2, Entry 3). As such, moving forward we planned to use anhydrides for esterification transformations whenever possible.

*Table 5.2 Comparison of different conditions for esterification of diol **230***

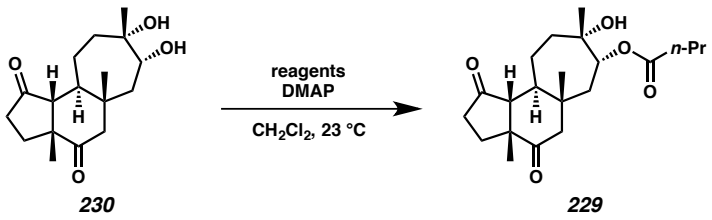

230 ***229***

Entry	Reagents	Yield
1	*n*-PrCOOH, EDCI	53%
2	*n*-PrCOCl	54%
3	$(n\text{-PrCO})_2O$, NEt_3	73%

For the preparation of cyanthiwigin–gagunin hybrid **227a**, we wondered if a global esterification strategy might be feasible through tetra-hydroxylated intermediate **232** (Scheme 5.5A). To investigate this possibility, we treated diol **230**, this time prepared through a catalytic dipotassium osmate dihydrate protocol, with excess sodium borohydride. Despite good conversion of starting material, the tetra-hydroxylated product **232** proved to be intractable, likely due to its high polarity and resistance to

extraction from the aqueous layer. As such, we determined that a global esterification strategy through a tetra-hydroxylated intermediate was not a viable approach for the preparation of cyanthiwigin–gagunin hybrids containing three identical ester substituents.

*Scheme 5.5 A) Alternate retrosynthesis for **227a** and B) attempted preparation of **232***

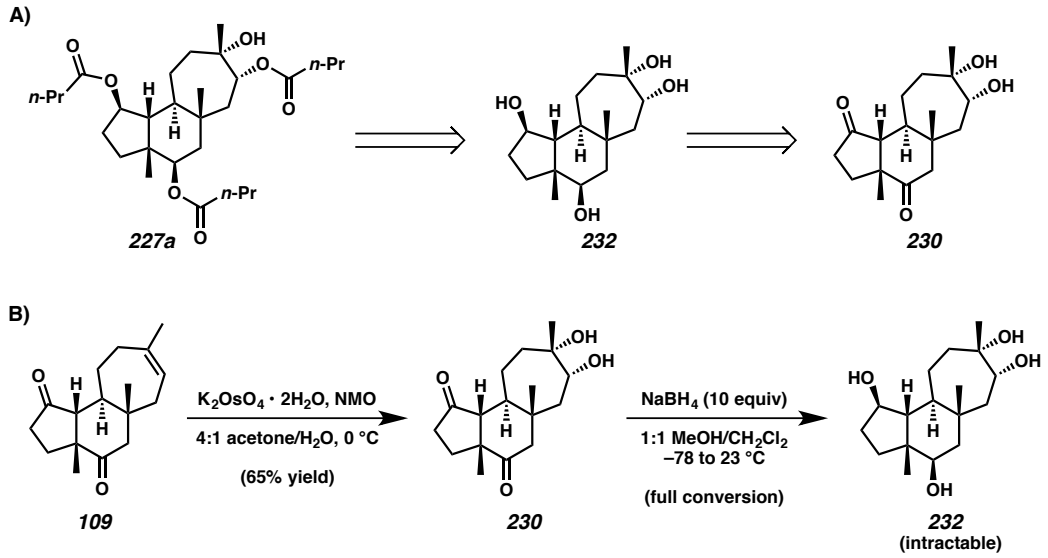

5.2.2 ANTI DIOL ROUTE

We next turned our attention to the preparation of cyanthiwigin–gagunin hybrids through the *anti*-diol route, which would enable access to compounds differing from the *syn*-diol route hybrids (**227**) at one stereocenter (C12). We reasoned that these molecules could be constructed in a similar fashion to **227**, except the route would begin with *anti*-diol instead of *syn*-diol formation. To this end, we treated tricycle **109** with dimethyldioxirane (DMDO) at 0 °C, forming epoxide **233** in excellent yield as a single diastereomer (Scheme 5.6). The high stereoselectivity of epoxidation resembles the

previously observed selectivity in the dihydroxylation of **109** (cf. Scheme 5.3), supporting our hypothesis that the β-face of the cyanthiwigin core is less accessible due to steric constraints. After unsuccessful attempts to open the epoxide under basic conditions (e.g., NaOH, $LiEt_3BH$), we found that treatment of epoxide **233** with catalytic perchloric acid delivered the desired *anti*-diol (**234**) in excellent yield.

*Scheme 5.6 Preparation of anti-diol **234** via acid-catalyzed epoxide-opening of **233***

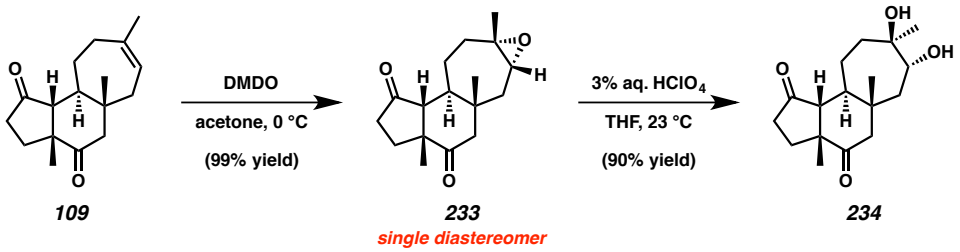

*Scheme 5.7 Formation of multiple products (**234–239**) from epoxide-opening of **233** (50 mg)*

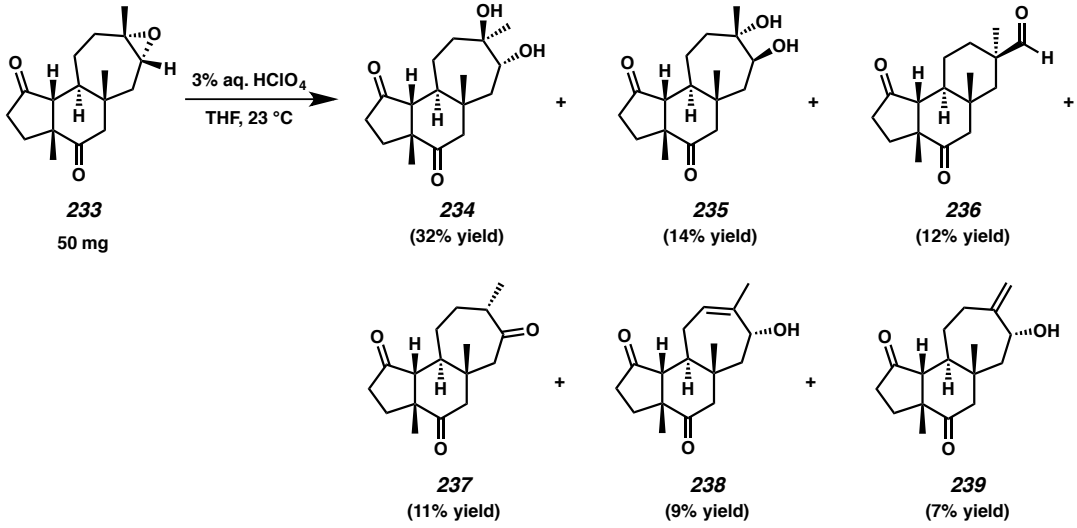

Pleased with this result, we proceeded to repeat the sequence on a larger scale. While epoxidation of **109** consistently occurred in excellent yield, the acid-catalyzed epoxide-

opening of **233** proved to be less reliable. When 50 mg of epoxide **233** was subjected to conditions that had been effective on 5 mg, the formation of multiple products was observed. These compounds were isolated by column chromatography and characterized as compounds **234**–**239**. The desired *anti*-diol (**234**) comprised the major product at 32% yield while diastereomeric *anti*-diol **235** constituted the next most abundant product. Meinwald rearrangement[16] products **236** and **237** were formed in roughly equal amounts, and elimination products **238** and **239** were obtained in the smallest quantities.

*Scheme 5.8 Esterification of **234** and future efforts toward cyanthiwigin–gagunin hybrids **242***

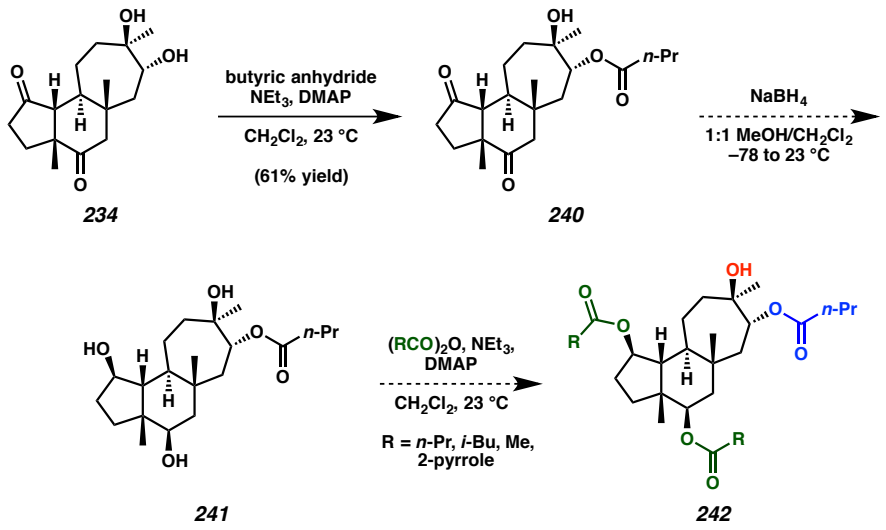

As evidenced by the low selectivity in the epoxide-opening reaction of **233**, further exploration will be required to identify a scalable procedure for the preparation of *anti*-diol **234**. A potential alternative to the two-step sequence outlined in Scheme 5.6 would be a Prévost reaction[17] on tricycle **109** to install the *anti*-diol directly. In the meantime, we have progressed diol **234** to mono-ester **240** using the previously optimized

esterification conditions. Future directions will entail the elaboration of **240** to cyanthiwigin–gagunin hybrids **242** (Scheme 5.8).

5.3 BIOLOGICAL STUDIES

While efforts are currently ongoing toward elucidating the biological properties of the cyanthiwigin–gagunin hybrid molecules, biological evaluation of synthetic intermediates has been initiated through collaboration with investigators at the City of Hope cancer research hospital. Preliminary results indicate that the compounds depicted in Figure 5.5 show no appreciable potency against melanoma cell line A2058 or prostate cancer cell line DU145. Further evaluation of these compounds and other intermediates in addition to the cyanthiwigin–gagunin hybrids (**227a**–**c**) against other cell lines and disease agents will be pursued through collaborations with other biological screening programs (e.g., National Cancer Institute, Eli Lilly and Co.).

Figure 5.5 Compounds sent to the City of Hope for biological testing to date

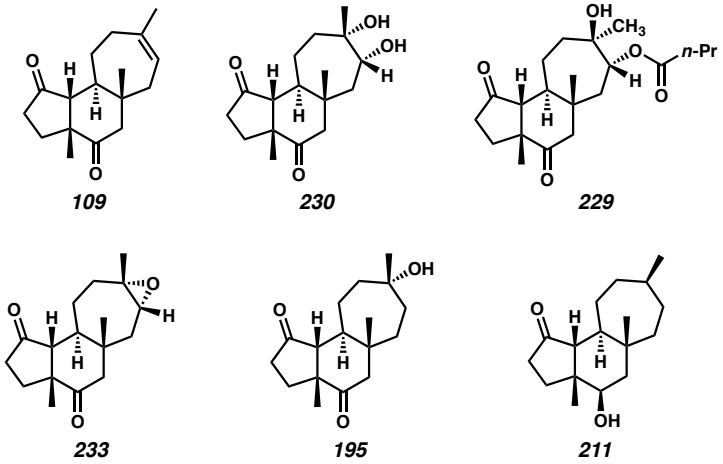

5.4 FUTURE DIRECTIONS

True to the nature of most late-stage diversification research programs, this project is quite open-ended with many avenues for cyanthiwigin–gagunin hybrid synthesis and biological evaluation yet to be explored. For each synthetic route to a hybrid molecule (e.g., *syn*-diol route, *anti*-diol route, etc.), there are nearly infinite combinations of ester functionalities that can be appended to the tricyclic core. Initial investigations have centered around butanoate, acetate, and isovalerate substituents based on their ubiquity among the natural gagunins, but as more insights into the activities of these compounds are generated, the ester functionalities can be re-designed as appropriate.

An alternative synthetic pathway that could be explored in future work involves the manipulation of stereochemistry at the C3 and C8 positions via carbonyl reduction. While SmI_2 and all hydride-based conditions examined (e.g., $NaBH_4$, L-selectride, K-selectride) have delivered exclusively α-face reduction products (i.e., **228**), preliminary results suggest that treatment of **109** with sodium metal in boiling ethanol effects rapid reduction of both carbonyls from the β-face, enabling access to diol **243** (Scheme 5.9), which features C3 and C8 stereochemistry opposite to what is generally observed with hydride reduction (cf. Scheme 5.3).

Notably, however, a drawback of this synthetic route is that carbonyl reduction would need to occur as the first step to avoid later reduction of ester carbonyl moieties under the strongly reducing conditions. Necessarily, this entails an earlier common intermediate for divergence (diol **243**, green box) and consequently a greater number of transformations to be performed in parallel afterwards, beginning with bis-esterification of **243** using various anhydrides (Scheme 5.9). The bis-esterified compounds (**244**)

would then serve as an additional bifurcation point (red box), as addition to the C-ring olefin could be effected through either a *syn* or *anti* pathway, as previously described. Finally, esterification of diols **245** and **246** (blue boxes) using a variety of anhydrides would furnish the hybrid molecules **247** and **248** (Scheme 5.9).

*Scheme 5.9 Future direction: preparation of hybrids **247** and **248** via β-face carbonyl reduction route, with boxes indicating points of divergence*

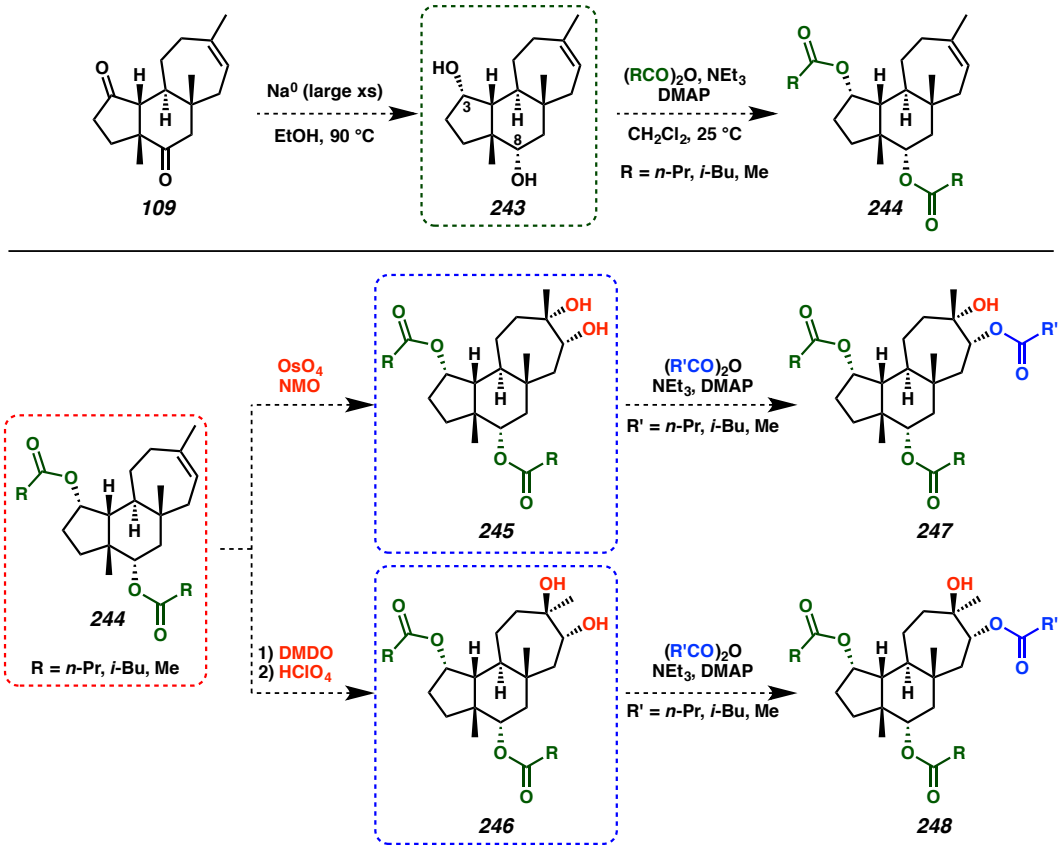

Another opportunity for further exploration involves the installation of an additional ester substituent on the carbocyclic core. Conversion of tricycle **109** to a silyl enol ether (**249**) and subsequent Rubottom oxidation with concurrent epoxidation of the C-ring olefin would afford C2-hydroxylated epoxide **250**, the first point of divergence in the

sequence (blue box, Scheme 5.10). Epoxide rupture followed by esterification using various anhydrides would yield bis-esterified compounds **251** (green box), which could be subjected to hydride reduction and esterfication with an array of anhydrides to generate the tetra-esterified hybrid molecules (**252**). Possessing an additional ester subsituent compared to the previously targeted hybrids (e.g., **227**, **242**, **247**, **248**), these highly oxygenated molecules would provide a unique perspective for biological study.

*Scheme 5.10 Future direction: preparation of hybrids **252** via Rubottom oxidation route*

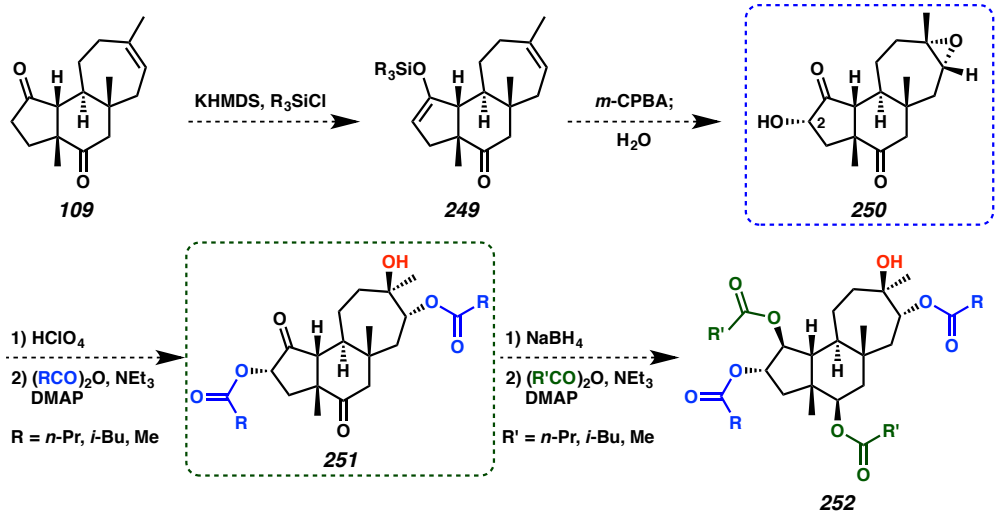

5.5 CONCLUDING REMARKS

These investigations have revealed noteworthy patterns of reactivity in the complex tricyclic framework of the cyanthiwigin natural products. Findings from our studies into the reactivities of the C-ring olefin and the A- and B-ring carbonyls in **109** have enabled us to conclude that the β-face of the molecule is substantially less accessible than the α-face due to steric hindrance originating from the C9 and C6 methyl substituents. We

have prepared three cyanthiwigin–gagunin hybrid molecules (**227a–c**) using a common late-stage intermediate available in three steps from the cyanthiwigin natural product core. These compounds arose through a *syn*-dihydroxylation pathway, and we are currently applying this strategy to the preparation of hybrids from an *anti*-dihydroxylation pathway. Although initial biological studies have not indicated any appreciable cytotoxicity among several synthetic intermediates, evaluation of new compounds, including cyanthiwigin–gagunin hybrids and synthetic intermediates thereto, is underway.

In conclusion, a vast number of compounds are accessible through a multitude of synthetic pathways, including those yet to be examined. We anticipate that the synthetic insights derived from these exploratory studies will provide a strong foundation on which to expand in future efforts toward the synthesis and biological evaluation of non-natural cyanthiwigin–gagunin hybrid molecules.

5.6 EXPERIMENTAL SECTION

5.6.1 MATERIALS AND METHODS

Unless noted in the specific procedure, reactions were performed in flame-dried glassware under argon atmosphere. Dried and deoxygenated solvents (Fisher Scientific) were prepared by passage through columns of activated aluminum before use.[18] Methanol (Fisher Scientific) was distilled from magnesium methoxide immediately prior to use. Commercial reagents (Sigma Aldrich or Alfa Aesar) were used as received. Triethylamine (Oakwood Chemical) was distilled from calcium hydride immediately prior to use. Dimethyldioxirane (DMDO)[19] was prepared according to known procedures immediately prior to use. Brine is defined as a saturated aqueous solution of sodium chloride. Reactions requiring external heat were modulated to the specified temperatures using an IKAmag temperature controller. Reaction progress was monitored by thin-layer chromatography (TLC) or Agilent 1290 UHPLC-LCMS. TLC was performed using E. Merck silica gel 60 F254 precoated plates (0.25 mm) and visualized by UV fluorescence quenching, potassium permanganate, or *p*-anisaldehyde staining. Silia*Flash* P60 Academic Silica gel (particle size 0.040–0.063 mm) was used for flash chromatography. NMR spectra were recorded on a Varian Mercury 300 spectrometer (at 300 MHz for ^{1}H NMR and 75 MHz for ^{13}C NMR), a Varian Inova 500 spectrometer (at 500 MHz for ^{1}H NMR and 126 MHz for ^{13}C NMR), or a Bruker AV III HD spectrometer equipped with a Prodigy liquid nitrogen temperature cryoprobe (at 400 MHz for ^{1}H NMR and 101 MHz for ^{13}C NMR), and are reported in terms of chemical shift relative to residual $CHCl_3$ (δ 7.26 and δ 77.16 ppm, respectively). Data for ^{1}H NMR spectra are reported as follows: chemical shift (δ ppm) (multiplicity, coupling constant (Hz), integration). Abbreviations

are used as follows: s = singlet, bs = broad singlet, d = doublet, t = triplet, q = quartet, m = complex multiplet. Infrared (IR) spectra were recorded on a Perkin Elmer Paragon 1000 spectrometer using thin film samples on KBr plates, and are reported in frequency of absorption (cm^{-1}). High-resolution mass spectra (HRMS) were obtained from the Caltech Mass Spectral Facility using a JEOL JMS-600H High Resolution Mass Spectrometer with fast atom bombardment (FAB+) ionization mode or were acquired using an Agilent 6200 Series TOF with an Agilent G1978A Multimode source in electrospray ionization (ESI+) mode. Optical rotations were measured with a Jasco P-1010 polarimeter at 589 nm using a 100 mm path-length cell.

5.6.2 PREPARATIVE PROCEDURES

5.6.2.1 PREPARATION OF SYN-DIOL-DERIVED HYBRIDS

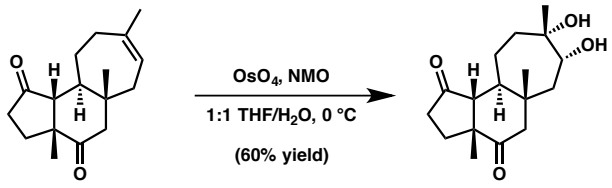

109 *230*
single diastereomer

Tricyclic Diol 230. To a solution of tricyclic diketone **109** (10 mg, 0.0384 mmol, 1.0 equiv) in 1:1 THF/H_2O (3.5 mL total volume) at 0 °C were added NMO (4 wt % solution in H_2O, 50 μL, 8.5 μmol, 0.22 equiv) and osmium tetroxide (50 wt % solution in H_2O, 0.1 mL, 0.410 mmol, 10.7 equiv). The resulting mixture was stirred at 0 °C for 4 hours, after which time TLC analysis showed full consumption of **109**. The reaction was quenched at 0 °C with saturated aq. $Na_2S_2O_3$ and stirred vigorously for 4 hours before

being diluted with dichloromethane (15 mL). The layers were separated, and the aqueous layer was extracted with dichloromethane (2 x 10 mL). The combined organic layers were washed with brine (20 mL) and dried over Na_2SO_4, filtered, and concentrated under reduced pressure. The crude residue was purified by silica gel column chromatography (30% → 50% → 70% → 90% ethyl acetate in hexanes) to afford tricyclic diol **230** as a colorless oil (6.7 mg, 60% yield). R*f* = 0.10 (25% hexanes in ethyl acetate); ^{1}H NMR ($CDCl_3$, 500 MHz) δ 3.62 (d, *J* = 10.1 Hz, 1H), 2.73 (d, *J* = 15.2 Hz, 1H), 2.50 (dd, *J* = 19.6, 10.2 Hz, 1H), 2.35 (dd, *J* = 19.6, 9.5 Hz, 1H), 2.29–2.23 (m, 1H), 2.14 (d, *J* = 16.2 Hz, 1H), 2.05–1.98 (m, 2H), 1.95 (d, *J* = 14.5 Hz, 1H), 1.86 (m, 1H), 1.79 (d, *J* = 11.3 Hz, 1H), 1.76–1.72 (m, 1H), 1.32 (d, *J* = 14.6 Hz, 1H), 1.28 (s, 3H), 1.12 (s, 3H), 1.06–0.98 (m, 1H), 0.82 (s, 3H); ^{13}C NMR ($CDCl_3$, 126 MHz) δ 218.2, 212.4, 74.2, 72.9, 61.2, 53.1, 51.0, 46.6, 45.5, 40.9, 40.1, 34.3, 31.0, 27.9, 21.8, 20.2, 19.3; IR (Neat Film, KBr) 3448 (br), 2961, 2934, 1735, 1702, 1466, 1384, 1176, 1125, 916, 731 cm^{-1}; HRMS (FAB+) *m/z* calc'd for $C_{17}H_{25}O_3$ $[M–OH]^+$: 277.1804, found 277.1804; $[\alpha]^{25}_D$ –225.2 (*c* 1.00, $CHCl_3$).

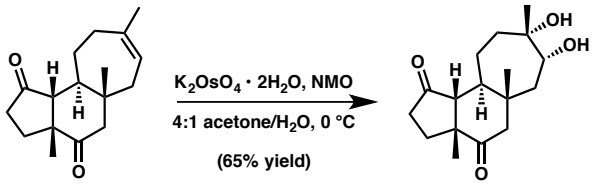

109 ***230***

Dihydroxylation of 109 using Dipotassium Osmate Dihydrate. To a solution of tricyclic diketone **109** (50 mg, 0.192 mmol, 1.0 equiv) in 4:1 acetone/H_2O (10 mL total volume) at 0 °C were added NMO (45.0 mg, 0.384 mmol, 2.0 equiv) and dipotassium osmate dihydrate (7.1 mg, 0.0192 mmol, 0.1 equiv). The resulting mixture was stirred at

0 °C for 7 hours, after which time TLC analysis showed full consumption of **109**. The reaction was quenched with saturated aq. $Na_2S_2O_3$ at 0 °C and stirred vigorously for 30 minutes before being diluted with dichloromethane (15 mL). The layers were separated, and the aqueous layer was extracted with dichloromethane (2 x 10 mL). The combined organic layers were washed with brine (20 mL) and dried over Na_2SO_4, filtered, and concentrated under reduced pressure. The crude residue was purified by silica gel column chromatography (50% → 75% → 100% ethyl acetate in hexanes) to afford tricyclic diol **230** as a colorless oil (36.8 mg, 65% yield).

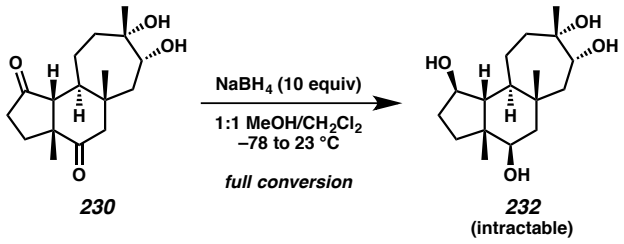

230 ***232*** **(intractable)**

Sodium Borohydride Reduction of 230. To a solution of diol **230** (5.7 mg, 0.0194 mmol, 1.0 equiv) in 1:1 CH_2Cl_2/MeOH (2.0 mL total volume) was added a solution of sodium borohydride (7.3 mg, 0.194 mmol, 10.0 equiv) in 1:1 CH_2Cl_2/MeOH (0.5 mL total volume) at –78 °C. The reaction mixture was allowed to warm to 23 °C over the course of six hours. When TLC analysis indicated full consumption of starting material, the reaction was quenched with acetone (1.0 mL) and 2N NaOH (1.0 mL). The phases were separated, and the organic layer was immediately washed with brine (10 mL) and dried over sodium sulfate. After filtration and concentration under reduced pressure, the crude residue was subjected to silica gel column chromatography (100% ethyl acetate), but tetra-hydroxylated compound **232** was not obtained.

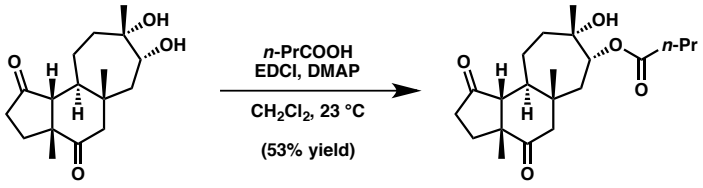

230
single diastereomer

229

Tricyclic Monoester 229. To a solution of diol **230** (6.7 mg, 0.0228 mmol, 1.0 equiv) in dichloromethane (1.0 mL) at 23 °C were added EDCI (6.5 mg, 0.0342 mmol, 1.5 equiv), DMAP (2.8 mg, 0.0228 mmol, 1.0 equiv), and butyric acid (3.2 μL, 0.0342 mmol, 1.5 equiv). The resulting mixture was stirred at 23 °C for 24 hours, after which time the reaction was diluted with ethyl acetate (5 mL) and washed with 0.5 M HCl (3 mL), sat. aq. $NaHCO_3$ (3 mL), and brine (3 mL). The combined organics were dried over Na_2SO_4, filtered, and concentrated, and the crude residue was purified by silica gel column chromatography (15% → 25% → 35% → 55% ethyl acetate in hexanes) to afford monoester **229** as a colorless oil (4.4 mg, 53% yield). R*f* = 0.33 (25% hexanes in ethyl acetate); ^{1}H NMR ($CDCl_3$, 500 MHz) δ 4.86 (d, *J* = 10.6 Hz, 1H), 2.55 (d, *J* = 15.1 Hz, 1H), 2.53–2.46 (m, 1H), 2.41–2.34 (m, 1H), 2.32 (t, *J* = 7.4 Hz, 2H), 2.27–2.17 (m, 2H), 2.14 (d, *J* = 15.2 Hz, 1H), 2.07–2.01 (m, 1H), 2.01–1.95 (m, 1H), 1.88 (d, *J* = 12.6 Hz, 1H), 1.79–1.73 (m, 1H), 1.70–1.64 (m, 3H), 1.55 (m, 1H), 1.20 (s, 3H), 1.17 (d, *J* = 14.3 Hz, 1H), 1.14 (s, 3H), 1.13–1.07 (m, 1H), 0.94 (t, *J* = 7.4, 14.8 Hz, 3H), 0.95 (s, 3H); ^{13}C NMR ($CDCl_3$, 126 MHz) δ 218.0, 211.8, 172.7, 74.6, 73.5, 61.1, 52.6, 50.9, 47.4, 43.3, 40.2, 40.0, 36.5, 34.3, 31.1, 28.6, 21.8, 20.2, 18.6, 18.0, 13.8 ; IR (Neat Film, KBr) 3503 (br), 2964, 2934, 2875, 1735, 1705, 1458, 1379, 1258, 1177, 988, 732 cm^{-1};

HRMS (FAB+) *m/z* calc'd for $C_{21}H_{31}O_4$ $[M–OH]^+$: 347.2222, found 347.2229; $[\alpha]^{25}_D$ – 277.4 (*c* 1.00, $CHCl_3$).

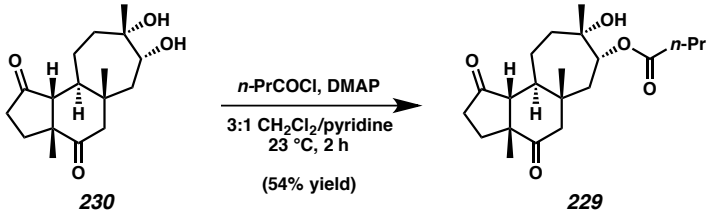

230 ***229***

Esterification of 230 using Butyryl Chloride. To a solution of diol **230** (30.0 mg, 0.102 mmol, 1.0 equiv) in 3:1 CH_2Cl_2/pyridine (4.0 mL total volume) at 23 °C were added butyryl chloride (53 μL, 0.510 mmol, 5.0 equiv) and DMAP (12.5 mg, 0.102 mmol, 1.0 equiv). The resulting mixture was stirred at 23 °C for 2 hours, after which time the reaction was cooled to 0 °C and quenched with H_2O (5.0 mL) and saturated aq. NH_4Cl (5.0 mL), then extracted with ethyl acetate (2 x 10 mL). The combined organics were washed with brine, dried over Na_2SO_4, filtered, and concentrated in vacuo. The crude residue was purified by silica gel column chromatography (15% → 30% → 45% ethyl acetate in hexanes) to afford monoester **229** as a colorless oil (20.2 mg, 54% yield).

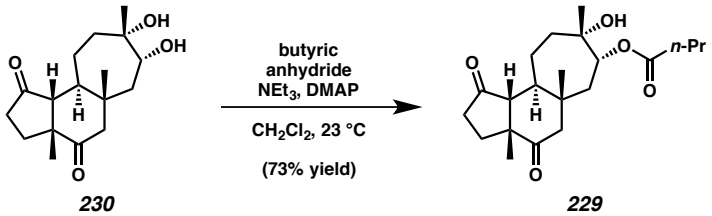

230 ***229***

Esterification of 230 using Butyric Anhydride. To a solution of diol **230** (36.8 mg, 0.125 mmol, 1.0 equiv) in dichloromethane (6.5 mL) was added triethylamine (70 μL, 0.500 mmol, 4.0 equiv), butyric anhydride (60 μL, 0.375 mmol, 3.0 equiv), and DMAP

(7.6 mg, 0.0625 mmol, 0.5 equiv) at 23 °C. The resulting mixture was stirred for 1 hour, after which time TLC analysis indicated full consumption of **230**. The reaction was diluted with dichloromethane (10 mL) and washed with water (2 x 20 mL). The organic layer was dried over $MgSO_4$, filtered, and concentrated under reduced pressure, and the resulting crude residue was purified by silica gel column chromatography (25% → 40% → 60% ethyl acetate in hexanes) to afford monoester **229** as a colorless oil (33.3 mg, 73% yield).

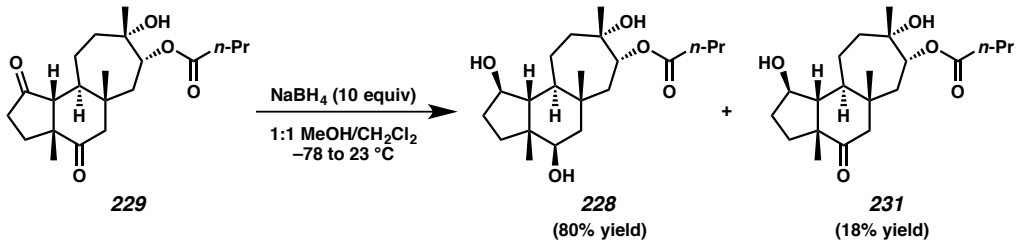

229 ***228*** (80% yield) ***231*** (18% yield)

Tris-hydroxylated Tricycle 228. To a solution of diketone **229** (31.0 mg, 0.0851 mmol, 1.0 equiv) in dichloromethane (2.0 mL) and methanol (2.0 mL) was added a solution of sodium borohydride (32.2 mg, 0.851 mmol, 10.0 equiv) in dichloromethane (1.0 mL) and methanol (1.0 mL) at –78 °C. The reaction mixture was allowed to warm to 23 °C over the course of 6 hours. When TLC analysis indicated full consumption of starting material, the reaction was quenched with acetone (2.0 mL) and 2N NaOH (2.0 mL). The phases were separated, and the organic layer was immediately washed with brine (10 mL) and dried over sodium sulfate. After filtration and concentration under reduced pressure, the crude residue was purified by silica gel column chromatography (15% ethyl acetate in hexanes), furnishing triol **228** (25.0 mg, 80% yield) and diol **231**

(5.6 mg, 18% yield). **Triol 228:** R*f* = 0.19 (25% hexanes in ethyl acetate); ^{1}H NMR ($CDCl_3$, 400 MHz) δ 4.87 (dd, *J* = 11.1, 2.5 Hz, 1H), 4.01 (td, *J* = 6.2, 2.9 Hz, 1H), 3.69 (dd, *J* = 8.7, 5.8 Hz, 1H), 2.31 (t, *J* = 7.4 Hz, 2H), 2.06–1.99 (m, 1H), 1.99–1.95 (m, 1H), 1.94–1.88 (m, 1H), 1.84–1.78 (m, 1H), 1.73–1.62 (m, 6H), 1.60 (m, 1H), 1.53–1.50 (m, 2H), 1.38–1.35 (m, 1H), 1.34–1.32 (m, 1H), 1.26–1.23 (m, 1H), 1.18 (s, 3H), 1.13 (s, 3H), 1.12 (s, 3H), 0.96 (t, *J* = 7.4 Hz, 3H); ^{13}C NMR ($CDCl_3$, 101 MHz) δ 172.8, 80.5, 76.4, 74.2, 73.3, 57.6, 46.4, 45.9, 45.7, 45.1, 39.3, 37.5, 36.6, 35.0, 33.4, 29.6, 23.2, 22.5, 21.5, 18.7, 13.9; IR (Neat Film, KBr) 3402 (br), 2933, 2874, 1715, 1463, 1384, 1307, 1263, 1196, 1097, 1032, 916, 732 cm^{-1}; HRMS (ESI+) *m/z* calc'd for $C_{21}H_{36}O_5K$ $[M+K]^+$: 407.2194, found 407.2196; $[\alpha]^{25}_D$ –20.7 (*c* 1.00, $CHCl_3$). **Diol 231:** R*f* = 0.25 (25% hexanes in ethyl acetate); ^{1}H NMR ($CDCl_3$, 400 MHz) δ 4.90 (d, *J* = 10.7 Hz, 1H), 4.19 (t, *J* = 5.3, 2.1 Hz, 1H), 2.35–2.26 (m, 4H), 2.14–2.06 (m, 3H), 1.81–1.76 (m, 2H), 1.75–1.71 (m, 1H), 1.70–1.65 (m, 3H), 1.63–1.59 (m, 2H), 1.31 (s, 3H), 1.27–1.24 (m, 2H), 1.22 (s, 3H), 1.18–1.13 (m, 1H), 0.96 (t, *J* = 7.1, 14.8 Hz, 3H), 0.95 (s, 3H); ^{13}C NMR ($CDCl_3$, 101 MHz) δ 214.7, 172.7, 80.5, 74.8, 73.7, 60.5, 53.7, 53.1, 52.5, 43.3, 40.7, 38.3, 36.9, 36.6, 34.5, 28.8, 23.9, 22.6, 18.6, 18.2, 13.8; IR (Neat Film, KBr) 3443 (br), 2964, 2934, 1731, 1694, 1463, 1384, 1264, 1190, 1140, 1030, 992, 920, 732 cm^{-1}; HRMS (FAB+) *m/z* calc'd for $C_{21}H_{35}O_5$ $[M+H]^+$: 367.2484, found 367.2471; $[\alpha]^{25}_D$ –21.9 (*c* 1.21, $CHCl_3$).

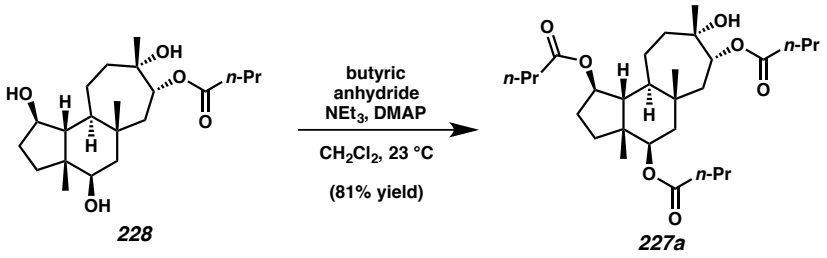

Cyanthiwigin–Gagunin Hybrid 227a. To a solution of tricyclic triol **228** (10.2 mg, 0.0277 mmol, 1.0 equiv) in dichloromethane (2.0 mL) was added triethylamine (30 μL, 0.222 mmol, 8.0 equiv), butyric anhydride (30 μL, 0.166 mmol, 6.0 equiv), and DMAP (3.4 mg, 0.0277 mmol, 1.0 equiv) at 23 °C. The resulting mixture was stirred for 2 hours, after which time TLC analysis indicated full consumption of **228**. The reaction was diluted with dichloromethane (5 mL) and washed with water (2 x 10 mL). The organic layer was dried over $MgSO_4$, filtered, and concentrated under reduced pressure, and the resulting crude residue was purified by silica gel column chromatography (10% → 40% → 60% ethyl acetate in hexanes) to afford cyanthiwigin–gagunin hybrid **227a** as a colorless oil (11.4 mg, 81% yield). Rf = 0.16 (20% ethyl acetate in hexanes); ^{1}H NMR ($CDCl_3$, 500 MHz) δ 5.10–5.06 (m, 1H), 4.95–4.89 (m, 2H), 2.32–2.29 (m, 2H), 2.28–2.23 (m, 4H), 2.01 (ddd, J = 14.9, 7.4, 3.1 Hz, 1H), 1.94 (dd, J = 13.9, 10.9 Hz, 1H), 1.88–1.82 (m, 1H), 1.74–1.69 (m, 2H), 1.69–1.61 (m, 8H), 1.59 (d, J = 4.3 Hz, 1H), 1.56–1.51 (m, 3H), 1.24 (m, 2H), 1.19 (s, 3H), 1.11 (s, 3H), 1.08 (s, 3H), 1.06–1.01 (m, 1H), 0.99–0.92 (m, 9H); ^{13}C NMR ($CDCl_3$, 126 MHz) δ 173.2, 173.2, 172.8, 81.4, 75.7, 74.0, 73.9, 53.5, 46.8, 45.1, 44.4, 41.9, 40.6, 36.9, 36.8, 36.6, 36.1, 34.6, 29.5, 29.5, 23.7, 22.8, 19.2, 18.6, 18.6, 18.5, 13.9, 13.8 (x2); IR (Neat Film, KBr) 3506 (br), 2966, 2936, 2876, 1731, 1461, 1384, 1258, 1184, 1144, 1092, 981 cm^{-1}; HRMS (FAB+) *m/z* calc'd for $C_{29}H_{49}O_7$ $[M+H]^+$: 509.3478, found 509.3464; $[\alpha]^{25}_D$ –11.4 (*c* 1.14, $CHCl_3$).

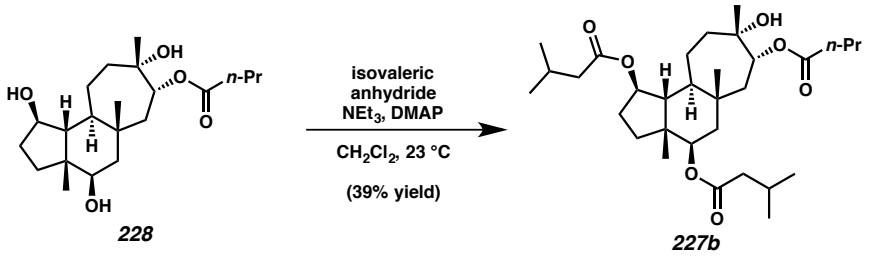

Cyanthiwigin–Gagunin Hybrid 227b. To a solution of tricyclic triol **228** (5.4 mg, 0.0147 mmol, 1.0 equiv) in dichloromethane (1.0 mL) was added triethylamine (16 μL, 0.118 mmol, 8.0 equiv), isovaleric anhydride (17 μL, 0.0879 mmol, 6.0 equiv), and DMAP (1.8 mg, 0.0147 mmol, 1.0 equiv) at 23 °C. The resulting mixture was stirred for 1 hour, after which time TLC analysis indicated full consumption of **228**. The reaction was diluted with dichloromethane (5 mL) and washed with water (2 x 10 mL). The organic layer was dried over $MgSO_4$, filtered, and concentrated under reduced pressure, and the resulting crude residue was purified by silica gel column chromatography (10% → 30% ethyl acetate in hexanes) to afford cyanthiwigin–gagunin **227b** as a colorless oil (3.1 mg, 39% yield): R*f* = 0.70 (50% ethyl acetate in hexanes); ^{1}H NMR ($CDCl_3$, 500 MHz) δ 5.11–5.08 (m, 1H), 4.98–4.91 (m, 2H), 2.32 (t, *J* = 7.4, 14.8 Hz, 2H), 2.27–2.21 (m, 1H), 2.21 (s, 1H), 2.20–2.16 (m, 4H), 2.16–2.08 (dddd, *J* = 12.9, 9.5, 8.1, 6.3 Hz, 2H), 2.05–1.99 (m, 1H), 1.96 (dd, *J* = 14.0, 11.0 Hz, 1H), 1.85 (m, 1H), 1.83 (s, 1H), 1.74–1.71 (m, 1H), 1.71–1.67 (m, 2H), 1.66–1.60 (m, 2H), 1.57–1.52 (m, 2H), 1.31–1.28 (m, 1H), 1.28–1.23 (m, 2H), 1.21 (s, 3H), 1.12 (s, 3H), 1.10 (s, 3H), 1.00–0.95 (m, 15H); ^{13}C NMR ($CDCl_3$, 126 MHz) δ 172.8, 172.7, 172.7, 81.3, 75.7, 74.0, 73.9, 53.5, 46.6, 45.1, 44.4, 44.2, 44.0, 42.0, 40.5, 36.6, 36.2, 34.7, 29.6, 29.5, 25.9, 25.7, 23.8, 22.9, 22.7, 22.7, 22.6, 22.6, 19.3, 18.7, 13.9; IR (Neat Film, KBr) 3499 (br), 2961, 2874, 1731, 1466,

1384, 1294, 1257, 1189, 1120, 1095, 990 cm^{-1}; HRMS (ESI+) *m/z* calc'd for $C_{31}H_{51}O_6$ $[M–OH]^+$: 519.3686, found 519.3700; $[\alpha]^{25}_D$ –13.7 (*c* 0.31, $CHCl_3$).

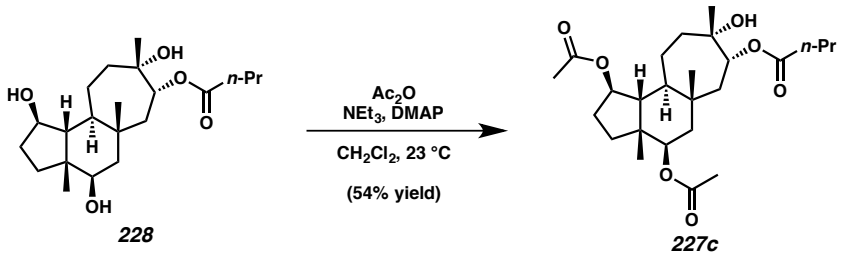

Cyanthiwigin–Gagunin Hybrid 227c. To a solution of tricyclic triol **228** (7.0 mg, 0.0190 mmol, 1.0 equiv) in dichloromethane (2.0 mL) was added triethylamine (21 μL, 0.152 mmol, 8.0 equiv), acetic anhydride (11 μL, 0.114 mmol, 6.0 equiv), and DMAP (2.3 mg, 0.0190 mmol, 1.0 equiv) at 23 °C. The resulting mixture was stirred for 1 hour, after which time TLC analysis indicated full consumption of **228**. The reaction was diluted with dichloromethane (5 mL) and washed with water (2 x 10 mL). The organic layer was dried over $MgSO_4$, filtered, and concentrated under reduced pressure, and the resulting crude residue was purified by silica gel column chromatography (20% → 40% ethyl acetate in hexanes) to afford cyanthiwigin–gagunin **227c** as a colorless oil (4.5 mg, 54% yield): R*f* = 0.56 (40% hexanes in ethyl acetate); ^{1}H NMR ($CDCl_3$, 500 MHz) δ 5.08–5.05 (m, 1H), 4.93 (dd, *J* = 10.9, 1.8 Hz, 1H), 4.89 (t, *J* = 4.1 Hz, 1H), 2.31 (t, *J* = 7.4 Hz, 2H), 2.26–2.17 (m, 1H), 2.04 (s, 3H), 2.03 (s, 3H), 2.02–1.98 (m, 1H), 1.94 (dd, *J* = 13.9, 10.9 Hz, 1H), 1.81 (s, 1H), 1.75–1.70 (m, 2H), 1.69–1.65 (m, 2H), 1.64–1.60 (m, 1H), 1.59–1.52 (m, 4H), 1.26–1.22 (m, 2H), 1.20 (s, 3H), 1.12 (s, 3H), 1.09 (s, 3H), 1.05 (ddd, *J* = 11.9, 9.7, 1.7 Hz, 1H), 0.97 (t, *J* = 7.4 Hz, 3H); ^{13}C NMR ($CDCl_3$, 126 MHz) δ 172.8, 170.7, 170.6, 81.6, 75.7, 74.3, 74.0, 53.4, 46.8, 45.0, 44.4, 41.8, 40.6, 36.6, 36.1,

34.7, 29.5, 29.5, 23.6, 22.9, 21.6, 21.5, 19.2, 18.7, 13.9; IR (Neat Film, KBr) 3457 (br), 2966, 2934, 2877, 1732, 1463, 1384, 1245, 1184, 1145, 1022, 982, 908 cm^{-1}; HRMS (FAB+) *m/z* calc'd for $C_{25}H_{41}O_7$ $[M+H]^+$: 453.2852, found 453.2835; $[\alpha]^{25}_D$ –12.3 (*c* 0.42, $CHCl_3$).

5.6.2.2 PREPARATION OF ANTI-DIOL-DERIVED INTERMEDIATES

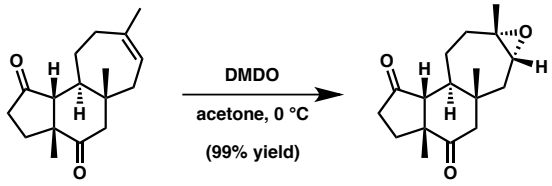

109 ***233***
single diastereomer

Epoxide 233. To a solution of tricyclic diketone **109** (50.0 mg, 0.192 mmol, 1.0 equiv) in acetone (2.0 mL) at 0 °C was added a solution of DMDO (0.0125M in acetone, 16.9 mL, 0.211 mmol, 1.1 equiv). The resulting mixture was stirred at 0 °C for 90 minutes, after which time the volatiles were removed under reduced pressure, affording epoxide **233** as a pale yellow oil (52.0 mg, 99% yield). This material was used without further purification. R*f* = 0.36 (50% ethyl acetate in hexanes); ^{1}H NMR ($CDCl_3$, 500 MHz) δ 2.72 (t, *J* = 7.5, 14.4 Hz, 1H), 2.65 (d, *J* = 14.7 Hz, 1H), 2.52 (dddd, *J* = 19.5, 10.3, 2.0, 0.9 Hz, 1H), 2.37 (dddd, *J* = 19.4, 10.2, 9.1, 1.2 Hz, 1H), 2.30–2.22 (m, 1H), 2.12 (td, *J* = 7.3, 2.8 Hz, 1H), 2.07 (d, *J* = 14.8 Hz, 1H), 2.05–1.94 (m, 2H), 1.90 (d, *J* = 12.2 Hz, 1H), 1.80–1.73 (m, 1H), 1.66 (ddd, *J* = 12.3, 11.1, 2.8 Hz, 1H), 1.55–1.48 (m, 1H), 1.45–1.37 (m, 1H), 1.33 (s, 3H), 1.30–1.24 (m, 1H), 1.11 (s, 3H), 0.88 (s, 3H); ^{13}C NMR ($CDCl_3$, 126 MHz) δ 217.7, 211.9, 62.5, 60.3, 59.3, 52.2, 50.7, 47.4, 43.8, 41.8,

34.4, 34.3, 31.3, 23.9, 22.2, 21.7, 17.0; IR (Neat Film, KBr) 2958, 2932, 1736, 1705, 1466, 1383, 1171, 1007, 875, 735 cm^{-1}; HRMS (ESI+) *m/z* calc'd for $C_{17}H_{25}O_3$ $[M+H]^+$: 277.1798, found 277.1789; $[\alpha]^{25}_D$ –68.4 (*c* 0.12, $CHCl_3$).

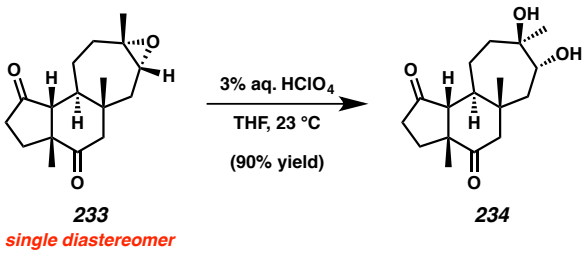

Anti Diol 234. To a solution of epoxide **233** (5.0 mg, 0.0181 mmol, 1.0 equiv) in THF (1.0 mL) at 23 °C was added perchloric acid (3 wt % solution in H_2O, 20 μL, 5.43 μmol, 0.3 equiv). The resulting mixture was stirred at 23 °C for 72 hours, after which time the reaction was diluted with ethyl acetate (5 mL) and washed with sat. aq. $NaHCO_3$ (5 mL), and brine (5 mL). The combined organics were dried over $MgSO_4$, filtered, and concentrated, and the crude residue was purified by silica gel column chromatography (30% → 40% → 50% → 60% → 75% ethyl acetate in hexanes) to afford monoester **234** as a colorless oil (4.8 mg, 90% yield). R*f* = 0.10 (25% hexanes in ethyl acetate); ^{1}H NMR ($CDCl_3$, 600 MHz) δ 3.88 (d, *J* = 10.1 Hz, 1H), 2.66 (d, *J* = 15.0 Hz, 1H), 2.53–2.44 (m, 1H), 2.41–2.33 (m, 1H), 2.27–2.21 (m, 1H), 2.16 (d, *J* = 15.0 Hz, 1H), 1.97–1.88 (m, 3H), 1.78–1.74 (m, 1H), 1.70–1.66 (m, 1H), 1.65 (m, 1H), 1.51 (m, 1H), 1.43 (m, 2H), 1.22 (s, 3H), 1.13 (s, 3H), 0.90 (s, 3H); ^{13}C NMR ($CDCl_3$, 126 MHz) δ 217.9, 212.2, 75.9, 74.1, 61.4, 52.9, 51.0, 46.5, 46.0, 41.8, 40.0, 34.3, 31.0, 24.5, 21.8, 19.9, 19.1; IR (Neat Film, KBr) 3444 (br), 2959, 2933, 1735, 1702, 1464, 1385, 1176, 1085,

992, 735 cm^{-1}; HRMS (EI+) *m/z* calc'd for $C_{17}H_{27}O_4$ $[M+H]^+$: 295.1909, found 295.1887; $[\alpha]^{25}_D$ –48.1 (*c* 1.62, $CHCl_3$).

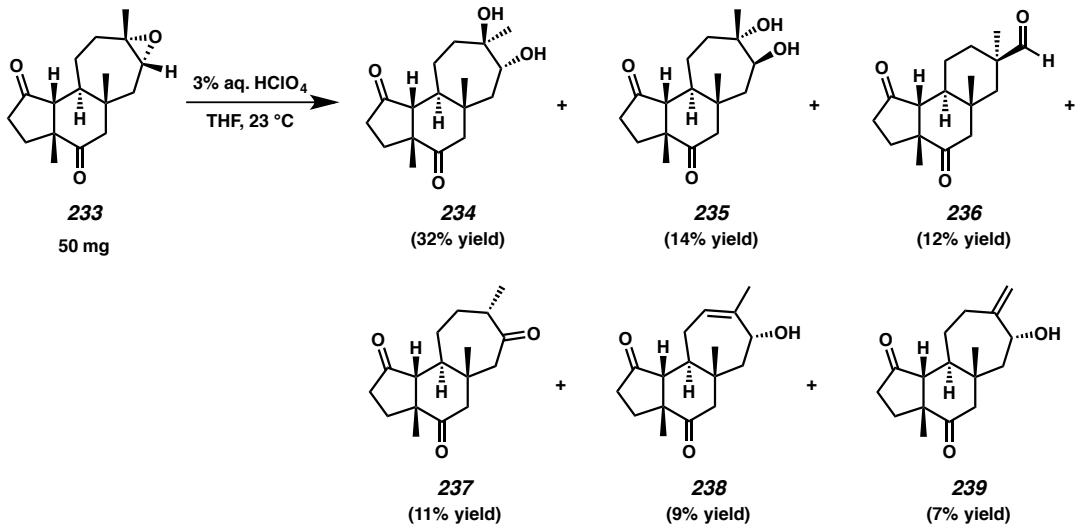

Epoxide-Opening Products 234–239. To a solution of epoxide **233** (47.2 mg, 0.171 mmol, 1.0 equiv) in THF (8.5 mL) at 23 °C was added perchloric acid (3 wt % solution in H_2O, 0.17 mL, 0.0512 mmol, 0.3 equiv). The resulting mixture was stirred at 23 °C for 72 hours, after which time the reaction was diluted with ethyl acetate (10 mL) and washed with sat. aq. $NaHCO_3$ (10 mL), and brine (10 mL). The combined organics were dried over $MgSO_4$, filtered, and concentrated, and the crude residue was purified by silica gel column chromatography (30% → 50% → 60% → 75% → 100% ethyl acetate in hexanes) to afford diol **234** (16.3 mg, 32% yield) along with side products **235**–**239**. Yields and chacaterization data for **235**–**239** are listed below.

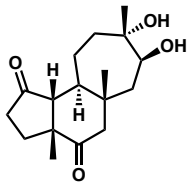

235

Diol 235: 7.2 mg, 14% yield. R*f* = 0.15 (25% hexanes in ethyl acetate); ^{1}H NMR ($CDCl_3$, 400 MHz) δ 3.85 (d, *J* = 10.3 Hz, 1H), 2.86 (d, *J* = 15.8 Hz, 1H), 2.60 (d, *J* = 6.7 Hz, 1H), 2.40–2.33 (m, 2H), 2.17 (d, *J* = 16.1 Hz, 1H), 2.08–2.04 (m, 1H), 1.96–1.91 (m, 2H), 1.86–1.83 (m, 1H), 1.73 (m, 1H), 1.60–1.54 (m, 1H), 1.51–1.46 (m, 2H), 1.29–1.27 (m, 1H), 1.20 (s, 3H), 1.19 (s, 3H), 1.08 (s, 3H); ^{13}C NMR ($CDCl_3$, 101 MHz) δ 221.7, 214.9, 75.8, 73.8, 60.1, 50.1, 49.0, 46.5, 44.9, 42.2, 39.8, 37.2, 32.4, 30.6, 24.8, 24.0, 21.5; IR (Neat Film, KBr) 3451 (br), 2958, 2932, 1737, 1704, 1455, 1384, 1268, 1169, 1147, 1087, 1070, 1036, 735 cm^{-1}; HRMS (EI+) *m/z* calc'd for $C_{17}H_{27}O_4$ $[M+H]^+$: 295.1909, found 295.1938; $[\alpha]^{25}_{D}$ –6.3 (*c* 0.72, $CHCl_3$).

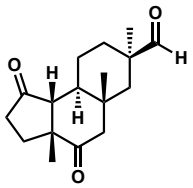

236

Aldehyde 236: 5.5 mg, 12% yield. R*f* = 0.65 (25% hexanes in ethyl acetate); ^{1}H NMR ($CDCl_3$, 500 MHz) δ 9.49 (d, *J* = 1.5 Hz, 1H), 2.52–2.46 (m, 2H), 2.42–2.36 (m, 1H), 2.35–2.30 (m, 1H), 2.29–2.23 (m, 2H), 2.19 (d, *J* = 14.8 Hz, 1H), 1.97 (dd, *J* = 14.2, 2.4 Hz, 1H), 1.88–1.83 (m, 2H), 1.81–1.75 (m, 1H), 1.54 (m, 1H), 1.23–1.17 (m, 1H), 1.12 (s, 3H), 1.11–1.07 (m, 1H), 0.94 (s, 3H), 0.64 (s, 3H); ^{13}C NMR ($CDCl_3$, 126 MHz) δ 217.2, 211.5, 205.0, 61.0, 52.4, 51.3, 48.4, 45.9, 41.3, 39.0, 34.3, 31.8, 31.3, 25.0, 21.8,

21.8, 18.4; IR (Neat Film, KBr) 2957, 2931, 1738, 1704 (overlapping peaks), 1456, 1384, 1135, 839 cm^{-1}; HRMS (EI+) *m/z* calc'd for $C_{17}H_{25}O_3$ $[M+H]^+$: 277.1804, found 277.1819; $[\alpha]^{25}_D$ –41.5 (*c* 0.55, $CHCl_3$).

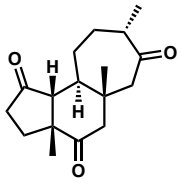

237

Triketone 237: 5.2 mg, 11% yield. R*f* = 0.50 (25% hexanes in ethyl acetate); ^1H NMR ($CDCl_3$, 400 MHz) δ 2.80 (d, *J* = 11.7 Hz, 1H), 2.74 (d, *J* = 15.0 Hz, 1H), 2.53 (dddd, *J* = 19.4, 10.3, 2.0, 0.8 Hz, 1H), 2.42 (m, 1H), 2.38–2.34 (m, 1H), 2.34–2.29 (m, 1H), 2.28–2.24 (m, 1H), 2.16–2.10 (m, 2H), 2.01–1.89 (m, 2H), 1.82–1.75 (m, 2H), 1.38–1.30 (m, 1H), 1.25–1.19 (m, 1H), 1.13 (s, 3H), 1.07 (d, *J* = 7.1 Hz, 3H), 0.76 (s, 3H); ^{13}C NMR ($CDCl_3$, 101 MHz) δ 217.6, 214.4, 211.4, 61.4, 54.2, 52.2, 50.9, 48.3, 46.5, 40.3, 34.3, 32.6, 31.2, 25.7, 21.7, 19.0, 18.6; IR (Neat Film, KBr) 2960, 2930, 1738, 1704 (overlapping peaks), 1456, 1384, 1222, 1176, 1053 cm^{-1}; HRMS (EI+) *m/z* calc'd for $C_{17}H_{25}O_3$ $[M+H]^+$: 277.1804, found 277.1814; $[\alpha]^{25}_D$ –5.4 (*c* 0.52, $CHCl_3$).

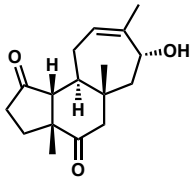

238

Allylic Alcohol 238: 4.3 mg, 9% yield. R*f* = 0.37 (25% hexanes in ethyl acetate); ^1H NMR ($CDCl_3$, 400 MHz) δ 5.56–5.51 (m, 1H), 4.52 (d, *J* = 9.5 Hz, 1H), 2.93 (d, *J* = 14.9

Hz, 1H), 2.56–2.48 (m, 1H), 2.43–2.30 (m, 3H), 2.10 (d, *J* = 14.7 Hz, 1H), 1.97–1.90 (m, 2H), 1.87 (m, 1H), 1.77 (s, 3H), 1.75–1.69 (m, 2H), 1.58–1.54 (m, 1H), 1.11 (s, 3H), 0.92 (s, 3H); ^{13}C NMR ($CDCl_3$, 101 MHz) δ 218.2, 212.3, 143.1, 124.7, 69.6, 61.1, 52.9, 51.5, 49.1, 41.7, 41.6, 34.4, 31.1, 24.3, 21.7, 20.7, 19.6; IR (Neat Film, KBr) 3453 (br), 2960, 2923, 1737, 1704, 1462, 1384, 1164, 1124, 1051, 1002, 890, 735 cm^{-1}; HRMS (EI+) *m/z* calc'd for $C_{17}H_{25}O_3$ $[M+H]^+$: 277.1804, found 277.1796; $[\alpha]^{25}_D$ –46.1 (*c* 0.43, $CHCl_3$).

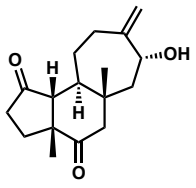

239

Allylic Alcohol 239: 3.4 mg, 7% yield. R*f* = 0.31 (25% hexanes in ethyl acetate); ^{1}H NMR ($CDCl_3$, 400 MHz) δ 5.05 (s, 1H), 4.97 (s, 1H), 4.31 (dd, *J* = 10.1, 5.5 Hz, 1H), 2.71 (d, *J* = 14.6 Hz, 1H), 2.60–2.49 (m, 1H), 2.43–2.22 (m, 5H), 2.09 (d, *J* = 14.6 Hz, 1H), 1.89–1.81 (m, 1H), 1.80–1.71 (m, 4H), 1.22 (m, 1H), 1.10 (s, 3H), 0.80 (s, 3H); ^{13}C NMR ($CDCl_3$, 101 MHz) δ 217.8, 212.3, 153.6, 113.6, 71.1, 62.6, 53.0, 50.9, 49.1, 45.1, 41.1, 34.4, 31.3 (x2), 28.9, 21.7, 17.3; IR (Neat Film, KBr) 3437 (br), 2928, 2871, 1732, 1704, 1455, 1384, 1262, 1165, 1019, 995, 905 cm^{-1}; HRMS (EI+) *m/z* calc'd for $C_{17}H_{25}O_3$ $[M+H]^+$: 277.1804, found 277.1803; $[\alpha]^{25}_D$ –47.6 (*c* 0.34, $CHCl_3$).

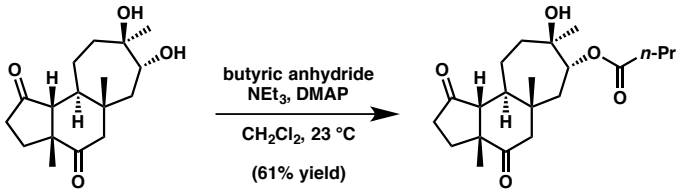

234 ***240***

Monoester 240. To a solution of diol **234** (13.0 mg, 0.0442 mmol, 1.0 equiv) in dichloromethane (4.0 mL) was added triethylamine (25 μL, 0.177 mmol, 4.0 equiv), butyric anhydride (22 μL, 0.132 mmol, 3.0 equiv), and DMAP (2.7 mg, 0.0221 mmol, 0.5 equiv) at 23 °C. The resulting mixture was stirred for 30 minutes, after which time TLC analysis indicated full consumption of **234**. The reaction was diluted with dichloromethane (5 mL) and washed with water (2 x 10 mL). The organic layer was dried over $MgSO_4$, filtered, and concentrated under reduced pressure, and the resulting crude residue was purified by silica gel column chromatography (10% → 30% → 50% ethyl acetate in hexanes) to afford monoester **240** as a colorless oil (9.8 mg, 61% yield). R*f* = 0.30 (50% ethyl acetate in hexanes); ^{1}H NMR ($CDCl_3$, 500 MHz) δ 4.99 (d, *J* = 10.7 Hz, 1H), 2.55 (d, *J* = 15.0 Hz, 1H), 2.52–2.44 (m, 1H), 2.41–2.34 (m, 1H), 2.33 (t, *J* = 7.4 Hz, 2H), 2.21 (m, 1H), 2.13 (d, *J* = 15.1 Hz, 1H), 2.00–1.88 (m, 3H), 1.82–1.72 (m, 2H), 1.67 (q, *J* = 7.5 Hz, 2H), 1.61 (m, 1H), 1.50–1.37 (m, 3H), 1.14 (s, 3H), 1.14 (s, 3H), 0.96 (t, *J* = 7.4 Hz, 3H), 0.94 (s, 3H); ^{13}C NMR ($CDCl_3$, 126 MHz) δ 217.7, 211.8, 174.4, 78.5, 75.1, 60.9, 52.7, 51.0, 47.2, 44.4, 41.6, 40.1, 36.6, 34.3, 31.1, 25.5, 21.8, 19.6, 18.6, 18.5, 13.8; IR (Neat Film, KBr) 3459 (br), 2963, 2933, 1732, 1705, 1463, 1456, 1380, 1260, 1177, 1086, 985 cm^{-1}; HRMS (ESI+) *m/z* calc'd for $C_{21}H_{31}O_4$ $[M–OH]^+$: 347.2217, found 347.2218; $[\alpha]^{25}_D$ –44.4 (*c* 0.26, $CHCl_3$).

5.7 NOTES AND REFERENCES

(1) Green, D.; Goldberg, I.; Stein, Z.; Ilan, M.; Kashman, Y. *Nat. Prod. Lett.* **1992**, *1*, 193–199.

(2) (a) Peng, J.; Walsh, K.; Weedman, V.; Bergthold, J. D.; Lynch, J.; Lieu, K. L.; Braude, I. A.; Kelly, M.; Hamann, M. T. *Tetrahedron* **2002**, *58*, 7809–7819; (b) Peng, J.; Avery, M. A.; Hamann, M. T. *Org. Lett.* **2003**, *5*, 4575–4578; (c) Peng, J.; Kasanah, N.; Stanley, C. E.; Chadwick, J.; Fronczek, F. R.; Hamann, M. T. *J. Nat. Prod.* **2006**, *69*, 727–730.

(3) (a) Obara, Y.; Nakahata, N.; Kita, T.; Takaya, Y.; Kobayashi, H.; Hosoi, S.; Kiuchi, F.; Ohta, T.; Oshima, Y.; Ohizumi, Y. *Eur. J. Pharmacol.* **1999**, *370*, 79–84; (b) Obara, Y.; Kobayashi, H.; Ohta, T.; Ohizumi, Y.; Nakahata, N. *Mol. Pharmacol.* **2001**, *59*, 1287–1297.

(4) Enquist, J. A., Jr.; Stoltz, B. M. *Nat. Prod. Rep.* **2009**, *26*, 661–680.

(5) Pfeiffer, M. W. B.; Phillips, A. J. *J. Am. Chem. Soc.* **2005**, *127*, 5334–5335.

(6) Pfeiffer, M. W. B.; Phillips, A. J. *Tetrahedron Lett.* **2008**, *49*, 6860–6861.

(7) Reddy, T. J.; Bordeau, G.; Trimble, L. *Org. Lett.* **2006**, *8*, 5585–5588.

(8) Enquist, J. A., Jr.; Stoltz, B. M. *Nature* **2008**, *453*, 1228–1231.

(9) Enquist, J. A., Jr.; Virgil, S. C.; Stoltz, B. M. *Chem.–Eur. J.* **2011**, *17*, 9957–9969.

(10) (a) Rho, J.-R.; Lee, H.-S.; Sim, C. J.; Shin, J. *Tetrahedron* **2002**, *58*, 9585–9591; (b) Jang, K. H.; Jeon, J.; Ryu, S.; Lee, H.-S.; Oh, K.-B.; Shin, J. *J. Nat. Prod.* **2008**, *71*, 1701–1707.

(11) Shibuya, G. M.; Enquist, J. A., Jr.; Stoltz, B. M. *Org. Lett.* **2013**, *15*, 3480–3483.

(12) Kim, K. E.; Stoltz, B. M. *Org. Lett.* **2016**, *18*, 5720–5723.

(13) Fatta-Kassinos, D.; Vasquez, M. I.; Kümmerer, K. *Chemosphere* **2011**, *85*, 693–709.

(14) For details on these investigations, see Chapter 4.

(15) Bürgi, H. B.; Dunitz, J. D.; Lehn, J. M.; Wipff, G. *Tetrahedron* **1974**, *30*, 1563–1572.

(16) Meinwald, J.; Labana, S. S.; Chadha, M. S. *J. Am. Chem. Soc.* **1963**, *85*, 582–585.

(17) Emmanuvel, L; Shaikh, T. M. A.; Sudalai, A. *Org. Lett.* **2005**, *7*, 5071–5074.

(18) Pangborn, A. B.; Giardello, M. A.; Grubbs, R. H.; Rosen, R. K.; Timmers, F. J. *Organometallics* **1996**, *15*, 1518–1520.

(19) Taber, D. F.; DeMatteo, P. W.; Hassan, R. A. *Org. Synth.* **2013**, *90*, 350–357.

APPENDIX 10

Synthetic Summary for Cyanthiwigin–Gagunin Hybrid Preparation

Scheme A10.1 Synthesis of diversification intermediate ***228*** *through a syn-dihydroxylation pathway*

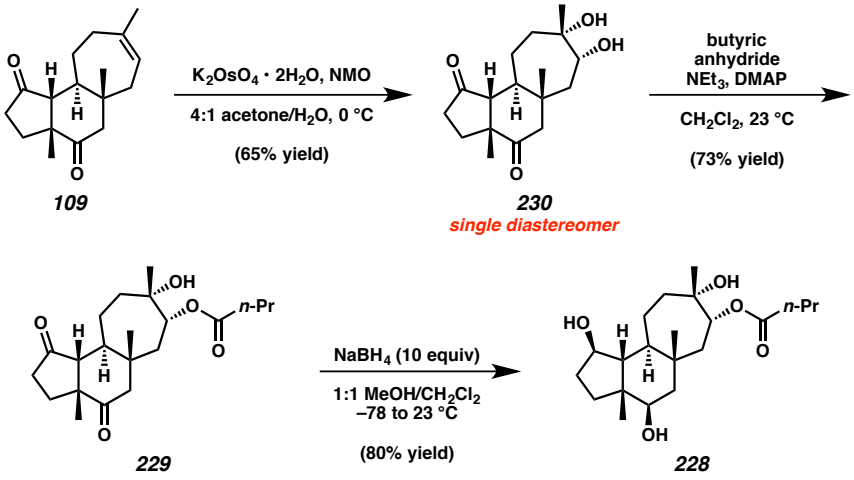

Scheme A10.2 Synthesis of cyanthiwigin–gagunin hybrids ***227a–c*** *from common intermediate* ***228***

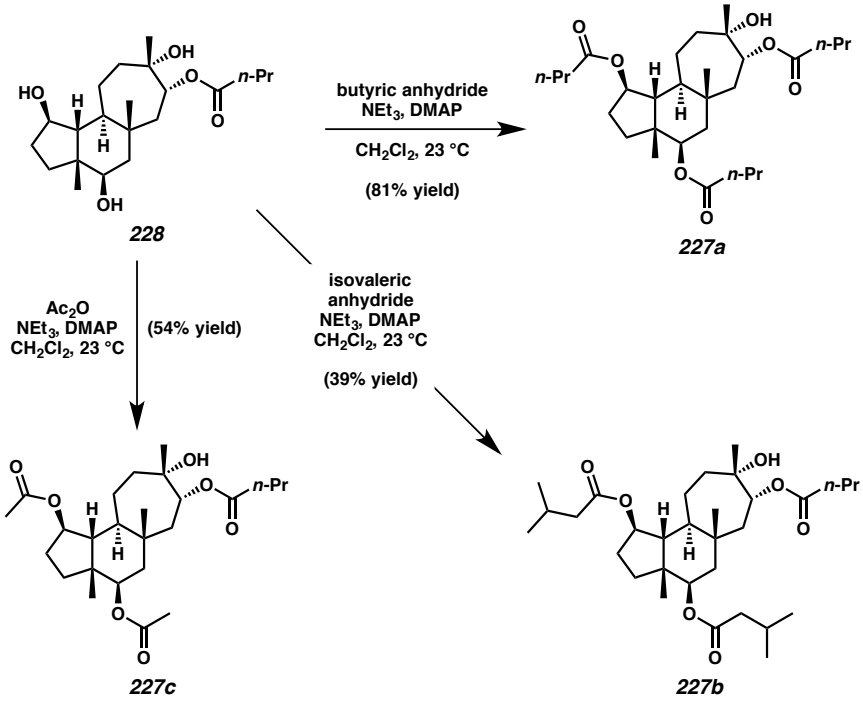

*Scheme A10.3 Progress toward hybrids **242** through an anti-dihydroxylation route*

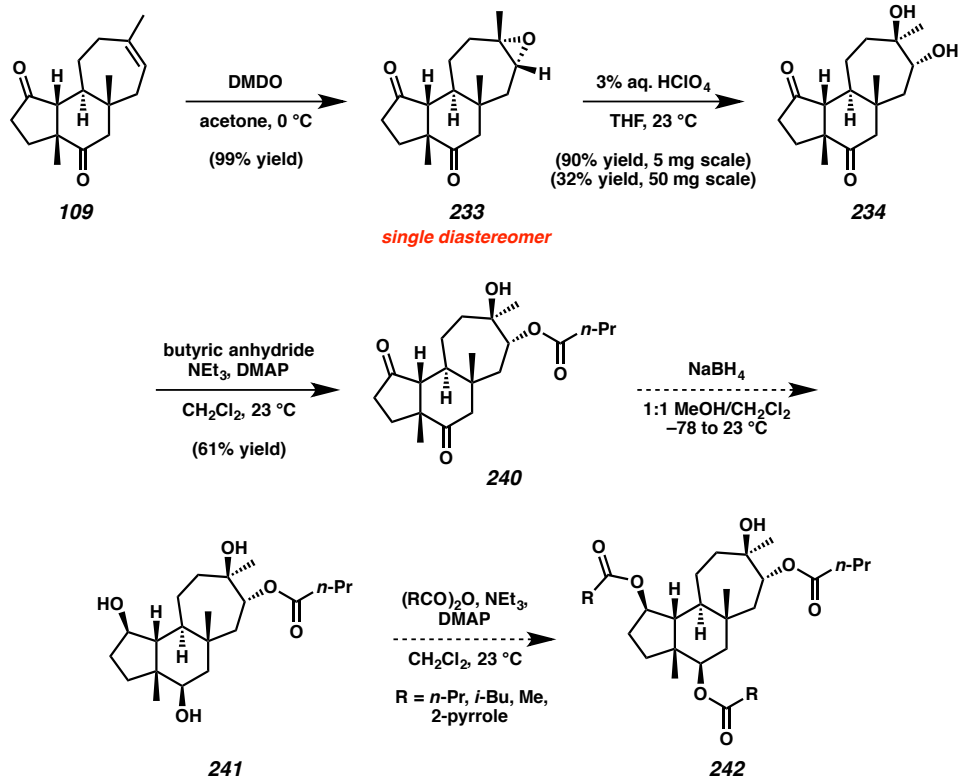

APPENDIX 11

Spectra Relevant to Chapter 5:

Synthesis of Non-natural Cyanthiwigin–Gagunin Hybrids through

Late-Stage Diversification of the the Cyanthiwigin Natural Product Core

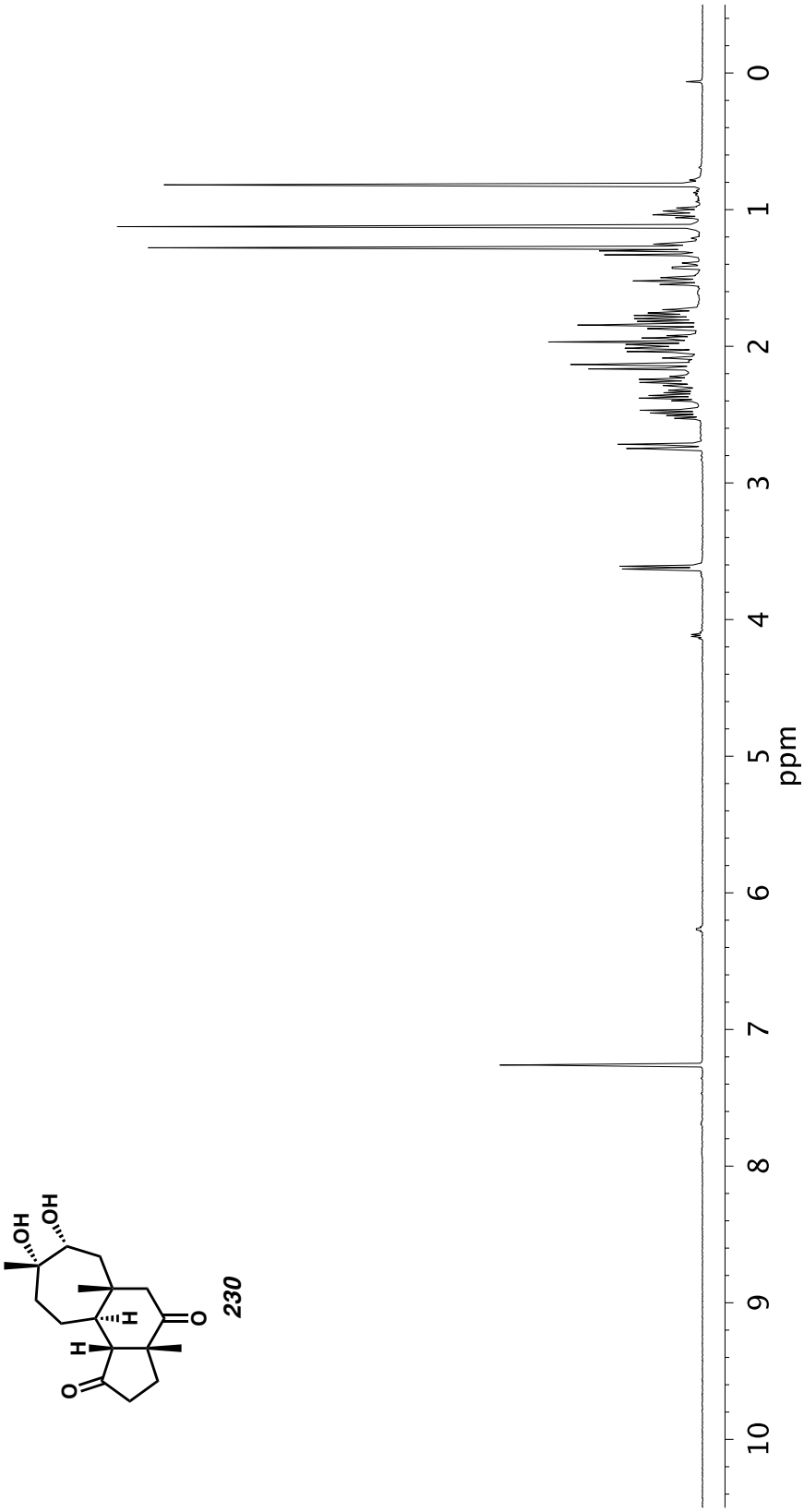

Figure A11.1. ^{1}H NMR (500 MHz, $CDCl_3$) of compound **230**.

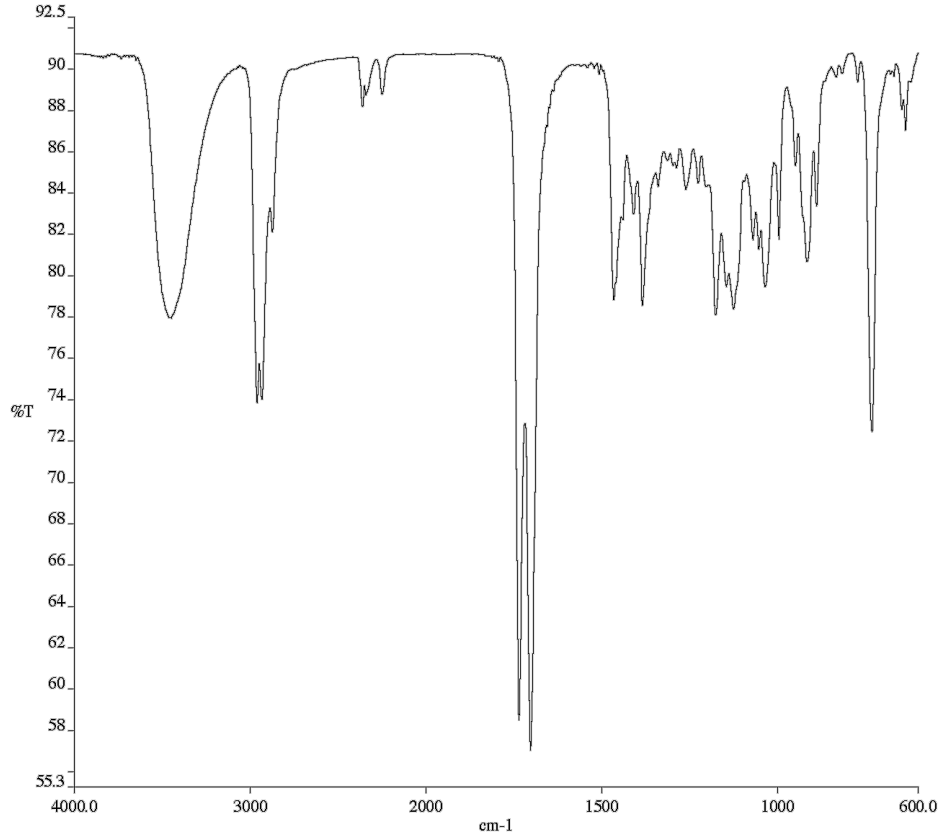

Figure A11.2. Infrared spectrum (Thin Film, KBr) of compound **230**.

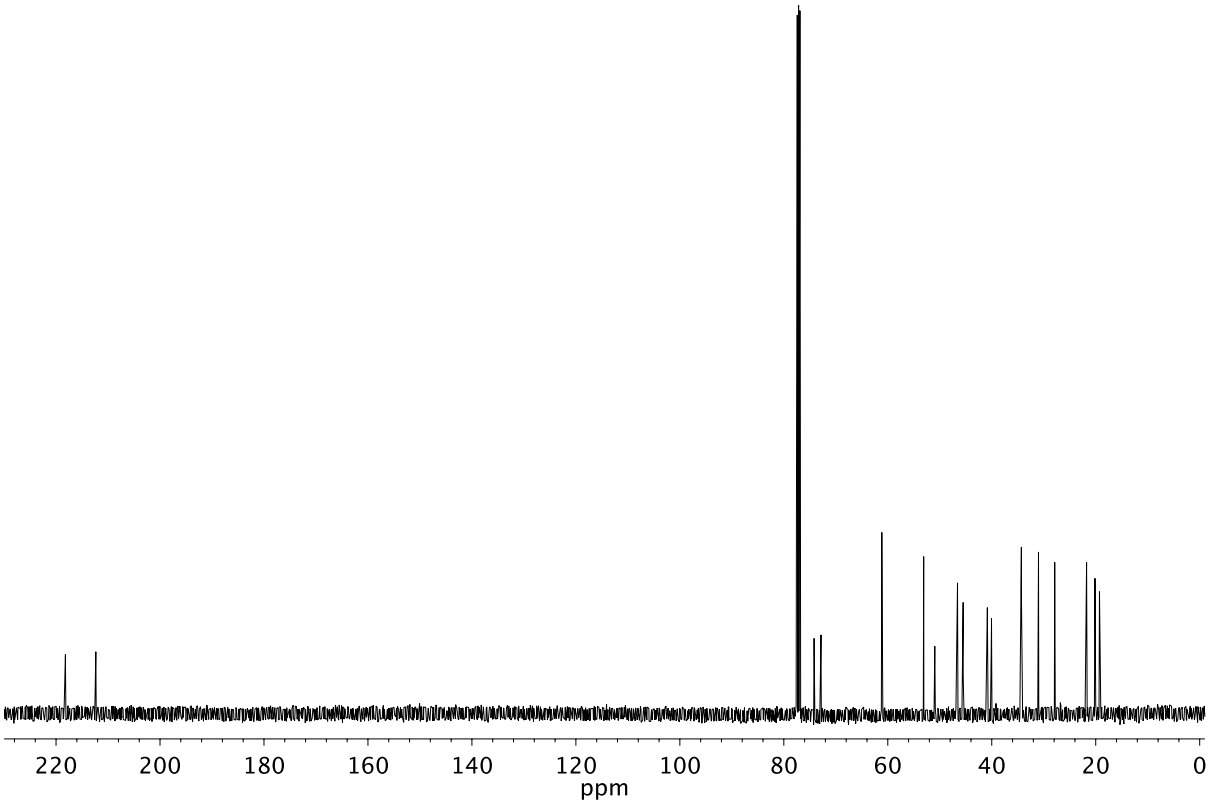

Figure A11.3. ^{13}C NMR (126 MHz, $CDCl_3$) of compound **230**.

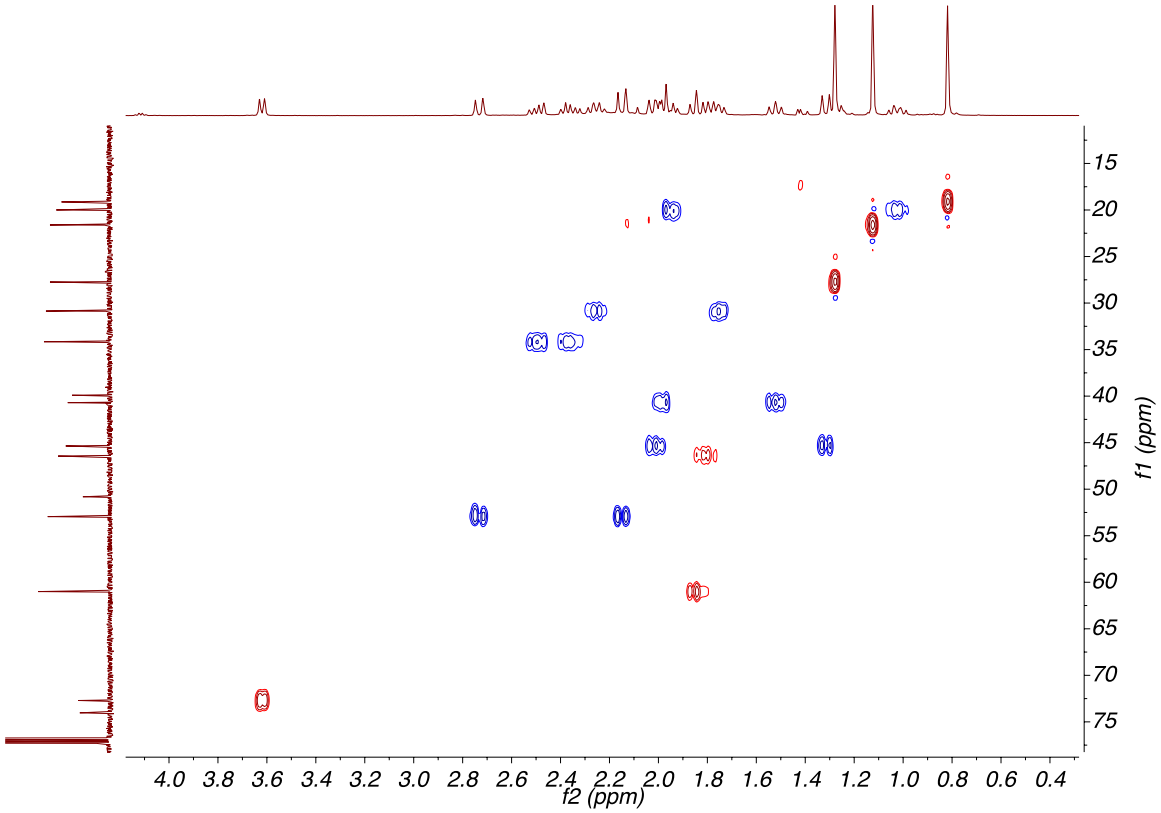

Figure A11.4. HSQC (500, 126 MHz, $CDCl_3$) of compound **230**.

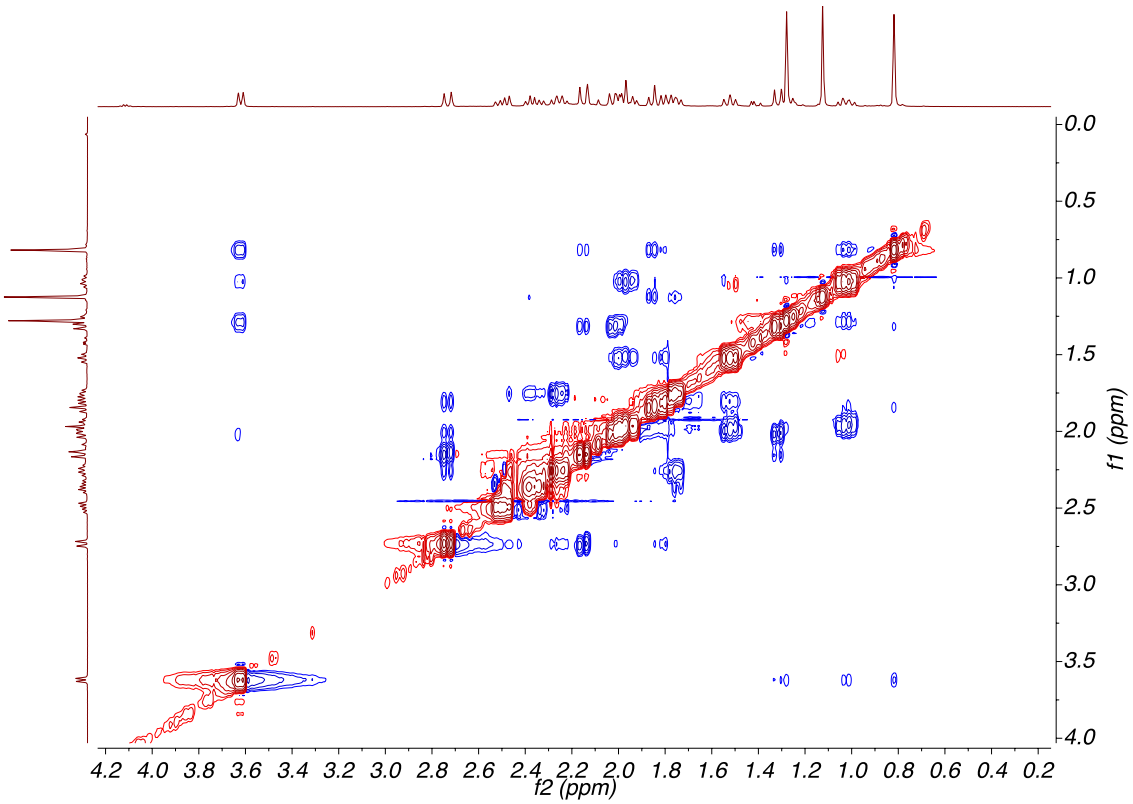

Figure A11.5. NOESY (500 MHz, $CDCl_3$) of compound **230**.

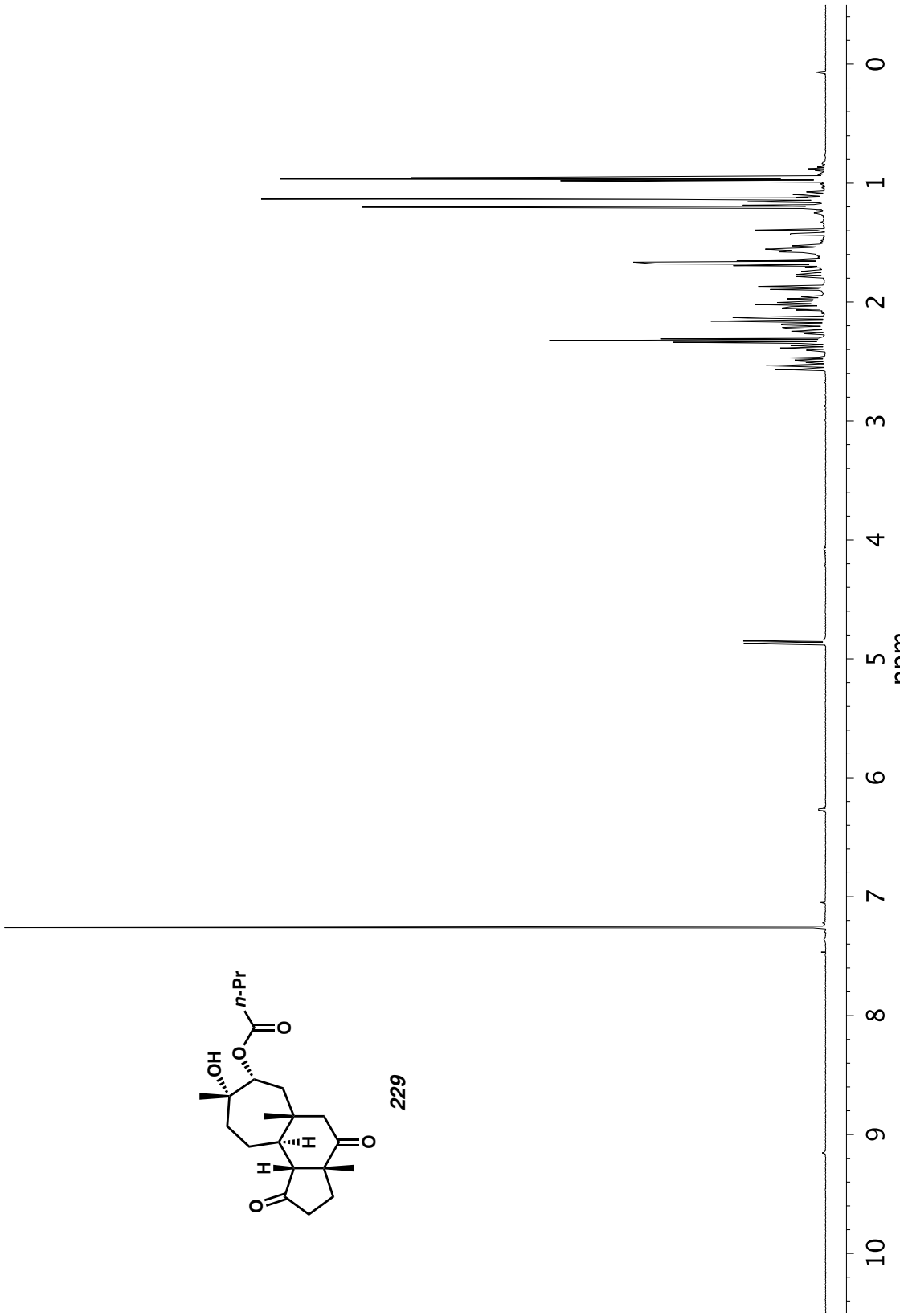

Figure A11.6. ^{1}H NMR (500 MHz, $CDCl_3$) of compound **229**.

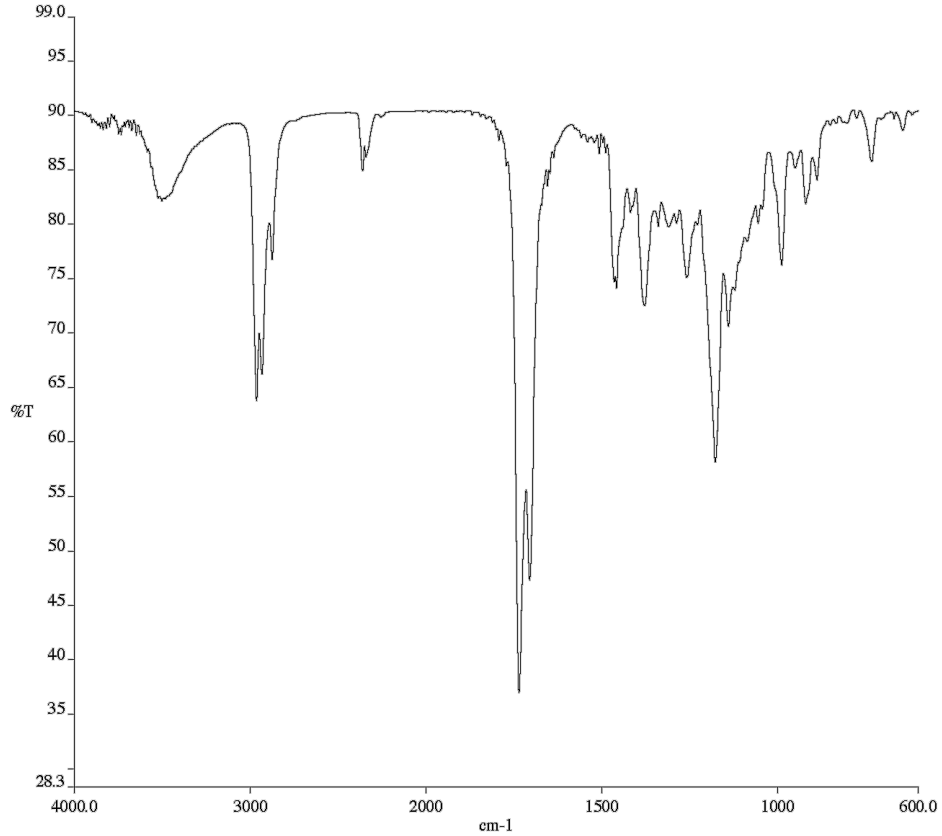

Figure 11.7. Infrared Spectrum (Thin Film, KBr) of compound **229**.

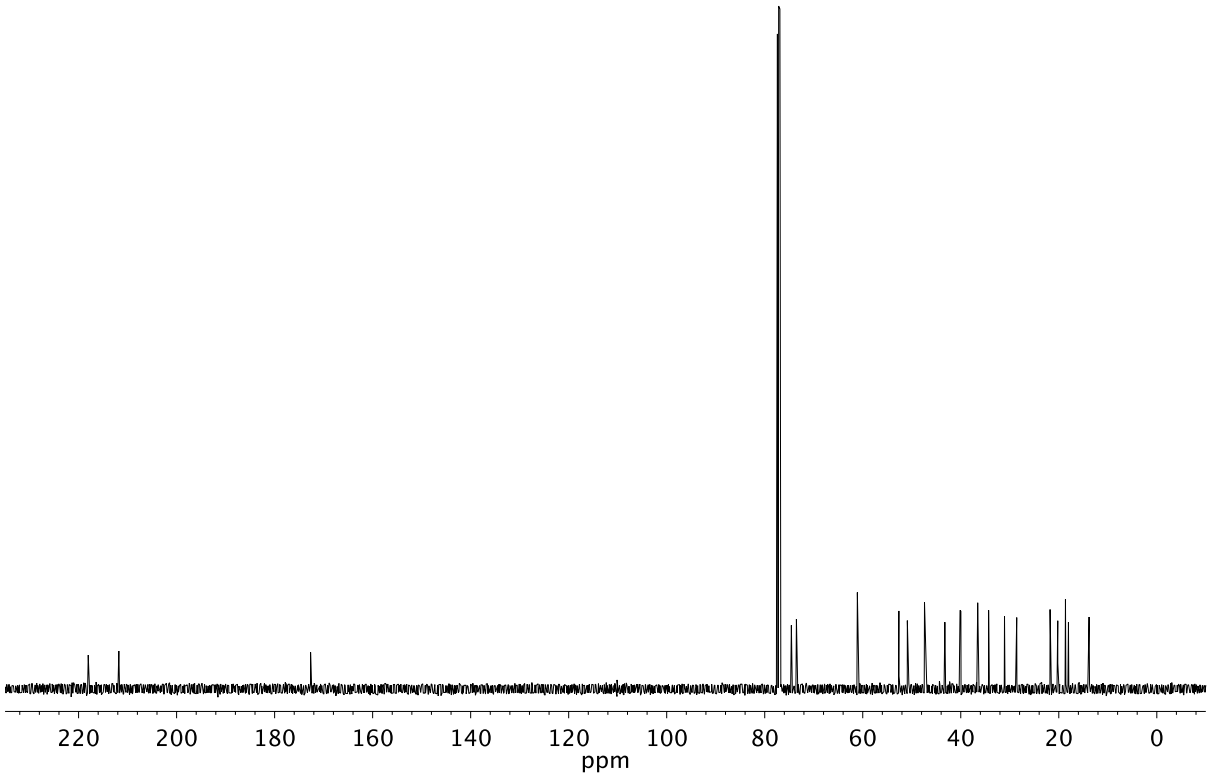

Figure A11.8. ^{13}C NMR (126 MHz, $CDCl_3$) of compound **229**.

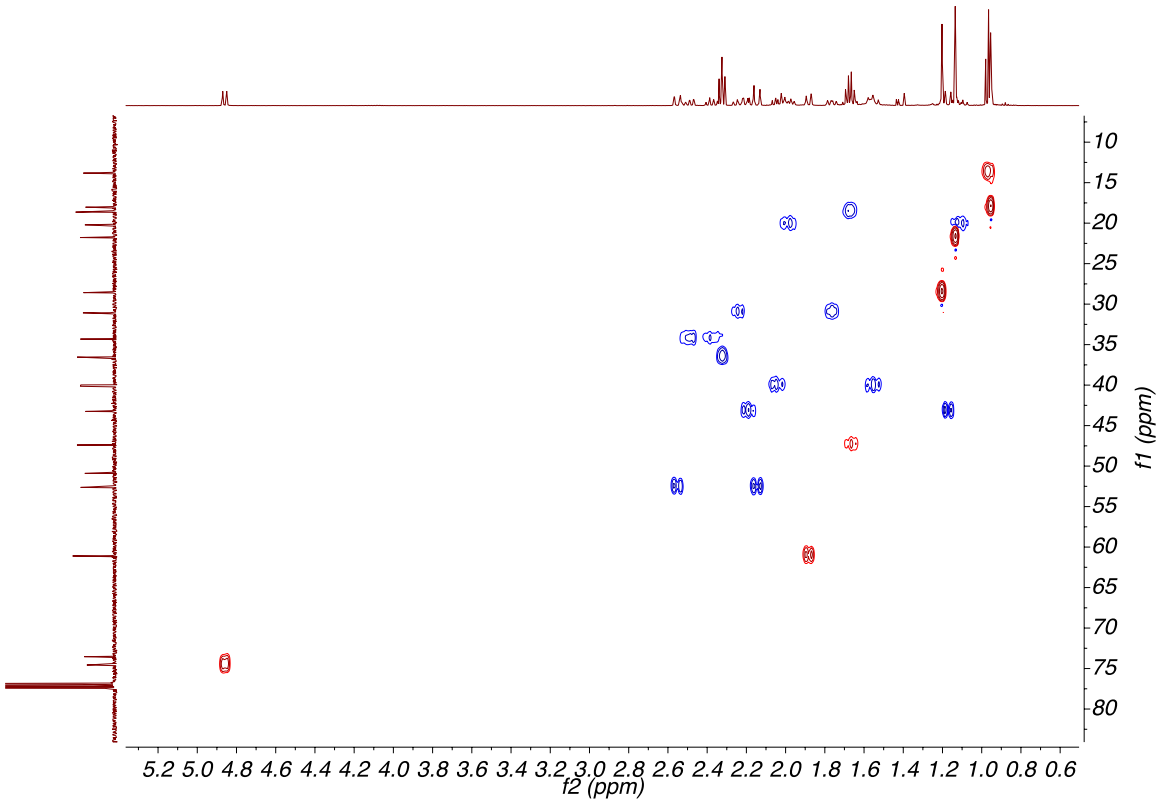

Figure A11.9. HSQC (500, 126 MHz, $CDCl_3$) of compound **229**.

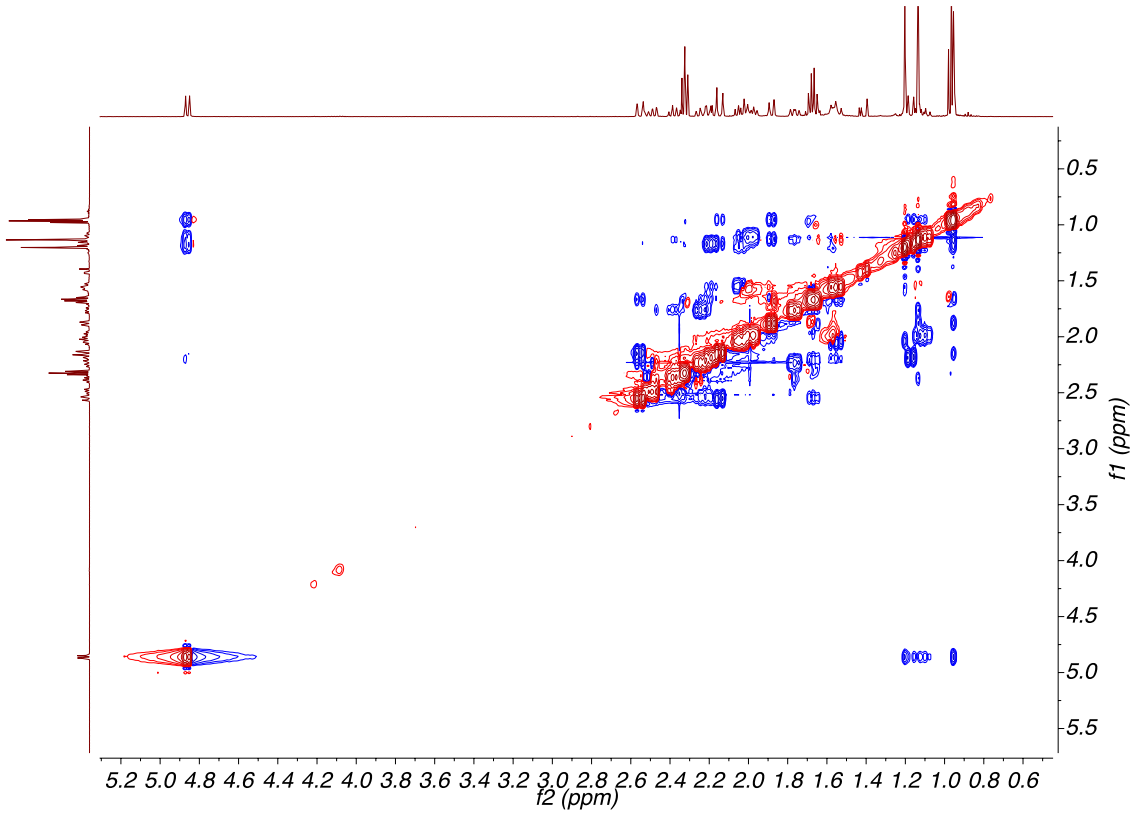

Figure A11.10. NOESY (500 MHz, $CDCl_3$) of compound **229**.

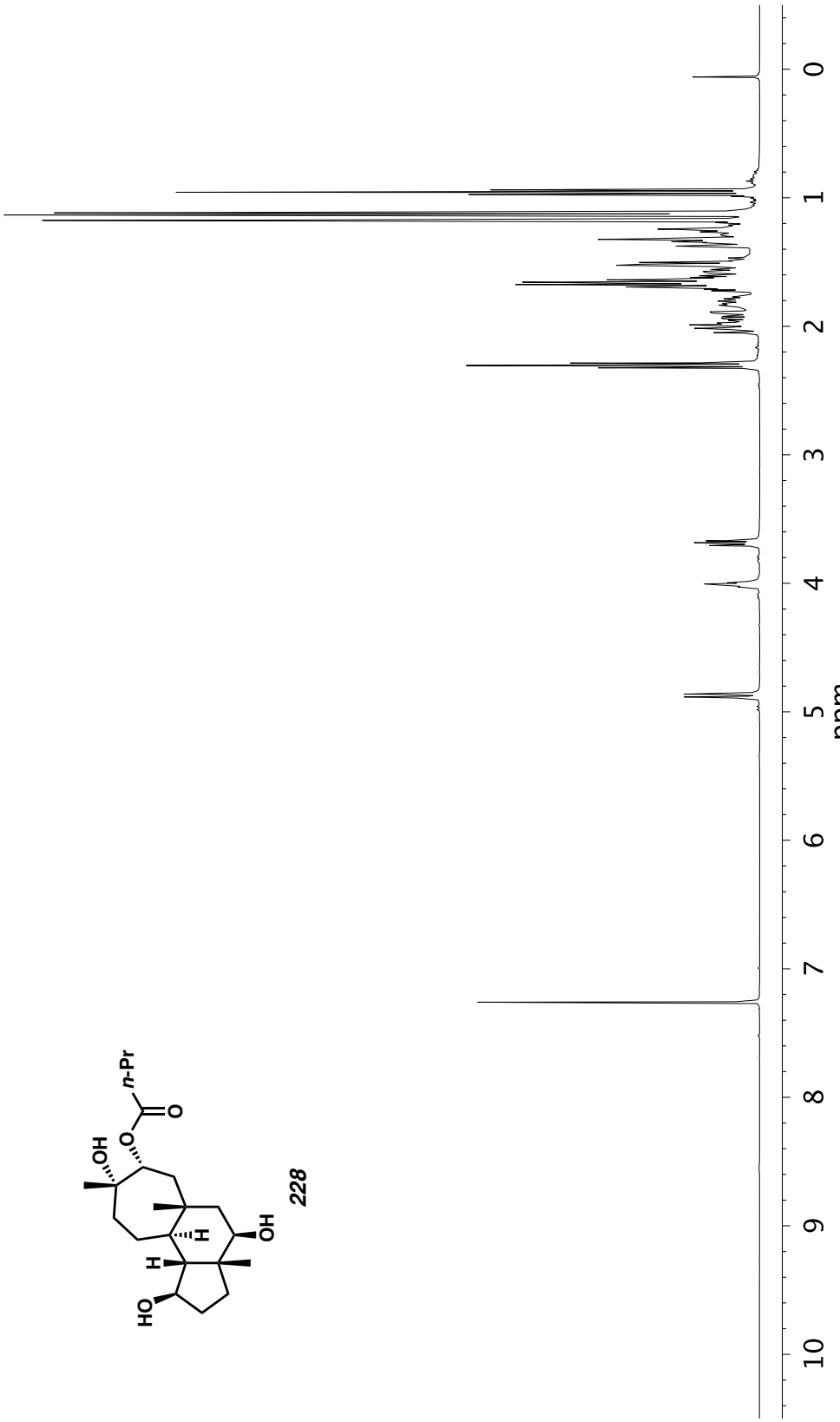

Figure A11.11. ^{1}H NMR (400 MHz, $CDCl_3$) of compound **228**.

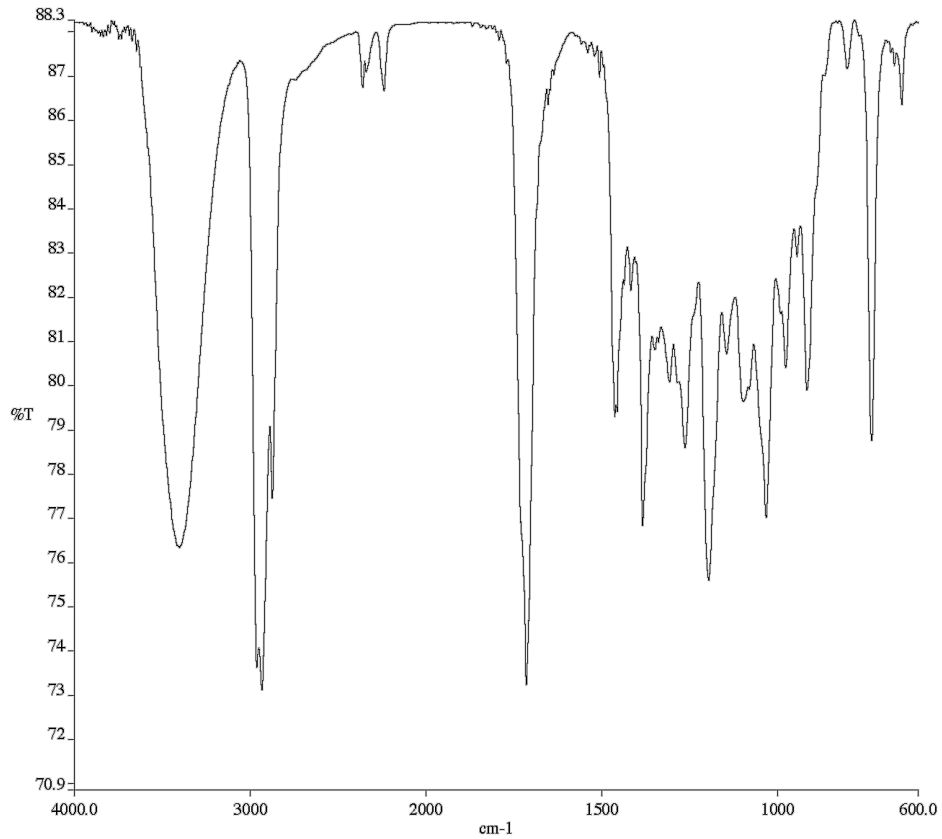

Figure A11.12. Infrared Spectrum (Thin Film, KBr) of compound **228**.

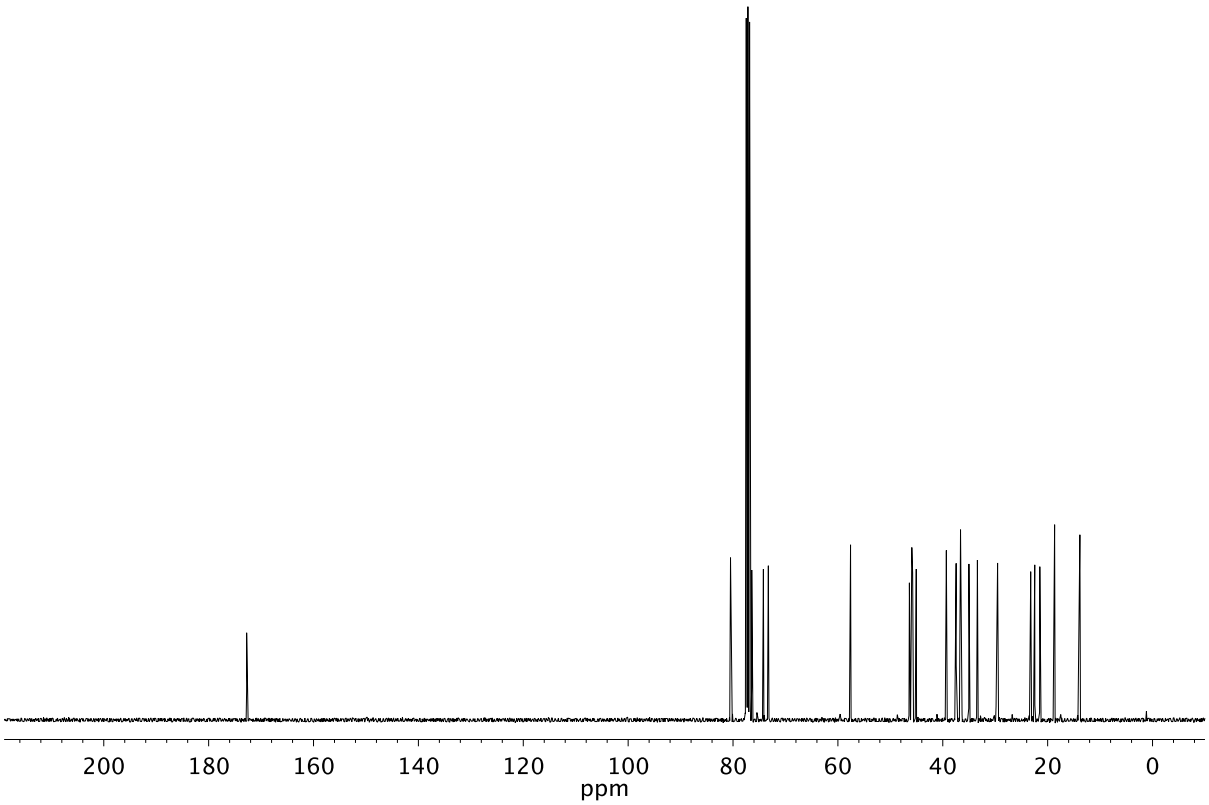

Figure A11.13. ^{13}C NMR (101 MHz, $CDCl_3$) of compound **228**.

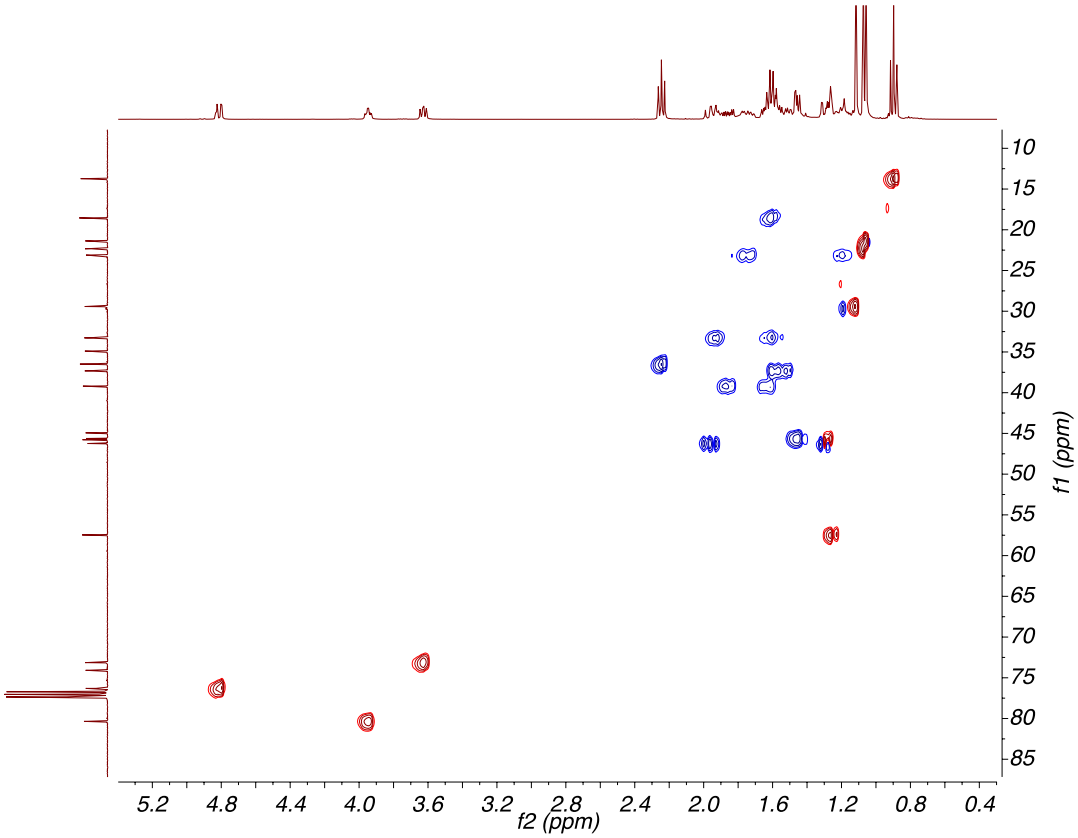

Figure A11.14. HSQC (400, 101 MHz, $CDCl_3$) of compound **228**.

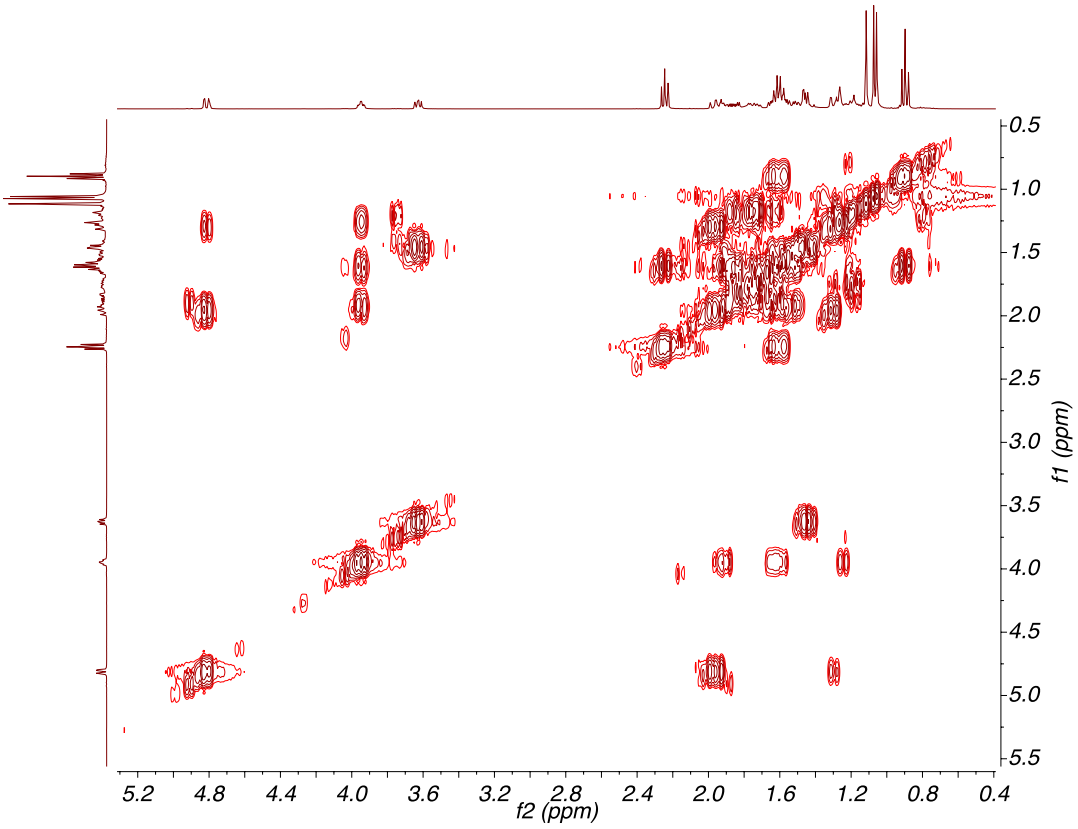

Figure A11.15. COSY (400 MHz, $CDCl_3$) of compound **228**.

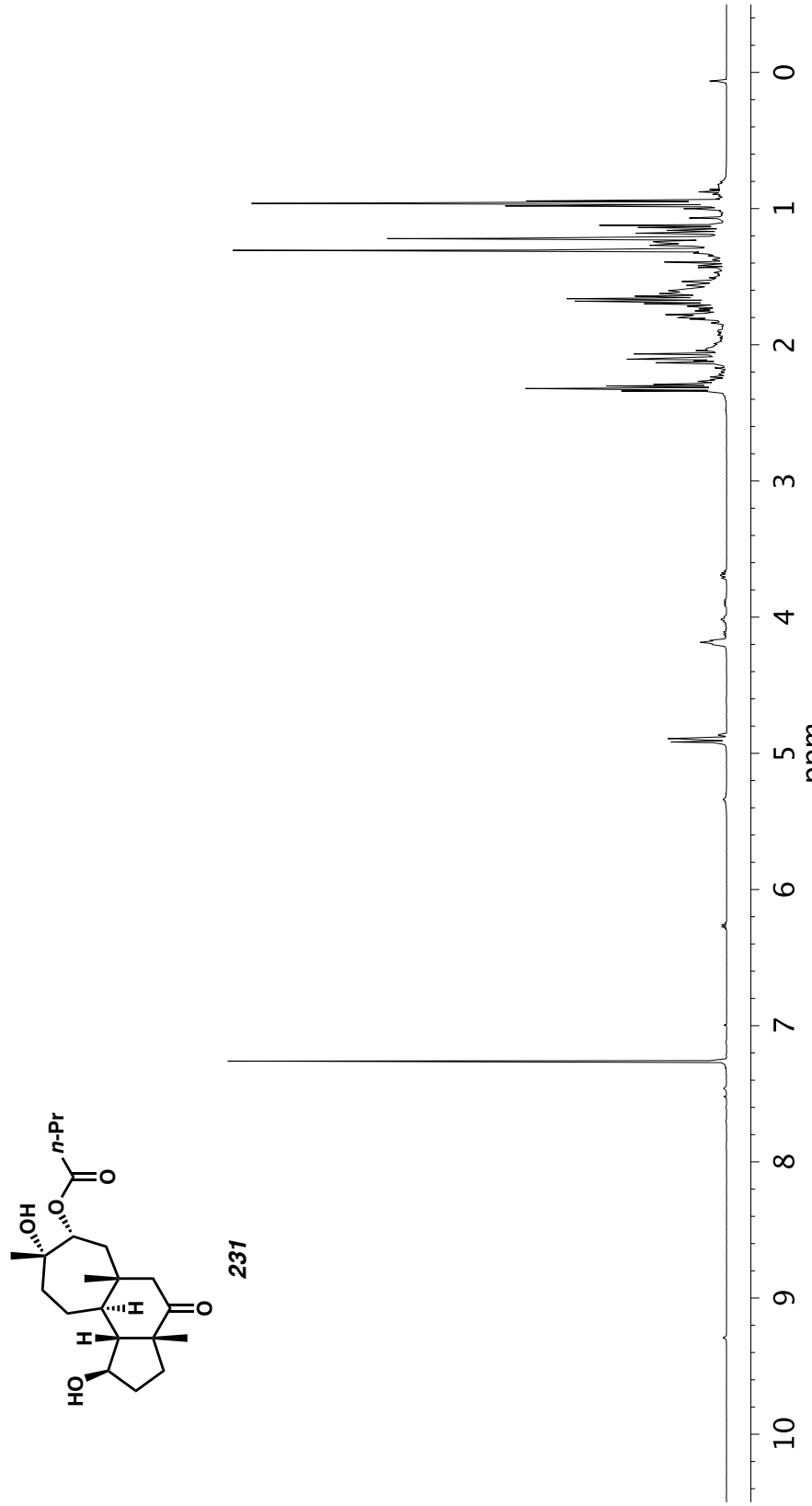

Figure A11.16. ^{1}H NMR (400 MHz, $CDCl_3$) of compound **231**.

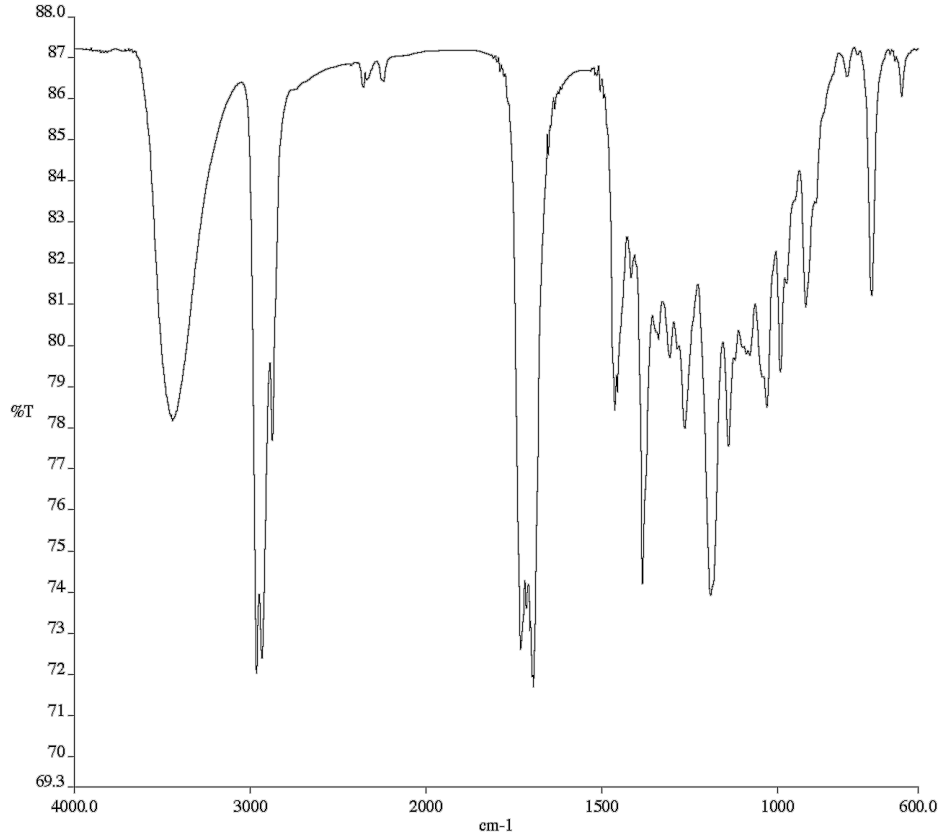

Figure A11.17. Infrared Spectrum (Thin Film, KBr) of compound **231**.

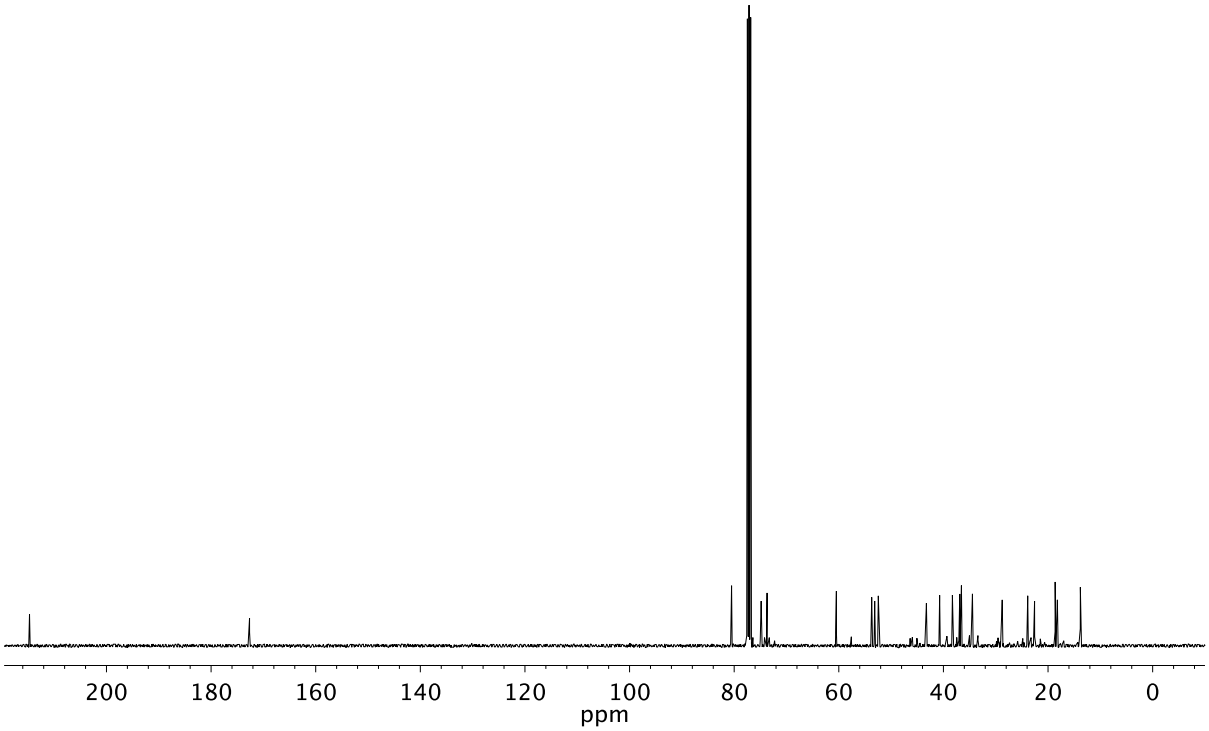

Figure A11.18. ^{13}C NMR (101 MHz, $CDCl_3$) of compound **231**.

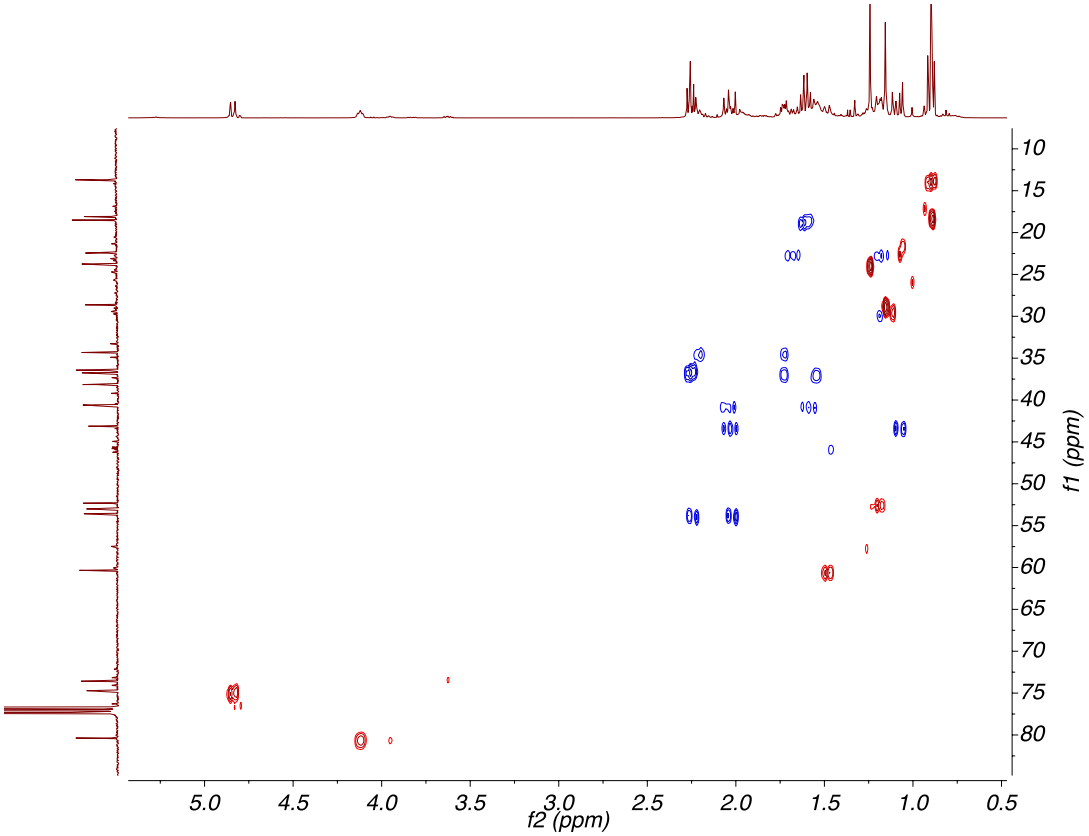

Figure A11.19. HSQC (400, 101 MHz, $CDCl_3$) of compound **231**.

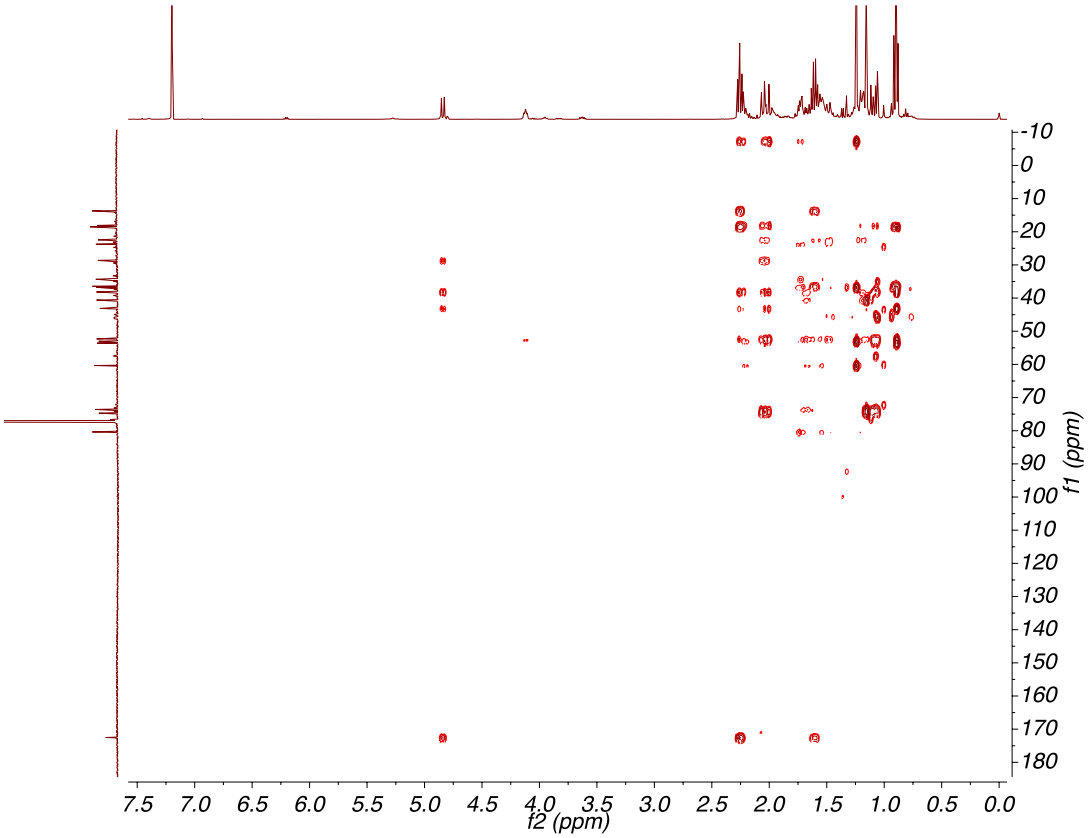

Figure A11.20. HMBC (400, 101 MHz, $CDCl_3$) of compound **231**.

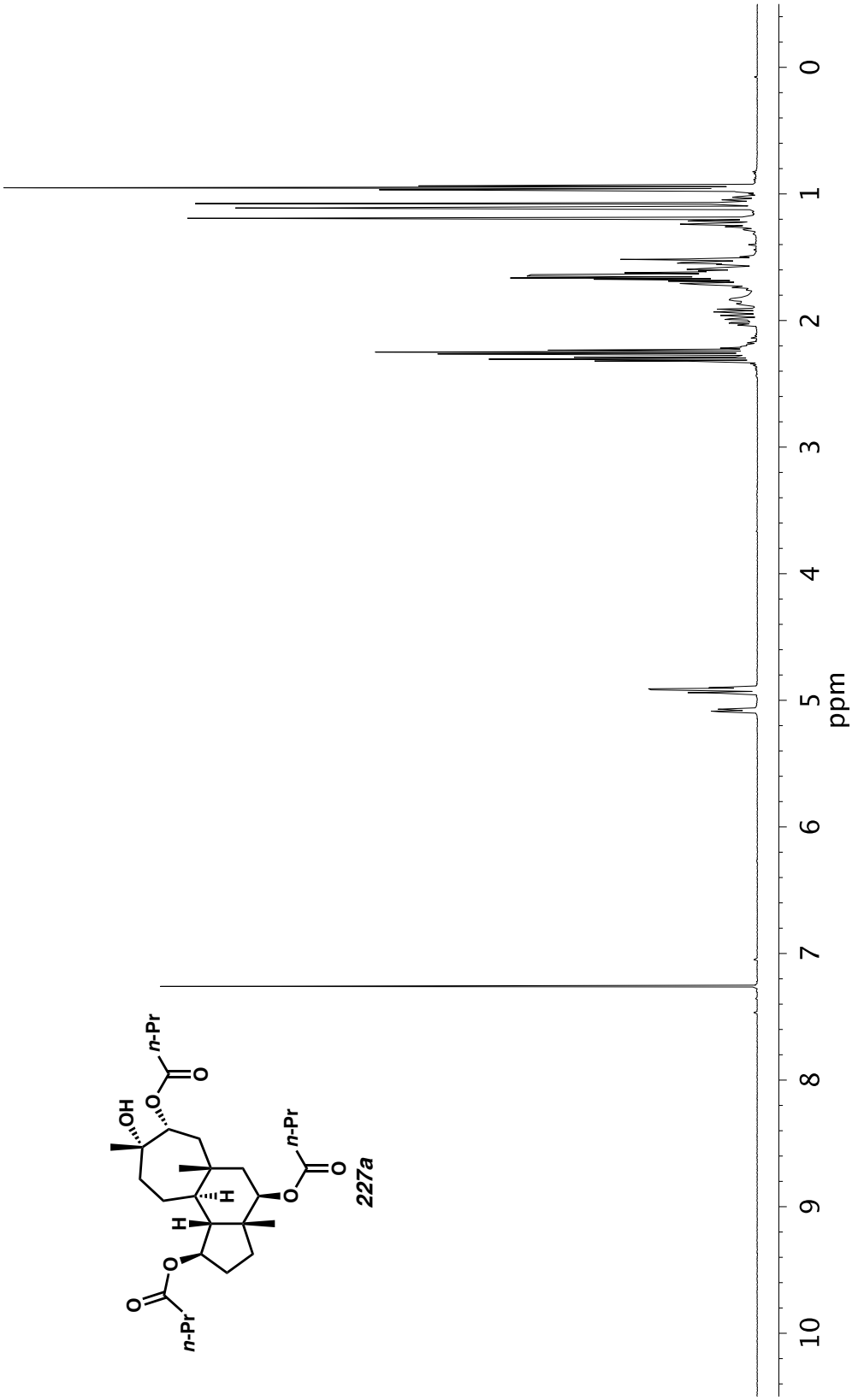

Figure A11.21. ^{1}H NMR (500 MHz, $CDCl_3$) of compound **227a**.

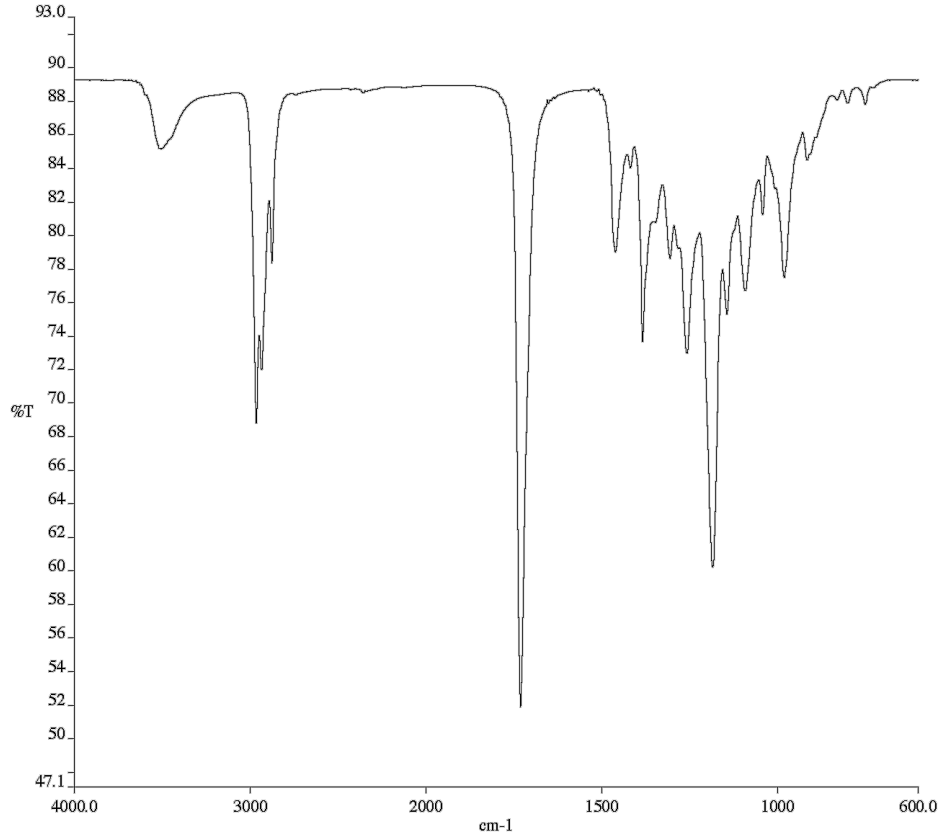

Figure A11.22. Infrared Spectrum (Thin Film, KBr) of compound **227a**.

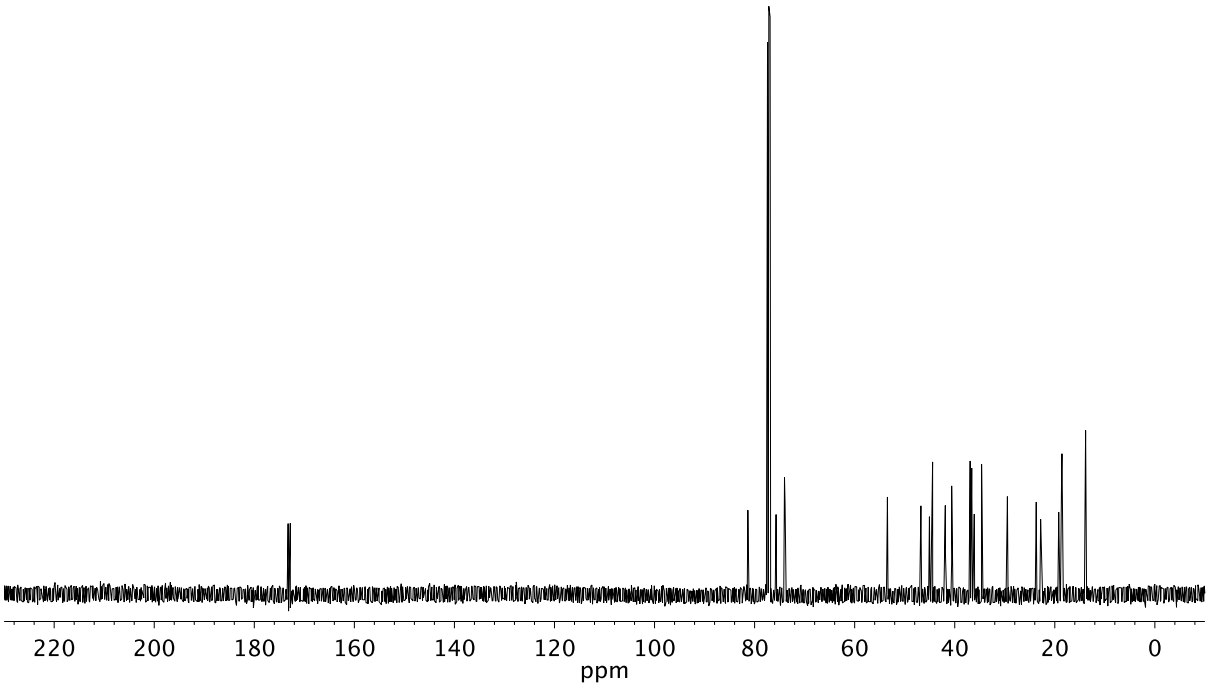

Figure A11.23. ^{13}C NMR (126 MHz, $CDCl_3$) of compound **227a**.

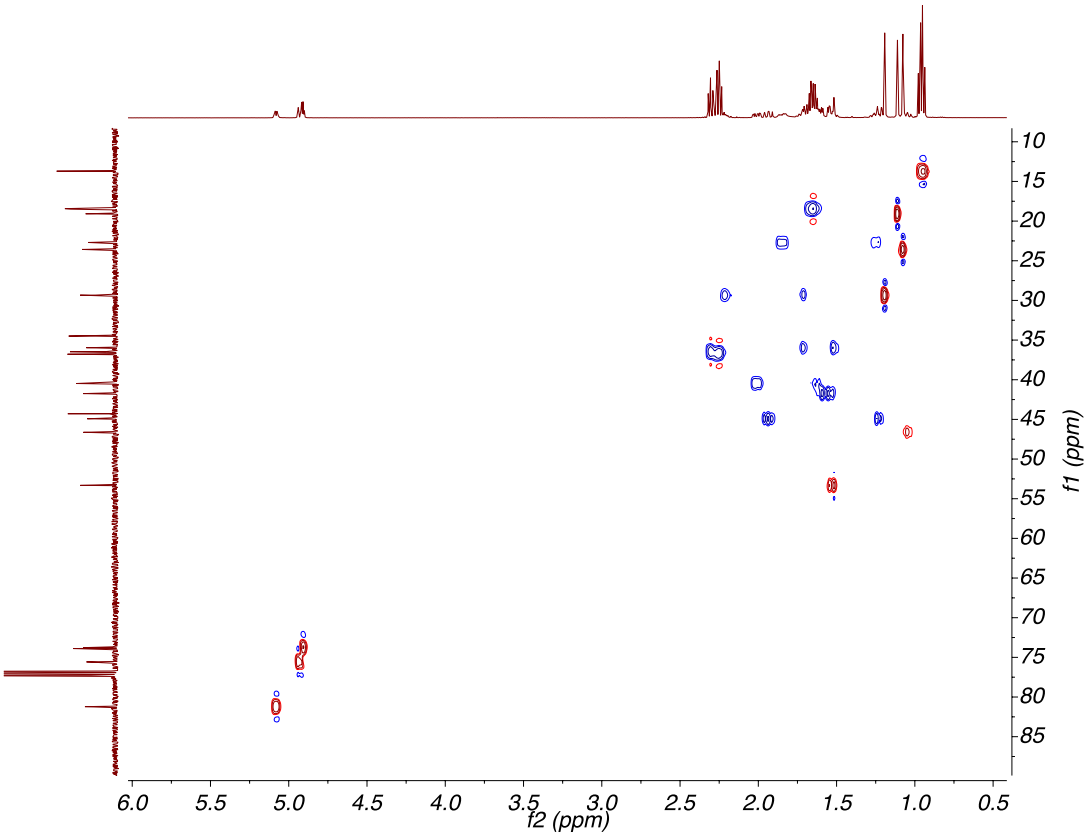

Figure A11.24. HSQC (500, 126 MHz, $CDCl_3$) of compound **227a**.

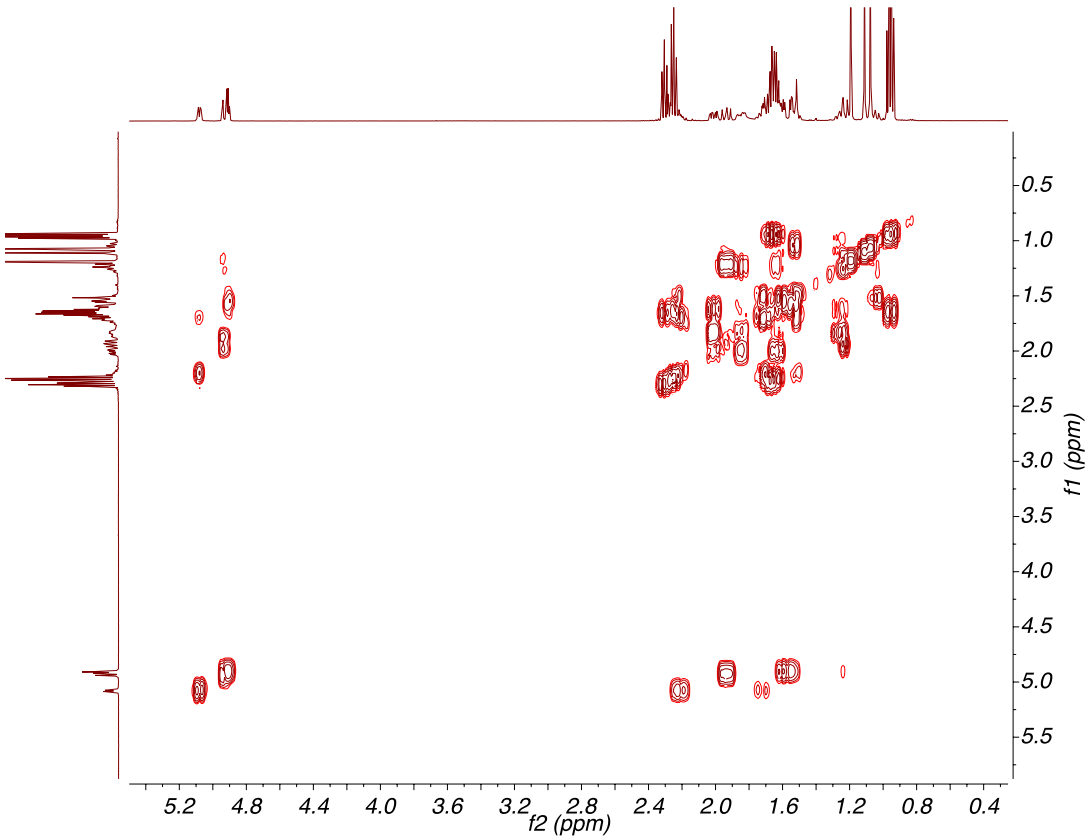

Figure A11.25. COSY (500 MHz, $CDCl_3$) of compound **227a**.

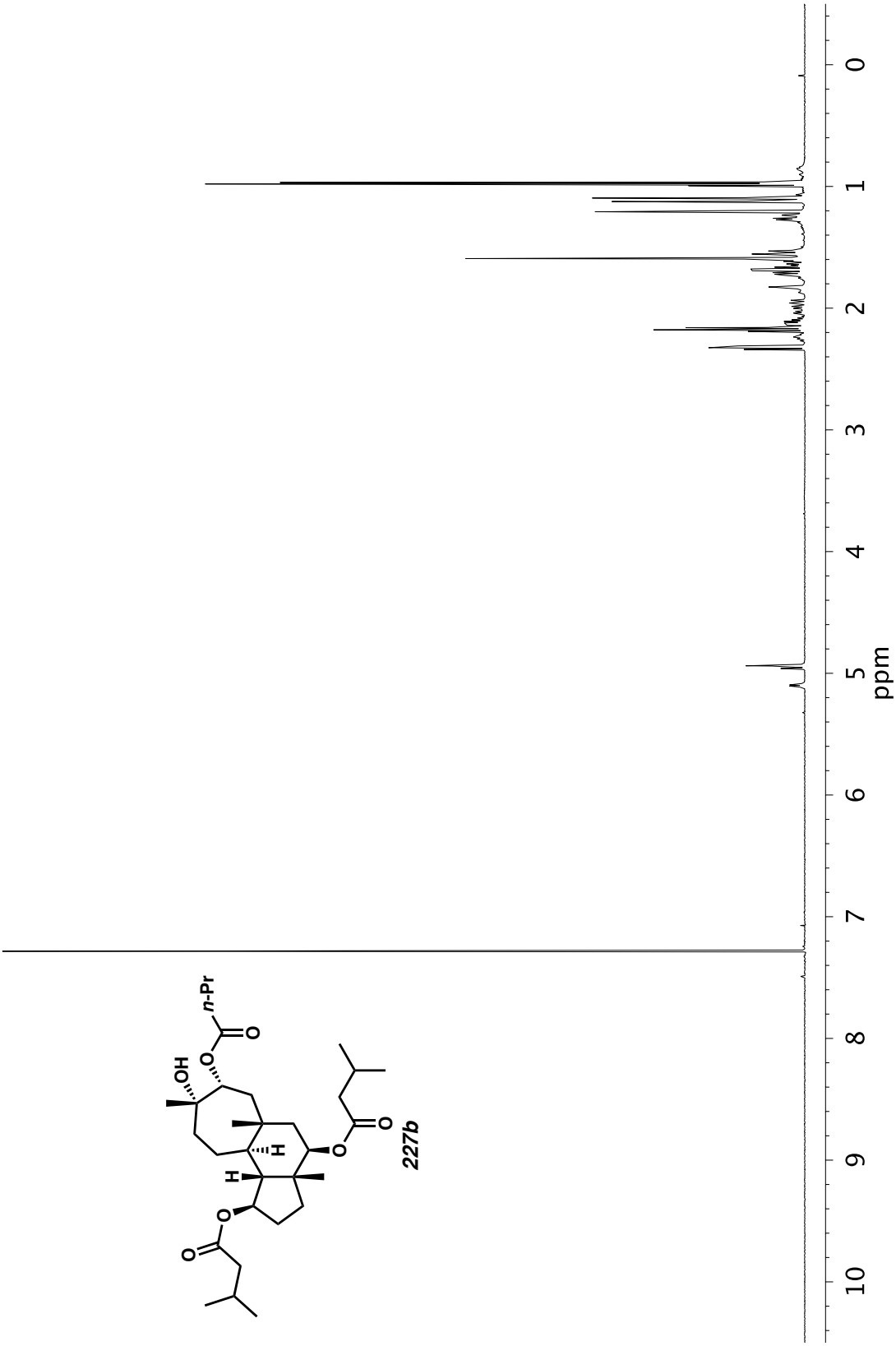

Figure A11.26. ^{1}H NMR (500 MHz, $CDCl_3$) of compound **227b**.

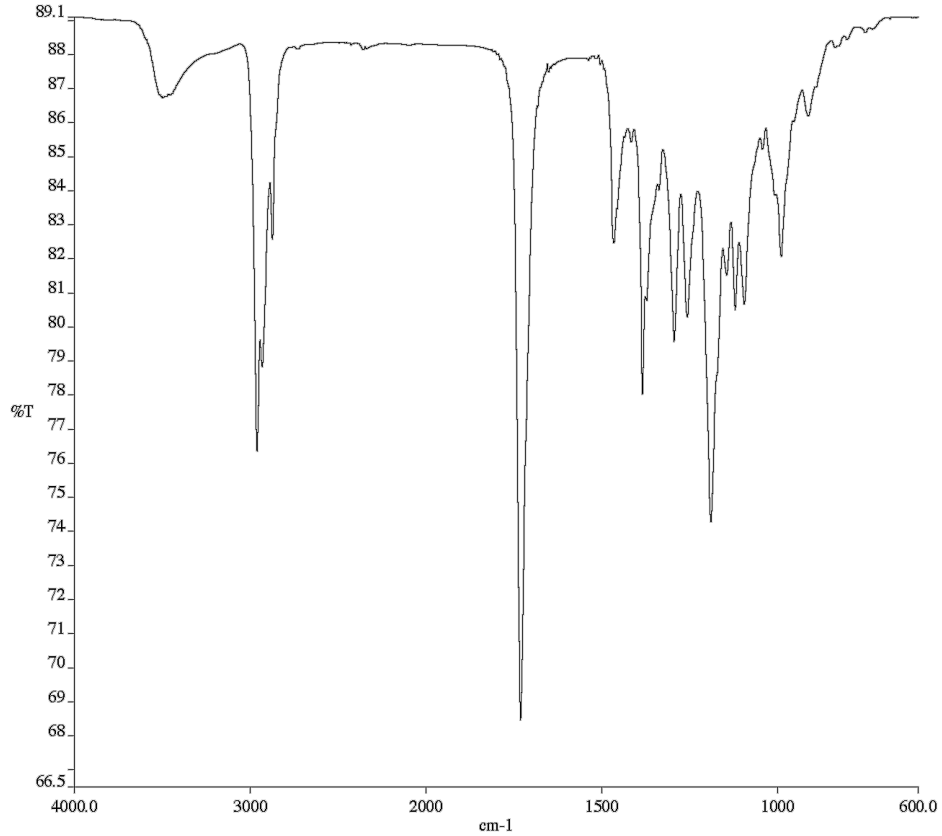

Figure A11.27. Infrared Spectrum (Thin Film, KBr) of compound **227b**.

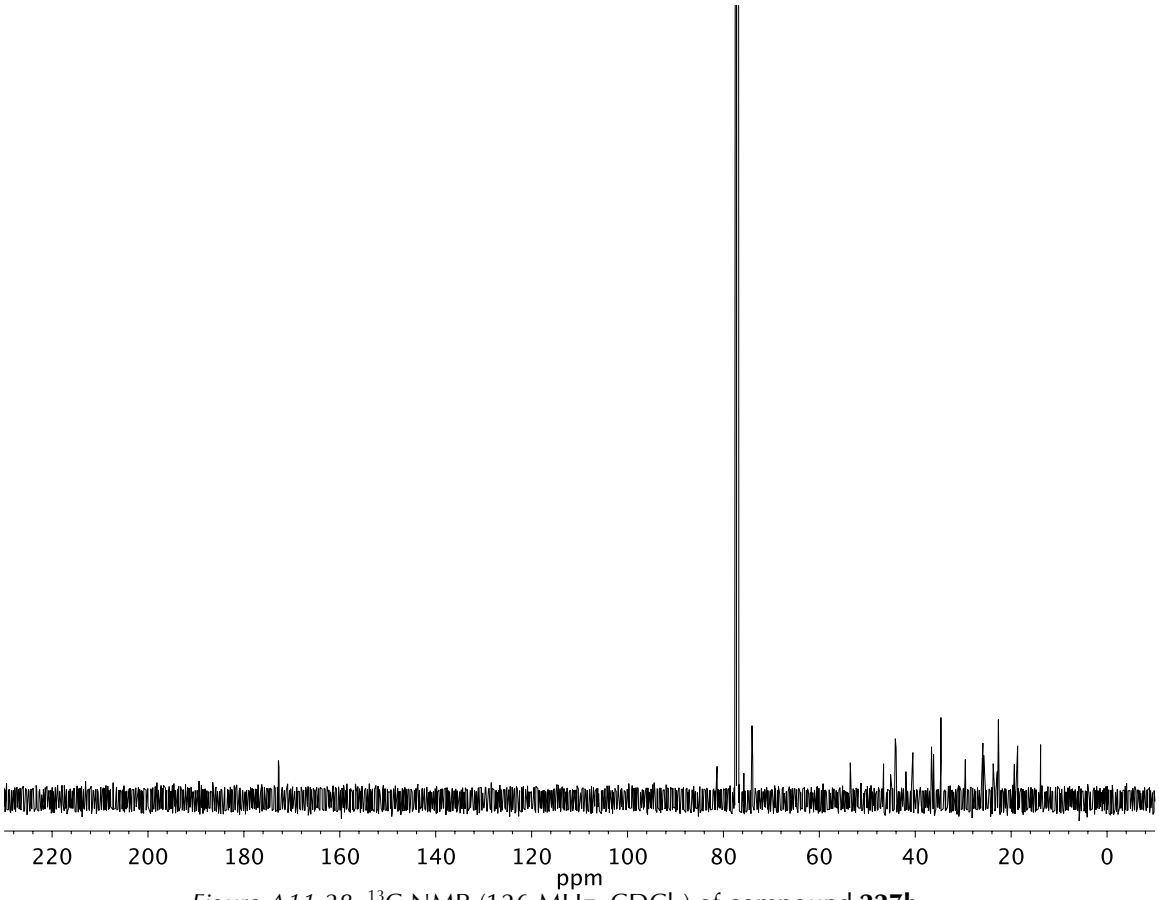

Figure A11.28. ^{13}C NMR (126 MHz, $CDCl_3$) of compound **227b**.

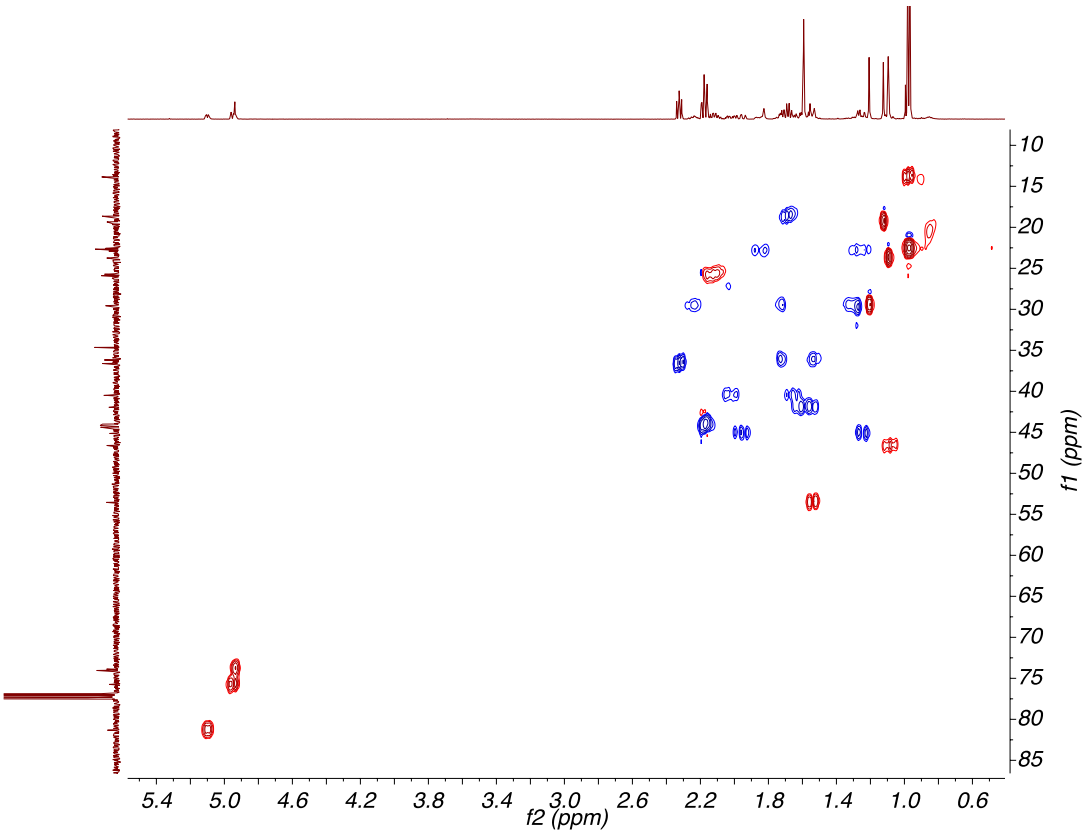

Figure A11.29. HSQC (400, 126 MHz, $CDCl_3$) of compound **227b**.

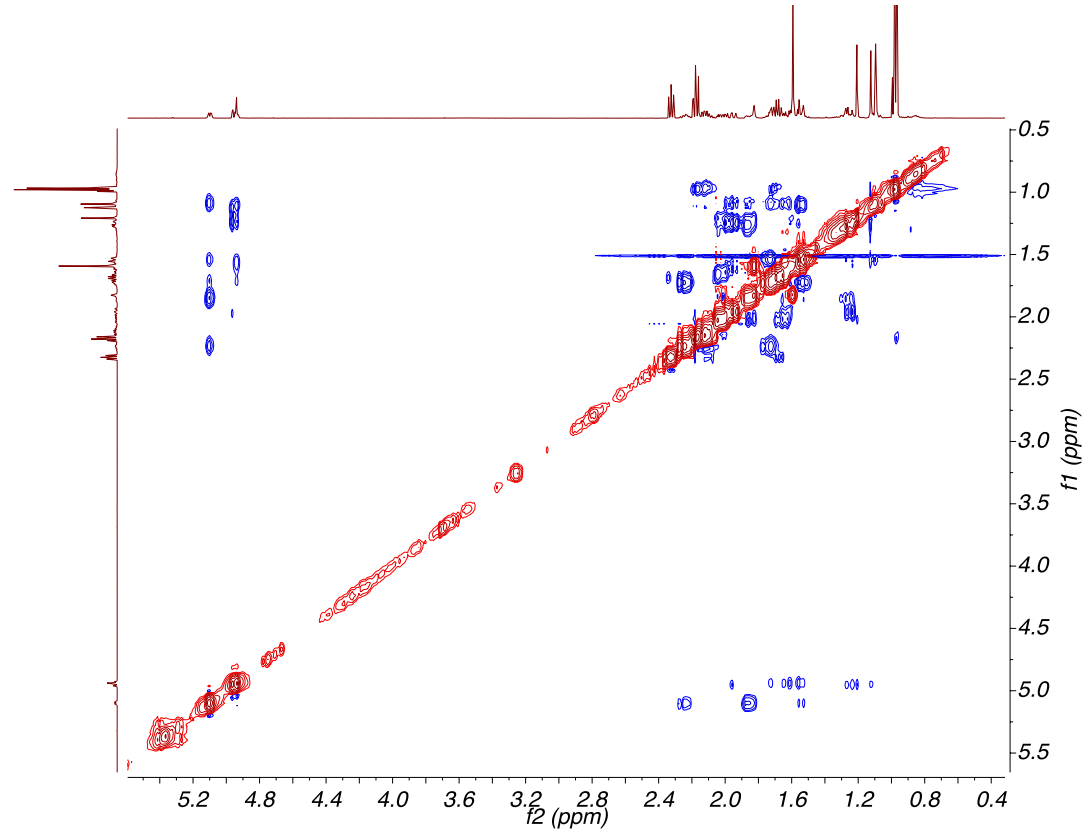

Figure A11.30. NOESY (400 MHz, $CDCl_3$) of compound **227b**.

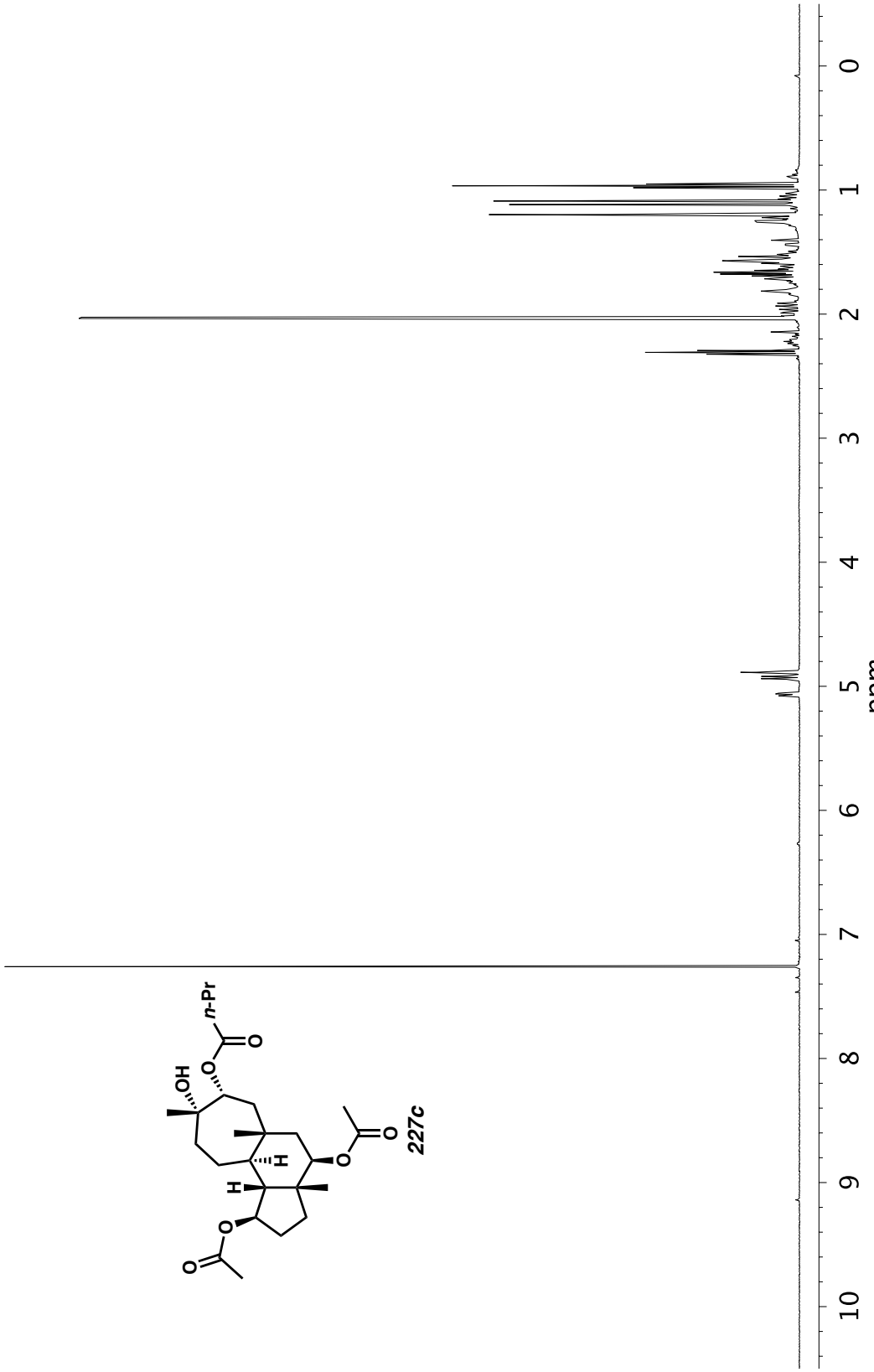

Figure A11.31. ^{1}H NMR (500 MHz, $CDCl_3$) of compound **227c**.

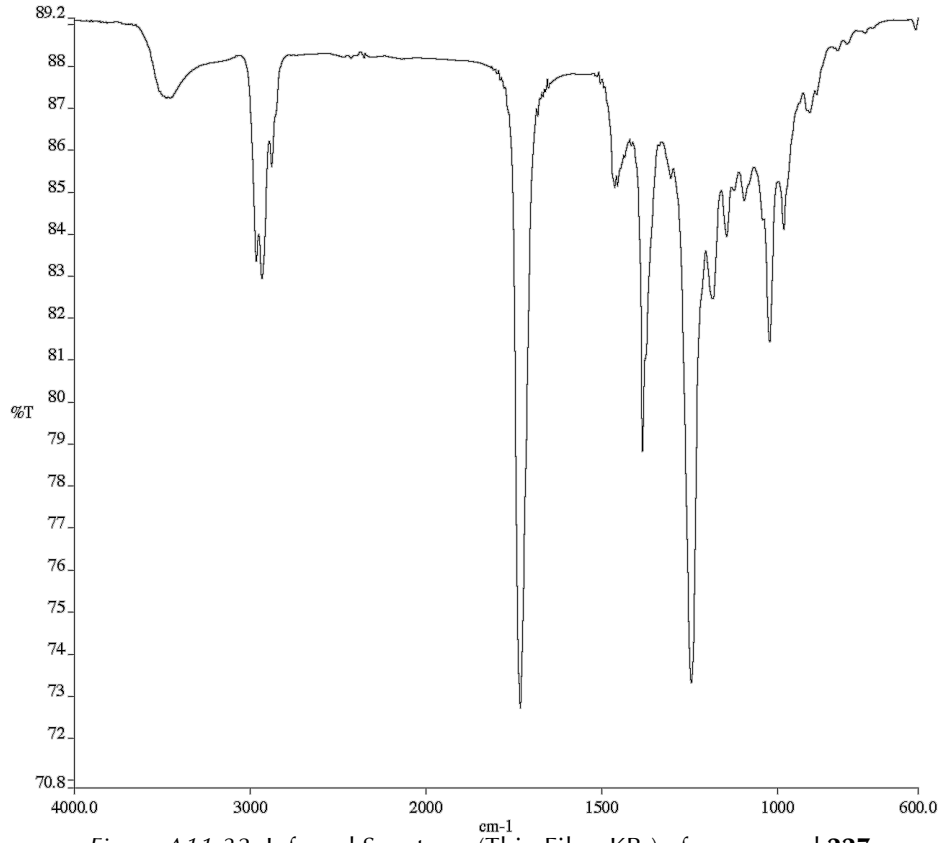

Figure A11.32. Infrared Spectrum (Thin Film, KBr) of compound **227c**.

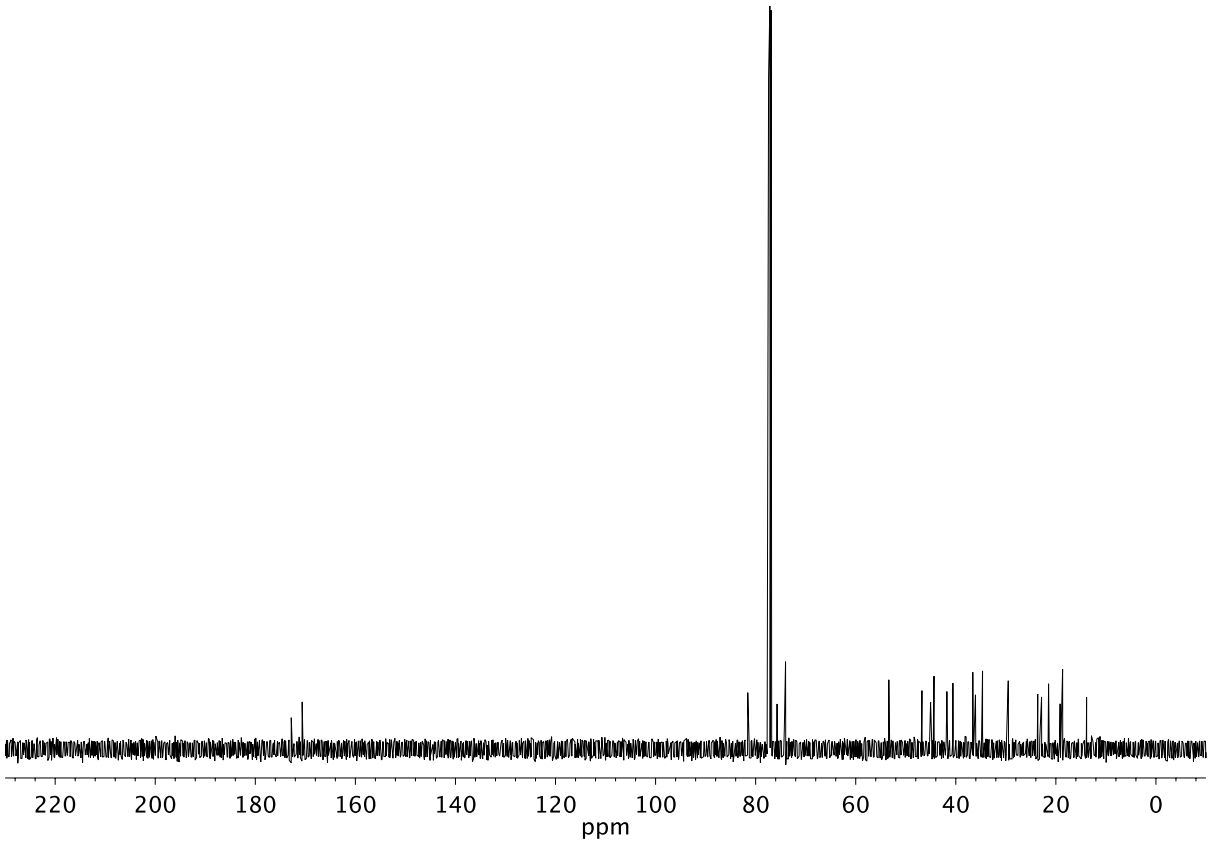

Figure A11.33. ^{13}C NMR (126 MHz, $CDCl_3$) of compound **227c**.

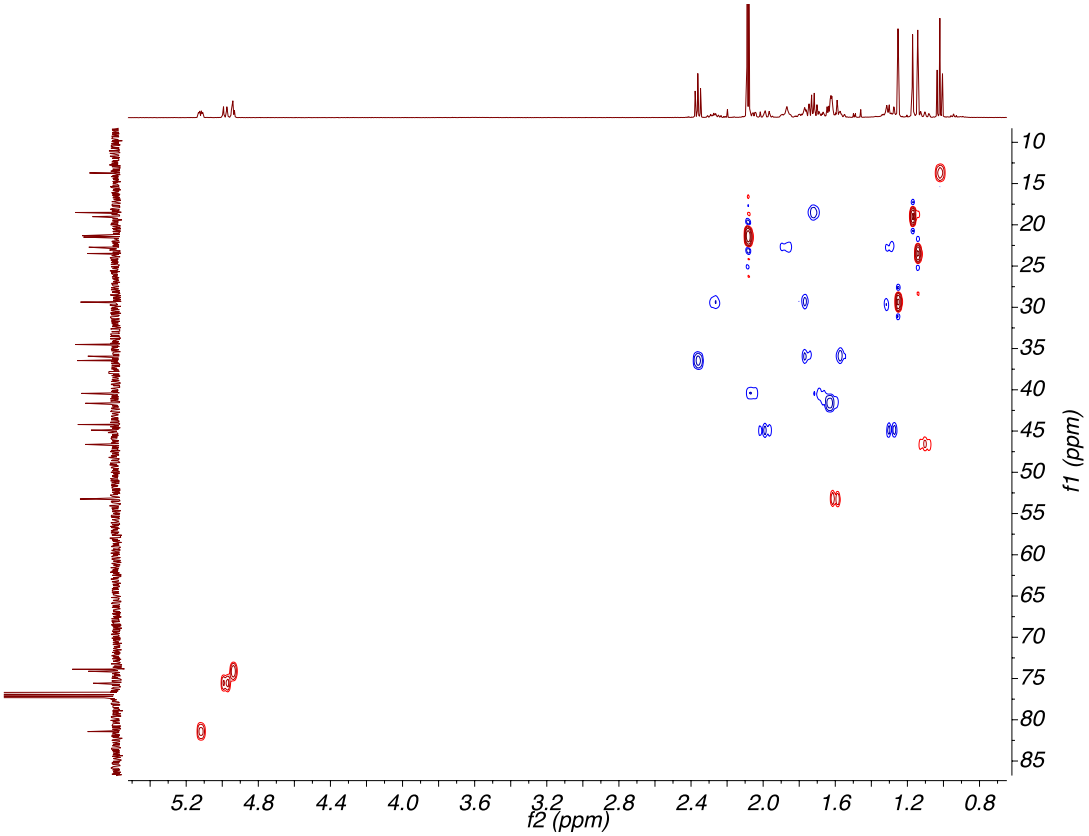

Figure A11.34. HSQC (500, 126 MHz, $CDCl_3$) of compound **227c**.

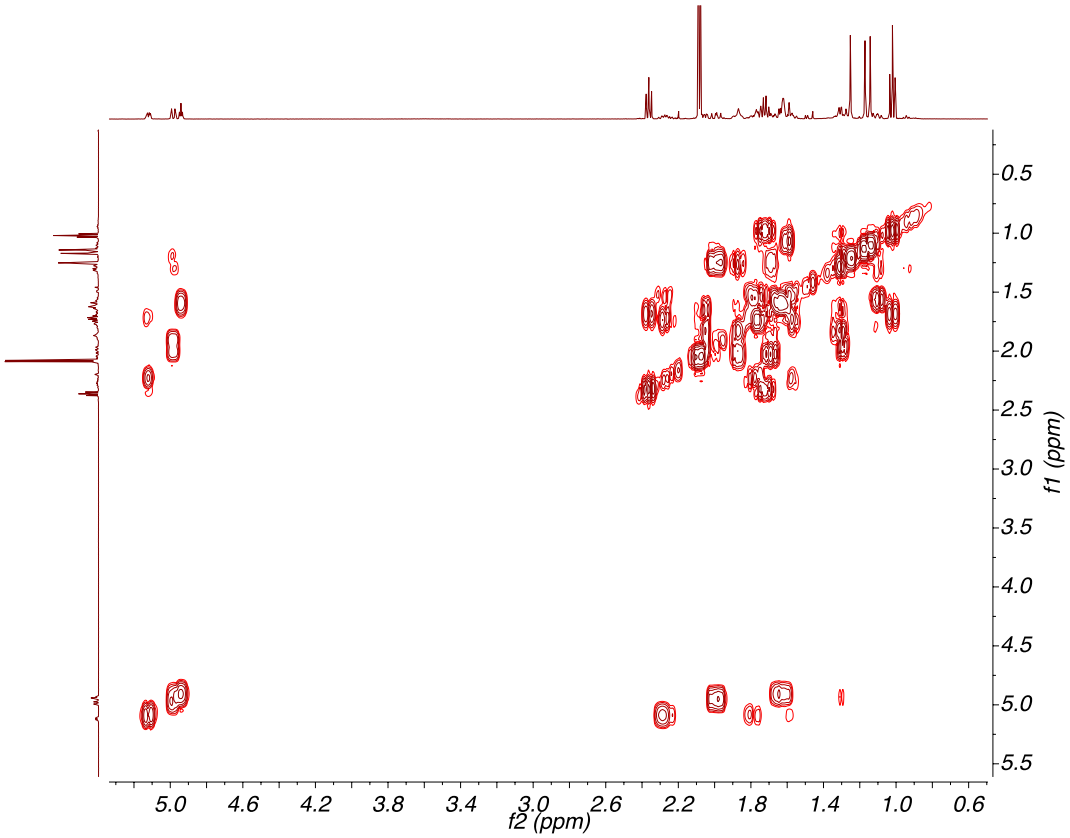

Figure A11.35. COSY (500 MHz, $CDCl_3$) of compound **227c**.

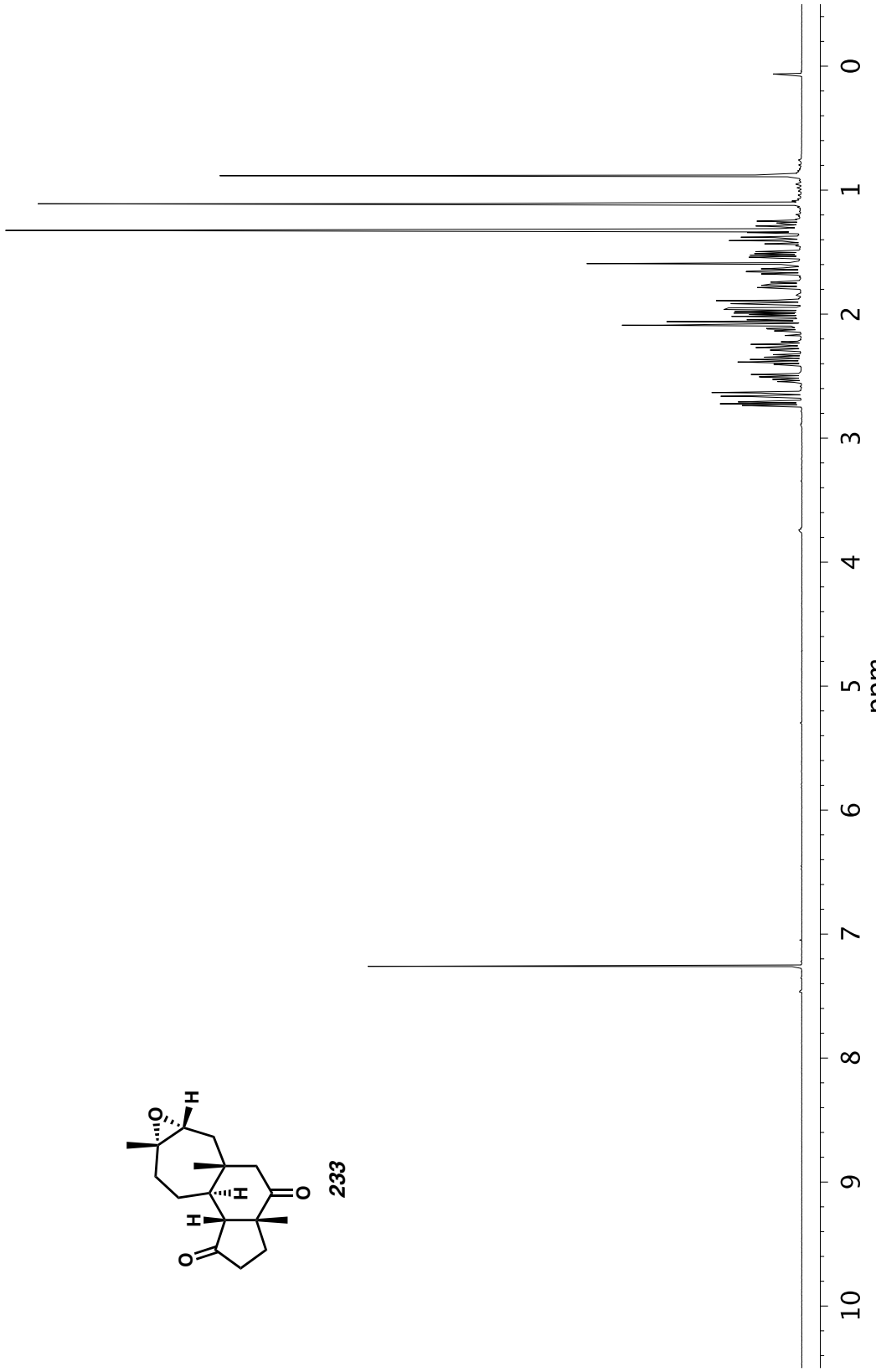

233

Figure A11.36. ^{1}H NMR (500 MHz, $CDCl_3$) of compound **233**.

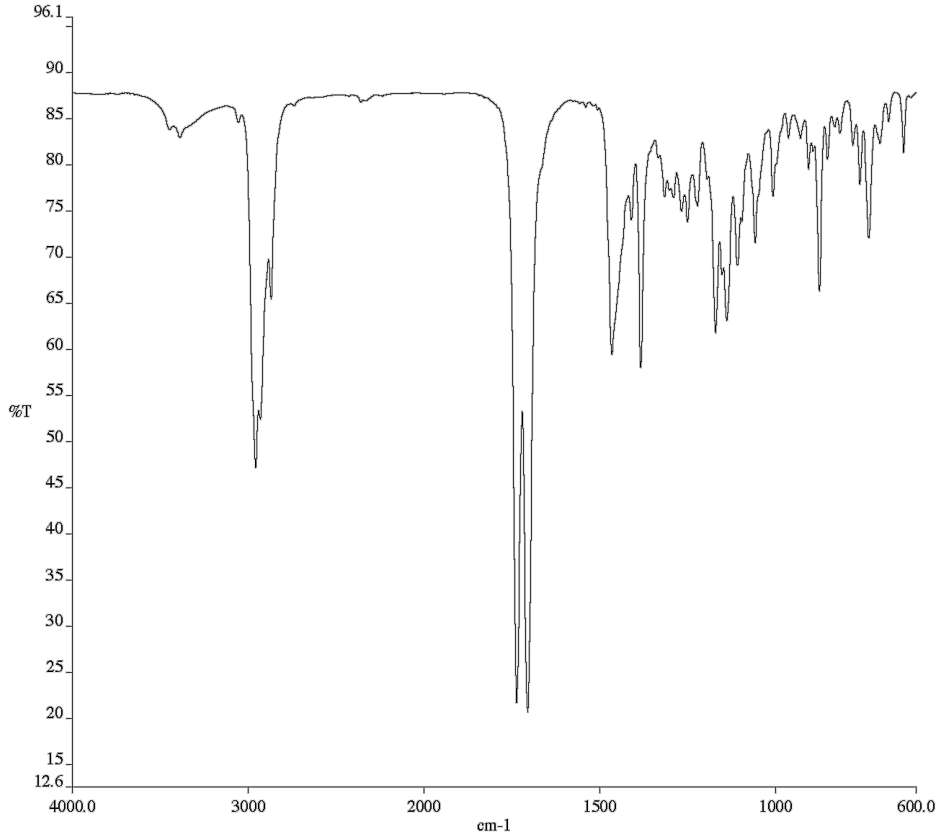

Figure A11.37. Infrared Spectrum (Thin Film, KBr) of compound **233**.

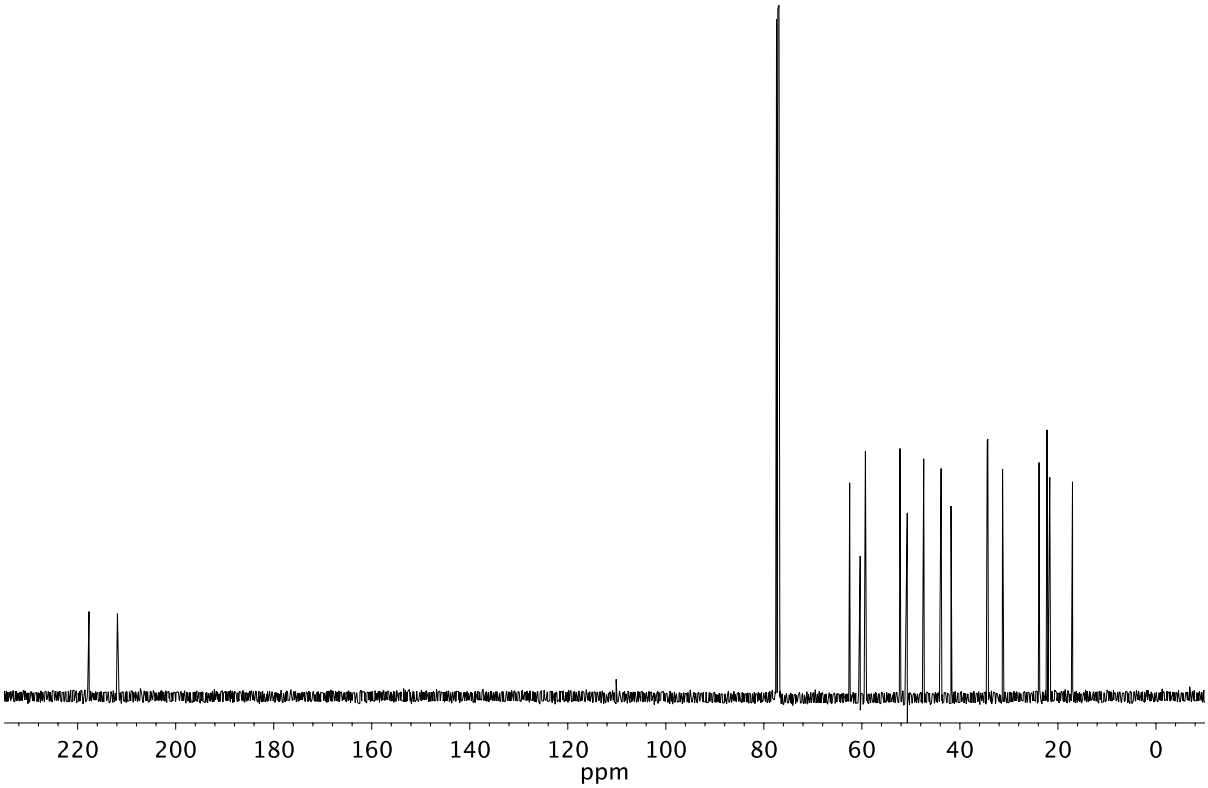

Figure A11.38. ^{13}C NMR (126 MHz, $CDCl_3$) of compound **233**.

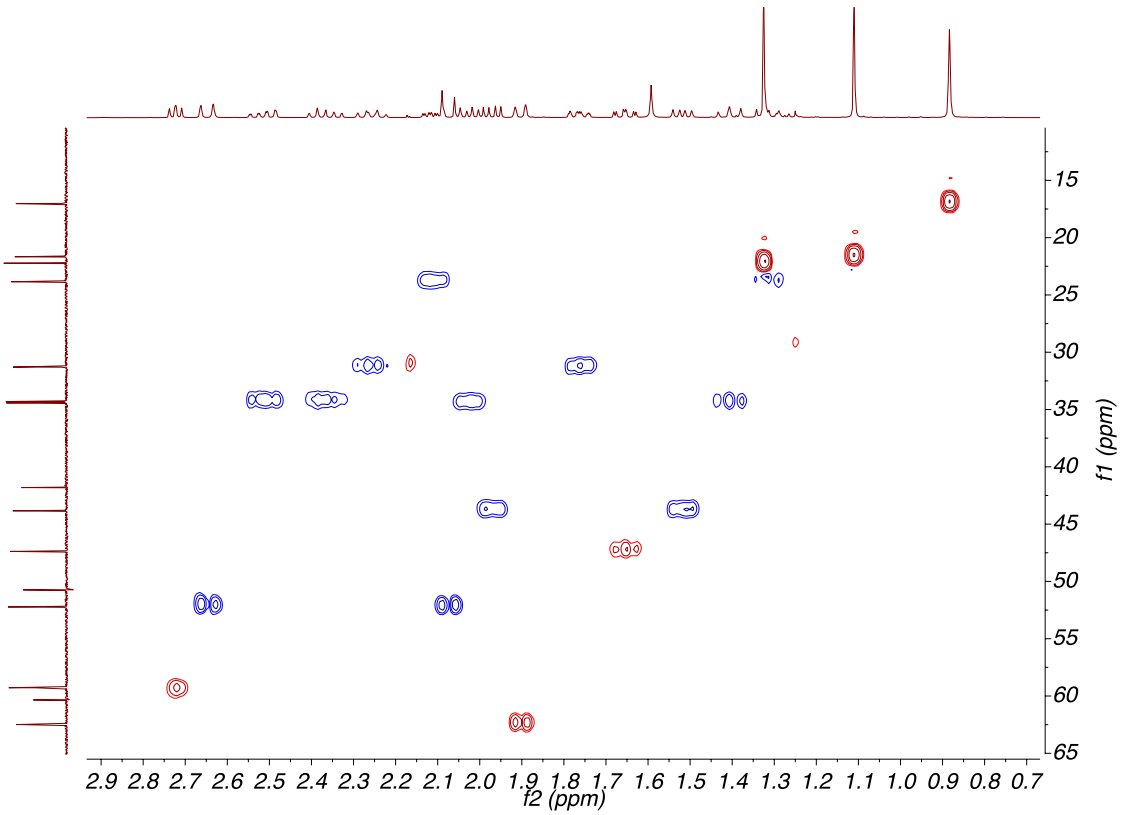

Figure A11.39. HSQC (500, 126 MHz, $CDCl_3$) of compound **233**.

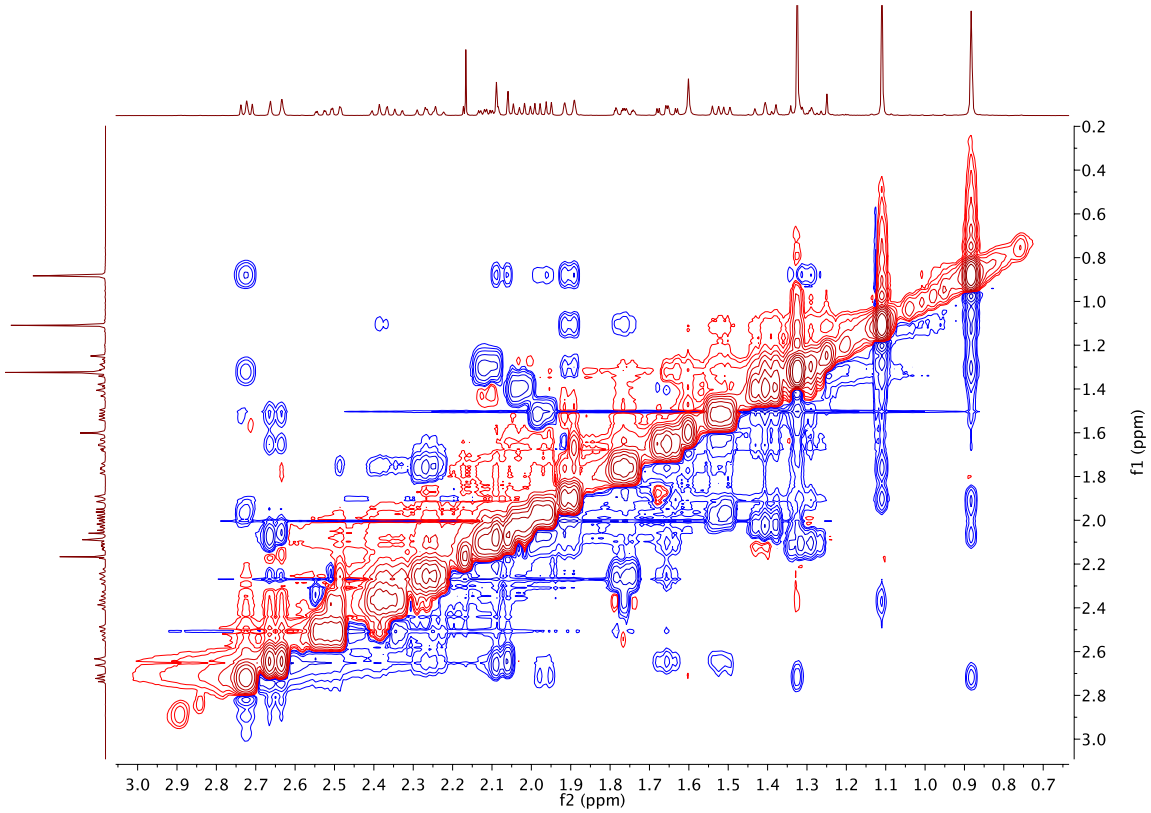

Figure A11.40. NOESY (500 MHz, $CDCl_3$) of compound **233**.

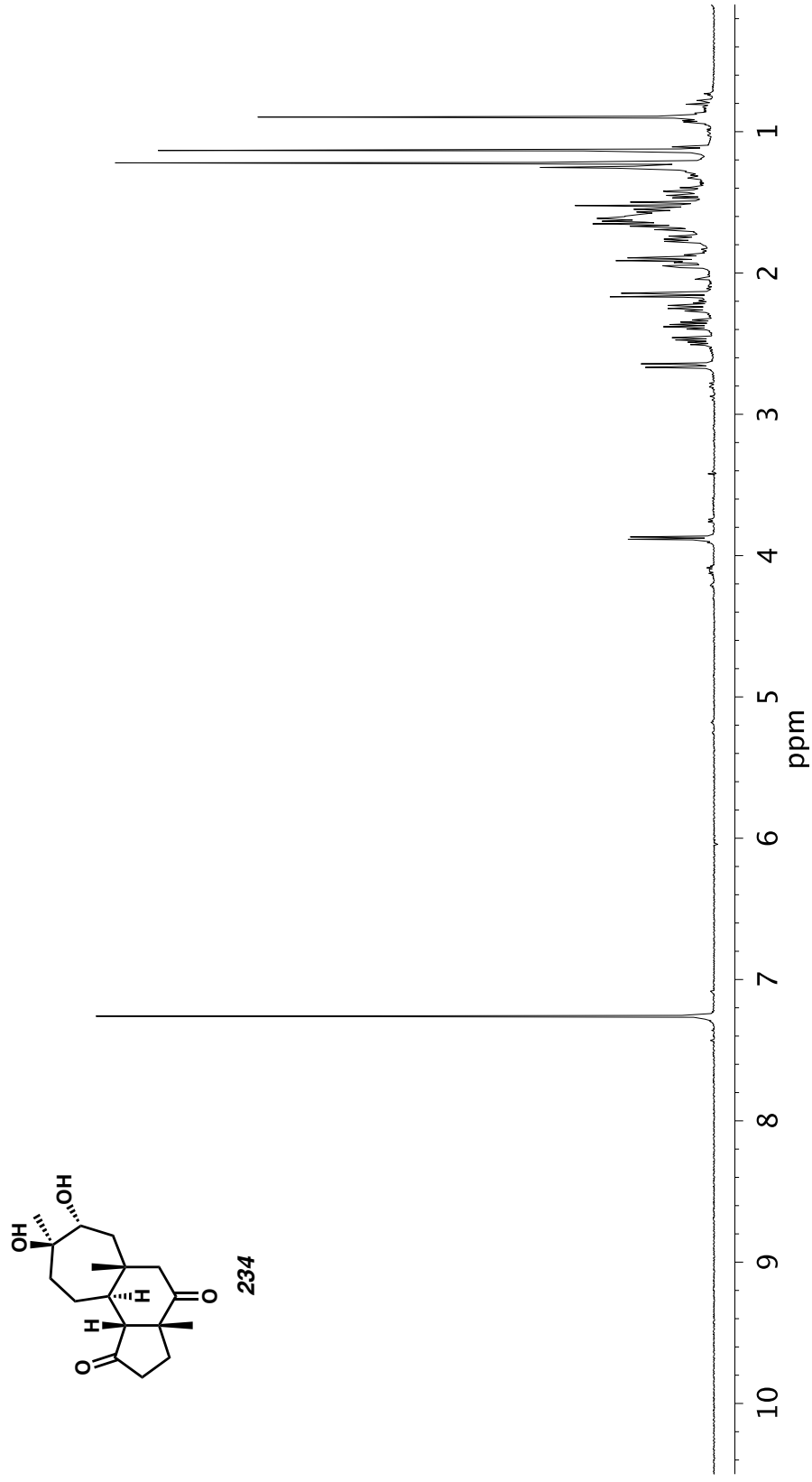

Figure A11.41. ^{1}H NMR (600 MHz, $CDCl_3$) of compound **234**.

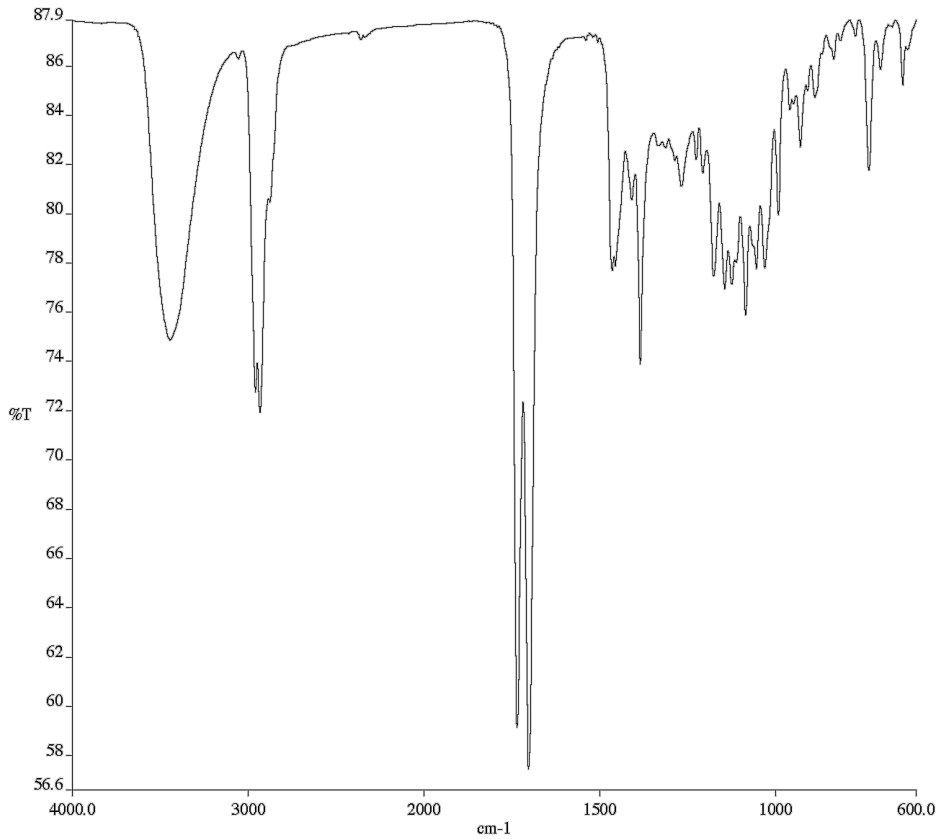

Figure A11.42. Infrared Spectrum (Thin Film, KBr) of compound **234**.

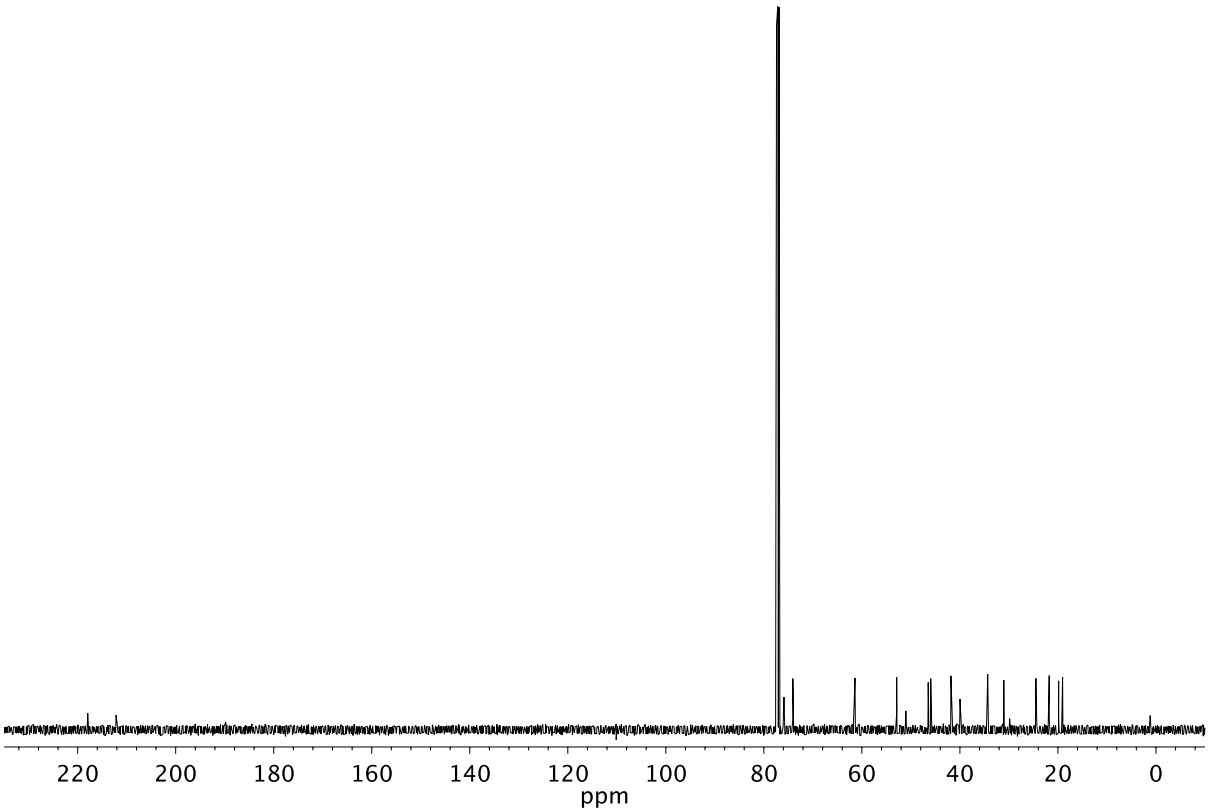

Figure A11.43. ^{13}C NMR (126 MHz, $CDCl_3$) of compound **234**.

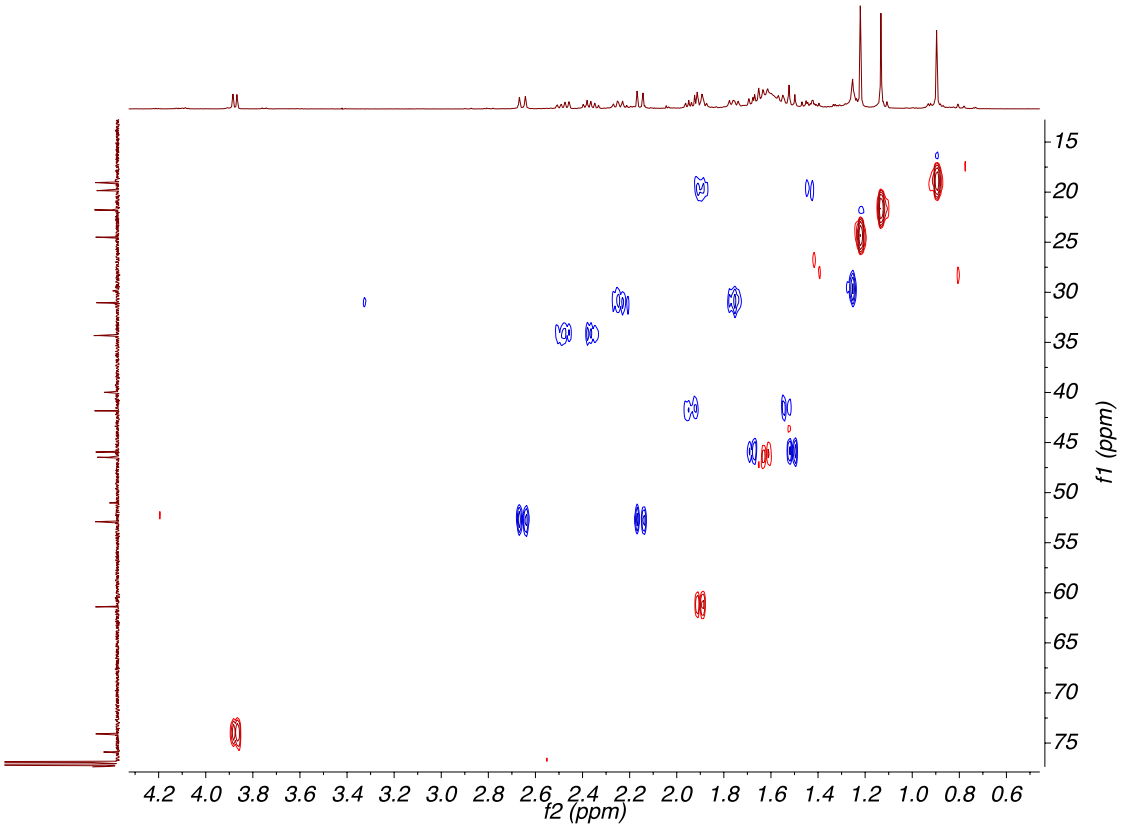

Figure A11.44. HSQC (600, 126 MHz, $CDCl_3$) of compound **234**.

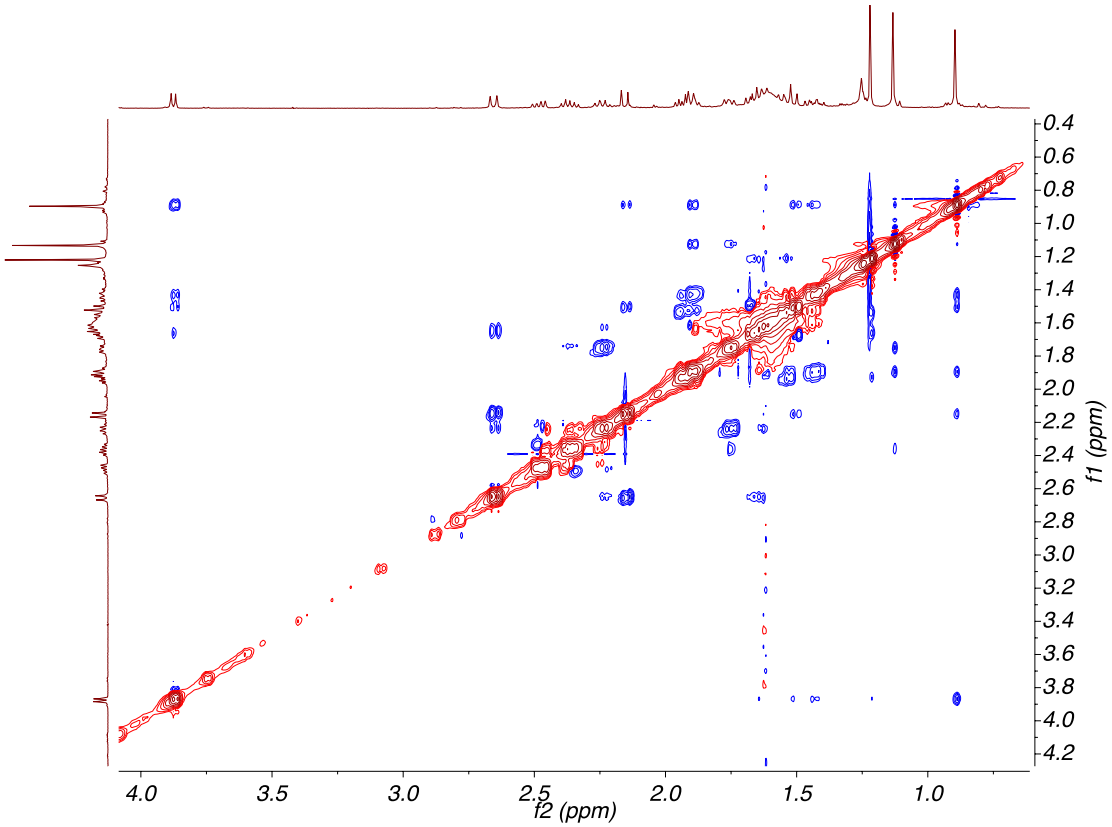

Figure A11.45. NOESY (600 MHz, $CDCl_3$) of compound **234**.

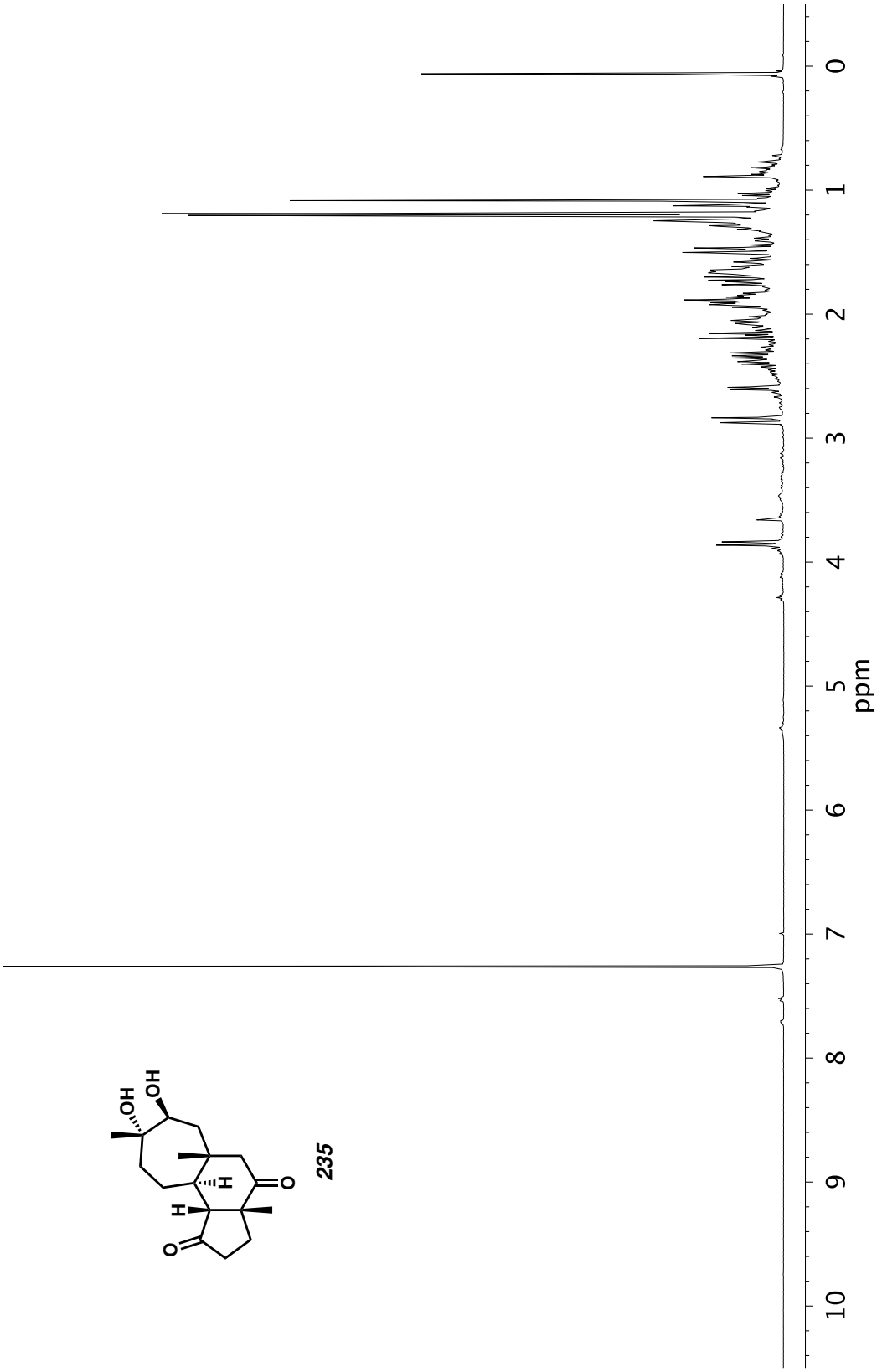

Figure A11.46. ^{1}H NMR (400 MHz, $CDCl_3$) of compound **235**.

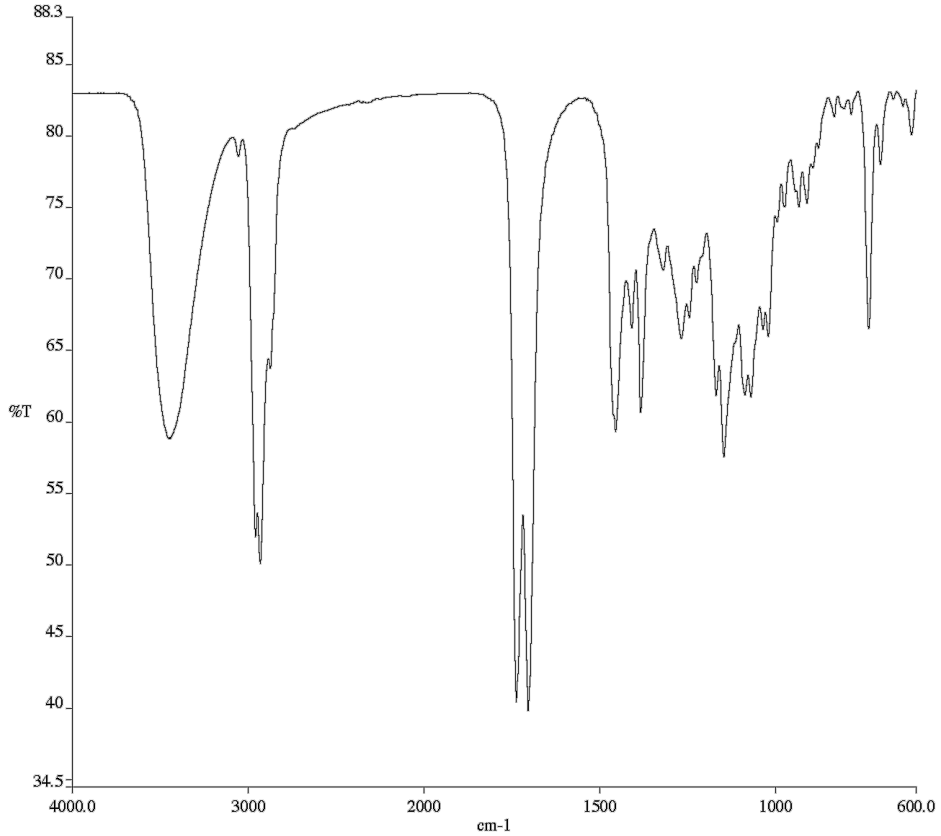

Figure A11.47. Infrared Spectrum (Thin Film, KBr) of compound **235**.

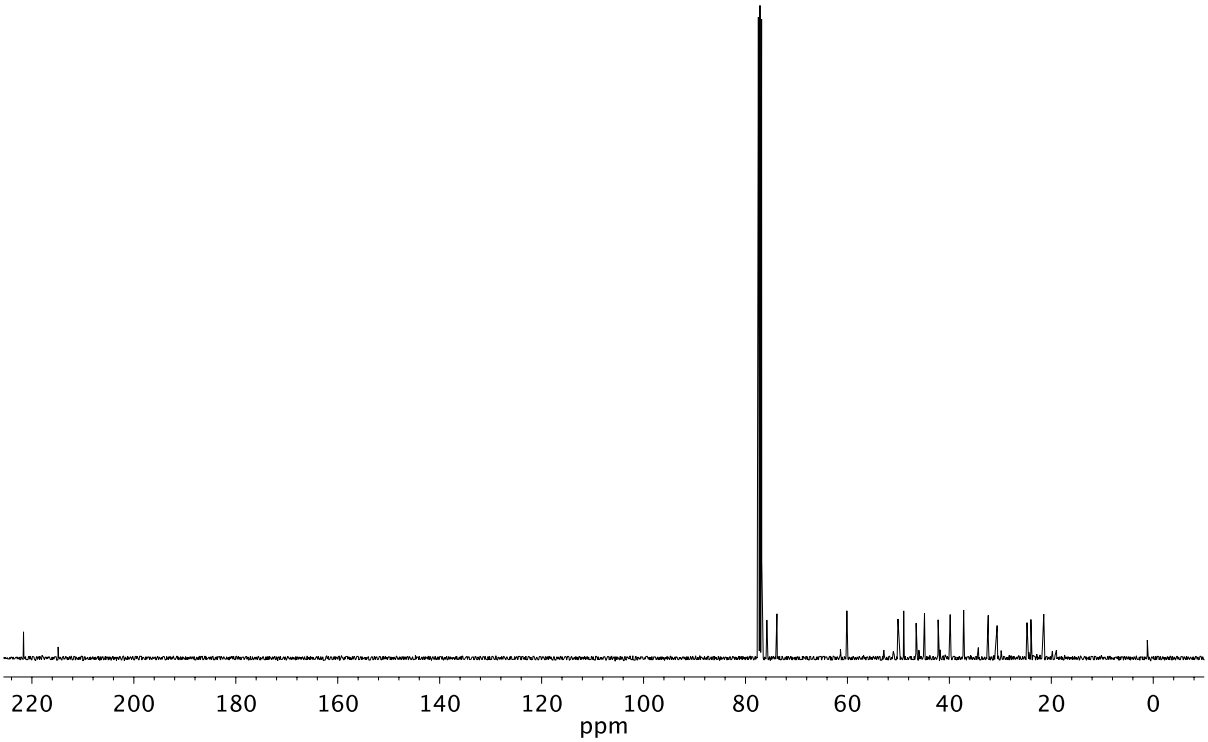

Figure A11.48. ^{13}C NMR (101 MHz, $CDCl_3$) of compound **235**.

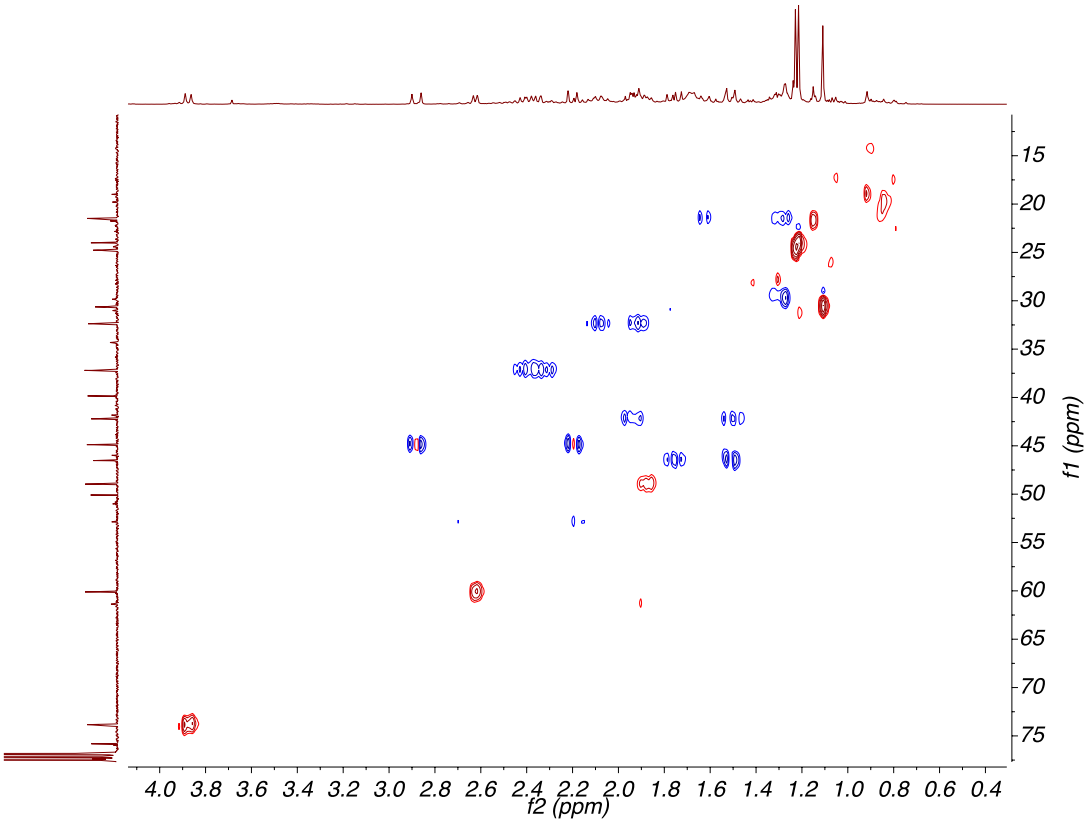

Figure A11.49. HSQC (400, 101 MHz, $CDCl_3$) of compound **235**.

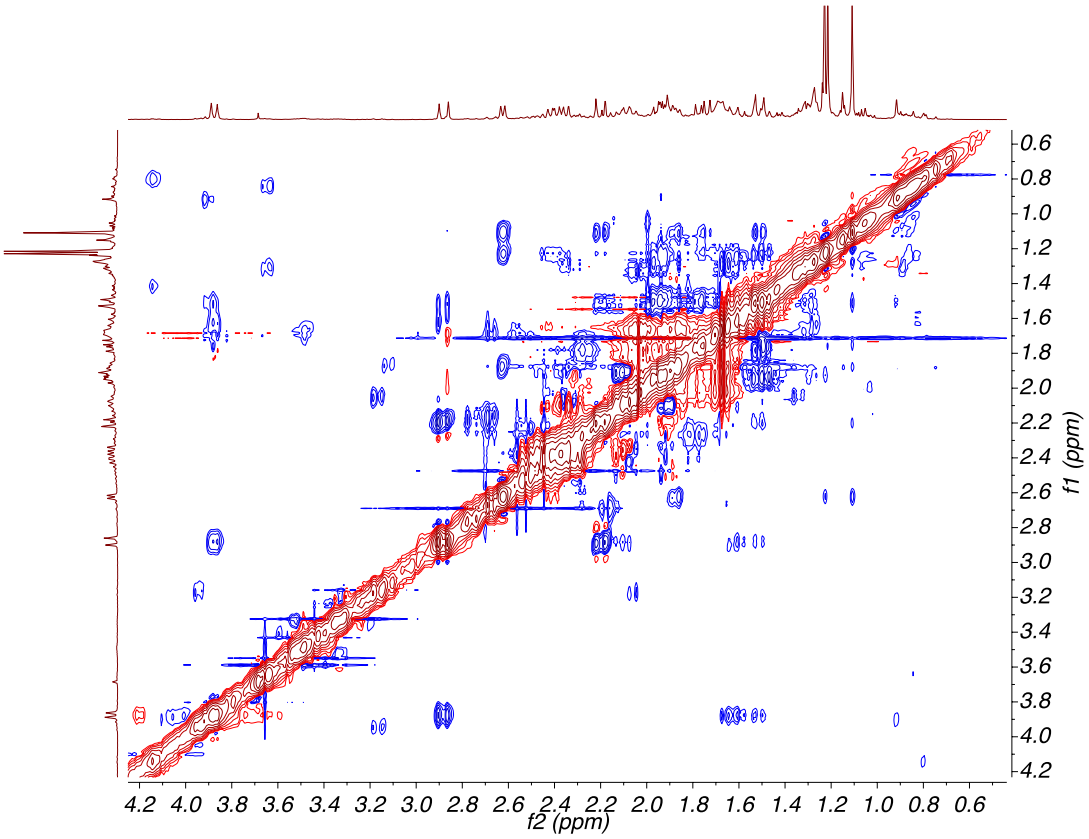

Figure A11.50. NOESY (400 MHz, $CDCl_3$) of compound **235**.

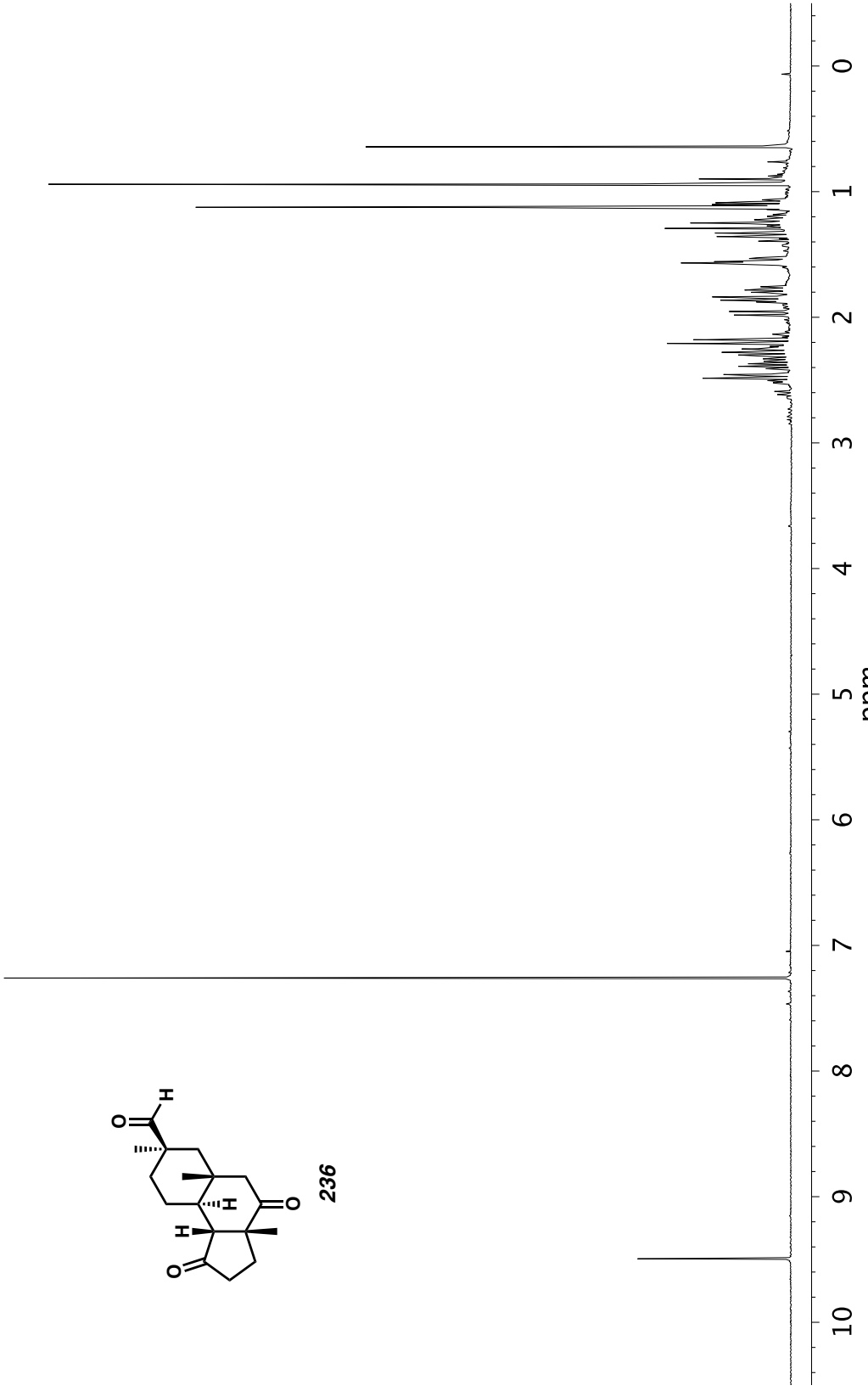

Figure A11.51. ^{1}H NMR (500 MHz, $CDCl_3$) of compound **236**.

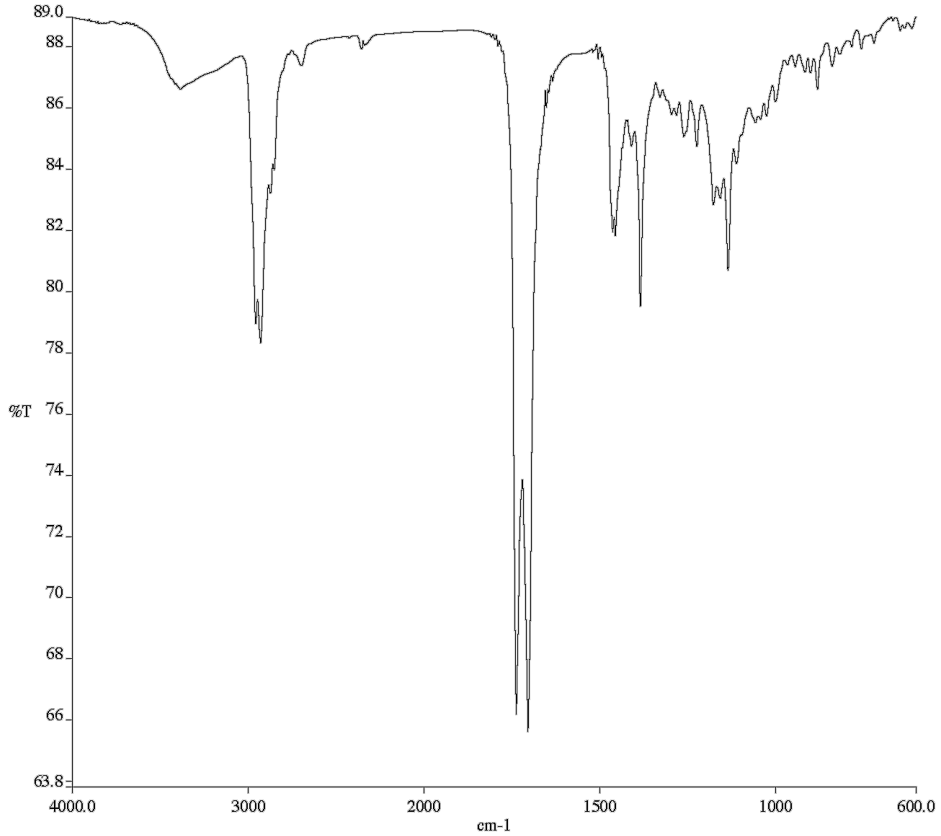

Figure A11.52. Infrared Spectrum (Thin Film, KBr) of compound **236**.

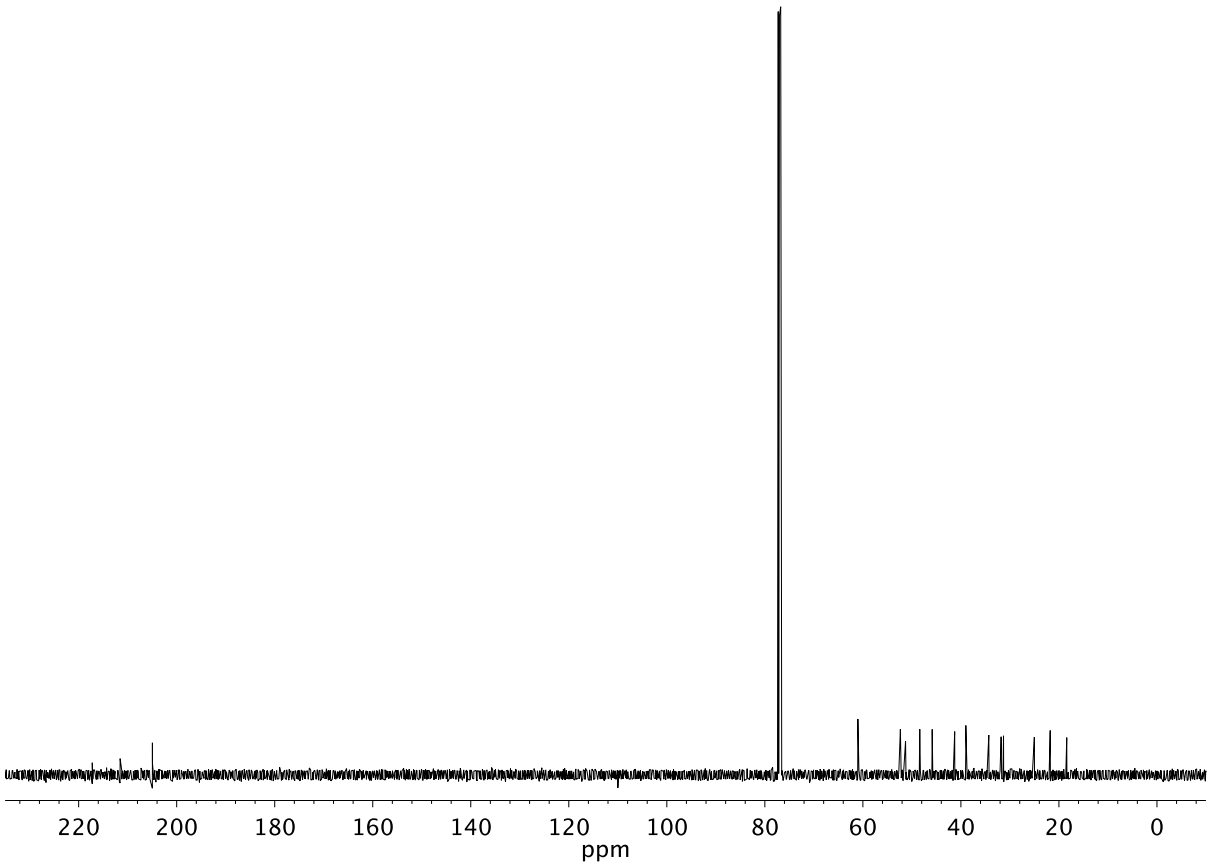

Figure A11.53. ^{13}C NMR (126 MHz, $CDCl_3$) of compound **236**.

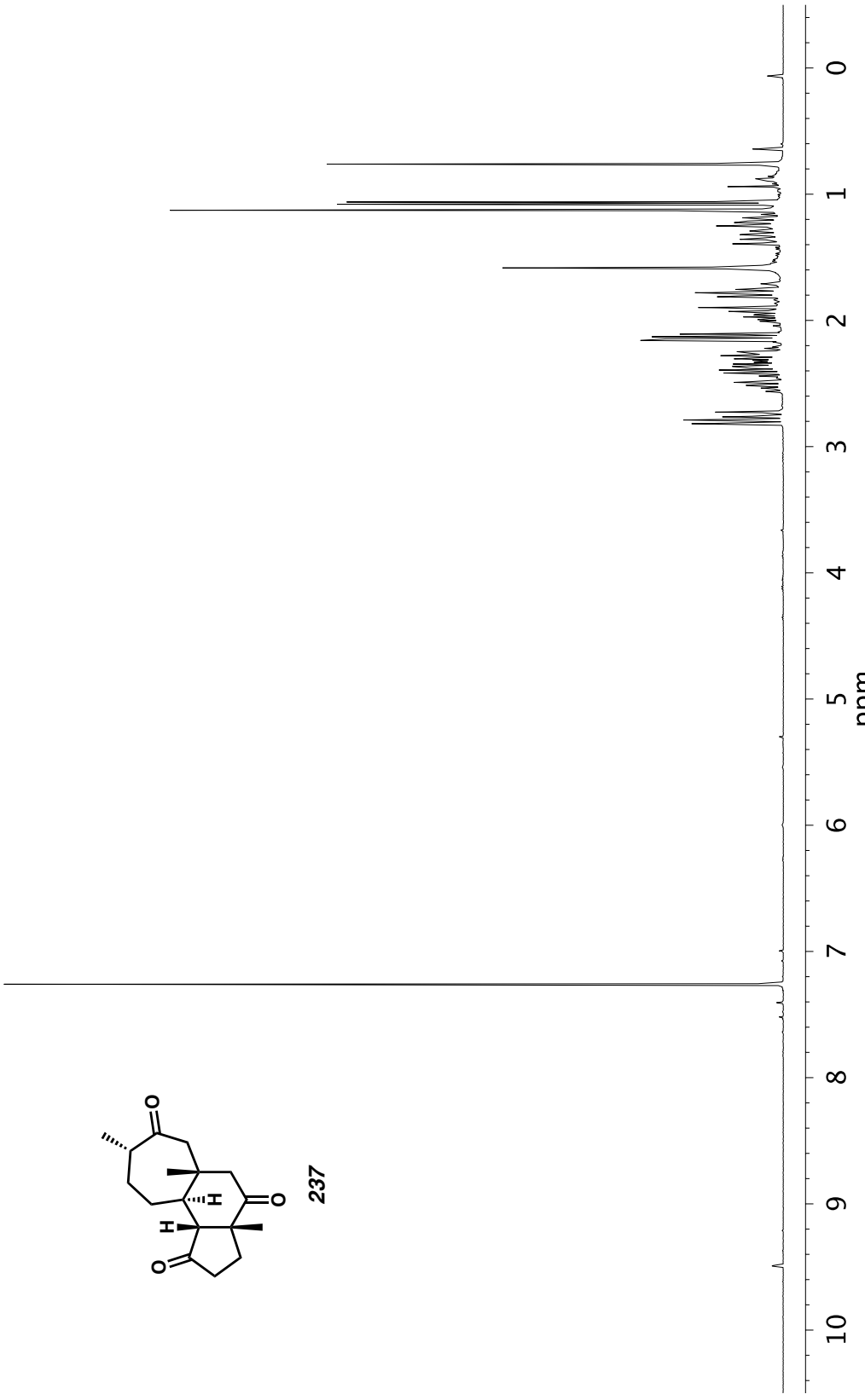

Figure A11.54. ^{1}H NMR (400 MHz, $CDCl_3$) of compound **237**.

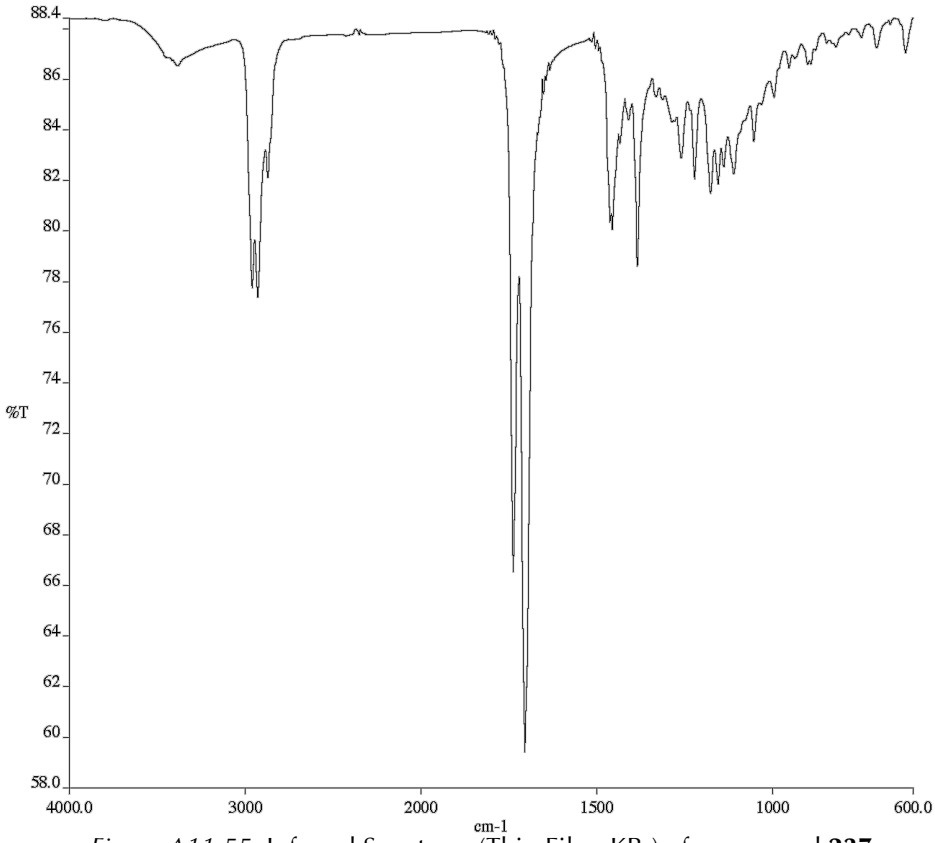

Figure A11.55. Infrared Spectrum (Thin Film, KBr) of compound **237**.

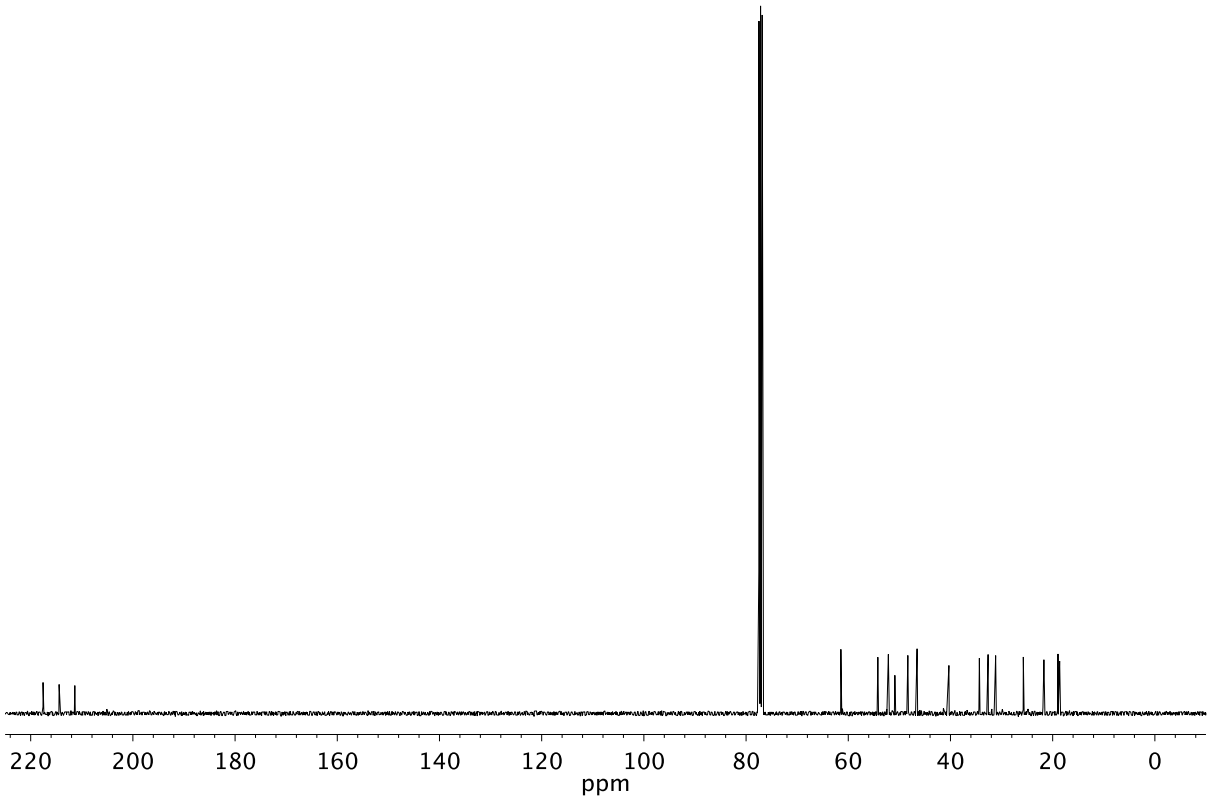

Figure A11.56. ^{13}C NMR (101 MHz, $CDCl_3$) of compound **237**.

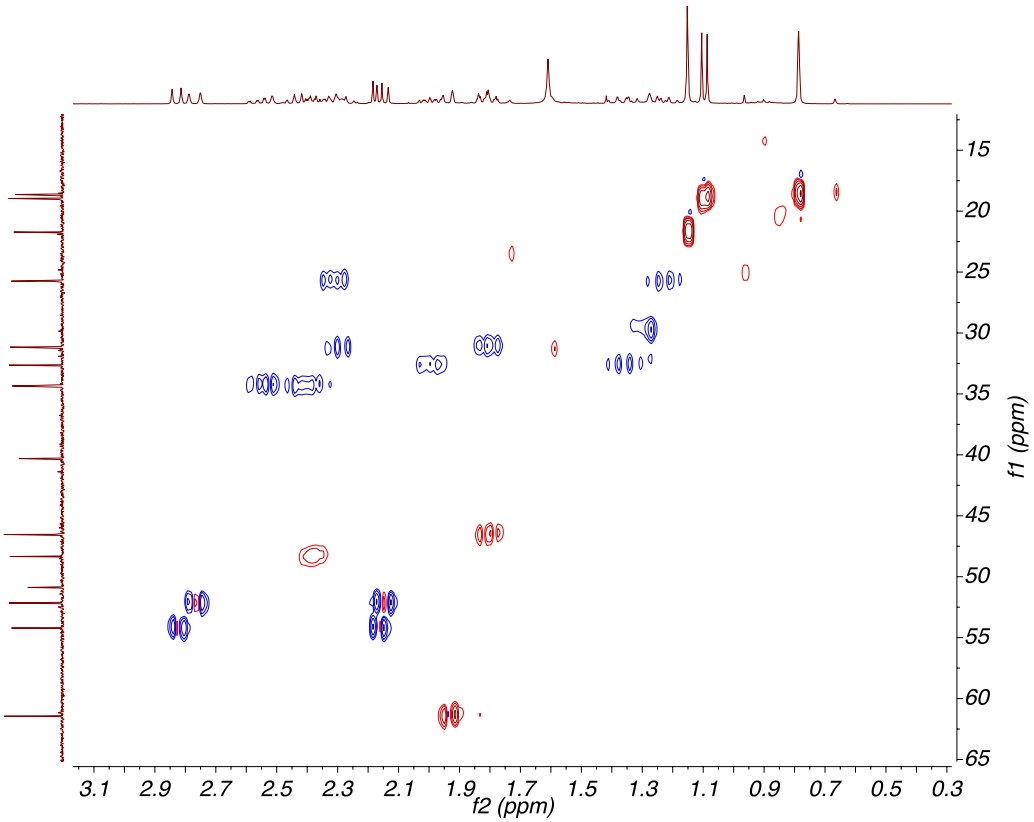

Figure A11.57. HSQC (400, 101 MHz, $CDCl_3$) of compound **237**.

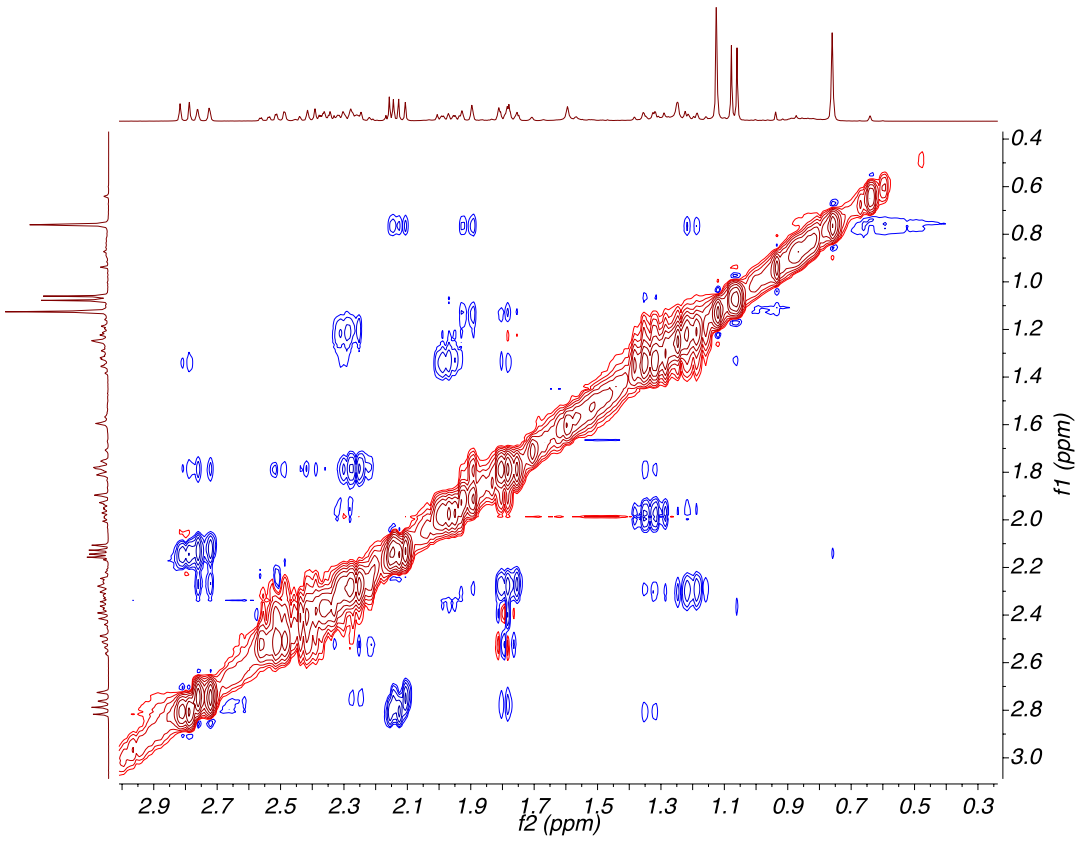

Figure A11.58. NOESY (400 MHz, $CDCl_3$) of compound **237**.

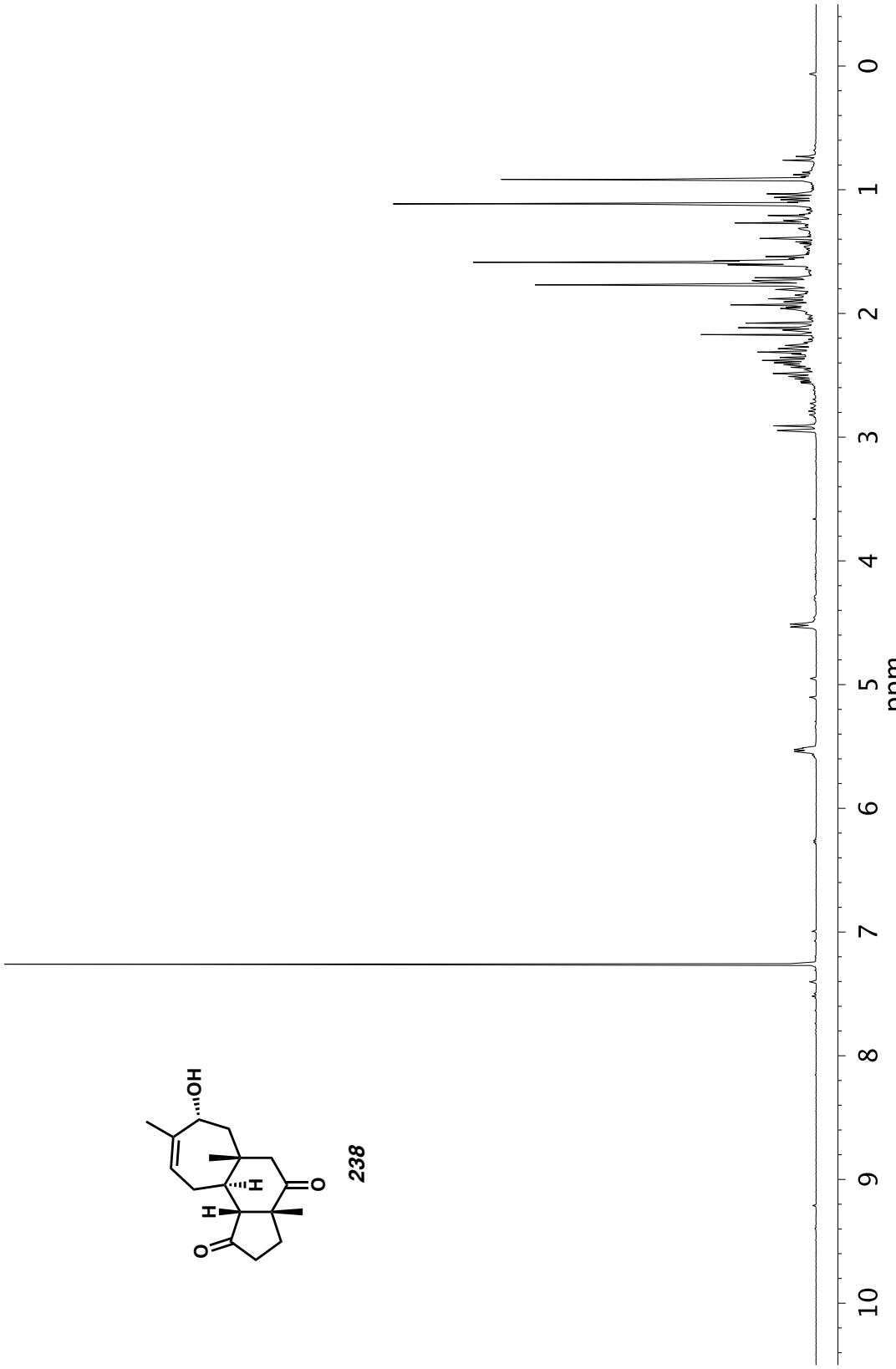

Figure A11.59. ^{1}H NMR (400 MHz, $CDCl_3$) of compound **238**.

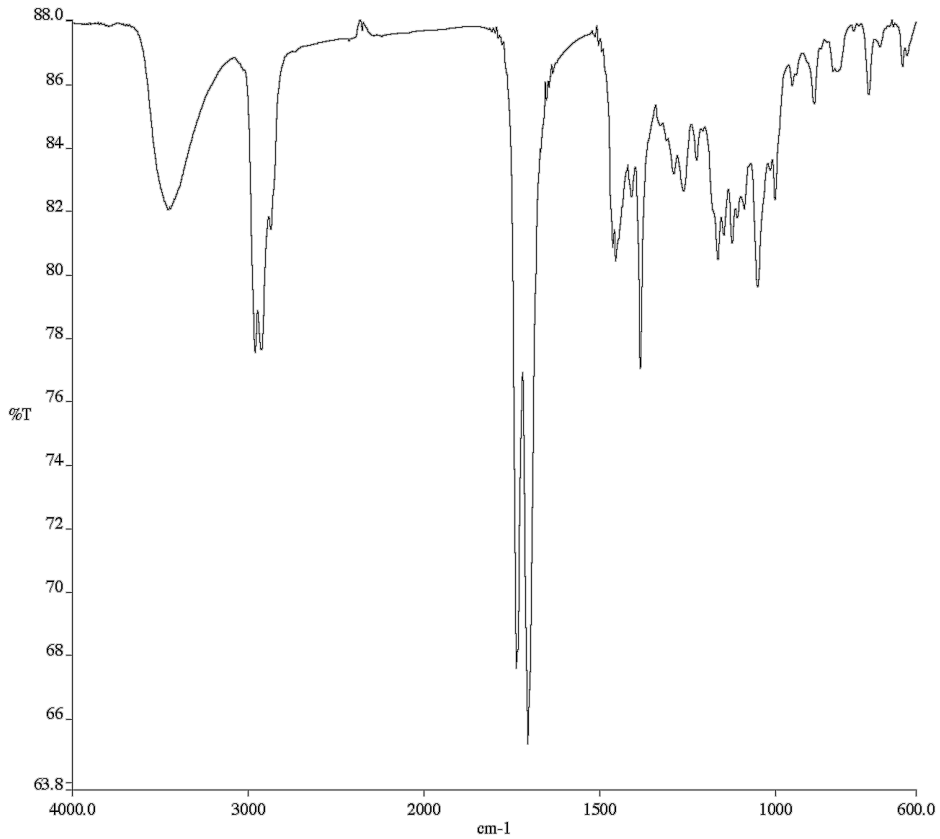

Figure A11.60. Infrared Spectrum (Thin Film, KBr) of compound **238**.

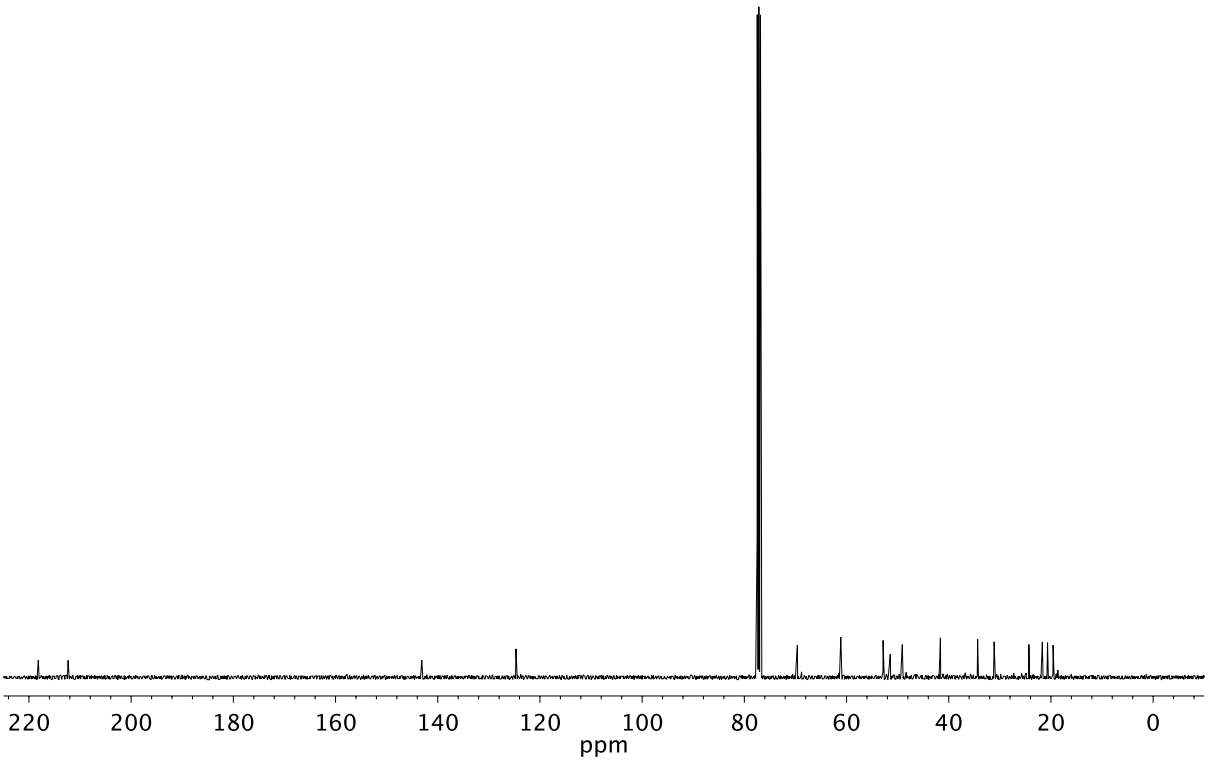

Figure A11.61. ^{13}C NMR (101 MHz, $CDCl_3$) of compound **238**.

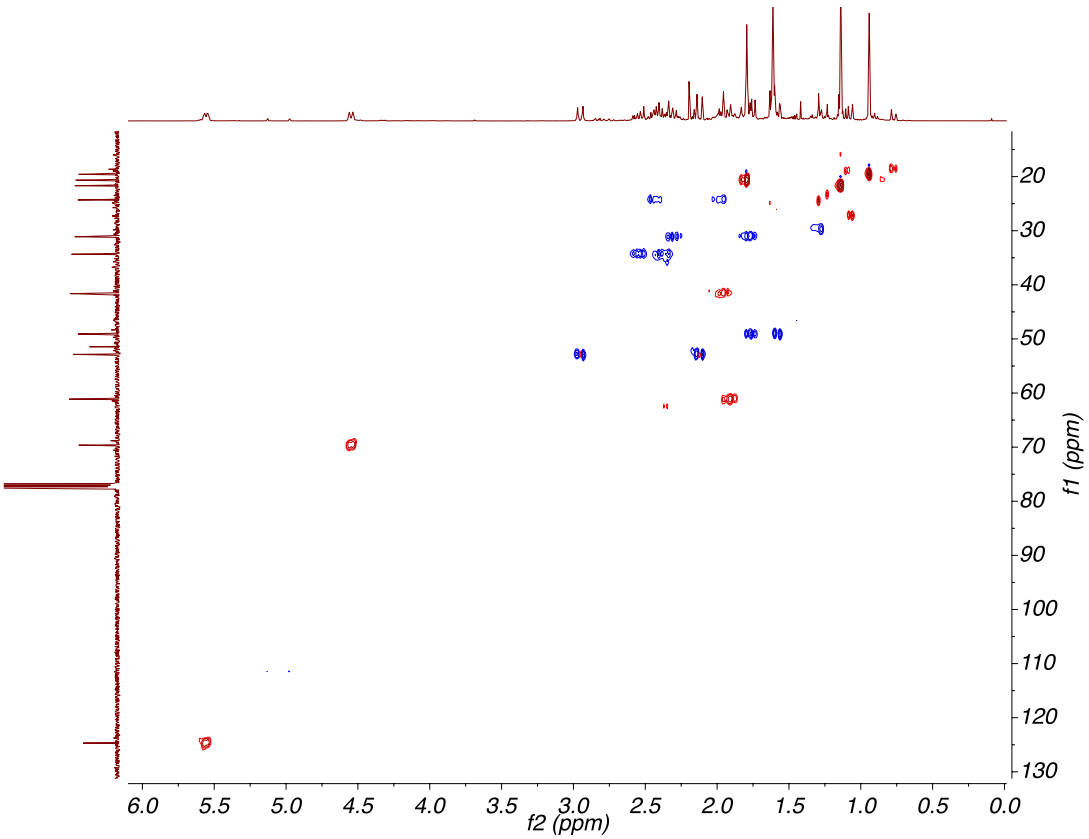

Figure A11.62. HSQC (400, 101 MHz, $CDCl_3$) of compound **238**.

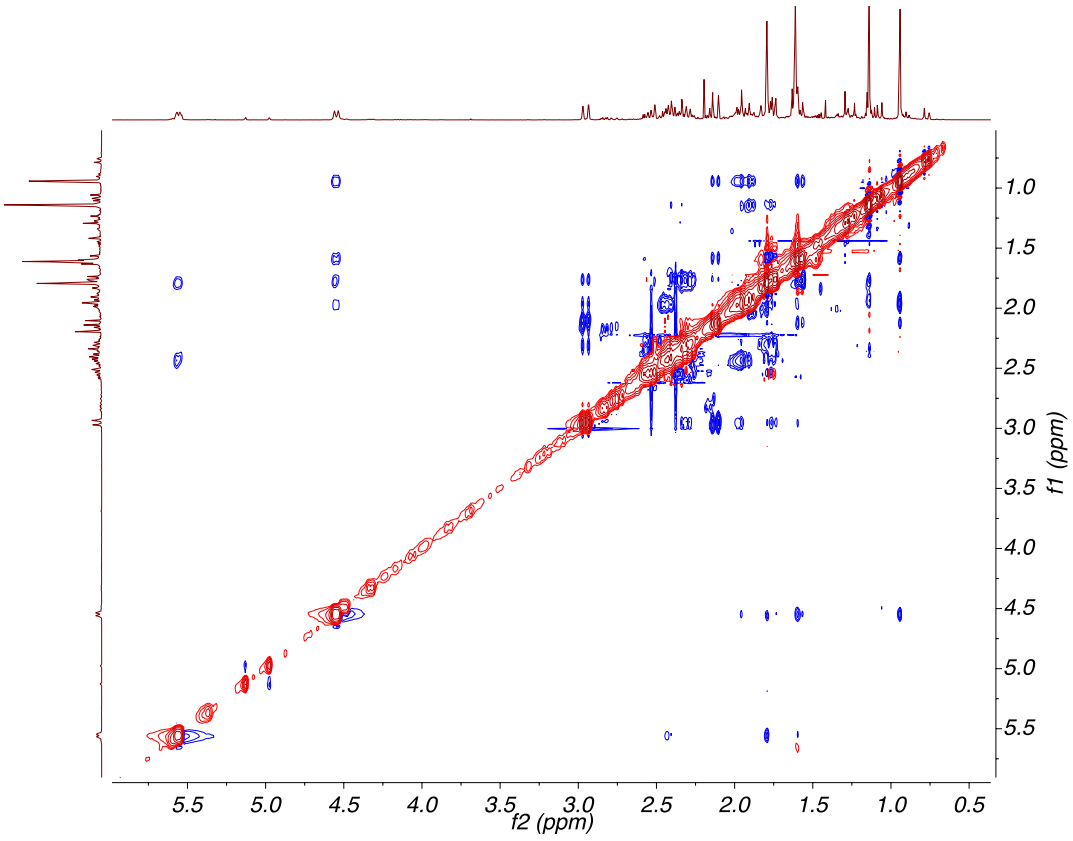

Figure A11.63. NOESY (400 MHz, $CDCl_3$) of compound **238**.

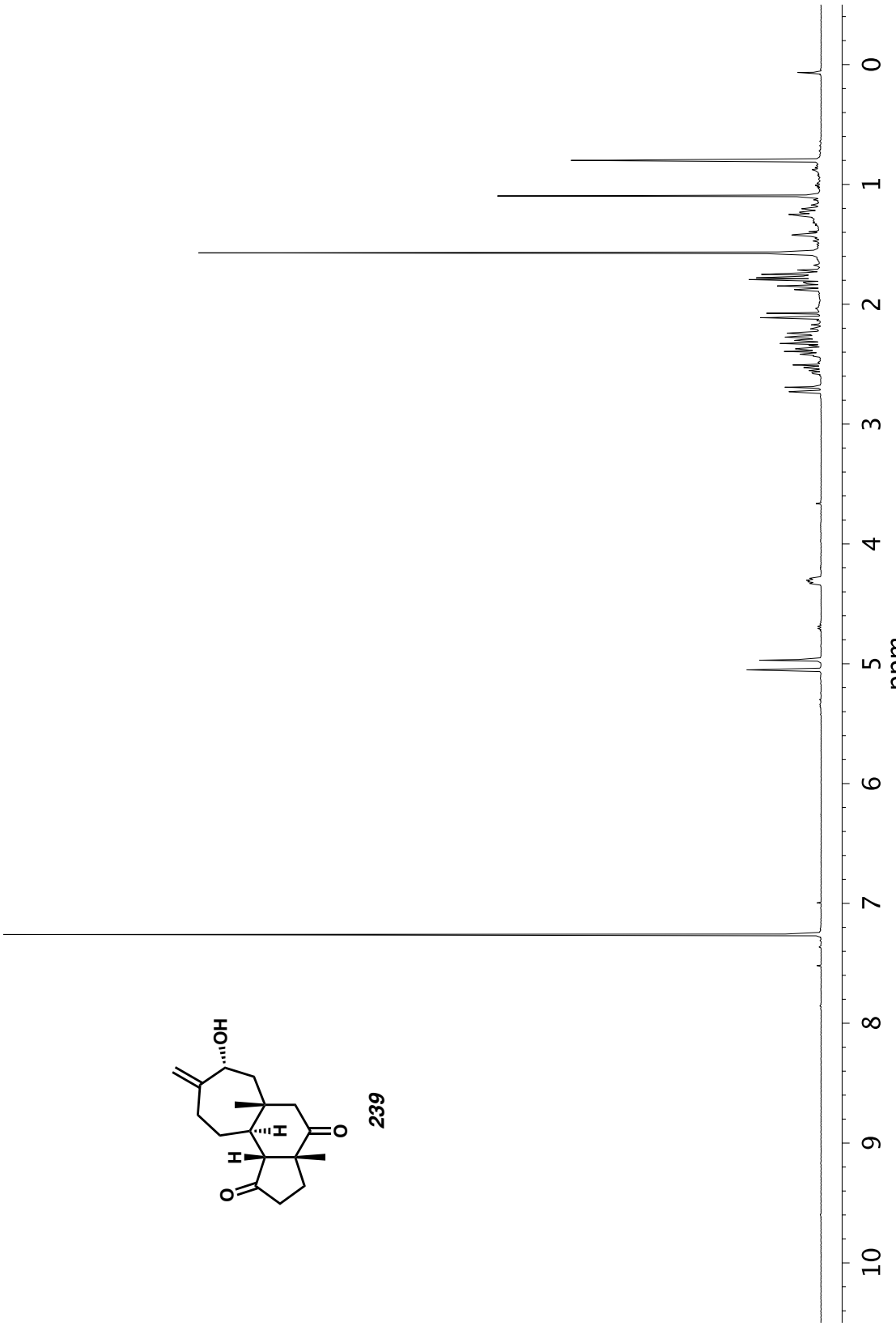

Figure A11.64. ^{1}H NMR (400 MHz, $CDCl_3$) of compound **239**.

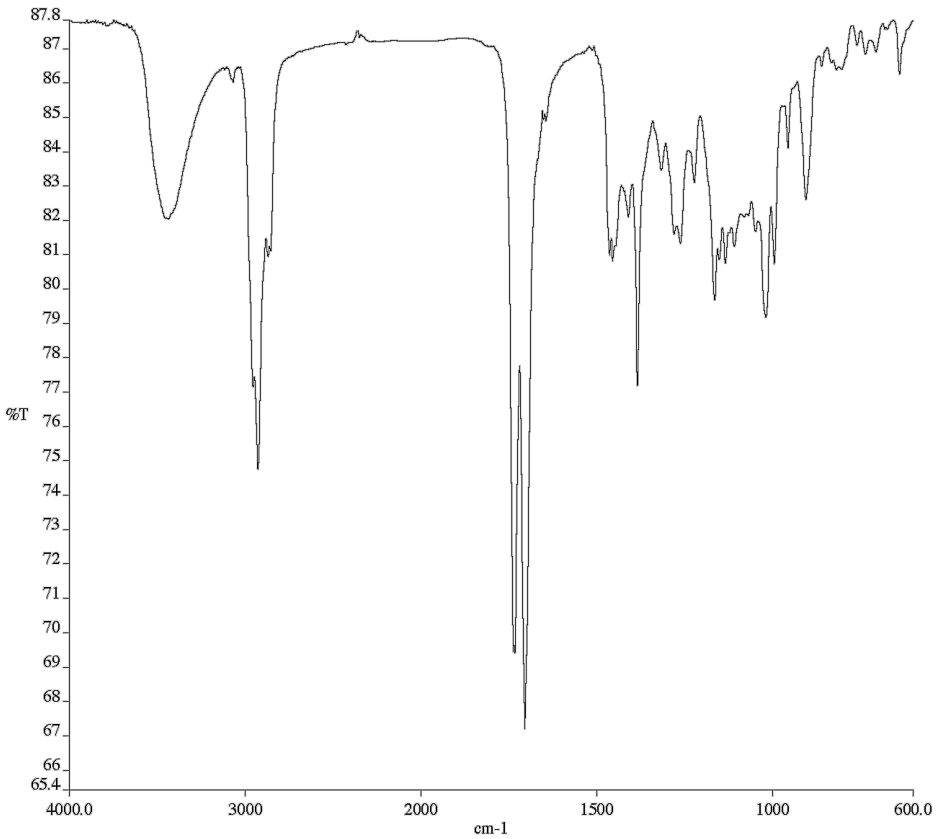

Figure A11.65. Infrared Spectrum (Thin Film, KBr) of compound **239**.

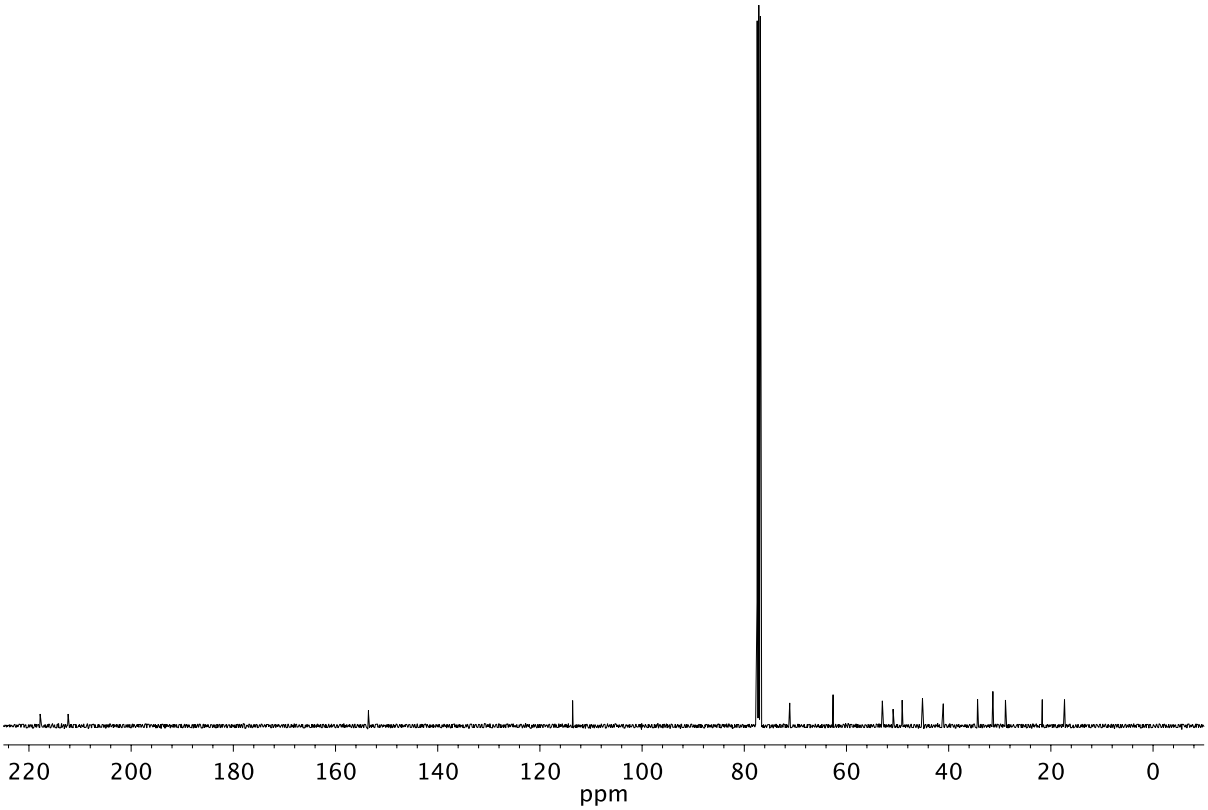

Figure A11.66. ^{13}C NMR (101 MHz, $CDCl_3$) of compound **239**.

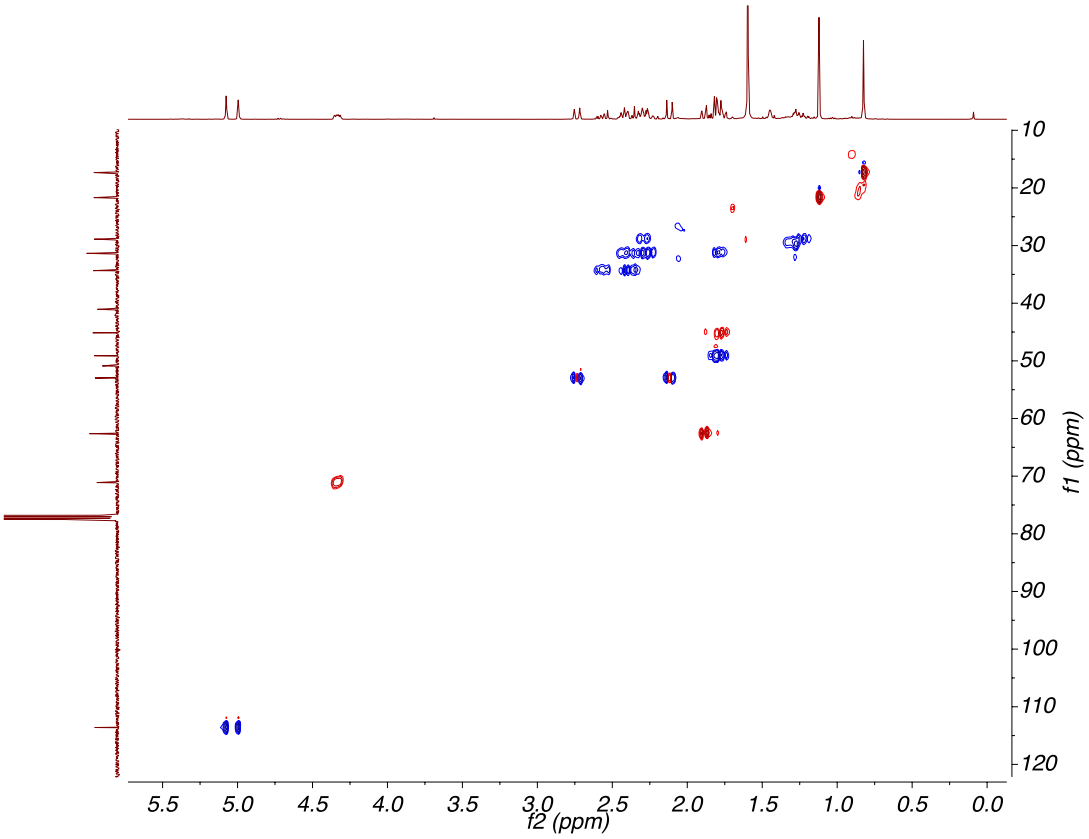

Figure A11.67. HSQC (400, 101 MHz, $CDCl_3$) of compound **239**.

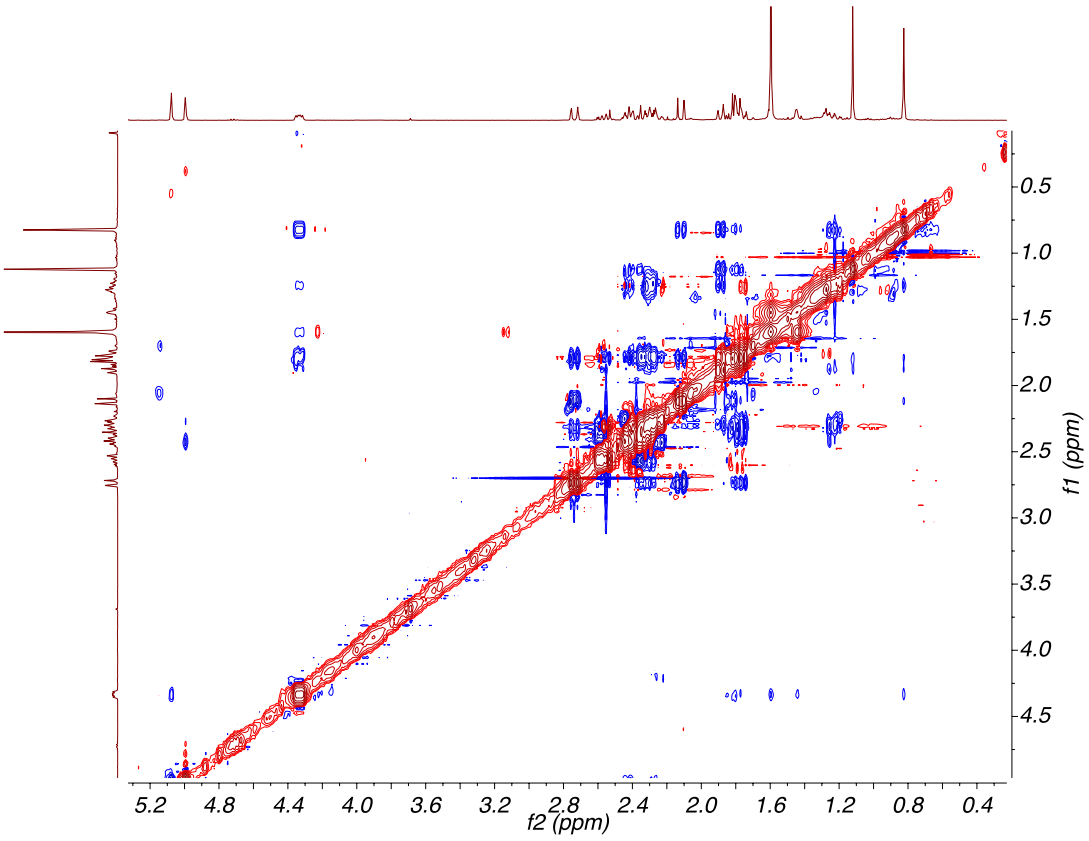

Figure A11.68. NOESY (400 MHz, $CDCl_3$) of compound **239**.

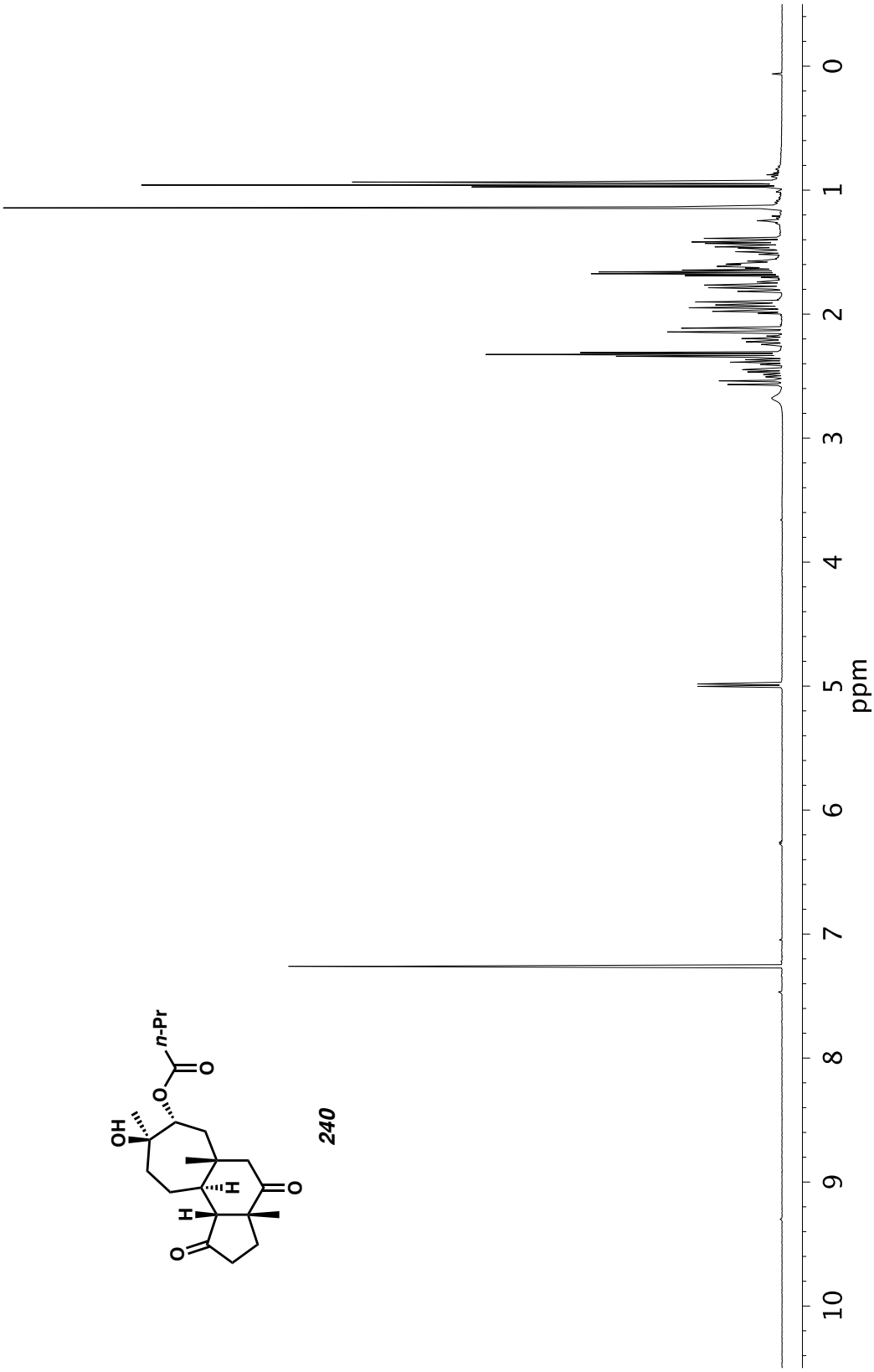

Figure A11.69. ^{1}H NMR (500 MHz, $CDCl_3$) of compound **240**.

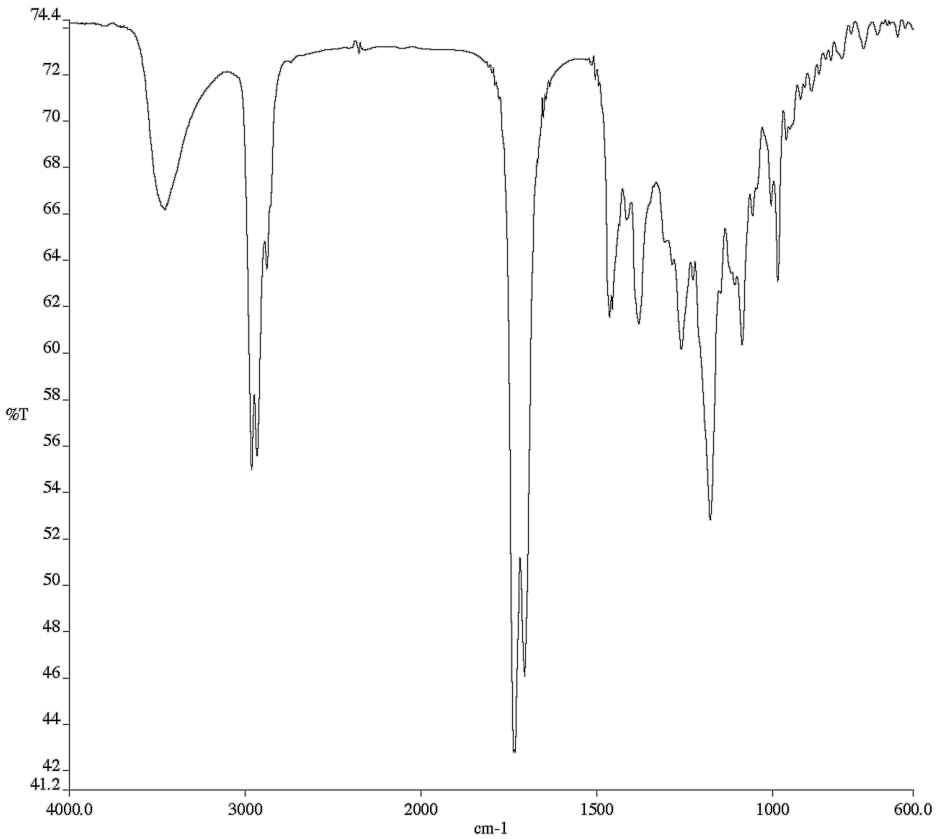

Figure A11.70. Infrared Spectrum (Thin Film, KBr) of compound **240**.

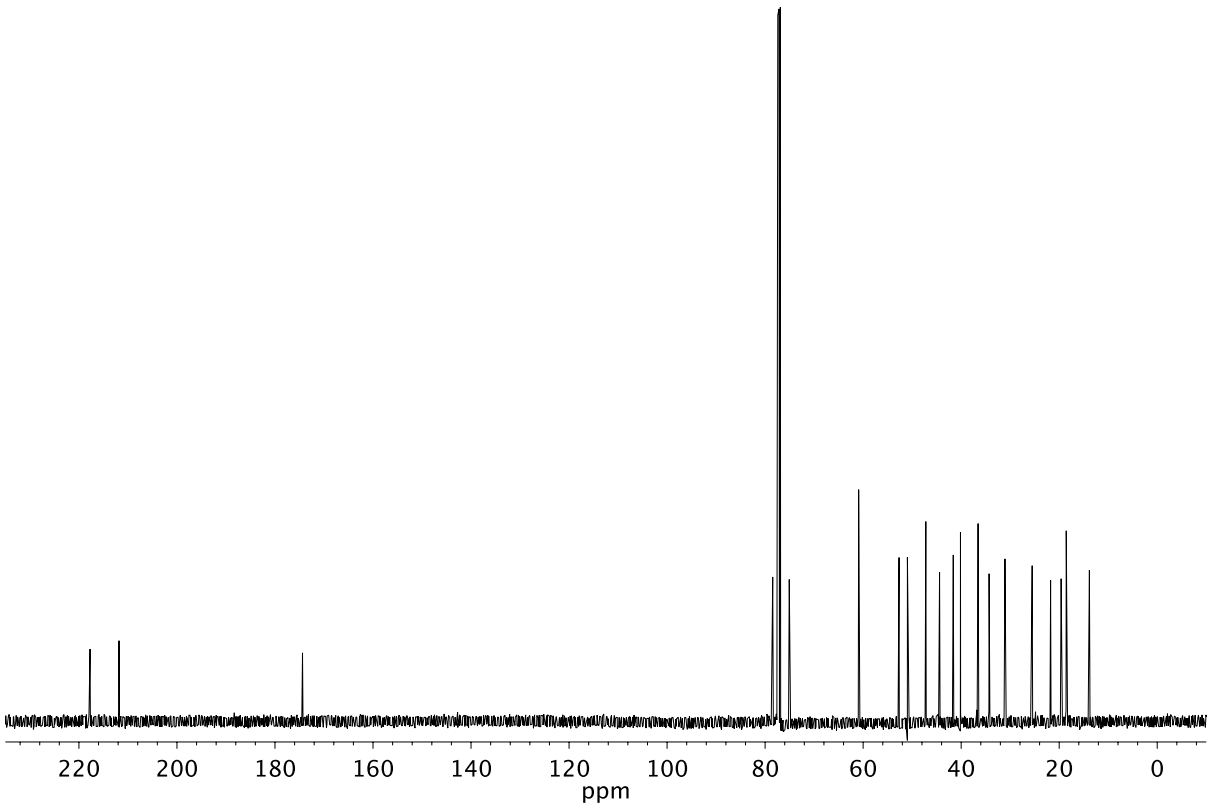

Figure A11.71. ^{13}C NMR (126 MHz, $CDCl_3$) of compound **240**.

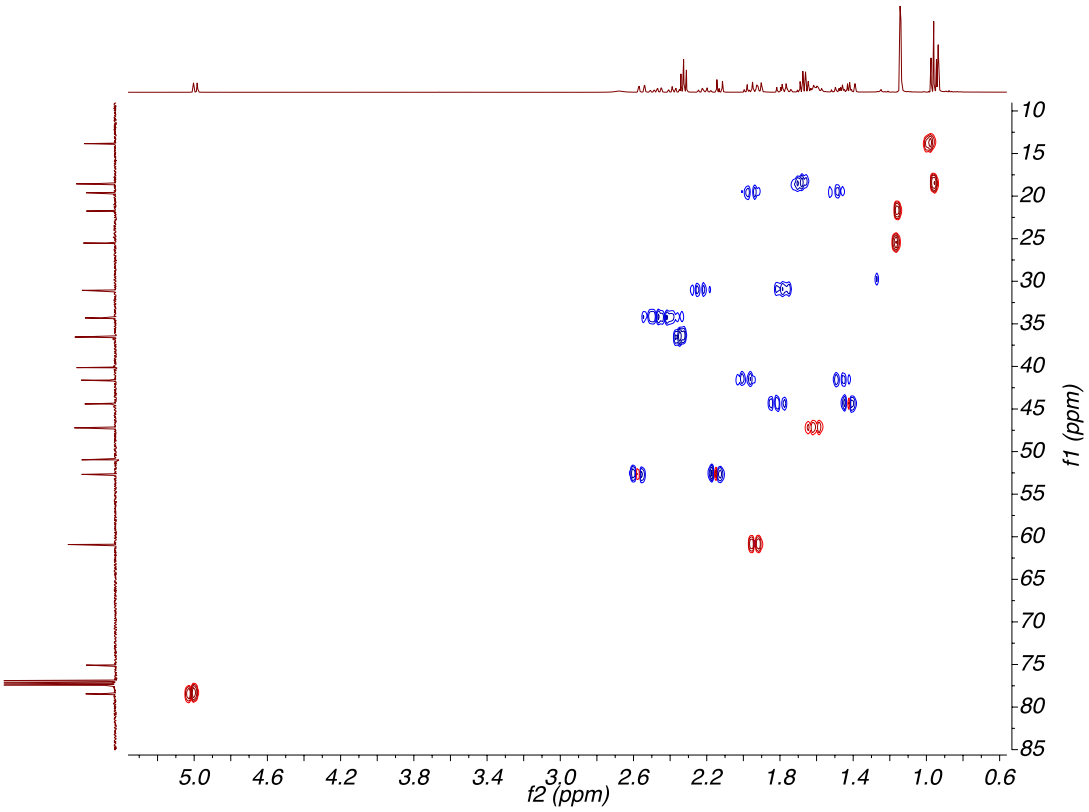

Figure A11.72. HSQC (400, 101 MHz, $CDCl_3$) of compound **240**.

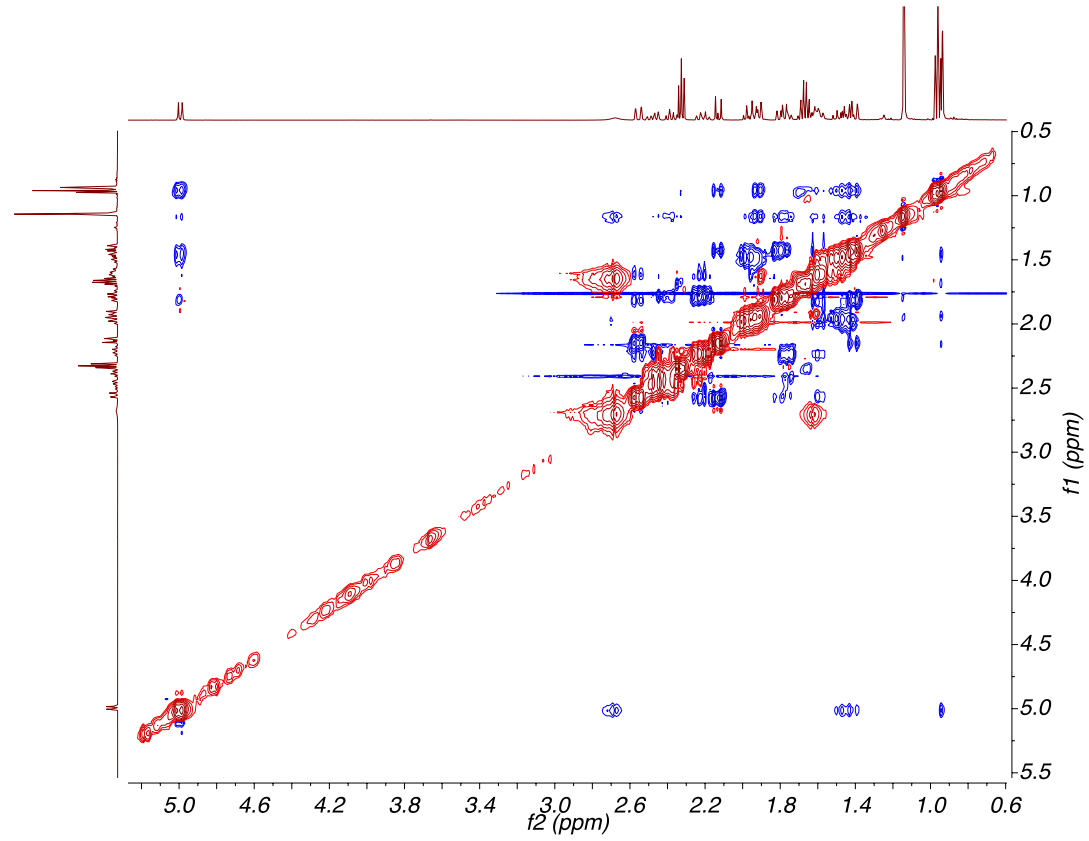

Figure A11.73. NOESY (400 MHz, $CDCl_3$) of compound **240**.

APPENDIX 12

Notebook Cross-Reference

NOTEBOOK CROSS-REFERENCE FOR NEW COMPOUNDS

The following cross-reference provides the file name for each piece of original spectroscopic data obtained for the compounds presented in this thesis. For each compound, both hard copy and electronic characterization folders containing the original ^{1}H NMR, ^{13}C NMR, ^{19}F NMR, COSY, HSQC, HMBC, NOESY, and IR spectra have been created. All notebooks and spectroscopic data are stored in the Stoltz research group archive.

Table A12.1 Notebook Cross-Reference for Compounds in Appendix 2

Compound	Chemical Structure	^{1}H NMR	^{13}C NMR	IR
129	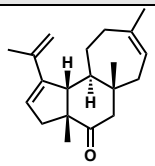	KK-5-293-4S	KK-5-293-4S	KK-5-293-4S
130	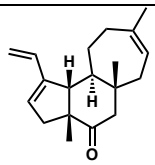	KK-4-211-4S	KK-4-211-4S	KK-4-211-4S

Table A12.2 Notebook Cross-Reference for Compounds in Chapter 3

Compound	Chemical Structure	^{1}H NMR	^{13}C NMR	IR
143b	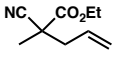	KK-5-55-1S	KK-5-55-1S	KK-5-55-1S

143c	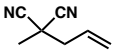	KK-5-87-2S	KK-5-87-2S	KK-5-87-2S
143d	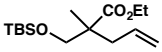	KK-5-167-1S	KK-5-167-1S	KK-5-167-1S
161	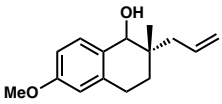	KK-5-263-2S	KK-5-263-2S	KK-5-263-2S
143j	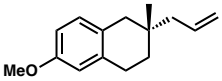	KK-5-265-2S	KK-5-265-2S	KK-5-265-2S
144a	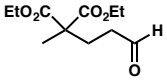	KK-4-291-2S	KK-4-291-2S	KK-4-291-2S
144b	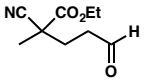	KK-5-57-2S	KK-5-57-2S	KK-5-57-2S
144c	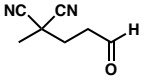	KK-5-73-2S	KK-5-73-2S	KK-5-73-2S
144d	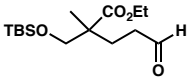	KK-5-169-2S	KK-5-169-2S	KK-5-169-2S
144e	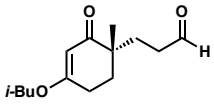	KK-5-161-3S	KK-5-161-3S	KK-5-161-3S
144f	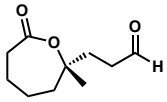	KK-5-165-3S	KK-5-165-3S	KK-5-165-3S
144g	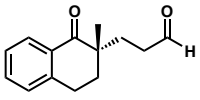	KK-4-185-2S	KK-4-185-2S	KK-4-185-2S
144h	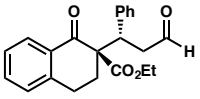	KK-5-75-2S	KK-5-75-2S	KK-5-75-2S

144i	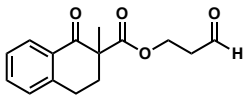	KK-5-233-3S	KK-5-233-3S	KK-5-233-3S
144j	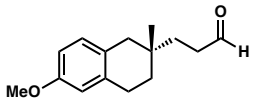	KK-5-271-2S	KK-5-271-2S	KK-5-271-2S
147a	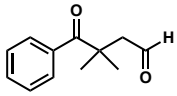	KK-5-129-3S	KK-5-129-3S	KK-5-129-3S
147b	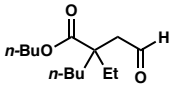	KK-6-143-3S	KK-6-143-3S	KK-6-143-3S
147c	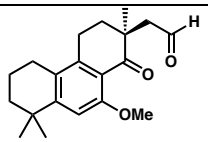	KK-6-149-2S	KK-6-149-2S	KK-6-149-2S
148a	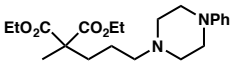	KK-5-211-2S	KK-5-211-2S	KK-5-211-2S
148b	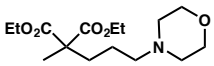	KK-5-223-2S	KK-5-97-2S	KK-5-97-2S
148c	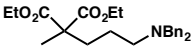	KK-5-221-2S	KK-5-221-2S	KK-5-221-2S
148d	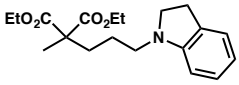	KK-5-39-2S	KK-5-39-2S	KK-5-39-2S
148e	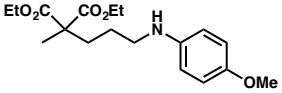	KK-5-215-2S	KK-5-215-2S	KK-5-215-2S
148f	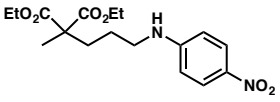	KK-5-219-2S	KK-5-219-2S	KK-5-219-2S
145a	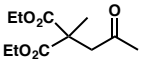	KK-5-151-2S	KK-5-151-2S	KK-5-151-2S

149	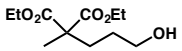	KK-5-51-4S	KK-5-51-4S	KK-5-51-4S
150	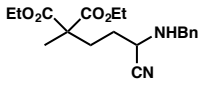	KK-5-193-3S	KK-5-193-3S	KK-5-193-3S
151	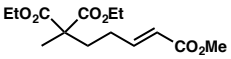	KK-5-89-2S	KK-5-89-2S	KK-5-89-2S
152	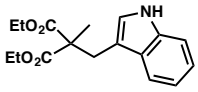	KK-5-295-2S	KK-5-295-2S	KK-5-295-2S
153	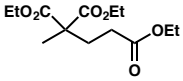	KK-5-225-6S	KK-5-225-6S	KK-5-225-6S
154	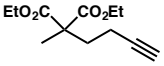	KK-5-147-1S	KK-5-147-1S	KK-5-147-1S

Table A12.3 Notebook Cross-Reference for Compounds in Chapter 4

Compound	Chemical Structure	^{1}H NMR	^{13}C NMR	IR
189	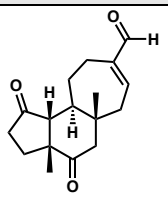	KK-6-183-6S	KK-6-183-6S	KK-6-183-6S
190	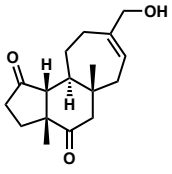	KK-6-245-4S	KK-6-183-5S	KK-6-183-5S

191	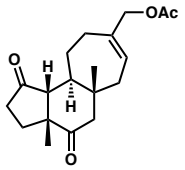	KK-6-89-5S	KK-6-89-5S	KK-6-89-4S
193	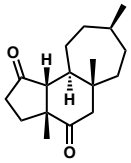	KK-3-287-3S	KK-3-287-3S	KK-6-91-3S
194	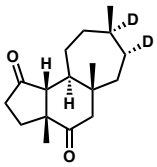	KK-6-179-1S	KK-3-249-1S	KK-6-179-1S
195	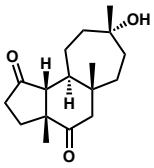	KK-4-263-5S	KK-4-263-6S	KK-3-283-3S
197	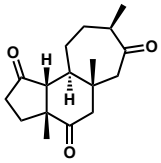	KK-6-267-2S	KK-6-267-2S	KK-6-267-2S
198a	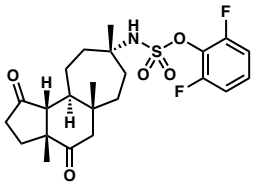	KK-4-175-5S	KK-4-175-5S	KK-4-175-5S
198b	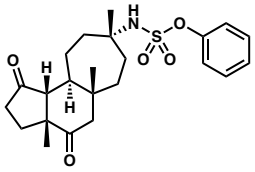	KK-6-73-5S	KK-6-73-5S	KK-6-73-5S
198c	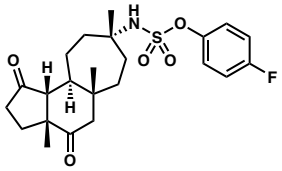	KK-6-75-7S	KK-6-75-7S	KK-6-75-7S

199a	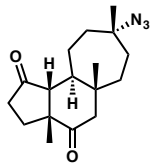	KK-6-63-2S	KK-4-93-2S	KK-6-63-2S
199b	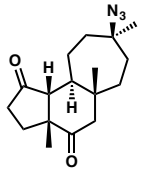	KK-6-67-3S	KK-6-63-3S	KK-6-67-3S
202	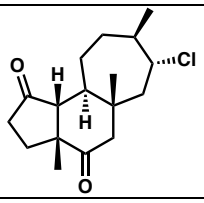	KK-6-199-3S	KK-6-199-3S	KK-6-199-3S

Table A12.4 Notebook Cross-Reference for Compounds in Appendix 6

Compound	Chemical Structure	^{1}H NMR	^{13}C NMR	IR
210	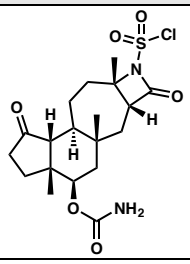	KK-4-39-2S	KK-4-39-2S	KK-4-39-2S
211	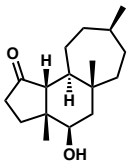	KK-4-43-6S	KK-4-43-6S	KK-6-55-1S
212	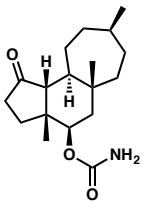	KK-4-61-5S	KK-4-61-5S	KK-4-61-5S

217	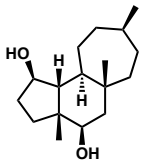	KK-6-55-4S	KK-6-55-4S	KK-6-55-4S
218	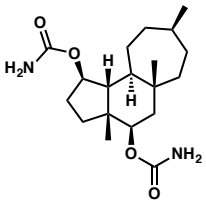	KK-4-303-3S	KK-4-303-3S	KK-4-303-3S
220	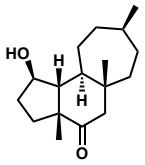	KK-6-269-3S	KK-6-269-3S	KK-6-269-3S

Table A12.5 Notebook Cross-Reference for Compounds in Chapter 5

Compound	Chemical Structure	^{1}H NMR	^{13}C NMR	IR
230	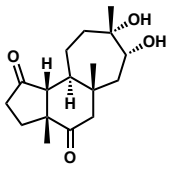	KK-3-225-2S	KK-3-225-2S	KK-5-269-4S
229	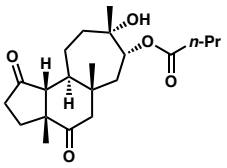	KK-3-237-2S	KK-3-237-2S	KK-5-275-4S

228	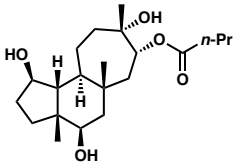	KK-5-289-5S	KK-5-289-5S	KK-5-289-5S
231	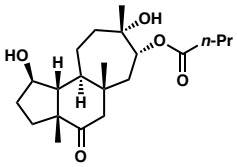	KK-6-207-4S	KK-6-207-4S	KK-6-207-4S
227a	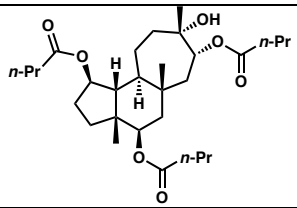	KK-6-209-3S	KK-6-209-3S	KK-6-209-3S
227b	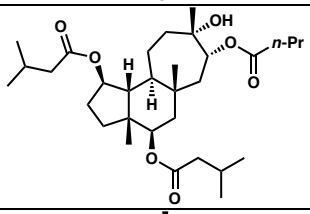	KK-6-259-2S	KK-6-259-2S	KK-6-259-2S
227c	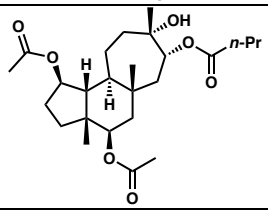	KK-6-211-3S	KK-6-211-3S	KK-6-211-3S
233	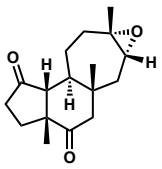	KK-3-191-char	KK-3-191-char	KK-3-191-char
234	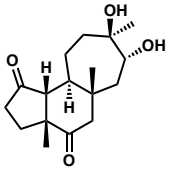	KK-3-209-2S	KK-3-209-2S	KK-6-225-3S
235	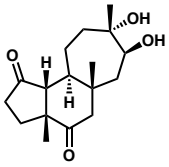	KK-6-225-4S	KK-6-225-4S	KK-6-225-4S

236	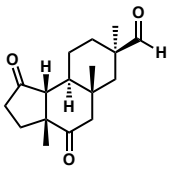	KK-6-225-2S	KK-6-225-2S	KK-6-225-2S
237	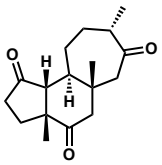	KK-6-225-6S	KK-6-225-6S	KK-6-225-6S
238	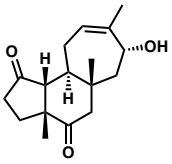	KK-6-225-7S	KK-6-225-7S	KK-6-225-7S
239	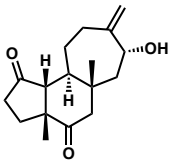	KK-6-225-8S	KK-6-225-8S	KK-6-225-8S
240	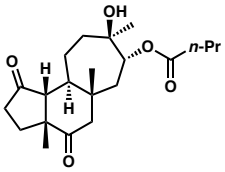	KK-6-227-3S	KK-6-227-3S	KK-6-227-3S

COMPREHENSIVE BIBLIOGRAPHY

Adams, A. M.; Du Bois, J. *Chem. Sci.* **2014**, *5*, 656–659.

Adams, A. M.; Du Bois, J.; Malik, H. A. *Org. Lett.* **2015**, *17*, 6066–6069.

Allred, G. D.; Liebeskind, L. S. *J. Am. Chem. Soc.* **1996**, *118*, 2748–2749.

Altstadt, T. J.; Fairchild, C. R.; Golik, J.; Johnston, K. A.; Kadow, J. F.; Lee, F. Y.; Long, B. H.; Rose, W. C.; Vyas, D. M.; Wong, H.; Wu, M.-J.; Wittman, M. D. *J. Med. Chem.* **2001**, *44*, 4577–4583.

Anderson, B. J.; Keith, J. A.; Sigman, M. S. *J. Am. Chem. Soc.* **2010**, *132*, 11872–11874.

Appendino, G.; Tron, G. C.; Cravotto, G.; Palmisano, G.; Jakupovic, J. *J. Nat. Prod.* **1999**, *62*, 76–79.

Appendino, G.; Tron, G. C.; Jarevång, T.; Sterner, O. *Org. Lett.* **2001**, *3*, 1609–1612.

Arndtsen, B. A.; Bergman, R. G.; Mobley, T. A.; Peterson, T. H. *Acc. Chem. Res.* **1995**, *28*, 154–162.

Bäckvall, J.-E. *Acc. Chem. Res.* **1983**, *16*, 335–342.

Baldino, C. M.; Parr, J.; Wilson, C. J.; Ng, S.-C.; Yohannes, D.; Wasserman, H. H. *Bioorg. Med. Chem. Lett.* **2006**, *16*, 701–704.

Balthaser, B. R.; Maloney, M. C.; Beeler, A. B.; Porco, J. A., Jr.; Snyder, J. K. *Nat. Chem.* **2011**, *3*, 969–973.

Baltz, R. H. *Curr. Opin. Pharmacol.* **2008**, *8*, 557–563.

Barker, E. C.; Gatbonton-Schwager, T. N.; Han, Y.; Clay, J. E.; Letterio, J. J.; Tochtrop, G. P. *J. Nat. Prod.* **2010**, *73*, 1064–1068.

Barrett, A. G. M.; Brinkmann, C.; Crimmin, M. R.; Hill, M. S.; Hunt, P.; Procopiou, P. A. *J. Am. Chem. Soc.* **2009**, *131*, 12906–12907.

Barve, I. J.; Dalvi, P. B.; Thikekar, T. U.; Chanda, K.; Liu, Y.-L.; Fang, C.-P.; Liu, C.-C.; Sun, C.-M. *RSC Adv.* **2015**, *5*, 73169–73179.

Behenna, D. C.; Liu, Y.; Yurino, T.; Kim, J.; White, D. E.; Virgil, S. C.; Stoltz, B. M. *Nat. Chem.* **2012**, *4*, 130–133.

Behenna, D. C.; Mohr, J. T.; Sherden, N. H.; Marinescu, S. C.; Harned, A. M.; Tani, K.; Seto, M.; Ma, S.; Novák, Z.; Krout, M. R.; McFadden, R. M.; Roizen, J. L.; Enquist, J. A., Jr.; White, D. E.; Levine, S. R.; Petrova, K. V.; Iwashita, A.; Virgil, S. C.; Stoltz, B. M. *Chem.–Eur. J.* **2011**, *17*, 14199–14223.

Behenna, D. C.; Stoltz, B. M. *J. Am. Chem. Soc.* **2004**, *126*, 15044–15045.

Beller, M.; Seayad, J.; Tillack, A.; Jiao, H. *Angew. Chem., Int. Ed.* **2004**, *43*, 3368–3398.

Beller, M.; Trauthwein, H.; Eichberger, M.; Breindl, C.; Herwig, J.; Müller, T. E.; Thiel, O. R. *Chem.–Eur. J.* , **1999**, *5*, 1306–1319.

Beydoun, K.; Zaarour, M.; Williams, J. A. G.; Doucet, H.; Guerchais, V. *Chem. Commun.* **2012**, *48*, 1260–1262.

Boers, R. B.; Randulfe, Y. P.; van der Haas, H. N. S.; van Rossum-Baan, M.; Lugtenburg, J. *Eur. J. Org. Chem.* **2002**, *2002*, 2094–2108.

Boger, D. L.; Patel, M. *J. Org. Chem.* **1988**, *53*, 1405–1415.

Bohacek, R. S.; McMartin, C.; Guida, W. C. *Med. Res. Rev.* **1996**, *16*, 3–50.

Bronner, S. M.; Grubbs, R. H. *Chem. Sci.* **2014**, *5*, 101–106.

Brückl, T.; Baxter, R. D.; Ishihara, Y.; Baran, P. S. *Acc. Chem. Res.* **2012**, *45*, 826–839.

Brummond, K. M.; Chen, H.; Fisher, K. D.; Kerekes, A. D.; Rickards, B.; Sill, P. C.; Geib, S. J. *Org. Lett.* **2002**, *4*, 1931–1934.

Buey, R. M.; Barasoain, I.; Jackson, E.; Meyer, A.; Giannakakou, P.; Paterson, I.; Mooberry, S.; Andreu, J. M.; Díaz, J. F. *Chem. Biol.* **2005**, *12*, 1269–1279.

Bürgi, H. B.; Dunitz, J. D.; Lehn, J. M.; Wipff, G. *Tetrahedron* **1974**, *30*, 1563–1572.

Burke, M. D.; Schreiber, S. L. *Angew. Chem., Int. Ed.* **2003**, *43*, 46–58.

Butler, M. S. *Nat. Prod. Rep.* **2008**, *25*, 475–516.

Campbell, A. N.; Stahl, S. S. *Acc. Chem. Res.* **2012**, *45*, 851–863.

Campbell, A. N.; White, P. B.; Guzei, I. A.; Stahl, S. S. *J. Am. Chem. Soc.* **2010**, *132*, 15116–15119.

Camps, F.; Castells, J.; Ferrando, M. J.; Font, J. *Tetrahedron Lett.* **1971**, *12*, 1713–1714.

Canales, A.; Matesanz, R.; Gardner, N. M.; Andreu, J. M.; Paterson, I.; Díaz, J. F.; Jiménez-Barbero, J. *Chem.–Eur. J.* **2008**, *14*, 7557–7569.

Cernak, T.; Dykstra, K. D.; Tyagarajan, S.; Vachal, P.; Krska, S. W. *Chem. Soc. Rev.* **2016**, *45*, 546–576.

Challacombe, J. M.; Suhrbrier, A.; Parsons, P. G.; Jones, B.; Hampson, P.; Kavanagh, D.; Rainger, G. E.; Morris, M.; Lord, J. M.; Le, T. T. T.; Hoang-Le, D.; Ogbourne, S. M. *J. Immunol.* **2006**, *177*, 8123–8132.

Chaudhary, A. G.; Rimoldi, J. M.; Kingston, D. G. I. *J. Org. Chem.* **1993**, *58*, 3798–3799.

Chen, D. Y.-K.; Youn, S. W. *Chem.–Eur. J.* **2012**, *18*, 9452–9474.

Chen, H.; Yang, W.; Wu, W.; Jiang, H. *Org. Biomol. Chem.* **2014**, *12*, 3340–3343.

Chen, K.; Baran, P. S. *Nature* **2009**, *459*, 824–828.

Chen, M. S.; White, M. C. *J. Am. Chem. Soc.* **2004**, *126*, 1346–1347.

Chen, M. S.; White, M. C. *Science* **2007**, *318*, 783–787.

Chen, P.; Cao, L.; Li, C. *J. Org. Chem.* **2009**, *74*, 7533–7535.

Chiba, S.; Kitamura, M.; Narasaka, K. *J. Am. Chem. Soc.* **2006**, *128*, 6931–6937.

Chiba, S.; Kitamura, M.; Saku, O.; Narasaka, K. *Bull. Chem. Soc. Jpn.* **2004**, *77*, 785–796.

Cooper, T. W.; Campbell, I. B.; Macdonald, S. J. *Angew. Chem., Int. Ed.* **2010**, *49*, 8082–8091.

Cornell, C. N.; Sigman, M. S. *Inorg. Chem.* **2007**, *46*, 1903–1909.

Crabtree, R. H.; Felkin, H.; Fillebeen-Khan, T.; Morris, G. E. *J. Organomet. Chem.* **1979**, *168*, 183–195.

Cragg, G. M.; Kingston, D. G. I.; Newman, D. J. *Anticancer Agents From Natural Products*, Taylor&Francis, Boca Raton, **2005**.

Craig, R. A., II; Loskot, S. A.; Mohr, J. T.; Behenna, D. C.; Harned, A. M.; Stoltz, B. M. *Org. Lett.* **2015**, *17*, 5160–5163.

Crimmin, M. R.; Casely, I. J.; Hill, M. S. *J. Am. Chem. Soc.* **2005**, *127*, 2042–2043.

Crowley, J. I.; Rapoport, H. *J. Am. Chem. Soc.* **1970**, *92*, 6363–6365.

Cruz, D.; Wang, Z.; Kibbie, J.; Modlin, R.; Kwon, O. *Proc. Natl. Acad. Sci. U.S.A.* **2011**, *108*, 6769–6774.

Cui, Y.; He, C. *Angew. Chem., Int. Ed.* **2004**, *43*, 4210–4212.

Curci, R.; D'Accolti, L.; Fusco, C. *Acc. Chem. Res.* **2006**, *39*, 1–9.

Dai, H.-X.; Stepan, A. F.; Plummer, M. S.; Zhang, Y.-H.; Yu, J.-Q. *J. Am. Chem. Soc.* **2011**, *133*, 7222–7228

D'Alessio, R.; Bargiotti, A.; Carlini, O.; Colotta, F.; Ferrari, M.; Gnocchi, P.; Isetta, A.; Mongelli, N.; Motta, P.; Rossi, A.; Rossi, M.; Tibolla, M.; Vanotti, E. *J. Med. Chem.* **2000**, *43*, 2557–2565.

Dairi, K.; Tripathy, S.; Attardo, G.; Lavallée, J.-F. *Tetrahedron Lett.* **2006**, *47*, 2605–2606.

Dao, H. T.; Li, C.; Michaudel, Q.; Maxwell, B. D.; Baran, P. S. *J. Am. Chem. Soc.* **2015**, *137*, 8046–8049.

Darabi, H. R.; Mirzakhani, M.; Aghapoor, K.; Jadidi, K.; Faraji, L; Sakhaee, N. *J. Organomet. Chem.* **2013**, *740*, 131–134.

Davies, H. M. L.; Hansen, T.; Churchill, M. R. *J. Am. Chem. Soc.* **2000**, *122*, 3063–3070.

D'Costa, A. M.; Robinson, J. K.; Maududi, T.; Chaturvedi, V.; Nickoloff, B. J.; Denning, M. F. *Oncogene* **2006**, *25*, 378–386.

de la Torre, M. C.; García, I.; Sierra, M. A. *J. Org. Chem.* **2003**, *68*, 6611–6618.

de la Torre, M. C.; García, I.; Sierra, M. A. *Chem.–Eur. J.* **2005**, *11*, 3659–3667.

DeLuca, R. J.; Edwards, J. L.; Steffens, L. D.; Michel, B. W.; Qiao, X.; Zhu, C.; Cook, S. P.; Sigman, M. S. *J. Org. Chem.* **2013**, *78*, 1682–1686.

Dess, D. B.; Martin, J. C. *J. Org. Chem.* **1983**, *48*, 4155–4156.

Dhar, D. N.; Murthy, K. S. K. *Synthesis* **1986**, *1986*, 437–449.

Döbler, C.; Mehltretter, G. M.; Sundermeier, U.; Beller, M. *J. Am. Chem. Soc.* **2000**, *122*, 10289–10297.

Dong, J. J.; Fañanás-Mastral, M.; Alsters, P. L.; Browne, W. R.; Feringa, B. L. *Angew. Chem., Int. Ed.* **2013**, *52*, 5561–5565.

Dröge, T.; Notzon, A.; Fröhlich, R.; Glorius, F. *Chem.–Eur. J.* **2011**, *17*, 11974–11977.

Dupuis, S. N.; Robertson, A. W.; Veinot, T.; Monro, S. M. A.; Douglas, S. E.; Syvitski, R. T.; Goralski, K. B.; McFarland, S. A.; Jakeman, D. L. *Chem. Sci.* **2012**, *3*, 1640–1644.

Emmanuvel, L.; Shaikh, T. M. A.; Sudalai, A. *Org. Lett.* **2005**, *7*, 5071–5074.

Enquist, J. A., Jr.; Stoltz, B. M. *Nature* **2008**, *453*, 1228–1231.

Enquist, J. A., Jr.; Stoltz, B. M. *Nat. Prod. Rep.* **2009**, *26*, 661–680.

Enquist, J. A., Jr.; Virgil, S. C.; Stoltz, B. M. *Chem.–Eur. J.* **2011**, *17*, 9957–9969.

Ernet, T.; Haufe, G. *Synthesis* **1997**, *1997*, 953–956.

Espino, C. G.; Du Bois, J. *Angew. Chem., Int. Ed.* **2001**, *40*, 598–600.

Espino, C. G.; Wehn, P. M.; Chow, J.; Du Bois, J. *J. Am. Chem. Soc.* **2001**, *123*, 6935–6936.

Fairlamb, I. J. S.; Kapdi, A. R.; Lee, A. F. *Org. Lett.* **2004**, *6*, 4435–4438.

Fatta-Kassinos, D.; Vasquez, M. I.; Kümmerer, K. *Chemosphere* **2011**, *85*, 693–709.

Flatt, B.; Martin, R.; Wang, T.-L.; Mahaney, P.; Murphy, B.; Gu, X.-H.; Foster, P.; Li, J.; Pircher, P.; Petrowski, M.; Schulman, I.; Westin, S.; Wrobel, J.; Yan, G.; Bischoff, E.; Daige, C.; Mohan, R. *J. Med. Chem.* **2009**, *52*, 904–907.

Fujiwara, M.; Ijichi, K.; Tokuhisa, K.; Katsuura, K.; Shigeta, S.; Konno, K.; Wang, G. Y.; Uemura, D.; Yokota, T.; Baba, M. *Antimicrob. Agents Chemother.* **1996**, *40*, 271–273.

Fürstner, A. *Angew. Chem., Int. Ed.* **2003**, *42*, 3582–3603.

Fürstner, A.; Grabowski, J.; Lehmann, C. W. *J. Org. Chem.* **1999**, *64*, 8275–8280.

Fürstner, A.; Krause, H. *J. Org. Chem.* **1999**, *64*, 8281–8286.

Fürstner, A.; Radkowski, K.; Peters, H.; Seidel, G.; Wirtz, C.; Mynott, R.; Lehmann, C. W. *Chem.–Eur. J.* **2007**, *13*, 1929–1945.

Galli, C.; Mandolini, L. *Eur. J. Org. Chem.* **2000**, 3117–3125.

Galloway, W. R. J. D.; Isidro-Llobet, A.; Spring, D. R. *Nat. Commun.* **2010**, *1*, 80.

Gaoni, Y. *J. Org. Chem.* **1994**, *59*, 6853–6855.

García, P.; Ramallo, I. A.; Salazar, M. O.; Furlan, R. L. E. *RSC Adv.* **2016**, *6*, 57245–57252.

Gerber, N. N. *J. Antibiot.* **1975**, *28*, 194–199.

Ghorai, M. K.; Talukdar, R.; Tiwari, D. P. *Org. Lett.* **2014**, *16*, 2204–2207.

Gligorich, K. M.; Sigman, M. S. *Chem. Commun.* **2009**, 3854–3867.

Goess, B. C.; Hannoush, R. N.; Chan, L. K.; Kirchhausen, T.; Shair, M. D. *J. Am. Chem. Soc.* **2006**, *128*, 5391–5403.

Gormisky, P. E.; White, M. C. *J. Am. Chem. Soc.* **2013**, *135*, 14052–14055.

Green, D.; Goldberg, I.; Stein, Z.; Ilan, M.; Kashman, Y. *Nat. Prod. Lett.* **1992**, *1*, 193–199.

Gribble, G. W. *Naturally Occurring Organohalogen Compounds: A Comprehensive Update*; Springer-Verlag: Weinheim Germany, **2010**.

Groves, J. T.; Quinn, R. *J. Am. Chem. Soc.* **1985**, *107*, 5790–5792.

Grue-Sørensen, G.; Liang, X.; Månsson, K.; Vedsø, P.; Sørensen, M. D.; Soor, A.; Stahlhut, M.; Bertelsen, M.; Engell, K. M.; Högberg, T. *Bioorg. Med. Chem. Lett.* **2014**, *24*, 54–60.

Grue-Sørensen, G.; Spenser, I. D. *J. Am. Chem. Soc.* **1983**, *105*, 7401–7404.

Gueritte-Voegelein, F.; Guenard, D.; Lavelle, F.; Le Goff, M. T.; Mangatal, L.; Potier, P. *J. Med. Chem.* **1991**, *34*, 992–998.

Gunasekera, S. P.; Gunasekera, M.; Longley, R. E.; Schulte, G. K. *J. Org. Chem.* **1990**, *55*, 4912–4915

Gutekunst, W. R.; Baran, P. S. *Chem. Soc. Rev.* **2011**, *40*, 1976–1991.

Handbook of Organopalladium Chemistry for Organic Synthesis (Ed.: Negishi, E.), Wiley New York, **2002**.

Han, X.; Stoltz, B. M.; Corey, E. J. *J. Am. Chem. Soc.* **1999**, *121*, 7600–7605.

Hann, M. M.; Leach, A. R.; Harper, G. *J. Chem. Inf. Comput. Sci.* **2001**, *41*, 856–864.

Hanson, F. R.; Eble, T. E. *US Patent* 2652356, 1950.

He, J.; Hamann, L. G.; Davies, H. M. L.; Beckwith, R. E. J. *Nat. Comms.* **2015**, *6*, 5943.

Hecker, E. *Cancer Res.* **1968**, *28*, 2338–2348.

Heeg, M. J.; Moore, T. L.; Rigby, J. H. *Acta Cryst.* **1991**, *C47*, 198–200.

Helmboldt, H.; Köhler, D.; Hiersemann, M. *Org. Lett.* **2006**, *8*, 1573–1576.

Henkel, T.; Brunne, R. M.; Müller, H.; Reichel, F. *Angew. Chem., Int. Ed.* **1999**, *38*, 643–647.

Hert, J.; Irwin, J. J.; Laggner, C.; Keiser, M. J.; Shoichet, B. K. *Nat. Chem. Biol.* **2009**, *5*, 479–483.

Hili, R.; Yudin, A. K. *Nat. Chem. Biol.* **2006**, *2*, 284–287.

Hong, A. Y.; Krout, M. R.; Jensen, T.; Bennett, N. B.; Harned, A. M.; Stoltz, B. M. *Angew. Chem., Int. Ed.* **2011**, *50*, 2756–2760.

Hong, A. Y.; Stoltz, B. M. *Angew. Chem., Int. Ed.* **2012**, *51*, 9674–9678.

Hong, A. Y.; Stoltz, B. M. *Eur. J. Org. Chem.* **2013**, 2745–2759.

Horrillo-Martínez, P.; Hultzsch, K. C.; Gil, A.; Branchadell, V. *Eur. J. Org. Chem.* **2007**, *2007*, 3311–3325.

Huigens, R. W., III; Morrison, K. C.; Hicklin, R. W.; Flood, T. A., Jr.; Richter, M. F.; Hergenrother, P. J. *Nat. Chem.* **2013**, *5*, 195–202.

Hultzsch, K. C. *Adv. Synth. Catal.* **2005**, *347*, 367–391.

Ignatenko, V. A.; Han, Y.; Tochtrop, G. P. *J. Org. Chem.* **2013**, *78*, 410–418.

Ignatenko, V. A.; Tochtrop, G. P. *J. Org. Chem.* **2013**, *78*, 3821–3831.

Inanaga, J.; Hirata, K.; Saeki, H.; Katsuki, T.; Yamaguchi, M. *Bull. Chem. Soc. Jpn.* **1979**, *52*, 1989–1993.

Isbrucker, R. A.; Cummins, J.; Pomponi, S. A.; Longley, R. E.; Wright, A. E. *Biochem. Pharmacol.* **2003**, *66*, 75–82.

Jang, K. H.; Jeon, J.; Ryu, S.; Lee, H.-S.; Oh, K.-B.; Shin, J. *J. Nat. Prod.* **2008**, *71*, 1701–1707.

Jiang, Y.-Y.; Zhang, Q.; Yu, H.-Z.; Fu, Y. *ACS Catal.* **2015**, *5*, 1414–1423.

Jin, Y.; Yeh, C.-H.; Kuttruff, C. A.; Jørgensen, L.; Dünstl, G.; Felding, J.; Natarajan, S. R.; Baran, P. S. *Angew. Chem., Int. Ed.* **2015**, *54*, 14044–14048.

Jira, R. *Angew. Chem., Int. Ed.* **2009**, 48, 9034–9037.

Jo, T. S.; Kim, S. H.; Shin, J.; Bae, C. *J. Am. Chem. Soc.* **2009**, *131*, 1656–1657.

Jørgensen, L.; McKerrall, S. J.; Kuttruff, C. A.; Ungeheuer, F.; Felding, J.; Baran, P. S. *Science* **2013**, *341*, 878–882.

Jung, W.-H.; Harrison, C.; Shin, Y.; Fournier, J.-H.; Balachandran, R.; Raccor, B. S.; Sikorski, R. P.; Vogt, A.; Curran, D. P.; Day, B. W. *J. Med. Chem.* **2007**, *50*, 2951–2966.

Keith, J. A.; Nielsen, R. J.; Oxgaard, J.; Goddard, W. A., III *J. Am. Chem. Soc.* **2007**, *129*, 12342–12343.

Kierkus, P. C.; Rigby, J. H.; Heeg, M. J. *Acta Cryst.* **1990**, *C46*, 521–522.

Kim, K. E.; Li, J.; Grubbs, R. H.; Stoltz, B. M. *J. Am. Chem. Soc.* **2016**, *138*, 13179–13182.

Kim, K. E.; Stoltz, B. M. *Org. Lett.* **2016**, *18*, 5720–5723.

Kingston, D. G. I.; Chaudhary, A. G.; Chordia, M. D.; Gharpure, M.; Gunatilaka, A. A. L.; Higgs, P. I.; Rimoldi, J. M.; Samala, L.; Jagtap, P. G.; Giannakakou, P.; Jiang, Y. Q.; Lin, C. M.; Hamel, E.; Long, B. H.; Fairchild, C. R.; Johnston, K. A. *J. Med. Chem.* **1998**, *41*, 3715–3726.

Koehn, F. E.; Carter, G. T. *Nat. Rev. Drug Discov.* **2005**, *4*, 206–220.

Kondo, Y.; García-Cuadrado, D.; Hartwig, J. F.; Boaen, N. K.; Wagner, N. L.; Hillmyer, M. A. *J. Am. Chem. Soc.* **2002**, *124*, 1164–1165.

Kowalski, R. J.; Giannakakou, P.; Gunasekera, S. P.; Longley, R. E.; Day, B. W.; Hamel, E. *Mol. Pharmacol.* **1997**, *52*, 613–622.

Krout, M. R.; Mohr, J. T.; Stoltz, B. M. *Org. Synth.* **2009**, *86*, 181–193.

Kuehne, M. E.; Bohnert, J. C.; Bornmann, W. G.; Kirkemo, C. L.; Kuehne, S. E.; Seaton, P. J.; Zebovitz, T. C. *J. Org. Chem.* **1985**, *50*, 919–924.

Kumar, K.; Michalik, D.; Castro, I. G.; Tillack, A.; Zapf, A.; Arlt, M.; Heinrich, T.; Böttcher, H.; Beller, M. *Chem.–Eur. J.* **2004**, *10*, 746–757.

Kuttruff, C. A.; Eastgate, M. D.; Baran, P. S. *Nat. Prod. Rep.* **2014**, *31*, 419–432.

Kuwajima, I.; Tanino, K. *Chem. Rev.* **2005**, *105*, 4661–4670.

Laatsch, H.; Kellner, M.; Weyland, H. *J. Antibiot.* **1991**, *44*, 187–191.

Lacaná, E.; Amur, S.; Mummanneni, P.; Zhao, H.; Frueh, F. W. *Clin. Pharmacol. Ther.* **2007**, *82*, 466–471.

Lachance, H.; Wetzel, S.; Kumar, K.; Waldmann, H. *J. Med. Chem.* **2012**, *55*, 5989–6001.

Lewis, J. C.; Mantovani, S. M.; Fu, Y.; Snow, C. D.; Komor, R. S.; Wong, C.-H.; Arnold, F. H. *Chembiochem* **2010**, *11*, 2502–2505.

Leznoff, C. C.; Wong, J. Y. *Can. J. Chem.* **1972**, *50*, 2892–2893.

Li, J. W.-H.; Vederas, J. C. *Science* **2009**, *325*, 161–165.

Li, L.; Wang, C.-Y.; Huang, R.; Biscoe, M. R. *Nat. Chem.* **2013**, *5*, 607–612.

Lin, H.; Xiao, L.-J.; Zhou, M.-J.; Yu, H.-M.; Xie, J.-H.; Zhou, Q.-L. *Org. Lett.* **2016**, *18*, 1434–1437.

Liu, W.-B.; Reeves, C. M.; Virgil, S. C.; Stoltz, B. M. *J. Am. Chem. Soc.* **2013**, *135*, 10626–10629.

Liu, Y.; Han, S.-J.; Liu, W.-B.; Stoltz, B. M. *Acc. Chem. Res.* **2015**, *48*, 740–751.

Liu, Y.; Virgil, S. C.; Grubbs, R. H.; Stoltz, B. M. *Angew. Chem., Int. Ed.* **2015**, *54*, 11800–11803.

López, S. N.; Ramallo, I. A.; Sierra, M. G.; Zacchino, S. A.; Furlan, R. L. E. *Proc. Natl. Acad. Sci. U.S.A.* **2007**, *104*, 441–444.

Lyons, T. W.; Sanford, M. S. *Chem. Rev.* **2010**, *110*, 1147–1169.

Magae, J.; Miller, M. W.; Nagai, K.; Shearer, G. M. *J. Antibiot.* **1996**, *49*, 86–90.

Maisonneuve, I. M.; Glick, S. D. *Pharmaol. Biochem. Behav.* **2003**, *75*, 607–618.

Manderville, R. A. *Curr. Med. Chem. Anti-Cancer Agents* **2001**, *1*, 195–218.

Marziale, A. N.; Duquette, D. C.; Craig, R. A., II; Kim, K. E.; Liniger, M.; Numajiri, Y.; Stoltz, B. M. *Adv. Synth. Catal.* **2015**, *357*, 2238–2245.

McDougal, N. T.; Streuff, J.; Mukherjee, H.; Virgil, S. C.; Stoltz, B. M. *Tetrahedron Lett.* **2010**, *51*, 5550–5554.

McFadden, R. M.; Stoltz, B. M. *J. Am. Chem. Soc.* **2006**, *128,* 7738–7739.

McMurray, L.; O'Hara, F.; Gaunt, M. J. *Chem. Soc. Rev.* **2011**, *40*, 1885–1898.

McNeill, E.; Du Bois, J. *Chem. Sci.* **2012**, *3*, 1810–1813.

McNeill, E.; Du Bois, J. *J. Am. Chem. Soc.* **2010**, *132*, 10202–10204.

Meinwald, J.; Labana, S. S.; Chadha, M. S. *J. Am. Chem. Soc.* **1963**, *85*, 582–585.

Melvin, M. S.; Calcutt, M. W.; Noftle, R. E.; Manderville, R. A.; *Chem. Res. Toxicol.* **2002**, *15*, 742–748.

Melvin, M. S.; Tomlinson, J. T.; Saluta, G. R.; Kucera, G. L.; Lindquist, N.; Manderville, R. A. *J. Am. Chem. Soc.* **2000**, *122*, 6333–6334.

Merrifield, R. B. *J. Am. Chem. Soc.* **1963**, *85*, 2149–2154.

Meyer, C.; Schepmann, D.; Yanagisawa, S.; Yamaguchi, J.; Itami, K.; Wünsch, B. *Eur. J. Org. Chem.* **2012**, *2012*, 5972–5979.

Meyer, S. D.; Schreiber, S. L. *J. Org. Chem.* **1994**, *59*, 7549–7552.

Michaudel, Q.; Journot, G.; Regueiro-Ren, A.; Goswami, A.; Guo, Z.; Tully, T. P.; Zou, L.; Ramabhadran, R. O.; Houk, K. N.; Baran, P. S. *Angew. Chem., Int. Ed.* **2014**, *53*, 12091–12096.

Michaudel, Q.; Thevenet, D.; Baran, P. S. *J. Am. Chem. Soc.* **2012**, *134*, 2547–2550.

Michel, B. W.; Camelio, A. M.; Cornell, C. N.; Sigman, M. S. *J. Am. Chem. Soc.* **2009**, *131*, 6076–6077.

Michel, B. W.; McCombs, J. R.; Winkler, A.; Sigman, M. S. *Angew. Chem., Int. Ed.* **2010**, *49*, 7312–7315.

Mickel, S. J.; Niederer, D.; Daeffler, R.; Osmani, A.; Kuesters, E.; Schmid, E.; Schaer, K.; Gamboni, R.; Chen, W.; Loeser, E.; Kinder, F. R., Jr.; Konigsberger, K.; Prasad, K.; Ramsey, T. M.; Repič, O.; Wang, R.-M.; Florence, G.; Lyothier, I.; Paterson, I. *Org. Process Res. Dev.* **2004**, *8*, 122–130.

Minisci, F.; Galli, R.; Galli, A.; Bernardi, R. *Tetrahedron Lett.* **1967**, *8*, 2207–2209.

Mita, A.; Lockhart, A. C.; Chen, T. *Proc. Am. Soc. Clin. Oncol.* **2004**, *23*, 133.

Mita, A.; Lockhart, A. C.; Chen, T.-L.; Bochinski, K.; Curtright, J.; Cooper, W.; Hammond, L.; Rothenberg, M.; Rowinsky, E.; Sharma, S. *J. Clin. Oncol.* **2004**, *22*, 2025–2025.

Mitsudome, T.; Mizumoto, K; Mizugaki, T; Jitsukawa, K; Kaneda, K. *Angew. Chem., Int. Ed.* **2010**, *49*, 1238–1240.

Mitsudome, T.; Umetani, T; Nosaka, N.; Mori, K.; Mizugaki, T.; Ebitani, K.; Kaneda, K. *Angew. Chem., Int. Ed.* **2006**, *45*, 481–485.

Mitsudome, T.; Yoshida, S; Mizugaki, T.; Jitsukawa, K.; Kaneda, K. *Angew. Chem., Int. Ed.* **2013**, *52*, 5961–5964.

Mitsudome, T.; Yoshida, S.; Tsubomoto, Y; Mizugaki, T.; Jitsukawa, K.; Kaneda, K. *Tetrahedron Lett.* **2013**, *54*, 1596–1598.

Młochowski, J.; Wójtowicz-Młochowska, H. *Molecules* **2015**, *20*, 10205–10243.

Moloney, G. P.; Martin, G. R.; Matthews, N.; Milne, A.; Hobbs, H.; Dosworth, S.; Sang, P. Y.; Knight, C.; Williams, M.; Maxwell, M.; Glen, R. C. *J. Med. Chem.* **1999**, *42*, 2504–2526.

Morandi, B.; Wickens, Z. K.; Grubbs, R. H. *Angew. Chem., Int. Ed.* **2013**, *52*, 2944–2948.

Morandi, B.; Wickens, Z. K.; Grubbs, R. H. *Angew. Chem., Int. Ed.* **2013**, *52*, 9751–9754.

Morrill, C.; Funk, T. W.; Grubbs, R. H. *Tetrahedron Lett.* **2004**, *45*, 7733–7736.

Morrill, C.; Grubbs, R. H. *J. Org. Chem.* **2003**, *68*, 6031–6034.

Morrison, K. C.; Hergenrother, P. J. *Nat. Prod. Rep.* **2014**, *31*, 6–14.

Mortellaro, A.; Songia, S.; Gnocchi, P.; Ferrari, M.; Fornasiero, C.; D'Alessio, R.; Isetta, A.; Colotta, F.; Golay, J. *J. Immunol.* **1999**, *162*, 7102–7109.

Mountford, P. in *Green Chemistry in the Pharmaceutical Industry*, Dunn, P. J.; Wells, A. S.; Williams, M. T., Eds. Wiley, Weinheim, Germany, **2010**: pp. 145–160.

Müller, P. *Crystallography Reviews* **2009**, *15*, 57–83.

Müller, T. E.; Hultzsch, K. C.; Yus, M.; Foubelo, F.; Tada, M. *Chem. Rev.* **2008**, *108*, 3795–3892.

Muzart, J. *Tetrahedron* **2007**, *63*, 7505–7521.

Nakamura, A.; Magae, J.; Tsuji, R. F.; Yamasaki, M.; Nagai, K. *Transplantation* **1989**, *47*, 1013–1016.

Narasaka, K.; Kitamura, M. *Eur. J. Org. Chem.* **2005**, 4505–4519.

Nelson, A. L.; Dhimolea, E.; Reichert, J. M. *Nat. Rev. Drug Discovery* **2010**, *9*, 767–774.

Neumann, R.; Dahan, M. *Nature* **1997**, *388*, 353–355.

Newhouse, T.; Baran, P. S. *Angew. Chem., Int. Ed.* **2011**, *50*, 3362–3374.

Newman, D. J.; Cragg, G. M. *J. Nat. Prod.* **2007**, *70*, 461–477.

Newman, D. J.; Cragg, G. M. *J. Nat. Prod.* **2012**, *75*, 311–335.

Ng, P. Y.; Tang, Y.; Knosp, W. M.; Stadler, H. S.; Shaw, J. T. *Angew. Chem., Int. Ed.* **2007**, *46*, 5352–5355.

Nickel, A.; Maruyama, T.; Tang, H.; Murphy, P. D.; Greene, B.; Yusuff, N.; Wood, J. L. *J. Am. Chem. Soc.* **2004**, *126*, 16300–16301.

Nicolaou, K. C.; Dai, W.-M.; Guy, R. K. *Angew. Chem., Int. Ed. Engl.* **1994**, *33*, 15–44.

Nicolaou, K. C.; Pfefferkorn, J. A.; Barluenga, S.; Mitchell, H. J.; Roecker, A. J.; Cao, G.-Q. *J. Am. Chem. Soc.* **2000**, *122*, 9968–9976.

Ning, X.-S.; Wang, M.-M.; Yao, C.-Z.; Chen, X.-M.; Kang, Y.-B. *Org. Lett.* **2016**, *18*, 2700–2703.

Njardarson, J. T.; Biswas, K.; Danishefsky, S. J. *Chem. Commun.* **2002**, 2759–2761.

Njardarson, J. T.; Gaul, C.; Shan, D.; Huang, X.-Y.; Danishefsky, S. J. *J. Am. Chem. Soc.* **2004**, *126*, 1038–1040.

Noisier, A. F. M.; Brimble, M. A. *Chem. Rev.* **2014**, *114*, 8775–8806.

Obara, Y.; Kobayashi, H.; Ohta, T.; Ohizumi, Y.; Nakahata, N. *Mol. Pharmacol.* **2001**, *59*, 1287–1297.

Obara, Y.; Nakahata, N.; Kita, T.; Takaya, Y.; Kobayashi, H.; Hosoi, S.; Kiuchi, F.; Ohta, T.; Oshima, Y.; Ohizumi, Y. *Eur. J. Pharmacol.* **1999**, *370*, 79–84.

Ochiai, M.; Miyamoto, K.; Kaneaki, T.; Hayashi, S.; Nakanishi, W. *Science* **2011**, *332*, 448–451.

O'Connor, C. J.; Beckmann, H. S. G.; Spring, D. R. *Chem. Soc. Rev.* **2012**, *41*, 4444–4456.

O'Connor, C. J.; Laraia, L.; Spring, D. R. *Chem. Soc. Rev.* **2011**, *40*, 4332–4345.

Ogbourne, S. M.; Suhrbier, A.; Jones, B.; Cozzi, S.-J.; Boyle, G. M.; Morris, M.; McAlpine, D.; Johns, J.; Scott, T. M.; Sutherland, K. P.; Gardner, J. M.; Le, T. T.

T.; Lenarczyk, A.; Aylward, J. H.; Parsons, P. G. *Cancer Res*. **2004**, *64*, 2833–2839.

Oguri, H.; Hiruma, T.; Yamagishi, Y.; Oikawa, H.; Ishiyama, A.; Otoguro, K.; Yamada, H.; Omura, S. *J. Am. Chem. Soc*. **2011**, *133*, 7096–7105.

Ojima, I.; Habus, I.; Zhao, M.; Zucco, M.; Park, Y. H.; Sun, C. M.; Brigaud, T. *Tetrahedron* **1992**, *48*, 6985–7012.

Ojima, I.; Sun, C. M.; Zucco, M.; Park, Y. H.; Duclos, O.; Kuduk, S. *Tetrahedron Lett*. **1993**, *34*, 4149–4152.

Orr, G. A.; Verdier-Pinard, P.; McDaid, H.; Horwitz, S. B. *Oncogene* **2003**, *22*, 7280–7295.

Oxygenases and Model Systems (Ed.: Funabiki, T.), Kluwer, Boston, **1997.**

Paddon, C. J.; Westfall, P. J.; Pitera, D. J.; Benjamin, K.; Fisher, K.; McPhee, D.; Leavell, M. D.; Tai, A.; Main, A.; Eng, D.; Polichuk, D. R.; Teoh, K. H.; Reed, D. W.; Treynor, T.; Lenihan, J.; Jiang, H.; Fleck, M.; Bajad, S.; Dang, G.; Dengrove, D.; Diola, D.; Dorin, G.; Ellens, K. W.; Fickes, S.; Galazzo, J.; Gaucher, S. P.; Geistlinger, T.; Henry, R.; Hepp, M.; Horning, T.; Iqbal, T.; Kizer, L.; Lieu, B.; Melis, D.; Moss, N.; Regentin, R.; Secrest, S.; Tsuruta, H.; Vasquez, R.; Westblade, L. F.; Xu, L.; Yu, M.; Zhang, Y.; Zhao, L.; Lievense, J.; Covello, P. S.; Keasling, J. D.; Reiling, K. K.; Renninger, N. S.; Newman, J. D. *Nature* **2013**, *496*, 528–532.

Pangborn, A. B.; Giardello, M. A.; Grubbs, R. H.; Rosen, R. K.; Timmers, F. J. *Organometallics* **1996**, *15*, 1518–1520.

Park, G.; Tomlinson, J. T.; Melvin, M. S.; Wright, M. W.; Day, C. S.; Manderville, R. A. *Org. Lett.* **2003**, *5*, 113–116.

Paterson, I.; Anderson, E. A. *Science* **2005**, *310*, 451–453.

Paterson, I.; Britton, R.; Delgado, O.; Wright, A. E. *Chem. Commun.* **2004**, 632–633.

Paterson, I.; Gardner, N. M.; Poullennec, K. G.; Wright, A. E. *Bioorg. Med. Chem. Lett.* **2007**, *17*, 2443–2447.

Paterson, I.; Naylor, G. J.; Gardner, N. M.; Guzmán, E.; Wright, A. E. *Chem.–Asian J.* **2011**, *6*, 459–473.

Pathak, T. P.; Miller, S. J. *J. Am. Chem. Soc.* **2013**, *135*, 8415–8422.

Pérez-Tomás, R.; Montaner, B.; Llagostera, E.; Soto-Cerrato, V. *Biochem. Pharmacol.* **2003**, *66*, 1447–1452.

Peng, J.; Avery, M. A.; Hamann, M. T. *Org. Lett.* **2003**, *5*, 4575–4578.

Peng, J.; Kasanah, N.; Stanley, C. E.; Chadwick, J.; Fronczek, F. R.; Hamann, M. T. *J. Nat. Prod.* **2006**, *69*, 727–730.

Peng, J.; Walsh, K.; Weedman, V.; Bergthold, J. D.; Lynch, J.; Lieu, K. L.; Braude, I. A.; Kelly, M.; Hamann, M. T. *Tetrahedron* **2002**, *58*, 7809–7819.

Pettit, G. R.; Cichacz, Z. A.; Goa, F.; Boyd, M. R.; Schmidt, J. M. *J. Chem. Soc., Chem. Commun.* **1994**, 1111–1112.

Pfeiffer, M. W. B.; Phillips, A. J. *J. Am. Chem. Soc.* **2005**, *127*, 5334–5335.

Pfeiffer, M. W. B.; Phillips, A. J. *Tetrahedron Lett*. **2008**, *49*, 6860–6861.

Pietruszka, J.; Witt, A. *Synthesis* **2006**, *24*, 4266–4268.

Popik, P.; Glick, S. D. *Drugs Future* **1996**, *21*, 1109–1115

Quinn, R. K.; Könst, Z. A.; Michalak, S. E.; Schmidt, Y.; Szklarski, A. R.; Flores, A. R.; Nam, S.; Horne, D. A.; Vanderwal, C. D.; Alexanian, E. J. *J. Am. Chem. Soc*. **2016**, *138*, 696–702.

Qiu, Y.; Gao, S. *Nat. Prod. Rep*. **2016**, *33,* 562–581.

Reddy, T. J.; Bordeau, G.; Trimble, L. *Org. Lett*. **2006**, *8*, 5585–5588.

Reeves, C. M.; Eidamshaus, C.; Kim, J.; Stoltz, B. M. *Angew. Chem., Int. Ed*. **2013**, *52*, 6718–6721.

Repke, D. B.; Artis, D. R.; Nelson, J. T.; Wong, E. H. F. *J. Org. Chem*. **1994**, *59*, 2164–2171.

Rho, J.-R.; Lee, H.-S.; Sim, C. J.; Shin, J. *Tetrahedron* **2002**, *58*, 9585–9591.

Rigby, J. H.; Moore, T. L. *J. Org. Chem*. **1990**, *55*, 2959–2962.

Roizen, J. L.; Zalatan, D. N.; Du Bois, J. *Angew. Chem., Int. Ed*. **2013**, *52*, 11343–11346.

Rottmann, M.; McNamara, C.; Yeung, B. K. S.; Lee, M. C. S.; Zou, B.; Russell, B.; Seitz, P.; Plouffe, D. M.; Dharia, N. V.; Tan, J.; Cohen, S. B.; Spencer, K. R.; González-Páez, G. E.; Lakshminarayana, S. B.; Goh, A.; Suwanarusk, R.; Jegla, T.; Schmitt, E. K.; Beck, H.-P.; Brun, R.; Nosten, F.; Renia, L.; Dartois, V.;

Keller, T. H.; Fidock, D. A.; Winzeler, E. A.; Diagana, T. T. *Science* **2010**, *329*, 1175–1180.

Rucker, R. P.; Whittaker, A. M.; Dang, H.; Lalic, G. *J. Am. Chem. Soc.* **2012**, *134*, 6571–6574.

Ryu, J.-S.; Li, G. Y.; Marks, T. J. *J. Am. Chem. Soc.* **2003**, *125*, 12584–12605.

Sakuda, Y. *Bull. Chem. Soc. Jpn.* **1969**, *42*, 3348–3349.

Salamone, M.; Ortega, V. B.; Bietti, M. *J. Org. Chem.* **2015**, *80*, 4710–4715.

Schmidt, R. J. *J. Linn. Soc. Bot.* **1987**, *94*, 221–230.

Schreiber, S. L. *Bioorg. Med. Chem.* **1998**, *6*, 1127–1152.

Schreiber, S. L. *Chem. Eng. News* **2003**, *81*, 51–60.

Schreiber, S. L. *Science* **2000**, *287*, 1964–1969.

Scriven, E. F. V.; Turnbull, K. *Chem. Rev.* **1988**, *88*, 297–368.

Sergent, D.; Wang, Q.; Sasaki, N. A.; Ouazzani, J. *Bioorg. Med. Chem. Lett.* **2008**, *18*, 4332–4335.

Sharma, A.; Hartwig, J. F. *Nature* **2015**, *517*, 600–604.

Shelat, A. A.; Guy, R. K. *Nat. Chem. Biol.* **2007**, *3*, 442–446.

Sheldrick, G. M. *Acta. Cryst.* **1990**, A46, 467–473.

Sheldrick, G. M. *Acta Cryst*. **2008**, A64, 112–122.

Shibuya, G. M.; Enquist, J. A., Jr.; Stoltz, B. M. *Org*. *Lett*. **2013**, *15*, 3480–3483.

Shibuya, K. *Synth*. *Commun*. **1994**, *24*, 2923–2941.

Shimokawa, J. *Tetrahedron Lett*. **2014**, *55*, 6156–6162.

Shin, Y.; Choy, N.; Balachandran, R.; Madiraju, C.; Day, B. W.; Curran, D. P. *Org*. *Lett*. **2002**, *4*, 4443–4446.

Sigman, M. S.; Werner, E. W. *Acc*. *Chem*. *Res*. **2012**, *45*, 874–884.

Smidt, J.; Hafner, W.; Jira, R.; Sedlmeier, J.; Sieber, R.; Rüttinger, R.; Kojer, H. *Angew*. *Chem*. **1959**, *71*, 176–182.

Somsák, L.; Kovács, L.; Tóth, M.; Ösz, E.; Szilágyi, L.; Györgydeák, Z.; Dinya, Z.; Docsa, T.; Tóth, B.; Gergely, P. *J*. *Med*. *Chem*. **2001**, *44*, 2843–2848.

Song, C. E. *Cinchona Alkaloids in Synthesis and Catalysis*. Wiley: 2009.

Spring, D. R. *Org*. *Biomol*. *Chem*. **2003**, *1*, 3867–3870.

Stepkowski, S. M.; Erwin-Cohen, R. A.; Behbod, F.; Wang, M.-E.; Qu, X.; Tejpal, N.; Nagy, Z. S.; Kahan, B. D.; Kirken, R. A. *Blood* **2002**, *99*, 680–689.

Stahl, S. S. *Angew*. *Chem*., *Int*. *Ed*. **2004**, *43*, 3400–3420.

Stepkowski, S. M.; Nagy, Z. S.; Wang, M.-E.; Behbod, F.; Erwin-Cohen, R.; Kahan, B. D.; Kirken, R. A. *Transplant*. *Proc*. **2001**, *33*, 3272–3273.

Stewart, I. C.; Ung, T.; Pletnev, A. A.; Berlin, J. M.; Grubbs, R. H.; Schrodi, Y. *Org. Lett.* **2007**, *9*, 1589–1592.

Stockwell, B. R. *Nat. Rev. Genet.* **2000**, *1*, 116–125.

Strom, A. E.; Hartwig, J. F. *J. Org. Chem.* **2013**, *78*, 8909–8914.

Sun, Y.-H.; Sun, T.-Y.; Wu, Y.-D.; Zhang, X.; Rao, Y. *Chem. Sci.* **2016**, *7*, 2229–2238.

Taber, D. F.; DeMatteo, P. W.; Hassan, R. A. *Org. Synth.* **2013**, *90*, 350–357.

Tan, D. S. *Nat. Chem. Biol.* **2005**, *1*, 74–84.

Tanino, K.; Onuki, K.; Asano, K.; Miyashita, M.; Nakamura, T.; Takahashi, Y.; Kuwajima, I. *J. Am. Chem. Soc.* **2003**, *125*, 1498–1500.

Tarbell, D. S.; Carman, R. M.; Chapman, D. D.; Cremer, S. E.; Cross, A. D.; Huffman, K. R.; Kunstmann, M.; McCorkindale, N. J.; McNally, J. G., Jr.; Rosowsky, A.; Varino, F. H. L.; West, R. L. *J. Am. Chem. Soc.* **1961**, *83*, 3096–3113.

Teo, P.; Wickens, Z. K.; Dong, G.; Grubbs, R. H. *Org. Lett.* **2012**, *14*, 3237–3239.

ter Haar, E.; Kowalski, R. J.; Hamel, E.; Lin, C. M.; Longley, R. E.; Gunasekera, S. P.; Rosenkranz, H. S.; Day, B. W. *Biochemistry* **1996**, *35*, 243–250.

Thenmozhiyal, J. C.; Wong, P. T.-H.; Chui, W.-K. *J. Med. Chem.* **2004**, *47*, 1527–1535.

Tran, B. L.; Li, B.; Driess, M.; Hartwig, J. F. *J. Am. Chem. Soc.* **2014**, *136*, 2555–2563.

Trost, B. M.; Pissot-Soldermann, C.; Chen, I.; Schroeder, G. M. *J. Am. Chem. Soc.* **2004**, *126*, 4480–4481.

Trost, B. M.; Van Vranken, D. L. *Chem. Rev.* **1996**, *96*, 395–422.

Tsao, S.-W.; Rudd, B. A. M.; He, X.-G.; Chang, C.-J.; Floss, H. G. *J. Antibiot.* **1985**, *38*, 128–131.

Tschaen, B. A.; Schmink, J. R.; Molander, G. A. *Org. Lett.* **2013**, *15*, 500–503.

Tsuji, J. *Palladium Reagents and Catalysts: Innovations in Organic Synthesis*, Wiley, New York, **1996.**

Tsuji, J. *Synthesis* **1984**, *1984*, 369–384; (b) Takacs, J.M.; Jiang, X.-T. *Curr. Org. Chem.* **2003**, 7, 369–396.

Tsutsui, H.; Kitamura, M.; Narasaka, K. *Bull. Chem. Soc. Jpn.* **2002**, *75*, 1451–1460.

Tsutsui, H.; Narasaka, K. *Chem. Lett.* **1999**, 45–46.

Tsutsui, H.; Narasaka, K. *Chem. Lett.* **2001**, 526–527.

Umbreit, M. A.; Sharpless, K. B. *J. Am. Chem. Soc.* **1977**, *99*, 5526–5528.

U.S. Food and Drug Administration, *2012 Novel New Drugs Summary* (FDA, Washington, DC, 2013); www.fda.gov/downloads/Drugs/DevelopmentApprovalProcess/DrugInnovation/UCM337830.pdf.

Utsunomiya, M.; Hartwig, J. F. *J. Am. Chem. Soc.* **2004**, *126*, 2702–2703.

Utsunomiya, M.; Kuwano, R.; Kawatsura, M.; Hartwig, J. F. *J. Am. Chem. Soc.* **2003**, *125*, 5608–5609.

Varseev, G. N.; Maier, M. E. *Angew. Chem., Int. Ed.* **2009**, *48*, 3685–3688.

Vasas, A.; Rédei, D.; Csupor, D.; Molnár, J.; Hohmann, J. *Eur. J. Org. Chem.* **2012**, *2012*, 5115–5130.

Vita, M. V.; Waser, J. *Org. Lett.* **2013**, *15*, 3246–3249.

Walsh, C. T. *Science* **2004**, *303*, 1805–1810.

Waser, J.; Gaspar, B.; Nambu, H.; Carreira, E. M. *J. Am. Chem. Soc.* **2006**, *128*, 11693–11712.

Welsch, M. E.; Snyder, S. A.; Stockwell, B. R. *Curr. Opin. Chem. Biol.* **2010**, *14*, 347–361.

Weiner, B.; Baeza, A.; Jerphagnon, T.; Feringa, B. L. *J. Am. Chem. Soc.* **2009**, *131*, 9473–9474.

Wencel-Delord, J.; Glorius, F. *Nat. Chem.* **2013**, *5*, 369–375.

Wickens, Z. K.; Morandi, B.; Grubbs, R. H. *Angew. Chem., Int. Ed.* **2013**, *52*, 11257–11260.

Wickens, Z. K.; Skakuj, K.; Morandi, B.; Grubbs, R. H. *J. Am. Chem. Soc.* **2014**, *136*, 890–893.

Wilde, N. C.; Isomura, M.; Mendoza, A.; Baran, P. S. *J. Am. Chem. Soc.* **2014**, *136*, 4909–4912.

Winkler, J. D.; Rouse, M. B.; Greaney, M. F.; Harrison, S. J.; Jeon, Y. T. *J. Am. Chem. Soc.* **2002**, *124*, 9726–9728.

Wright, J. A.; Gaunt, M. J.; Spencer, J. B. *Chem.–Eur. J.* **2006**, *12*, 949–955.

Xing, X.; O'Connor, N. R.; Stoltz, B. M. *Angew. Chem., Int. Ed.* **2015**, *54*, 11186–11190.

Yamamoto, M.; Nakaoka, S.; Ura, Y.; Kataoka, Y. *Chem. Commun.* **2012**, *48*, 1165–1167.

Yang, Z.; Yu, P.; Houk, K. N. *J. Am. Chem. Soc.* **2016**, *138*, 4237–4242.

Yedida, V.; Leznoff, C. C. *Can. J. Chem.* **1980**, *58*, 1144–1150.

Yoganathan, S.; Miller, S. J. *J. Med. Chem.* **2015**, *58*, 2367–2377.

Yoshikai, K.; Hayama, T.; Nishimura, K.; Yamada, K.; Tomioka, K. *J. Org. Chem.* **2005**, *70*, 681–683.

Yu, J.-Q.; Corey, E. J. *J. Am. Chem. Soc.* **2003**, *125*, 3232–3233.

Zaman, S.; Kitamura, M.; Narasaka, K. *Bull. Chem. Soc. Jpn.* **2003**, *76*, 1055–1062.

Zhang, M.; Zhang, Y.; Jie, X.; Zhao, H.; Li, G.; Su, W. *Org. Chem. Front.* **2014**, *1*, 843–895.

Zhang, X.; Jia, X.; Fang, L.; Liu, N.; Wang, J.; Fan, X. *Org. Lett.* **2011**, *13*, 5024–5027.

Zhang, X.; Yang, H.; Tang, P. *Org. Lett.* **2015**, *17*, 5828–5831.

Zhu, C.; Cook, S. P. *J. Am. Chem. Soc.* **2012**, *134*, 13577–13579.

Zheng, L.; Xiang, J.; Bai, X. *J. Heterocycl. Chem.* **2006**, *43*, 321–324.

Zhu, S.; Niljianskul, N.; Buchwald, S. L. *J. Am. Chem. Soc.* **2013**, *135*, 15746–15749.

INDEX

A

B

C

D

E

F

G

H

I

J

L

M

N

O

P

Q

R

S

T

U

V

W

X

Y

Z

ABOUT THE AUTHOR

Kelly Eun-Jung Kim was born in Buffalo, NY, on January 18th, 1990 to Jessie and Brian Kim. After a brief move to Torrance, CA, the Kim family settled in Fort Myers, FL, in 1994. Kelly's childhood years were spent enjoying video and card games with her older brother Roger and playing with Amber and Cookie, the four-legged members of the Kim family. At Saint Michael Lutheran School, Kelly was especially enthusiastic about her 7th-grade Earth science course. After enrolling at Bishop Verot High School in 2003, Kelly was dismayed by the dearth of Earth science course offerings and thus vowed to study geology in college. Outside of the classroom, Kelly played the flute in band, participated in varsity cross-country, and founded the BVHS chess club.

In the fall of 2007, Kelly moved to New Haven, CT, to attend Yale University. Despite her intention to study geology, Kelly was quickly seduced by chemistry through Prof. J. Michael McBride's Freshman Organic Chemistry course. Fascinated by this unique introduction to organic chemistry and enamored with the associated lab course, Kelly decided to major in chemistry. A 2009 summer research internship in organic synthesis in Jülich, Germany, inspired Kelly to pursue graduate studies in chemistry. Kelly carried out her senior thesis research in the group of Prof. Nilay Hazari, studying the synthesis and reactivities of Ir, Rh, and Mg organometallic complexes.

After graduating from Yale in 2011, Kelly relocated to Pasadena, CA, to begin her doctoral studies at the California Institute of Technology. Craving a return to organic synthesis, she joined the group of Prof. Brian M. Stoltz, where her research efforts have been focused on the applications of transition metal catalysis in organic synthesis and the late-stage diversification of the cyanthiwigin natural product core.

Alongside her scientific interests, Kelly has nurtured a passion for music since beginning piano lessons at age 5. Exhilarated by her experience at the National High School Music Institute after her junior year of high school, Kelly continued her musical training in college, completing the music major and studying with Yale School of Music piano faculty. Throughout graduate school, Kelly has maintained her musical interests through regular participation in the Caltech Chamber Music Program.

Kelly will begin a postdoctoral position in the laboratories of Prof. Karen I. Goldberg at the University of Washington in January 2017.